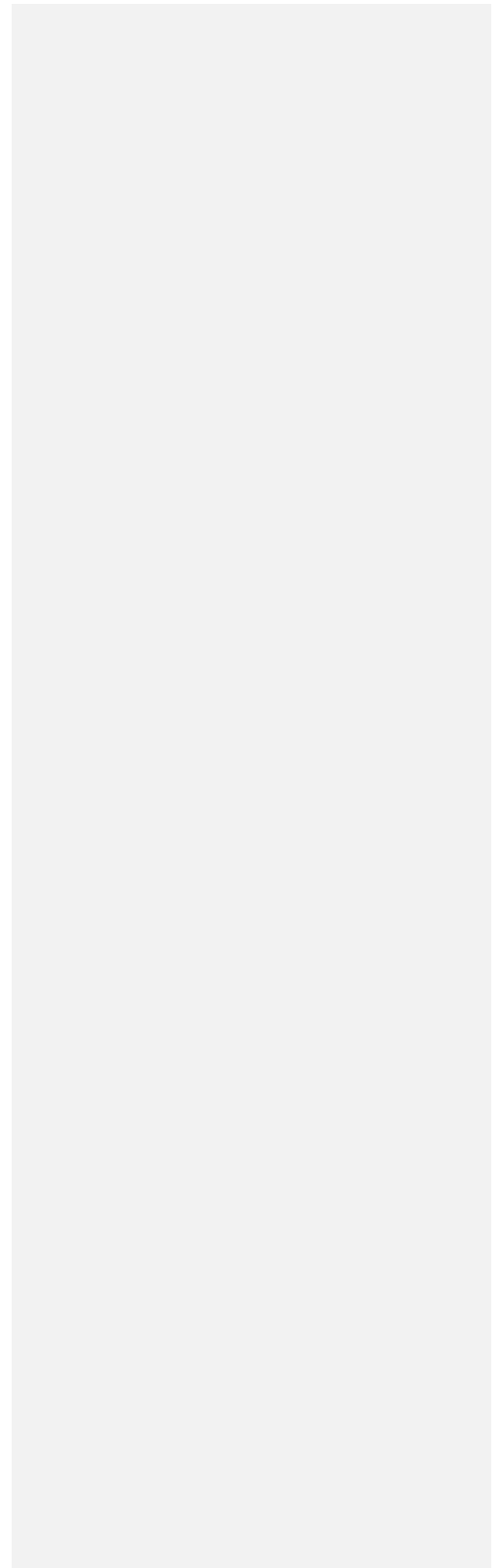


**Translating the effects of dietary flavonoids on energy
metabolism into physical activity benefits**

Daniel George Sadler

A thesis submitted in partial fulfilment of the requirements of Liverpool John
Moore's University for the degree of Doctor of Philosophy

May 2021



LIST OF CONTENTS

List of figures.....	9
List of tables.....	30
List of equations.....	33
Abbreviations.....	34
Abstract.....	38
Declaration.....	40
Acknowledgement.....	41
Dedication.....	42
Chapter 1: Introduction & Literature Review.....	43
1.1 General Introduction.....	44
1.2 Literature Review.....	48
1.2.1 Mitochondria – an overview.....	48
1.2.2 Mitochondrial oxidative phosphorylation.....	49
1.2.3 Mitochondrial turnover.....	50
1.2.4 Mitochondria morphology.....	52
1.2.5 Mitochondrial (& extra-mitochondrial) reactive oxygen species.....	53
1.2.6 Section Summary & link to thesis objectives.....	54
1.2.7 Mechanisms of age-related mitochondrial dysfunction.....	54
1.2.7.1 Skeletal muscle mitochondrial (dys)function.....	54
1.2.7.2 Vascular endothelial mitochondrial dysfunction.....	57
1.2.8 Evidence of age-related impairments in the capacity to deliver and utilise oxygen <i>in vivo</i>	60
1.2.8.1 Impaired O ₂ utilisation.....	60
1.2.8.2 Impaired O ₂ delivery.....	62
1.2.9 Consequences of impaired capacity for the delivery and utilisation of O ₂ : $\dot{V}O_2$ kinetics and exercise tolerance.....	65
1.2.9.1 $\dot{V}O_2$ kinetics offers insights into skeletal muscle metabolism.....	65
1.2.10 $\dot{V}O_2$ kinetics: Deleterious effects of ageing (and inactivity).....	66
1.2.11 Section Summary.....	68
1.2.12 Dietary flavonoids: An overview.....	69
1.2.13 Evidence for flavonoids purported health benefits on vascular and skeletal muscle health: Reported effects and associated mechanisms.....	72
1.2.14 Cocoa-flavanols.....	72
1.2.15 Quercetin.....	74
1.2.16 EGCG.....	75
1.2.17 (-)-Epicatechin (EPI).....	77
1.2.18 Section Summary.....	79
1.3 Thesis Perspective.....	81
1.4 Thesis Aims & Objectives.....	81
Chapter 2: Materials and Methods.....	83
2.1 Cell culture.....	84
2.2 Cell culture reagents.....	84
2.3 C ₂ C ₁₂ skeletal muscle cells.....	85

2.3.1	Passaging C ₂ C ₁₂ cells	85
2.3.2	Replicatively aged C ₂ C ₁₂ myoblasts	86
2.4	Primary Human Umbilical Vein Endothelial Cells	87
2.4.1	Passaging HUVEC.....	87
2.5	Cell counting	88
2.6	Cell cryopreservation and resuscitation.....	89
2.7	Cell viability.....	90
2.8	Mitochondrial ROS production (MitoSOX assay)	92
2.9	CellROX Assay.....	93
2.10	Assessing mitochondrial bioenergetics.....	94
2.10.1	Mitochondrial stress test protocol.....	95
2.10.2	Bioenergetic parameters analysis.....	97
2.11	Rates of ATP production and proton production.....	99
2.12	RT-qPCR Gene expression	101
2.12.1	RNA extraction	101
2.12.2	Assessment of RNA Concentration and Purity.....	102
2.12.3	Principle of the polymerase chain reaction.....	103
2.12.4	Procedure	106
2.12.5	Quantification of Relative Gene Expression.....	106
2.12.6	Primer Design	108
2.13	SDS-PAGE and immunoblotting.....	109
2.13.1	Principle.....	109
2.13.2	Procedures.....	110
2.14	SRB Assay	112
2.15	BCA Assay	113
2.16	Statistical Analysis.....	113
Chapter 3: Cocoa-flavanols enhance moderate-intensity pulmonary $\dot{V}O_2$ kinetics but not exercise tolerance in sedentary middle-aged adults.....		115
3.1	Abstract.....	116
3.2	Introduction.....	117
3.3	Methodology	118
3.3.1	Participants.....	118
3.3.2	Procedures.....	119
3.3.3	Preliminary trial(s).....	120
3.3.4	Experimental trials.....	122
3.3.5	Measurements	123
3.3.6	Data analysis	124
3.3.7	Statistics	126
3.4	Results.....	126
3.4.1	Heart rate kinetics, blood lactate profiles and blood pressure	127
3.4.2	$\dot{V}O_2$ kinetics and exercise tolerance	129
3.5	Discussion	132
3.6	Limitations	135
3.7	Conclusion	136
Chapter 4: The impact of dietary flavonoids on mitochondrial function and reactive oxygen and nitrogen species in HUVECs		137
4.1	Abstract.....	138
4.2	Introduction.....	140

4.3 Methodology	143
4.3.1 Cell culture and treatment	143
4.3.2 Cell viability assay	143
4.3.3 MitoSOX assay	144
4.3.4 CellROX Assay	145
4.3.5 DAF-FM (Nitric oxide detection)	145
4.3.6 RT-qPCR – Gene expression quantification	146
4.3.7 Mitochondrial Bioenergetics	148
4.3.8 SDS-PAGE and immunoblotting	149
4.3.9 Statistical analysis	150
4.4 Results	151
4.4.1 Flavonoids do not impair vascular endothelial cell viability	151
4.4.2 Mitochondrial ROS production is differentially impacted by flavonoids in vascular endothelial cells	152
4.4.2.1 Quercetin dose-dependently modulates mitochondrial ROS production	153
4.4.2.2 EGCG attenuates mitochondrial ROS production	153
4.4.2.3 EPI dose-dependently modulates mitochondrial ROS production	154
4.4.3 Non-mitochondrial specific ROS production is not impacted by flavonoid treatment	156
4.4.4 Flavonoids differentially impact the production of nitric oxide in vascular endothelial cells	157
4.4.5 Dietary flavonoids differentially impact the expression of genes associated with energy metabolism in vascular endothelial cells	159
4.4.6 Acute flavonoid treatment has limited impact on mitochondrial bioenergetics in vascular endothelial cells	164
4.4.7 Acute dietary flavonoid treatment does not impact ATP production or proton efflux rates in vascular endothelial cells	167
4.4.8 The effects of EPI on endothelial cell signalling responses	168
4.4.8.1 CaMKII is not modulated by EPI in endothelial cells	168
4.4.8.2 Acute EPI treatment inhibits AMPK activity in endothelial cells	169
4.4.8.3 EPI temporally augments p44/42 MAPK (ERK1/2) signalling	171
4.4.8.4 Epicatechins impact on ERK1/2 signalling is independent of eNOS activity in vascular endothelial cells	173
4.5 Discussion	174
4.5.1 Flavonoids differentially affect the production of mitochondrial ROS and NO	174
4.5.2 Flavonoids differentially modulate gene expression of vascular endothelial cells	176
4.5.3 Acute dietary flavonoid treatment does not modulate indices of mitochondrial function	178
4.5.4 EPI transiently stimulates ERK1/2 signalling whilst suppressing AMPK activity	180
4.6 Limitations	181
4.7 Conclusion	182
Chapter 5: The effects of replicative ageing and dietary flavonoids on mitochondrial function, nitric oxide bioavailability and gene expression of C₂C₁₂ skeletal myoblasts	184
5.1 Abstract	185
5.2 Introduction	187
5.3 Methodology	190
5.3.1 Cell culture and treatment	190
5.3.2 Cell viability assay	190
5.3.3 Nitric oxide availability	191

5.3.4 Mitochondrial Bioenergetics.....	191
5.3.5 ATP Production Rates.....	192
5.3.6 Mitochondrial bioenergetics normalisation procedures.....	193
5.3.6.1 CyQuant® Direct Cell Proliferation Assay	193
5.3.6.2 dsDNA PicoGreen	194
5.3.7 Complex I Activity	196
5.3.8 RT-qPCR – Gene expression Quantification.....	198
5.3.9 Statistical analysis.....	200
5.4 Results.....	200
5.4.1 Mitochondrial bioenergetics of control and aged skeletal muscle myoblasts.....	200
5.4.2 Rates of ATP production: Control vs aged myoblasts.....	202
5.4.3 Mitochondrial bioenergetics of control and aged C ₂ C ₁₂ skeletal myoblasts: Effects of dietary flavonoids.....	204
5.4.4 Rates of ATP and proton production in skeletal myoblasts.....	208
5.4.5 The impact of flavonoids on myoblast mitochondrial bioenergetics may relate to modulation of complex I activity.....	209
5.4.6 Intracellular nitric oxide levels are not impacted by flavonoid treatment in control and aged skeletal muscle cells	210
5.4.7 Gene expression of control and aged skeletal myoblasts under CTRL conditions..	211
5.4.8 Summary of the effects of replicative ageing on gene expression in myoblasts	215
5.4.9 Flavonoids modulate gene expression of control and aged skeletal myoblasts.....	215
5.4.9.1 Expression of mitochondrial genes following Quercetin treatment in skeletal myoblasts	215
5.4.9.2 Expression of mitochondrial genes following EGCG treatment in skeletal myoblasts	217
5.4.9.3 Expression of mitochondrial genes following EPI treatment in skeletal myoblasts	218
5.4.9.4 Expression of antioxidant related genes following Quercetin treatment in skeletal myoblasts	221
5.4.9.5 Expression of antioxidant related genes following EGCG treatment in skeletal myoblasts	222
5.4.9.6 Expression of antioxidant related genes following EPI treatment in skeletal myoblasts	223
5.4.10 Summary of the impact of dietary flavonoids upon control and aged skeletal myoblasts	226
5.5 Discussion.....	229
5.5.1 Replicative ageing does not compromise mitochondrial function in myoblasts	230
5.5.2 Flavonoids do not cause alterations in myoblast mitochondrial respiration.....	231
5.5.3 Flavonoids do not rescue impairments to NO bioavailability in replicatively aged myoblasts	232
5.5.4 Replicative ageing attenuates myoblast PARKIN and SOD2 mRNA expression....	233
5.5.5 Flavonoids modulate the expression of genes associated with mitochondrial remodelling and the antioxidant response.....	234
5.6 Limitations	238
5.7 Conclusion	238
Chapter 6: The effects of replicative ageing and dietary flavonoids on mitochondrial function, reactive oxygen species production and cell signalling in C₂C₁₂ skeletal myotubes.....	240
6.1 Abstract.....	241
6.2 Introduction.....	243

6.3 Methodology	244
6.3.1 Cell culture and treatment	244
6.3.2 Mitochondrial ROS production	245
6.3.3 Cellular ROS	245
6.3.4 Mitochondrial Bioenergetics	246
6.3.5 ATP Production Rates	247
6.3.6 Mitochondrial bioenergetics normalisation procedures	248
6.3.6.1 dsDNA PicoGreen	248
6.3.7 RT-qPCR – Gene expression Quantification	250
6.3.8 SDS-PAGE and immunoblotting – Cell signalling	252
6.3.9 Statistical analysis	253
6.4 Results	254
6.4.1 Mitochondrial bioenergetics of control and aged skeletal muscle myotubes	254
6.4.2 Rates of ATP production: Control vs. aged myotubes	256
6.4.3 Proton production rates: Control vs. aged myotubes	257
6.4.4 Mitochondrial bioenergetics of control and aged skeletal myotubes: Impact of dietary flavonoids	258
6.4.5 Rates of ATP and proton production in skeletal myotubes with flavonoid treatment	261
6.4.6 Replicative ageing augments the production of mitochondrial reactive oxygen species	261
6.4.7 Quercetin does not attenuate antimycin A-induced mitochondrial ROS in control and aged myotubes	263
6.4.8 EGCG does not impact mitochondrial ROS production in control or aged myotubes	264
6.4.9 EPI does not attenuate age-related increases in mitochondrial ROS production	265
6.4.10 No role for dietary flavonoids in mitigating age-related increases in cellular ROS	266
6.4.11 Flavonoids differentially modulate gene expression of control and aged skeletal myotubes	269
6.4.12 Summary of replicative ageing’s impact upon gene expression in control and aged myotubes	273
6.4.13 Mitochondrial-related gene expression following Quercetin treatment in skeletal myotubes	274
6.4.14 Mitochondrial-related gene expression following EGCG treatment in skeletal myotubes	275
6.4.15 Mitochondrial-related gene expression following EPI treatment in skeletal myotubes	276
6.4.16 Antioxidant-related transcriptional responses following Quercetin treatment in skeletal myotubes	279
6.4.17 Antioxidant-related transcriptional responses following EGCG treatment in skeletal myotubes	280
6.4.18 Antioxidant-related transcriptional responses following EPI treatment in skeletal myotubes	281
6.4.19 Summary of flavonoid effects upon the transcriptional responses of skeletal myotubes	284
6.4.20 The effects of EPI on CaMKII protein content in control and aged myotubes	287
6.4.21 Acute EPI treatment augments AMPK phosphorylation in control and aged myotubes	288

6.4.22 EPI does not impact p44/42 MAPK (Erk1/2) phosphorylation in skeletal myotubes	290
6.4.23 EPI treatment does not augment eNOS phosphorylation in control and aged skeletal myotubes	292
6.4.24 Summary of the impact of dietary flavonoids upon control and aged skeletal myotubes	294
6.5 Discussion	294
6.5.1 Flavonoids do not rescue age-related impairments to mitochondrial function.....	294
6.5.2 Flavonoids do not mitigate age-related increases in ROS production	297
6.6 Flavonoids distinctly alter the expression of genes associated with energy metabolism	298
6.6.1 EPI augments AMPK activity in skeletal muscle cells, independent of Erk1/2	301
6.7 Limitations	303
6.8 Conclusion	304
Chapter 7: The effects of replicative ageing and dietary flavonoids on the metabolome of skeletal myoblasts and myotubes.....	306
7.1 Introduction.....	307
7.2 Materials and methods	309
7.2.1 Cell culture.....	309
7.2.2 Flavonoid treatments and controls	310
7.2.3 Sample preparation for ¹ H NMR acquisition.....	311
7.2.4 ¹ H NMR acquisition and sample processing.....	313
7.2.5 Metabolite annotation and identification	313
7.2.6 Spectral Normalisation.....	314
7.2.7 Data scaling and centring.....	315
7.2.8 Statistical Analysis.....	316
7.2.9 Principal component analysis	317
7.2.10 Partial least square discriminant analysis (PLS-DA).....	318
7.2.11 Variable importance of the projection (VIP)	319
7.2.12 Correlation reliability score	319
7.2.13 Univariate analysis.....	320
7.2.14 Metabolite set enrichment analysis (MSEA) and interpretation.....	321
7.3 Results.....	321
7.3.1 Age-specific differences in skeletal myoblasts.....	321
7.3.2 Age-specific differences in skeletal myotubes	327
7.3.3 Control vs. aged myoblasts and myotubes section summary	331
7.3.4 Quercetin effects in control and aged skeletal myoblasts.....	332
7.3.5 Quercetin effects in control and aged skeletal myotubes.....	338
7.3.6 Summary of Q effects upon the metabolome of control and aged myoblasts and myotubes	344
7.3.7 EGCG effects in control and aged skeletal myoblasts.....	345
7.3.8 EGCG effects in control and aged skeletal myotubes	351
7.3.9 Summary of EGCG effects upon the metabolome of control and aged myoblasts and myotubes	356
7.3.10 Epicatechin effects in control and aged skeletal myoblasts.....	357
7.3.11 Epicatechin effects in control and aged skeletal myotubes	362
7.3.12 Summary of EPI effects upon the metabolome of control and aged myoblasts and myotubes	367
7.4 Discussion	368

7.4.1 Control vs. aged myoblast comparisons (untreated CTRL conditions).....	368
7.4.2 Control vs. aged myotube comparisons (untreated CTRL conditions).....	371
7.4.3 Quercetin effects on the metabolome of skeletal myoblasts.....	374
7.4.4 Quercetin effects on the metabolome of skeletal myotubes	377
7.4.5 EGCG effects in control and aged myoblasts	380
7.4.6 EGCG effects in control and aged myotubes.....	383
7.4.7 EPI effects in control and aged myoblasts.....	386
7.4.8 EPI effects in control and aged myotubes.....	388
7.5 Limitations	391
7.6 Conclusion	392
Chapter 8: Thesis synthesis.....	394
8.1 Realisation of Aims.....	395
8.2 General findings.....	398
8.3 Future Directions	401
8.3.1 Chapter 3:.....	401
8.3.2 Chapter 4:.....	402
8.3.3 Chapter 5:.....	403
8.3.4 Chapter 6:.....	404
8.3.5 Chapter 7:.....	405
8.4 Thesis Implications and conclusion	406
Chapter 9: Appendices	408
Chapter 10: References	472

List of figures

- Figure 1. 1** Graphical representation of the relationship between ageing and functional capacity. Adapted from WHO, 2000.45
- Figure 1. 2** Pathway of O₂ and CO₂ transport from mouth to mitochondria. Physiologic mechanisms that link respiration at the cellular and whole-body levels. Red bars denote inhibitory effects of sedentary ageing upon O₂ delivery and utilisation pathways.....46
- Figure 1. 3** Flavonoid ingestion may promote beneficial effects upon target tissues such as the vascular endothelium and skeletal muscle tissue.47
- Figure 1. 4** Schematic of the molecular machinery responsible for oxidative phosphorylation within the mitochondrion. Electron (e⁻) transfer along the electron transport chain (comprising complex I, II, III and IV embedded in the inner mitochondrial membrane [IMM]) drives protons (H⁺) from the mitochondrial matrix into the inner membrane space (IMS). The electrochemical potential created by accumulation of H⁺ within the mitochondrial membranes is used by ATP synthase (complex V) to produce ATP. Proton leak allows H⁺ to re-enter the matrix, bypassing ATP synthase, such that oxygen (O₂) consumption is not entirely coupled to ATP synthesis. Electron leakage from complex I and III leads to partial reduction of O₂ to form superoxide (O₂⁻), which is rapidly quenched to form hydrogen peroxide (H₂O₂) by superoxide dismutase (SOD). H₂O₂ is further metabolised to water (H₂O) by catalase (CAT).....50
- Figure 1. 5** Highly interconnected cellular network of mitochondria. HUVEC mitochondria stained with Mitotracker Green (25 nM) and image captured at 63x magnification by confocal microscopy.53
- Figure 1. 6** Impact of sedentary ageing upon on skeletal muscle mitochondria. In older, physically inactive skeletal muscle, mitochondria display lowered respiratory function, reduced mitochondrial content, and increased production of mitochondrial-derived reactive oxygen species (ROS). Ultimately, these effects lead to a diminished capacity for oxygen utilisation.....57
- Figure 1. 7** Impact of advancing age on the vascular endothelium. In younger endothelial cells (**top**), eNOS (endothelial NO synthase) produces NO through the conversion of L-arginine to L-citrulline, to facilitate endothelium-dependent vasodilation (EDD). Reactive oxygen species (ROS), for example, O₂⁻ and H₂O₂, are produced by the mitochondrial electron transport chain (ETC) or cytosolic oxidant enzymes, such as NOX (NADPH oxidase). These reactive molecules are quenched by endogenous antioxidant enzymes such as superoxide dismutase (SOD) and catalase (CAT). In older endothelial cells (**bottom**), ROS production increases due

to increased mitochondrial and NOX-derived ROS. Increased O_2^- diminishes NO bioavailability, through its conversion to peroxynitrite ($ONOO^-$). Ultimately, these effects lead to a reduction in endothelial-dependent vasodilation in the aged endothelium. Figure adapted from (Donato et al., 2018).....59

Figure 1. 8 Schematic depicting the impact of sedentary ageing upon skeletal muscle and vascular endothelial function. Impairments to skeletal muscle and vascular endothelial cells manifest as reduced O_2 transport and utilisation.....64

Figure 1. 9 Schematic depicting typical pulmonary oxygen uptake response during constant-rate moderate-intensity exercise. After phase I which represents the time taken for deoxygenated blood to reach pulmonary circulation, oxygen uptake rises in a mono-exponential fashion (phase II, primary response), before reaching a steady-state (phase III).66

Figure 1. 10 Idealised portrayal of the relationship between the speed of $\dot{V}O_2$ kinetics (given by the time constant, τ) and muscle(s) O_2 delivery. Note the presence of O_2 dependent (leftwards) and O_2 -independent (rightwards) zones falling either side of the “Tipping Point”. When O_2 delivery falls below the tipping point $\dot{V}O_2$ kinetics become progressively slowed as evidenced by increasing τ . In young healthy individuals conventional locomotory activities such as walking, running, and cycling lie to the right of the tipping point. However, $\dot{V}O_2$ kinetics become demonstrably slowed with aging (black downward arrow), by moving the individual leftward into the O_2 -delivery dependent region. Figure adapted from (D. C. Poole & Jones, 2012).68

Figure 1. 11 Chemical structure of dietary flavonoids: A) quercetin, B) epigallocatechin-gallate, C) (-)-epicatechin.69

Figure 1. 12 Basic overview of flavonoid absorption and metabolism.70

Figure 1. 13 Schematic overview of the known effects of dietary flavonoids on skeletal muscle and vascular endothelial cells, as they relate to mitochondrial function and RONS production.80

Figure 2. 1 Murine C2C12 myoblasts in culture. A) Skeletal myoblasts. B) Late differentiating skeletal myotubes (96 hours). Images taken at 10x magnification (Olympus, CKX31).86

Figure 2. 2 Replicatively aged murine C2C12 myoblasts in culture. A) Aged skeletal myoblasts (24 hours) B) Late differentiating aged skeletal myotubes (96 hours). Images taken at 10x magnification (Olympus, CKX31).....87

Figure 2. 3 Primary human umbilical vein endothelial cells (HUVEC) in monolayer. Typical cobblestone morphology. Image taken at 10x magnification (Olympus, CKX31).88

Figure 2. 4 Standard curve generated for C₂C₁₂ myoblasts and HUVECs using CyQUANT® Cell Proliferation Assay. Cells were seeded at densities of 0-50,000 cells per well and grown in GM for 24 h. C₂C₁₂ myoblasts were then switched to DM for a further 24 h before freezing and subsequent processing on the day of assay. HUVECs remained in GM for an additional 24 h before freezing and processing. Data are representative of one experiment performed with 5 replicates for each cell number.91

Figure 2. 5 Mitochondrial superoxide production was estimated from rates of MitoSOX oxidation, in the absence and presence of 15 µM antimycin A. Fluorescence was recorded at ~30-second intervals for 30 minutes. Probe oxidation rates were calculated from the slopes of the progress curves. Relative fluorescence units (RFU) were normalised to cell number.93

Figure 2. 6 Typical mitochondrial stress test profile. Rates of oxygen consumption expressed in pmol/min and recorded over 120 minutes. Sequential additions of oligomycin, uncoupler (e.g., FCCP or BAM15), and mixture of rotenone and antimycin A were performed in order to interrogate mitochondrial function.97

Figure 2. 7 Diagram illustrating the main processes in the real time polymerase chain reaction (RT-qPCR). A) cDNA generation from a single strand of mRNA (from the 3' to 5' end) isolated from an experimental sample. B) Outline of RT-qPCR, where three key steps occur, including: Denaturation, annealing of primers, and extension of primers. Primers specific to the gene of interest anneal at both of the 3' end of the sense (top) and anti-sense (bottom) strand. The PCR reaction amplifies the amount of DNA over 40 cycles.105

Figure 2. 8 Setting of cycle threshold (C_T) to derive C_T values for genes of interest.108

Figure 2. 9 Melt curve analysis to determine specific target amplification. An example of melt curves analysed to determine primer specificity. A) A single peak suggesting no unspecific amplification whereas B) A double peak suggesting amplification of unintended targets and/or primer dimer issues.109

Figure 3. 1 CONSORT diagram showing the flow of participants through each stage of the randomised trial.119

Figure 3. 2 Schematic of experimental design.123

Figure 3. 3 Pulmonary $\dot{V}O_2$ and best-fit modelled responses of a representative participant to moderate-intensity exercise following PL (solid black circles) and CF (clear circles)

supplementation. $\tau\dot{V}O_2$ values are displayed for each transition, with the solid grey lines representing the modelled fits. 129

Figure 3. 4 Pulmonary $\dot{V}O_2$ and best-fit modelled responses to severe-intensity exercise following PL (solid black circles) and CF (clear black circles) supplementation. Panel A) Pulmonary $\dot{V}O_2$ responses of a representative participant displayed with associated $\tau\dot{V}O_2$. Panel B) Group mean $\dot{V}O_2$ responses during the rest-to-exercise transition following PL and CF supplementation. Group mean \pm SD $\dot{V}O_2$ at limit of exercise tolerance also shown. Solid grey lines represent the modelled fits. 130

Figure 4. 2 Schematic of the cellular and molecular processes investigated in this study. ... 142

Figure 4. 3 Standard curve generated for HUVECs using CyQUANT® Cell Proliferation Assay. Cells were seeded at densities of 0-50,000 cells per well and grown in EGM for 48 h before performing the assay. 151

Figure 4. 4 Vascular endothelial cell viability is not impaired by acute flavonoid treatment. HUVECs were treated with 0-20 μ M A) Quercetin, B) EGCG or C) EPI for 24 h. Data are means \pm SEM, representative of 3 independent repeats with 3 replicates of each condition. Statistical significance was tested for by one-way ANOVA and Dunnett's test for multiple comparisons. * P <0.05. ^a Significant main effect of dose (P <0.05). 152

Figure 4. 5 Dietary flavonoids differentially impact the rate of mitochondrial ROS production in vascular endothelial cells. MitoSOX oxidation rates were determined in HUVECs in the absence of presence of Q, EPI or EGCG. Cells were treated for 24 h with 0, 5 and 10 μ M Q, EGCG or EPI. After 24 h, cells were incubated with or without antimycin A for 30 minutes, before MitoSOX was loaded into cells (2.5 μ M final concentration). Rates of MitoSOX oxidation were measured in 30 second intervals over 30 minutes in a plate reader and normalised to cell density. A) Q treated; B) EGCG treated and C) EPI treated. Data are means \pm SEM of three independent repeats with two replicates per treatment. Statistical significance was tested for by a two-way ANOVA, with dose and antimycin A as factors: ^a Significant main effect of dose; ^d Significant main effect of AA (P <0.05). *** P <0.001 and **** P <0.0001. 155

Figure 4. 6 Dietary flavonoids do not regulate ROS production in vascular endothelial cells. CellROX oxidation was determined in HUVECs in the absence of presence of A) Q, B) EGCG or C) EPI. Cells were treated over 24 h with 0, 5 and 10 μ M Q, EGCG or EPI After 24 h, cells were incubated with or without antimycin A for 30 minutes, before CellROX was loaded into cells (2.5 μ M final concentration). CellROX oxidation was measured at 640/665 nm (Ex/Em) in a plate reader and normalised to cell density. Data are means \pm SEM of three independent

repeats with two replicates per treatment. Statistical significance was tested for by a two-way ANOVA, with dose and antimycin A as factors for each flavonoid individually: ^a Significant main effect of dose; ^d Significant main effect of AA ($P<0.05$)..... 157

Figure 4. 7 Flavonoid supplementation distinctly affects intracellular nitric oxide in vascular endothelial cells. NO levels (DAF-FM oxidation) were determined in HUVECs in the absence and presence of Q, EGCG and EPI. Cells were treated with 0, 5 and 10 μ M of flavonoids for 24 h. After 24 h, cells were trypsinised and resuspended in PBS. Median fluorescence intensity was determined with background signal (cell-free signal) subtracted. Data are presented as means \pm SEM of three independent repeats with two replicates per experimental condition. Statistical significance was tested for by one-way ANOVA for each flavonoid separately, and multiple comparisons by Dunnett's multiple comparison test. * $P<0.05$ significant versus CTRL. 158

Figure 4. 8 Heatmap representation of vascular endothelial cell mRNA responses in the absence of presence of flavonoids. 159

Figure 4. 9 Expression of genes associated with the antioxidant response in vascular endothelial cells following acute dietary flavonoid treatment. HUVECs were treated with 0, 5 and 10 μ M of Q, EPI or EGCG over 48 h and lysed for analysis of gene expression. A) CAT, B) SOD2, C) eNOS, D) NOX4 and E) NRF2. Data are means \pm SEM from 3 independent experiments run in duplicate. Statistical significance was determined by a two-way ANOVA, with dose and time as factors. Multiple comparisons were performed by Dunnett's test to determine differences in gene expression between conditions. ^a main effect of dose; ^b main effect of time ($P<0.05$); * $P<0.05$ 161

Figure 4. 10 Expression of genes associated with mitochondrial function in vascular endothelial cells following acute dietary flavonoid treatment. HUVECs were treated with 0, 5 and 10 μ M of Q, EPI or EGCG over 48 h and lysed for analysis of gene expression. A) DRP1, B) MFN2, C) PARKIN, D) PGC-1 α , E) SIRT1 and F) TFAM. Data are means \pm SEM from 3 independent experiments run in duplicate. Statistical significance was determined by a two-way ANOVA, with dose and time as factors. Multiple comparisons were performed by Dunnett's test to determine differences in gene expression between conditions. ^a main effect of dose; ^b main effect of time ($P<0.05$); * $P<0.05$, ** $P<0.01$, *** $P<0.001$, **** $P<0.0001$ 164

Figure 4. 11 Mitochondrial bioenergetics of HUVECs following acute dietary flavonoid treatment. A) Basal respiration. B) Maximal respiration after FCCP addition. C) Proton leak. D) ADP. phosphorylation. E) Spare respiratory capacity F) Spare respiratory capacity (%). G)

Coupling efficiency (%). Data from 3 independent experiments are normalised to cell number (1×10^3) and presented as mean \pm SEM. 166

Figure 4. 12 ATP production and proton efflux rates in HUVECs following 24 h dietary flavonoid treatment. A) Rates of ATP_{glyc} production B) ATP_{ox} production. C) Proton production rates. Data from 3 independent experiments are normalised to cell number (1×10^3) and presented as mean \pm SEM. 168

Figure 4. 13 CaMKII levels are not impacted by EPI treatment. A) Total CaMKII in HUVECs in the absence (-; clear bars) or presence (+; green bars) of EPI. B) Representative images of n=3 independent experiments. Cell lysates were analysed by SDS-PAGE and western blotting with indicated antibodies. Data are expressed as means \pm SEM. 169

Figure 4. 14 AMPK phosphorylation at Thr172 is acutely blunted by EPI. A) AMPK phosphorylation at Thr172 in HUVECs in the absence (-; clear bars) or presence (+; green bars) of EPI. B) Representative images of n=3 independent experiments. Cell lysates were analysed by SDS-PAGE and western blotting with indicated antibodies. Representative images of n=3 independent experiments are shown. Data are expressed as means \pm SEM; * $P < 0.05$ and *** $P < 0.001$. ^a significant main effect of treatment; ^b significant main effect of time ($P < 0.05$). 171

Figure 4. 15 EPI transiently stimulates ERK1/2 phosphorylation. A) ERK1/2 phosphorylation at Thr202/Tyr204 in HUVECs in the absence (-; clear bars) or presence (+; green bars) of EPI. B) Representative images of n=3 independent experiments. Cell lysates were analysed by SDS-PAGE and western blotting with indicated antibodies. Data are expressed as means \pm SEM; * $P < 0.05$ and ** $P < 0.01$ compared to CTRL. ^a significant main effect of treatment; ^b significant main effect of time ($P < 0.05$). 172

Figure 4. 16 EPI does not stimulate eNOS signalling in HUVECs. A) eNOS phosphorylation at Ser1177 in HUVECs in the absence (-; clear bars) or presence (+; green bars) of EPI. B) Representative images of n=3 independent experiments. Cell lysates were analysed by SDS-PAGE and western blotting with indicated antibodies. Data are expressed as means \pm SEM; * $P < 0.05$, compared to CTRL. 174

Figure 4. 17 Schematic of the potential mechanisms by which EPI exerts its biological effects in vascular endothelial cells. Dashed arrows represent no, or unknown activity of EPI on protein activity. Solid lines represent reported stimulatory or inhibitory effects of EPI. 181

Figure 5. 1 DNA standard curve generated using CyQUANT[®] Cell Proliferation Assay. Bacteriophage λ DNA standards (0-1000 ng/mL) fluorescence was measured using a filter

combination of 480 nm excitation and 520 nm emission and corrected for the background fluorescence determined for the no-DNA control. Data are from one independent experiment from 3 technical replicates. 194

Figure 5. 2 Standard curve of Lambda dsDNA detected with QuantiT™ PicoGreen® dsDNA reagent. Cell Proliferation Assay. Lambda DNA was diluted to create standards of known concentrations (0-2000 ng/mL) and were quantified using QuantiT™ PicoGreen® dsDNA reagent. Samples were excited at 480 nm and fluorescence emission intensity measured at 520 nm. Relative fluorescent units were plotted as a function of dsDNA and fitted with linear regression. 196

Figure 5. 3 Mitochondrial bioenergetics of control and aged C₂C₁₂ myoblasts. A) Non-mitochondrial respiration, B) Basal respiration, C) Proton leak, D) ADP phosphorylation and E) Coupling efficiency (%). Data are mean±SEM, representative of 3 independent experiments and normalised to DNA content. Differences between groups determined by independent t-test. 201

Figure 5. 4 ATP production rates of control and aged C₂C₁₂ myoblasts A) Absolute J_{ATPproduction}. B) Relative contribution of J_{ATPglyc} to J_{ATPproduction} and C) Relative contribution of J_{ATPox} to J_{ATPproduction}. Data from 3 independent experiments are presented as mean±SEM and normalised to DNA content. Differences between groups establish by independent t-test... 203

Figure 5. 5 Proton production rates in control and aged C₂C₁₂ myoblasts. Data from 3 independent experiments are presented as mean±SEM and normalised to DNA content. Differences between groups determined by independent t-test. 204

Figure 5. 6 Cell viability following 24 h differentiation +/- flavonoid treatment with A) Quercetin, B) EGCG and C) EPI. Data are means±SEM, representative of 3 independent repeats performed using 5 replicates of each condition. 205

Figure 5. 7 Mitochondrial bioenergetics of control and aged skeletal muscle cells in the absence and presence of dietary flavonoids. A) Basal respiration, B) Proton leak, C) ADP phosphorylation, D) Coupling efficiency (%). Data representative of 3 independent experiments (presented as mean±SEM) and normalised to DNA content. *P<0.05, significant vs. CTRL. ^a significant effect of dose. ^c significant main effect of age (P<0.05). 207

Figure 5. 8 ATP production rates of control and aged myoblasts following acute dietary flavonoid treatment. Data from 3 independent experiments are presented as mean±SEM and normalised to DNA content. *P<0.05, significant vs. CTRL. ^a significant main effect of dose. 208

Figure 5. 9 Limited impact of flavonoid treatment on complex I activity in control and aged skeletal muscle cells. Control and aged skeletal muscle cells were cultured in the absence and presence of Q, EPI or EGCG for 24 h, at 0, 5 and 10 μ M. After 24 h, cells were harvested and assayed for complex I activity by spectrophotometry. Immediately following analysis, the protein content of cell lysates was determined so that complex I activity could be normalised to cell lysate protein content. Data are means \pm SEM from 3 independent experiments. A two-way ANOVA was performed with dose and age as factors to test for statistical significance between conditions, using Dunnett's test for multiple comparisons. ^c significant main effect of age. Black and transparent grey solid circles represent control and aged myoblasts, respectively.210

Figure 5. 10 Flavonoid supplementation does not impact intracellular nitric oxide in control and aged skeletal muscle cells. DAF-FM oxidation was determined in control and replicatively aged skeletal muscle cells in the absence and presence of Q, EPI and EGCG. Cells were treated with 0, 5 and 10 μ M of flavonoids for 24 h. After 24 h, cells were trypsinised and resuspended in PBS. Median fluorescence intensity was determined with background signal (cell-free signal) subtracted. Data are presented as means \pm SEM of three independent repeats with two-three replicates per experimental condition. Black and transparent grey solid circles represent control and aged myoblasts, respectively. Statistical significance was tested for by two-way ANOVA and multiple comparisons by Tukey's test. ^c significant main effect of age ($P<0.05$).211

Figure 5. 11 Expression of genes associated with mitochondrial remodelling in control and aged skeletal myoblasts under CTRL conditions. C₂C₁₂ myoblasts were lysed over 0-48 h of differentiation for analysis of gene expression. A) DRP1, B) MFN2, C) PARKIN, D) PGC-1 α , E) SIRT1 and F) TFAM. Data are means \pm SEM from 3 independent experiments run in duplicate. Statistical significance was determined by a two-way ANOVA, with age and time as factors. Multiple comparisons performed by Sidak's test to determine differences in gene expression between ages within each time point. ^b main effect of time; ^c main effect of age. **** $P<0.0001$. Control and aged myoblasts are denoted by solid black and grey bars, respectively.213

Figure 5. 12 Expression of genes associated with the antioxidant response in control and aged skeletal myoblasts under CTRL conditions. C₂C₁₂ myoblasts were lysed over 0-48 h of differentiation for analysis of gene expression. A) CAT, B) SOD2, C) eNOS, D) NOX4 and E) NRF2. Data are means \pm SEM from 3 independent experiments run in duplicate. Statistical significance was determined by a two-way ANOVA, with age and time as factors. Multiple

comparisons performed by Sidak's test to determine differences in gene expression between ages within each time point. ^b main effect of time; ^c main effect of age. ***P*<0.01 and ****P*<0.001. Control and aged myoblasts are denoted by solid black and grey bars, respectively.215

Figure 5. 13 Expression of genes associated with mitochondrial function in control and aged skeletal myoblasts following acute dietary flavonoid treatment. Myoblasts were treated with 0, 5 and 10 μM of Q, EPI or EGCG over 48 h and lysed for analysis of gene expression. A) DRP1, B) MFN2, C) PARKIN, D) PGC1a, E) SIRT1 and F) TFAM. Data are means±SEM from 3 independent experiments run in duplicate. Statistical significance was determined by a three-way ANOVA, with dose, time and age as factors. Multiple comparisons performed by Dunnett's test, to determine within-age differences in gene expression between experimental conditions. ^a main effect of dose; ^b main effect of time; ^c main effect of age. **P*<0.05, ***P*<0.01, ****P*<0.001, *****P*<0.0001. Control and aged myoblasts are denoted by solid black and transparent circles, respectively.221

Figure 5. 14 Expression of genes associated with the antioxidant response in control and aged skeletal muscle myoblasts following acute dietary flavonoid treatment. C₂C₁₂ myoblasts were treated with 0, 5 and 10 μM of Q, EPI or EGCG over 48 h and lysed for analysis of gene expression. A) CAT, B) SOD2, C) eNOS, D) NOX4 and E) NRF2. Data are means±SEM from 3 independent experiments run in duplicate. Statistical significance was determined by a three-way ANOVA, with dose, time and age as factors. Multiple comparisons performed by Dunnett's test, to determine within-age differences in gene expression between experimental conditions. ^a main effect of dose; ^b main effect of time; ^c main effect of age. ***P*<0.05, ***P*<0.01, ****P*<0.001, *****P*<0.0001. Control and aged myoblasts are denoted by solid black and transparent circles, respectively.226

Figure 5. 15 Heatmap representation of myoblast mRNA responses in the absence of presence of flavonoids.228

Figure 5. 16 Impact of replicative ageing upon skeletal myoblasts. Replicative ageing does not impair indices of mitochondrial function but lowers NO bioavailability and alters gene expression (SOD2 and PARKIN lower and MFN2 and eNOS higher in aged vs. control myoblasts).230

Figure 5. 17 Schematic of the potential mechanisms by which flavonoids exert their biological effects in skeletal myoblasts. Genes differentially expressed by Q, EGCG and EPI treatment are highlighted in purple, red and green, respectively.237

Figure 6. 1 Standard curve of Lambda dsDNA detected with QuantiT™ PicoGreen® dsDNA reagent. Cell Proliferation Assay. Lambda DNA was diluted to create standards of known concentrations (0-2000 ng/mL) and were quantified. Samples were excited at 480 nm and fluorescence emission intensity measured at 520 nm. Relative fluorescent units were plotted as a function of dsDNA and fitted with linear regression.250

Figure 6. 2 Mitochondrial bioenergetics of control and aged C₂C₁₂ myotubes. A) Non-mitochondrial respiration, B) Basal respiration, C) Maximal respiration, D) Proton leak, E) ADP phosphorylation, F) Spare respiratory capacity G) Coupling efficiency (%). Data are mean±SEM, representative of 3 independent experiments and normalised to DNA content. ***P*<0.01, significance between groups by independent t-test.256

Figure 6. 3 ATP production rates of control and aged C₂C₁₂ myotubes. A) Absolute J_{ATPproduction}. B) Relative contribution of J_{ATPglyc} to J_{ATPproduction} and C) Relative contribution of J_{ATPox} to J_{ATPproduction}. Data from 3 independent experiments are presented as mean±SEM and normalised to DNA content. **P*<0.05, significant between groups by independent t-test.257

Figure 6. 4 Proton production rates in control and aged C₂C₁₂ myoblasts and myotubes. Data from 3 independent experiments are presented as mean±SEM and normalised to DNA content. Differences between groups determined by independent t-test.258

Figure 6. 5 Mitochondrial bioenergetics of control and aged skeletal myotubes following 96 h differentiation and 24 h dietary flavonoid treatment. A) Basal respiration, B) Proton leak, C) ADP phosphorylation, D) Coupling efficiency (%). Data representative of 3 independent experiments and are normalised to DNA content and presented as mean±SEM. ^c significant main effect of age (*P*<0.05).261

Figure 6. 6 Replicative ageing increases the rate of mitochondrial ROS production in skeletal muscle cells. MitoSOX oxidation rates were determined in control and replicatively aged skeletal myotubes in the absence of presence of antimycin A. Cells were incubated with or without antimycin A for 30 minutes, prior to the immediate loading of MitoSOX (2.5 μM final concentration). Rates of MitoSOX oxidation were immediately measured in 30 second intervals over 30 minutes. Data are means ± SEM of three independent repeats with twelve replicates per condition. Statistical significance of mean differences was tested for by two-way ANOVA and adjusted for multiple comparisons: ^c main effect of age (*P*<0.05); ^d main effect of Antimycin A (*P*<0.05); **P*<0.05, ***P*<0.01, *** *P*<0.001 and **** *P*<0.0001.262

Figure 6. 7 Quercetin supplementation increases the rate of mitochondrial ROS production in control skeletal muscle cells. MitoSOX oxidation rates were determined in control and

replicatively aged skeletal myotubes in the absence of presence of dietary flavonoids. Cells were treated with 0, 5 and 10 μM Q for 24 h. After 24 h, antimycin A was added to cells for 30 minutes, before 2.5 μM MitoSOX was loaded into cells in KRB. Rates of MitoSOX oxidation were measured in 30 second intervals over 30 minutes. Data are means \pm SEM of three independent repeats with two replicates per treatment. Statistical significance of mean differences was tested for by two-way ANOVA: ^a Significant main effect of dose; ^c Significant main effect of age; ^d Significant main effect of AA.....264

Figure 6. 8 EGCG supplementation does not impact the rate of mitochondrial ROS production in control or aged skeletal muscle cells. MitoSOX oxidation rates were determined in control and replicatively aged skeletal myotubes in the absence of presence of dietary flavonoids. Cells were treated with 0, 5 and 10 μM EGCG for 24 h. After 24 h, antimycin A was added to cells for 30 minutes, before 2.5 μM MitoSOX was loaded into cells in KRB. Rates of MitoSOX oxidation were measured in 30 second intervals over 30 minutes. Data are means \pm SEM of three independent repeats with two replicates per treatment. Statistical significance of mean differences was tested for by two-way ANOVA: ^c Significant main effect of age; ^d Significant main effect of AA.265

Figure 6. 9 EPI supplementation does not impact the rate of mitochondrial ROS production in control or aged skeletal muscle cells. MitoSOX oxidation rates were determined in control and replicatively aged skeletal myotubes in the absence of presence of dietary flavonoids. Cells were treated with 0, 5 and 10 μM EPI for 24 h. After 24 h, antimycin A was added to cells for 30 minutes, before 2.5 μM MitoSOX was loaded into cells in KRB. Rates of MitoSOX oxidation were measured in 30 second intervals over 30 minutes. Data are means \pm SEM of three independent repeats with two replicates per treatment. Statistical significance of mean differences was tested for by two-way ANOVA: ^a Significant main effect of dose; ^c Significant main effect of age; ^d Significant main effect of AA.....266

Figure 6. 10 Replicative ageing increases ROS production in skeletal muscle cells. CellROX oxidation was measured in control and replicatively aged skeletal myotubes in the absence of presence of antimycin A. Cells were incubated with or without antimycin A for 30 minutes, prior to the loading of CellROX (2.5 μM final concentration) for 30 minutes. Rates of CellROX oxidation were subsequently measured at 640/665 nm (Ex/Em) in a plate reader. The gain was kept constant between independent experiments. Data are means \pm SEM of three independent repeats with two replicates per condition. Statistical significance was determined by a two-way ANOVA with age and antimycin A as factors. Multiple comparisons were corrected for using Sidak's test. ^c main effect of age ($P < 0.05$). ^{*} $P < 0.05$267

Figure 6. 11 Dietary flavonoids do not regulate ROS production in control and aged skeletal muscle cells. CellROX oxidation was determined in control and replicatively aged skeletal myotubes in the absence of presence of Q, EPI or EGCG. Cells were treated over 24 h with 0, 5 and 10 μ M Q, EPI or EGC. After 24 h, cells were incubated with or without antimycin A for 30 minutes, before CellROX was loaded into cells (2.5 μ M final concentration). CellROX oxidation was measured at 640/665 nm (Ex/Em) in a plate reader and normalised to cell density. A) Q treated; B) EPI treated and C) EGCG treated. Data are means \pm SEM of three independent repeats with two replicates per treatment. Statistical significance was tested for by a three-way ANOVA, with dose, age and antimycin A as factors: ^c main effect of age ($P < 0.05$).

.....268

Figure 6. 12 Expression of genes associated with mitochondrial remodelling in control and aged skeletal muscle myotubes under CTRL conditions. C₂C₁₂ myotubes were lysed over 72-120 h for analysis of gene expression. A) DRP1, B) MFN2, C) PARKIN, D) PGC-1 α , E) SIRT1 and F) TFAM. Data are means \pm SEM from 3 independent experiments run in duplicate. Statistical significance was determined by a two-way ANOVA, with age and time as factors. Multiple comparisons performed by Sidak's test to determine differences in gene expression between ages within each time point. ^c main effect of age. * $P < 0.05$ and ** $P < 0.01$. Control and aged myotubes are denoted by solid black and grey bars, respectively.....271

Figure 6. 13 Expression of genes associated with the antioxidant response in control and aged skeletal muscle myotubes under CTRL conditions. C₂C₁₂ myotubes were lysed over 72-120 h for analysis of gene expression. A) CAT, B) SOD2, C) eNOS, D) NOX4 and E) NRF2. Data are means \pm SEM from 3 independent experiments run in duplicate. Statistical significance was determined by a two-way ANOVA, with age and time as factors. Multiple comparisons performed by Sidak's test to determine differences in gene expression between ages within each time point. ^b main effect of time; ^c main effect of age. *** $P < 0.001$ and **** $P < 0.0001$. Control and aged myotubes are denoted by solid black and grey bars, respectively.....273

Figure 6. 14 Expression of genes associated with mitochondrial function in control and aged skeletal muscle myotubes following acute dietary flavonoid treatment. Myotubes were treated with 0, 5 and 10 μ M Q, EPI or EGCG over 48 h and lysed for analysis of gene expression. A) DRP1, B) MFN2, C) PARKIN, D) PGC-1 α , E) SIRT1 and F) TFAM. Data are means \pm SEM from 3 independent experiments run in duplicate. Statistical significance was determined by a three-way ANOVA, with dose, time and age as factors. Multiple comparisons performed by Dunnett's test, to determine within-age differences in gene expression between experimental conditions. ^a main effect of dose; ^b main effect of time; ^c main effect of age. * $P < 0.05$, ** $P < 0.01$,

*** $P < 0.001$, **** $P < 0.0001$. Control and aged myotubes are denoted by solid black and transparent triangles, respectively.....279

Figure 6. 15 Expression of genes associated with the antioxidant response in control and aged skeletal myotubes following acute dietary flavonoid treatment. Myotubes were treated with 0, 5 and 10 μM Q, EPI or EGCG over 48 h and lysed for analysis of gene expression. A) CAT, B) SOD2, C) eNOS, D) NOX4 and E) NRF2. Data are means \pm SEM from 3 independent experiments run in duplicate. Statistical significance was determined by a three-way ANOVA, with dose, time and age as factors. Multiple comparisons performed by Dunnett's test, to determine within-age differences in gene expression between experimental conditions. ^a main effect of dose; ^b main effect of time; ^c main effect of age. * $P < 0.05$, ** $P < 0.01$, *** $P < 0.001$, **** $P < 0.0001$. Control and aged myotubes are denoted by solid black and transparent triangles, respectively.284

Figure 6. 16 Heatmap representation of myotube mRNA responses in the absence of presence of flavonoids.286

Figure 6. 17 EPI treatment does not impact CaMKII levels in control and aged muscle cells. A) Total CaMKII in control and aged myotubes in the absence (-; clear bars) or presence (+; green bars) of EPI. B) Representative images of $n=3$ independent experiments. Cell lysates were analysed by SDS-PAGE and western blotting with indicated antibodies. Data are expressed as means \pm SEM; ^c significant main effect of age.....288

Figure 6. 18 AMPK phosphorylation at Thr172 in control and aged skeletal muscle cells. A) AMPK phosphorylation at Thr172 in control and aged myotubes in the absence (-; clear bars) or presence (+; green bars) of EPI. B) Representative images of $n=3$ independent experiments. Cell lysates were analysed by SDS-PAGE and western blotting with indicated antibodies. Data are expressed as means \pm SEM; * $P < 0.05$ compared to 0 h CTRL. ^a significant main effect of treatment; ^b significant main effect of time; ^c significant main effect of age.289

Figure 6. 19 Erk1/2 phosphorylation is not enhanced by EPI in control cells and aged muscle cells. A) ERK1/2 phosphorylation at Thr202/Tyr204 in control and aged myotubes in the absence (-; clear bars) or presence (+; green bars) of EPI. B) Representative images of $n=3$ independent experiments. Cell lysates were analysed by SDS-PAGE and western blotting with indicated antibodies. Data are expressed as means \pm SEM; * $P < 0.05$ compared to 0 h CTRL. ^b significant main effect of time; ^c significant main effect of age.291

Figure 6. 20 eNOS phosphorylation is not impacted by EPI treatment. A) eNOS phosphorylation at Ser1177 in control and aged myotubes in the absence (-; clear bars) or presence (+; green bars) of EPI. B) Representative images of $n=3$ independent experiments.

Cell lysates were analysed by SDS-PAGE and western blotting with indicated antibodies. Data are expressed as means \pm SEM. ° significant main effect of age.....293

Figure 6. 21 Impact of replicative ageing upon mitochondrial form and function of skeletal myotubes.296

Figure 6. 22 Schematic of the potential mechanisms by which EPI exerts its biological effects in skeletal myotubes.....303

Figure 7. 1 Two plates were prepared per condition per dose for both myoblast and myotube cultures for seven groups: A – DM only, B – Quercetin 5 μ M, C – EGCG 5 μ M, D – Epicatechin 5 μ M, E – Quercetin 10 μ M, F – EGCG 10 μ M, G – Epicatechin 10 μ M, and one plate for the cell free control group H – No cells, matrix only. Each letter coded plate e.g. “A” contained 3x wells of “control” and 3x wells of “aged” cells = 6 samples in total for each condition. Two control plates (24 h and 96 h, for myoblast and myotube timeframes, respectively) contained replicates of cell-free media with and without 0.1% DMSO.....311

Figure 7. 2 Method of extraction from stored samples. The extraction required addition of solvent, followed by an incubation over ice to ensure solvent penetration through the sample. Homogenisation was critical for the separation of protein and small molecules. Homogenised samples were centrifuged to separate the debris and precipitants (this allowed the solution of metabolites to be extracted). The supernatant was lyophilized and metabolites were either immediately stored or prepared for analysis. Dry pellets were mixed with the appropriate buffer (see section 7.2.3) prior to acquisition.312

Figure 7. 3 Raw and normalised data using TotArea and PQN methods. Representative of 168 NMR spectra. A) Raw data – no normalisation. B) TotArea normalisation. C) PQN.....315

Figure 7. 4 Comparison of scaling methods. A) Normalisation by TotArea and Auto-scaling. B) Normalisation by TotArea and Pareto scaling.316

Figure 7. 5 Overview of quality control and statistical analysis workflow employed.....317

Figure 7. 6 Multivariate analyses of control and aged skeletal myoblasts. Panel A) PCA scores of control vs. aged myoblasts, coloured by age (control cells in ED black circles, $n=6$; aged cells in ED grey circles, $n=6$). Brackets report the percentage variance explained by the PC. Six PCs were required to achieve 95% explained variance. Only PC1 and PC2 are shown for simplicity/clarity. Ellipses represent 95% confidence region. Panel B) PLS-DA density plot to verify metabolite selection in myoblasts discriminated by age (control = 6 and aged = 6). Model complexity of one variate (32.87% explained variance) was determined to be optimal.322

Figure 7. 7 VIP scores of PLS-DA model (ROC = 1) built on age-dependent differences in skeletal myoblasts. A lower threshold of 1 was used on latent variable one to select metabolites from the model. The top 20 representative metabolites/bins are presented for clarity.....323

Figure 7. 8 Selected metabolite boxplots of control (black fill, n=6) and aged (grey fill, n=6) skeletal myoblasts. ** and *** represent *P*-value less than 0.01 and 0.001 respectively. * in the boxplot title represent denotes overlapping bin.325

Figure 7. 9 Multivariate analyses of control and aged myotubes. Panel A) PCA scores of control vs. aged myotubes, coloured by age (control cells, black triangles in LD n=6 and aged cells, grey triangles in LD n=5). Brackets report the variance explained by the PC. Six PCs were required to achieve 95% explained variance. Only PC1 and PC2 are show in the Figure for simplicity/clarity. Ellipses represent 95% confidence region. Panel B) PLS-DA density plot to verify metabolite selection in myotubes discriminated by age (control, n=6 and aged, n=5). Model complexity of one variate (34.30% explained variance) was determined to be optimal.327

Figure 7. 10 VIP scores of PLS-DA model (ROC = 1) built on age-dependent differences in skeletal myotubes. A lower threshold of 1 was used on latent variable one to select metabolites from the model. The top 20 representative metabolites/bins are presented for clarity.....328

Figure 7. 11 Selected metabolite boxplots of control (black outline, n=6) and aged (grey outline, n=5) skeletal myotubes. *, **, *** and **** represent *P*-value less than 0.05, 0.01, 0.001 and 0.0001, respectively. * in the boxplot title represent denotes overlapping bin.330

Figure 7. 12 Venn diagram reporting metabolites with VIP scores >1 between control and aged myoblasts and myotubes comparisons.....332

Figure 7. 13 Multivariate analysis of control and aged myoblasts +/- Q treatment. A) PCA scores of control and aged myoblasts coloured by dose. A total of ten principal components were required to achieve 95% explained variance. Brackets report the variance explained by the PC. Only PC1 and PC2 are shown in the Figure for simplicity/clarity. Ellipses represent 95% confidence region. B) PLS-DA scores of control- and C) aged-myoblasts coloured by dose. A model complexity of two variates was employed for control and aged myoblasts. Closed and open circles represent control and aged cells, respectively.333

Figure 7. 14 VIP scores of PLS-DA model built on Q treatment-dependent differences in A) control- and B) aged- skeletal myoblasts. AUC scores for control myoblasts were 0.986, 0.972 and 0.486, and 1.0, 0.5 and 1.0 for aged myoblasts for 0 μ M vs. others, 5 μ M vs. others and 10 μ M vs. others, respectively. A lower threshold of 1 was used on latent variable one and two to select metabolites from the model. The top 20 metabolites/bins are presented for clarity....335

Figure 7. 15 Selected metabolite boxplots of control and aged skeletal myoblasts following 0, 5 and 10 μ M Quercetin treatment. *, **, *** and **** represent *P*-value less than 0.05, 0.01, 0.001 and 0.0001, respectively. * in the boxplot title represent denotes overlapping bin.....336

Figure 7. 16 Multivariate analysis of control and aged cells myotubes +/- Quercetin treatment. A) PCA scores of control and aged myotubes coloured by dose. A total of twelve principal components were required to achieve 95% explained variance. Brackets report the variance explained by the PC. Only PC1 and PC2 are shown in the Figure for simplicity/clarity. Ellipses represent 95% confidence region. B) PLS-DA scores of control- and C) aged-myotubes coloured by dose. A model complexity of two variates was employed for control and aged myotubes. Closed and open triangles represent control and aged cells, respectively.....339

Figure 7. 17 VIP scores of PLS-DA model built on Q treatment-dependent differences in A) control- and B) aged- skeletal myotubes. AUC scores for control myotubes were 1.0, 0.583 and 0.912, and 0.917, 0.576 and 0.955 for aged myotubes for 0 μ M vs. others, 5 μ M vs. others and 10 μ M vs. others, respectively. A lower threshold of 1 was used on latent variable one and two to select metabolites from the model. The top 20 metabolites/bins are presented for clarity.340

Figure 7. 18 Selected metabolite boxplots of control and aged myotubes following 0, 5 and 10 μ M Quercetin treatment. *, ** and *** represent *P*-value less than 0.05, 0.01 and 0.001, respectively. * in the boxplot title represent denotes overlapping bin.....342

Figure 7. 19 Venn diagram reporting metabolites with VIP scores >1 between control and aged myoblasts and myotubes following Q treatment. Four metabolites were commonly represented between ages and differentiation stage (myoblast vs. myotube).345

Figure 7. 20 Multivariate analysis of control and aged myoblasts +/- EGCG treatment. A) PCA scores of control and aged myoblasts coloured by dose. A total of twelve principal components were required to achieve 95% explained variance. Brackets report the variance explained by the PC. Only PC1 and PC2 are shown in the Figure for simplicity/clarity. Ellipses represent 95% confidence region. B) PLS-DA scores of control- and, C) aged-myoblasts, coloured by dose. A model complexity of three- and two-components was employed for of control and aged myoblasts, respectively. Closed and open circles represent control and aged cells, respectively.346

Figure 7. 21 VIP scores of PLS-DA model built on EGCG treatment-dependent differences in A) control- and B) aged- skeletal myoblasts. AUC scores for control myoblasts were 0.944, 0.889 and 0.556, and 0.972, 0.625 and 0.847 for aged myoblasts for 0 μ M vs. others, 5 μ M vs. others and 10 μ M vs. others, respectively. A lower threshold of 1 was used on latent variable

one and two to select metabolites from the model. The top 20 representative metabolites/bins are presented for clarity.348

Figure 7. 22 Selected metabolite boxplots of control and aged skeletal myoblasts following 0, 5 and 10 μ M EGCG treatment. *, ** and *** represent *P*-values less than 0.05, 0.01 and 0.001, respectively. * in the boxplot title represent denotes overlapping bin. Closed and open circles represent control and aged cells, respectively.....349

Figure 7. 23 Multivariate analysis of control and aged myotubes +/- EGCG treatment. A) PCA scores of control and aged myotubes coloured by dose. A total of eleven principal components were required to achieve 95% explained variance. Brackets report the variance explained by the PC. Only PC1 and PC2 are shown in the Figure for simplicity/clarity. Ellipses represent 95% confidence region. B) PLS-DA scores of control myotubes and C) aged myotubes, coloured by dose. A model complexity of three variates was employed. Closed and open triangles represent control and aged cells, respectively.....352

Figure 7. 24 VIP scores of PLS-DA model built on EGCG treatment-dependent differences in A) control- and B) aged- skeletal myotubes. AUC scores for control myotubes were 0.931, 0.583 and 0.843, and 0.750, 0.727 and 0.955 for aged myotubes for 0 μ M vs. others, 5 μ M vs. others and 10 μ M vs. others, respectively. A lower threshold of 1 was used on latent variable one and to select metabolites from the model. The top representative 20 metabolites/bins are presented for clarity.353

Figure 7. 25 Selected metabolite boxplots of control and aged skeletal myotubes following 0, 5 and 10 μ M EGCG treatment. *, ** and *** represent *P*-values less than 0.05, 0.01 and 0.001, respectively. * in the boxplot title represent denotes overlapping bin. Closed and open triangles represent control and aged cells, respectively.....354

Figure 7. 26 Venn diagram reporting metabolites with VIP scores >1 between control and aged myoblast and myotubes following EGCG treatment. Three metabolites were commonly represented between ages and differentiation stage (myoblast vs. myotube).....357

Figure 7. 27 Multivariate analysis of control and aged myoblasts +/- EPI treatment. A) PCA scores of control and aged myoblasts coloured by dose. A total of thirteen principal components were required to achieve 95% explained variance. Brackets report the variance explained by the PC. Only PC1 and PC2 are shown in the Figure for simplicity/clarity. Ellipses represent 95% confidence region. B) PLS-DA scores of control- and C) aged-myoblasts coloured by dose. A model complexity of two-variates was employed for control and aged myoblasts. Closed and open triangles represent control and aged cells, respectively.358

Figure 7. 28 VIP scores of PLS-DA model built on EPI treatment-dependent differences in A) control- and B) aged- skeletal myoblasts. AUC scores for control myoblasts were 1.0, 0.653 and 0.847, and 0.986, 0.903 and 0.583 for aged myoblasts for 0 μ M vs. others, 5 μ M vs. others and 10 μ M vs. others, respectively. A lower threshold of 1 was used on latent variable one and two to select metabolites from the model. The top 20 representative metabolites/bins are presented for clarity.359

Figure 7. 29 Selected metabolite boxplots of control and aged skeletal myoblasts following 0, 5 and 10 μ M EPI treatment. *, ** and *** represent *P*-values less than 0.05, 0.01 and 0.001, respectively. * in the boxplot title represent denotes overlapping bin. Closed and open circles represent control and aged cells, respectively.....361

Figure 7. 30 Multivariate analysis of control and aged myotubes +/- EPI treatment. A) PCA scores of control and aged myotubes coloured by dose. A total of ten principal components were required to achieve 95% explained variance. Brackets report the variance explained by the PC. Only PC1 and PC2 are shown in the Figure for simplicity/clarity. Ellipses represent 95% confidence region. B) PLS-DA scores of control myotubes and C) aged myotubes coloured by dose. A model complexity of two- variates was employed for control and aged myotubes. Closed and open triangles represent control and aged cells, respectively.....363

Figure 7. 31 VIP scores of PLS-DA model built on EPI treatment-dependent differences in A) control- and B) aged- skeletal myotubes. AUC scores for control myoblasts were 0.847, 0.583 and 0.931, and 0.850, 1.0 and 0.682 for aged myoblasts for 0 μ M vs. others, 5 μ M vs. others and 10 μ M vs. others, respectively. A lower threshold of 1 was used on latent variable one and two to select metabolites from the model. The top 20 metabolites/bins are presented for clarity.364

Figure 7. 32 Selected metabolite boxplots of control and aged skeletal myotubes following 0, 5 and 10 μ M EPI treatment. *, ** and *** represent *P*-values less than 0.05, 0.01 and 0.001, respectively. * in the boxplot title represent denotes overlapping bin. Closed and open triangles represent control and aged cells, respectively.....365

Figure 7. 33 Venn diagram reporting metabolites with VIP scores >1 between control and aged myoblasts and myotubes following EPI treatment. Five metabolites were commonly represented between ages and differentiation stage (myoblast vs. myotube).....368

Figure 7. 34 Schematic representation of metabolic signatures of control and aged myoblasts. Metabolites in green and red are higher and lower in aged versus control, respectively. Metabolites in black are similar between control and aged.371

Figure 7. 35 Schematic representation of metabolic signatures of control and aged myotubes. Metabolites in green and red are higher and lower in aged versus control, respectively. Metabolites in black are similar between control and aged.....374

Figure 7. 36 Schematic representation of metabolic signatures in A) control and B) aged myoblasts, in the presence of 0, 5 and 10 μ M Q. Metabolites in green and red are higher and lower with Q treatment vs. untreated CTRL. Metabolites in bold are significantly different vs. CTRL with 5 and 10 μ M Q, whereas metabolites in regular font are only different vs. CTRL at one Q dose. Metabolites in black are similar between treatment conditions.....376

Figure 7. 37 Schematic representation of metabolic signatures in A) control and B) aged myotubes, in the presence of 0, 5 and 10 μ M Q. Metabolites in green and red are higher and lower with Q treatment vs. untreated CTRL. Metabolites in bold are significantly different vs. CTRL with 5 and 10 μ M Q, whereas metabolites in regular font are only different vs. CTRL at one Q dose. Metabolites in black are similar between treatment conditions.....380

Figure 7. 38 Schematic representation of metabolic signatures in A) control and B) aged myoblasts in the presence of 0, 5 and 10 μ M EGCG. Metabolites in green and red are higher and lower with EGCG treatment vs. untreated CTRL. Metabolites in bold are significantly different vs. CTRL with 5 and 10 μ M EGCG, whereas metabolites in regular font are only different vs. CTRL at one EGCG dose. Metabolites in black are similar between treatment conditions.....382

Figure 7. 39 Schematic representation of metabolic signatures in A) control and B) aged myotubes in the presence of 0, 5 and 10 μ M EGCG. Metabolites in green and red are higher and lower with EGCG treatment vs. untreated CTRL. Metabolites in bold are significantly different vs. CTRL with 5 and 10 μ M EGCG, whereas metabolites in regular font are only different vs. CTRL at one EGCG dose. Metabolites in black are similar between treatment conditions.....385

Figure 7. 40 Schematic representation of metabolic signatures in A) control and B) aged myoblasts in the presence of 0, 5 and 10 μ M EPI. Metabolites in green and red are higher and lower with EPI treatment vs. untreated CTRL. Metabolites in bold are significantly different vs. CTRL with 5 and 10 μ M EPI, whereas metabolites in regular font are only different vs. CTRL at one EPI dose. Metabolites in black are similar between treatment conditions.....388

Figure 7. 41 Schematic representation of metabolic signatures in A) control and B) aged myotubes in the presence of 0, 5 and 10 μ M EPI. Metabolites in green and red are higher and lower with EPI treatment vs. untreated CTRL. Metabolites in bold are significantly different

vs. CTRL with 5 and 10 μ M EPI, whereas metabolites in regular font are only different vs. CTRL at 5 μ M EPI dose. Metabolites in black are similar between treatment conditions. ...391

Figure 9. 1 Baseline C_T values of genes of interest in control and aged muscle A) myoblasts and B) myotubes. Control and aged myoblast/myotube are denoted by solid black and grey bars, respectively. * P <0.05409

Figure 9. 2 Heatmap representation of myotube mRNA responses (without eNOS) in the absence of presence of flavonoids.410

Figure 9. 3 Phosphorylation of CaMKII at Thr286 is not detectable under control conditions in C_2C_{12} myotubes and HUVECs. Representative images of pThr286-CaMKII (60, 50 kDa) in control and aged C_2C_{12} myotubes and HUVECs under control conditions, alongside positive control (mouse brain extract).411

Figure 9. 4 Total eNOS is not detectable under control conditions in C_2C_{12} myotubes. Representative images of eNOS (140 kDa) in control and aged C_2C_{12} myotubes and HUVECs under control conditions, alongside positive control (Bovine arterial endothelial cells + vascular endothelial growth factor).411

Figure 9. 5 pThr172-AMPK α and AMPK α primary and secondary antibody optimisation under control conditions in HUVECs. Representative image of pThr172-AMPK α and AMPK α (62 kDa) with primary dilution 1:500 to 1:4,000 and secondary dilution 1:2,000 to 1:10,000.412

Figure 9. 6 pThr202/Tyr204-p44/42 MAPK and p44/42 MAPK primary and secondary antibody optimisation under control conditions in HUVECs. Representative image of pThr202/Tyr204-p44/42 MAPK and p44/42 MAPK (44/42 kDa) with primary dilution 1:1000 to 1:8,000 and secondary dilution 1:2,000 to 1:10,000.....412

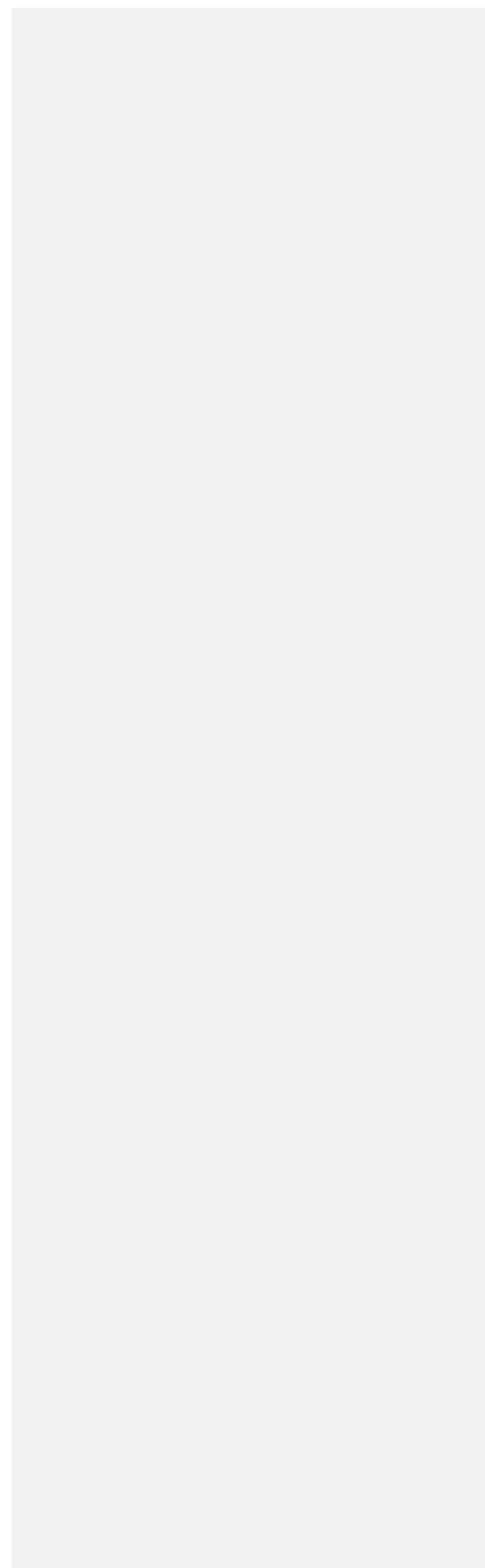
Figure 9. 7 pSer1177-eNOS and eNOS primary and secondary antibody optimisation under control conditions in HUVECs. Representative image of pSer1177-eNOS and eNOS (140 kDa) with primary dilution 1:500 to 1:4,000 and secondary dilution 1:2,000 to 1:10,000.413

Figure 9. 8 CaMKII primary and secondary antibody optimisation under control conditions in C_2C_{12} myotubes. Representative image of CaMKII (60, 50 kDa) with primary dilution 1:500 to 1:4,000 and secondary dilution 1:2,000 to 1:10,000.....413

Figure 9. 9 pThr172-AMPK α and AMPK α primary and secondary antibody optimisation under control conditions in C_2C_{12} myotubes. Representative image of pThr172-AMPK α and AMPK α (62 kDa) with primary dilution 1:500 to 1:4,000 and secondary dilution 1:2,000 to 1:10,000.414

Figure 9. 10 pThr202/Tyr204-p44/42 MAPK and p44/42 MAPK primary and secondary antibody optimisation under control conditions in C₂C₁₂ myotubes. Representative image of pThr202/Tyr204-p44/42 MAPK and p44/42 MAPK (44/42 kDa) with primary dilution 1:1000 to 1:8,000 and secondary dilution 1:2,000 to 1:10,000.....414

Figure 9. 11 pSer1177-eNOS and eNOS primary and secondary antibody optimisation under control conditions in C₂C₁₂ myotubes. Representative image of pSer1177-eNOS and eNOS (140 kDa) with primary dilution 1:500 to 1:4,000 and secondary dilution 1:2,000 to 1:10,000.415



List of tables

Table 2. 1 Modified KRH Buffer Composition	96
Table 2. 2 Mitochondrial Stress Test parameters and associated calculations.....	98
Table 3. 2 Heart rate and blood lactate responses during moderate- and severe-intensity exercise following CF and PL supplementation.....	128
Table 3. 3 Pulmonary O ₂ uptake responses to moderate- and severe-intensity exercise following CF and PL supplementation	131
Table 4. 1 Primer sequences for homo sapiens with product length. All primers were used under the same cycling conditions.....	147
Table 4. 2 List of antibodies and dilutions used.....	150
Table 5. 1 Cuvette contents to assay complex I activity	197
Table 5. 2 Primer sequences for Mus musculus with product length. All primers were used under the same cycling conditions.....	199
Table 6. 1 Primer sequences for Mus musculus with product length. All primers were used under the same cycling conditions.....	251
Table 6. 2 List of antibodies and dilutions used.....	253
Table 7. 1 Pathway analysis results for control and aged skeletal myoblasts. Reporting raw & BH adjusted <i>P</i> values, number of hits, pathway impact and matches.	326
Table 7. 2 Pathway analysis results for control and aged skeletal myotubes. Reporting raw & BH adjusted <i>P</i> values, number of hits, pathway impact and matches.	331
Table 7. 3 Pathway analysis results for control skeletal muscle myoblasts treated with Q. Reporting raw & BH adjusted <i>P</i> values, number of hits, pathway impact and matches.	337

Table 7. 4 Pathway analysis results for aged skeletal muscle myoblasts treated with Q. Reporting raw & BH adjusted <i>P</i> values, number of hits, pathway impact and matches.	338
Table 7. 5 Pathway analysis results for control skeletal muscle myotubes treated with Q. Reporting raw & BH adjusted <i>P</i> values, number of hits, pathway impact and matches.	343
Table 7. 6 Pathway analysis results for aged skeletal muscle myotubes treated with Q. Reporting raw & BH adjusted <i>P</i> values, number of hits, pathway impact and matches.	344
Table 7. 7 Pathway analysis results for control skeletal myoblasts treated with EGCG. Reporting raw & BH adjusted <i>P</i> values, number of hits, pathway impact and matches.	350
Table 7. 8 Pathway analysis results for aged skeletal myoblasts treated with EGCG. Reporting raw & BH adjusted <i>P</i> values, number of hits, pathway impact and matches.	350
Table 7. 9 Pathway analysis results for control skeletal myotubes treated with EGCG. Reporting raw & BH adjusted <i>P</i> values, number of hits, pathway impact and matches.	355
Table 7. 10 Pathway analysis results for aged skeletal myotubes treated with EGCG. Reporting raw & BH adjusted <i>P</i> values, number of hits, pathway impact and matches.	356
Table 7. 11 Pathway analysis results for control skeletal myoblasts treated with EPI. Reporting raw & BH adjusted <i>P</i> values, number of hits, pathway impact and matches.	361
Table 7. 12 Pathway analysis results for control skeletal myotubes treated with EPI. Reporting raw & BH adjusted <i>P</i> values, number of hits, pathway impact and matches.	366
Table 7. 13 Pathway analysis results for aged skeletal myotubes treated with EPI. Reporting raw & BH adjusted <i>P</i> values, number of hits, pathway impact and matches.	366
Table 9. 1 Genes of interest investigated and their known function.	409
Table 9. 2 Metabolites with VIP scores >1 and entered for pathway analysis for comparison of control and aged skeletal myoblasts under CTRL conditions.	416
Table 9. 3 Metabolites with VIP scores >1 and entered for pathway analysis for comparison of control and aged skeletal myotubes under CTRL conditions.	417

Table 9. 4 Metabolites with VIP scores >1 and entered for pathway analysis for comparison of Q treated control skeletal myoblasts.	418
Table 9. 5 Metabolites with VIP scores >1 and entered for pathway analysis for comparison of Q treated aged skeletal myoblasts.	419
Table 9. 6 Metabolites with VIP scores >1 and entered for pathway analysis for comparison of Q treated control skeletal myotubes.	420
Table 9. 7 Metabolites with VIP scores >1 and entered for pathway analysis for comparison of Q treated aged skeletal myotubes.	421
Table 9. 8 Metabolites with VIP scores >1 and entered for pathway analysis for comparison of EGCG treated control skeletal myoblasts.	422
Table 9. 9 Metabolites with VIP scores >1 and entered for pathway analysis for comparison of EGCG treated aged skeletal myoblasts.	424
Table 9. 10 Metabolites with VIP scores >1 and entered for pathway analysis for comparison of EGCG treated control myotubes.	425
Table 9. 11 Metabolites with VIP scores >1 and entered for pathway analysis for comparison of EGCG treated aged skeletal myotubes.	426
Table 9. 12 Metabolites with VIP scores >1 and entered for pathway analysis for comparison of EPI treated control skeletal myoblasts.	427
Table 9. 13 Metabolites with VIP scores >1 and entered for pathway analysis for comparison of EPI treated aged myoblasts.	429
Table 9. 14 Metabolites with VIP scores >1 and entered for pathway analysis for comparison of EPI treated control myotubes.	430
Table 9. 15 Metabolites with VIP scores >1 and entered for pathway analysis for comparison of EPI treated aged skeletal myotubes.	431
Table 9. 16 Statistical analyses of control and aged myoblast metabolites following Q treatment.	432
Table 9. 17 Statistical analyses of control and aged myotube metabolites following Q treatment.	438
Table 9. 18 Statistical analyses of control and aged myoblast metabolites following EGCG treatment.	443
Table 9. 19 Statistical analyses of control and aged myotube metabolites following EGCG treatment.	449
Table 9. 20 Statistical analyses of control and aged myoblast metabolites following EPI treatment.	455

Table 9. 21 Statistical analyses of control and aged myotube metabolites following EPI treatment.	460
Table 9. 22 Comparison of metabolites with VIP scores >1 between control and aged myoblasts treated with Q, EGCG and EPI and modelled via PLS-DA.	466
Table 9. 23 Comparison of metabolites with VIP scores >1 between control and aged myotubes treated with Q, EGCG and EPI and modelled via PLS-DA.	469

List of equations

Equation 2. 1 Cell counting equations.....	89
Equation 2. 2 Total rate of glycolysis.....	99
Equation 2. 3 Total rate of oxidative phosphorylation.....	100
Equation 2. 4 Normalised mitochondrial respiration.....	100
Equation 2. 5 Total proton production rate.....	100
Equation 2. 6 Respiratory portion of PPR.....	101
Equation 2. 7 The glycolytic portion of PPR.....	101
Equation 2. 8 Beer-Lambert equation.....	103
Equation 2. 9 Delta Delta C_T ($2^{-\Delta\Delta CT}$) Equation used to calculate relative gene expression against a reference gene and control group.....	107
Equation 3. 1 Mono-exponential model.....	125
Equation 3. 2 Monoexponential function with no time delay.....	126
Equation 5. 1 Enzyme activity determination.....	198

Abbreviations

AA	Antimycin A
AHR	Amplitude of the fundamental heart rate response
AMPK	Adenosine monophosphate activated protein kinase
ANOVA	Analysis of variance
ATP	Adenosine triphosphate
$\dot{A}V\dot{O}_2$	Amplitude of phase II oxygen uptake response
BAM15	N5,N6-bis(2-Fluorophenyl)[1,2,5]oxadiazolo[3,4-b]pyrazine-5,6-diamine
BCA	Bicinchoninic acid
BCAA	Branched chain amino acid
BSA	Bovine serum albumin
CaMKII	Ca ²⁺ /calmodulin-dependent protein kinase
cDNA	Complimentary DNA
CFs	Cocoa flavanols
CK	creatine kinase
CO ₂	Carbon dioxide
CoA	Coenzyme A
COX	Cytochrome c oxidase
CPMG	Carr-Purcell-Meiboom-Gill
CRS	Correlation reliability score
C _T	Cycle threshold
CTRL	Untreated control condition
CVD	Cardiovascular disease
DM	Differentiation medium
DMEM	Dulbecco's modified minimum essential medium
DMSO	Dimethyl sulfoxide
DNA	Deoxyribonucleic acid
DRP1	Dynamamin-related protein 1
ECAR	Extracellular acidification rate
ECG	Epicatechin-3-gallate
ECL	Enhanced chemiluminescence

EDTA	Ethylenediaminetetraacetic acid
EGC	Epigallocatechin
EGCG	Epigallocatechin-3-gallate
EGM	Complete endothelial cell growth medium
eNOS	Endothelial nitric oxide synthase
EPI	Epicatechin
ERK1/2	Extracellular Regulated Kinases 1/2
ETS	Electron transport system
FCCP	2-[2-[4-(trifluoromethoxy)phenyl]hydrazinylidene]-propanedinitrile
FMD	Flow-mediated dilation
GET	Gas exchange threshold
GM	Growth medium
GPER	G-protein-coupled estrogen receptor
GSH	Glutathione
H ₂ O	Water
H ₂ O ₂	Hydrogen peroxide
hiFBS	Heat-inactivated fetal bovine serum
hiNBCS	Heat-inactivated newborn calf serum
HR _b	Baseline heart rate
HS	Horse serum
HUVEC	Human umbilical vein endothelial cells
IMM	Inner mitochondrial membrane
IPAQ	International Physical Activity Questionnaire
KRH	Krebs-Ringer buffer
L-NAME	N(ω)-nitro-L-arginine methyl ester
LCFA	Long-chain fatty acids
LG	L-glutamine
LN ₂	Liquid nitrogen
MFN2	Mitofusin-2
mRNA	Messenger ribonucleic acid
MRS	³¹ P-magnetic resonance spectroscopy
MSEA	Metabolite set enrichment analysis
mtDNA	Mitochondrial DNA

mTORC1	Mammalian target of rapamycin complex 1
NAD	Nicotinamide adenine dinucleotide
NFDM	Non-fat dried milk
NIRS	near-infrared spectroscopy
NMR	Nuclear magnetic resonance
NO	Nitric oxide
NOX4	NADPH oxidase 4
NRF2	Nuclear respiratory factor 2
O ₂	Oxygen
OAT	Organic anion transporters
OCR	Oxygen consumption rate
OLI	Oligomycin
OMM	Outer mitochondrial membrane
OXPHOS	Oxidative phosphorylation
PBS	Phosphate buffered saline
PC	Principal component
PCA	Principal component analysis
PCr	Phosphocreatine
PCR	Polymerase chain reaction
PDH	pyruvate dehydrogenase
PGC-1 α	Peroxisome proliferator activated receptor γ coactivator 1 α
PINK1	PTEN-induced kinase 1
PL	Placebo
PLS-DA	Partial least square – discriminant analysis
RP2 β	RNA Polymerase II Subunit B
PPR	Proton production rate
PQN	Probabilistic quotient normalisation
PS	Penicillin and streptomycin
Q	Quercetin
QC	Quality control
RIPA	Radioimmunoprecipitation assay
RNA	Ribonucleic acid
RONS	Reactive oxygen and nitrogen species

ROS	Reactive oxygen species
RT	Room temperature
SC $\dot{V}O_2$	Magnitude of the slow component
SD	Standard deviation
SDS-PAGE	Sodium dodecyl sulphate polyacrylamide gel electrophoresis
SEM	Standard error of the mean
SIRT1	Sirtuin-1
SRB	Sulforhodamine B
TBS	Tris-buffered saline
TCA	Tricarboxylic acid
TD _{SC$\dot{V}O_2$}	Time delay of the oxygen uptake slow component
TD _{$\dot{V}O_2$}	Time delay of the primary response
Tfam	Mitochondrial transcription factor A
T _{lim}	Time to exhaustion
T _m	Melting temperature
TotArea	Total area
TSP	Trimethylsilyl propionate
UV	Ultraviolet
$\dot{V}CO_2$	CO ₂ production
$\dot{V}E$	Minute ventilation
VIP	Variable importance of the projection
$\dot{V}O_2$	Pulmonary oxygen uptake
$\dot{V}O_{2\text{ peak}}$	Peak oxygen uptake
$\dot{V}O_{2b}$	Baseline oxygen uptake
τ_{HR}	Time constant of the primary response
$\tau\dot{V}O_2$	Phase II oxygen uptake time-constant

Abstract

Introduction: Exercise tolerance gradually declines with sedentary ageing, which contributes to reduced quality of life. With ageing, slower pulmonary oxygen uptake kinetics manifest as a consequence of impairments along the oxygen transport and utilisation pathways. Consequently, there is a mismatch between metabolic demand and O₂ delivery, and the oxygen deficit is exacerbated during exercise. Strategies that target the vascular endothelium and skeletal muscle are therefore required to respectively improve O₂ delivery and utilisation. Flavonoids may provide therapeutic value through their interaction with cellular processes associated with energy metabolism, but their exact effects on vascular endothelial and skeletal muscle cells are yet to be fully described.

Objective: The overall objective of this thesis is to investigate whether flavonoid supplementation impacts $\dot{V}O_2$ kinetics and exercise tolerance *in vivo*, and to examine whether flavonoids modulate vascular endothelial and/or skeletal muscle cell (control and aged) function as it relates to energy metabolism, *in vitro*.

Methods: Three models were used to achieve the thesis objectives: 1) Randomised, double-blind placebo-controlled trial to investigate whether flavonoid supplementation modulates $\dot{V}O_2$ kinetics and exercise tolerance in physically inactive middle-aged adults, 2) human vascular endothelial cell model to investigate the effects of flavonoids on RONS production, mitochondrial function and cells signalling. 3) Replicative ageing skeletal myoblast/myotube model to investigate the impact of ageing on the effects of micromolar concentrations of flavonoids on RONS production, mitochondrial function, cell signalling and metabolic signatures.

Results: *Model 1:* Cocoa-flavanol supplementation sped phase II $\dot{V}O_2$ kinetics by 15% during moderate-intensity exercise in physically inactive middle-aged adults, but did not alter exercise tolerance. *Model 2:* In vascular endothelial cells, antimycin A augmented ROS emission, which was modulated by flavonoids in a dose-dependent manner. However, flavonoids did not impact mitochondrial respiration. EPI treatment augmented NRF2 expression and genes associated with mitochondrial remodelling. NRF2 induction in vascular endothelial cells appeared downstream of increased ERK1/2 signalling and may relate to increased NO bioavailability. *Model 3:* Ageing attenuated coupling efficiency and OXPHOS in myotubes, but not myoblasts, whilst increasing mitochondrial ROS production. Flavonoid treatment did not rescue age-related mitochondrial dysfunction. However, flavonoids upregulated NRF2 in skeletal muscle cells, and in the presence of EPI, NRF2 induction appeared downstream of increased AMPK

Commented [HJ1]: A little more info here on how this was done. E.g. cells in 1 and 2 and humans in 3. Think your under selling your self here by being too breif

Commented [HJ2]: Are these the order you present the studies in the thesis? Need to be in the order you present in thesis

Commented [TD3]: Correct addition?

Commented [TD4]: Would like to see a stronger link to the three studies. What relates to model 1, etc... It is now difficult to read, without its relation to the studies.

Commented [HJ5R4]: I agree and also useful to put some data in the abstract

signalling, but independent of NO bioavailability. Replicative ageing significantly altered the metabolic signatures of myoblasts and myotubes, which were only partially affected by flavonoid treatment.

Conclusion(s): Cocoa-flavanols speed $\dot{V}O_2$ kinetics during moderate intensity exercise, but do not enhance exercise tolerance. The speeding of $\dot{V}O_2$ kinetics with cocoa flavanols *in vivo* may relate to the action of flavonoids on vascular endothelial and skeletal muscle cellular processes. Flavonoids differentially impact mitochondrial ROS production and gene expression profiles in skeletal muscle and vascular endothelial cells. However, flavonoids do not play a major role in modulating mitochondrial respiration, regardless of cell type. EPI in-particular may afford mitochondrial adaptations via induction of NRF2 and ERK1/2 or AMPK signalling in vascular endothelial and skeletal muscle cells, respectively, potentially through the effects of hormesis. In the context of sedentary ageing, flavonoid supplementation may enhance quality of life through effects on $\dot{V}O_2$ kinetics, and the modulation of ROS production and adaptive responses at the cellular level.

Commented [HJ6]: This reads like 3 different conclusions to 3 separate studies., Which is ok if you separate out as 1, 2, 3 like in methods and results but also need to add a overall statement about flavonoids and ageing at the end.

Declaration

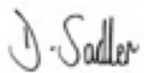
I declare that the work in this thesis was carried out in accordance with the regulations of Liverpool John Moores University. Apart from the help and advice acknowledged, the work within was solely completed and carried out by the author.

Any views expressed in this thesis are those of the author and in no way represent those of Liverpool John Moores University and the School of Sport and Exercise Science.

This thesis has not been presented to any other University for examination either in the United Kingdom or overseas. No portion of the work referred to in this research project has been submitted in support of an application for another degree or qualification of this or any other university or institute of learning.

Copyright in text of this research project rests with the author. The ownership of any intellectual property rights, which may be described in this research project, is vested in Liverpool John Moores University and may not be made available for use to any third parties without the written permission of the University.

Signed

A handwritten signature in black ink that reads "J. Sadler". The signature is written in a cursive style with a large initial 'J'.

Date: 15/05/2021

Acknowledgement

This thesis would not have been possible without the support and guidance from my supervisory team. Prof. Claire Stewart, my 'academic mother', has been inspirational and central to my development and the completion of this thesis. I have greatly valued your mentorship throughout this PhD program. I would like to thank my co-supervisors Prof. Dick Thijssen and Prof. Helen Jones for their support and resourcefulness. Both of you have provided practical advice that helped me stay on track and complete the research program. Thank you to my external supervisor Dr. Richard Draijer (Unilever), who provided honest and valuable advice throughout. I also wish to acknowledge the amazing support from Dr. Marie Phelan (University of Liverpool) and Dr. Jonathan Barlow (University of Birmingham) in facilitating key experiments within their respective departments.

I am grateful to my fellow researchers and friends at LJMU, who have supported and inspired me. I feel privileged to have completed this thesis alongside such talented researchers and great human beings. A special thank you to members of the SCAMP research group. It's been fun learning, failing and developing alongside you. I also wish to thank the LJMU academic staff who I've had the pleasure to teach and conduct research alongside during my studies. Finally, I would like to thank the non-academic staff in the Life Sciences Building, Dr. Nicola Browning and Jennifer Thompson, and those in the Tom Reilly building, including Dr. Gemma Miller, Dean Morrey and George Savage. I appreciate your help in ensuring research activities ran smoothly.

Dedication

My parents, siblings and family. I cannot put into words how much your love and support mean to me. Thank you for supporting me throughout this rollercoaster journey. You continue to remind me what is most important.

Chapter 1: Introduction & Literature

Review

Commented [TD7]: Overall a really good read and structure. Nicely linked to the chapters and nice additions of summary-paragraphs and figures.

1.1 General Introduction

Ageing and physical inactivity are two bio-cultural trends at the forefront of public interest. Physical inactivity itself is identified as the fourth leading risk factor for global mortality (WHO, 2010), and a major contributing factor for disability and poor health (Peterson et al., 2009). Moreover, physical inactivity is related to approximately 3 million deaths per year globally and accounts for the occurrence of 6–10% of the major non-communicable diseases (Lim et al., 2012). In the UK alone, it is estimated that around 20 million adults are insufficiently active, putting them at significantly greater risk of cardiovascular disease (CVD) and premature death than their active counterparts (BHF, 2017). Older adults typically have a more sedentary lifestyle, spending more than 9 hours inactive per day (Harvey et al., 2015). The high rate of physical inactivity that characterises the older adult population compounds impairments to physiological systems typically observed with chronological ageing. Indeed, living an inactive lifestyle into older age can lead to a greater loss of functional capacity, due to exacerbated deficits in strength, endurance, and flexibility (Chodzko-Zajko et al., 2009). Ultimately, the non-adherence to physical exercise in adults, which is as prevalent as non-adherence to medicines (Barnett, 2014; Jefferis et al., 2014), can not only negatively impact activities of daily living but also lead to life-threatening conditions (Figueiredo et al., 2016).

Commented [TD8]: Do you have a reference for this?

Whilst inactivity is a major cause of poor physiological fitness and disease in older age (Booth et al., 2012), maintaining a physically active lifestyle through middle and older age is associated with improved health and longevity (Hamer et al., 2014) (Manini et al., 2006; Stessman et al., 2009). Fortunately, the trajectory towards frailty is directly modifiable through physical activity habits earlier in life (Department of Health and Social Care, 2011; Tak et al., 2013). For instance, beginning a new exercise regimen in middle age is associated with healthy ageing (Sabia et al., 2012; Sun et al., 2010). Despite the well-known benefits of physical

activity, the adoption of a physically active lifestyle has remained low for reasons including limitations in self-efficacy and lack of free time (Lavie et al., 2019). One frequently reported barrier to engagement in physical activity is perceived physical exertion or fatigue (Jones & Nies, 1996; Malone et al., 2012; Thomson et al., 2016). Acknowledging such barriers to engagement in physical activity is important, but ultimately, the poor/insufficient adherence levels of the general population to physical activity guidelines are unacceptable, emphasising the need for alternate strategies to help individuals engage with physical activity and maintain functional capacity and independence into older age (see Figure 1.1).

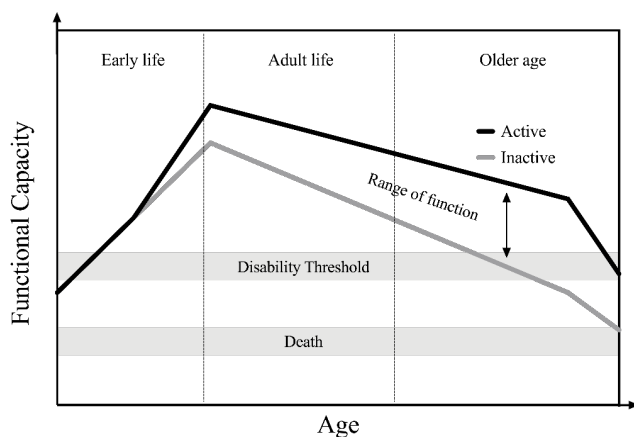


Figure 1. 1 Graphical representation of the relationship between ageing and functional capacity. Adapted from WHO, 2000.

An individual's tolerance for the activities of daily living is compromised with sedentary ageing. Major determinants of exercise tolerance including cardio-pulmonary and muscle-energetic function are impaired with sedentary ageing, which culminates in reduced oxygen (O₂) transport and impaired utilisation (Ward, 2007). Indeed, lowered capacity for O₂ transport and utilisation manifests as reduced maximal O₂ uptake and slower pulmonary O₂ uptake ($\dot{V}O_2$)

Commented [DR9]: I can't find any reference to this figure in the text neither the term 'functional capacity'. Also, at the very end the two lines should come to one similar end point (death) at zero functional capacity

Commented [TD10]: Do you have a reference to support this?

kinetics during exercise. As a result, sedentary ageing increases the physical and cognitive burden of a given task. Physiologically, the vascular endothelium and skeletal muscle tissue play central roles in regulating the delivery and consumption of O₂, respectively. Evidence suggests that sedentary ageing impairs vascular endothelial and skeletal muscle function (and thus O₂ delivery and utilisation, respectively; see Figure 1.2), which is largely attributable to intricate mechanisms converging on cellular mitochondria. Both the vascular endothelium and skeletal muscle mitochondria, therefore, may represent important therapeutic targets for enhancing O₂ uptake, and ultimately exercise tolerance.

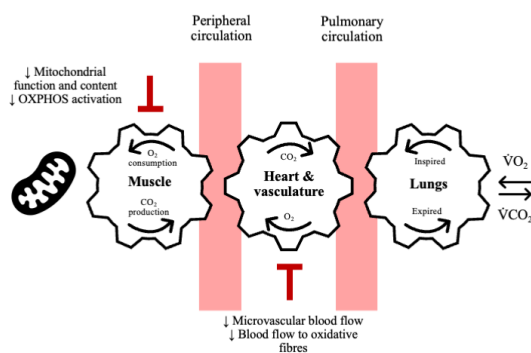


Figure 1. 2 Pathway of O₂ and CO₂ transport from mouth to mitochondria. Physiologic mechanisms that link respiration at the cellular and whole-body levels. Red bars denote inhibitory effects of sedentary ageing upon O₂ delivery and utilisation pathways.

Dietary interventions are increasingly considered for their potential as relatively inexpensive strategies to mitigate the burden of sedentary ageing. Polyphenols are bioactive constituents of foodstuffs, broadly categorised into four subclasses according to their molecular structure (Pandey & Rizvi, 2009). One class of naturally occurring polyphenols, flavonoids, account for the majority of known polyphenol compounds (~60%) (Manach et al., 2004). Flavonoids were first discovered in the 1930's by the Nobel laureate Dr. Albert Szent-Gyorgyi. After isolating unknown compounds from lemon juice and Hungarian red pepper, Szent-Gyorgyi restored

capillary resistance in man through intravenous administration of the compounds, which he subsequently classified as another vitamin group, 'P' (Rusznayak & Szent-Gyorgyi, 1936). Later, it was determined that vitamin P was rather a mixture of flavonoids, that would later belong to a class of over four thousand identified metabolites. Unlike micronutrients, there is no established disease associated with suboptimal flavonoid consumption. Nevertheless, flavonoids are considered essential for maintaining health across the life course (Holst & Williamson, 2008). A plethora of research has been published describing how flavonoids and flavonoid-rich products afford beneficial effects upon cardiovascular and metabolic health (see section 1.2.13 and Figure 1.3). Today, the consensus is that the health promoting effects of flavonoids can be owed to their capacity to modulate enzyme activities, activate signalling pathways and even interact with the energy-producing organelles of cells, the mitochondria (Kicinska & Jarmuszkiewicz, 2020; Williamson et al., 2018).

Commented [SD11]: Is this sentence best located here/?

Commented [DR12R11]: Yes, although you could argue to have this whole paragraph about flavonoids, health, and ageing as a starter of 15.1

Commented [TD13]: Ref needed?

Commented [TD14]: Can you enlarge the figure?

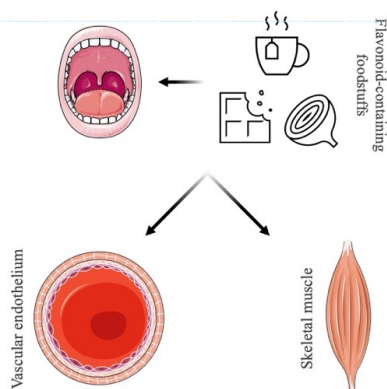


Figure 1. 3 Flavonoid ingestion may promote beneficial effects upon target tissues such as the vascular endothelium and skeletal muscle tissue.

Considering the therapeutic potential of flavonoids in the context of sedentary ageing, the aim of the experiments in this thesis were twofold: To assess 1. whether dietary flavonoids can

Commented [SD15]: Changed this paragraph

Commented [DR16]: ..the research...which would also include your theoretical work

speed $\dot{V}O_2$ kinetics and enhance exercise tolerance, *in vivo*, in physically inactive middle-aged adults and 2. Whether dietary flavonoids improve vascular endothelial and/or skeletal muscle function as it relates to energy metabolism *in vitro*. To achieve these aims, complementary *in vivo* (human) and *in vitro* (vascular endothelial and skeletal muscle cells) studies were conducted that investigated whether flavonoid supplementation impacted: 1. $\dot{V}O_2$ kinetics in inactive middle-aged adults, 2. Reactive oxygen and nitrogen species (RONS) production, mitochondrial function and signalling in vascular endothelial cells, 3. NO bioavailability, mitochondrial function and gene expression of C₂C₁₂ myoblasts, 4. Mitochondrial function, ROS production and cell signalling of C₂C₁₂ myotubes and 5. The metabolome of C₂C₁₂ skeletal myoblasts and myotubes. Together, these studies facilitated a critical appraisal of the literature that addressed four key areas: 1. The molecular processes underpinning vascular endothelial and skeletal muscle (dys)function during ageing, with a particular focus on the role of the mitochondria; 2. Evidence for impaired O₂ delivery and uptake with older age; 3. The impact of older age on $\dot{V}O_2$ kinetics and potential sites of regulation in the rest-to-work transition and 4. The known health benefits of dietary flavonoids *in vivo* and their biological activities at the cellular and molecular level.

Commented [HJ17]: This needs to in some way explain how you split the studies up into chapters. Each chapter your present in the thesis has an aim and hypothesis. I think they need to be reflected here. I am reading this like you have performed 2 studies.

1.2 Literature Review

1.2.1 Mitochondria – an overview

The mitochondrion is hailed as "the powerhouse of the cell" because it provides the majority of the cell's chemical energy currency, adenosine triphosphate (ATP). In doing so, mitochondria generate a small quantity of reactive molecules containing unpaired electrons, collectively known as reactive oxygen and nitrogen species (RONS). Yet, mitochondria are also involved in other critical cellular activities, such as retrograde signalling, cellular differentiation, apoptosis and cell senescence (Groschner et al., 2012; Hood et al., 2019). Given

Commented [DR18]: I had the same feeling as Helen (without having seen her comment). In general when you write down a text you have to get the reader curious about the topic, wanting eagerly to read further because he/she wants to know more. For me it is not clear why you go into so much depth describing mitochondrial function and mechanism. You need to have a paragraph on the relationship between ageing, oxygen consumption, mitochondrial function, and relate that to specific cells (muscle and endothelial). One self-made scheme/figure quite early in this chapter would say more than a thousand words. Introducing such a scheme would also help you say that you will address the relationship between these topics in more detail later. First 'paint' the context and then go in depth...

the multifaceted role of this organelle, it is no wonder that mitochondria are widely implicated in human health, disease and the ageing process.

1.2.2 Mitochondrial oxidative phosphorylation

Cellular energy requirements are met by the energy released in the oxidation of electron donors derived from reduced substrates (such as carbohydrates, fatty acids, and amino acids). This intricate process involves the entry of electrons into the electron transport system (ETS), and their subsequent movement down >20 reduction-oxidation (redox) couples to molecular O₂, which serves as the ultimate electron acceptor. The ETS is a highly refined molecular engine, made up of multi-protein complexes (Complex I-V) encoded by both nuclear and mitochondrial DNA (mtDNA), and are embedded in the inner mitochondrial membrane (see Figure 1.4). The movement of electrons down the gradient of redox potential in the ETS is tightly coupled to the energy-demanding reactions of ATP synthesis, and is achieved through a chemiosmotic mechanism (Mitchell, 1961). As electrons flow through the ETS, Complex I, Complex III and Complex IV translocate protons from the mitochondrial matrix to the inner membrane space. Through this mechanism, a proton-motive force is generated, consisting of an electrical gradient (membrane potential; $\Delta\psi$), accompanied by a small chemical gradient (ΔpH). The resultant proton motive force drives protons back into the matrix through the mitochondrial ATP synthase (Complex V), resulting in ATP synthesis. Together, this dynamic and orchestrated process is the mechanism of oxidative phosphorylation (OXPHOS).

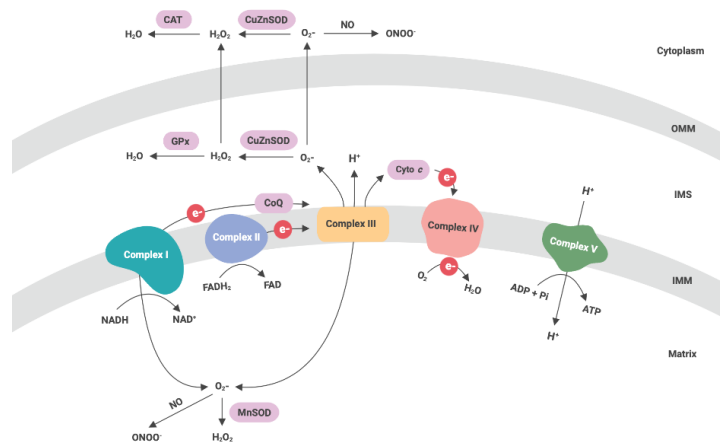


Figure 1. 4 Schematic of the molecular machinery responsible for oxidative phosphorylation within the mitochondrion. Electron (e^-) transfer along the electron transport chain (comprising complex I, II, III and IV embedded in the inner mitochondrial membrane [IMM]) drives protons (H^+) from the mitochondrial matrix into the inner membrane space (IMS). The electrochemical potential created by accumulation of H^+ within the mitochondrial membranes is used by ATP synthase (complex V) to produce ATP. Proton leak allows H^+ to re-enter the matrix, bypassing ATP synthase, such that oxygen (O_2) consumption is not entirely coupled to ATP synthesis. Electron leakage from complex I and III leads to partial reduction of O_2 to form superoxide (O_2^-), which is rapidly quenched to form hydrogen peroxide (H_2O_2) by superoxide dismutase (SOD). H_2O_2 is further metabolised to water (H_2O) by catalase (CAT).

1.2.3 Mitochondrial turnover

By virtue of their endosymbiotic origins, mammalian mitochondria maintain their own individual 16.5-kb genome which works in conjunction with nuclear DNA for the expression of mitochondrial proteins (Calvo et al., 2016). Of the nearly ~1500 proteins that make up mitochondria (Zhao et al., 2013), mtDNA is responsible for the transcription of just 13, albeit integral, ETS proteins, along with 2 rRNAs and 22 tRNAs (Anderson et al., 1981). Hence, the

vast majority (>99%) of the remaining mitochondrial proteins require transcription in the nucleus and import into their appropriate compartments via mitochondrial chaperones and protein import channels (Schwarz & Neupert, 1994; Takahashi & Hood, 1996).

The transcription of nuclear encoded mitochondrial proteins is highly regulated, and the transcriptional coactivator peroxisome proliferator activated receptor γ coactivator 1 α (PGC-1 α) is considered a major governor of this process (Handschin & Spiegelman, 2006; Lin et al., 2005; Scarpulla et al., 2012), despite its apparent dispensability for mitochondrial biogenesis (Rowe et al., 2012). PGC-1 α acts to upregulate gene transcription by docking with transcription factors and additional proteins on DNA promoters to regulate nuclear genes encoding mitochondrial proteins (Puigserver et al., 1999; Scarpulla, 2011a; Scarpulla et al., 2012). Once activated, PGC-1 α interacts with TFs including nuclear respiratory factor (NRF)-1/2, which induce the expression of mitochondrial transcription factor A (Tfam). Tfam is subsequently imported into the organelle and serves as the most important transcription factor to upregulate the transcription of mtDNA-derived proteins (Gordon et al., 2001; Scarpulla, 2011b). Besides activation of the mitochondrial biogenesis pathway leading to an increase in mitochondrial content, elimination of organelles via mitophagy is important to maintain or improve the quality of the mitochondrial pool (Erlich & Hood, 2019; Kim & Hood, 2017). Mitophagy involves the engulfment of damaged organelles by autophagosomes when they exhibit a decreased membrane potential and/or excessive increases in RONS production (Chen et al., 2018; Kim et al., 2019; Wei et al., 2015). One key regulatory pathway involved in mitophagy involves PINK1 and the E3 ligase Parkin. Initially, stabilisation of PTEN-induced kinase 1 (PINK1) on the outer membrane occurs, which recruits Parkin, and upon phosphorylation, targets membrane proteins such as mitofusin-2 (Mfn2) for selective degradation through a ubiquitin tag.

Commented [DR19]: Just a general comment: you don't have to show off telling everything you know about the mechanisms within the mitochondria. Try to focus on those aspects that are relevant to introduce your experiments and hypotheses. Too much information distracts from the message you want to get across.

1.2.4 Mitochondria morphology

Mitochondria comprise of four specific regions, including the outer mitochondrial membrane (OMM), intermembrane space, inner mitochondrial membrane (IMM), and the mitochondrial matrix. Although often depicted as stand-alone organelles, mitochondria exist as an interconnected network (see Figure 1.5), that is not static but rather highly dynamic, and dictated by the metabolic demands of the cell (Picard et al., 2013). The morphology of these organelle relies on the dynamic interplay between fission and fusion activities, where the fusion of smaller organelles allows for the sharing of cellular material and facilitates the expansion of the mitochondrial network (Liu et al., 2009). The primary proteins involved in mitochondrial fusion include mitofusin1/2 (Mfn1/2), which anchors adjacent OMMs, and optical atrophy 1 (OPA1), which plays a similar role in IMM fusion (Mishra & Chan, 2016). Conversely, fission is required to break the reticulum into smaller fragmented organelles, an important step in removing dysfunctional mitochondria from the mitochondrial pool for degradation. In a manner similar to Mfn2, the fission protein dynamin-related protein 1 (Drp1) resides on the OMM and works in conjunction with mitochondrial fission factor and fission protein 1 to wrap around and constrict the mitochondria to promote organellular separation (Losó n et al., 2013).

Commented [DR20]: Your definitions are not consistent OM, IM, IMM why not OMM?

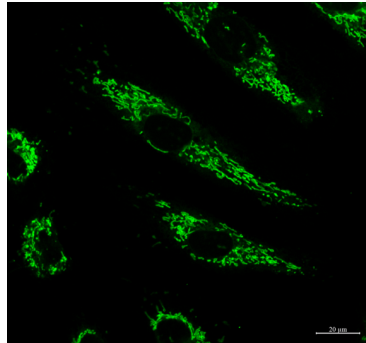


Figure 1. 5 Highly interconnected cellular network of mitochondria. HUVEC mitochondria stained with Mitotracker Green (25 nM) and image captured at 63x magnification by confocal microscopy.

Commented [DR21]: This text doesn't tell me what I am looking at. What has been stained? Extrusions of mitochondrial membranes?

Commented [SD22R21]: Have adjusted description to suit

Commented [HJ23]: Need to link to the sentence about static and dynamic in above paragraph

1.2.5 Mitochondrial (& extra-mitochondrial) reactive oxygen species

As electrons pass down the ETS during OXPHOS, a small proportion of them (~0.15%) will escape their destined path and react with O_2 , generating RONS (St-Pierre et al., 2002). Typically, this reaction results in the formation of the superoxide radical, that is rapidly dismutated to the freely diffusible oxidant hydrogen peroxide (H_2O_2) (St-Pierre et al., 2002). Despite their relatively short half-life, RONS can trigger key redox-sensitive signalling pathways and subsequently promote important cellular adaptations (Krylatov et al., 2018; Powers et al., 2010). The importance of RONS as beneficial signalling molecules for adaptation has been eloquently demonstrated by studies showing antioxidant supplementation regimes blunt vasodilation and mRNA responses following exercise (Gomez-Cabrera et al., 2008; Sindler et al., 2009; Strobel et al., 2011). In spite of their indispensability, excessive emission of RONS can increase oxidative stress, which may culminate in damage to lipids, DNA and proteins, and even impair mitochondrial function (Melov et al., 2000; Schriener et al., 2005). Indeed, RONS may compromise the activity of complexes within the ETS, which can be directly altered by oxidative modifications (Cobley et al., 2019; Mailloux et al., 2014). To help

Commented [TD24]: The balance and the delicacy of this may deserve a bit more attention?

Commented [SD25R24]: Subtly adjust sentences to make clearer

maintain appropriate cellular redox balance in the face of oxidative insults, specific antioxidant defence enzymes are deployed, including those within the glutathione system, superoxide dismutase and catalase (Dimauro et al., 2012; Jones, 2006).

1.2.6 Section Summary & link to thesis objectives

To summarise, mitochondrial form and function play a vital role in maintaining cellular function by serving the requirements for ATP, co-ordinating signalling responses and regulating the oxidative state. Ensuring a dense and robust cellular mitochondrial network is therefore of utmost importance for defending against the perils of ageing, physical inactivity and disease. In Chapters 4, 5 and 6 of this thesis, mitochondrial function will be interrogated in vascular endothelial cells and skeletal muscle cells.

1.2.7 Mechanisms of age-related mitochondrial dysfunction

1.2.7.1 Skeletal muscle mitochondrial (dys)function

Mitochondrial dysfunction is considered a major hallmark of the ageing process (López-Otín et al., 2013). Investigations into the mechanisms underlying skeletal muscle mitochondrial dysfunction with ageing have unveiled marked reductions in mitochondrial contents and capacity (Holloszy et al., 1991; Lyons et al., 2006; Zahn et al., 2006), as well as increased production of RONS (Palomero et al., 2013; Vasilaki et al., 2010). Early work studying mitochondrial turnover with ageing revealed a substantial decline (~40%) in the rate of mitochondrial protein synthesis from young- to middle-age that persisted into older age (Rooyackers et al., 1996). Subsequent studies have repeatedly shown older skeletal muscle displays lower expression of key proteins that regulate mitochondrial function, such as PGC-1 α (Chabi et al., 2008a; Konopka et al., 2014). It is thought that this reduction in mitochondrial content is partly attributable to blunted responses to stimuli that augment mitochondrial

Commented [HJ26]: Just a suggestion but instead on a section summary could the summaries be linked to the aims of the studies... with statements like for example in study ? of the present thesis mitochondrial function will be examined to

Commented [SD27R26]: I do like idea of making reference to studies, and will strive to do this in later stages where gaps in literature are identified.

biogenesis, such as contractile activity (Ljubicic et al., 2009; Ljubicic & Hood, 2009). In this regard, the deleterious effects of ageing can be observed at the level of energy sensing signalling pathways, where the activation of AMP-activated protein kinase (AMPK) is lower after endurance exercise in aged compared to young muscle (Reznick et al., 2007a). Remodelling of the mitochondrial network also involves targeted degradation (mitophagy) and dynamic quality control processes, fusion and fission. Both mitophagy and mitochondrial dynamics are altered in older compared to young skeletal muscle, evidenced by increased expression of autophagy- and mitochondrial fission-related proteins (Carter et al., 2018; Chen et al., 2018; Iqbal et al., 2013). Although conflicting data have been reported in older animals with respect to mitophagy and fission (Distefano et al., 2017; Joseph et al., 2013a; Leduc-Gaudet et al., 2015; Russ et al., 2012), an increased drive for mitophagy and fission activities may result in a less functional and more fragmented mitochondrial network (Gospillou et al., 2014).

On the issue of mitochondrial function, a wide range of studies have described the impact of ageing on the intrinsic capacities of mitochondria. Those reporting the activity of mitochondrial respiratory enzymes from ageing muscle tissue have shown a marked decline in some (Bass et al., 1975; Desai et al., 1996; Lezza et al., 1994), but not all cases (Barrientos et al., 1996; Örlander et al., 1978). Other integrated measures of functionality in cultured cells and isolated muscle mitochondria by respirometry have suggested age-related deficiencies. For example, isolated aged skeletal muscle mitochondria demonstrate altered indices of function, including reduced maximal ATP-generating capacity (Drew et al., 2003a), lower ADP-stimulated respiration (Picard et al., 2010a) and reduced maximal respiratory capacity (Chabi et al., 2008b). These altered indices of organelle function coincide with changes in metabolic pathways *in vitro*, where cultured skeletal muscle cells from older donors display greater

reliance on glycolysis for ATP synthesis compared to younger donors (Marrone et al., 2018a; Pääsuke et al., 2016). In this thesis, intrinsic mitochondrial function will be investigated in control and replicatively aged skeletal myoblasts (Chapter 5) and myotubes (Chapter 6).

Commented [SD28]: Adding links to studies/chapters

Aside from contents and capacity, another driver of dysfunctional mitochondria in ageing skeletal muscle is increased mitochondrial-derived RONS (Holloway et al., 2018; Jang et al., 2010). Mitochondrial peroxide generation has been repeatedly shown to be increased in skeletal muscle during ageing (Jang & Remmen, 2009; Martinez Guimera et al., 2018; Palomero et al., 2013). For instance, isolated skeletal muscle mitochondria demonstrate age-related increases in H₂O₂ production (Chabi et al., 2008b; Vasilaki et al., 2006), which is likely the result of excessive generation of superoxide from the ETS (Brand et al., 2013). Although the reported increase in ROS production with ageing may also manifest due to increased action of cytosolic NADPH oxidases (Jackson et al., 2015). However, increased mitochondrial RONS with ageing has not been consistently demonstrated *in vitro* (Distefano et al., 2017; Gouspillou et al., 2014a). Such discrepancies in study outcomes can partly be explained by a failure of some cellular models to closely mimic the *in vivo* environment. However, when physiological concentrations of ADP are employed, ageing skeletal muscle presents increased production of H₂O₂ (Holloway et al., 2018). Given that mitochondria are responsible for the bulk of oxygen consumption and ATP production (Rolfe & Brown, 1997), the aforementioned (age-related) perturbations to the abundance and overall function of these organelles (see Figure 1.6) has major implications for contractile bioenergetics and oxygen uptake *in vivo*.

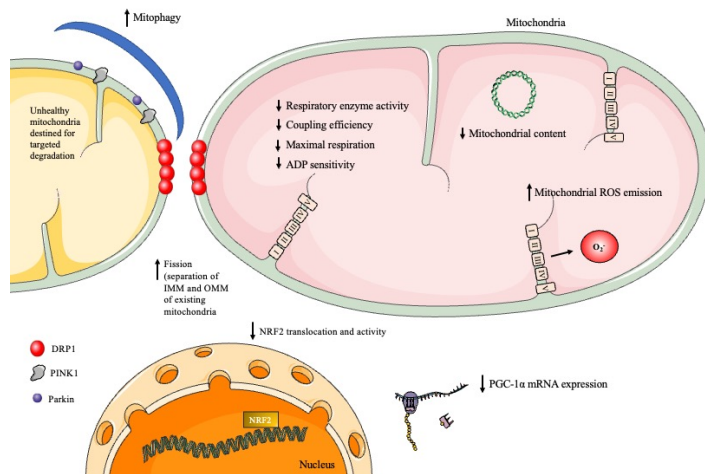


Figure 1. 6 Impact of sedentary ageing upon on skeletal muscle mitochondria. In older, physically inactive skeletal muscle, mitochondria display lowered respiratory function, reduced mitochondrial content, and increased production of mitochondrial-derived reactive oxygen species (ROS). Ultimately, these effects lead to a diminished capacity for oxygen utilisation.

1.2.7.2 Vascular endothelial mitochondrial dysfunction

From a mechanistic standpoint, endothelial dysfunction is characterised by several, interlinked factors, including mitochondrial dysfunction, elevated oxidative stress, reduced NO bioavailability and altered energy-sensing pathways (Ungvari et al., 2018). Of these factors, mitochondrial dysfunction has received the least attention in the recent literature, largely owed to early observations that endothelial cells contain relatively few mitochondria (2–5% of cell volume) in comparison to other cell types like skeletal muscle (2.5-9.5% of cell volume) (Howald et al., 1985; Ørtenblad et al., 2018; Vincent et al., 2019) and cardiomyocytes (~35% of cell volume) (Barth et al., 1992; Oldendorf et al., 1977). Nevertheless, mitochondria have emerged as having a potential key role in contributing to vascular endothelial dysfunction with

Commented [DR29]: It is not immediately clear why you include endothelial cells in your research. Muscle cells is easily to understand being related to physical activity and energy, but endothelial cells need some more introduction. Maybe relate it to long capacity and blood supply in the muscles?

Commented [HJ30]: Sentence on endothial function contributing to CVD risk?

ageing. Ageing is associated with reduced endothelial mitochondrial content, evidenced by reduced expression of PGC-1 α and citrate synthase, as well as lowered cytochrome c oxidase (COX) activity (Park et al., 2018a; Ungvari et al., 2008a). Such declines in mitochondrial content may contribute to increased production of mitochondrial ROS in the ageing endothelium. Associated with reductions in mitochondrial proteins, impairments to organelle quality control processes (fusion and fission) have been demonstrated in aged versus young human vascular endothelial cells (Jendrach et al., 2005) by light microscopy. Aside from content, it was recently shown that the respiratory function (complex I and I + II state 3 respiration) of aged human skeletal muscle feed arteries is impaired in old compared to young participants (Park et al., 2020). Therefore, age-related changes in mitochondrial content and function may contribute to vascular endothelial dysfunction with advancing age.

A second, well documented feature of vascular endothelial ageing is increased oxidative stress (see Figure 1.7), a state in which the production of RONS outweighs the buffering capacity of antioxidant defences (Cai & Harrison, 2000; Harrison, 1997). There is strong evidence for increased production of RONS in the ageing rodent and human endothelium (Adler et al., 2003a; Csizsar et al., 2002a; Eskurza et al., 2004; Jacobson et al., 2007), that is both cytosolic (e.g. NADPH oxidases) and mitochondrial in origin (Donato et al., 2007a; Durrant et al., 2009a; Ungvari et al., 2007; Zhou et al., 2009). It is thought that elevated oxidative stress within the ageing vascular endothelium is caused by defects in the ETS (Ungvari et al., 2008b), and/or compromised antioxidant responses (Csizsar et al., 2014; Ungvari et al., 2011; Van Der Loo et al., 2000a). Irrespective of the underlying cause, increased oxidative stress may culminate in critical modifications to DNA or proteins (Sastre et al., 2003), though one of its most potent effects is a reduction in NO bioavailability, caused by the reaction of superoxide with NO to produce peroxynitrite (Donato et al., 2007a; Durrant et al., 2009b; Lesniewski et al., 2009).

The lowered bioavailability of NO with ageing can also be explained by a reduced activity and expression of the enzyme responsible for its synthesis, endothelial nitric oxide synthase (eNOS) (Cernadas et al., 1998a; Chou et al., 1998; Donato et al., 2009a); although other work suggests ageing may elevate eNOS expression as a compensatory mechanism (Thijssen et al., 2016).

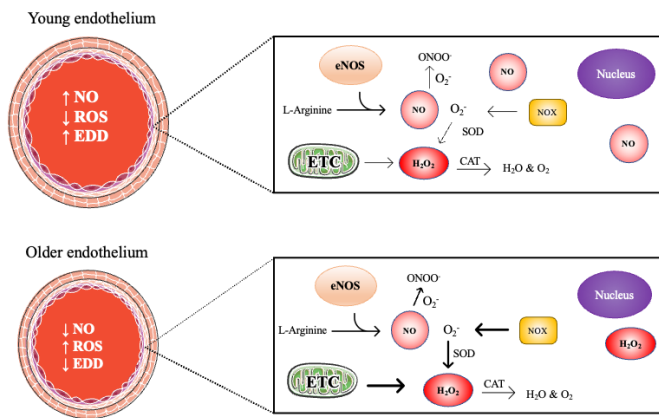


Figure 1. 7 Impact of advancing age on the vascular endothelium. In younger endothelial cells (**top**), eNOS (endothelial NO synthase) produces NO through the conversion of L-arginine to L-citrulline, to facilitate endothelium-dependent vasodilation (EDD). Reactive oxygen species (ROS), for example, O₂⁻ and H₂O₂, are produced by the mitochondrial electron transport chain (ETC) or cytosolic oxidant enzymes, such as NOX (NADPH oxidase). These reactive molecules are quenched by endogenous antioxidant enzymes such as superoxide dismutase (SOD) and catalase (CAT). In older endothelial cells (**bottom**), ROS production increases due to increased mitochondrial and NOX-derived ROS. Increased O₂⁻ diminishes NO bioavailability, through its conversion to peroxynitrite (ONOO⁻). Ultimately, these effects lead to a reduction in endothelial-dependent vasodilation in the aged endothelium. Figure adapted from (Donato et al., 2018).

Commented [HJ31]: Define EDD in legend

The energy-sensitive serine/threonine kinase AMPK plays an important role in regulating vascular endothelial mitochondrial function and biogenesis, thus determining sensitivity to

oxidative stresses (Ceolotto et al., 2007; Colombo & Moncada, 2009; Ido et al., 2002; Kukidome et al., 2006). Activation of AMPK requires phosphorylation of the α subunit and occurs downstream of two kinases, including liver kinase B1 (LKB1) and Ca^{2+} /calmodulin-dependent protein kinase (CaMKII) (Hawley et al., 2005; Stahmann et al., 2006). AMPK is also considered to regulate the activity of eNOS, through its phosphorylation at Ser1177 (Chen et al., 1999), amongst other sites. During ageing, AMPK expression and activity are reportedly downregulated in the vascular endothelium (Lesniewski et al., 2012), thus highlighting the therapeutic potential in targeting this protein kinase for ameliorating vascular endothelial dysfunction.

1.2.8 Evidence of age-related impairments in the capacity to deliver and utilise oxygen

in vivo

1.2.8.1 Impaired O_2 utilisation

The aforementioned age-related disruptions to mitochondria at the cellular and molecular level have implications for O_2 utilisation *in vivo*. In-fact, mitochondrial dysfunction is implicated in the causality of slower walking speeds, fatigability and slowing of $\dot{V}\text{O}_2$ kinetics with ageing (Choi et al., 2016a; Coen et al., 2013; Joseph et al., 2012; Murias & Paterson, 2015a; Sundberg et al., 2019; Zane et al., 2017). Reports of muscle oxidative capacity in older humans using ^{31}P -magnetic resonance spectroscopy (MRS) have suggested mitochondrial dysfunction by slowed phosphocreatine (PCr) resynthesis in resting (Fleischman et al., 2010) and contracting skeletal muscle (Choi et al., 2016b; Distefano et al., 2018). Nevertheless, no such impairments to PCr recovery were observed in the tibialis anterior muscle of aged compared to young subjects when matched for physical activity levels (Kent-Braun & Ng, 2000; Lanza et al., 2005). More invasive and direct examinations of mitochondrial function in permeabilised

Commented [DR32]: This kind of information needs to be at the forefront of your chapter illustrating your line of thinking before you go into depth

Commented [SD33R32]: Should it be if we start from mitochondrial cell level and go 'outwards' to in-vivo?

Commented [HJ34R32]: Agree with Richard. Your introduction section, the reader should be able to read and know what your going to do but also why you doing it? Why its important

Commented [DR35]: ^{31}P

Commented [TD36]: this suggests it is not ageing but physical inactivity?

Commented [SD37R36]: It does, and role of ageing on muscle mito is debated, could be due to reductions in content rather than functional deficits per se. Although dysfunction was indeed observed in a important paper (Holloway 2018) that used submax ADP cones relevant to in-vivo

myofibers by respirometry have also produced equivocal results. A decline in mitochondrial function with ageing has been evidenced by reduced basal and maximal respiration (Joseph et al., 2012; Tonkonogi et al., 2003a), as well as impaired coupling efficiency (Porter et al., 2015). On the other hand, some studies have found no such impediments to muscle mitochondrial respiration in isolated muscle fibres of aged human and rat skeletal muscle (Gousspillou, Sgarioto, et al., 2014b; Hütter et al., 2007; Picard et al., 2010a). The apparent discrepancies between study outcomes could be explained by the fitness or physical activity levels of older participants (Conley et al., 2013; Distefano et al., 2018; Gram et al., 2015), or even due to artefacts introduced by mitochondrial isolation procedures (Picard et al., 2010b). Using an alternative experimental approach involving modular control analysis, one study reported that activation of mitochondrial oxidative phosphorylation in response to a given increase in ATP demand, or affinity for ADP (during low contractile activity, reflecting daily living activity), is markedly reduced with skeletal muscle aging (Gousspillou et al., 2014a), adding support to the idea mitochondrial bioenergetics (and O₂ utilisation) are significantly impaired *in vivo* in aged skeletal muscle.

Besides potential limitations in mitochondrial function of older muscle, it has been reported that the key enzyme, pyruvate dehydrogenase (PDH), might also play a role in regulating O₂ utilisation. One study demonstrated blunted PDH activation in biopsy samples from the vastus lateralis 30 s into a moderate-intensity exercise transition in older adults, which the authors concluded was partly responsible for the slower $\dot{V}O_2$ kinetics observed compared to young adults (Gurd et al., 2008). Besides PDH, research has suggested that creatine kinase (CK) induced breakdown of phosphocreatine may also modulate mitochondrial respiration through feedback control (Grassi et al., 2011). In this way, CK appears to slow the signal responsible for the activation of OXPHOS in mammalian skeletal muscle, although this is yet to be

Commented [TD38]: In...?

Commented [SD39R38]: In compromising capacity for O₂ utilisation – at first half of sentence. Need changing?

Commented [TD40]: How? Assumption? Or did they demonstrate this?

Commented [SD41R40]: Authors showed a slower vo₂ kinetics in the older adults compared to young, and they measured pdh activity in muscle

Commented [DR42]: The 2 comments of Dick are indications that your message is not immediately clear. Rearranging the sentences may help here.

explored in older populations. Multiple groups have used ^{31}P -MRS to demonstrate close relationships between phosphocreatine kinetics and $\dot{V}\text{O}_2$ during moderate-intensity exercise (Barstow et al., 1994a, 1994b; McCreary et al., 1996; Rossiter et al., 2002). Collectively, the reported decrements in mitochondrial respiration and potentially impaired PDH activation reported in physically inactive older adults may contribute to the age-related decline in $\dot{V}\text{O}_2$ kinetics in the rest-to-work transition.

Commented [DR43]: ^{31}P

Another possible and noteworthy factor related to O_2 uptake is the influence of NO on mitochondrial function. In addition to its well-known role in the regulation of endothelium dependent vasodilation, NO has the potential to compete with O_2 for the binding site at COX (Brown, 2000; Schweizer & Richter, 1994), thereby inhibiting respiration and ATP synthesis (Takehara et al., 1995). Human based studies (Jones et al., 2003, Jones et al., 2004) have reported that inhibition of NO synthesis with N(ω)-nitro-L-arginine methyl ester (L-NAME) actually results in a significant speeding of the primary response of $\dot{V}\text{O}_2$ kinetics, albeit in young adults. Paradoxically, NO also stimulates mitochondrial biogenesis, and plays a critical role in vasodilation responses. With older age, NO levels markedly decline, yet $\dot{V}\text{O}_2$ kinetics are concurrently slowed during exercise (Bell et al., 1999; Gurd et al., 2008). Therefore, it seems that the potential inhibitory effects of NO on $\dot{V}\text{O}_2$ are intricate and not completely understood. Quite possibly, the relationship between NO and $\dot{V}\text{O}_2$ is complicated with older age due to changes in the muscle redox state (Casey et al., 2015; Kirby et al., 2009).

Commented [DR44]: Does NO from endothelial cells stimulate mitochondrial biogenesis in skeletal muscle cells? If so then this is your logic link to study both cell types. On what timespan does this happen? Over minutes, days or months?

Commented [SD45R44]: Good question,

Commented [SD46]: Expanded on this to make it clearer

1.2.8.2 Impaired O_2 delivery

It is thought that structural and functional changes in the O_2 transport system of older individuals negatively affect the matching of O_2 delivery to O_2 utilisation (see Figure 1.8), such that a greater O_2 deficit is incurred during the onset of exercise. Potential regulatory sites along

the O₂ transport pathway include limitations in cardiac output, heart rate, vascular reactivity, and capillarization (Chilibeck et al., 1996; Coggan et al., 1992; Harper et al., 2006; Murias & Paterson, 2015a). A substantial amount of research over the past three decades has attempted to decipher the relative contribution of these limitations to muscle O₂ delivery with ageing, which has underlined diminished microvascular blood flow as a major candidate.

The decline in vascular endothelial function with advancing age is well documented. In the femoral and brachial artery, measures of endothelial function by flow-mediated dilation (FMD) have shown impairments with older age (Black et al., 2009; Celermajer et al., 1994; Thijssen et al., 2006). Similar effects of ageing have been observed in the (cutaneous) microvasculature, where ageing leads to impaired vasodilatory responses to heating and local acetylcholine infusion (Black et al., 2008a; Tew et al., 2010). As previously discussed (see section 1.2.7.2), a primary mechanism underlying vascular dysfunction with ageing appears to be related to the bioavailability of NO and production of RONS. Support for reduced NO bioavailability *in vivo* is provided by studies showing lowered forearm vasoconstrictor responses to infusion of the NO-synthase inhibitor N G-monomethyl-L-arginine (L-NMMA) (Singh et al., 2002a; Taddei et al., 2000a), and impaired microvascular dilation response to local heating (Black et al., 2008b). Furthermore, L-arginine (NO precursor) supplementation in older adults improves peripheral flow-mediated vasodilation (Bode-Böger et al., 2003) and reflex cutaneous vasodilation (Holowatz et al., 2006).

Commented [HJ47]: And prolonged heating (Black)

Research examining macro- and micro-vascular blood flow responses to exercise with advancing age has yielded divergent results. Initial work hinted that macrovascular blood flow was unlikely to be limiting to $\dot{V}O_2$ kinetics, where researchers reported that femoral artery blood flow exhibited faster kinetics than $\dot{V}O_2$ kinetics during single-leg knee extension exercise

in older adults (Bell et al., 2001). More recent research supports the premise $\dot{V}O_2$ kinetics are not limited by macrovascular blood flow, where the dynamic adjustment of femoral artery blood flow in the rest-to-work transition was similar between young and older adults (Dumanoir et al., 2010). However, leg blood flow appears to be lower in sedentary older compared to young adults during cycling exercise (Poole et al., 2003). On the contrary to macro-vascular flow, capillary blood flow (micro-vascular) kinetics are in fact slower than those of $\dot{V}O_2$ (Harper et al., 2006) during exercise onset. Data derived from studies utilising near-infrared spectroscopy (NIRS) to measure deoxygenation of the vastus lateralis of older men and women have demonstrated a greater reliance on O_2 extraction for a given $\dot{V}O_2$ compared to younger or trained counterparts - indicative of poorer matching of O_2 delivery to utilisation (Dogra et al., 2013; Murias et al., 2010a, 2011). Additional support for microvascular blood flow impairments in ageing comes from rodent models that have shown lowered endothelium-dependent vasodilation in feed arteries and arterioles (Behnke & Delp, 2010a; Muller-Delp et al., 2002a) and increased blood flow distribution to glycolytic muscle (Musch et al., 2004a). Overall, microvascular delivery and/or distribution of O_2 within regions of active muscle fibres might not be satisfactory to meet imposed metabolic demands in older adults, potentially resulting in slowed $\dot{V}O_2$ kinetics.

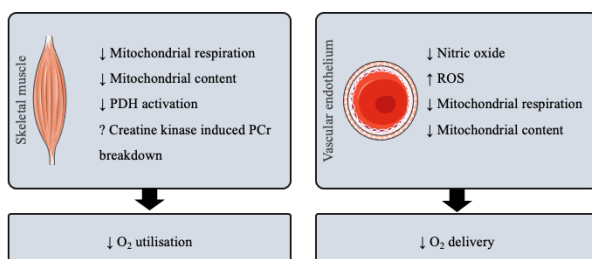


Figure 1. 8 Schematic depicting the impact of sedentary ageing upon skeletal muscle and vascular endothelial function. Impairments to skeletal muscle and vascular endothelial cells manifest as reduced O_2 transport and utilisation.

1.2.9 Consequences of impaired capacity for the delivery and utilisation of O₂: $\dot{V}O_2$ kinetics and exercise tolerance

1.2.9.1 $\dot{V}O_2$ kinetics offers insights into skeletal muscle metabolism

The first assessment of gas exchange kinetics in an exercising human was performed over a century ago by Krogh and Lindhard. Using the classic Douglas bag technique to measure pulmonary oxygen uptake ($\dot{V}O_2$), the authors administered an immediate, step increment in work rate and demonstrated that O₂ uptake increased relatively slowly in comparison to the onset of exercise (Krogh & Lindhard, 1913). Since this pioneering study, the non-invasive study of $\dot{V}O_2$ kinetics has significantly advanced our understanding of the mechanisms controlling the dynamic adjustment of OXPHOS. Actually, studying dynamic $\dot{V}O_2$ responses to submaximal exercise is often considered a more important outcome variable than peak exercise capacity ($\dot{V}O_{2\text{ peak}}$) in older adults (Alexander et al., 2003a). This is because submaximal activity is more translatable to everyday life activity and is relatively independent of motivation and effort, unlike $\dot{V}O_{2\text{ peak}}$ (Kitzman & Groban, 2011). Furthermore, below a particular $\dot{V}O_{2\text{ peak}}$ threshold ($\sim 30 \text{ mL/kg}^{-1}/\text{min}^{-1}$), daily life activities like brisk walking may be performed at submaximal intensities (Paterson et al., 2007). With this in mind, studying $\dot{V}O_2$ kinetics in sedentary adults offers the unique opportunity to decipher the effectiveness of targeted interventions in the context of physical activity that closely resembles that of daily life activity.

When assessed on a breath-by-breath basis, pulmonary $\dot{V}O_2$ displays three distinctive phases following the onset of moderate-intensity exercise (see Figure 1.9): phase I, an initial response phase of $\sim 19 \text{ s}$ reflecting the circulatory transit delay of O₂ from the active tissues to the lungs. Changes in $\dot{V}O_2$ during this phase represent an increase in pulmonary blood flow rather than

Commented [DR48]: What location?

increased O₂ extraction in active skeletal muscle; phase II (often termed the fundamental response), in which $\dot{V}O_2$ increases with approximately exponential response dynamics. It describes a mono-exponential increase until a steady state is achieved (Whipp et al., 1982, 2005); and phase III, the steady state (Whipp et al., 1982). When subjected to the appropriate data analysis, phase II pulmonary $\dot{V}O_2$ kinetics provides an accurate reflection of muscle $\dot{V}O_2$ kinetics during exercise (Barstow et al., 1990; Grassi et al., 1996; Rossiter et al., 1999). Specifically, the duration of the primary response of $\dot{V}O_2$ is characterised by the $\dot{V}O_2$ time-constant ($\tau\dot{V}O_2$), which describes the time required for $\dot{V}O_2$ to reach 63% of its steady state value. A lower $\tau\dot{V}O_2$ (i.e., faster $\dot{V}O_2$ kinetics) in the rest-to-work transition will attenuate the O₂ deficit incurred, thereby potentially causing less perturbations to intracellular homeostasis.

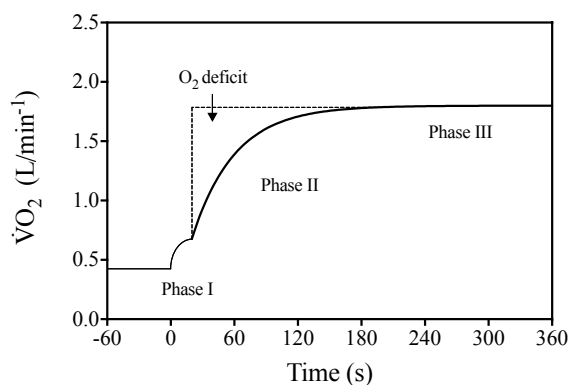


Figure 1. 9 Schematic depicting typical pulmonary oxygen uptake response during constant-rate moderate-intensity exercise. After phase I which represents the time taken for deoxygenated blood to reach pulmonary circulation, oxygen uptake rises in a mono-exponential fashion (phase II, primary response), before reaching a steady-state (phase III).

1.2.10 $\dot{V}O_2$ kinetics: Deleterious effects of ageing (and inactivity)

The study of $\dot{V}O_2$ kinetics across age groups has revealed that older adults typically display a slower dynamic adjustment of $\dot{V}O_2$ (Bell et al., 1999; Cunningham & Paterson, 1994; DeLorey et al., 2004a; Gurd et al., 2008; Murias et al., 2010a, 2011). As a result, older adults incur a greater O_2 deficit in the transition to physical activity, which may contribute to the reduced exercise tolerance observed in this demographic (Goulding et al., 2017; Grassi, et al., 2011). However, data are not fully conclusive on whether ageing *per se* slows $\dot{V}O_2$ kinetics, which could be explained by the confounding effect of physical activity levels in research participants. George and colleagues reported a slowing of $\dot{V}O_2$ kinetics in inactive, young and otherwise healthy individuals to similar levels of those in older inactive adults. Hence, the authors suggested that fitness level, and not ageing *per se*, determine the rate of $\dot{V}O_2$ kinetics (George et al., 2018). In spite of this, it is evident that ageing is associated with a progressive slowing of $\dot{V}O_2$ kinetics across the lifespan that coincides with exercise intolerance. With regards to the mechanisms underpinning the slower $\dot{V}O_2$ kinetics with ageing, research is not conclusive. There is strong support for the concept that a limitation in O_2 delivery to working muscles may, at least partly, be responsible for the greater $\tau\dot{V}O_2$ observed in older compared with young individuals (Murias et al., 2010a, 2011; Poole & Jones, 2012; Poole & Musch, 2010). Besides O_2 delivery through the (rapid) vasodilation of (feed) arteries to the active muscles, there is also experimental support that a key locus of control for $\dot{V}O_2$ kinetics resides intracellularly (see Figure 1.10), that is, one that pertains to an individual's capacity for O_2 utilisation within the mitochondria (Murias & Paterson, 2015a).

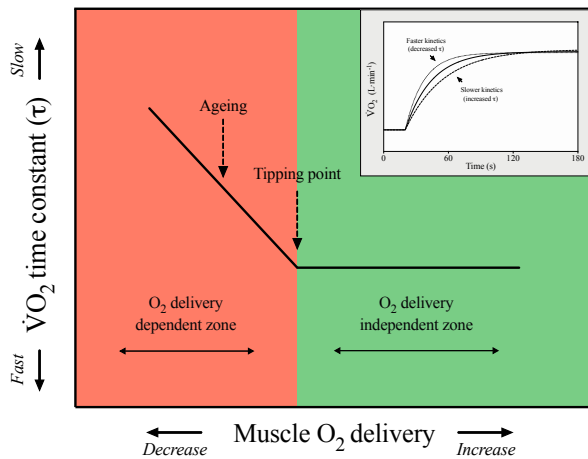


Figure 1.10 Idealised portrayal of the relationship between the speed of $\dot{V}O_2$ kinetics (given by the time constant, τ) and muscle(s) O_2 delivery. Note the presence of O_2 dependent (leftwards) and O_2 -independent (rightwards) zones falling either side of the “Tipping Point”. When O_2 delivery falls below the tipping point $\dot{V}O_2$ kinetics become progressively slowed as evidenced by increasing τ . In young healthy individuals conventional locomotory activities such as walking, running, and cycling lie to the right of the tipping point. However, $\dot{V}O_2$ kinetics become demonstrably slowed with aging (black downward arrow), by moving the individual leftward into the O_2 -delivery dependent region. Figure adapted from (D. C. Poole & Jones, 2012).

Commented [SD49]: Added new part of the figure, trying to decide whether it needs further adjustments

1.2.11 Section Summary

Advancing age and chronic physical inactivity impair pathways involved in the transport and utilisation of O_2 in active skeletal muscle, which culminates in relatively slow rates of $\dot{V}O_2$ kinetics compared to younger healthy counterparts. Therefore, there is a requirement for interventions targeted at pathways related to O_2 delivery and utilisation in ageing adults, with the aim of speeding $\dot{V}O_2$ kinetics and enhancing exercise tolerance. To meet this need, Chapter

Commented [HJ50]: Link to study aim/objective

Commented [TD51]: Can you think of a ‘summary figure’ where you link the various parts/topics to the oxygen kinetics (in older individuals)? Perhaps a rework of the figure above, with some additional mechanisms...?

Commented [SD52R51]: Tried to add and adjust, maybe panel C now needs adjusting... its not just O2 delivery that changes with ageing

3 of this thesis will test the effects of a nutritional intervention upon $\dot{V}O_2$ kinetics and exercise tolerance in sedentary middle-aged adults.

1.2.12 Dietary flavonoids: An overview

Flavonoids are a chemically defined class of polyphenols characterised by a common structure consisting of two aromatic rings (A and B) and an oxygenated heterocycle ring (see Figure 1.11). These compounds comprise of several subgroups according to their ascending degree of oxidation: flavanols, flavanones, isoflavones, flavonols, and anthocyanidins (Beecher, 2003; Bravo, 2009). The pattern of hydroxylation and conjugation in the aromatic rings further categorises individual flavonoids within these subclasses. These structurally diverse compounds exhibit a wide range of biological activity, that may explain their health-related effects. Whilst ubiquitous in plants, dietary flavonoids can be found in a wide variety of foods and beverages including fruit, vegetables, tea and cocoa (Arts et al., 1999).

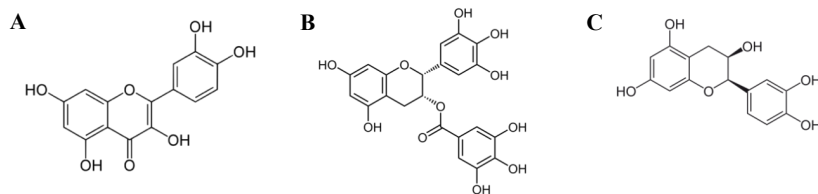


Figure 1. 11 Chemical structure of dietary flavonoids: A) quercetin, B) epigallocatechin-gallate, C) (-)-epicatechin.

After ingestion of flavonoid-containing foods or beverages, flavonoids must pass from the gut lumen before entering circulation (see Figure 1.12). Firstly, flavonoids are hydrolysed in the small intestine, and the resulting aglycones are subject to the action of phase I (hydrolysing

Commented [HJ53]: This section reads well and will link with the work you have performed in study 1. Again highlight throughout what you are doing to fill gaps in the literature with the studies in the current thesis.

e.g.
This comparison will be explored in chapter ?? of the present thesis
Or
This underpinned the hypothesis in study ??

Commented [SD54R53]: Have attempted to do this throughout below

and oxidising) and II (conjugating and detoxifying) enzymes that produce sulfate, glucuronide and/or methylated metabolites (Scalbert & Williamson, 2000; Spencer, 2003; Spencer et al., 1999). Upon entering circulation, flavonoid metabolites can be subjected to further phase II metabolism with biotransformation occurring in the liver, prior to urinary excretion. Those flavonoids not absorbed by the small intestine pass to the colon, in which the enzymes of the gut microflora induce the breakdown of flavonoids to simple phenolic acids that may then undergo absorption and are further metabolised in the liver (Spencer et al., 2008). Once taken up by target tissues, flavonoids may also be subject to specific types of intracellular metabolism, including oxidative metabolism, glutathione conjugation and even demethylation (Moridani et al., 2001; Spencer et al., 2003).

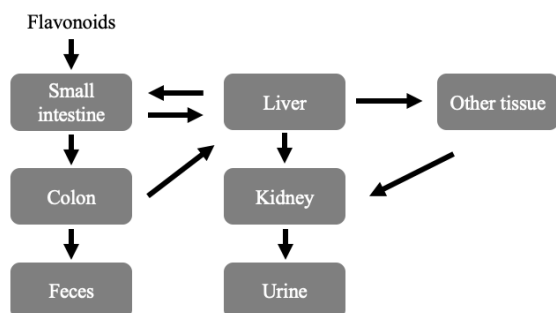


Figure 1. 12 Basic overview of flavonoid absorption and metabolism.

The total estimated flavonoid intake of adults living in western nations is ~430 mg/day (Peterson et al., 2015), and the concentration of flavonoid metabolites that reach systemic circulation is likely up to 10 μ M (Manach et al., 2005a). Some of the factors that likely affect flavonoid bioavailability *in vivo* include flavonoid dose, flavonoid structure, and the macronutrient composition of the ingested food matrix (Bohn et al., 2014). Once in circulation,

flavonoids may be taken up into cells via the organic anion transporters (OAT), which are specific for the class of flavonoid, its conjugated group and conjugation position (Wong et al., 2011). Studies describing the cellular uptake and metabolism of flavonoids by different cell types are very limited. Nonetheless, some research has examined how the flavonoids quercetin (Q) and (-)-epicatechin (EPI) are metabolised *in vitro*, using primary vascular cells as a model (Rodriguez-Mateos et al., 2014; Tribolo et al., 2013). One previous study demonstrated EPI is taken up and metabolised by HUVECs, resulting in the appearance of distinct metabolites conjugated with methyl and glucuronide groups (Rodriguez-Mateos et al., 2014). These data suggest that human endothelial cells contain enzymes (e.g., UDP-glucuronosyltransferases, sulfotransferases, or catechol O-methyl transferase) potentially capable of metabolising some phenolic compounds, whilst more research is needed to confirm the presence of such enzymes in other cell types. Taken together, flavonoids are bioactive food constituents that undergo extensive metabolism *in vivo*. Once in circulation, these compounds (or their metabolites) may have the potential to modulate cellular function, given their sustained bioavailability, and potential uptake and metabolism by target tissues.

Initial interest in flavonoids as health-promoting entities grew from epidemiological evidence suggesting the total daily consumption of flavonoids was associated with lower risk of cardiovascular disease (Arts et al., 2001; Geleijnse et al., 2002; Hertog et al., 1997; Knekt et al., 2002). For instance, in the Zutphen Elderly Study published in *The Lancet*, a significant inverse correlation between flavonoid intake and coronary heart disease was observed in 805 males aged between 65-84 years (Hertog et al., 1993a). However, other reports have found no such associations between flavonoid intake and lower cardiovascular disease risk (Lin et al., 2007; Rimm et al., 1996; Sesso et al., 2003). In addition, flavonoids were believed to play a causal role in the beneficial effects of the Mediterranean diet upon incidence of coronary heart

Commented [SD55]: Epidemiology

disease (Ferrières, 2004). Building upon these data, a plethora of research has focused on the possible health benefits of flavonoids and flavonoid-rich food, particularly with respect to cardiometabolic health. From these studies, the emerging consensus is that flavonoids are lifespan essential and help protect, at least in part, against the deleterious effects of ageing and disease (Ezzati & Riboli, 2013; Holst & Williamson, 2008). Although our understanding of the health benefits and mechanisms of action of flavonoids has transformed, our knowledge is far from complete.

1.2.13 Evidence for flavonoids purported health benefits on vascular and skeletal muscle health: Reported effects and associated mechanisms

1.2.14 Cocoa-flavanols

Cocoa is derived from seeds of the fruit of the *Theobroma cacao* tree and contains the monomeric cocoa flavanols (CFs) EPI and catechin, and oligomeric procyanidins (Holt et al., 2002). For many years, cocoa has been recognised for its therapeutic value, and some cocoas have been manufactured to be extra rich in flavanols, which may underlie their associated health benefits. It is established that CFs stimulate NO production, resulting in improved vascular endothelial function (Grassi et al., 2012, 2014; Heiss et al., 2005; Karim et al., 2000; Monahan et al., 2011; Phillips et al., 2016). Beyond augmenting NO production, CFs may also regulate oxidative stress and inflammation in the vasculature (Hermann et al., 2006; Monagas et al., 2009). Whilst the precise mechanisms of CFs actions remain to be defined, both acute (single bolus containing >600 mg flavanols) and chronic (12-weeks of daily flavanol supplementation [>900 mg]) CF intake has been demonstrated to augment endothelium-dependent vasodilation, as measured by FMD (Berry et al., 2010; Davison et al., 2008; Heiss et al., 2007). Other studies have reported reductions in diastolic and systolic blood pressure

Commented [DR56]: As indicated previously describe from general to specific. The previous chapter was about epicatechin and now you have another chapter about cocoa flavanols, which is largely again EC.

after CF intake, although this effect has not consistently been reproduced. A meta-analysis of randomised controlled trials reported a significant lowering of systolic blood pressure by 4 mmHg in hypertensive patients after cocoa intake, although normotensive patients did not exhibit a significant reduction (Ried et al., 2017). Furthermore, the blood-pressure lowering effect of CFs was found to be less effective with advancing [age](#) in the same study. EPI, the most commonly found CF monomer, seems primarily responsible for all of the above-mentioned beneficial effects (Schroeter et al., 2006). Indeed, it has been shown that ingestion of pure EPI mimics vascular effects observed after CF consumption (Schroeter et al., 2006), and that EPI, and not catechin, is capable of mediating vasodilatation *in vivo* (Ottaviani et al., 2011).

Commented [TD57]: Observed from that meta-analysis? Please clarify.

The effects of CFs on skeletal muscle adaptation have also been investigated, albeit to a lesser extent. Whilst research is still in its infancy, studies employing long-term CF supplementation regimes have reported enhanced mitochondrial adaptations (Taub et al., 2012, 2016) and attenuated oxidative stress (Ramirez-Sanchez et al., 2013). Taub and colleagues demonstrated that skeletal muscle citrate synthase activity increased 2.5-fold following 3 months CF supplementation in sedentary middle-aged adults (Taub et al., 2016). However, a more recent study, using a 7-day CF supplement regime, reported no impact of supplementation on the expression of mitochondrial-related genes in healthy older male skeletal muscle (Crossland et al., 2019). Taken together, CFs may enhance vascular endothelial function, primarily through effects on NO bioavailability, and may also enhance indices of mitochondrial function in skeletal muscle. [To further investigate the potential therapeutic effects of CFs *in vivo*, Chapter 3 will examine how CFs impact pulmonary \$\dot{V}O_2\$ kinetics and exercise tolerance.](#)

Commented [SD58]: Link to study

1.2.15 Quercetin

Quercetin is a naturally occurring flavonoid, found primarily in onions, apples and other foodstuffs (Wach et al., 2007), with documented health benefits (Arts & Hollman, 2005; Hertog et al., 1993a). Previous studies using quercetin supplementation in rodents or humans to examine muscle and/or vascular function have not always produced positive results. The treatment of rodents with quercetin apparently increased the mRNA and protein levels of markers of mitochondrial biogenesis, through the induction of PGC-1 α (Davis et al., 2009a; Sharma et al., 2015a). Likewise, in untrained humans, the supplementation of this flavanol marginally increased endurance performance, in concert with elevated mRNA expression of citrate synthase, sirtuin-1 (SIRT1) and PGC-1 α (Nieman et al., 2010). Results from studies investigating how quercetin supplementation impacts vascular endothelial function are equivocal. A randomised, placebo-controlled cross-over design trial in 12 healthy males demonstrated quercetin is able to augment indices of NO bioavailability (Loke et al., 2008a). However, 4 weeks quercetin supplementation in apparently healthy adults (40-80 years) had no measurable effect on flow-mediated dilation (Dower et al., 2015). In the same way, quercetin supplementation (50-400mg) had no impact on NO bioavailability or endothelial function of the brachial artery (Bondonno et al., 2016). Clearly, there is no consensus on whether quercetin improves vascular endothelial function in adults, although it may modulate energy metabolism.

Mechanistically, quercetin is thought to act by increasing AMPK activation (Hawley et al., 2010a), which occurs via its phosphorylation at Thr172 and also by increasing SIRT1 gene expression and activation (Howitz et al., 2003). These effects on AMPK activation are thought to occur by decreasing cellular ATP concentrations (and increasing the AMP:ATP ratio) and reducing O₂ consumption (Dorta et al., 2005; Hawley et al., 2010a). Given these data, it is

Commented [DR59]: I would have expected to see first a sum up of effects of flavonoid rich diets (e.g med diet), followed by flavonoid rich products (e.g. onions, grape, cocoa, tea) and finally specific flavonoids, so describing from general to specific

Commented [SD60R59]: I have started with cocoa-flavanols, then gone into individual flavonoids which I study in vitro in the thesis.

I have combined mechanistic literature into each flavonoid sub section, typically following in vivo research. I could keep it like this, or just keep in vivo research for each flavonoid separately, then start another section with each flavonoid separately for in vitro lit review only?

unsurprising quercetin has been shown to augment indices of mitochondrial biogenesis *in vivo*. Besides mitochondrial synthesis, quercetin has been shown to upregulate the targeted degradation of mitochondria by mitophagy. For instance, quercetin enhanced mitophagy through the reversion of Parkin inhibition and increased lysosome biogenesis and mitophagosome formation (Yu et al., 2016). Similar effects were reported in hepatic steatosis in mice, whereby quercetin enhanced LC3-II formation through the PINK1/Parkin pathway (Liu et al., 2018). Given that quercetin has been shown to accumulate within the mitochondria of cells (Fiorani et al., 2010a), and to impact the function of mitochondria in various cell types (Brookes et al., 2002; Fiorani et al., 2010a; Park et al., 2003), further research is necessary to understand how quercetin may regulate mitochondrial function. Chapters 4, 5 and 6 will describe how Q impacts mitochondrial functionality.

1.2.16 EGCG

The main catechins present in green tea are EPI, epigallocatechin (EGC), epicatechin-3-gallate (ECG) and epigallocatechin-3-gallate (EGCG). The most abundant catechin in green tea is EGCG (~59%), followed by EGC (~19%), ECG (~14%) and EPI (~6%) (Cabrera et al., 2006). One of the protective effects of tea consumption on health relates to blood pressure, where a number of studies have reported lowered blood pressure in response to black or green tea consumption in normo- and hyper-tensive patients (Grassi et al., 2015; Nogueira et al., 2017; Wasilewski et al., 2016). Tea consumption is also linked with enhanced vascular endothelial function (Ras et al., 2011), as measured by improved flow-mediated dilation. For instance, a randomised controlled trial conducted with 14 healthy participants reported that the intake of green tea polyphenol-enriched ice cream could immediately enhance vascular function and reduce oxidative stress (Sanguigni et al., 2017). Whilst it is unclear what exact constituents of green tea are responsible for the reported improvements in cardiovascular health, EGCG was

Commented [TD61]: After this summary of various flavonoids, I could do with a summary figure or table. Simply list them and indicate key aspects or differences between them. This would be really helpful

Commented [SD62R61]: See the example graphic at end of section – this is template ill perhaps use. Can continue in this style. I was unsure if using graphic like below, whether to include only effects known in muscle and endothelial cells, or effects in other cells too...

Commented [SD63]: linker

considered a major candidate. However, a randomised controlled trial involving 50 healthy men compared the endothelial protective effects of EGCG in three formulas, including a green tea beverage, green tea extract, and pure EGCG, and found that only the green tea beverage could improve flow-mediated dilation (Lorenz et al., 2017). In light of this, there is no clear consensus on whether EGCG has a major role in regulating endothelial function.

Data describing EGCG (or green tea) supplementation and skeletal muscle mitochondrial function are limited. Murase and colleagues observed that green tea extract supplementation led to increased activation of PGC-1 α mRNA in skeletal muscle, which coincided with increases in treadmill running time in mice (Murase et al., 2006). One study administered EGCG (282 mg/day⁻¹) over 3 days to overweight adults and observed a significant reduction in blood lactate concentrations of skeletal muscle using microdialysis, suggesting a potential shift towards oxidative metabolism (Most et al., 2015a). In the skeletal muscle of diabetic rats, the oral gavage of 100 mg EGCG/kg⁻¹/day⁻¹ for 3 months significantly reduced the expression levels of beclin1 and DRP1 (Yan et al., 2012), suggesting that EGCG regulates mitochondrial-involved autophagy. Here, chapters 5 and 6 will help to describe the effects of EGCG on mitochondrial function in skeletal muscle cells.

Commented [SD64]: Link to study

Several studies have sought to determine the mechanisms by which EGCG may impact endothelial function and muscle metabolism. Numerous reports have shown EGCG induces endothelial vasodilation, effects that are mediated in part by eNOS (Appeldoorn et al., 2009; Lorenz et al., 2004a, 2015; Ng et al., 2017; Romano & Lograno, 2009). Interestingly, these vasodilatory effects are hypothesised to partly depend on the activation of PI3-kinase and Akt pathways. In neuronal cells, EGCG was reported to interact with the mitochondria, where 90–95% of administered ³H-EGCG was found accumulated in the mitochondrial fraction,

suggesting that it may act as a free radical scavenger at the mitochondrial level (Schroeder et al., 2009). This proposition was supported by a study using murine skeletal muscle cells, where it was shown EGCG treatment repressed mitochondrial biogenesis, via reductions in PGC-1 α and AMPK activation, an effect attributed to reductions in cellular ROS (Wang et al., 2016). Further support for EGCG interacting with mitochondria came from a study examining EGCG and mitochondrial bioenergetics. In this study, EGCG inhibited mitochondrial oxidative phosphorylation, thereby decreasing ATP levels (Valenti et al., 2013). Similarly, increased AMPK activation was documented after EGCG treatment in cultured adipocytes (Hwang et al., 2005). When taken together, it is clear that EGCG can modulate endothelial function and muscle metabolism, which may be achieved through its actions on eNOS and AMPK activity. Chapters 4, 5 and 6 will help clarify the effects of EGCG on vascular endothelial and muscle cell energy metabolism.

Commented [SD65]: linker

1.2.17 (-)-Epicatechin (EPI)

The monomer EPI is particularly abundant in dark chocolate and cocoa products (Katz et al., 2011). As outlined above, EPI is reportedly responsible for the vasodilatory effects of CFs *in vivo*. Accordingly, EPI administration enhances FMD and leads to reductions in blood pressure (Fraga et al., 2011; Galleano et al., 2013; Karim et al., 2000; Schewe et al., 2008; Schroeter et al., 2006), effects attributable to the modulation of NO bioavailability. The augmentation of NO bioavailability after EPI supplementation is thought to occur primarily via increased activation and expression of eNOS (Ramirez-Sanchez et al., 2011, 2018). Support for this proposal comes from studies employing cell culture and rodent models, whereby EPI activates eNOS via increased phosphorylation at Ser-616, Ser-633 and Ser-1177 (Gómez-Guzmán et al., 2011, 2012; Ramirez-Sanchez et al., 2010). Additionally, EPI may also contribute to NO

production through its capacity to inhibit arginase, the arginine-degrading enzyme. By doing so, EPI may increase L-arginine bioavailability for NO synthesis (Schnorr et al., 2008).

Beyond regulating NO bioavailability, several lines of evidence suggest that EPI may impact mitochondrial function. Evidence for the modulation of mitochondria by EPI is unequivocal. In C₂C₁₂ muscle cells, EPI treatment produced negligible effects upon mitochondrial respiration (Bitner et al., 2018). Other studies in which isolated mitochondria or submitochondrial particles were exposed to EPI showed that different parameters of mitochondrial function and oxidant production, e.g. O₂ consumption, NADH oxidation, mitochondria membrane potential, and in few cases, H₂O₂ production, were only marginally affected (Dorta et al., 2005; Kopustinskiene et al., 2015a; Lagoa et al., 2011; Moini et al., 1999). In rodents and humans, EPI has been reported to induce adaptations typically associated with exercise, such as increased mitochondrial signalling, superior mitochondrial protein content and enzyme activity, and elevated fatigue resistance (Lee et al., 2015; Moreno-Ulloa et al., 2013; Nogueira et al., 2011; Ramirez-Sanchez et al., 2018; Taub et al., 2012). Although, one recent study reported blunted cycling-induced aerobic adaptations after 4 weeks EPI supplementation (Schwarz et al., 2018). To date, there is limited data available on the impact of EPI on mitochondrial bioenergetics in aged skeletal muscle and vascular endothelial cells; topics that will be addressed in Chapters 4, 5 and 6 of this thesis.

Commented [SD66]: Linker

Research attempting to dissect EPI effects on mitochondria function have highlighted its potential to regulate cell signalling responses. In 2014, Moreno-Ulloa and colleagues suggested EPI effects are mediated by a plasma membrane receptor, having demonstrated similar responses between cells treated with EPI alone, and EPI bound to dextran (preventing EPI cell

internalisation) in endothelial cells (Moreno-Ulloa et al., 2014). Further research from the group indeed highlighted a role for the G-protein-coupled estrogen receptor (GPER) as a target for EPI through a series of experiments using GPER agonists, selective blockers, and siRNA in endothelial (Moreno-Ulloa et al., 2015a), and murine skeletal muscle cells (Moreno-Ulloa et al., 2018). At least in endothelial cells, the authors highlighted EPI modulated its effects via the GPER in an extracellular signal-regulated protein kinase 1 and 2 (ERK1/2)- and CaMKII-dependent manner, although the precise mechanisms are yet to be fully elucidated in skeletal muscle cells. From current knowledge, it is thought EPI may evoke mitochondrial adaptations via an AMPK dependent signalling cascade in skeletal muscle (Murase et al., 2009; Si et al., 2011). However, further work is required to completely describe EPI's mechanism of action on the AMPK pathway, which will be addressed in Chapter 4 and 6.

Commented [SD67]: Link to thesis

1.2.18 Section Summary

Dietary flavonoids are bioactive compounds with the potential to regulate processes related to energy metabolism (see Figure 1.13). Currently, our knowledge of the mechanisms regulating the effects of flavonoids on vascular endothelial and skeletal muscle cells is limited. In spite of our incomplete understanding, it is emerging that flavonoids may impact indices of mitochondrial function, highlighting their potential therapeutic value in the context of sedentary ageing. Following this hypothesis, there is a need to examine the efficacy of flavonoid-based interventions in speeding $\dot{V}O_2$ kinetics and improving exercise tolerance *in vivo*, whilst simultaneously resolving their mechanisms of action, *in vitro*.

Commented [TD68]: For all these flavonoids, you directly dive into detail. It would be helpful to give some overview of studies that (epidemiologically) link flavonoids to beneficial health outcomes. Good to start this section with.

Individual sections are good (but linking them together is missing a bit).

Commented [SD69R68]: I have done this in paragraph 4 above Quercetin paragraph, is the epidemiology not done in enough detail here? If not I can expand more

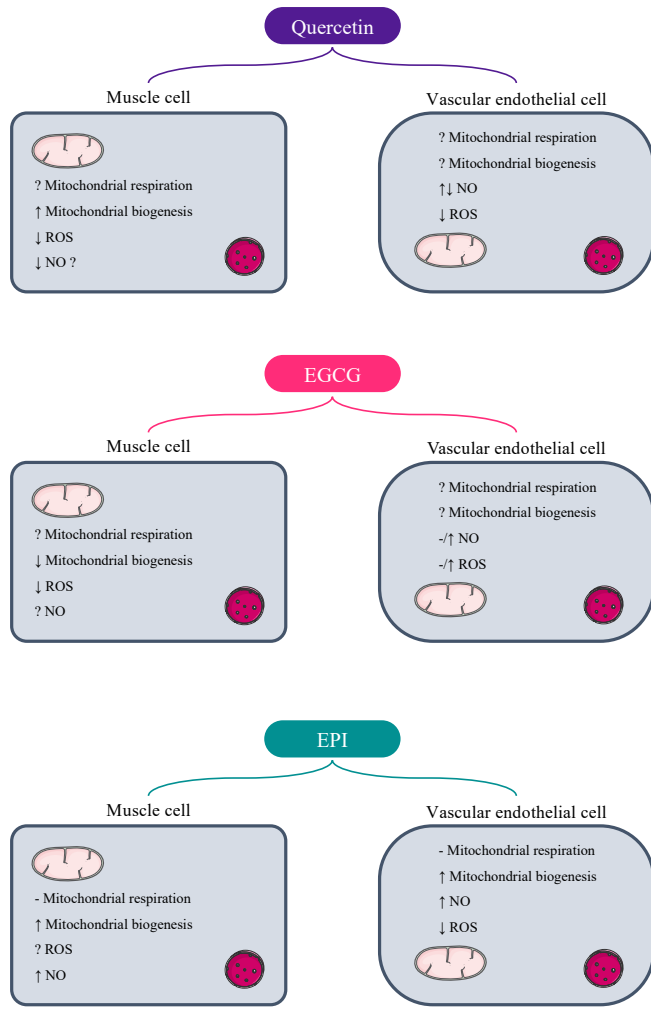


Figure 1. 13 Schematic overview of the known effects of dietary flavonoids on skeletal muscle and vascular endothelial cells, as they relate to mitochondrial function and RONS production.

1.3 Thesis Perspective

To summarise, the dynamic change in $\dot{V}O_2$ across a metabolic transient is highly coordinated, with major sites of regulation present both upstream of, and proximal to, the site of O_2 utilisation within the mitochondrion. Unfortunately, advancing age and physical inactivity compromise the capacity for O_2 transport and utilisation, partly due to impairments in mitochondrial function, which manifests as slower $\dot{V}O_2$ kinetics and impaired exercise tolerance. In light of this, there is a need for targeted interventions that mitigate these impairments and help maintain one's functional capacity into later life. Increasing evidence suggests a potential role for dietary flavonoids as compounds with therapeutic potential. The potential use of flavonoids to combat the deleterious effects of ageing and physical inactivity on O_2 delivery and consumption requires an in-depth understanding of their mechanisms of action, and appropriate randomised controlled trials to determine their effectiveness and translational potential to daily life.

1.4 Thesis Aims & Objectives

The central aim of this thesis is to use dietary flavonoid supplementation to speed $\dot{V}O_2$ kinetics and enhance exercise tolerance *in vivo*, and to enhance vascular endothelial and/or skeletal muscle energy metabolism, *in vitro*. To realise this aim, the following objectives will be addressed:

1. Investigate the impact of cocoa-flavanol supplementation on pulmonary $\dot{V}O_2$ kinetics and exercise tolerance in sedentary middle-aged adults (Chapter 3).

Commented [DR70]: Research is by definition uncertain so I won't say that the aim is to speed or enhance...the aim is to study whether/demonstrate that dietary flavonoids speed/enhance...

Commented [HJ71]: Is this the same wording in the abstract?

Commented [TD72]: Objectives are fairly broad... compensate with clear and sharp hypothesis...?

Commented [HJ73]: Include study specific aims and hypothesis and then use objective to show how going to do the study

Commented [HJ74]: These aims an hyptheiss are more conventional to what you have in the introduction to lit review. I suggest removing the aims from intro to lit review as the working is inconsistent with what you have here

2. Examine whether flavonoids regulate ROS production, NO bioavailability, mitochondrial function and signalling of endothelial cells, using human vascular endothelial cells as a model system (Chapter 4).
3. Determine the effects of replicative ageing and flavonoids on mitochondrial function, NO bioavailability and gene expression using C₂C₁₂ myoblasts as a model system (Chapter 5).
4. Investigate how replicative ageing and flavonoids impact mitochondrial function, ROS production and cell signalling using C₂C₁₂ myotubes as a model system (Chapter 6).
5. Explore how replicative ageing and dietary flavonoids impact the metabolome of C₂C₁₂ skeletal myoblasts and myotubes (Chapter 7).

The following hypotheses were tested:

1. Cocoa-flavanols will speed phase II $\dot{V}O_2$ kinetics during moderate and severe-intensity exercise and enhance exercise tolerance in physically inactive middle-aged adults.
2. Dietary flavonoids will attenuate ROS emission, increase NO production and enhance indices of mitochondrial function and cell signalling in vascular endothelial cells.
3. Replicative ageing will impair indices of mitochondrial function, lower NO bioavailability and blunt gene expression in C₂C₁₂ myoblasts, but these effects will be rescued by flavonoid treatment.
4. Dietary flavonoids will mitigate age-related impairments to mitochondrial function, and attenuate ROS production and enhance cell signalling in aged C₂C₁₂ myotubes.

Commented [DR75]: clear

Chapter 2: Materials and Methods

Commented [TD76]: only scanned this chapter (seen this before and little to add to this).

2.1 Cell culture

All cell culture procedures were undertaken in a Class II Microbiological Safety Cabinet (BSC; Kojair, Mänttä-Vilppula, Finland) under aseptic conditions. All cells were sub-cultured and incubated in a HERAcell 150i CO₂ humidified incubator (Thermo Fisher Scientific, Cheshire, UK) at 37°C and 5% CO₂ and were routinely monitored using an inverted light microscope (Olympus, CKX31, Japan). An extraction pump (Charles Austen Pumps Ltd, Surrey, UK) was used to remove waste media and supernatant.

2.2 Cell culture reagents

Dulbecco's modified Eagle's medium (DMEM) was purchased from Gibco (Life Technologies, California, US) and was used for murine C₂C₁₂ cells. All serum was purchased from Gibco (Life Technologies, California, US) and included: heat-inactivated horse serum (HS), heat-inactivated newborn calf serum (hiNCS) and heat-inactivated fetal bovine serum (hiFBS). The antibiotics penicillin and streptomycin (PS) were added to all media (1%: 50 U/mL penicillin and 50 µg/mL streptomycin). To wash the cells, phosphate buffered saline (PBS) or Dulbecco's phosphate-buffered saline (D-PBS; PBS without calcium and magnesium) was used. The PBS/D-PBS was purchased from Sigma-Aldrich (Poole, UK) in tablet or powder form, respectively. The tablet/powder was reconstituted to a working concentration of 10 mM phosphate buffer, 3 mM KCl and 140 mM NaCl at a pH of 7.4 in dH₂O. For cell adherence, gelatin type A from porcine skin was used (Sigma-Aldrich, Poole, UK) and reconstituted to create a working stock of 0.2% gelatin. The trypsin was composed of 0.05% trypsin and 0.02% ethylenediaminetetraacetic acid (EDTA) and purchased from Sigma-Aldrich (Poole, UK).

For murine C₂C₁₂ cells, growth media (GM) comprised: DMEM, 10% hiFBS, 10% hiNCS, 1% PS and 2 mM L-Glutamine (LG). Differentiation media (DM) included: DMEM, 2% HS,

Commented [SD77]: Add glucose conc?

1% PS and 2 mM LG. GM was used to promote cell proliferation and DM was used to induce cell differentiation. Complete Endothelial Cell Growth Medium (EGM; Cell Applications Inc, San Diego, USA) was used to sub-culture primary human umbilical vein endothelial cells (HUVEC) and contained 1 g/L glucose, 2% FBS and 1.461 g/L LG.

The flavonoids used throughout this thesis for *in vitro* experiments included quercetin (Q), epigallocatechin-gallate (EGCG) and (-)-epicatechin (EPI). All compounds were purchased in powder form from Sigma-Aldrich (Poole, UK). All supplements were reconstituted as 10 mM stocks in deionised H₂O or dimethyl sulfoxide (DMSO) and stored at -20°C. Compounds were diluted in appropriate medium for experimental procedures, and relevant compound vehicle concentrations were used in control conditions where appropriate. The final concentration of DMSO in experimental chapters did not exceed 0.1%. The specific concentrations of flavonoids used will be outlined in the methods section of each experimental chapter.

Commented [CS78]: This bit can probably stay here, as these are more generic compounds.

2.3 C₂C₁₂ skeletal muscle cells

Murine C₂C₁₂ skeletal muscle myoblasts were sourced from the American Tissue Culture Collection (ATCC; Rockville, USA), were passaged to increase cell yield and were stored in liquid nitrogen (LN₂) until required for experimentation. C₂C₁₂ cells are the C₁₂ sub-clone of the C₂ parental cell line, originally derived from the crush injured leg of the C3H mouse (Blau et al., 1985; Yaffe & Saxel, 1977). The C₁₂ sub-clone was selected for their differentiation capability, hence the extensive use of this cell line for *in vitro* research.

2.3.1 Passaging C₂C₁₂ cells

C₂C₁₂ cells were sub-cultured in T25 or T75 flasks (Nunc™, Thermo Fisher Scientific, Waltham, MA, USA) containing GM composed of high glucose Dulbecco's modified Eagle's

medium (DMEM, Lonza, UK), 10% hiFBS, 10% hiNBCS, 2 mM LG, 100 U/mL penicillin and 100 µg/mL streptomycin until 80% confluency was attained (see Figure 2.1). Here, existing GM was removed, and cells underwent 2 × PBS washes. Either 500 µL (for T25 flasks) or 1 mL (for T75 flasks) trypsin was added to the culture flask(s) and incubated for 5 minutes (37°C, 5% CO₂) in order to dissociate cells from the culture flask surface. Following detachment of cells, 2.5 mL (for T25 flasks) or 4 mL (for T75 flasks) GM was added to neutralise trypsin activity, and the cells were subsequently counted (see section 2.5).

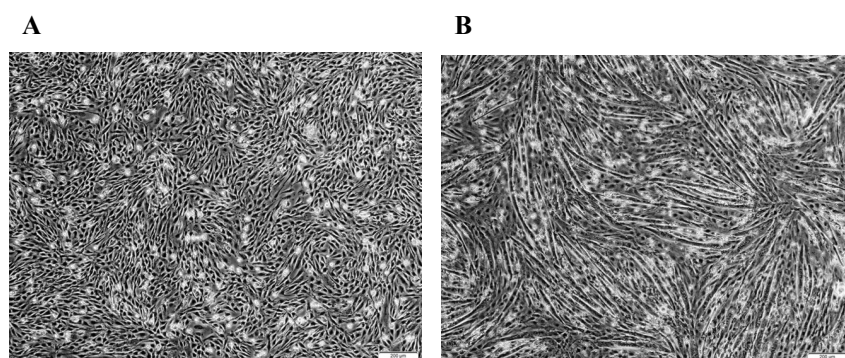


Figure 2. 1 Murine C₂C₁₂ myoblasts in culture. A) Skeletal myoblasts. B) Late differentiating skeletal myotubes (96 hours). Images taken at 10x magnification (Olympus, CKX31).

2.3.2 Replicatively aged C₂C₁₂ myoblasts

Given a global drive to reduce animal research, relevant cell models are required to inform relevant *in vivo* studies. To this end, we have developed a myoblast model, with an application to ageing muscle cell behaviour (Sharples et al., 2011a). C₂C₁₂ myoblasts underwent multiple population doublings (130-150) to passages 46-50 by repeatedly passaging cells (Sharples et al., 2011a). This model is used throughout the thesis and these cells are referred to as ‘replicatively aged’.

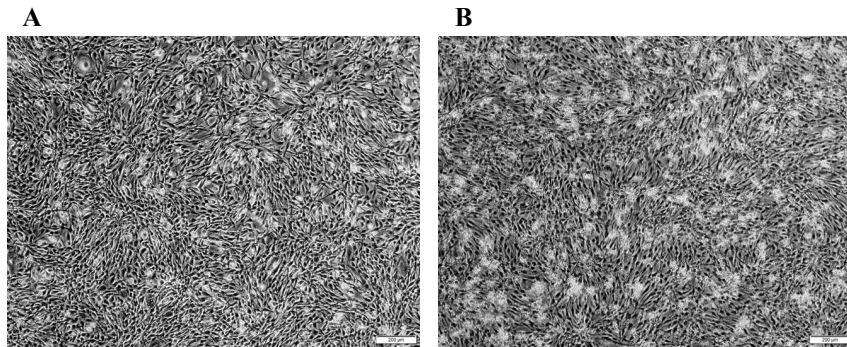


Figure 2. 2 Replicatively aged murine C₂C₁₂ myoblasts in culture. A) Aged skeletal myoblasts (24 hours) B) Late differentiating aged skeletal myotubes (96 hours). Images taken at 10x magnification (Olympus, CKX31).

2.4 Primary Human Umbilical Vein Endothelial Cells

HUVECs were purchased from Thermo Fisher Scientific, (Waltham, MA, USA), passaged to increase cell yield and were stored in LN₂ until required for experimentation. Cells were not passaged more than 8 times because changes in HUVEC phenotype can occur with multiple population doublings, that ultimately lead to cell senescence (Chang et al., 2005; Cheung, 2007; Grillari et al., 2000).

Commented [CS79]: I would move this to follow the passaging of the C2C12 cells, otherwise this is a bit disjointed – so move this paragraph down to come before the passaging of HUVECs

2.4.1 Passaging HUVEC

HUVECs were sub-cultured in T25 or T75 flasks (Nunc, Thermo Fisher Scientific, Waltham, MA, USA) containing complete endothelial cell growth medium (EGM; Cell Applications Inc, San Diego, CA, USA). Cells were grown to 70-80% confluency (see Figure 2.3), which was typically attained after 96 hours. Existing EGM was then removed, and cells underwent 2 × D-PBS (PBS without calcium and magnesium) washes. Either 500 μL (for T25 flasks) or 1 mL

Commented [CS80]: Move HUVEC info from above to precede this section

(for T75 flasks) trypsin was added to the culture flask(s) and incubated for 2-3 minutes (37°C, 5% CO₂) in order to dissociate cells from the culture flask surface. Following detachment of cells, 2.5 mL (for T25 flasks) or 4 mL (for T75 flasks) of EGM was added to neutralise trypsin activity. The cell suspension was transferred to a 15 mL flacon tube and centrifuged at 220 × g for 5 min at 20°C to obtain a cell pellet. The supernatant was discarded, and the cell pellet was resuspended in either 1 mL (T25 flasks) or 2 mL (T75 flasks) EGM ready for counting (see section 2.5).

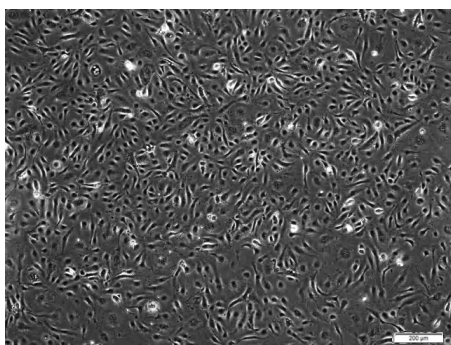


Figure 2. 3 Primary human umbilical vein endothelial cells (HUVEC) in monolayer. Typical cobblestone morphology. Image taken at 10x magnification (Olympus, CKX31).

2.5 Cell counting

After trypsinising cells, the suspension was dissociated 8 × using a 19G hypodermic needle (Becton Dickinson, USA). Cells were manually counted on a Neubauer haemocytometer (BLAUBRAND® Neubauer, Sigma-Aldrich, Poole, UK) using the trypan blue exclusion method, whereby 20 µL of cell suspension was mixed with 20 µL 0.4% trypan blue stain (Sigma-Aldrich, Poole, UK) in a 1:1 ratio. The mixture was pipetted onto either end of the haemocytometer, flooding both chambers via capillary action. Cells present within each quadrant were counted. Small, round and clearly visible cells were considered viable whereas

larger, darker/blue stained cells were considered non-viable cells or debris and were therefore excluded from cell counts. To determine the concentration of cells/mL present within the cell suspension, the mean number of cells in 8 × grids was calculated (average cell numbers per 0.1 mm³ grid) which was multiplied by 2 (to account for the trypan blue dilution factor) and 10⁴ (to convert the number of cells in 0.1 mm³ to 1 cm³). The total number of cells present within the cell suspension was calculated by simply multiplying the cells/mL by the cell suspension volume in mL (see Equation 2.1).

A

$$\text{Cells/mL} = \text{Average cell count of 8 grids} \times \text{dilution factor (2)} \times 10^4;$$

$$\text{Total number of cells} = \text{Cells/mL} \times \text{cell suspension volume (mL)}$$

B

$$\text{Cell suspension required (mL)} = \frac{\text{Desired cell concentration (cells/mL)}}{\text{current cell concentration (cells/ mL)}} \times \text{required cell suspension volume (mL)}$$

Equation 2. 1 Cell counting equations.

A) Equation used to calculate cell concentrations (cells/mL). B) Equation used to determine the cell suspension volume for the desired cell seeding concentration.

2.6 Cell cryopreservation and resuscitation

Once counted (see section 2.5), GM and EGM was added to existing cell suspension to ensure a concentration of 1×10^6 cells/mL or 5×10^5 cells/mL for C₂C₁₂ and HUVEC cells, respectively. Dimethyl sulfoxide (DMSO; Sigma-Aldrich, Poole, UK), a cryoprotectant that

prevents ice crystal formation, was added at 10% of the total cell suspension volume (Lovelock & Bishop, 1959) before distributing the cell suspension into labelled (name, cell type, passage number, concentration and date) 2 mL cryovials (Simport Scientific, Fisher Scientific, UK). The cryovials were transferred to a cryopreservation container ('Mr Frosty', Thermo Fisher Scientific, Waltham, MA, USA) containing isopropanol (Sigma-Aldrich, Poole, UK) which was placed in a -80°C freezer for 24 h to ensure a gradual freezing rate (-1°C/min⁻¹) before storing individual cryovials in liquid nitrogen (LN₂). When resuscitating cells, a cryovial was removed from LN₂, mist sprayed with 70% ethanol and placed in a BSC incubator to thaw at RT. Cell suspension was then pipetted onto a pre-gelatinised T75 flask(s) (5 mL of 0.2% gelatin (Sigma-Aldrich, Poole, UK) per T75, incubated at RT for 20 mins) containing 15 mL of preheated (37°C) GM and incubated at 37°C, 5% CO₂ to allow cell attachment and proliferation over the ensuing day(s). The time to reach ~80% confluency for 1 × 10⁶ C₂C₁₂ and 1 × 10⁶ HUVEC cells was approximately 72 and 96 h, respectively.

2.7 Cell viability

The fluorescent CyQUANT[®] Proliferation Assay kit (ThermoFisher, Waltham, MA, USA) was used to determine cell viability. Firstly, an experiment was performed to establish a cell number standard curve to enable the conversion of sample fluorescence values into cell numbers. This was completed for C₂C₁₂ myoblasts and HUVECs separately (see Figure 2.4A/B). For subsequent experiments, cells were treated for 24 h with specific doses of Q, EGCG and EPI (0, 0.5, 1.0, 5.0 10.0 and 20.0 μM). Wells were washed twice with PBS, aspirated, and the plate was frozen immediately at -80°C. On the day of the experiment, plates were thawed at room temperature, and 100 μL of CyQUANT[®] GR dye/cell-lysis buffer was added to each sample well. Plates were gently mixed on an orbital shaker for 5 minutes protected from light. Sample fluorescence was measured using a CLARIOStar plate reader (BMG Labtech, Bucks, Great

Commented [CS81]: Details of company – I wont write this again, but please update methods accordingly

Britain) with Excitation 485-12 and Emission EM520 filters in bottom reading, well scanning mode.

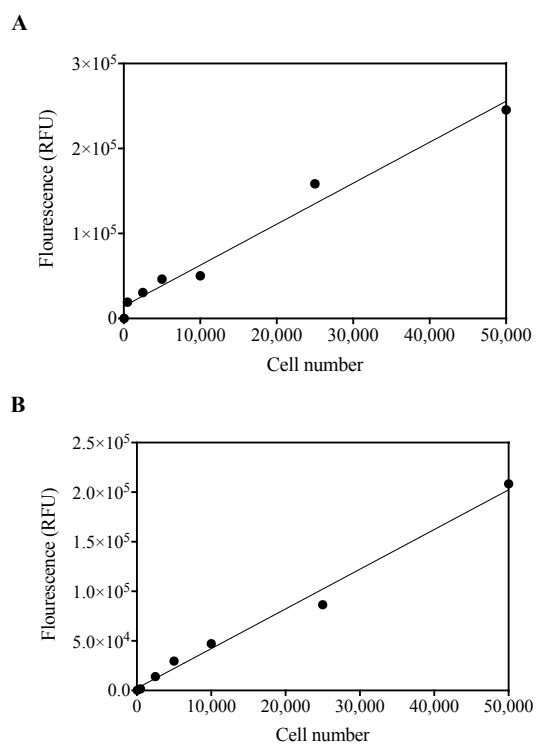


Figure 2. 4 Standard curve generated for C₂C₁₂ myoblasts and HUVECs using CyQUANT® Cell Proliferation Assay. Cells were seeded at densities of 0-50,000 cells per well and grown in GM for 24 h. C₂C₁₂ myoblasts were then switched to DM for a further 24 h before freezing and subsequent processing on the day of assay. HUVECs remained in GM for an additional 24 h before freezing and processing. Data are representative of one experiment performed with 5 replicates for each cell number.

Commented [CS82]: N=? replicates?

Commented [CS83]: This will become method text if you amend according to comment above.

2.8 Mitochondrial ROS production (MitoSOX assay)

Mitochondrial derived superoxide was detected in adherent skeletal muscle and vascular endothelial cells using MitoSOX, a hydroethidine probe which is targeted to the mitochondria by a conjugated triphenyl-phosphonium moiety. In the presence of mitochondrial superoxide, and to some extent hydrogen peroxide (Robinson et al., 2006; Zielonka & Kalyanaraman, 2010), MitoSOX is oxidised to fluorescent products which are readily detected fluorometrically. C₂C₁₂ myoblasts and HUVECs were seeded at 3×10^4 cells/mL into 12-well microplates until ~80% confluence. Next, C₂C₁₂ myoblasts were switched to DM for 96 h. Subsequently, skeletal myotubes or HUVECs were washed into pre-warmed Krebs-Ringer buffer (KRH) comprising: 135 mM NaCl, 3.6 mM KCl, 10 mM HEPES (pH 7.4), 0.5 mM MgCl₂, 1.5 mM CaCl₂, 0.5 mM NaH₂PO₄, 2 mM glutamine and 25/5.5 mM D(+)-glucose; with or without 15 μM antimycin A (AA), and incubated at 37°C for 30 minutes. After incubation, AA-containing KRH was removed, and MitoSOX was loaded into cells in fresh pre-warmed KRH to a final concentration of 2.5 μM. Plates were immediately transferred to a plate reader (BMG Labtech, Bucks, Great Britain), and fluorescence was monitored continuously at ~30-sec intervals over 30 min. Fluorescent MitoSOX oxidation products were excited at 510 nm and light emission was detected at 580 nm. The plate reader's focal height and gain was optimised and fixed between different experiments. Since MitoSOX is primarily oxidised by mitochondrial superoxide, the rate at which mitochondrial superoxide was produced could be determined from the slope of the resultant progress curve over the 30-minute period post MitoSOX loading (See Figure 2.5). Upon completion of the 30-min reading, plates were immediately fixed for the determination of cell density by the SRB assay (see section 2.14), which was used to normalise obtained fluorescence values.

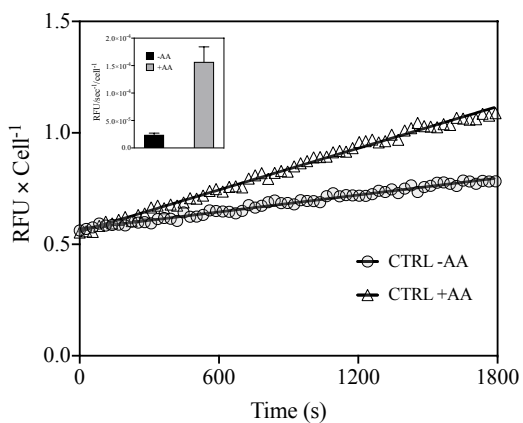


Figure 2. 5 Mitochondrial superoxide production was estimated from rates of MitoSOX oxidation, in the absence and presence of 15 μM antimycin A. Fluorescence was recorded at ~ 30 -second intervals for 30 minutes. Probe oxidation rates were calculated from the slopes of the progress curves. Relative fluorescence units (RFU) were normalised to cell number.

2.9 CellROX Assay

Cellular ROS were detected using the CellROX[®] Deep Red reagent by spectrophotometry. The cell-permeant dye is non-fluorescent while in a reduced state and exhibits bright fluorescence upon oxidation by ROS. C₂C₁₂ myoblasts and HUVECs were seeded at 3×10^4 cells/mL into 12-well microplates until $\sim 80\%$ confluence. Next, C₂C₁₂ myoblasts were switched to DM for 96 h. Both skeletal myotubes and HUVECs were then treated for 24 h with 0, 5 and 10 μM Q, EGCG or EPI. After treatment, myotubes and HUVECs were washed into KRH with or without 15 μM antimycin A (AA) and incubated at 37°C for 30 minutes. Next, KRH was removed, and CellROX was loaded into cells in fresh, pre-warmed KRH buffer, to a final concentration of 2.5 μM . Following 30 minutes incubation with the reagent, cells were washed 2 \times with PBS and immediately transferred to a plate reader (BMG Labtech, Bucks, Great Britain), where

fluorescent CellROX oxidation products were excited at 640 nm and light emission detected at 665 nm. The plate reader's focal height and gain was optimised and fixed between experiments. Upon completion of the reading, plates were immediately fixed for the determination of cell density by the SRB assay (see section 2.14), which was used to normalise obtained fluorescence values.

2.10 Assessing mitochondrial bioenergetics

The single most valuable general test of mitochondrial (dys)function in cell populations is the measurement of cell respiratory control (Brand & Nicholls, 2011). Until recently, the analysis of mitochondrial respiration had predominantly relied upon the classical oxygen electrode (Chance & Williams, 1955). Whilst the use of this system over the past 50 years has advanced understanding of mitochondrial respiratory function, the oxygen electrode has notable limitations with regard to signal stability, instrumental background noise, resolution, and throughput (Gnaiger, 2008). Addressing these limitations, the Seahorse XF Analyzer, first introduced during 2006/2007 (M. Wu et al., 2007), enabled a high-throughput system for the determination of mitochondrial (dys)function in adherent cells. The basic principle of the system is to measure the rate of mitochondrial oxidative phosphorylation (through determination of the oxygen consumption rate [OCR] measured in picomoles/minute) and glycolysis (through determination of the extracellular acidification rate measured in milli-pH units/minute; (Ferrick et al., 2008). These measurements are obtained through fluorescent sensors contained within a bio-cartridge that fits over a cell culture microplate. Pharmaceutical reagents or mitochondrial respiratory electron transport system inhibitors are distributed in ports surrounding the sensor, which can be sequentially injected to each well to interrogate components of mitochondrial function.

Commented [CS84]: Will data from these methods be in more than one data chapter e.g. will the HUVECs be in a separate chapter from the C2C12s or will blasts and tubes be separate etc etc? I only ask, because if all seahorse data are in 1 chapter, then all of this methodology should be in that chapter. However, if methods across more than one chapter, then keep it here.

2.10.1 Mitochondrial stress test protocol

Mitochondrial respiration was measured in adherent C₂C₁₂ myoblasts and myotubes, and in HUVECs using Seahorse XFe96 and XFe24 Analyzers, respectively (Agilent Technologies, Santa Clara, CA, USA). C₂C₁₂ myoblasts (passages 9-11 [control] and 47-50 [aged]) were seeded in XFe96 well plates at 5,000 or 10,000 cells per well in 100 µL of GM for 24 h to allow cell attachment. Whereas HUVECs (passages 4-6) were seeded at 30,000 cells per well in 200 uL and grown in EGM for 24 h. After 24 h, control and aged C₂C₁₂ myoblasts were washed twice with PBS and transferred to DM. For myoblast experiments, cells were dosed with specific concentrations (0, 1, 5 and 10 µM) of Q, EGCG and EPI in DM for 24 hours. In a separate experiment, myotubes were allowed to form over 96 h in DM, before being dosed with Q, EGCG and EPI (0, 1, 5 and 10 µM) in DM for a further 24 hours. After 24 h, HUVEC were washed twice with D-PBS and replaced with fresh EGM containing specific concentrations (0, 5 and 10 µM) of Q, EGCG and EPI for 24 hours. Sensor cartridges for the XFe96 and XFe24 Analyzer were hydrated by loading each well with deionised water and XF Calibrant (Agilent Technologies, Santa Clara, CA, USA) at 37°C in a non-CO₂ incubator in the 24 h preceding the assay, respectively.

On the day of the assay, C₂C₁₂ myoblasts and myotubes were washed into 200 µL pre-warmed modified KRH at pH 7.4. See Table 2.1 for composition of KRH. The cells were incubated in this buffer for 45 minutes at 37°C in a non-CO₂ incubator and then transferred to a Seahorse XFe96 extracellular flux analyser (maintained at 37°C). Similarly, on the day of the assay, HUVECs were washed into 500 µL pre-warmed unbuffered Seahorse DMEM (Agilent Technologies, Santa Clara, CA, USA) at pH 7.4. The cells were incubated in this buffer for 45 minutes at 37°C in a non-CO₂ incubator and then transferred to a Seahorse XFe24 extracellular flux analyser (maintained at 37°C).

Commented [CS85]: I have defined above – just check it is correct, please.

Commented [CS86]: Why spelling out here? I think you did this earlier in the text – if not, please do so on first mention of these products

Table 2. 1 Modified KRH Buffer Composition

Chemical	Final Concentration
NaCl	135 mM
KCl	3.6 mM
HEPES	10 mM
MgCl ₂	0.5 mM
CaCl ₂	1.5 mM
NaH ₂ PO ₄	0.5 mM
GlutaMAX	2 mM
BSA	0.1%

Following a 10-minute calibration step, OCRs were measured by 3-4 loop cycles, each consisting of a 1-min mix, 2-min incubate and 3-min measure to record cellular basal respiration (see Figure 2.6). After measuring basal respiration, 2 μ M OLI was added to selectively inhibit the mitochondrial ATP synthase. Subsequently, 2 μ M 2-[2-[4-(trifluoromethoxy)phenyl]hydrazinylidene]-propanedinitrile (FCCP) or 3 μ M N5,N6-bis(2-Fluorophenyl)[1,2,5]oxadiazolo[3,4-b]pyrazine-5,6-diamine (BAM15), followed by a mixture of 2 μ M rotenone and 2 μ M antimycin A were added sequentially to, 1) uncouple oxygen consumption rates to ATP synthesis rates to determine maximal respiration or 2) inhibit complex I and III of the electron transport chain to determine non-mitochondrial respiration (see Figure 2.6). Rates of oxygen consumption and proton production (PPR) were expressed relative to the DNA content or cell number of the appropriate well. Three independent experiments were performed to assess mitochondrial respiration.

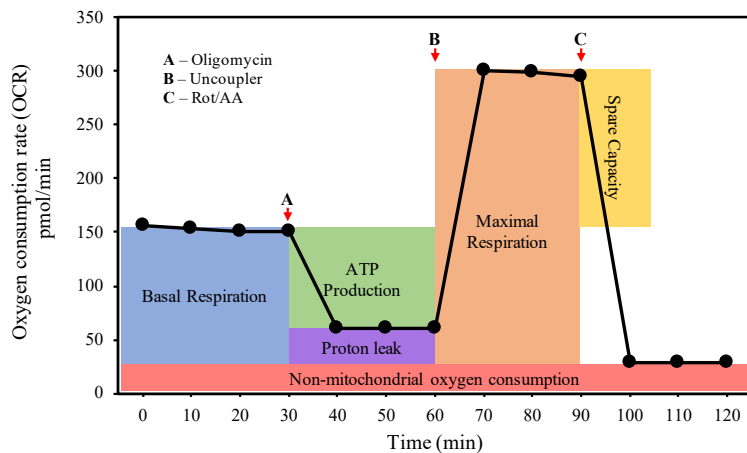


Figure 2. 6 Typical mitochondrial stress test profile. Rates of oxygen consumption expressed in pmol/min and recorded over 120 minutes. Sequential additions of oligomycin, uncoupler (e.g., FCCP or BAM15), and mixture of rotenone and antimycin A were performed in order to interrogate mitochondrial function.

2.10.2 Bioenergetic parameters analysis

Using the Wave Desktop 2.6.1 software (Agilent Technologies, Santa Clara, CA, USA) and in accordance with previously described methods, seven parameters of mitochondrial respiration, basal OCR, ATP-linked OCR, OCR due to proton leak, maximal OCR, spare respiratory capacity, non-mitochondrial OCR, and PPR were calculated from the bioenergetic profiles obtained from the XFe96 and XFe24 extracellular flux analyser (see Table 2.2). Briefly, basal OCR refers to the total baseline cellular respiration rate and includes respiration due to ATP production, proton leak (leak of protons across the inner mitochondrial membrane) and oxygen consumption due to nonmitochondrial processes. ATP-linked oxygen consumption is determined through the addition of the ATP synthase inhibitor oligomycin, which effectively shuts down ATP production due to oxidative phosphorylation. Any residual mitochondrial respiration/oxygen consumption noted at this point can then be attributed to proton leak.

Maximal OCR is determined through the addition of the proton ionophores (uncoupler) FCCP or BAM15, which increase inner mitochondrial membrane permeability to protons, increasing oxygen consumption and allowing for the assessment of the maximal oxygen consumption/respiration possible in the cells. Spare respiratory capacity is calculated through determining the difference between basal OCR and maximal OCR in the cells and this reflects the extra amount of oxygen consumption/ATP production that can be achieved by the cells in response to increased energy demand. Non-mitochondrial respiration is the oxygen consumption due to non-mitochondrial processes. Although not well defined, these have been attributed to such processes as hydrogen peroxide production and the enzymatic activity of oxygenases.

Table 2. 2 Mitochondrial Stress Test parameters and associated calculations.

Parameter	Equation
Non-mitochondrial O ₂ consumption	Minimum rate measurement after rotenone/antimycin A injection
Basal Respiration	(Last rate measurement before first injection) – (Non-Mitochondrial Respiration Rate)
Maximal Respiration	(Maximum rate measurement after FCCP injection) – (Non-Mitochondrial Respiration Rate)
Proton Leak	(Minimum rate measurement after Oligomycin injection) - (Non-Mitochondrial Respiration Rate)
ADP Phosphorylation	(Last rate measurement before Oligomycin injection) – (Minimum rate measurement after Oligomycin injection)
Spare Respiratory Capacity	(Maximal Respiration) – (Basal Respiration)
Spare Respiratory Capacity (%)	(Maximal Respiration) / (Basal Respiration) x 100
Coupling Efficiency (%)	(ATP Production Rate) / (Basal Respiration Rate) x 100

2.11 Rates of ATP production and proton production

Rates of ATP production and PPR were calculated post-hoc from the bioenergetic parameters obtained from the mitochondrial stress test. The raw values of extracellular acidification rate (ECAR) and OCR were sub-divided into component rates (Mookerjee & Brand, 2015). For ECAR, the total rate of change of pH was first converted to total proton production rate (PPR_{tot}), then divided into proton production rates originating from respiratory bicarbonate production (PPR_{resp}) (using OCR data) and glycolytic lactate production (PPR_{glyc}). For OCR, mitochondrial oxygen consumption rate (OCR_{mito}) was defined as total oxygen consumption rate (OCR_{tot}) minus the oxygen consumption rate (OCR_{R/AA}) in the presence of the respiratory chain poisons rotenone and antimycin A (OCR_{mito} = OCR_{tot} - OCR_{R/AA}), and the phosphorylating or coupled rate was defined as the total oxygen consumption rate minus the oligomycin-insensitive oxygen consumption rate (OCR_{oli}), with a small additional correction by 9.2% to compensate for changes in mitochondrial protonmotive force upon addition of oligomycin (Mookerjee & Brand, 2015). Thus, OCR_{coupled} = 0.908 × (OCR_{tot} - OCR_{oli}). The vast majority of ATP made in cells comes either from glycolysis (ATP_{glyc}) or from oxidative reactions (ATP_{ox}). The corresponding rates (denoted by J) are J_{ATPglyc} and J_{ATPox}. The total rate of ATP production (J_{ATPproduction}) is defined as the sum of J_{ATPglyc} + J_{ATPox}.

Total Rate of Glycolysis (J_{ATPglyc}) was calculated by equation 2.2:

$$\text{PPR}_{\text{glyc}} \times \text{ATP/lactate} + \text{OCR}_{\text{mito}} \times 2\text{P/O}_{\text{glyc}}$$

Equation 2.2 Total rate of glycolysis

Commented [CS87]: Determined how?

Commented [CS88]: I am guessing this is 100% - 9.2%? If so the additional correction, is actually a subtraction?

Total Rate of Oxidative Phosphorylation ($J_{ATP_{ox}}$) was calculated by Equation 2.3:

$$OCR_{coupled} \times 2P/O_{oxphos} + OCR_{mito} \times 2P/O_{TCA}$$

Equation 2. 3 Total rate of oxidative phosphorylation

Where P/O_{glyc} equals 0.242, P/O_{oxphos} equals 2.486, and P/O_{TCA} is equal to 0.121 (Mookerjee & Brand, 2015).

Normalised mitochondrial respiration was determined by Equation 2.4:

$$(OCR_{tot} - OCR_{R/AA}) / \text{Normalisation factor} = OCR_{mito}$$

Equation 2. 4 Normalised mitochondrial respiration

Total PPR was determined using Equation 2.5:

$$(ECAR_{tot} / \text{buffering power}) / \text{Normalisation factor} = PPR_{tot}$$

Equation 2. 5 Total proton production rate

The buffering power of each medium was determined a priori and was equal to 3.2- and 0.8- mM H^+ /pH for C_2C_{12} DM and HUVEC EGM, respectively.

The respiratory portion of PPR was calculated using Equation 2.6, assuming a max H^+/O_2 value of 1:

$$OCR_{\text{mito}} \times \max H^+/O_2 \times (10^{pH} - pK_1)(1 + 10^{pH} - pK_1) = PPR_{\text{resp}}$$

Equation 2. 6 Respiratory portion of PPR

Where, the combined hydration/dissociation constant (pK_1) is equal to 6.093, derived from the conversion of CO_2 to HCO_3^- at pH 7.4.

The glycolytic portion of PPR was determined using Equation 2.7:

$$PPR_{\text{tot}} - PPR_{\text{resp}} = PPR_{\text{glyc}}$$

Equation 2. 7 The glycolytic portion of PPR

2.12 RT-qPCR Gene expression

2.12.1 RNA extraction

Following experimental procedures (dosing with flavonoids as detailed above), cells were washed in cold PBS and lysed in TRIzol. All plasticware used in the following procedures was RNA free and laboratory space was cleaned with 70% ethanol. Once lysed, 0.1 mL chloroform (Sigma-Aldrich, Poole, UK) per 0.5 mL TRIzol reagent was added to the homogenates, followed by vigorous shaking by hand for 15 seconds. This separated the sample into a lower red organic layer (containing TRIzol and cell debris), a cloudy interphase layer (containing DNA and protein) and a clear upper aqueous layer (containing RNA and chloroform). Samples

were incubated at RT for 10 minutes, before centrifugation at $12,000 \times g$ for 15 minutes at 4°C . The aqueous layer was carefully transferred into a new Eppendorf tube, prior to the addition of isopropanol (ratio 1:2 of isopropanol to TRIzol reagent), and vigorous shaking, in order to precipitate the RNA. Following 10 minutes incubation at RT, the samples were centrifuged at $12,000 \times g$ for 10 minutes at 4°C . The supernatant was removed, and 1 mL 75% ethanol was added to the pellet. The samples were centrifuged $7,500 \times g$ for 8 minutes at 4°C and the supernatant decanted. A further 1 mL 75% ethanol was added to the pellet before another centrifugation step ($7,500 \times g$ for 8 minutes at 4°C), and subsequent decanting of the supernatant. The pellet was left to air dry to remove excess ethanol, before being resuspended in RNA storage solution (Ambion® RNA Storage Solution, Invitrogen, Thermo Fisher Scientific, Waltham, MA, USA). Lastly, samples were vortexed and placed in a block heater for 10 minutes at 35°C , before vortexing and storing at -20°C until further processing.

2.12.2 Assessment of RNA Concentration and Purity

RNA concentration and purity were assessed using a spectrophotometer (NanoDrop™ 2000, Thermo Fisher Scientific, Waltham, MA, USA). One microliter of extracted RNA was pipetted onto the NanoDrop probe and the amount of ultraviolet (UV) light absorbed at 260 nm (the wavelength at which nucleic acids best absorb light) was measured by a photodetector to determine the concentration of RNA inferred using the Beer-Lambert law (see Equation 2.8). Following assessment of RNA concentration, the purity of RNA was determined from the ratio of absorbance at 260 nm to 280 nm, the wavelengths at which RNA/DNA and protein best absorb UV light, respectively. A A_{260}/A_{280} ratio of ~ 2 is indicative of highly purified RNA, and a ratio of 1.8-2.2 was accepted. Other potential contaminants include ethanol, phenol or guanidine, which are measured at 230 nm. Therefore, the A_{260}/A_{230} ratio is measured where a

Commented [CS89]: Should this be ribonucleic?

Commented [CS90]: Is protein not at 230? I thought it was picked up with other contaminants e.g. EDTA etc at 230?

Commented [CS91]: I think for good quality RNA it should be 2 or above – DNA tends to be between 1.8 and 2.0. What were your actual values? May be worth putting in a range?

reading >1.5 of is accepted. RNA concentrations and purities are reported within the methods section of each experimental chapter throughout this thesis.

Commented [CS92]: I may be remembering incorrectly, but should the 260/230 – not be nearer to 2?

The data derived from the Nanodrop UV spectrophotometer were used to calculate RNA quantity based on the absorbance at 260 nm. A spectrophotometric reading of 1 at 260 nm is equivalent to 40 $\mu\text{g}/\text{mL}^{-1}$ RNA. The following Beer-Lambert equation was used by the Nanodrop software:

$$C = \frac{A \times \epsilon}{b}$$

Equation 2. 8 Beer-Lambert equation

Where C = nucleic acid concentration ($\mu\text{g}/\text{mL}^{-1}$), A = absorbance in AU, ϵ = extinction coefficient ($\text{ng}/\text{cm}/\mu\text{L}^{-1}$), which is 40 $\text{ng}/\text{cm}/\mu\text{L}^{-1}$ for RNA and b = path length in cm.

2.12.3 Principle of the polymerase chain reaction

The polymerase chain reaction (PCR), a technique widely used to amplify specific fragments of DNA, was first introduced in 1983 by Nobel prize recipient Kary Mullis (Mullis & Faloona, 1987). Fundamentally, a cells phenotype is dictated by its component proteins. The synthesis of functional protein first requires that its corresponding gene is transcribed to produce a messenger ribonucleic acid (mRNA). This mRNA can then be translated into protein when it associates with the ribosome. Therefore, assessment of mRNA responses following specific stimuli is necessary to shed light on the molecular processes underpinning cellular adaptation.

Commented [CS93]: Quite superficial – do you need a bit more detail and also some references?

Commented [SD94R93]:

Following isolation of mRNA from cells (see section 2.12.1), the single stranded RNA (ssRNA) must be reverse transcribed to form a complimentary DNA (cDNA) before the target sequence is amplified. In order for reverse transcription to occur, oligonucleotides (dNTPs) are added to the ssRNA using the enzyme reverse transcriptase and cDNA is synthesised from the 3' to 5' end of the mRNA molecule. Once synthesised, the cDNA is amplified in a process known as RT-PCR, via three distinct steps all of which represent 1 cycle of a PCR reaction that is repeated numerous times (30-40 cycles) to produce ~1 billion copies of the target sequence (see Figure 2.7). These steps include: 1) Denaturation, whereby the double stranded DNA (dsDNA) is subjected to high temperatures (95°C) in order to separate the DNA into two strands exposing the 3' end of the DNA. 2) Annealing, whereby the temperature is lowered (optimal temperature is primer specific, with all the primers used herein designed to anneal at approximately 60°C) to enable binding of short sequence (approximately 18-30 bp) primers to the DNA strands. 3) Extension, where *Taq* polymerase (an enzyme derived from the bacterium species *Thermus Aquaticus* that is able to withstand high temperatures) binds to the primers and synthesises the complimentary strand using free dNTPs.

During each PCR cycle, a fluorescent dye (SYBR Green was used in these experiments) binds to each dsDNA molecule after primers anneal to the 3' end. The amount of light excited and emitted from SYBR Green is able to provide a 'real-time' measurement of DNA amplification, as the amount of light measured by the fluorometer within the PCR thermocycler instrument is directly proportional to the amount of targeted DNA produced. The fluorescence is quantified following each PCR run according to the number of cycles required to exceed the fluorescence cycle threshold (C_T). Therefore, generally, the lower the C_T value the higher the expression levels of the gene of interest, as the fluorescence being detected earlier above background fluorescence reflects the larger amount of starting nucleic acid material. The resultant C_T values

Commented [CS95]: Is this true for both low and high expressed genes?

of the target gene in each sample are then compared to the C_T values of a housekeeper/reference gene (one of which should remain consistent, regardless of any given stimulus) to determine either absolute or relative quantities (Livak & Schmittgen, 2001).

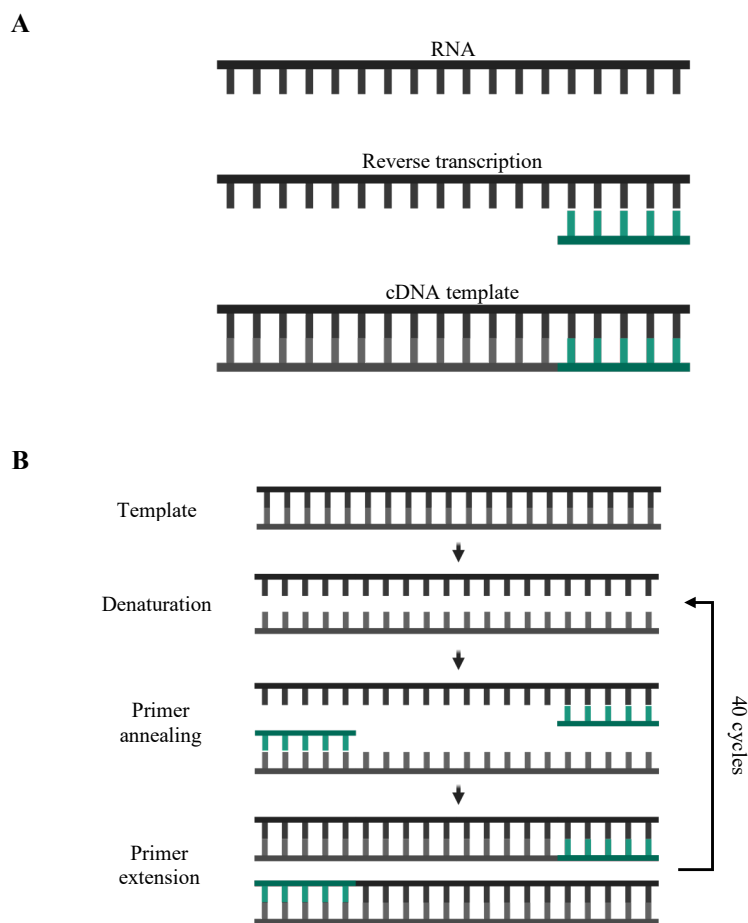


Figure 2. 7 Diagram illustrating the main processes in the real time polymerase chain reaction (RT-qPCR). A) cDNA generation from a single strand of mRNA (from the 3' to 5' end) isolated from an experimental sample. B) Outline of RT-qPCR, where three key steps occur, including: Denaturation, annealing of primers, and extension of primers. Primers specific to the gene of

interest anneal at both of the 3' end of the sense (top) and anti-sense (bottom) strand. The PCR reaction amplifies the amount of DNA over 40 cycles.

2.12.4 Procedure

Throughout this thesis, a one-step PCR method (QuantiFast SYBR[®] Green RT-PCR Kit, Qiagen, UK) was used to analyse mRNA expression whereby the cDNA synthesis and PCR steps were performed in the same reaction tube for time efficiency and reduced risk of cross contamination. Reaction tubes were either prepared manually by hand or automatically using the QIAgility robot (Qiagen, Crawley, UK). Each reaction included 5.6 μ L of master mix, containing 5 μ L 2x QuantiFast SYBR[®] Green (comprising HotStarTaq[®] DNA polymerase, SYBR[®] green RT-PCR buffer, dNTP mix and ROX[™] passive reference dye), 0.25 μ L of forward and reverse primers and 0.1 μ L reverse transcriptase (RT) and 4.4 μ L RNA (at a concentration of 7.9 ng/ μ L in nuclease-free H₂O) sample. The preparation method (i.e. manual or automatic using the QIAgility robot) used per reaction will be specified within the methods section of each experimental chapter. Prepared reaction tubes were transferred to a PCR thermal cycler (Rotor-Gene 3000Q, Qiagen, UK) to undergo reverse transcription/cDNA synthesis (hold 50°C for 10 min), transcriptase inactivation and initial denaturation (95°C for 5 min) followed by 40 \times amplification cycles consisting of: 95°C for 10 s (denaturation) and 60°C for 30 s (annealing and extension). For some products with low gene expression levels, the total number of cycles was extended by 5-10 cycles to enable sufficient amplification.

2.12.5 Quantification of Relative Gene Expression

Following the completion of 40 \times PCR cycles (see section 2.12.4), melt curve analysis was first performed to ensure that only the gene(s) of interest was amplified. Sample efficiencies were also analysed and are reported within the methods section of each experimental chapter.

An efficiency value of 2 represents a 2-fold increase (100% which is derived from dividing the efficiency value by 2 and multiplying by 100) of amplicon with each PCR cycle. To obtain the raw C_T values for each sample, a threshold line was self-adjusted on the amplification curve according to where an exponential rise in fluorescence occurred (see Figure 2.8). The lower the number of cycles required for the gene to achieve the fluorescent threshold, the higher the expression and vice versa. The C_T values were used to quantify relative gene expression using the comparative Delta Delta C_T ($2^{-\Delta\Delta C_T}$) equation (Livak & Schmittgen, 2001), whereby the expression of the gene of interest was determined relative to the internal control in the treated sample compared with the untreated control (see Equation 2.9). The C_T values of the reference gene and the zero-hour control were used.

Delta Delta C_T ($2^{-\Delta\Delta C_T}$) Equation:

$$\text{Expression fold change} = 2^{-\Delta\Delta C_T}$$

Where, $\Delta C_{T \text{ Treated}} = C_T \text{ (Gene of interest)} - C_T \text{ (Internal Control)}$, $\Delta C_{T \text{ Calibrator}} = C_T \text{ (Gene of interest)} - C_T \text{ (Internal Control)}$ and $\Delta\Delta C_T = \Delta C_{T \text{ Treated}} \text{ (Treated Sample)} - \Delta C_{T \text{ Calibrator}} \text{ (Control Sample)}$.

Equation 2. 9 Delta Delta C_T ($2^{-\Delta\Delta C_T}$) Equation used to calculate relative gene expression against a reference gene and control group.

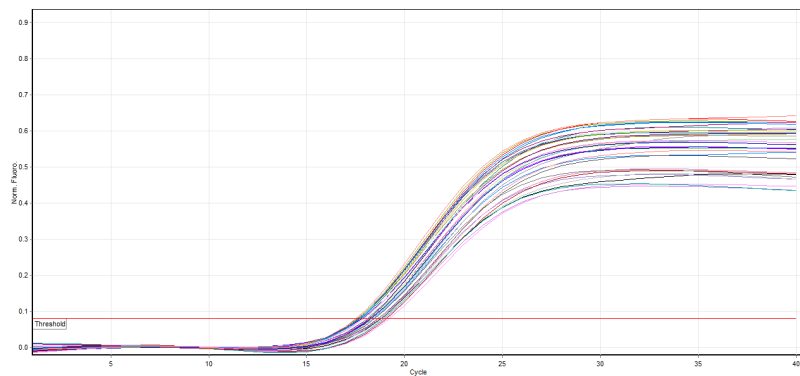


Figure 2. 8 Setting of cycle threshold (C_T) to derive C_T values for genes of interest.

2.12.6 Primer Design

All primers were custom designed according to several specific guidelines (Dieffenbach et al., 1993), where a balance between primer specificity and efficiency of amplification was the primary aim. This was achieved by considering primer length, PCR product length, oligonucleotide content and melting temperature. Primers were manufactured and ordered via Sigma-Aldrich (UK) or Primer Design (UK). All stock (desalted) primers were suspended in RNA free H_2O to a final concentration of 100 μM . For genes with multiple transcript variants, primers were designed to target all mRNA sequences of the main transcript and its variants to enable a global measure of gene expression. The Clustal Omega Multiple Sequence Alignment program (<https://www.ebi.ac.uk/Tools/msa/clustalo>) was used to identify gene regions which shared the same sequence across all transcript variants. Following primer design, specificity was confirmed via performing a Basic Local Alignment Search Tool (BLAST) online (<http://blast.ncbi.nlm.nih.gov>) search and conducting melt curve analysis. Melt curve analysis determines the melting temperature (T_m) and confirms that only the gene of interest was amplified (indicated by a single peak; Figure 2.8 B) without amplification of unintended targets

(indicated by a double melt curve peak; see Figure 2.8 A). Primer sequences for the gene(s) of interest are described in the methods section of each experimental chapter.

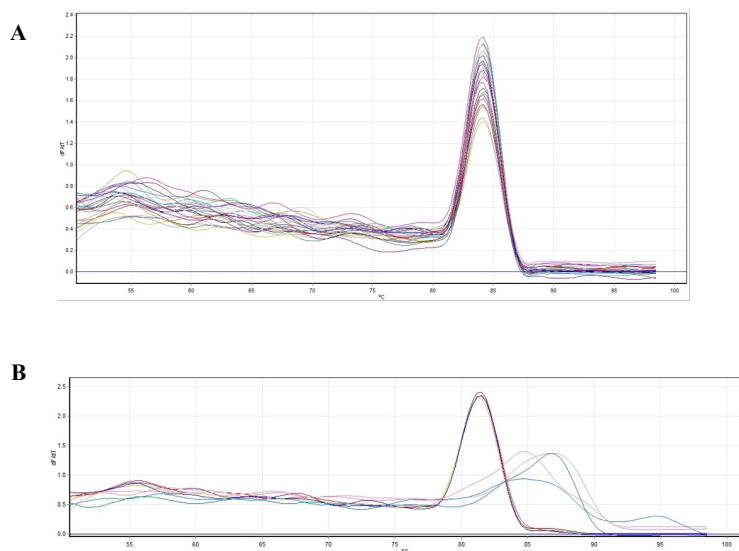


Figure 2.9 Melt curve analysis to determine specific target amplification. An example of melt curves analysed to determine primer specificity. A) A single peak suggesting no unspecific amplification whereas B) A double peak suggesting amplification of unintended targets and/or primer dimer issues.

2.13 SDS-PAGE and immunoblotting

2.13.1 Principle

Sodium dodecyl sulphate polyacrylamide gel electrophoresis (SDS-PAGE) is a discontinuous electrophoretic system that allows for separation of proteins by their molecular weight (kilo Daltons [kDa]) using an electrical current (Laemmli, 1970). To enable protein separation

during PAGE, proteins must be denatured with Laemmli buffer (and reducing agent) and coated with negative charges through addition of SDS. The denaturing process of secondary/tertiary structures in proteins permits their separation based upon the primary amino acid sequence, and theoretically, molecular weight. After these initial steps, PAGE is conducted in polyacrylamide gels using the frictional resistance of a protein as it migrates through pores formed between polymer chains within the gel (Ornstein, 1964). Polyacrylamide gels are comprised of polymerized acrylamide monomers along with cross-linking N,N'-Methylenebisacrylamide monomers (Raymond & Weintraub, 1959), creating uniformly sized pores. Proteins move through pores within the gel structure once an electrical current is passed through. Typically, gels comprise of two separate regions: a “stacking gel” above a “resolving or separating gel” with larger and smaller pores, respectively. As proteins migrate into the resolving gel containing smaller pores, protein migration occurs more slowly and is dependent upon protein size, as previously mentioned. Following separation, the proteins are electrophoretically transferred to an appropriate membrane, thereby immobilising the separated proteins. Similar to PAGE, the negatively charged proteins in the gel are transferred across onto a membrane when a lateral electric current is applied. Subsequently, proteins can be probed with antibodies, and providing additional durability compared to gels (Towbin et al., 1979).

2.13.2 Procedures

After relevant treatments, cells were lysed and scraped in ice-cold 1x radioimmunoprecipitation assay (RIPA) buffer containing: 25 mM Tris-HCl pH 7.6, 150 mM NaCl, 1% NP-40, 1% sodium deoxycholate and 0.1% SDS, supplemented with 1x Protease Inhibitor Cocktail Set V (Merck Life Science, UK). Cell lysates were centrifuged for 15 minutes at $18,000 \times g$ (4°C) and the supernatant was stored at -80°C before analysis for total

protein. Following determination of sample protein concentrations using the Pierce™ bicinchoninic acid (BCA) assay (see section 2.15), samples were resuspended in 4x Laemmli buffer (Bio-Rad laboratories, Hertfordshire, UK) containing reducing agent (1x working concentration: 31.5 mM Tris-HCl [pH 6.8], 10% glycerol, 1% SDS, 0.005% Bromophenol Blue and 355 mM 2-mercaptoethanol). After boiling samples for 5 minutes at 95°C, 22.5-25 µg sample was loaded and electrophoresed on 10% Mini-PROTEAN® TGX Stain-Free™ Precast Gels (Bio-Rad laboratories, Hertfordshire, UK). Samples were separated in Tris-glycine running buffer (1:10 10X Running buffer, Scientific Laboratory Supplies, Nottingham, UK) using Bio-Rad Mini-PROTEAN® Tetra vertical electrophoresis cell (Bio-Rad laboratories, Hertfordshire, UK). Voltage was set at 100 V for the entirety of electrophoresis. After protein separation, stain-free gels were activated by UV light for 5 minutes and subject to transfer.

Semi-dry transfer of proteins to a 0.2 µM nitrocellulose membrane (Bio-Rad laboratories, Hertfordshire, UK) was performed using the Trans-Blot® Turbo™ Transfer System. Next, the polyacrylamide stain-free gel was stacked on a nitrocellulose membrane. Filter paper was used to sandwich the membrane and gel together. The nitrocellulose membrane and filter paper were pre-soaked in transfer buffer (600 ml H₂O, 200 ml ethanol and 200 ml 5x transfer buffer (Bio-Rad laboratories, Hertfordshire, UK)). Care was taken to avoid bubbles in the transfer stack by using a roller. The transfer sandwich was placed into a transfer cassette and pressed evenly with the cassette lid. Proteins were transferred onto the nitrocellulose membrane at 25 V for 7 mins. To verify the transfer of proteins, fluorescent stain-free imaging of the membrane was performed (ChemiDoc™ MP imaging system, Bio-Rad Laboratories, Inc. CA, USA).

After protein transfer, membranes were blocked for 1 hour in 5% non-fat dried milk (NFDM) or 5% bovine serum albumin (BSA) at room temperature. Membranes were then incubated overnight at 4°C with primary antibodies. The concentration of primary antibodies used will be specified in the experimental chapters. After overnight incubation, membranes were washed 3 times in Tris-buffered saline with Tween 20 (TBST) (20 mM Tris [pH 7.5], 150 mM NaCl and 0.1% Tween 20) for 5 min and subsequently incubated for 1 hour in anti-rabbit IgG HRP-linked secondary antibody (Cell Signaling Technology Europe, B.V.) at a dilution of 1:2000-1:10,000 in 5% NFDM-containing TBST. Following secondary antibody incubation, membranes were again washed 3 times for 5 minutes in TBST. Proteins were visualised by enhanced chemiluminescence (ECL) (Pierce™ western blotting substrate, Thermo Fisher Scientific inc, Waltham, USA) by incubating membranes in reagents at a 1:1 dilution for ~3 minutes. The membrane was then imaged by the ChemiDoc™ MP imaging system (Bio-Rad Laboratories, Inc. CA, USA). Band densities were analysed using Image Lab software (Bio-Rad Laboratories, Inc. CA, USA). Stain-free image bands were measured for total lane protein levels. Bands of targeted proteins were measured and normalised to total protein in the relevant lane and made relative to the 0-hour CTRL condition. Detected phosphorylated proteins were normalised to their total protein expression before being compared between experimental conditions.

2.14 SRB Assay

The protein concentration of experimental samples was determined after relevant measurements to standardise ROS level/production as a function of the protein level (i.e., cell number) in each well of the culture plate. This was performed using the sulforhodamine B (SRB) assay, as described by (Vichai & Kirtikara, 2006). Directly after the measurement of ROS, cells were fixed by gently adding a cold solution of 1% (v/v) acetic acid in methanol and

incubating for at least 1 hour at -20°C. Next, plates were air-dried in an incubator for ~10 minutes. Following this, 0.5% (w/v) SRB solution in 1% acetic acid was added to each well and incubated for 1 hour at 37°C with gentle shaking. The SRB solution was then aspirated and cells were gently washed with 1% (v/v) acetic acid. This step was repeated two-three times or until the remaining SRB solution was removed. Next the plate was dried for 10 minutes (e.g., in an incubator), before adding add 1 mL of 10 mM Tris to dried wells and applying gentle shaking for 15 min in order to dissolve the dye. Finally, 200 µL of the solution from each well was transferred into a 96-well plate (in duplicate) and the absorbance was measured at 540 nm using a plate reader.

2.15 BCA Assay

The protein concentration of samples was determined, prior to, or after relevant assays. The BCA assay can be used to quantify protein concentrations, as described herein. The determination of sample protein concentration (mg/mL) was achieved by generating a standard curve using BSA at concentrations ranging between 0-2000 µg/mL. To create the protein standards, serial doubling dilutions were performed using the 2 mg/mL BSA stock and appropriate volumes of diluent (Milli-Q H₂O). For the assay, the Pierce™ BCA protein kit (Rockford, IL, USA) was used. Reagent A (sodium carbonate, sodium bicarbonate, BCA and sodium tartrate in 0.1 M sodium hydroxide) was mixed in a mixing trough with reagent B using a multichannel pipette (4% cupric acid sulphate) at a ratio of 50:1. In a 96 well plate, 20 µL of sample and standard were pipetted in each well followed by 200 µL BCA buffer. The plate was immediately shaken thoroughly on an orbital shaker for 30 seconds, prior to a 30-minute incubation at 37°C before measuring samples at 562 nm using a plate reader.

Commented [TD96]: I guess we made a decision earlier that the VO₂ kinetics data/analysis is presented in the individual chapter rather than in Chapter 2 – Methods.

2.16 Statistical Analysis

Data in this thesis are presented as means \pm SEM, unless otherwise stated. Statistical significance was accepted when $P < 0.05$. All statistical analyses were conducted using MiniTab Statistical Software (Minitab, Version 18, USA), GraphPad Software (Prism, Version 8.0, San Diego, CA) or R Studio (Version 1.3, RStudio, MA, USA). The software used and the specific statistical tests conducted will be specified in the methods section of each experimental chapter.

Commented [TD97]: This is fairly unusual...not for figures, but definitely in tables. Are you sure you didn't present SD... keep it as it is please (don't adjust your full thesis from SEM to SD), but I just wanted to check!

Chapter 3: Cocoa-flavanols enhance
moderate-intensity pulmonary $\dot{V}O_2$ kinetics
but not exercise tolerance in sedentary middle-
aged adults

3.1 Abstract

Introduction: Cocoa flavanols (CF) may exert health benefits through their potent vasodilatory effects, which are exerted by elevations in nitric oxide (NO) bioavailability, where NO diffuses and acts upon the smooth muscle layer. These vasodilatory effects may contribute to improved delivery of blood and oxygen (O₂) to exercising muscle.

Objective: Therefore, the objective of this study was to investigate how CF supplementation impacts pulmonary O₂ uptake ($\dot{V}O_2$) kinetics and exercise tolerance in sedentary middle-aged adults. It was hypothesised that CF supplementation would speed phase II $\dot{V}O_2$ kinetics during moderate and severe-intensity exercise and enhance exercise tolerance in healthy middle-aged individuals.

Methods: In a double-blind cross-over, placebo-controlled design, 17 participants (11 male, 6 female; mean±SD, 45±6 years) randomly received either 7 days of daily CF (400 mg) or placebo (PL) supplementation. On day 7, participants completed a series of 'step' moderate- and severe-intensity exercise tests for the determination of $\dot{V}O_2$ kinetics.

Results: During moderate-intensity exercise, the time constant of the phase II $\dot{V}O_2$ kinetics ($\tau\dot{V}O_2$) was decreased by 15% in CF as compared to PL (mean±SD; PL: 40±12 vs. CF: 34±9 s, $P=0.019$), with no differences in the amplitude of $\dot{V}O_2$ ($A\dot{V}O_2$; PL: 0.77±0.32 vs. CF: 0.79±0.34 l min⁻¹, $P=0.263$). However, during severe-intensity exercise, $\tau\dot{V}O_2$, the amplitude of the slow component ($SC\dot{V}O_2$) and exercise tolerance (PL: 435±58 vs. CF: 424±47 s, $P=0.480$) were unchanged between conditions.

Conclusion(s): The data show that acute CF supplementation enhanced phase II $\dot{V}O_2$ kinetics during moderate-, but not severe-intensity exercise in middle-aged participants. These effects of CFs, in this demographic, may reduce the O₂ deficit and contribute to improved tolerance of moderate-intensity physical activities, which appear commonly present in daily life.

Commented [TD98]: I've largely scanned the paper, rather than in-depth read as it is published and I assume you've largely copy-pasted that draft into your thesis. I've specifically looked into the intro and discussion how you linked it to the other chapters.

Commented [HJ99R98]: Same for me. Its already published so no point in making changes

Commented [HJ100]: Is this not aim?

Commented [DR101]: I think your objective can be much more specific. Your hypothesis is that CF supplementation improves pulmonary O₂ uptake ($\dot{V}O_2$) adjustments to a moderate exercise stimulus in healthy middle age people.

Commented [DR102]: Because you are stating here your main objective, to affect phase II $\dot{V}O_2$ kinetics, you expect that this term has been explained somewhere in the introduction. What is so special about phase II?

Commented [TD103]: SEM or SD (see previous comment) Think all of this is SD.... Right?

Commented [DR104]: You list here a number of parameters related to oxygen uptake, which is not wrong, but it doesn't give any clue why you have done it. Your hypothesis was that impact would be noticeable with moderate exercise and not severe. Despite that you 'treat the findings at a similar level'. You could even choose to write one simple sentence: 'CF had no impact on $\dot{V}O_2$ kinetics under severe -intensity exercise'.

Commented [DR105]: Can't you include a concluding sentence what it means when $\tau\dot{V}O_2$ decreases, whilst $\dot{V}O_2$ amplitude, HR etc are not affected?

3.2 Introduction

Skeletal muscle contraction and force production form the basis for the ability to perform physical activity, both for daily life activities as well as during sports-related events. Repeated muscle contractions require continuous regeneration of adenosine triphosphate (ATP). The production of ATP during (prolonged) physical activity is driven through the mechanism of oxidative phosphorylation, which depends on sufficient availability of oxygen (O_2) amongst other key substrates (Poole et al., 2008). Impairment to pathways involved in the delivery of O_2 to working skeletal muscle, like that observed in older and physically-inactive adults, leads to slower rates of phase II (the exponential rise in oxygen uptake following exercise onset) pulmonary O_2 uptake ($\dot{V}O_2$) and therefore greater O_2 deficit (Cunningham & Paterson, 1994; DeLorey et al., 2004a; Dumanoir et al., 2010; George et al., 2018; Whipp & Rossiter, 2013). Slower phase II $\dot{V}O_2$ kinetics in response to physical activity are associated with lower exercise tolerance (Goulding et al., 2017, 2018; Grassi, et al., 2011), and may affect the capacity to perform daily life activities that require moderate-intensity physical activity.

The slower dynamic adjustment of $\dot{V}O_2$ across a metabolic transient observed in older adults is thought to be due to a mismatch of O_2 delivery to O_2 utilisation (George et al., 2018; Murias et al., 2010a; Murias & Paterson, 2015a). This possible imbalance could be due to reductions in the supply of microvascular blood flow and/or lowered mitochondrial sensitivity to ADP (Gouspillou et al., 2014b; Murias & Paterson, 2015b). Indeed, attenuations in microvascular blood flow supply and distribution (and thus O_2 delivery) within aged skeletal muscle are well documented (Behnke & Delp, 2010a; Dumanoir et al., 2010; Muller-Delp et al., 2002a; Musch et al., 2004a). These reductions in O_2 delivery to active skeletal muscle are likely caused by impaired vascular endothelial function and diminished nitric oxide (NO) bioavailability (Muller-Delp et al., 2002a; Sindler et al., 2009; Spier et al., 2004; Woodman et al., 2002).

Interestingly, lifestyle interventions, such as exercise training and dietary strategies (Schreuder et al., 2015; Vanhatalo et al., 2010), have demonstrated potent effects to enhance NO bioavailability and improve endothelial function. Consequently, a number of studies have shown faster $\dot{V}O_2$ kinetics in concert with increased O_2 availability (Bailey et al., 2015; Goulding et al., 2017; Murias et al., 2010a).

Cocoa flavanols (CFs) represent a group of flavonoids present in cocoa derived from seeds of the fruit of the *Theobroma cacao* tree. Previous studies have found CFs (700-900 mg range) act primarily through the monomer (-)-epicatechin, to stimulate NO production, resulting in improved vasodilation and endothelial function in healthy adults (Berry et al., 2010; Davison et al., 2008; Schroeter et al., 2006). Given the direct impact of CFs on NO production and vascular endothelial function, and the negative effects of sedentary ageing on O_2 delivery and $\dot{V}O_2$ kinetics at the onset of exercise, the study objective was to test the hypothesis that, compared with placebo (PL), CF supplementation speeds phase II $\dot{V}O_2$ kinetics during moderate- and severe-intensity physical activity and enhances exercise tolerance in healthy middle-aged individuals.

3.3 Methodology

3.3.1 Participants

Seventeen healthy middle-aged adults (11 male: mean \pm SD, age 45 \pm 6 years; body mass 87.7 \pm 13.5 kg; height 1.75 \pm 0.07 m; and 6 female: aged 47 \pm 5 years; body mass 68.2 \pm 17.7 kg; height 1.62 \pm 0.09 m) volunteered and gave written informed consent to participate in the study (see Figure 3.1). All procedures conformed to the Declaration of Helsinki and were approved by Liverpool John Moores University Research Ethics Committee (approval reference number: 18/SPS/014). Participants engaged in less than two hours of structured exercise training per

Commented [DR106]: Because you are stating here your main objective, to affect phase II $\dot{V}O_2$ kinetics, you expect that this term has been explained somewhere in the introduction. What is so special about phase II?

Commented [SD107R106]: Have added small detail in brackets about phase II $\dot{V}O_2$ kinetics in first paragraph

Commented [HJ108]: Is this wording the same as what is at the end of the literature review? If not make the wording the same

week. All participants were non-smokers and had no history of cardiovascular, respiratory or metabolic diseases. Participants were not taking any dietary supplements or medication.

Participants reported to the laboratory at least 3 hours postprandial in a rested state, having completed no strenuous exercise within the previous 24 hours and avoided alcohol and caffeine for 24 and 6 hours, preceding each exercise test, respectively. Participants were advised to avoid consumption of flavonoid-rich foodstuffs (e.g. green tea, dark chocolate and berries) in the 24 hours preceding each experimental trial.

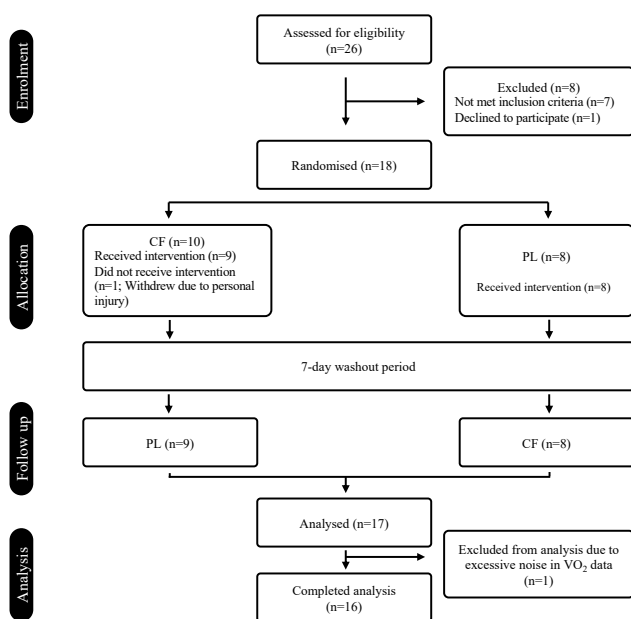


Figure 3. 1 CONSORT diagram showing the flow of participants through each stage of the randomised trial.

3.3.2 Procedures

Participants visited the temperature-controlled laboratory (19-22°C) on 4 occasions during a 4-5-week period, with each test scheduled at the same time of day (± 1 h) and at least 48 h between visits. Participants completed two preliminary trials and two experimental trials. Exercise bouts were performed on an electrically operated cycle ergometer (Lode Corival, Groningen, The Netherlands). Saddle and handlebar height/angle were recorded at the first visit and replicated during each subsequent visit for each individual participant. Throughout all exercise tests, participants were instructed to maintain a cadence of 65-80 rpm, and exhaustion was defined as when the participants cadence dropped 10 rev min⁻¹ below the target work rate. Time to exhaustion was measured to the nearest second (s) in all tests.

3.3.3 Preliminary trial(s)

Upon arrival to the laboratory, participants height and weight were recorded. Subsequently, each participant undertook an incremental step test until the limit of tolerance to establish $\dot{V}O_2$ peak, the gas exchange threshold (GET) and the power outputs for later tests. The incremental step test consisted of 3-min of baseline pedalling at 0 W, followed by a continuous, stepped increase in power output of 30 or 25 W every minute (for males and females, respectively) until the limit of tolerance was established. Gas exchange and ventilatory variables were measured continuously at the mouth breath-by-breath throughout each test. $\dot{V}O_2$ peak was defined as the highest $\dot{V}O_2$ value obtained over 30 s. The GET was determined using a collection of previously established criteria (Beaver et al., 2016) including 1) a disproportionate rise in $\dot{V}CO_2$ relative to $\dot{V}O_2$; 2) an increase in minute ventilation ($\dot{V}E$) relative to $\dot{V}O_2$ ($\dot{V}E/\dot{V}O_2$) without an increase in $\dot{V}E$ relative to $\dot{V}CO_2$ ($\dot{V}E/\dot{V}CO_2$); and 3) an increase in end tidal O_2 tension without decreasing end tidal CO_2 tension.

During the familiarisation trial (visit 2), participants were requested to perform two bouts of severe-intensity exercise at a fixed power output to exhaustion (e.g. T_{lim}), each separated by 45 min of seated rest. The power outputs of these severe-intensity bouts were selected based upon performance during the incremental test and were calculated to be 60% Δ (i.e., a work rate calculated to require 60% of the difference between GET and $\dot{V}O_2$ peak). On occasion, adjustments were made to the power output of the subsequent exercise tests based upon performance in the familiarisation trials; the prescribed power output was lowered for participants who failed to exercise for up to 360 s during the severe-intensity bouts.

After completion of the familiarisation trial, participants were randomly assigned (computer generated), using a double-blind cross-over design (see Figure 3.2), to receive 7 consecutive days of CF supplementation or a PL that was matched for caffeine and theobromine content. Nine participants began with the CF condition, and eight participants began with the PL condition. Participants were advised to consume 4 capsules daily. Each CF capsule contained 316 mg CocoActiv (Naturex, Netherlands; ~100 mg total flavanols of which 22 mg DP1 = catechin + epicatechin) whereas PL capsules contained 0 mg CocoActiv product. This CF dose was selected based on the knowledge that ~400 mg CF's are required to improve vascular function during exercise (Decroix et al., 2018a). Both PL and CF capsules contained 2.9 mg caffeine and 22.5 mg theobromine (Fagron, Netherlands). Remaining empty volumes of PL and CF capsules were filled with microcrystalline cellulose (Fagron, Netherlands). Two capsules were taken in the morning and two in the evening following ingestion of a mixed meal (Cifuentes-Gomez et al., 2015). A 7-day wash-out period separated the supplementation periods and the order between CF and PL supplementation was randomised. Throughout the study period participants were instructed to maintain their normal daily activities and diet. Participants kept a food diary and were instructed to consume an identical diet in the two

periods of exercise testing. Physical activity levels were measured by accelerometry in the 6 days preceding testing via a hip-mounted activity monitor (Actigraph GT3X).

3.3.4 Experimental trials

On the 7th day of supplementation, participants were advised to consume 4 capsules 45 min prior to arrival at the laboratory. The supplementation protocol was chosen so that participants commenced exercise testing ~90 min following supplement ingestion, which coincided with reported peak plasma flavanol concentrations (Cifuentes-Gomez et al., 2015). The participants completed a series of separate “step” exercise tests from an unloaded (0 W) baseline to moderate or severe-intensity work rates for the determination of pulmonary $\dot{V}O_2$ kinetics. Tests began with 3 minutes of 0 W baseline cycling, before a step change in power output to 80% GET for 6 minutes or 60% Δ until T_{lim} . Participants sequentially completed three bouts of moderate- and one bout of severe-intensity exercise, each separated by 10 min of passive recovery. This protocol was employed with the knowledge that multiple bouts of moderate-intensity exercise do not impact the $\dot{V}O_2$ kinetics of subsequent moderate- and heavy-intensity exercise (Burnley et al., 2000a; Spencer et al., 2011a).

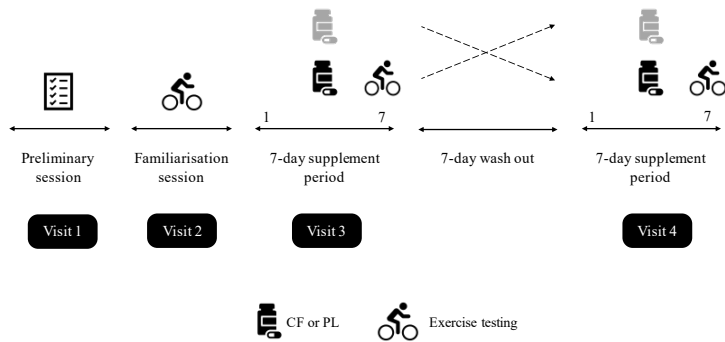


Figure 3. 2 Schematic of experimental design.

3.3.5 Measurements

After arrival to the laboratory, participants underwent an assessment of the previous 7 days physical activity levels and sedentary behaviour by the International Physical Activity Questionnaire (IPAQ) and by accelerometry (ActiGraph GTX3). Following 10 min of seated rest, participants blood pressure was measured in the brachial artery. Blood pressure was measured three times and the mean of the responses was recorded.

During all exercise tests, pulmonary gas exchange and ventilation were measured at the mouth breath-by-breath using a metabolic cart (Jaeger Oxycon Pro, Hoechberg, Germany). Participants wore a facemask and breathed through a low dead space (90 ml), low resistance ($0.75 \text{ mmHg l}^{-1} \text{ s}^{-1}$ at 15 l/s) impeller turbine assembly (Jaeger Triple V, Hoechberg, Germany). The inspired and expired gas volumes and gas concentration signals were continuously sampled at 100 Hz, the latter using paramagnetic (O_2) and infrared (CO_2) analysers (Jaeger Oxycon Pro, Hoechberg, Germany) via a capillary line connected to the mouthpiece. These analysers were calibrated before each test with gases of known

concentrations (16% O₂ and 4% CO₂), and the turbine volume transducer was calibrated using a 3-liter syringe (Hans Rudolph, Kansas City, MO). The volume and concentration signals were time aligned by accounting for the delay in capillary gas transit and analyser rise time relative to the volume signal. Breath-by-breath fluctuations in lung gas stores were corrected for by computer algorithms (Beaver et al., 1981). Heart rate was measured during all tests via short-range radiotelemetry (Polar H10, Polar Electro, Kempele, Finland). During one of the transitions to moderate- and severe-intensity exercise for both supplementation periods, a blood sample was collected from a fingertip over the last 30 s preceding the step transition in work rate and within the last 15 s of exercise. Blood samples were immediately analysed using a hand-held device (Lactate Pro, Nova Biomedical, USA) to determine blood lactate concentration. Blood lactate accumulation was calculated as the difference between blood lactate at end exercise and blood lactate at baseline.

3.3.6 Data analysis

Breath-by-breath $\dot{V}O_2$ data were edited to remove data points lying more than 3 standard deviations (SD) outside the local 5-breath mean (Lamarra et al., 1987). The resultant data were then linearly interpolated to provide second-by-second values. For $\dot{V}O_2$ and heart rate data in response to moderate exercise transitions, second-by-second data for the three transitions were averaged together to produce a single dataset. The severe-intensity exercise bout for each condition was not repeated and was modelled separately. For each exercise transition, the first 20 s of data after the onset of exercise (i.e., the cardiodynamic or phase I response) were deleted (Benson et al., 2017; McNarry et al., 2012) and a mono-exponential model (Equation 3.1) with time delay was then fitted to the data (Whipp & Rossiter, 2013), as follows:

$$\dot{V}O_{2(t)} = \dot{V}O_{2(b)} + A\dot{V}O_2 \left(1 - e^{-(t-TD\dot{V}O_2/\dot{V}O_2)}\right)$$

Equation 3. 1 Mono-exponential model

Where $\dot{V}O_2(t)$ is the $\dot{V}O_2$ at any time t , $\dot{V}O_{2b}$ is the baseline $\dot{V}O_2$, which was taken as the mean $\dot{V}O_2$ over the final 30 s of the baseline period preceding the transition, $A\dot{V}O_2$ is the amplitude of the primary response above baseline, $TD_{\dot{V}O_2}$ is the time delay of the primary response relative to the onset of exercise, and $\tau\dot{V}O_2$ is the time constant of the primary response. For moderate intensity exercise, data were modelled to 360s. For severe intensity exercise, the onset of the $\dot{V}O_2$ slow component ($TD_{SC\dot{V}O_2}$) was determined using purpose-designed programming in Microsoft Excel (Microsoft Corporation, Redmond, WA, USA), which iteratively fits a monoexponential function to the $\dot{V}O_2$ data, starting at 60 s until the window encompasses the entire response. The resulting primary time constants are plotted against time, and the $TD_{SC\dot{V}O_2}$ was identified as the point at which $\tau\dot{V}O_2$ consistently deviates from a previously 'flat' profile, and the demonstration of a local threshold in the χ^2 value (Rossiter et al., 2001). This method allows the fitting of Equation 1 to the primary component of the response isolated from the slow component, thus avoiding the possibility of arbitrarily parameterizing the slow component. The amplitude of the $\dot{V}O_2$ slow component was determined by calculating the difference between the end-exercise $\dot{V}O_2$ (i.e., mean $\dot{V}O_2$ over final 30 s of exercise) and $(A\dot{V}O_2 + \dot{V}O_{2b})$. In instances where exercise duration was too short to allow the slow component to be discerned the $\dot{V}O_2$ response was modelled using Equation 1 to the end of exercise and the slow component was assigned a value of 0.

Heart rate kinetics were modelled for each exercise transition using a monoexponential function (Equation 3.2) with the response constrained to the start of exercise (at $t = 0$; i.e., with no time delay):

Commented [DR109]: Seems to be not part of the formula

$$HR_{(t)} = HR_b + AHR * (1 - e^{(-t/\tau HR)})$$

where HR_b is the mean HR measured over the final 30 s of baseline cycling, and AHR and τHR are the amplitude and the time constant of the response, respectively.

Equation 3. 2 Monoexponential function with no time delay

3.3.7 Statistics

Based on previous knowledge of a meaningful change in $\dot{V}O_2$ during intervention studies (5 s), and a common standard deviation of 4.3 s (Benson et al., 2017), the necessary calculated sample size was 12. Differences in the cardiorespiratory variables between conditions were determined with two-tailed, paired-samples *t*-tests (GraphPad, Prism, USA). Data are presented as means±SD. Statistical significance was accepted when $P < 0.05$.

3.4 Results

Peak $\dot{V}O_2$ was $2.45 \pm 0.61 \text{ l min}^{-1}$ ($28.1 \pm 5.7 \text{ ml kg}^{-1} \text{ min}^{-1}$), with the mean GET occurring at $1.51 \pm 0.46 \text{ l min}^{-1}$ ($108 \pm 39 \text{ W}$). The peak work rate attained from the incremental test was $207 \pm 49 \text{ W}$ and the work rates calculated to require 80% of the GET and 60%Δ were $87 \pm 29 \text{ W}$ and $166 \pm 40 \text{ W}$, respectively. Levels of moderate-to-vigorous intensity physical activity were similar in the 7 days preceding experimental testing under PL and CF conditions (PL: 44.8 ± 17.9 vs. CF: $50.1 \pm 14.8 \text{ min/day}^{-1}$). Total moderate-to-vigorous physical activity (MVPA) over the 7-day supplementation period was also similar between conditions (PL: 308.4 ± 126.3 vs. CF: $332.9 \pm 99.7 \text{ min}$).

Commented [DR110]: I am not sure what is meant with this. Is this another way of presenting the peak VO2? Kg refers to body weight?

Commented [SD111R110]: Correct, peak or max VO2 is typically expressed relative to subject to body weight

Commented [DR112]: Explain term

3.4.1 Heart rate kinetics, blood lactate profiles and blood pressure

There were no differences in the primary τ HR between PL and CF for moderate- or severe-intensity bouts ($P=0.219$ and 0.956 , respectively, Table 3.1). Despite significant changes in blood lactate concentrations at T_{lim} compared to baseline ($P<0.05$; Table 3.1), there were no significant differences in blood [lactate] from pre- to post-exercise between conditions during moderate- and severe-intensity exercise (see Table 3.1). Overall, there were no differences between resting systolic (PL: 128 ± 12 vs. CF: 127 ± 12 mmHg, $P=0.66$) or diastolic (PL: 78 ± 7 vs. 78 ± 7 mmHg, $P=0.75$) blood pressure following either PL or CF administration.

Table 3. 1 Heart rate and blood lactate responses during moderate- and severe-intensity exercise following CF and PL supplementation

Parameter	HR _b (b min ⁻¹)	AHR (b min ⁻¹)	τHR (s)	End exercise HR (b min ⁻¹)	Baseline blood lactate (mM)	End exercise blood lactate (mM)	Δ blood lactate (mM)	Blood lactate at exhaustion (mM)
<i>Moderate-intensity exercise</i>								
PL	83±13	31±8	53±22	114±16	1.5±0.7	2.6±0.5	1.2±0.9	-
CF	83±14	32±8	47±13	115±18	1.3±0.4	2.5±0.7	1.3±0.8	-
<i>Severe-intensity exercise</i>								
PL	89±15	69±16	89±17	159±14	1.9±0.9	8.8±2.0	7.4±2.5	9.5±2.3 [#]
CF	92±17	67±17	89±29	160±17	1.8±0.9	8.4±2.3	7.1±2.8	9.7±1.9 [#]

HR_b, baseline heart rate; AHR, amplitude of the fundamental response; τHR, time constant of the fundamental response; PL, placebo; CF, cocoa flavanol. Values are mean±SD. [#]Significantly different from baseline blood lactate ($P<0.05$).

3.4.2 $\dot{V}O_2$ kinetics and exercise tolerance

The $\dot{V}O_2$ kinetic parameters for moderate intensity exercise are presented in Table 3.2, and the $\dot{V}O_2$ response of a representative participant to moderate-intensity exercise is shown in Figure 3.3. Compared with PL, $\tau\dot{V}O_2$ was faster during moderate-intensity exercise following CF supplementation (PL: 40 ± 12 vs. CF: 34 ± 9 s, $P=0.019$). However, there were no differences in $\dot{V}O_{2b}$ ($P=0.175$), $A\dot{V}O_2$ ($P=0.263$), $TD\dot{V}O_2$ ($P=0.961$) or end exercise $\dot{V}O_2$ ($P=0.565$) between PL and CF.

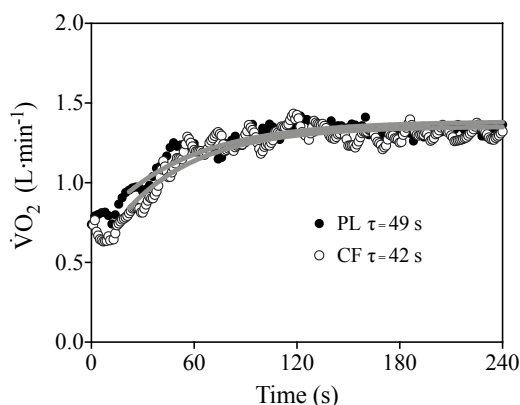


Figure 3. 3 Pulmonary $\dot{V}O_2$ and best-fit modelled responses of a representative participant to moderate-intensity exercise following PL (solid black circles) and CF (clear circles) supplementation. $\tau\dot{V}O_2$ values are displayed for each transition, with the solid grey lines representing the modelled fits.

The pulmonary $\dot{V}O_2$ response to severe-intensity exercise for a representative participant is shown in Figure 3.4A and group mean responses are shown in Figure 3.4B. The associated modelled parameters are presented in Table 3.2. No impact of CF supplementation on the $\tau\dot{V}O_2$ ($P=0.799$) for exercise initiated at 60% Δ over PL was evident. There were no differences in $\dot{V}O_{2b}$ ($P=0.246$), $A\dot{V}O_2$ ($P=0.427$), $TD\dot{V}O_2$ ($P=0.617$), $SC\dot{V}O_2$ ($P=0.887$) or end exercise $\dot{V}O_2$

Commented [DR113]: any reviewer may argue that you have to correct for multiple comparisons (table 2). What is exactly your argument that $\tau\dot{V}O_2$ was initially the parameter defined to look at? It feels a bit like pick and choose because you sum up a lot of different parameters and this is just a lucky finding (by chance)

Commented [SD114R113]: when modelling $\dot{V}O_2$ kinetics two-four variables are derived from the procedures. Adjustment for multiple comparisons could be considered, but I think the small number of derived $\dot{V}O_2$ kinetics parameters between two experimental conditions would not necessarily warrant multiple comparisons

($P=0.954$) between conditions. $TD_{SC\dot{V}O_2}$ was lower following CF vs. PL supplementation (PL: 110 ± 15 vs. CF: 95 ± 13 s, $P=0.002$). Both end-exercise $\dot{V}O_2$ ($P=0.959$) and T_{lim} ($P=0.480$) were not significantly different following PL and CF supplementation during severe-intensity exercise (see Table 3.2).

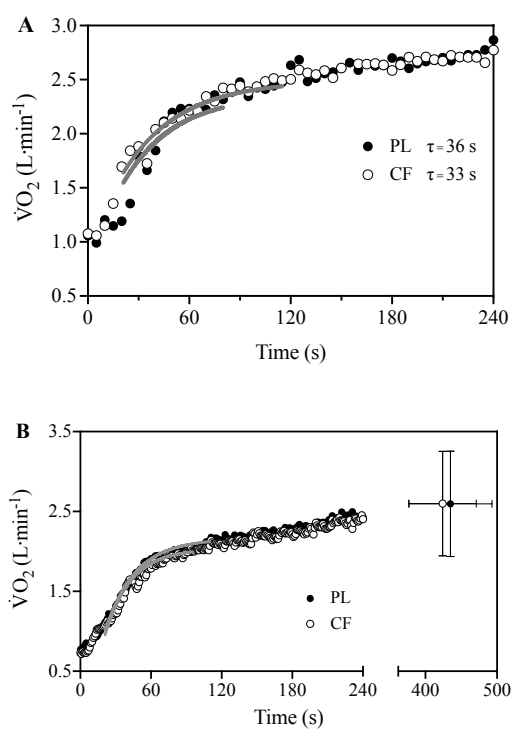


Figure 3. 4 Pulmonary $\dot{V}O_2$ and best-fit modelled responses to severe-intensity exercise following PL (solid black circles) and CF (clear black circles) supplementation. Panel A) Pulmonary $\dot{V}O_2$ responses of a representative participant displayed with associated $\tau\dot{V}O_2$. Panel B) Group mean $\dot{V}O_2$ responses during the rest-to-exercise transition following PL and CF supplementation. Group mean \pm SD $\dot{V}O_2$ at limit of exercise tolerance also shown. Solid grey lines represent the modelled fits.

Table 3. 2 Pulmonary O₂ uptake responses to moderate- and severe-intensity exercise following CF and PL supplementation

Parameter	$\dot{V}O_{2b}$ (l min ⁻¹)	$A\dot{V}O_2$ (l min ⁻¹)	TD $\dot{V}O_2$ (s)	$\tau\dot{V}O_2$ (s)	End exercise $\dot{V}O_2$ (l min ⁻¹)	TD _{SC$\dot{V}O_2$} (s)	SC $\dot{V}O_2$ (l min ⁻¹)	T _{lim} (s)
<i>Moderate-intensity exercise</i>								
PL	0.69±0.12	0.77±0.32	13±6	40±12	1.50±0.35	-	-	-
CF	0.66±0.13	0.79±0.34	13±7	34±9*	1.50±0.38	-	-	-
<i>Severe-intensity exercise</i>								
PL	0.78±0.14	1.40±0.40	17±4	27±9	2.60±0.66	110±15	0.50±0.20	435±58
CF	0.74±0.13	1.50±0.52	16±4	28±6	2.60±0.65	95±13*	0.50±0.20	424±47

$\dot{V}O_{2b}$, baseline oxygen uptake; $A\dot{V}O_2$, amplitude of the primary response; TD $\dot{V}O_2$, time delay of the primary response; $\tau\dot{V}O_2$, time constant of the primary response; TD_{SC $\dot{V}O_2$} , time delay of the $\dot{V}O_2$ slow component; SC $\dot{V}O_2$, magnitude of the slow component; T_{lim}, limit of exercise tolerance; PL, placebo; CF, cocoa flavanol. Values are mean±SD. *Significantly different from PL ($P<0.05$).

3.5 Discussion

The objective of this study was to investigate the impact of CFs on pulmonary $\dot{V}O_2$ kinetics during two intensities of cycling exercise in healthy, normotensive middle-aged individuals. Congruent with the hypothesis, the major finding of this study was that 7-days CF supplementation sped pulmonary $\dot{V}O_2$ kinetics during moderate-intensity exercise as demonstrated by a significant reduction in $\tau\dot{V}O_2$. These effects of CFs, however, were not apparent during severe-intensity exercise when compared with a PL. Ultimately, the findings of the present study may have clinical potential in contributing to improved tolerance of daily life activity in middle-aged adults.

This study is the first to investigate whether CFs modulate pulmonary $\dot{V}O_2$ kinetics. Here, 7 days CF supplementation significantly reduced the $\tau\dot{V}O_2$ (40 vs. 34 s) associated with the transition from unloaded to moderate intensity cycling in middle-aged adults. Notably, the magnitude of change in $\tau\dot{V}O_2$ (~6 s) reported is important, as it exceeds the minimum physiologically relevant change of ~5 s (Benson et al., 2017). The reduction in $\tau\dot{V}O_2$ observed after CF supplementation in our middle-aged individuals reflects a shift towards values typically observed in younger healthy individuals (B. Grassi et al., 2009), whereby $\dot{V}O_2$ kinetics are not limited by O_2 delivery *per se* (Poole & Jones, 2012). Theoretically, a lowered $\tau\dot{V}O_2$ would reduce the O_2 deficit incurred during the exercise transition, thereby causing less perturbations to the intracellular milieu (i.e., Δ phosphocreatine, ADP, H^+ , inorganic phosphate, glycogen) and enhancing exercise tolerance (Goulding et al., 2017, 2018; Grassi et al., 2011). Therefore, the data suggest CFs may lower the O_2 deficit incurred during moderate-intensity activity by negating age-associated impairments to pulmonary $\dot{V}O_2$ kinetics.

Since the purpose of the study was to examine the impact of CFs on $\dot{V}O_2$ kinetics, the data raise questions about the potential underlying mechanisms contributing to the lowered $\tau\dot{V}O_2$ with CF supplementation. It is acknowledged $\tau\dot{V}O_2$ is sensitive to manipulations in O_2 delivery (DeLorey et al., 2004b; Gurd et al., 2009), and, that the slowing of $\dot{V}O_2$ kinetics with advancing age occurs at least partly as a consequence of lowered O_2 availability in oxidative skeletal muscle (Behnke & Delp, 2010a; DeLorey et al., 2004a; Musch et al., 2004a). Given that CFs exert potent NO-dependent vasodilatory effects (Cifuentes-Gomez et al., 2015; Decroix, et al., 2018a; Schroeter et al., 2006), CF supplementation may have sped $\dot{V}O_2$ kinetics by augmenting muscle blood flow and O_2 availability. Although, it is important to acknowledge CFs can alter indices of mitochondrial biogenesis and function (Kopustinskiene et al., 2015a; Taub et al., 2012), as well as lower markers of oxidative stress (Ahmed et al., 2020). Together these factors may also influence $\dot{V}O_2$ responses to exercise by augmenting the capacity for O_2 utilisation and delivery. Clearly, further work is required to determine the mechanisms by which CFs may regulate blood flow and changes in $\dot{V}O_2$ kinetics.

In spite of differences in the kinetics of $\dot{V}O_2$, no changes in the O_2 cost of moderate-intensity exercise were observed after CF supplementation. Similarly, Patel and colleagues (2015) demonstrated no significant reduction in $\dot{V}O_2$ during twenty minutes of moderate-intensity cycling after 14 days dark chocolate supplementation (Patel et al., 2015). Together these findings contrast those published employing alternate dietary means of augmenting NO bioavailability, such as dietary nitrate, which reduces the O_2 cost of moderate-intensity activity (Bailey et al., 2009; Lansley et al., 2011; Larsen et al., 2007; Vanhatalo et al., 2010). Such discrepancies may be explained by recent evidence linking dietary nitrate to improved contractile function (Bailey et al., 2019), an effect that has not been reported with CF

supplementation. Possibly, the mechanisms by which CFs impact physiological responses to exercise relate to muscle O₂ delivery rather than contractile function. Given that measures of NO or redox biomarkers were not taken, it is not clear to what extent CFs sped phase II $\dot{V}O_2$ kinetics through processes associated with reactive O₂ and nitrogen species. Additional research will help delineate CFs mode of action in the context of exercise.

In contrast to the observations during moderate-intensity exercise, acute CF supplementation had no measurable impact on pulmonary $\dot{V}O_2$ kinetics during severe-intensity cycling. For instance, the $\tau\dot{V}O_2$ of the phase II response was similar between PL and CF (27 vs. 28 s, respectively). The kinetics of $\dot{V}O_2$ are considered an important determinant of exercise tolerance (Grassi et al., 2011; Whipp & Ward, 1992). In line with this principle, no effect of CF supplementation on T_{lim} during severe-intensity exercise was found. Whilst no previous studies have examined the impact of CF supplementation on $\dot{V}O_2$ kinetics in the severe-intensity exercise domain, a number have studied their effects on exercise performance. The present findings corroborate these data, showing no beneficial impact of acute or sub-chronic CF supplementation on time-trial or time-to-exhaustion performance in healthy male adults (Allgrove et al., 2011; Davison et al., 2012; Decroix, Tonoli, et al., 2018; Peschek et al., 2013; Stellingwerff et al., 2014).

The data demonstrate divergent effects of CFs on $\dot{V}O_2$ kinetics between moderate- and severe-intensity exercise domains. Given that the pattern of muscle-fibre activation within moderate- and severe-intensity exercise domains differs (type I and type II predominant, respectively) (Krustrup et al., 2004), future studies should investigate a potential muscle fibre-type dependency of CF supplementation on the physiological responses to exercise. Another potential explanation for the differences between exercise intensity domains presented herein

relates to the dose of CFs administered. Recent published evidence suggests that the 400 mg CF prescribed is the minimum dose necessary to exert beneficial effects during exercise (Decroix et al., 2018a). Therefore, the dose used in the present study may not have been high enough to raise blood flow sufficiently to detect a measurable effect upon $\dot{V}O_2$ kinetics during severe-intensity exercise. In addition, CFs had no beneficial impact on resting systolic or diastolic blood pressure over PL, which may be attributable to insufficient dosage and the normotensive population studied (Hooper et al., 2012).

3.6 Limitations

The experimental design of this study did not include measures of any blood or muscle biomarkers. Therefore, no biochemical or mechanistic information could be derived that may have afforded explanations of the faster $\dot{V}O_2$ kinetics observed with acute cocoa-flavanol supplementation. More specifically, it could not be established whether NO or redox markers were influenced by cocoa-flavanol supplementation. Besides these markers, vascular endothelial function and/or muscle oxygenation were also not measured as part of this randomised placebo-controlled study. Such measures would have been valuable in providing information on whether cocoa-flavanols sped $\dot{V}O_2$ kinetics due to changes along the O_2 transport pathway. Another limitation of this experimental design was the inclusion of a single severe-intensity exercise bout to model the phase II $\dot{V}O_2$ kinetics. This single bout reduced the confidence in the modelling parameters, but additional bouts would have required a minimum of two additional testing days that were not feasible with the chosen study design and population. Here, a single severe-intensity exercise bout was performed following three bouts of moderate-intensity exercise, with prior knowledge that moderate exercise does not influence the phase II $\dot{V}O_2$ kinetics of subsequent heavy intensity exercise (Burnley et al., 2000b; Spencer et al., 2011b). Nevertheless, it is possible that prior moderate intensity exercise, through its

Commented [CS115]: We did have ethics to take blood samples and I thought you did do some early measures?

effects on (muscle) perfusion, sped the phase II $\dot{V}O_2$ kinetics response during severe-intensity exercise in the population studied (Scheuermann et al., 2002). A 400 mg daily cocoa-flavanol dose was prescribed in this study, which is the minimum dose necessary to exert beneficial vascular effects during exercise (Decroix, Soares, et al., 2018b). Therefore, the dose administered may not have been high enough to raise blood flow sufficiently to detect a measurable effect upon $\dot{V}O_2$ kinetics during severe-intensity exercise, although vasodilation responses may already have been maximised by the severe-intensity exercise stimulus.

3.7 Conclusion

In the present study, seven days supplementation with a flavanol-rich cocoa-extract resulted in a reduced $\tau\dot{V}O_2$ during moderate-, but not severe-intensity exercise in normotensive, middle-aged adults. Whilst the O_2 cost of exercise was similar between CF and PL conditions, the phase II $\dot{V}O_2$ kinetics were sped at the onset of moderate-intensity exercise after acute CF intake. Such effects on phase II $\dot{V}O_2$ kinetics were not found during severe-intensity exercise with CF. Whilst the mechanism(s) responsible for CFs effects upon phase II $\dot{V}O_2$ kinetics are not known, subsequent chapters in this thesis will determine whether flavonoids impact vascular endothelial and skeletal muscle cell function. Overall, CF supplementation may reduce the metabolic perturbations associated with moderate-intensity exercise in middle-aged adults through speeding phase II $\dot{V}O_2$ kinetics.

Commented [TD116]: would be nice if you could link the findings from this chapter to the next ones. You find some interesting things. How can you explain them? You can highlight it may relate to some mechanisms, that you then indicate you will explore in the next chapters (and then be very specific on the mechanisms and chapters).

Chapter 4: The impact of dietary flavonoids on mitochondrial function and reactive oxygen and nitrogen species in HUVECs

4.1 Abstract

Introduction: Sedentary ageing is associated with impaired vascular endothelial function that is characterised by lowered nitric oxide (NO) bioavailability. Several factors contribute to lowered NO bioavailability with older age, including increased production of reactive oxygen species (ROS), mitochondrial dysfunction and altered cell signalling. Flavonoids may mitigate oxidative stress and interact with mitochondria *in vivo*, but their effects on vascular endothelial cells *in vitro* are poorly understood.

Objective(s): The primary objectives of this study were: 1) To examine whether flavonoid treatment modulates ROS production and NO bioavailability of human vascular endothelial cells (HUVECs). 2) To investigate the impact of flavonoid treatment on indices of mitochondrial function and cell signalling of HUVECs. It was hypothesised that flavonoids would attenuate ROS production, increase NO bioavailability and enhance indices of mitochondrial function and cell signalling.

Methods: HUVECs were treated with the flavonoids quercetin (Q), epigallocatechin-gallate (EGCG) or (-)-epicatechin (EPI) at micromolar concentration for up to 48 h. Mitochondrial and non-mitochondrial specific ROS was measured in the absence and presence of antimycin A (AA). Genes associated with mitochondrial remodelling and the antioxidant response were quantified over 48 h using RT-qPCR. Mitochondrial bioenergetics were investigated by respirometry after 24 h and signalling responses examined, by western blotting, in the presence or absence of EPI.

Results: In the absence of AA, MitoSOX oxidation was 54% lower, but 280% higher vs. CTRL with 5 and 10 μM Q ($P=0.035$ and $P=0.011$, respectively). EGCG lowered MitoSOX oxidation by ~85% in the absence of AA ($P<0.0001$), regardless of dose. With AA, 5 and 10 μM EGCG lowered MitoSOX oxidation by 42 and 74%, respectively ($P<0.0001$). MitoSOX oxidation without AA was increased 32% and decreased 53% after 5 and 10 μM EPI vs. CTRL. With AA, only 10 μM EPI increased MitoSOX oxidation vs. CTRL (25%, $P<0.0001$). NO bioavailability was increased by 45% with 10 μM EPI vs. CTRL ($P=0.01$). NRF2 expression was increased 1.5- and 1.6-fold with 5 and 10 μM EPI over 48 h vs. CTRL ($P=0.015$ and $P=0.001$, respectively). However, flavonoids did not impact mitochondrial respiration. EPI transiently increased ERK1/2 signalling (2.9 and 3.2-fold over 15 min and 1 h vs. 0 h, respectively; $P=0.035$ and $P=0.011$) and suppressed AMPK.

Conclusion(s): Despite flavonoids differentially impacting mitochondrial ROS production and gene expression profiles in HUVECs, they did not directly modulate mitochondrial respiration.

Commented [CS117]: This may change slightly, depending on chapter order

Commented [CS118]: What was the hypothesis that these objectives underpin? Please add.

Commented [DR119]: Or: 'human endothelial cells' (explaining later in methods which type)

Commented [HJ120]: Again is this the wording at the end of the literature review

Commented [DR121]: Too specific for an abstract

Commented [DR122]: Why, what is the function of AA?

Commented [SD123R122]: Save explanation for methods?

Commented [CS124]: What genes – provide loose categories, if nothing else

Commented [DR125]: Define as you mention this here for the first time

Commented [SD126R125]: Name of assay probe, could refer to as mitochondrial ROS instead if this better suits?

Commented [CS127]: If your abstract were the only thing published, this results section would not really tell your reader what your findings were, it is nicely written but descriptive. Ideally, include some data e.g. key and significant fold changes with p values.

EPI may afford mitochondrial adaptations via induction of NO, NRF2 and ERK1/2 signalling, independent of AMPK activation. EPI shows potential as a hormetic compound and requires further study in the context of sedentary ageing.

Commented [CS128]: First mention of this. Need this sort of info in the results before you can draw a conclusion.

Commented [CS129]: Would be nice to add an impact statement e.g. what is the benefit of this new knowledge.

Commented [DR130]: Why quercetin not, also showing opposing effects on MitoSOX

Commented [SD131R130]: Have focused on EPI in conclusion given the focus on this towards the end of the chapter, can add more detail if you feel necessary

4.2 Introduction

One of the primary limitations to $\dot{V}O_2$ kinetics in older adults is alleged to reside along the O_2 transport pathway (Murias & Paterson, 2015a). Indeed, both reduced flow and altered distribution of microvascular blood to glycolytic (type II) skeletal muscle fibres contributes to reduced O_2 delivery during exercise (Behnke & Delp, 2010b; Muller-Delp et al., 2002b; Murias et al., 2010b; Musch et al., 2004b). Consequently, the precise coupling of metabolic demand with O_2 delivery is dysregulated in older age, which exacerbates the O_2 deficit during the rest-to-work transition (Alexander et al., 2003b; Murias et al., 2010b). The vascular endothelium plays a central role in the regulation of vasodilation and blood flow (and therefore O_2 delivery), but advancing age is known to impair endothelium-dependent vasodilation (Celermajer et al., 1994; Thijssen et al., 2006; Vita et al., 1990), which is partly dependent on lowered NO bioavailability (Singh et al., 2002b; Taddei et al., 2000b).

Nitric oxide is essential for vasodilatory responses, and its availability in the endothelium is modulated by eNOS content, activation and the production of ROS (Cernadas et al., 1998a; Chou et al., 1998; Donato et al., 2007b, 2009b). Critically, the ageing vascular phenotype is characterised by lowered eNOS expression and activity (Cernadas et al., 1998b; Chou et al., 1998; Donato et al., 2009a). In addition, the ageing vasculature is associated with increased ROS production and elevated oxidative stress (Csiszar et al., 2002b, 2007; Donato et al., 2007b; Hamilton et al., 2001; Jablonski et al., 2007; Sun et al., 2004; Van Der Loo et al., 2000b), that may be cytosolic (Adler et al., 2003b; Csiszar et al., 2002a; Van Der Loo et al., 2000a) and/or mitochondrial in origin (Donato et al., 2007a; Durrant et al., 2009a; Ungvari et al., 2007; Zhou et al., 2009).

Commented [CS132]: I wonder if it is worth putting an additional paragraph in the intro to cover the genes you assess and their relevance – that way your examiners know what is coming. At the moment, I think the genes are undersold.

Commented [CS133]: Same comment as above for the signalling e.g. relating to the proteins you have selected and how they fit into the story.

Commented [DR134]: This OK for thesis but a bit of a strange start when you expect to read about in vitro experiments. Can't you describe this in more layman words, e.g., 'adapting the use and consumption of oxygen to the metabolic demand'?

Commented [SD135R134]: I agree about being an odd intro, would definitely change this if it were intro for a paper

Commented [DR136]: Yes these are better layman's words 😊

Commented [DR137]: Where?

Commented [SD138R137]: Have added detailed here

Although endothelial cells are considered to meet two thirds of their energy requirements via glycolysis (Culic et al., 1997), mitochondrial dysfunction can pose significant challenges to the maintenance of vascular endothelial cell health. For instance, ageing is associated with lowered mitochondrial contents in endothelial cells of conduit and feed arteries, as well as capillaries (Burns et al., 1979; Park et al., 2018b; Park et al., 2018; Ungvari et al., 2008a). Reductions in vascular endothelial mitochondrial protein with older age may be due to blunted transcriptional responses (Park et al., 2018; Ungvari et al., 2008a), as a result of diminished [NO] bioavailability (Gouill et al., 2007; Miller et al., 2013) and/or lowered AMP-activated protein kinase (AMPK) signalling (Lesniewski et al., 2012). Consequently, aged organelles exhibit impaired bioenergetics compared to young counterparts. Indeed, the mitochondrial oxidative respiratory capacity and coupling efficiency of aged human skeletal muscle feed arteries is lowered in middle-aged (55 years) and old (70 years) adults compared to young (Park et al., 2018b, 2020). Taken together, vascular endothelial mitochondria and ROS may represent therapeutic targets for interventions aimed at improving vascular endothelial function in advancing age.

Dietary flavonoids are a class of polyphenols linked with positive health effects, particularly in relation to cardiovascular function (Arts et al., 2001; Hertog et al., 1993b). Whilst the antioxidant potential of flavonoids has long been appreciated (Williamson et al., 2018), less is known about their potential interaction with mitochondria. Interestingly, flavonoids have been reported to interact with mitochondrial proteins (Lagoa et al., 2011; Lang & Racker, 1974a; Zheng & Ramirez, 2000a), and even regulate mitochondrial bioenergetics (Dorta et al., 2005; Keller et al., 2020; Rowley et al., 2017a). Although the potential of flavonoids to interact with these organelles is recognised, the precise mode of action of flavonoids on vascular endothelial mitochondria is not known, with only limited data available on how specific flavonoids such as quercetin (Q), epigallocatechin-gallate (EGCG) and (-)-epicatechin (EPI) modulate

Commented [CS139]: Production or availability?

Commented [CS140]: Age and gender

Commented [CS141]: Age and gender

Commented [CS142]: Initial reference with his finding or a current review

Commented [CS143]: If this is spelled out on the first use in each chapter, you can just use the abbreviations here for all flavonoids.

mitochondrial bioenergetics in vascular endothelial cells. In chapter 3, cocoa-flavanol supplementation sped phase II pulmonary oxygen uptake ($\dot{V}O_2$) kinetics during moderate-intensity exercise, but the underlying mechanisms are not well understood.

Commented [TD144]: Good one!!

Commented [SD145]: Linker to human study

To this end, the primary aim of this study was to use dietary flavonoids to enhance mitochondrial function and attenuate ROS production in human vascular endothelial cells (see Figure 4.1). The two main study objectives were: 1) To examine whether flavonoid treatment modulates ROS production and NO bioavailability of HUVECs. 2) To investigate the impact of acute flavonoid treatment on indices of mitochondrial function and cell signalling in HUVECs. We hypothesised that flavonoid treatment would attenuate ROS production, augment NO bioavailability and enhance indices of mitochondrial function and signalling of HUVECs.

Commented [HJ146]: Now use aim again? Check wording matches abstract and lit review

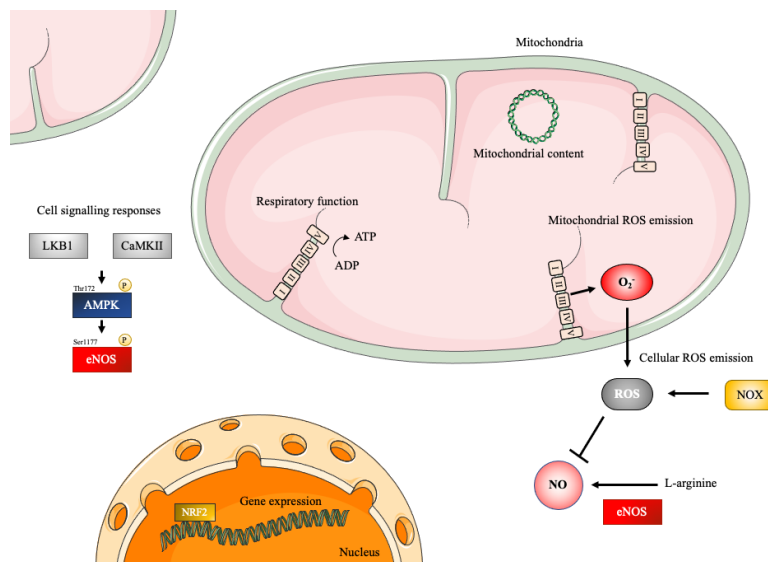


Figure 4. 1 Schematic of the cellular and molecular processes investigated in this study.

4.3 Methodology

4.3.1 Cell culture and treatment

Human umbilical endothelial vein endothelial cells (HUVECs; Thermo Fisher Scientific, Waltham, MA, USA) were purchased from), at passages 3-7 were used in this study. HUVECs were not passaged more than 8 times because changes in HUVEC phenotype can occur with multiple population doublings, that ultimately lead to cell senescence (Chang et al., 2005; Cheung, 2007; Grillari et al., 2000). For standardised cell culture procedures, see section 2.4. Following the plating of cells onto appropriate well-plates in complete endothelial cell growth medium (EGM; Cell Applications Inc, San Diego, CA, USA), ~80% confluent HUVECs were washed twice with D-PBS and switched to pre-warmed (37°C) EGM in the absence, or presence of specific concentrations of Q, EGCG and EPI (0-20 µM) over 24 h (cell viability, ROS production, NO bioavailability, gene expression, respiration and western blotting) and 48 h (gene expression) with Q, EGCG and EPI (0-20 µM). Gene expression was quantified over 48 h to understand whether repeated flavonoid doses over a longer time course would alter mRNA levels, which would somewhat mimic the repeated ingestion of cocoa flavanols over days in Chapter 3.

Commented [CS147]: Worth putting in () after each timepoint what was measured? Eg 24 (a,b, and c were assessed) and 48 h (x and y were assessed)

4.3.2 Cell viability assay

The fluorescent CyQUANT® Proliferation Assay kit was used to determine cell viability. HUVECs were grown to 60-70% confluency in Endothelial Cell Growth Medium (EGM) (Cell Applications Inc, San Diego, USA) in 96-well plates. Cells were dosed for 24 h in EGM +/- Q, EGCG or EPI at 0-20 µM. After 24 h, wells were aspirated, washed twice with Dulbecco's phosphate-buffered saline (D-PBS), and then frozen immediately at -80°C. On the day of the assay, plates were thawed at room temperature and 100 µL CyQUANT® GR dye/cell-lysis

Commented [CS148]: All your sections and subsections will need numbering e.g. if this is chapter three, methodology would be 3.2 and viability would be 3.2.1 etc. Figures will be 3.1 to 3. X etc

Commented [SD149R148]: Will sort this in the full thesis draft

Commented [DR150]: This section should start with the source of HUVEC. Also, very important here, where they primary? If not, which passage? Did you use different passages and if so was there an ageing effect noticeable with later passages?

Commented [CS151]: Spell out on first use

buffer was added to each well. Plates were gently mixed on an orbital shaker (80 rpm) for 5 minutes protected from light. Sample fluorescence was measured using a CLARIOStar Plate Reader (BMG Labtech, Ortenberg, Germany) with Excitation 485-12 and Emission EM520 filters in bottom reading, well scanning mode.

4.3.3 MitoSOX assay

Mitochondrial derived superoxide was detected in adherent HUVECs using MitoSOX (Thermo Fisher Scientific, Waltham, USA), a hydroethidine probe which is targeted to the mitochondria by a conjugated triphenyl-phosphonium moiety. In the presence of mitochondrial superoxide, and to some extent hydrogen peroxide (Robinson et al., 2006; Zielonka & Kalyanaraman, 2010), MitoSOX is oxidised to fluorescent products which are readily detected fluorometrically. HUVECs were seeded at 3×10^4 cells/mL in 12-well microplates and at ~80% confluence (typically 48 h later), washed in Krebs-Ringer buffer (KRH; 135 mM NaCl, 3.6 mM KCl, 10 mM HEPES (pH 7.4), 0.5 mM MgCl₂, 1.5 mM CaCl₂, 0.5 mM NaH₂PO₄, 2 mM glutamine and 5 mM D(+)-glucose) prior to incubation at 37°C for 30 minutes, with or without 15 µM of the complex III inhibitor antimycin A (AA) as a positive control. Next, AA-containing KRH was removed and MitoSOX was loaded into cells in fresh pre-warmed KRH to a final concentration of 2.5 µM. Plates were immediately transferred to a multimode plate reader (ClarioStar, BMG Labtech), and fluorescence was monitored continuously at 30-sec intervals over 30 min. Fluorescent MitoSOX oxidation products were excited at 510 nm and light emission was detected at 580 nm. The plate reader's focal height and gain were optimised and fixed between different experiments. Since MitoSOX is primarily oxidised by mitochondrial superoxide, the rate at which mitochondrial superoxide was produced could be determined from the slope of the resultant progress curve over the 30-minute period post MitoSOX loading. Upon completion of the 30-min reading, plates were immediately fixed for

Commented [CS152]: Rpm?

Commented [CS153]: (manufacturer details)

Commented [CS154]: (source details)

Commented [CS155]: Could you explain this at viva if asked?

Commented [DR156]: It is not immediately clear from this text why you are doing this

Commented [SD157R156]: Have put in text saying this is a positive control

Commented [CS158]: Why this time frame – random or is there a purpose – may get asked at viva

the determination of cell density by the SRB assay (see section 2.14), which was used to normalise obtained fluorescence values.

4.3.4 CellROX Assay

Cellular reactive oxygen species (ROS) were detected using the CellROX[®] Deep Red reagent by spectrophotometry. The cell-permeant dye is non-fluorescent while in a reduced state and exhibits bright fluorescence upon oxidation by cellular ROS. Briefly, HUVECs were seeded at 3×10^4 cells/mL into 12-well microplates and at ~80% confluence treated with flavonoids for 24 h. After treatment, HUVECs were washed in Krebs-Ringer buffer (KRH) with or without 15 μ M antimycin A (AA) and incubated at 37°C for 30 minutes, prior to KRH removal and CellROX loading using fresh, pre-warmed KRH buffer, to a final concentration of 2.5 μ M. Following 30 minutes CellROX incubation, cells were washed 2 \times with D-PBS and immediately transferred to a plate reader (ClarioStar, BMG Labtech), where fluorescent CellROX oxidation products were excited at 640 nm and light emission detected at 665 nm. The plate reader's focal height and gain were optimised and fixed between experiments. Upon completion of the reading, plates were immediately fixed for the determination of cell density by the SRB assay (see section 2.14, Chapter 2), which was used to normalise obtained fluorescence values.

4.3.5 DAF-FM (Nitric oxide detection)

For the determination of intracellular NO bioavailability, HUVECs were plated in gelatin-coated 12-well plates in EGM and incubated (37°C, 5% CO₂) until ~80% confluency. Once confluent, cells were treated with 0, 5 or 10 μ M Q, EGCG or EPI for 24 h. After treatment, HUVECs were washed 2 \times with D-PBS and loaded with DAF-FM[™] diacetate (4-amino-5-methylamino-2',7'-difluorofluorescein diacetate; Molecular Probes, Invitrogen). Cells were

Commented [CS159]: At what wavelength?

Commented [DR160]: Did you check the effect of the single flavonoids on the fluorescence signal without the cells?

Commented [SD161R160]: Good point, because of washes and switching cells to flavonoid free KRH buffer, did not include cell free flavonoid only conditions – although did do a cell free KRH buffer only condition

Commented [CS162]: On first use in each chapter, please also detail the sources of the flavonoids

Commented [DR163]: Why did you incubate for 24 hours? Usually, flavonoid blood concentration peak within a hour and are rapidly metabolized. In 24 hours the flavonoids may also become metabolized

Commented [SD164R163]: Great point and it is a limitation. Further work should consider performing a time-course experiment. We chose 24 h because same time course was used for ROS/gene expression experiments and wanted to keep this consistent

loaded with DAF-FM™ to a final concentration of 1 μM in KRH buffer and incubated at 37°C for 45 minutes protected from light. Following dye loading, cells were washed 2 × with D-PBS and immediately trypsinised prior to pelleting and resuspension in D-PBS, before measuring sample fluorescence by flow cytometry (BD Accuri C6, BD Biosciences, Wokingham, UK). Data were recorded from 5,000 events.

4.3.6 RT-qPCR – Gene expression quantification

HUVECs were lysed in 125 μL TRIzol and total RNA was then extracted using the phenol-chloroform method (see section 2.12.1). RNA concentration (300.5 ± 101.1 ng/μL; n=3, in duplicate, per condition) and purity (1.96 ± 0.14 A₂₆₀/A₂₈₀) were determined by spectrophotometry (NanoDrop™ 2000, Thermo Fisher Scientific, Waltham, USA). Samples were diluted in nuclease-free H₂O to a concentration of 7.95 ng/μL, enabling the addition of 35 ng RNA per PCR. Total reaction volume equalled 10 μL/sample, which contained 5.6 μL of master mix (5 μL QuantiFast Sybr® Green, 0.5 μL primer, 0.1 μL reverse transcriptase) and 4.4 μL RNA sample. Specific primers used in each PCR are outlined in Table 4.1. After preparation, reaction tubes (Qiagen, UK) were transferred to a Rotor-Gene Q PCR thermal cycler for product amplification using a one-step protocol (QuantiFast SYBR® Green RT-PCR Kit, Qiagen, UK). The amplification protocol was as follows: reverse transcription (10 minutes at 50°C), transcriptase inactivation and initial denaturation (95°C for 5 min) followed by 40 × amplification cycles consisting of: 95°C for 10 s (denaturation) and 60°C for 30 s (annealing and extension); followed by melt curve detection. Critical threshold (C_T) values were derived from setting a threshold of 0.09 for all genes (see Figure 2.8). The amplification efficiencies were analysed for all reactions (90.0 ± 4.7%) and values between 80-100% were accepted as efficient. To quantify gene expression, C_T values were used to quantify relative gene expression using the comparative Delta Delta C_T (2^{-ΔΔCT}) equation (Livak & Schmittgen, 2001), whereby

Commented [CS165]: Why different to the first 2 assays? Could this have been via plate reader as above?

Commented [CS166]: N=? replicates=?

Commented [CS167]: Same question as above

Commented [CS168]: What kit and which manufacturer?

Commented [CS169]: Could you explain this to the examiners? Would the annealing temp ever change – primer dependent?

Commented [CS170]: This would not mean anything to someone who does not run PCR – worth putting in a representative figure here and showing where the C_T is and explaining why 0.09 was selected and maintained e.g. not changed across different genes

Commented [SD171R170]: Will refer to chapter 2 for this?

Commented [CS172]: N=? replicates=?

Commented [CS173]: Is this the real range, or was it from 85%?

the expression of the gene of interest was determined relative to the internal reference gene (RPL13a) in the treated sample, compared with the untreated zero-hour control.

Table 4. 1 Primer sequences for *homo sapiens* with product length. All primers were used under the same cycling conditions.

Gene	Accession	Sequence		Product length (bp)
		Forward/Reverse or Anchor	Nucleotide	
RPL13a	NM_012423.4	F: GGCTAAACAGGTA	CTGCTGGG R: GGAAAGCCAGGTA	104
CAT	NM_001752	AN: 1649		134
SOD2	NM_000636	AN: 194		132
DNM1L (DRP1)	NM_012062.5	F: CACCCGGAGACCTCTCATTC	R: CCCATTCTTCTGCTTCCAC	99
MFN2	NM_014874.4	F: CCCCTTGCTTTTATGCTGATGT	R: TTTGGGAGAGGTGTGCTTATT	168
PPARGC1A (PGC-1 α)	NM_001330751.2	F: TGCTAAACGACTCCGAGAA	R: TGCAAAGTTCCCTCTCTGCT	67
SIRT1	NM_012238	AN: 1382		109
TFAM	NM_003201	AN: 462		143
NOS3 (eNOS)	NM_000603.5	F: AACTATTCCTGTCCCCGGC	R: AGGATGTGCGCTTCACTCG	173
CYBB (NOX2)	NM_000397.4	F: GGGCTGTTCAATGCTTGTGG	R: GGCCATCAACCGCTATCTT	80
NOX4	NM_016931.5	F: CAGTCCTCCGTTGGTTTGC	R: CAAAAGTTTCCACCGAGGACG	189
PRKN (PARKIN)	NM_004562	AN: 747		91
GABPA (NRF2)	NM_002040.4	F: AAATTGAGATTGATGGAACAGAGAA	R: TATGGCCTGGCTTACACATTCA	95

Commented [DR174]: I can't find any explanation in the text why you are interested to measure these genes specifically. Explain their potential role in mitochondrial activity (see also next table)

4.3.7 Mitochondrial Bioenergetics

Mitochondrial respiration was measured in adherent HUVECs using a Seahorse XFe24 Analyzer (Agilent, Santa Clara, CA, USA). HUVECs (passages 4-6) were seeded in XFe24 well plates (Agilent, Santa Clara, CA, USA) at 30,000 cells per well in 200 μ L EGM over 48 h for measurements. After 48 h, HUVECs were washed twice with D-PBS and replaced with fresh EGM containing 0, 5 and 10 μ M of Q, EGCG or EPI for 24 hours. Sensor cartridges for the XFe24 Analyzer were hydrated by loading each well with 1 mL XF Calibrant (Agilent, Santa Clara, CA, USA) solution at 37°C in a non-CO₂ incubator in the 24 h preceding the assay.

Commented [CS175]: ?EGM Please replace growth medium with EGM throughout, after your first definition in this chapter

On the day of the assay, HUVECs were washed with 500 μ L pre-warmed unbuffered Dulbecco's Modified Eagle Medium (DMEM) (Agilent, Santa Clara, CA, USA), pH 7.4. The cells were incubated in this buffer for 45 minutes at 37°C in a non-CO₂ incubator and then transferred to a Seahorse XFe24 extracellular flux analyser (maintained at 37°C). After an initial 10-minute calibration, oxygen consumption rates (OCR) were measured by a 3-4 loop cycle consisting of a 1-min mix, 2-min incubate and 3-min measure to record cellular basal respiration. After measuring basal respiration, 2 mM oligomycin was added to selectively inhibit the mitochondrial ATP synthase. Subsequently, 3 μ M BAM15 and a mixture of 2 μ M rotenone and 2 μ M antimycin A were added sequentially to, respectively, 1. uncouple oxygen consumption rates with ATP synthesis rates to determine maximal respiration or 2. inhibit complex I and III of the electron transport chain to determine non-mitochondrial respiration. Rates of oxygen consumption and extracellular acidification (ECAR) were expressed relative to the cell number of the appropriate well. Three independent experiments were performed to

Commented [CS176]: Already spelled out? If not, do so here.

assess mitochondrial respiration, each containing at least two technical replicates. The Wave software native to the XF Analyzer was used to extract OCR's and ECAR.

4.3.8 SDS-PAGE and immunoblotting

Total protein and phosphoprotein levels were detected in HUVECs by Western blot (see section 2.13 for further details). Following treatment (vehicle CTRL or 5 μ M EPI), HUVECs were lysed and scraped in ice-cold 1x radioimmunoprecipitation assay (RIPA) buffer containing: 25 mM Tris-HCl pH 7.6, 150 mM NaCl, 1% NP-40, 1% sodium deoxycholate and 0.1% SDS, supplemented with 1x Protease Inhibitor Cocktail Set V (Merck Life Science, UK). Cell lysates were centrifuged for 15 minutes at $18,000 \times g$ (4°C) and the supernatant was stored at -80°C before analyses for total protein. Protein concentrations of samples were determined by the Pierce BCA™ assay (section 2.15), and samples were subsequently resuspended in 4x Laemmli buffer (Bio-Rad laboratories, Hertfordshire, UK) containing reducing agent (1x working concentration: 31.5 mM Tris-HCl [pH 6.8], 10% glycerol, 1% SDS, 0.005% Bromophenol Blue and 355 mM 2-mercaptoethanol). Samples (22.5 μ g) were loaded and electrophoresed on 10% SDS-stain-free polyacrylamide gels. Semi-dry transfer of proteins to a nitrocellulose membrane was performed using the Trans-Blot® Turbo™ Transfer System. Following blocking for 1-hour in Tris-buffered saline Tween-20 (TBS-T) containing 5% non-fat dried milk (NFDM), membranes were incubated overnight with rabbit anti-phosphorylated or total antibodies: CaMKII, pThr286-CaMKII, AMPK α , pThr172-AMPK, p44/42 MAPK, pThr202/Tyr204-p44/42 MAPK, eNOS and pSer1177-eNOS, at a dilution of 1:500-1:4000 (see table 4.2; all antibodies were tested at different dilutions for optimisation purposes before the experimental gels were run) in 5% bovine serum albumin (BSA) made up in TBS-T (Cell Signaling Technology, London, UK). After overnight incubation, the membrane was washed 3 times in TBS-T for 5 minutes and incubated for 1 hour in HRP-conjugated anti-rabbit

antibodies (Cell Signaling Technology, London, UK) at dilution of 1:5000-1:10,000, following appropriate optimisation. Proteins were visualised by enhanced chemiluminescence (Thermo Fisher Scientific inc, Waltham, USA) and quantified by densitometry (ChemiDoc™ MP imaging system, Bio-Rad Laboratories, Inc. CA, USA). Stain-free image bands were measured for total lane protein levels so that bands of targeted proteins could be normalised to total protein in the relevant lane. Detected phosphorylated proteins were normalised to their total protein expression before being compared between experimental conditions.

Commented [CS177]: It would be good to have the optimisation blots presented somewhere. Maybe in the main methods or perhaps referenced in an appendix. You spent a lot of time and effort getting things right, this warrants reporting.

Commented [SD178R177]: Can put these together for the appendix if they add value

Commented [DR179]: Reading the comment of Claire: was it so much work and did you gain any insights that it is worth publishing it as a methodology paper?

Table 4. 2 List of antibodies and dilutions used.

Antibody	Primary Ab Dilution	Secondary Ab Dilution	Company
CaMKII	1:1000	1:5000	Cell Signaling Technology
pThr286-CaMKII	1:500	1:5000	Cell Signaling Technology
AMPK α	1:1000	1:5000	Cell Signaling Technology
pThr172-AMPK	1:1000	1:10,000	Cell Signaling Technology
p44/42 MAPK	1:2000	1:10,000	Cell Signaling Technology
pThr202/Tyr204-p44/42 MAPK	1:2000	1:10,000	Cell Signaling Technology
eNOS	1:500	1:5000	Cell Signaling Technology
pSer1177-eNOS	1:500	1:5000	Cell Signaling Technology

4.3.9 Statistical analysis

One-way ANOVAs were performed for specific flavonoids separately, using dose as the main factor. Two-way ANOVAs were performed to determine statistical significance when using two main independent factors in the following experiments: ROS production, with dose and antimycin A as factors; RT-qPCR, using dose and time as factors; and western blotting, where treatment and time were the main factors. Multiple comparisons were performed to determine differences between experimental conditions by adjusting for multiple tests, using Dunnett's

or Sidak's test where appropriate. All data are presented as mean \pm SEM and significance accepted when $P < 0.05$.

4.4 Results

4.4.1 Flavonoids do not impair vascular endothelial cell viability

Firstly, a cell number standard curve was generated to convert sample fluorescence values into cell numbers, where the coefficient of correlation (R^2) was 0.988 (see Figure 4.2).

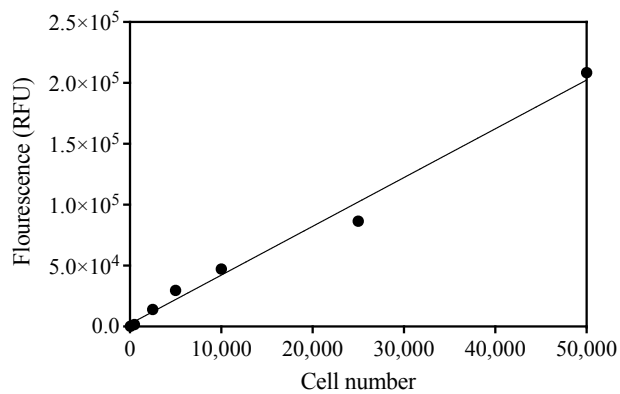


Figure 4. 2 Standard curve generated for HUVECs using CyQUANT® Cell Proliferation Assay. Cells were seeded at densities of 0-50,000 cells per well and grown in EGM for 48 h before performing the assay.

After 24 h dietary flavonoid treatments (0-20 μ M dose responses), no main effect of dose was found on cell viability (measured by cell density) in the presence of Q ($P=0.095$) and EGCG ($P=0.142$; Figure 4.3). However, in the presence of EPI, there was a significant main effect of dose on cell viability ($P=0.018$). Multiple comparisons revealed that only 0.5 μ M Q increased cell viability 37% compared to CTRL conditions ($P=0.03$). Given that the flavonoid doses tested did not cause cell toxicity, along with the knowledge of attainable *in vivo* flavonoid

concentrations (up to 10 μM), subsequent experiments were conducted with doses of 5 and 10 μM .

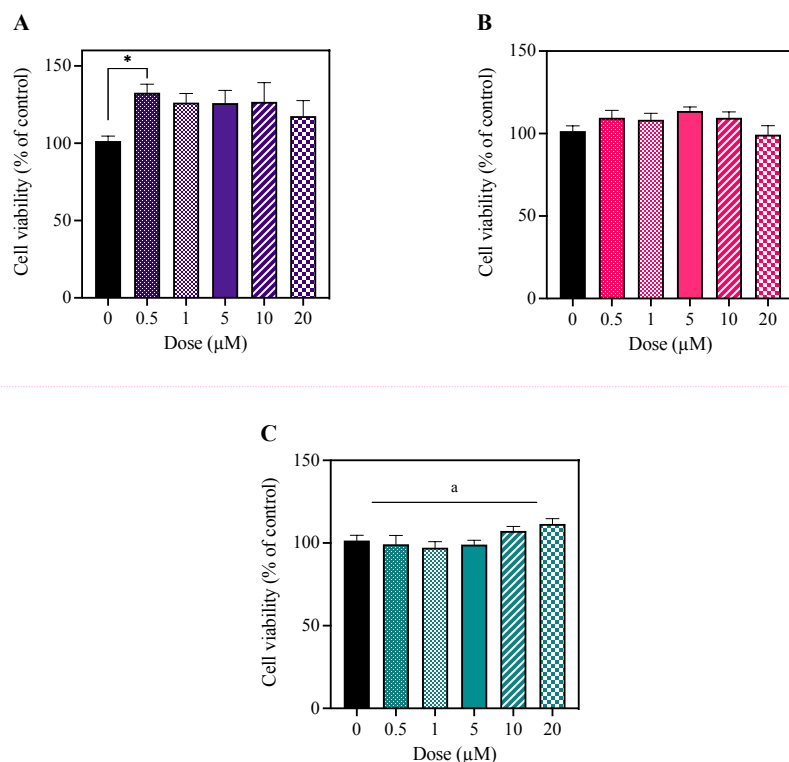


Figure 4.3 Vascular endothelial cell viability is not impaired by acute flavonoid treatment. HUVECs were treated with 0-20 μM A) Quercetin, B) EGCG or C) EPI for 24 h. Data are means \pm SEM, representative of 3 independent repeats with 3 replicates of each condition. Statistical significance was tested for by one-way ANOVA and Dunnett's test for multiple comparisons. * P <0.05. ^a Significant main effect of dose (P <0.05).

4.4.2 Mitochondrial ROS production is differentially impacted by flavonoids in vascular endothelial cells

Commented [DR180]: The overall picture is that the flavonoids increase cell viability, which seems to me to good to be true: the viability assay is fluorescence-based. These cyclic structured flavonoids may affect the fluorescence signal. Did you check/and if needed adjust whether the flavonoids affect the signal (without cells)?

Commented [CS181]: I am not convinced as to why this dose was selected based on the preceding data. The only sig for Q was 0.5um. Maybe think of rephrasing? Words along the lines of: No dose was found to be toxic, therefore based on other publications (refs) and the c2c12 data, it was decided to use 5 and 10 μM for further experimentation – or some such info.

Commented [SD182R181]: We chose the dose because it was in possible physiological range in-vivo, and because these doses didn't impair viability i.e. no impairment to proportion of live healthy cells compared to CTRL. increase in 'viability' might represent stimulation of proliferation, but main message is no cell death compared to CTRL

Commented [CS183R181]: Maybe add some of the text above re the possible physiological range in vivo

Commented [CS184]: Only 05um sig dif? Seems odd t me that the other doses are not also significantly increased.

Commented [CS185]: Do you put this level of detail in all figure legends in all chapters? If not, please amend to include or remove the specifics from here

Commented [CS186]: For the C2c12s you originally started with seahorse data and ROS came later. I know you are reworking order of the the data, but is it worth matching the order between the two cell types, for the data that are shared?

Having ascertained that physiological flavonoid concentrations do not cause toxicity to vascular endothelial cells, experiments were performed to investigate whether flavonoids, in the absence or presence of the complex III inhibitor Antimycin A (AA), regulate vascular endothelial cell ROS emission. These experiments were performed with the knowledge dietary flavonoids may have antioxidant properties that contribute to their health benefits *in vivo*.

Commented [CS187]: Why? What is the driving force for doing this? Is it human data and you want to ascertain how flavonoids may work at the level of endothelial cells, or is there another reason?
You want to lay this out clearly but succinctly, or the reader wont know, why, if the flavonoids haven't done much, you then go on to look at ROS.

Commented [SD188R187]: I've added a small sentence and hope that the introduction sets the scene for this work too

4.4.2.1 Quercetin dose-dependently modulates mitochondrial ROS production

There was a significant main effect of dose ($P<0.0001$) and AA ($P<0.0001$) on rates of MitoSOX oxidation in Q treated endothelial cells, and a significant dose \times AA interaction ($P<0.0001$). Post-hoc tests revealed that AA significantly increased the rate of MitoSOX oxidation under CTRL conditions (-AA: $8.1 \times 10^{-5} \pm 0.2 \times 10^{-5}$ vs. +AA: $35.4 \times 10^{-5} \pm 0.5 \times 10^{-5}$ RFU/sec⁻¹/cell⁻¹; $P<0.0001$). In the absence of AA, 5 and 10 μ M Q significantly decreased and increased MitoSOX oxidation, respectively, compared to -AA CTRL (CTRL: $8.1 \times 10^{-5} \pm 0.2 \times 10^{-5}$; 5 μ M Q: $3.7 \times 10^{-5} \pm 0.2 \times 10^{-5}$; 10 μ M Q: $30.7 \times 10^{-5} \pm 0.4 \times 10^{-5}$ RFU/sec⁻¹/cell⁻¹; $P<0.0001$; see Figure 4.4B). In the presence of AA, rates of MitoSOX oxidation were significantly increased with 5 and 10 μ M Q versus +AA CTRL (CTRL: $35.4 \times 10^{-5} \pm 0.49 \times 10^{-5}$ RFU/sec⁻¹/cell⁻¹; 5 μ M Q: $38.1 \times 10^{-5} \pm 0.4 \times 10^{-5}$; 10 μ M Q: $56.1 \times 10^{-5} \pm 0.8 \times 10^{-5}$; $P=0.0005$ and $P<0.0001$, respectively).

Commented [CS189]: Spell out as Antimycin A – should you put in a line as to why it was used

Commented [DR190]: This whole paragraph contains so much data that I would personally choose to put this in one big table.

Commented [SD191R190]: I have split this up into sections with the hope this makes better reading

Commented [CS192]: worth stating that basal rates were sig increased e.g. control vs AA? Then go onto the comparison with AA

Commented [CS193]: When you say Ctrl here, do you actually mean the AA control – I would add this for clarity for your examiners.

4.4.2.2 EGCG attenuates mitochondrial ROS production

There was a significant main effect of dose ($P<0.0001$) and AA ($P<0.0001$) on rates of MitoSOX oxidation in EGCG treated endothelial cells, and a significant dose \times AA interaction ($P<0.0001$). In EGCG treated endothelial cells, MitoSOX oxidation rates were attenuated

Commented [CS194]: Spell out as Antimycin A – should you put in a line as to why it was used

across conditions with and without AA (see Figure 4.4B). In the absence of AA, MitoSOX oxidation rates were significantly lower with 5 and 10 μM EGCG versus -AA CTRL (5 μM EGCG: $0.6 \times 10^{-5} \pm 0.1 \times 10^{-5}$ and 10 μM EGCG: $0.7 \times 10^{-5} \pm 0.1 \times 10^{-5}$ vs. CTRL: $4.5 \times 10^{-5} \pm 0.1 \times 10^{-5}$ RFU/sec⁻¹/cell⁻¹; $P < 0.0001$ and $P < 0.0001$, respectively). Similarly, in the presence of AA, MitoSOX oxidation rates was significantly lowered with 5 and 10 μM EGCG versus +AA CTRL (5 μM EGCG: $14.2 \times 10^{-5} \pm 0.3 \times 10^{-5}$ and 10 μM EGCG: $6.3 \times 10^{-5} \pm 0.2 \times 10^{-5}$ vs. CTRL: $24.5 \times 10^{-5} \pm 0.3 \times 10^{-5}$ RFU/sec⁻¹/cell⁻¹; $P < 0.0001$ and $P < 0.0001$, respectively).

4.4.2.3 EPI dose-dependently modulates mitochondrial ROS production

There was a significant main effect of dose ($P < 0.0001$) and AA ($P < 0.0001$) on rates of MitoSOX oxidation in EPI treated endothelial cells, and a significant dose \times AA interaction ($P < 0.0001$). Post-hoc comparisons revealed that, in the absence of AA, 5 and 10 μM EPI significantly increased and decreased rates of MitoSOX oxidation compared to -AA CTRL, respectively (CTRL: $8.1 \times 10^{-5} \pm 0.2 \times 10^{-5}$; 5 μM EPI: $10.7 \times 10^{-5} \pm 0.2 \times 10^{-5}$; 10 μM EPI: $3.8 \times 10^{-5} \pm 0.2 \times 10^{-5}$ RFU/sec⁻¹/cell⁻¹; $P < 0.0001$). In the presence of AA, 5 μM EPI did not affect MitoSOX oxidation versus +AA CTRL (5 μM EPI: $35.4 \times 10^{-5} \pm 0.4 \times 10^{-5}$ vs. CTRL: $35.4 \times 10^{-5} \pm 0.5 \times 10^{-5}$ RFU/sec⁻¹/cell⁻¹; see Figure 4.4C). Whereas 10 μM EPI significantly increased rates of MitoSOX oxidation compared to +AA CTRL (10 μM EPI: $44.4 \times 10^{-5} \pm 0.6 \times 10^{-5}$ vs. CTRL: $35.4 \times 10^{-5} \pm 0.5 \times 10^{-5}$ RFU/sec⁻¹/cell⁻¹; $P < 0.0001$).

Commented [CS195]: Opposite to Q

Commented [CS196]: Same re aa control comment above. I wont mention again, but please amend accordingly/

Commented [CS197]: Please move control to the end of the brackets, to follow the text – please amend throughout, I wont mention again.

Commented [CS198]: AA above is at 35, why is it so much lower here?

Commented [SD199R198]: Thanks for pointing this out Claire – the control values condition values may have been distorted in EGCG treated plate for some reason... these EGCG data had to be repeated on separate days due to issues with cells in plates. So, what ive done is pool control values obtained from EGCG plates with Q and EPI plates and took the average, and have amended the data accordingly. This made the control values between EGCG and EPI/Q plates more comparable and likely better reflection of true control values – hope this makes sense, and tell me if this isn't appropriate

Commented [CS200R198]: Thank you

Commented [CS201]: Please move control to the end of the brackets, to follow the text – please amend throughout, I wont mention again.

Commented [CS202]: AA above is at 35, why is it so much lower here?

Commented [CS203]: Spell out as Antimycin A – should you put in a line as to why it was used

Commented [CS204]: What about 5?

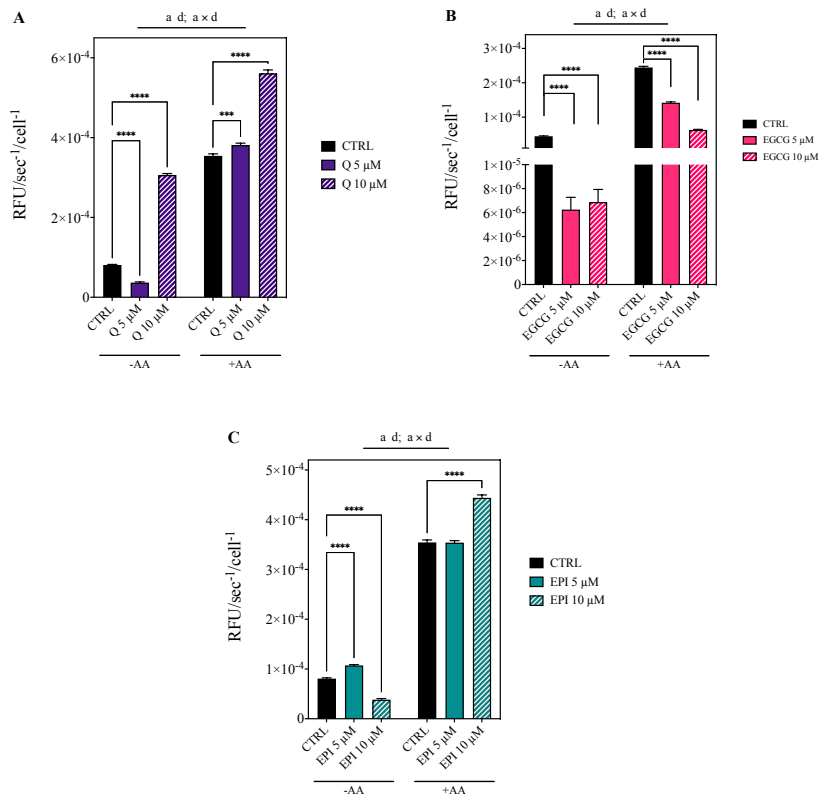
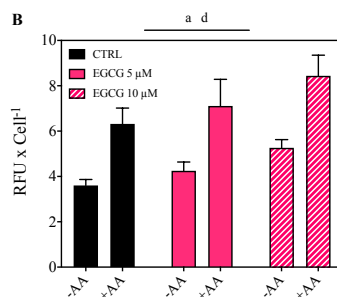
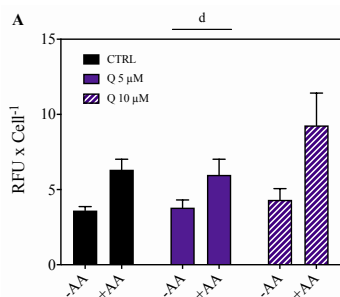


Figure 4. Dietary flavonoids differentially impact the rate of mitochondrial ROS production in vascular endothelial cells. MitoSOX oxidation rates were determined in HUVECs in the absence of presence of Q, EPI or EGCG. Cells were treated for 24 h with 0, 5 and 10 μM Q, EGCG or EPI. After 24 h, cells were incubated with or without antimycin A for 30 minutes, before MitoSOX was loaded into cells (2.5 μM final concentration). Rates of MitoSOX oxidation were measured in 30 second intervals over 30 minutes in a plate reader and normalised to cell density. A) Q treated; B) EGCG treated and C) EPI treated. Data are means \pm SEM of three independent repeats with two replicates per treatment. Statistical significance was tested for by a two-way ANOVA, with dose and antimycin A as factors: ^a Significant main effect of dose; ^d Significant main effect of AA ($P < 0.05$). *** $P < 0.001$ and **** $P < 0.0001$.

4.4.3 Non-mitochondrial specific ROS production is not impacted by flavonoid

treatment

Following the findings that rates of MitoSOX oxidation were differentially impacted by flavonoid treatment, the emission of cellular ROS (not mitochondrial-specific) was determined with and without dietary flavonoids. In Q treated endothelial cells, there was no main effect of dose, but a significant main effect of AA ($P=0.0003$; see Figure 4.5A). Whilst there was an upward trend in ROS production in the presence of 10 μM Q and AA versus AA alone, this did not reach statistical significance (CTRL +AA: 6.32 ± 0.70 vs. Q 10 μM + AA: 9.27 ± 2.15 RFU/Cell $^{-1}$; $P=0.073$). With EGCG treatment, there was a main effect of dose ($P=0.030$) and AA ($P<0.0001$). Multiple comparisons revealed no significant main effect of EGCG treatment on ROS production between conditions (see Figure 4.5B). In EPI treated cells, there was a significant main effect of AA only ($P<0.0001$).



Commented [DR205]: Same question mark for me: the antimycin MitoSOX experiment should basically be similar to the emission of cellular ROS?? If not, then please specify exactly in your introduction how they differ. Are the assays measure different aspects of ROS?

Commented [SD206R205]: Yes, mitosox mitochondrial ROS whereas cellROX is general cellular ROS, this is stated in methods.

Commented [CS207]: Am I missing something? Differences are evident in the data above, why not here? This needs a short transition sentence

Commented [DR208]: Also, I am missing a positive control in this assay, e.g. a known chemical inhibitor of ROS. Maybe your assay is not sensitive for inhibition?

Commented [SD209R208]: Great point, this would have been a worthwhile addition, and is a limitation

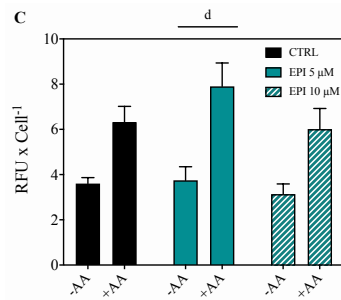


Figure 4. 5 Dietary flavonoids do not regulate ROS production in vascular endothelial cells. CellROX oxidation was determined in HUVECs in the absence of presence of A) Q, B) EGCG or C) EPI. Cells were treated over 24 h with 0, 5 and 10 μM Q, EGCG or EPI. After 24 h, cells were incubated with or without antimycin A for 30 minutes, before CellROX was loaded into cells (2.5 μM final concentration). CellROX oxidation was measured at 640/665 nm (Ex/Em) in a plate reader and normalised to cell density. Data are means \pm SEM of three independent repeats with two replicates per treatment. Statistical significance was tested for by a two-way ANOVA, with dose and antimycin A as factors for each flavonoid individually: ^a Significant main effect of dose; ^d Significant main effect of AA ($P < 0.05$).

Together, these findings demonstrate divergent effects of flavonoids on the rate of mitochondrial ROS production, and further, demonstrate no role for flavonoids in the emission of cellular ROS. Of the flavonoids tested, Q and EPI demonstrated dose-dependent effects on ROS production in the absence of AA. Whereas EGCG lowered the rate of mitochondrial ROS production, regardless of dose and the presence of AA.

4.4.4 Flavonoids differentially impact the production of nitric oxide in vascular endothelial cells

Commented [DR210]: OK so now I understand that one assay measures ROS intracellularly and the other extracellularly?

Commented [SD211R210]: One is mitochondrial specific ROS, and other is general cellular ROS

Commented [CS212]: I would move this text to follow the ROS data and then transition into why you then look at NO. If you unmove it, you will need to add text here re the findings of NO and the relevance before transitioning to mitogenesis.

However, if you change the order of reporting, it may be your transition will be a bit different.

After describing the effects of flavonoids on (mitochondrial and non-mitochondrial specific) ROS emission, NO production was investigated with and without flavonoid treatment. There was no main effect of Q dose on NO levels (see Figure 4.6). Although, there was a significant main effect of dose on NO levels in EGCG and EPI treated vascular endothelial cells ($P=0.035$ and $P=0.003$, respectively). Multiple comparisons revealed no significant impact of EGCG treatment on NO levels (see Figure 4.6). Whilst 5 μM EPI did not impact NO production (5 μM EPI: $2.78 \times 10^5 \pm 0.20 \times 10^5$ vs. CTRL: $3.02 \times 10^5 \pm 0.18 \times 10^5$ AU; $P=0.784$), 10 μM EPI significantly increased NO production compared to CTRL conditions (10 μM EPI: $4.38 \times 10^5 \pm 0.43 \times 10^5$ vs. CTRL: $3.02 \times 10^5 \pm 0.18 \times 10^5$ AU; $P=0.010$).

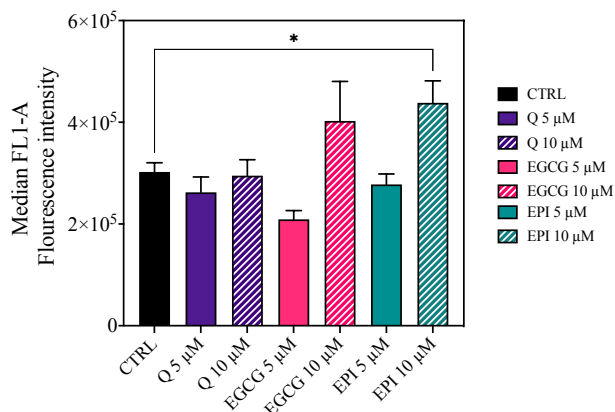


Figure 4. 6 Flavonoid supplementation distinctly affects intracellular nitric oxide in vascular endothelial cells. NO levels (DAF-FM oxidation) were determined in HUVECs in the absence and presence of Q, EGCG and EPI. Cells were treated with 0, 5 and 10 μM of flavonoids for 24 h. After 24 h, cells were trypsinised and resuspended in PBS. Median fluorescence intensity was determined with background signal (cell-free signal) subtracted. Data are presented as means \pm SEM of three independent repeats with two replicates per experimental condition. Statistical significance was tested for by one-way ANOVA for each flavonoid separately, and multiple comparisons by Dunnett's multiple comparison test. * $P<0.05$ significant versus CTRL.

Commented [CS213]: Why no 5um? If not reporting it any more, then make a statement somewhere early on to explain why.

Commented [SD214R213]: Because it was not significant, does it need to entered too?

Commented [CS215R213]: Probably not.

4.4.5 Dietary flavonoids differentially impact the expression of genes associated with energy metabolism in vascular endothelial cells

In light of findings that flavonoids distinctly impact the rate of mitochondrial ROS emission and NO production, experiments were performed to resolve whether flavonoids regulate genes linked with mitochondrial function and the antioxidant response in vascular endothelial cells.

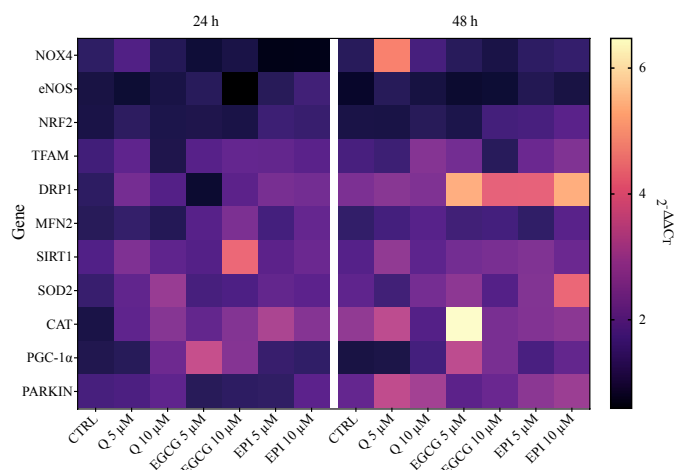


Figure 4. 7 Heatmap representation of vascular endothelial cell mRNA responses in the absence of presence of flavonoids. Fold changes ($2^{-\Delta\Delta CT}$) in gene expression over 48 h presented as heat map.

A visual overview of the mRNA responses to flavonoid treatment can be seen in Figure 4.7. Firstly, the expression of genes associated with the antioxidant response were quantified. There was no effect of dose or time on catalase expression in Q and EPI treated endothelial cells (see Figure 4.8A). Though, a main effect of time on catalase expression was found in EGCG treated cells ($P=0.032$). Multiple comparisons revealed a 5 μ M EGCG increased catalase expression 2.4-fold compared to CTRL conditions over 48 h ($P=0.029$). Similarly, a 2.6-fold increase in

Commented [DR216]: In genral: I miss you line of thinking, why you are measuring all these different genes/enzymes? Why did you choose these and explain in the introduction section

Commented [DR217]: Nice figure! You may even want to consider to start with this figure and add a table with the exact number (leaving out the bar graphs). Based on this I would conclude that DRP1 is affected by EC and EGCG. All others seem quite irrelevant (observing effects at one concentration but none at another concentration of the same flavonoid is questionable; 5 and 10 uM is more or less the same concentration)

Commented [SD218]: Have added in additional heatmap, can remove if needed

Commented [CS219R218]: I really like the heatmap.

Commented [CS220]: I think this does not follow the EPI alone above. Needs a rethink for order.

Being out there a bit, if we started with the human study and EPI, could you then finish that chapter by speculating that EPI could elicit the impact by acting at the level of the endothelial cell and hence look at relevant signalling pathways. Then, as a result of the signalling data being confounding, assessed it at a mito level – lack of any big impact meant that you wanted to determine whether the cells were simply not responsive, or just not responsive to EPI. Then come in with the other flavonoids and mito and then ROS etc

What do you think? This could then lead into the c2c12 and all flavonoids....

Commented [SD221R220]: I do like this idea, would potentially help the order of results and not having to worry about signalling being EPI alone.

For now, I have made the order this: RONS<Genes<Mito<Signalling, which i think can make sense, with possible change to what you suggest above

Commented [CS222R220]: Sounds good

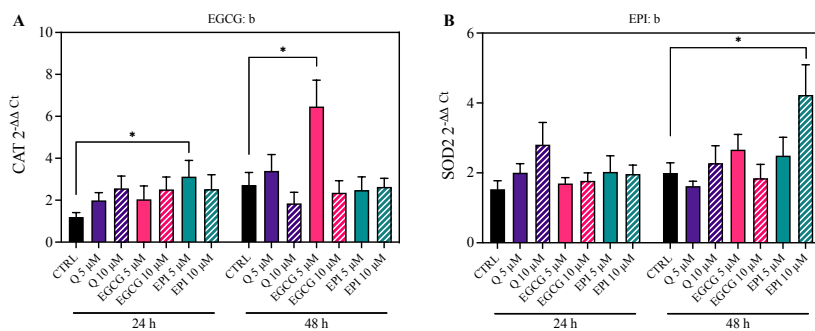
Commented [CS223]: We need a table of the basal CT values for all genes tested, to get a feel fo how well or not they are expressed int hje cells e.g. if very low expression and no change, differen t story to very high level and no change.....also need ct table for the genes in the c2c12 chapters.

Commented [CS224]: Why? What were the data that led to this being undertaken?

Commented [CS225]: Why catalase, specifically? What was the logic/hypothesis?

Might be worth putting together a figure of the pathways of interest (within a cell) and how your huvec data expand or challenge current knowledge

catalase expression over 24 h was found with 5 μ M EPI over versus CTRL conditions ($P=0.045$). No main effect of dose or time was observed on SOD2 mRNA abundance in Q and EGCG treated cells. Though, there was a significant effect of time on SOD2 expression in EPI treated cells only ($P=0.024$). Multiple comparisons revealed that SOD2 expression was increased 2.1-fold in the presence of 10 μ M EPI versus CTRL conditions ($P=0.040$). There was no main effect of dose or time on eNOS expression in the presence of Q, EGCG or EPI. Multiple comparisons revealed that eNOS expression was decreased 1.9-fold with 5 μ M EGCG compared to CTRL ($P=0.032$). There was a significant main effect of dose and time on NOX4 expression in Q and EPI treated cells, respectively ($P=0.015$ and $P=0.006$). Over 48 h, 5 μ M Q increased NOX4 expression 3.4-fold compared to CTRL ($P=0.0190$). A significant main effect of dose was found on NRF2 expression in the presence of EPI ($P=0.0003$), but not Q or EGCG (see Figure 4.8E). NRF2 mRNA abundance was increased 1.5-fold and 1.6-fold with 5 and 10 μ M EPI over 48 h when compared to CTRL ($P=0.015$ and $P=0.001$, respectively).



Commented [CS226]: Why studied – I think you want to lay this all out in an opening paragraph

Commented [CS227]: As above

Commented [CS228]: As above

Commented [CS229]: This was the only dose and treatment that impacted mito data – does this make sense with that story?

Commented [CS230]: As above

Commented [HJ231]: Take care with decimal places 3 is enough. Be consistent throughout.

Commented [CS232]: Did you look at sig vs. 24 hr control (eg for epi 10 at 48 h), or only to the 48 h control?

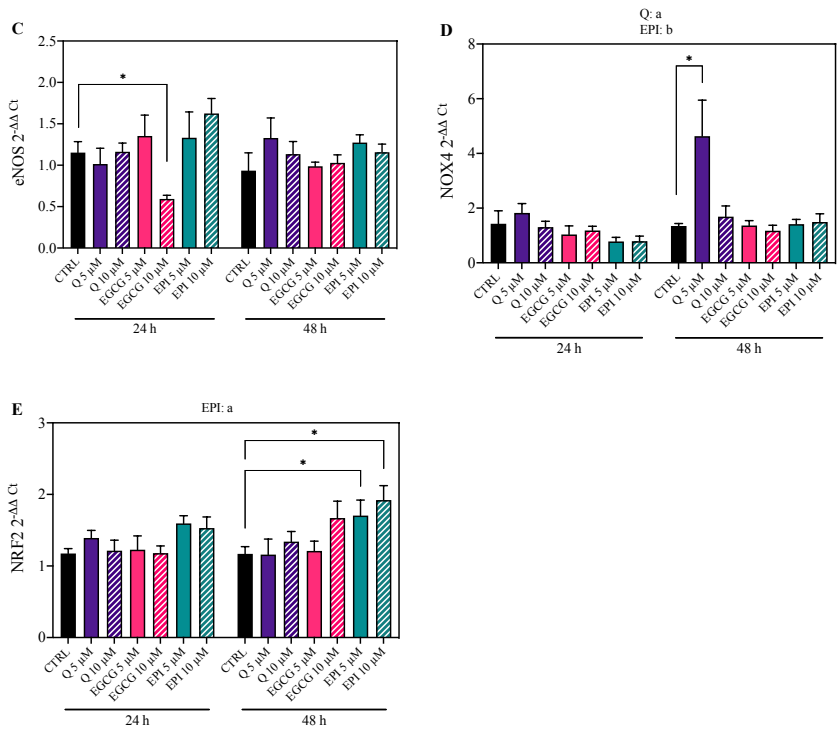


Figure 4. 8 Expression of genes associated with the antioxidant response in vascular endothelial cells following acute dietary flavonoid treatment. HUVECs were treated with 0, 5 and 10 μM of Q, EPI or EGCG over 48 h and lysed for analysis of gene expression. A) CAT, B) SOD2, C) eNOS, D) NOX4 and E) NRF2. Data are means ± SEM from 3 independent experiments run in duplicate. Statistical significance was determined by a two-way ANOVA, with dose and time as factors. Multiple comparisons were performed by Dunnett's test to determine differences in gene expression between conditions. ^a main effect of dose; ^b main effect of time ($P < 0.05$); * $P < 0.05$. |

From the previous data, it was evident that flavonoids play a limited role in regulating the expression of antioxidant related genes. The enhancement of NOX4 with Q may partially explain its reported pro-oxidant effects. Additionally, EPI enhanced NRF2 expression over 48

Commented [CS233]: Need a concluding statement of the above studies, whether they fit with any of the data collected so far and then an explanation of why the following genes were selected for analyses.

h. To investigate whether flavonoids impact mitochondrial remodelling at the level of transcription, gene expression was investigated with and without dietary flavonoids.

Next, the expression of genes associated with mitochondrial function were quantified. In the presence of Q, there was no main effect of dose or time on DRP1 expression. There was a main effect of dose ($P=0.025$) and time ($P<0.0001$) on DRP1 expression in cells treated with EGCG (see Figure 4.9A), and a significant dose x time interaction ($P=0.0004$). Over 48 h, DRP1 expression was increased 2.2-fold and 1.7-fold by 5 and 10 μM EGCG, respectively ($P=0.0002$ and $P=0.0188$, respectively). In the presence of EPI, there was a significant main effect of dose ($P=0.0180$) and time ($P=0.0016$) on DRP1 expression. At 48 h, 10 μM EPI increased DRP1 expression 2.2-fold compared to CTRL ($P=0.010$). There was a significant main effect of time on MFN2 expression in Q treated cells ($P=0.026$), and a main effect of dose on MFN2 in cells treated with EGCG and EPI ($P=0.027$ and $P=0.035$; see Figure 4.9B). At 24 h, 10 μM EGCG increased MFN2 expression 1.8-fold versus CTRL ($P=0.0031$). Whereas 10 μM EPI increased MFN2 expression 1.6-fold versus CTRL ($P=0.0244$). There was a significant main effect of time on PARKIN expression in cells cultured in the presence of Q, EGCG and EPI ($P=0.001$, $P=0.015$ and $P=0.004$, respectively). At 24 h, 5 μM EGCG increased PARKIN expression 1.3-fold compared to CTRL ($P=0.040$). There was a significant main effect of dose on PGC-1 α expression in cells cultured with Q and EGCG ($P=0.023$ and $P<0.0001$). Multiple comparisons revealed that PGC-1 α expression was increased 2.8-fold and 2.0-fold over 24 h with 5 and 10 μM EGCG, respectively ($P<0.0001$ and $P=0.004$, respectively). Over 48 h, PGC-1 α was increased 2.9-fold and 2.0-fold in the presence of 5 and 10 μM EGCG compared to CTRL, respectively ($P<0.0001$ and $P=0.0003$, respectively). There was a significant main effect of dose on SIRT1 expression in cells cultured in the presence of EGCG ($P=0.0007$), and a significant dose \times time interaction ($P=0.0448$). At 24 h, 10 μM EGCG increased SIRT1

Commented [DR234]: Again, I would choose for one large table showing all data for flavonoids and genes. This text is almost not readable.

Commented [CS235]: Why chosen?

Commented [CS236]: What about Q? If without effect, then state this

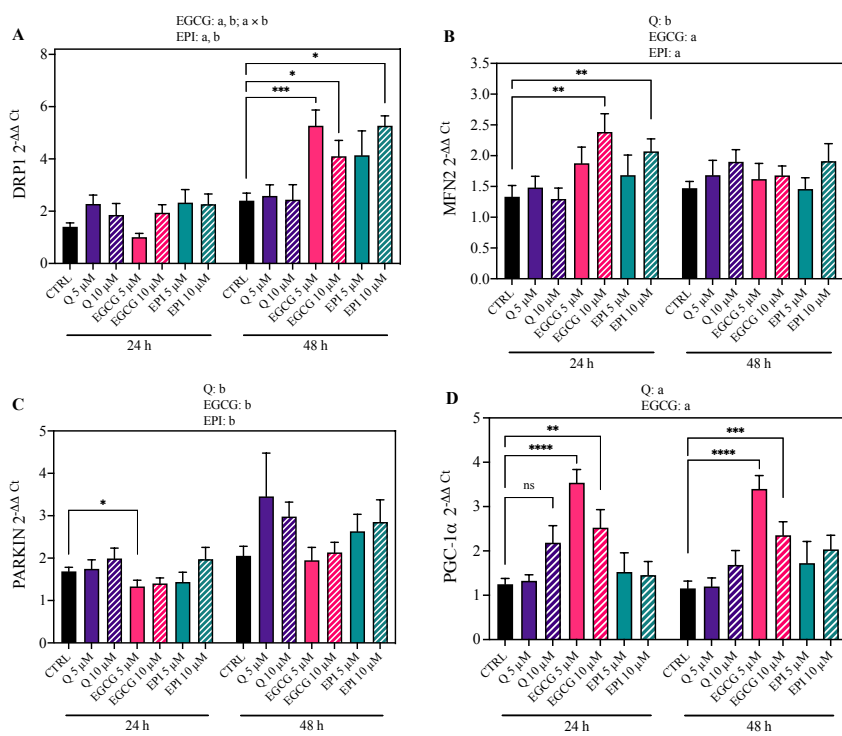
Commented [CS237]: Why chosen?

Commented [CS238]: As above

Commented [CS239]: As above.....having an intro para on why the genes were chosen will alleviate this question in the actual results presentation

expression 2.3-fold compared to CTRL ($P=0.0001$). There was a significant dose \times time interaction ($P=0.0013$) on TFAM expression in cells cultured with Q. Multiple comparisons revealed no significant impact of flavonoid treatment on TFAM expression, regardless of the flavonoid tested.

Commented [CS240]: As above



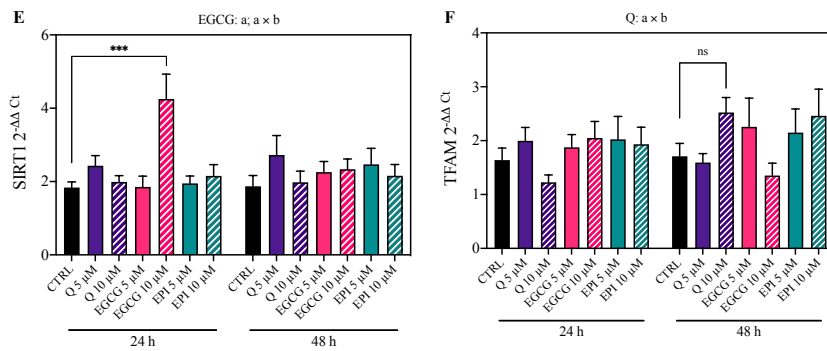


Figure 4.9 Expression of genes associated with mitochondrial function in vascular endothelial cells following acute dietary flavonoid treatment. HUVECs were treated with 0, 5 and 10 μM of Q, EPI or EGCG over 48 h and lysed for analysis of gene expression. A) DRP1, B) MFN2, C) PARKIN, D) PGC-1 α , E) SIRT1 and F) TFAM. Data are means \pm SEM from 3 independent experiments run in duplicate. Statistical significance was determined by a two-way ANOVA, with dose and time as factors. Multiple comparisons were performed by Dunnett's test to determine differences in gene expression between conditions. ^a main effect of dose; ^b main effect of time ($P < 0.05$); * $P < 0.05$, ** $P < 0.01$, *** $P < 0.001$, **** $P < 0.0001$.

Overall, these data highlight that flavonoids are capable of increasing the expression of genes associated with mitochondrial function and the antioxidant stress response in vascular endothelial cells (see Figure 4.8). More specifically, Q increased NOX4 expression, which may relate to its pro-oxidant activity. On the other hand, EGCG increased the transcription of key genes associated with mitochondrial biogenesis and dynamics. Lastly, EPI enhanced NRF2 expression concomitantly with increased expression of genes related to mitochondrial dynamics.

4.4.6 Acute flavonoid treatment has limited impact on mitochondrial bioenergetics in vascular endothelial cells

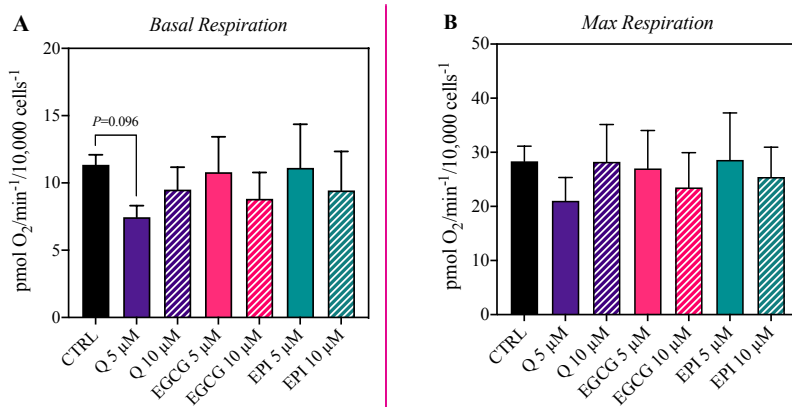
Commented [CS241]: Is this really a good summary? It seems that EGCG had the greatest impact, generally. Worth looking at the pathways in a figure (as suggested above) as this may help in deciding what/if anything the flavonoids do.

Interesting that epi and egcg did not have an impact at a mito level, when tested by Seahorse, but having an impact at the gene level – what is this telling you? Q was inhibitory at Seahorse level, but no impact to speak of at gene level – why?

Commented [CS242]: Reference also the figure below, which is great.

Having described that flavonoids differentially impact RONS production and alter the expression of genes linked with mitochondrial remodelling, the impact of flavonoids on vascular endothelial cell bioenergetics were investigated. There was no significant main effect of flavonoid treatment on rates of basal respiration. Although 5 μM Q treatment caused a 34% reduction in basal respiration vs. CTRL, this did not reach statistical significance ($P=0.096$). Similarly, there was no main effect of treatment on maximal respiration or ADP phosphorylation, irrespective of the flavonoids tested (see Figure 4.10). Despite that 5 μM Q lowered maximal respiration and ADP phosphorylation by 26% and 37% versus CTRL, respectively, these did not reach statistical significance. There was no significant effect of treatment on proton leak, spare respiratory capacity (%) or coupling efficiency, regardless of the flavonoid tested.

Commented [DR243]: Your in vitro work is quite complex, here you introduce another stepwise approach. Therefore I would strongly advise you to introduce an overview figure what aspects you are going to study and how they are interrelated (introduction section)



Commented [CS244]: Instead of Ns, put the actual P value in both graphs.

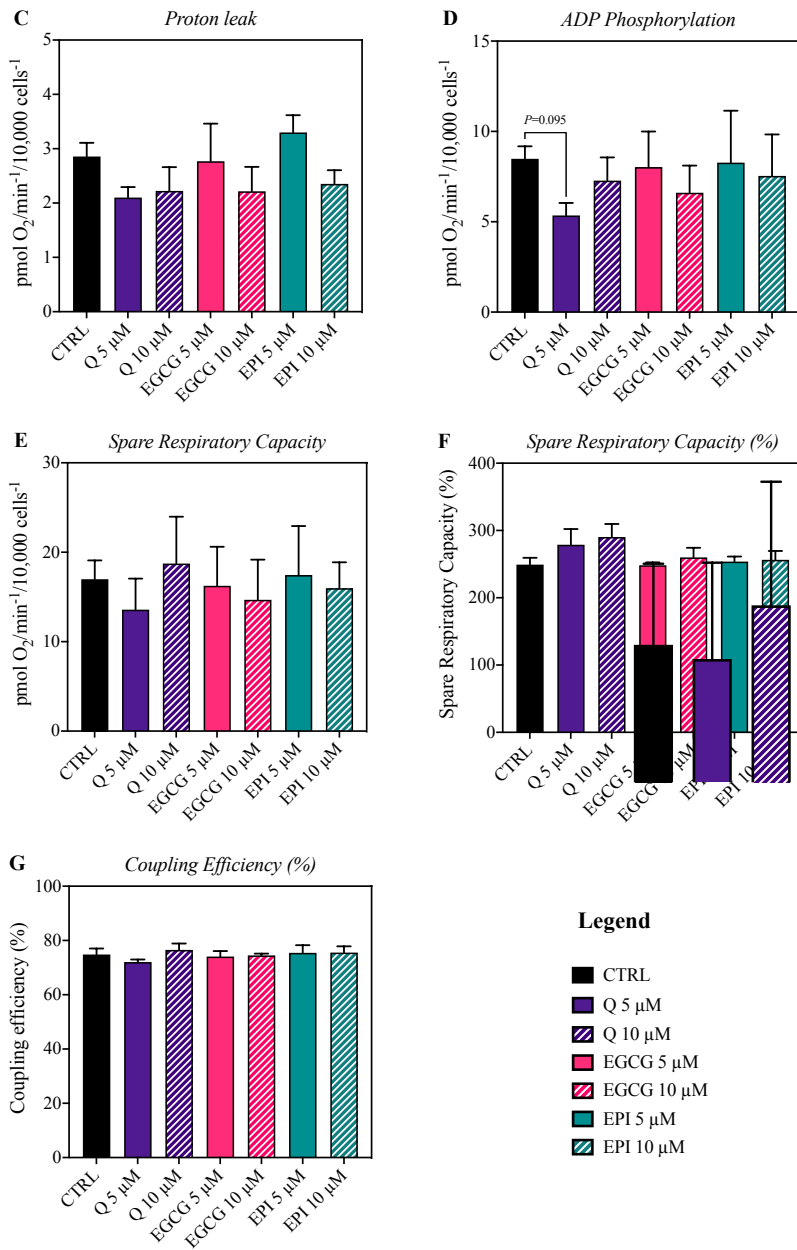


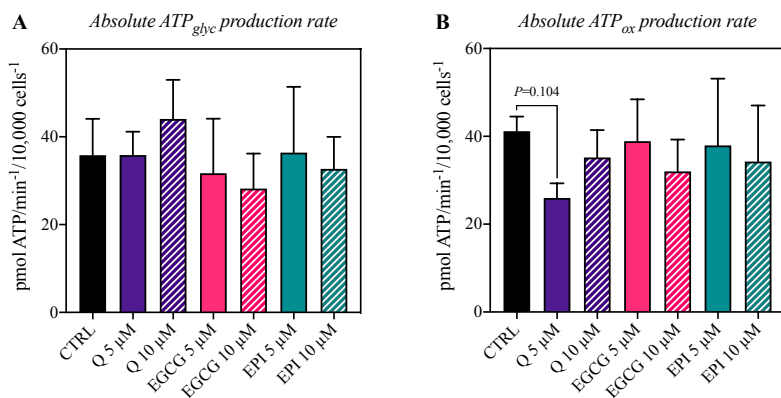
Figure 4. 10 Mitochondrial bioenergetics of HUVECs following acute dietary flavonoid treatment. A) Basal respiration. B) Maximal respiration after FCCP addition. C) Proton leak.

D) ADP phosphorylation. E) Spare respiratory capacity F) Spare respiratory capacity (%). G) Coupling efficiency (%). Data from 3 independent experiments are normalised to cell number (1×10^3) and presented as mean \pm SEM.

4.4.7 Acute dietary flavonoid treatment does not impact ATP production or proton efflux rates in vascular endothelial cells

Following the examination of mitochondrial bioenergetics in the presence of dietary flavonoids, the impact of flavonoid treatment on $J_{ATP_{production}}$ and the contribution of $J_{ATP_{glyc}}$ and $J_{ATP_{ox}}$ was investigated. In line with the mitochondrial respiration data, no significant impact of flavonoid treatment was found on absolute rates of ATP_{glyc} production or ATP_{ox} production (see Figure 4.11). Likewise, there was no main effect of flavonoid treatment on proton production rates (see Figure 4.11B) or relative rates of ATP production (data not shown).

Commented [CS245]: If the studies above showed no differences, would you expect these to? How inter-related are the data. If you would not expect to see differences, based on the initial data, state this and then prove it right or wrong.



Commented [CS246]: Put in the actual P value, particularly since it is not in the text.

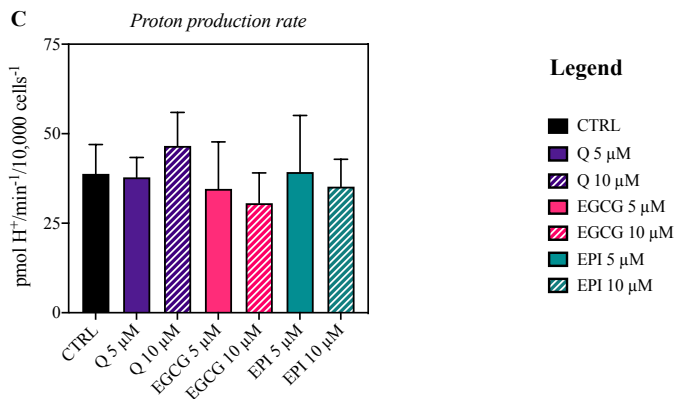


Figure 4. 11 ATP production and proton efflux rates in HUVECs following 24 h dietary flavonoid treatment. A) Rates of ATP_{glyc} production B) ATP_{ox} production. C) Proton production rates. Data from 3 independent experiments are normalised to cell number (1x10³) and presented as mean ± SEM.

Overall, the findings indicate little significance of a role for dietary flavonoids in impacting indices of mitochondrial function in vascular endothelial cells, with similar observations at the level of ATP and proton production rates.

Commented [CS247]: 5 um q reduces basal and max respiration, ADP phosphorylation and absolute ATP ox. None of the others do anything much of anything. What does this tell you about 5um Q? Why was this dose not studied further?

4.4.8 The effects of EPI on endothelial cell signalling responses

4.4.8.1 CaMKII is not modulated by EPI in endothelial cells

EPI dose-dependently impacted the rate of mitochondrial ROS production and augmented NO production, in parallel with changes in mitochondrial and stress response related genes. Consequently, the potential contribution of EPI to intracellular signalling responses was investigated. Firstly, CaMKII signalling was assessed because this kinase sits upstream of AMPK and may underpin EPI's effects upon eNOS phosphorylation in vascular endothelial cells. Total levels of CaMKII were similar across time-points and between conditions (see

Commented [SD248]: If we keep this overall order, does this justify our reasons for studying EPI only well enough? Also, does it seem slightly odd just studying EPI here, and then all flavonoids in the gene expression work in next section?

Commented [CS249R248]: Difficult one – I would find it strange as an examiner to return to all flavonoids, if you have justified the signalling for just one. Remind me why we did just Epi?

Maybe you want to shift the order and put the signalling to follow the ROS NO and come before the mito data?

If shifting the order to follow the same order as the c2c12s, maybe we should have this discussion again then? Easiest would be if you finished on the signalling with just one flavonoid....

Commented [CS250]: Why CAMK? Add 1 sentence to guide the reader as to why this was the first phosphoprotein you looked at, following the derived data.

Figure 4.12). Accordingly, there was no main effect of treatment or time on total CaMKII levels, and no significant treatment \times time interaction. The phosphorylation of CaMKII at Thr286 was not detectable in vascular endothelial cells under any conditions. The inclusion of positive controls confirmed the effectiveness of the antibody and substantiates the lack of phosphorylation of CaMKII at Thr286 (see Chapter 9, Figure 9.3).

Commented [DR251]: Did you include here the basal 0h value as covariate of the three independent experiments (there seems to be quite some variants between experiments)

Commented [CS252]: Why CAMK? Add 1 sentence to guide the reader as to why this was the first phosphoprotein you looked at, following the derived data.

Commented [CS253]: Is this what you show in the appendix? If not, remove.

Commented [CS254]: I think I would prefer this as the -TC first then the + timecourse, but that is just me. Probably if you had done that, I would have asked for this format.....

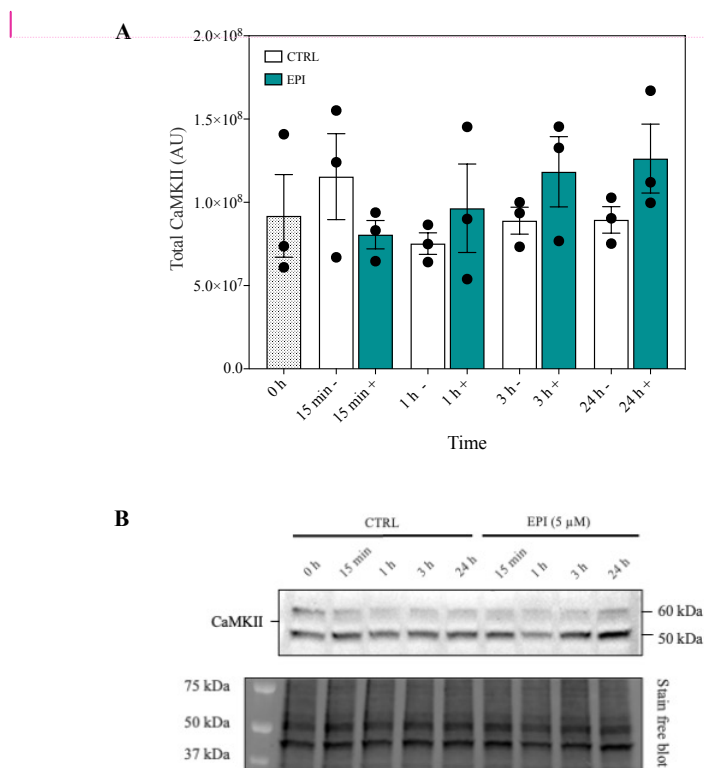
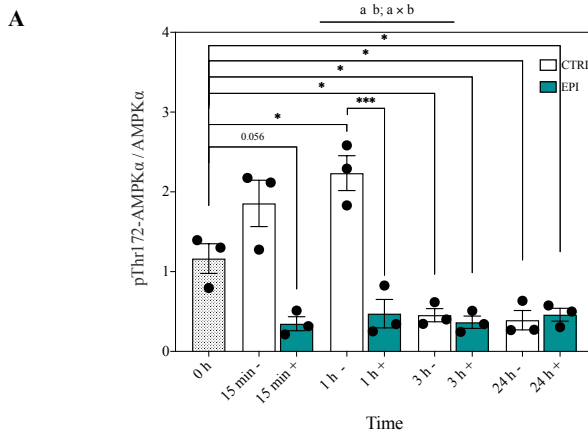


Figure 4. 12 CaMKII levels are not impacted by EPI treatment. A) Total CaMKII in HUVECs in the absence (-; clear bars) or presence (+; green bars) of EPI. B) Representative images of n=3 independent experiments. Cell lysates were analysed by SDS-PAGE and western blotting with indicated antibodies. Data are expressed as means \pm SEM.

4.4.8.2 Acute EPI treatment inhibits AMPK activity in endothelial cells

After obtaining data on CaMKII, the effects of EPI on the downstream kinase, AMPK, were subsequently investigated. Following acute EPI treatment, there was a significant main effect of treatment ($P<0.0001$) and time ($P<0.0001$) on AMPK activity (see Figure 4.13), and a significant interaction ($P<0.0001$). Multiple comparisons revealed a significant increase in phosphorylation of AMPK at Thr172 at 1 h versus 0 h (1 h: 2.24 ± 0.22 vs. 0 h: 1.16 ± 0.19 AU) under CTRL conditions ($P=0.0057$), whereas there was no significant change at 1 h versus 0 h following EPI treatment (1 h: 0.47 ± 0.18 vs. 0 h: 1.16 ± 0.19 AU; $P=0.157$). Further, there was a significant reduction in activation in the presence of EPI vs. CTRL at 15 min (EPI: 0.35 ± 0.09 vs. CTRL: 1.86 ± 0.29 AU; $P=0.0001$) and 1 h (EPI: 0.47 ± 0.18 vs. CTRL: 2.24 ± 0.22 AU; $P<0.0001$). From 3 hours, AMPK phosphorylation was suppressed under both control (3 h: 0.54 ± 0.08 and 24 h: 0.39 ± 0.12 AU vs. 0 h: 1.16 ± 0.19 AU; $P=0.046$ and $P=0.026$, respectively) and treatment conditions compared to 0 h CTRL (3 h: 0.37 ± 0.08 and 24 h: 0.46 ± 0.08 AU vs. 0 h: 1.16 ± 0.19 AU; $P=0.021$ and $P=0.049$, respectively).



Commented [CS255]: Add some text before the results. Having attained these data for CaMKII and wishing to determine.....AMPK activation was subsequently investigated. Following acute.....

Commented [CS256]: Switch order to follow text order

Commented [CS257]: As above re order

Commented [CS258]: Switch order to follow new text

Commented [CS259]: Switch order to follow text.

Commented [CS260]: Switch order to follow text order

Commented [CS261]: Is the reduction significant if compared to 1 hour control, where levels were peak? If so can write

From 3 hours, AMPK phosphorylation was significantly suppressed under both control and treatment conditions, when compared with peak phosphorylation at 1 hour.

If sig vs 0 h, then this is even better.

Commented [CS262]: Switch order to follow text order

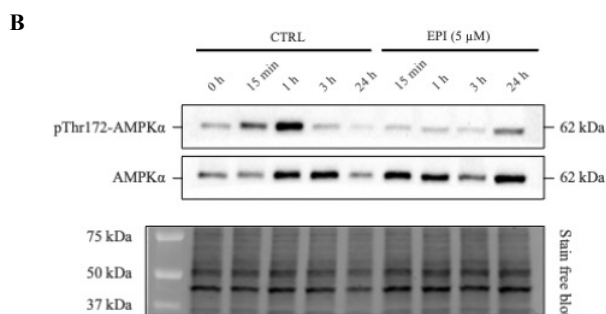


Figure 4. 13 AMPK phosphorylation at Thr172 is acutely blunted by EPI. A) AMPK phosphorylation at Thr172 in HUVECs in the absence (-; clear bars) or presence (+; green bars) of EPI. B) Representative images of n=3 independent experiments and associated stain free blot used for total lane protein normalisation. Cell lysates were analysed by SDS-PAGE and western blotting with indicated antibodies. Representative images of n=3 independent experiments are shown. Data are expressed as means \pm SEM; * P <0.05 and *** P <0.001. ^a significant main effect of treatment; ^b significant main effect of time (P <0.05).

4.4.8.3 EPI temporally augments p44/42 MAPK (ERK1/2) signalling

Having described how EPI impacts AMPK activation, the effects of EPI on ERK1/2 activity were investigated. Whilst ERK1/2 is not involved in the canonical CaMKII/AMPK/eNOS pathway, ERK1/2 signalling may be involved in mediating the effects of EPI on vascular endothelial cells. There was no significant main effect of treatment (P =0.141), but a significant main effect of time (P =0.039) for ERK1/2 activity (see Figure 4.14). There was also a significant treatment \times time interaction (P =0.003). Under CTRL conditions, despite a 2.7-fold increase in ERK1/2 phosphorylation at 3 h, ERK1/2 phosphorylation did not reach significance vs. 0 h until 24 hours post treatment (0 h: 0.38 ± 0.10 vs. 24 h: 1.15 ± 0.28 AU; P =0.022). By contrast, EPI treatment resulted in a significant increase in ERK1/2 phosphorylation at 15 minutes vs 0 h (15 min: 1.09 ± 0.24 vs. 0 h: 0.38 ± 0.10 AU; P =0.035), which was retained at 1 hour (1 h: 1.22 ± 0.07 vs. 0 h: 0.38 ± 0.10 AU; P =0.011), before returning to baseline levels,

Commented [CS263]: Why? Talk about the pathway and what MAPK may provide to the story.

Commented [CS264]: Switch order

Commented [CS265]: Switch order

Commented [CS266]: Switch order

suggesting a change in the temporal pattern of ERK1/2 activation as a result of EPI treatment. Indeed at 1 hour, EPI treatment resulted in a 4.3-fold increase in ERK1/2 phosphorylation vs. CTRL at that time point ($P=0.007$).

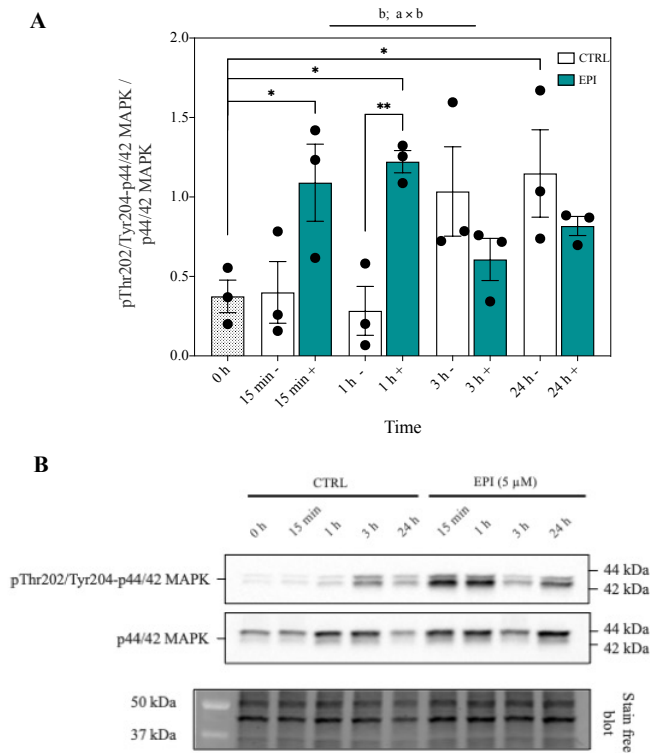


Figure 4. 14 EPI transiently stimulates ERK1/2 phosphorylation. A) ERK1/2 phosphorylation at Thr202/Tyr204 in HUVECs in the absence (-; clear bars) or presence (+; green bars) of EPI. B) Representative images of n=3 independent experiments and associated stain free blot used for total lane protein normalisation. Cell lysates were analysed by SDS-PAGE and western blotting with indicated antibodies. Data are expressed as means \pm SEM; * $P<0.05$ and ** $P<0.01$ compared to CTRL. ^a significant main effect of treatment; ^b significant main effect of time ($P<0.05$).

4.4.8.4 Epicatechins impact on ERK1/2 signalling is independent of eNOS activity in vascular endothelial cells

To help further establish whether EPI elevated NO levels independent of the AMPK axis, eNOS phosphorylation was subsequently determined. There was no significant main effect of treatment ($P=0.469$) or time ($P=0.515$) on phosphorylation of eNOS at Ser1177 in endothelial cells (see Figure 4.15). Likewise, there was no significant treatment \times time interaction ($P=0.100$). At 3 h, eNOS phosphorylation was $\sim 60\%$ higher under CTRL versus EPI conditions (CTRL: 0.38 ± 0.10 vs EPI: 1.15 ± 0.28 AU, $P=0.038$).

Commented [CS267]: Again, put in a linker having made these findings, the next phosphoprotein to be investigated was eNOS as a result of....There was no significant...

Commented [CS268]:

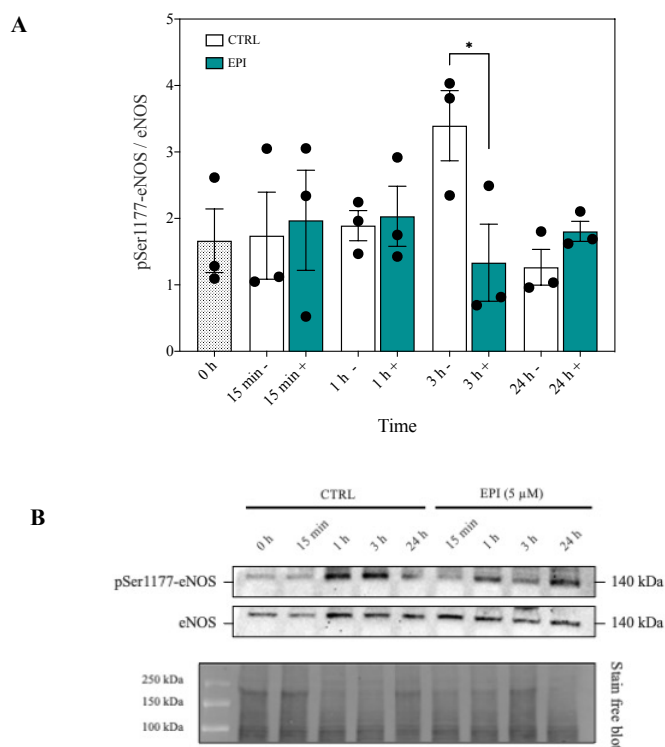


Figure 4. 15 EPI does not stimulate eNOS signalling in HUVECs. A) eNOS phosphorylation at Ser1177 in HUVECs in the absence (-; clear bars) or presence (+; green bars) of EPI. B) Representative images of n=3 independent experiments and associated stain free blot used for total lane protein normalisation. Cell lysates were analysed by SDS-PAGE and western blotting with indicated antibodies. Data are expressed as means \pm SEM; * P <0.05, compared to CTRL.

Commented [CS269]: Amend legend as suggested above.

Together, these findings demonstrate that EPI, at the doses investigated, suppressed AMPK activation, was without impact on eNOS phosphorylation and elicited an altered temporal pattern of ERK1/2 activation, resulting in early and enhanced activation, in HUVECs.

4.5 Discussion

The aim of this study was to enhance mitochondrial function and attenuate ROS in vascular endothelial cells using dietary flavonoids. It was hypothesised that acute flavonoid treatment would attenuate ROS production, increase NO bioavailability and enhance indices of mitochondrial function. The main findings of this chapter were: 1) RONS emission are differentially impacted by flavonoid treatment, in a dose-dependent manner. 2) flavonoids do not significantly impact indices of mitochondrial function. 3) genes linked with mitochondrial remodelling and the antioxidant response were differentially expressed with acute flavonoid treatment, in a dose-dependent manner. 4) EPI transiently stimulates ERK1/2 signalling, independent of AMPK activity.

Commented [DR270]: If you decide on including an 'overview' scheme in the introduction, you could repeat the same scheme here and adding the findings with '+', '--', '0' effects

Commented [CS271]: 5um Q?

Commented [CS272]: This is very vague – once you draw some sort of interactive picture of the pathways, maybe you can put this more explicitly?

Commented [CS273]: Worth putting somewhere, in the absence of a stressor, these were the data, but they may well have been different in the presence of age/inflammation for example.

Commented [SD274R273]: Have included small line later on, first line of mitochondrial respiration paragraph, mentioning this, and was going to include this in the limitations section of synthesis chapter

Commented [CS275R273]: Makes sense, thank you.

4.5.1 Flavonoids differentially affect the production of mitochondrial ROS and NO

Flavonoids possess antioxidant properties and may contribute to control of the redox state *in-vivo*. Here, flavonoids evoked dose-dependent effects upon the production of mitochondrial

ROS. In conditions of elevated oxidative stress brought about by AA, Q acted in a pro-oxidant manner. Whereas under control conditions, higher Q doses (10 μ M) were pro-, and lower doses anti-oxidant. Several studies have investigated the potential of Q to mitigate the production of vascular endothelial ROS in response to stressors like H₂O₂, high glucose, and palmitate. Despite using a range of doses (from nM to μ M), these studies have repeatedly reported attenuated ROS production in vascular endothelial cells treated with Q (Chao et al., 2009; Chen et al., 2020; Guo et al., 2013; Yang et al., 2015). However, these studies used a non-targeted probe for the examination of ROS. By contrast, a mitochondrial targeted probe (MitoSOX) was used in the present study, which may partly explain the differences between the findings. Furthermore, Q (at 100 μ M) has been shown to interact with commonly used cell culture media and acutely augment H₂O₂ production (Long et al., 2000), which may have also contributed to the observed increase in ROS production in the present study with higher micromolar doses. In the present study, EGCG attenuated rates of mitochondrial ROS production in vascular endothelial cells, with and without elevated oxidative stress. These data contrast previous findings reporting that 25-50 μ M EGCG does not contribute to the regulation of angiotensin II-induced ROS production in HUVECs (Ahn et al., 2010). Further, the current findings do not support previous observations that low micromolar doses of EGCG stimulate intracellular ROS production and activate redox sensitive signalling pathways (Collins et al., 2007; Elbling et al., 2010). Again, the inconsistencies in findings may relate to the methodological approaches employed to measure ROS production. The current study demonstrated EPI did not mitigate AA-induced ROS production, although, the rate of mitochondrial ROS production was attenuated under control conditions. Conversely, Keller and colleagues reported that 1 μ M EPI blunted the production of mitochondrial superoxide in vascular endothelial cells after AA treatment (Keller et al., 2020). In this way, the antioxidant actions of EPI *in vitro* may be largely dependent upon the dose administered. Besides ROS, NO levels were also impacted by EPI

Commented [CS276]: Add a few words to suggest the limitations of interpreting such data

Commented [SD277R276]: No major limitations per se, differences in probe specificity exist for mitochondrial or general cellular ROS. Wanted to try explain differences in our and other findings

Commented [DR278]: It feels to me that you have measured ROS in different compartments of the cell, although this is still not completely clear for me when reading your text. If so, then there is no discrepancy but just an explanation that you have measured another aspect/compartment of ROS production

Commented [CS279]: Validity?

Commented [CS280]: How could this be studied in future?

treatment in this study. At 10 μ M, EPI increased NO production, which lends support to the premise that EPI is a potent stimulator of NO in cell, human and rodent models (Loke et al., 2008b; Moreno-Ulloa, Mendez-Luna, et al., 2015a; Ramirez-Sanchez et al., 2011, 2018; Schroeter et al., 2006). Taken together, these findings emphasise the potential dose-dependent effects of flavonoids on RONS production and raise further questions about the underlying mechanisms of EPI's antioxidant actions. Possibly, EPI's mechanistic effects (increased NO and altered mitochondrial ROS) could translate to improved vascular endothelial function and increased O₂ delivery to active muscle during exercise when ingested *in vivo*, thus providing a potential mechanism by which cocoa-flavanols sped phase II $\dot{V}O_2$ kinetics in Chapter 3.

4.5.2 Flavonoids differentially modulate gene expression of vascular endothelial cells

To help establish whether the effects of flavonoids on RONS production in vascular endothelial cells relates to the cellular adaptive response, the transcription of genes associated with energy metabolism was determined in the presence and absence of Q, EGCG and EPI. Coincubation of vascular endothelial cells with Q upregulated the expression of NOX4, at least over 48 h. NOX4 is one isoform of the NADPH oxidase family that generates cellular ROS (Montezano et al., 2011). Therefore, the apparent increase in NOX4 expression may provide some causal explanation for the pro-oxidative effects of Q reported in this study. In contrast to these data, other studies have demonstrated that Q lowers the expression of NADPH oxidase subunits in endothelial cells in the presence of elevated ROS (Hung et al., 2015; Jones et al., 2016; Luo et al., 2020; Sanchez et al., 2007; Wan et al., 2009). Aside from NOX4, PGC-1 α and TFAM expression were not altered by Q treatment. This observation supports the respiration data reported, where Q did not significantly alter indices of mitochondrial function. Therefore, the transcriptional profiles of endothelial cells cultured with Q suggest altered ROS production, but no impact on mitochondrial functionality. It is currently thought that EGCG stimulates NO

Commented [CS281]: What about the actual use of EPI for suggested health benefits – worth having a bold statement r the pros/cons based on what your findings add to the literature and how they associate with your human study?

Commented [SD282R281]: Have added in line one summary

production via phosphorylation of eNOS, and these effects occur independent of changes in eNOS content (Kim et al., 2007; Lorenz et al., 2004b). This premise is partially supported by findings of the present study, where eNOS mRNA was similar or decreased with EGCG supplementation when compared to control conditions. Therefore, EGCG may modulate NO production in vascular endothelial cells via a post-translational mechanism, rather than effects mediated at the level of transcription; this warrants further investigation. Mitochondrial remodelling involves the synthesis of mitochondrial proteins and concurrent changes in organelles dynamics, mediated by fusion and fission activities. Here, coincubation of endothelial cells with EGCG upregulated the expression of genes linked with mitochondrial remodelling, including PGC-1 α , SIRT1, DRP1 and MFN2. This observation is consistent with previous studies reporting enhanced expression of molecular markers of mitochondrial biogenesis in skeletal muscle, brown adipose tissue and PC12 cells (Lee et al., 2017; Yan et al., 2012; Ye et al., 2012). Regarding the mechanism, the data suggest increased ROS production above basal conditions is not a prerequisite for the action of EGCG on mitochondrial adaptations. Although, increased CAT mRNA was observed with EGCG treatment, which could be indicative of augmented ROS, that may not have been captured by the techniques employed in this study. Of note, previous reports using specific ROS inhibitors have demonstrated that ROS are at least required for EGCG-induced mitochondrial biogenesis in hepatocytes and endothelial cells via AMPK (Collins et al., 2007; Kim et al., 2013). Thus, the precise mechanisms by which EGCG mediates transcription of vascular endothelial cells are yet to be fully elucidated. In the presence of EPI, vascular endothelial cells also exhibited increased expression of genes associated with mitochondrial dynamics. The elevated mRNA levels of MFN2 and DRP1 following EPI treatment suggests increased remodelling of endothelial mitochondria via fusion and fission activities. Along these lines, some studies have shown EPI (0.002 - 1 μ M) augments markers of mitochondrial biogenesis in endothelial cells

Commented [CS283]: Why might the differences occur? Were the Collins studies also in HUVECs? What were the doses? What were the timepoints assessed? Were there additional stressors included?

Commented [CS284]: Dose?

(Moreno-Ulloa et al., 2013; Ramirez-Sanchez et al., 2018; Ramírez-Sánchez et al., 2016a), although others have reported reductions in HUVEC mitochondrial complex I and V abundance after acute EPI supplementation (0.1-1 μ M) in the presence of AA and high glucose, respectively (Keller et al., 2020). The current study, therefore, seems to be the first to demonstrate that EPI may contribute to the remodelling of mitochondria at the level of transcription on genes associated with fusion and fission. Interestingly, EPI augmented the expression of the redox sensitive transcription factor NRF2 in the present study. There has been evidence for EPI mediated induction of NRF2, and its nuclear translocation, documented previously (Moreno-Ulloa, Nogueira, et al., 2015; Rowley et al., 2017a). Together, these data suggest that EPI may increase NRF2 activity in endothelial cells, although the exact underlying processes are not clear. In the presence of NO and ROS, modifications of cysteine residues on Keap1 relieve NRF2 inhibition, resulting in nuclear accretion of NRF2 and subsequent upregulation of antioxidant and mitochondrial related genes (Gao et al., 2020; Gureev et al., 2019; Tebay et al., 2015). Considering the increased production of NO and altered mitochondrial ROS levels in the presence of EPI found in this study, induction of NRF2 expression with EPI could be mediated by RONS. Evidently, further work is necessary to elucidate the potential signalling pathways by which EPI exerts its biological effects in vascular endothelial cells.

4.5.3 Acute dietary flavonoid treatment does not modulate indices of mitochondrial function

One main outcome of the present chapter was that dietary flavonoids do not directly impact indices of mitochondrial function in vascular endothelial cells, in the absence of additional stressors. In recent years, mitochondria have emerged as potential molecular targets of dietary flavonoids (Duluc et al., 2012). Here, the function of vascular endothelial mitochondria was

Commented [CS285]: If this chapter does follow the human study, then you should tie the findings back. If not and the human study is the last one, you should precede it with predictions on what may happen, based on the huvec and c2c12 data and then conclude whether the hypotheses were supported or not and if not why not.

Commented [SD286R285]: I agree makes sense, need to finalise the order of the data

not directly impacted by physiological flavonoid concentrations. Although 5 μM Q lowered rates of basal respiration and oxidative ATP synthesis versus CTRL, this reduction was not significant. The observation that Q did not measurably impact mitochondrial bioenergetics supports a previous study reporting that Q doses up to 10 μM do not affect rates of oxygen consumption in rat brain and heart mitochondria (Lagoa et al., 2011). However, other research has provided evidence that Q may in-fact impair state 3 supported respiration, at least in isolated rat liver and heart mitochondria (Dorta et al., 2005; Trumbeckaite et al., 2006). In a similar way, the precise effects of EGCG on mitochondrial function are not entirely clear. Whilst some research has documented enhanced state 3 respiration/ADP supported respiration in rat cardiomyocytes treated with EGCG, others have reported negligible effects of 10 μM EGCG on respiration in isolated hepatocyte mitochondria (Kucera et al., 2015). The aforementioned discrepancies, between study outcomes, emphasise the potential cell-specific and dose-dependent effects of flavonoids on mitochondrial function. Studies on the effects of EPI on mitochondrial respiration in cells have also produced equivocal results. Whilst some studies have demonstrated increased state 3 respiration in rat β cells following EPI (0.1-2.5 μM) supplementation (Kener et al., 2018a; Rowley et al., 2017a), others have demonstrated inhibited/similar state 3 respiration rates with EPI, depending on the substrates provided during respirometry (Kopustinskiene et al., 2015b). Notably, one recent investigation examined the impact of EPI on mitochondrial function in vascular endothelial cells (HUVECs). Similar to the findings in the present study, the authors reported that 0.1 and 1 μM EPI supplementation over 2 hours had no impact on mitochondrial respiration as assessed by respirometry (Keller et al., 2020). Taken together, it seems that flavonoids do not directly impact indices of mitochondrial function when used in the low micromolar range (1-10 μM). Future studies could investigate whether nanomolar flavonoid concentrations impact vascular endothelial cell

Commented [SD287]: Have added in short sentence saying 5 μM Q lowered mito respiration but it didn't reach significance

Commented [CS288]: Species?

Commented [CS289]: Dose/time?

Commented [CS290]: And so? End with a conclusion and potential for future investigations? Just a couple of sentences, not a huge amount of additional text.

bioenergetics, and also, study alternate modes of action that potentially converge on mitochondria.

4.5.4 EPI transiently stimulates ERK1/2 signalling whilst suppressing AMPK activity

One important pathway upstream of mitochondria is the AMPK signalling axis. Interestingly, enhanced phosphorylation of AMPK has been reported in various tissues in the presence of EPI, though not including endothelial cells (Murase et al., 2009; Papadimitriou et al., 2014; Si et al., 2011). One recent study using HUVECs demonstrated 2 h EPI treatment (1 μM) had no effect upon the phosphorylation of AMPK (Keller et al., 2020). In a similar fashion, the data presented here demonstrate that AMPK phosphorylation at Thr172 is suppressed up to 1 h in the presence of 5 μM EPI, and up to 24 h, no impact of EPI was observed on AMPK activity. Aside from AMPK, the effects of EPI on vascular endothelial function could relate to the activation of ERK1/2 signalling. Accordingly, ERK1/2 phosphorylation at Thr202/Tyr204 was acutely increased following EPI supplementation here, supporting recent observations of increased ERK1/2 activity after 0.1 μM EPI treatment in bovine coronary artery endothelial cells, that may be associated with phosphorylation of CaMKII (Moreno-Ulloa, Mendez-Luna, et al., 2015a). Regarding CaMKII, it has been postulated that EPI may induce ergogenic effects via phosphorylation at Thr286 (Moreno-Ulloa, Mendez-Luna, et al., 2015a; Ramirez-Sanchez et al., 2010). However, the present investigation reported no phosphorylation of CaMKII at Thr286 in vascular endothelial cells. In this way, more research is necessary to better define the signalling mechanisms associated with EPI in vascular endothelial cells, but the data suggest that ERK1/2 activation is independent, at least of Thr286 phosphorylation of CaMKII in HUVECs. Downstream of the aforementioned kinases, there was no significant change in eNOS phosphorylation at Ser1177 in the presence of EPI. These data agree with the recent findings of Keller and colleagues (Keller et al., 2020), and dispute previous reports of increased

Commented [CS291]: In what cells?

Commented [CS292]: This is a bit confusing – the sentence before say phosphorylation was blunted for 24 hours, how can you say here there was no impact?

eNOS phosphorylation in vascular endothelial cells following EPI treatment at low micromolar doses (Carnevale et al., 2014; Ramirez-Sanchez et al., 2010, 2012, 2018; Ramirez-Sánchez et al., 2016b). Given that EPI was capable of augmenting NO production in this study, it is possible that EPI increased NO levels via inhibition of arginase (thus increasing the availability of L-arginine for NO synthesis) as opposed to acting via eNOS activity (Schnorr et al., 2008). These findings demonstrate that EPI augments ERK1/2 signalling in vascular endothelial cells independent of AMPK phosphorylation. However, it remains to be determined whether EPI's acute activation of ERK1/2 signalling is a prerequisite for the induction of NRF2 in vascular endothelial cells.

Commented [SD293]: We would need to adjust this sentence if the signalling work stays here, as we have not yet discussed NRF2?

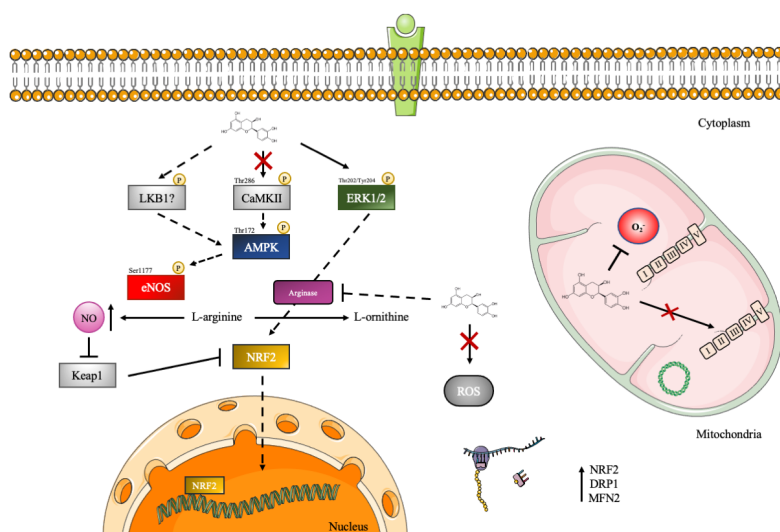


Figure 4. 16 Schematic of the potential mechanisms by which EPI exerts its biological effects in vascular endothelial cells. Dashed arrows represent no, or unknown activity of EPI on protein activity. Solid lines represent reported stimulatory or inhibitory effects of EPI.

Commented [SD294]: Have focused on EPI here, given the focus on this compound for signalling work, and given it's the primary compound present in the cocoa-flavanol supplement in vivo. Option is there to include Q and EPI also, but would be hard to incorporate too, at least into this single figure. Perhaps separate ones could be made

4.6 Limitations

Parent flavonoid compounds were used in this study rather than metabolites that typically reach circulation following the ingestion of flavonoid-containing foods/beverages or supplements (Ottaviani et al., 2016). Therefore, it is not known whether the reported effects of flavonoids on vascular endothelial cells in this study will be subsequently replicated using their associated metabolites. In this study, HUVECs were used a model vascular endothelial cell system. These cells are venous in nature and as such their physiology may not well reflect the arterial vasculature where flavonoids potentially exert their beneficial effects. Thus, caution should be taken when interpreting the results obtained with flavonoids in these cells. A noteworthy limitation of this study was that flavonoids were administered in some assays, without any additional cell stressor. Given that ageing is associated with perturbations to cellular function, it is possible that flavonoids may have evoked different effects to those observed upon gene expression and mitochondrial bioenergetics in the presence of additional cell stress. Whilst attempts were made to replicatively age HUVECs as part of this programme of work, the cells very rapidly become senescent and therefore no meaningful studies could be performed due to insufficient cell numbers. Finally, western blotting was used to determine relative protein phosphorylation in a semi-quantitative manner, which does not provide a direct measure of protein activity.

Commented [CS295]: Can they be purchased – if not, state this e.g. is it better to make an attempt at the understanding in the absence of flavonoid metabolites or should we do nothing because no ethics would ever be granted to do relevant human mechanistic studies....

4.7 Conclusion

To summarise, this chapter demonstrates that dietary flavonoids, at the doses tested, do not directly impact mitochondrial bioenergetics, but rather modulate signalling and transcriptional activities of vascular endothelial cells. One key theme of this work was that flavonoids evoked dose-dependent effects upon energy metabolism. Interestingly, EPI evoked dose-dependent effects upon RONS production, which occurred in parallel with enhanced, transient ERK1/2 signalling (see Figure 4.16). Moreover, all flavonoids tested evoked changes in gene

transcription indicative of mitochondrial remodelling and the stress response. Taken together, EPI may promote favourable mitochondrial adaptations in vascular endothelial cells through activation of stress response pathways and increases in NO, when ingested *in vivo*. With that said, dietary EPI supplementation *in vivo* may improve vascular endothelial function, and potentially, augment O₂ delivery during physical activity. Future translational research will help define the exact mechanisms by which EPI regulates ERK1/2 activity, NRF2 induction, and mitochondrial remodelling. Further, clinical trials will help establish whether EPI supplementation can improve vascular endothelial function and increase exercise tolerance in sedentary older adult populations.

Commented [CS296]: If you have generated a figure of the pathways and how the different flavonoids increase or decrease them, then you may be able to have a tighter conclusion here with specific recommendations for either future studies or human prescription.....what is your gut, is there a benefit to taking any of these flavonoids, from a vascular endothelial perspective and based on your studies – how could you address this further (come back to the sorts of experiments that could be done in e.g. humans in the future directions chapter)

Commented [SD297R296]: Have attempted to improve this...

Chapter 5: The effects of replicative ageing
and dietary flavonoids on mitochondrial
function, nitric oxide bioavailability and gene
expression of C₂C₁₂ skeletal myoblasts

5.1 Abstract

Introduction: The capacity for oxygen (O₂) utilisation is compromised with advancing age, which contributes to exercise intolerance. Mitochondrial dysfunction is a feature of sedentary ageing, thought to be partly responsible for impairments in O₂ utilisation, characterised by lowered respiratory capacity and lowered mitochondrial contents. Flavonoids have emerged as health promoting entities that may modulate mitochondrial function, but little is known how they impact ageing skeletal muscle mitochondria.

Objective(s): The primary objectives were to determine whether replicative ageing and dietary flavonoids (quercetin [Q], epigallocatechin-gallate [EGCG] or (-)-epicatechin [EPI]) impacted mitochondrial function, nitric oxide (NO) bioavailability and gene expression using C₂C₁₂ myoblasts as a model system. It was hypothesised that replicative ageing would cause mitochondrial dysfunction, lower NO bioavailability and blunt gene expression and that these effects would be mitigated by dietary flavonoid supplementation.

Methods: Control and replicatively aged C₂C₁₂ myoblasts were treated in the absence (CTRL) or presence of micromolar concentrations of Q, EGCG or EPI for up to 48 h. Mitochondrial bioenergetics were investigated by respirometry after 24 h flavonoid treatment. Complex I activity was measured spectrophotometrically over 24 h. NO bioavailability was determined by DAF-FM oxidation using flow cytometry over 24 h. Genes related to mitochondrial remodelling and the antioxidant response were quantified by RT-qPCR over 48 h.

Results: Indices of mitochondrial function, including basal respiration, proton leak and coupling efficiency were similar between control and aged myoblasts. Generally, flavonoids did not impact mitochondrial respiration, but EPI inhibited basal respiration by 27.6% (5 μM EPI: 1.31±0.14 vs. CTRL: 1.81±0.15 pmol O₂/min⁻¹/ng DNA⁻¹; *P*=0.041). A downward trend in complex I activity (28.3%) was found in the presence of EPI (5 μM: 49.4±3.9 vs. CTRL: 35.4±4.4 nmol/min⁻¹/mg⁻¹ protein; *P*=0.079) vs. CTRL in aged myoblasts. NO levels were 50% lower in aged versus control myoblasts (*P*=0.024) and were not impacted by flavonoids. Flavonoids augmented the expression of genes associated with mitochondrial remodelling and the antioxidant response, in a dose- and compound dependent manner. PARKIN and SOD2 mRNA levels were 3.9-fold and 3.2-fold lower in aged vs. control myoblasts over 48 and 24 h, respectively, but were not rescued by flavonoids. NRF2 expression was upregulated by EPI treatment in control (1.6-fold increase over 24 h after 5 μM EPI vs. CTRL; *P*=0.045) and aged (1.6-fold increase with 5 μM EPI over 48 h vs. CTRL, *P*=0.032) myoblasts.

Commented [CS298]: Very nice scene setting

Commented [HJ299]: Same comment ... is this consistent throughout?

Commented [SD300]: why study this?

Commented [CS301]: Please can you track and change your thesis and remove , before and

Commented [CS302]: Somewhere early you need to spell out that CTRL is not the same as control e.g. the latter is non-passaged. I don't mean in the abstract, but somewhere early on define CTRL as untreated, regardless of whether aged or not.

Conclusion(s): Replicative ageing does not impair indices of mitochondrial function but lowers NO bioavailability and attenuates mitochondrial (PARKIN and SOD2) gene expression in skeletal myoblasts. Generally, flavonoids did not modulate mitochondrial respiration, although EPI may inhibit respiration in aged myoblasts. Further, flavonoids did not mitigate age-related impairments to NO bioavailability. Flavonoids may instigate cell adaptations at the transcriptional level, partly via NRF2, that could be related to respiratory inhibition in the presence of EPI.

Commented [CS303]: Not mentioned in the results – move this info up and then rejig the conclusion

Commented [SD304R303]: Need to do this!

Commented [CS305]: Very nice abstract. All should take on this sort of format.

5.2 Introduction

Advancing age and physical inactivity are strongly associated with a decline in tolerance of daily life activity, that is largely owed to reductions in maximal oxygen uptake (Fitzgerald et al., 1997; Paterson et al., 2007) and slowed pulmonary oxygen uptake ($\dot{V}O_2$) kinetics during submaximal exercise (DeLorey et al., 2004a; Dumanoir et al., 2010; George et al., 2018; B. Grassi, Porcelli, et al., 2011). The detrimental impact of sedentary ageing on $\dot{V}O_2$ kinetics is thought to be due to changes in the systems responsible for the delivery and utilisation of oxygen (O_2). Oxygen utilisation during exercise is controlled by numerous factors, including pyruvate dehydrogenase (PDH) activation, phosphocreatine kinetics and mitochondrial functionality. Of these factors, the function (and content) and activation of skeletal muscle mitochondria may be of central importance in the kinetics of $\dot{V}O_2$, because these organelles house the molecular machinery required for ATP synthesis that is achieved through the generation of a proton motive force and consumption of molecular O_2 .

Mitochondrial dysfunction is considered a major hallmark of ageing. Yet, the role of chronological ageing in regulating skeletal muscle mitochondrial function has been subject to much debate. Several *in vitro* studies have reported an age-related decline in maximal oxidation rates in isolated mitochondria from rodent skeletal muscle (Kumaran et al., 2005; Mansouri et al., 2006), and also in permeabilised fibres from human skeletal muscle tissue (Tonkonogi et al., 2003a). Similarly, the maximum capacity for ATP production in isolated mitochondria from rat and human skeletal muscle reportedly declines with older age (Drew et al., 2003a; Short et al., 2005), which could relate to lowered complex I activity (Boffoli et al., 1994; Cooper et al., 1992). In contrast, a handful of studies have found no age-related impairments to organelle functionality. For instance, mitochondria isolated from human vastus lateralis had comparable respiratory function in the presence of various metabolic substrates between young

Commented [CS306]: Spell out all abbreviations on first use

and older individuals (Rasmussen et al., 2003). Moreover, rates of ADP-stimulated respiration were unchanged between young and old rat skeletal muscle tissue (Chabi et al., 2008b; Picard et al., 2010b). These inconsistent findings can partially be explained by potential artefacts introduced by the *in vitro* isolation procedures, that may affect mitochondrial function independent of the ageing process (Picard et al., 2010b). To circumvent the effects of mitochondrial isolation, mitochondrial respiratory function was examined in intact skeletal myoblasts in this chapter.

Beyond functionality, older human skeletal muscle displays lowered mitochondrial contents compared to young (Rooyackers et al., 1996; Short et al., 2005), which may be due to blunted transcriptional responses to relevant stimuli. For example, the expression of peroxisome proliferator-activated receptor gamma coactivator 1-alpha (PGC-1 α), an important regulator of mitochondrial adaptations, is reportedly lower following exercise in older compared to younger adults (Ljubicic & Hood, 2009; Reznick et al., 2007b). Older adults also demonstrate diminished nitric oxide (NO) bioavailability in muscle tissue (Nyberg et al., 2012), which may exacerbate reductions in PGC-1 α activation. Additionally, lower NO levels could attenuate the nuclear translocation of nuclear factor erythroid 2-related factor 2 (NRF2), and subsequently impair the transcription of several mitochondrial and antioxidant related genes. Organelle's quality control processes, including mitophagy and mitochondrial dynamics, also play important roles in maintaining mitochondrial health. With ageing, both mitophagy and fusion:fission activities (ratio of mitofusin-1 (MFN2): dynamin-related protein 1 (DRP1) are reportedly dysregulated (Carter et al., 2018; Chen et al., 2018b; Iqbal et al., 2013), which may compromise mitochondrial functionality. Together, targeting molecular pathways that converge on mitochondria may offer promise in mitigating age- and (in)activity related declines in O₂ utilisation, and ultimately may improve exercise tolerance.

Commented [CS307]: In humans? If so state, if not, provide the model

Dietary flavonoids are increasingly recognised for their potential to modulate indices of mitochondrial function. Although evidence for direct flavonoid and skeletal muscle mitochondria interactions is lacking, flavonoids accumulate within the mitochondrial compartments of different cell types (Fiorani et al., 2010a; Mukai et al., 2016; Schroeder et al., 2009). Some flavonoids have been reported to modulate mitochondrial respiration (Dorta et al., 2005; Rowley et al., 2017b; Vilella et al., 2020a), although data in skeletal muscle cells is very limited (Bitner et al., 2018). Moreover, flavonoids may stimulate pathways responsible for mitochondrial turnover in skeletal muscle (Davis et al., 2009b; Hüttemann et al., 2013; Moreno-Ulloa et al., 2018; Murase et al., 2009). Another reported role for flavonoids relates to the modulation of NO production. Several studies have documented that flavonoids and their associated metabolites stimulate NO production in vascular endothelial cells (Ramirez-Sanchez et al., 2018; Shen et al., 2012), but more research is needed to establish whether these effects occur in skeletal muscle. Evidently, it remains to be determined whether flavonoids modulate mitochondrial function and NO bioavailability of skeletal muscle cells.

One major utility of cell models lies in the non-invasive investigation of mechanisms that are associated with health and disease *in vivo*. Previously, a murine skeletal muscle cell model of ageing was established that somewhat recapitulates ageing muscle behaviour (Sharples et al., 2011, Bigot et al 2008). Although this model has been characterised with respect to ageing muscle hypertrophy, it is not currently known how this model captures ageing human muscle behaviour as it relates to energy metabolism. Consequently, the main aim of the present study was to characterise how replicative ageing impact's mitochondrial function, NO bioavailability and gene expression of aged vs. control skeletal myoblasts. The study objective was to determine whether replicative ageing and dietary flavonoids (quercetin [Q], epigallocatechin-

Commented [CS308]: Are any of these in skeletal muscle?

Commented [SD309]: Check all refs are skeletal muscle based

Commented [CS310]: No oversight of any of the genes you want to study nor of the signalling pathways to be investigated. If this has been done in the main intro (sorry, I cant remember), then refer the reader to the relevant sections. If not, please add a couple of paragraphs to this intro to let your reader know these parameters will be investigated and why they are relevant.

Commented [CS311]: Comment as above re genes of interest. They have not been introduced, so unexpected to have them in the abstract. If introduced in the main intro, please reference that text somewhere in this chapter and also the coming chapters that investigate the genes of interest.

Commented [CS312]: nice

gallate [EGCG] or (-)-epicatechin [EPI]) impact mitochondrial function, nitric oxide (NO) bioavailability and gene expression using C₂C₁₂ myoblasts as a model system. It was hypothesised that replicative ageing would cause mitochondrial dysfunction, lower NO bioavailability and blunted gene expression, and that these effects would be mitigated by dietary flavonoid supplementation.

5.3 Methodology

5.3.1 Cell culture and treatment

Commercially available C₂C₁₂ murine skeletal myoblasts at passages 8-12 (referred to as ‘control’) and passages 47-50 (replicative aged and referred to as ‘aged’, having undergone 130-140 population doublings) were used in this study. For standardised cell culture procedures, see section 2.3. Following the plating of cells onto appropriate well-plates in growth medium (GM), confluent C₂C₁₂ cells were washed twice with phosphate-buffered saline (PBS) and switched to pre-warmed (37°C) differentiation medium (DM). For experiments in myoblasts, C₂C₁₂ cells were switched to DM in the absence, or presence of specific concentrations of Q, EGCG and EPI (0-20 µM) over 24 and 48 h.

5.3.2 Cell viability assay

Following generation of a standard curve (see section 2.7), cell viability was determined in response to acute dietary flavonoid treatment using the fluorescent CyQUANT® Proliferation Assay kit (ThermoFisher, Waltham, MA, USA). C₂C₁₂ myoblasts were grown to ~80% confluency in 96-well plates before being transferred to DM +/- flavonoids. Dose responses were performed with Q, EGCG and EPI at 0-20 µM for 24 h, prior to aspiration, washing twice with PBS, and then freezing immediately at -80°C. On the day of the experiment, plates were

Commented [SD313]: why study this? Something like this may be a good linker: <https://journals.physiology.org/doi/full/10.1152/japplphysiol.00490.2011> or this one: <https://pubmed.ncbi.nlm.nih.gov/22950758/> or maybe this review: <https://link.springer.com/article/10.1007/s10068-020-00816-5>

Commented [CS314]: If your general cell methods are in a general chapter, then your first couple of methods on how you work with cells would be referred to here e.g. see 2.2.1 for general methods on cell culture etc – see Alex’s thesis for clarification of what I mean.

For a paper you would need to add the relevant info to your methods, but you know that already.

Commented [CS315]: Details of company eg ThermoFisher Scientific, XXXX, UK

Commented [CS316]: Ensure these are spelled out somewhere in the chapter – if this is the first mention, spell out here

Commented [CS317]: If cold, specify

thawed at room temperature, and 100 μ L of CyQUANT® GR dye/cell-lysis buffer was added to each sample well. Plates were gently mixed on an orbital shaker for 5 minutes protected from light. Sample fluorescence was measured using a CLARIOStar Plate Reader (BMG Labtech, Bucks, Great Britain) with Excitation 485-12 and Emission EM520 filters in bottom reading, well scanning mode.

Commented [CS318]: Details of company – I wont write this again, but please update methods accordingly

5.3.3 Nitric oxide availability

For the determination of intracellular nitric oxide (NO) bioavailability, C₂C₁₂ myoblasts were plated in gelatin-coated 12-well plates in GM and incubated (37°C, 5% CO₂) until ~80% confluency. Once confluent, cells were switched to DM, containing 0, 5 and 10 μ M Q, EGCG or EPI, for 24 h. Next, myoblasts were washed 2 \times with PBS and loaded with DAF-FM™ diacetate (4-amino-5-methylamino- 2',7'-difluorofluorescein diacetate; Molecular Probes, Invitrogen). DAF-FM™ was loaded in myoblasts to a final concentration of 1 μ M in pre-warmed KRH buffer and incubated at 37°C for 30 minutes protected from light. Following dye loading, cells were washed 2 \times with PBS and immediately trypsinised. After trypsin neutralisation, cells were pelleted and resuspended in PBS, before measuring sample fluorescence by flow cytometry (BD Accuri C6, BD Biosciences, Wokingham, UK). Data were recorded from 5,000 events.

5.3.4 Mitochondrial Bioenergetics

Mitochondrial respiration was measured in adherent C₂C₁₂ myoblasts using a Seahorse XFe96 Analyzer (Agilent, Santa Clara, CA, USA). Control (passages 9-11) and replicatively aged (passages 47-50) C₂C₁₂ myoblasts were seeded in XFe96 well plates (Agilent, Santa Clara, CA, USA) at 5,000 cells per well in 100 μ L of GM for 24 h to allow cell attachment. After 24 h,

C₂C₁₂ myoblasts were washed twice with PBS and transferred to DM. Myoblasts were dosed with specific concentrations (0, 1, 5 and 10 μ M) of Q, EGCG and EPI in DM for 24 hours.

Sensor cartridges for the XFe96 Analyzer were hydrated with deionised water at 37°C in a non-CO₂ incubator in the 24 h preceding the assay. On the day of the assay, C₂C₁₂ myoblasts were washed into 200 μ L pre-warmed modified KRH at pH 7.4 (see table 2.1 for KRH composition). The cells were incubated in this buffer for 45 minutes at 37°C in a non-CO₂ incubator and then transferred to a Seahorse XFe96 extracellular flux analyser (maintained at 37°C). Following 10-minute calibration, oxygen consumption rates (OCR) were measured by a 3-4 loop cycle consisting of a 1-min mix, 2-min incubate and 3-min measure to record cellular basal respiration (Figure 2.6). After measuring basal respiration, 2 μ M oligomycin was added to selectively inhibit the mitochondrial ATP synthase. Subsequently, 2 μ M carbonyl cyanide-4-phenylhydrazone (FCCP) followed by a mixture of 2 μ M rotenone and 2 μ M antimycin A were added sequentially to, 1. uncouple oxygen consumption rates to ATP synthesis rates to determine maximal respiration or 2. inhibit complex I and III of the electron transport chain to determine non-mitochondrial respiration. Rates of oxygen consumption and extracellular acidification (ECAR) were expressed relative to the DNA content of the appropriate well (see section 5.3.6). Three independent experiments were performed to assess mitochondrial respiration, each containing four technical replicates. The Wave software native to the XF Analyzer was used to extract OCR's and ECAR.

5.3.5 ATP Production Rates

A full description of the method used for calculation of total cellular ATP production rates from ECAR and OCR is in section 2.11, chapter 2. Briefly, to calculate J_{ATPglyc} , the ECAR was first converted to total proton production rate (PPR). The contribution of respiratory CO₂ to

Commented [CS319]: Remember to add the full name before the (FCCP)

Commented [CS320]: What is the F an abbreviation of?

total PPR was subtracted to yield glycolytic rate of glucose catabolism terminating in lactate. This rate was multiplied by the ratio of ATP produced in glycolysis terminating in lactate per extracellular H^+ (the P/H^+ ratio). Additional glycolytic flux generating the pyruvate that is later fully oxidised in the mitochondria generates additional ATP and is represented in the mitochondrial respiration rate (see below). Mitochondrial respiration rate was multiplied by the ratio of ATP produced in glycolysis terminating in pyruvate per O_2 consumed for each substrate (P/O_{glyc}). Glycolytic ATP production ($J_{ATP_{glyc}}$) was calculated as the sum of these two rates. To calculate $J_{ATP_{ox}}$, mitochondrial respiration rate was isolated by subtracting from the total OCR any additional oxygen consumption in the presence of rotenone and antimycin A ($OCR_{R/AA}$). Mitochondrial respiration rate was further divided into ATP-coupled and uncoupled respiration rates using the mitochondrial ATP synthase inhibitor oligomycin. The ATP-coupled respiration rate was multiplied by the portion of the P/O ratio attributable to the mitochondrial ATP synthase (P/O_{OXPHOS}). To account for oxidative substrate-level phosphorylation in the TCA cycle, the mitochondrial respiration rate was multiplied by the P/O ratio attributable to succinyl CoA synthetase (P/O_{TCA}). Oxidative ATP production ($J_{ATP_{ox}}$) was calculated as the sum of these two rates. Finally, $J_{ATP_{glyc}}$ and $J_{ATP_{ox}}$ were summed to yield the total cellular ATP production rate, $J_{ATP_{production}}$.

5.3.6 Mitochondrial bioenergetics normalisation procedures

5.3.6.1 CyQuant® Direct Cell Proliferation Assay

The 2x detection reagent was made by combining KRH buffer (assay media) with CyQuant® Direct nucleic acid stain and CyQUANT® Direct background suppressor, prior to removal of assay media from each well of the Seahorse microplate, whilst ensuring to leave appropriate necessary volume (25 μ L). To each well, 25 μ L ~~2X~~ detection reagent was added. Cells were incubated in the dark for 60 minutes at 37°C without CO_2 , prior to fluorescence measures being

Commented [CS321]: How was this done accurately between wells? Did you have a method of aspirating 175 ul from each well? If not precise, then the dilution of your detection reagent would be impacted well to well.

Commented [CS322]: How can this be 2x if being added to 25ul?

Commented [CS323R322]: Hans will pick you up on this – if adding 12.5 ul to 25 ul, while it may be a 2x stock, you are actually diluting it 3x eg 12.5/37.5

captured using a FLUOstar Omega Plate Reader with Excitation 485-12 and Emission EM520 filters in bottom reading, well scanning mode. DNA content in each sample was quantified by interpolating unknown X values by comparing RFU values with those on a standard curve of known DNA concentrations (see Figure 5.1).

Commented [CS324]: Vague – this needs expanding and clarifying.

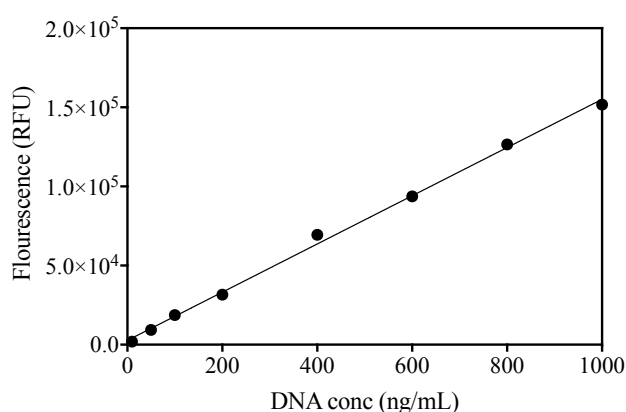


Figure 5. 1 DNA standard curve generated using CyQUANT[®] Cell Proliferation Assay. Bacteriophage λ DNA standards (0-1000 ng/mL) fluorescence was measured using a filter combination of 480 nm excitation and 520 nm emission and corrected for the background fluorescence determined for the no-DNA control. Data are from one independent experiment from 3 technical replicates.

5.3.6.2 dsDNA PicoGreen

QuantiT[™] PicoGreen[®] dsDNA reagent (ThermoFisher, Waltham, MA, USA) was used as a fluorescent nucleic acid stain for quantifying dsDNA in solution. Upon completion of mitochondrial stress tests, C₂C₁₂ myotubes were immediately removed from the Seahorse Analyzer and existing assay media (KRH buffer) carefully removed, ensuring that ~25 μ L remained. Subsequently, 200 μ L RIPA buffer was added to each well of the 96-well plate and plates were shaken vigorously on an orbital shaker for 10 minutes. Plates were immediately

Commented [CS325]: Same comment above re precision of remaining volume

frozen at -80°C until further processing. On the day of the assay, 96-well plates were allowed to thaw at room temperature. Meanwhile, a 1X Tris-EDTA (TE) buffer (10 mM Tris-HCl (pH 7.5), 1 mM EDTA) was prepared in DNase free H_2O and left to reach room temperature. A working concentration of QuantiT™ PicoGreen® dsDNA reagent was prepared by making a 200-fold dilution of the concentrated stock solution using TE buffer. To avoid the reagent absorbing to glass surfaces or being susceptible to photo degradation it was prepared in a plastic container and stored away from direct light. A 5-point high-range DNA standard curve was created using a 100 $\mu\text{g}/\text{mL}$ Lambda DNA stock solution diluted in 1x TE buffer supplemented with 50 RIPA buffer (see Figure 5.2). 50 μL of each DNA standard (0, 2, 20, 200, 2000 ng/mL) was added to wells of a black solid-bottom 96-well microplate (Greiner Bio-One, Kremsmünster, Austria) in duplicate. Next, 50 μL of each sample was added to appropriate wells, followed by 50 μL 1x TE buffer. Finally, 100 μL PicoGreen reagent was added to each well. Following a 5-minute incubation at room temperature in the dark, endpoint fluorescence was measured by exciting fluorescent products at 485 nm and recording emitted light at 520 nm using a multi-plate reader (OMEGA FluoSTAR, BMG Labtech). To ensure all sample readings remained in the detection range of the fluorometer, the gain was set to that of the sample containing the highest DNA concentration (i.e., the 2 $\mu\text{g}/\text{mL}$ Lambda DNA stock). DNA content in each sample was quantified by interpolating unknown X values by comparing RFU values with those on a standard curve of known dsDNA concentrations.

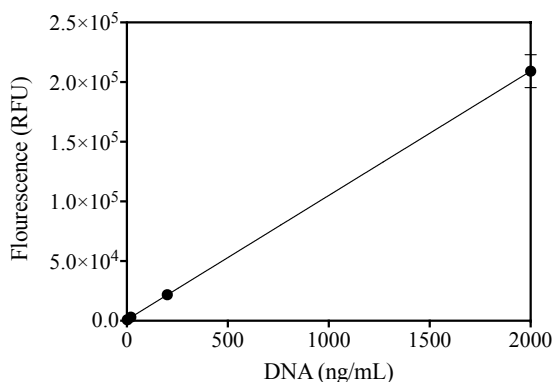


Figure 5. 2 Standard curve of Lambda dsDNA detected with QuantiT™ PicoGreen® dsDNA reagent. Cell Proliferation Assay. Lambda DNA was diluted to create standards of known concentrations (0-2000 ng/mL) and were quantified using QuantiT™ PicoGreen® dsDNA reagent. Samples were excited at 480 nm and fluorescence emission intensity measured at 520 nm. Relative fluorescent units were plotted as a function of dsDNA and fitted with linear regression.

5.3.7 Complex I Activity

Mitochondrial complex I catalyses NADH oxidation. Electrons are transferred from NADH through complex I to ubiquinone (CoQ10), which is reduced to ubiquinol. Complex I activity was measured as the rotenone-sensitive decrease in NADH at 340nm. Control and aged C₂C₁₂ myoblasts were grown to ~80% confluence in 6-well plates before being washed twice with PBS and transferred to DM. Cells were allowed to differentiate for 24 h, +/- Q, EGCG and EPI at 0, 5 and 10 μM. After 24 h treatment, cells were washed twice with PBS and trypsinised for 5 minutes at RT. Detachment was confirmed by microscopy, prior to the addition of fresh GM to neutralise the trypsin. The resultant cell suspension was aliquoted into Eppendorf tubes and centrifuged for 5 minutes at 230 × g. The supernatant was carefully aspirated, and cell pellets were resuspended in 100 μL PBS and immediately frozen at -80°C. On the day of the assay, cell suspensions were thawed and refrozen twice in liquid N₂, to enable cell lysis, before being

Commented [CS326]: Should this be moved to follow the mito methods? It seems a bit out of synch otherwise – unless this is the order your results are going to be in, but I cant remember.

diluted 1 in 5 in Milli-Q H₂O and kept on ice prior to assay. Samples were assayed as follows (total cuvette volume 1 mL; Table 5.1):

Table 5. 1 Cuvette contents to assay complex I activity

	Sample (μL)	Reference (μL)
Phosphate buffer	800	800
BSA	50	50
NADH	30	30
KCN	10	10
Cell homogenate	20	20
H ₂ O	80	90

Commented [CS327]: I assume the sample sample also had 10 ul of lysate? Add this to the table

Cuvette (Sigma-Aldrich, Poole, UK) contents were mixed gently and placed in a spectrophotometer (Uvikon 941 plus, NorthStar Scientific, Leeds, USA) for 1-2 minutes to reach 30°C, prior to ubiquinone (10 μL) addition to non-reference samples, before gentle mixing and measuring absorbance every 30 seconds over 5 minutes at 340 nm. Samples were mixed in cuvettes by covering the top of the cuvette with parafilm and inverting three times. After 5 minutes, rotenone (20 μL) was added to each cuvette and gently mixed. After allowing 2-3 minutes for the rotenone to take effect, measurements were continued at 340 nm for a further 5 minutes. Enzyme activity was determined using Equation 5.1:

Commented [CS328]: For how long

$$\Delta A = C \times \epsilon \times b \quad C = \frac{\Delta A}{b}$$

Where C = enzyme concentration (Mole/min⁻¹/L), A = absorbance in AU, ΔA = ΔA₁ - ΔA₂ (ΔA₁ = change in absorbance/min⁻¹ before rotenone addition and ΔA₂ = change in absorbance/min⁻¹ after rotenone addition); ε = extinction coefficient (Mole/cm⁻¹), which is 6.81

$\times 10^3 \text{ M/cm}^{-1}$ and b = path length in cm (1 cm). Complex I activity was normalised relative to protein content (see section 2.15).

Equation 5. 1 Enzyme activity determination

5.3.8 RT-qPCR – Gene expression Quantification

C₂C₁₂ myoblasts were lysed in 250 μL TRIzol and total RNA was extracted using the phenol-chloroform method (see section 2.12.1). RNA concentration of control and aged myoblasts ($n=3$, in duplicate per condition; Control myoblasts: 792.7 ± 120.8 ; Aged myoblasts: $1841.8 \pm 592 \text{ ng}/\mu\text{L}$) and purity (All samples $2.0 \pm 0.0 A_{260}/A_{280}$, respectively) was determined by spectrophotometry (NanoDrop™ 2000, Thermo Fisher Scientific, Waltham, USA). Samples were diluted in nuclease-free H₂O to a concentration of $7.95 \text{ ng}/\mu\text{L}$, enabling the addition of 35 ng RNA per PCR. Total reaction volume equalled 10 $\mu\text{L}/\text{sample}$, which contained 5.6 μL of master mix (5 μL QuantiFast Sybr® Green, 0.5 μL primer, 0.1 μL reverse transcriptase) and 4.4 μL RNA sample. Specific primers used in each PCR are outlined in Table 5.2, and their associated function in Chapter 9, table 9.1. After preparation, reaction tubes (Qiagen, UK) were transferred to a Rotor-Gene Q PCR thermal cycler for product amplification using a one-step protocol (see section 2.12.4). The amplification protocol was as follows: reverse transcription (10 minutes at 50°C), transcriptase inactivation and initial denaturation (95°C for 5 min) followed by 40 \times amplification cycles consisting of: 95°C for 10 s (denaturation) and 60°C for 30 s (annealing and extension); followed by melt curve detection. Critical threshold (C_T) values were derived from setting a threshold of 0.08 for all genes. The amplification efficiencies were analysed for all reactions (Control myoblasts: 92.5 ± 5.4 ; Aged myoblasts: $92.0 \pm 6.0 \%$) and values between 80-100% were accepted as efficient. To quantify gene expression, C_T values

were used to quantify relative gene expression using the comparative Delta Delta C_T ($2^{-\Delta\Delta C_T}$) equation (Livak & Schmittgen, 2001), whereby the expression of the gene of interest was determined relative to the internal reference gene (RP2 β) in the treated sample, compared with the untreated zero-hour control. RP2 β was selected as an internal reference gene because its expression was stable across experimental conditions (19.76 ± 0.69).

Table 5. 2 Primer sequences for *Mus musculus* with product length. All primers were used under the same cycling conditions.

Gene	Accession	Sequence		Product length (bp)
		Forward/Reverse or Anchor nucleotide		
Polr2b (RP2 β)	NM_153798.2	F: GGTCAGAAGGGAACCTGTGGTAT	R: GCATCATTAATGGAGTAGCGTC	197
CAT	NM_009804	AN: 324		96
SOD2	NM_013671	AN: 1769		103
Dnm1 (DRP1)	NM_152816	AN: 1337		104
MFN2	NM_113201	AN: 1709		93
Ppargc1a (PGC-1 α)	NM_008904	AN: 4601		122
Sirt1	NM_001159589.2	F: ACAATTCCTCCACCTGAG	R: GTAACCTCACAGCATCTTCAA	124
Tfam	NM_009360.4	F: TCTTGGGAAGAGCAGATGGC	R: GTCTCCGGATCGTTTCACACT	72
eNOS	NM_008713.4	F: GGTGCAAGGCTGCCAATTT	R: TAACTACCACAGCCGGAGGA	106
Nox2	NM_007807.5	F: CAGAACCAACACTTAACCTT	R: CAACCACACCAGAATGAC	84
Nox4	NM_015760.5	F: TCCCTCCTATGGGCAATGTG	R: TGCACATCAAGCCTGGACAA	177

Prkn (PARKIN)	NM_001317726.1	AN: 724	92
Nrf2	NM_010902.4	F: GGACATGGAGCAAGTTTGGC R: CCAGCGAGGAGATCGATGAG	164

5.3.9 Statistical analysis

To compare differences in outcome measures between control and aged cells only, independent t-tests were used. For the comparison of replicative ageing and flavonoid dose upon outcome measures, a two-way ANOVA was employed. A three-way ANOVA was used for comparisons of ageing, flavonoid dose and other factors such as time or antimycin A. When main effects and interactions were present, multiple comparisons were performed using Dunnett's or Sidak's test where appropriate. For within age comparisons, a one-way ANOVA was used. Data are presented as means \pm SEM, and significance was accepted when $P < 0.05$.

5.4 Results

5.4.1 Mitochondrial bioenergetics of control and aged skeletal muscle myoblasts

Indices of mitochondrial function were compared between control and aged myoblasts under CTRL conditions. No significant differences were revealed in mitochondrial energetics of control vs. replicatively aged myoblasts (see Figure 5.3). Rates of basal respiration (Control: 1.67 ± 0.13 vs. Aged: 1.81 ± 0.15 pmol/min⁻¹/ng DNA⁻¹, $P = 0.653$), proton leak (Control: 0.54 ± 0.05 vs. Aged: 0.54 ± 0.07 pmol/min⁻¹/ng DNA⁻¹, $P > 0.999$), ADP phosphorylation (Control: 1.12 ± 0.10 vs. Aged: 1.27 ± 0.14 pmol/min⁻¹/ng DNA⁻¹, $P = 0.497$) and coupling efficiency (%) (Control: $67.1 \pm 2.2\%$ vs. Aged: $70.1 \pm 1.3\%$, $P = 0.297$) were similar between control and aged cells.

Commented [CS329]: No comparisons provided for young blasts vs young tubes and old blasts vs old tubes – have you done any of these analyses? Would it be worth adding e.g. these are the differences in blasts con vs aged) the fusion process causes changes in the parameters examined (or not) within con and aged. As a result of or despite no differences, con vs aged tubes then show x.

Essentially, what is the impact of fusion within the control cells and within the aged cells (blasts vs tubes) and finally are there diffs between con vs aged tubes.

Blasts vs blasts; blasts vs tubes; tubes vs tubes

If this is a huge amount of work, forget I suggested it, but I think it is an important consideration e.g. if the aged blasts are not too different from the control, but the aged tubes are, are they also different to the blasts from which they started....

Commented [SD330R329]: I would like to but this comparison isn't possible due to different normalisation strategies used for blasts and tubes in seahorse. Although I've used DNA content as normaliser, the blasts were initially relative to cell density. When this was converted to DNA content through interpolation of fluorescence from cell density to DNA from a similar assay we had in our lab (in attempt to make comparison blast vs tube), the respiration data was hugely different between blasts and tubes, and I don't trust it (at all) for a comparison between blasts and tubes

Commented [CS331R329]: Thank you.

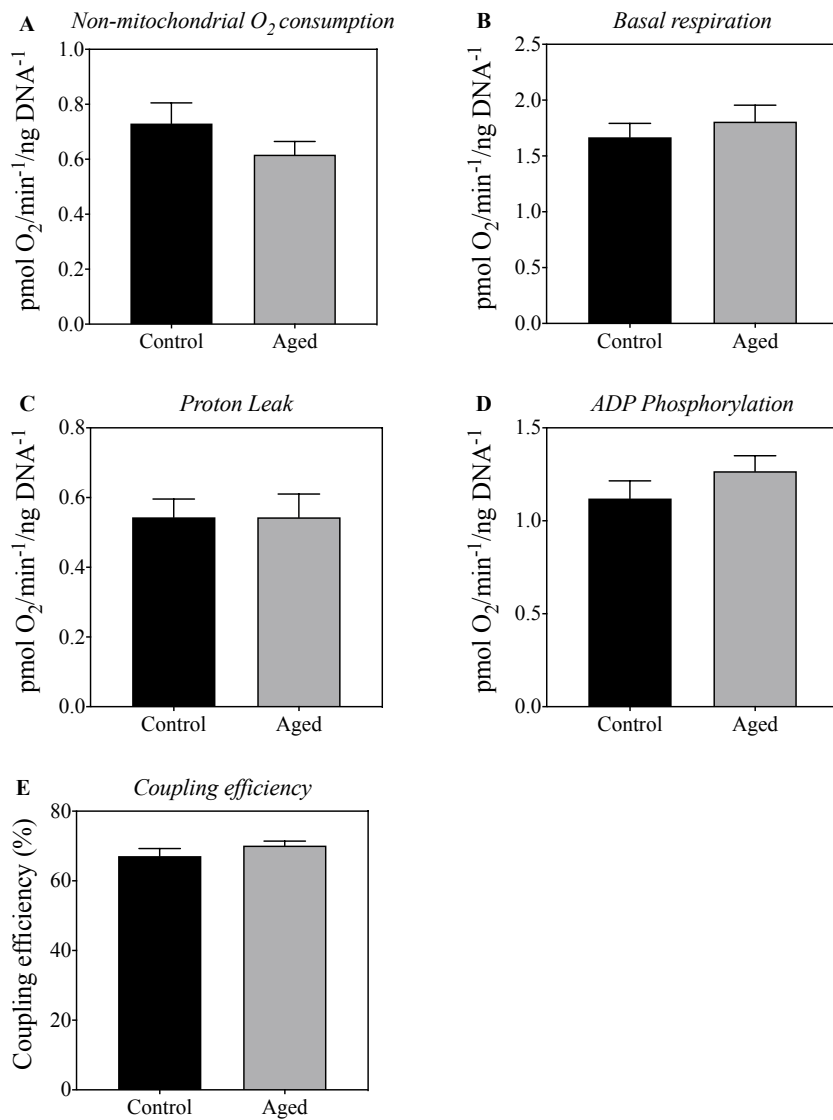


Figure 5.3 Mitochondrial bioenergetics of control and aged C₂C₁₂ myoblasts. A) Non-mitochondrial respiration, B) Basal respiration, C) Proton leak, D) ADP phosphorylation and E) Coupling efficiency (%). Data are mean±SEM, representative of 3 independent experiments and normalised to DNA content. Differences between groups determined by independent t-test.

Commented [SD332]: Relaised ive done stats wrong. Changed control aged comparisons to an unpaired rather than paired t test throughout, so p values have changed accordingly

Commented [CS333R332]: Well caught.

5.4.2 Rates of ATP production: Control vs aged myoblasts

In the absence of significant differences between control and aged myoblasts, in terms of mitochondrial function, it was hypothesised that no differences would prevail in the processes underpinning energy production. The glycolytic ($J_{ATP_{glyc}}$), oxidative ($J_{ATP_{ox}}$) and total ($J_{ATP_{production}}$) rates of ATP production were therefore calculated. Accordingly, there were no differences in absolute $J_{ATP_{production}}$ between control and aged myoblasts (mean \pm SEM; Control: 16.97 ± 2.23 vs. Aged: 15.90 ± 2.75 pmol ATP/min⁻¹/ng DNA⁻¹, $P=0.713$). Along similar lines, the relative contribution of $J_{ATP_{glyc}}$ (Control: 66.6 ± 4.2 vs. Aged: 60.1 ± 4.2 %; $P=0.337$) and $J_{ATP_{ox}}$ (Control: 33.4 ± 4.2 vs. Aged: 39.9 ± 4.2 %; $P=0.337$) to $J_{ATP_{production}}$ was similar between in control and aged cells (see Figure 5.4). Therefore, indices of mitochondrial function were similar between control and aged myoblasts, and both absolute and relative rates of $J_{ATP_{production}}$ were comparable between control and aged cells. Replicative ageing does not appear to alter pathways associated with energy metabolism in skeletal myoblasts. Overall, the mitochondrial respiration data indicate that aged myoblasts display comparable mitochondrial function when compared to control.

Commented [CS334]: What I was getting at with the "and so" comment was that despite no differences in ATP production, the means by which the ATP was produced were sig dif e.g. via glycolytic pathway in control blasts and via oxidative in the aged blasts – state this and then comment on what the relevance may be e.g. in control cells using glycolysis more than in aged, but in aged then converting to oxidative phosphorylation more than in control – higher energy demands? More efficient? What might that specific difference mean in terms of the two cells – that is the and so question – one to two liner response in the text.

Commented [SD335R334]: Have added one liner at end but haven't speculated too much. Do I need to go further?

Commented [CS336R334]: I still think the differences between the modes is interesting, but are they now not sig dif? In which case what you have is sufficient

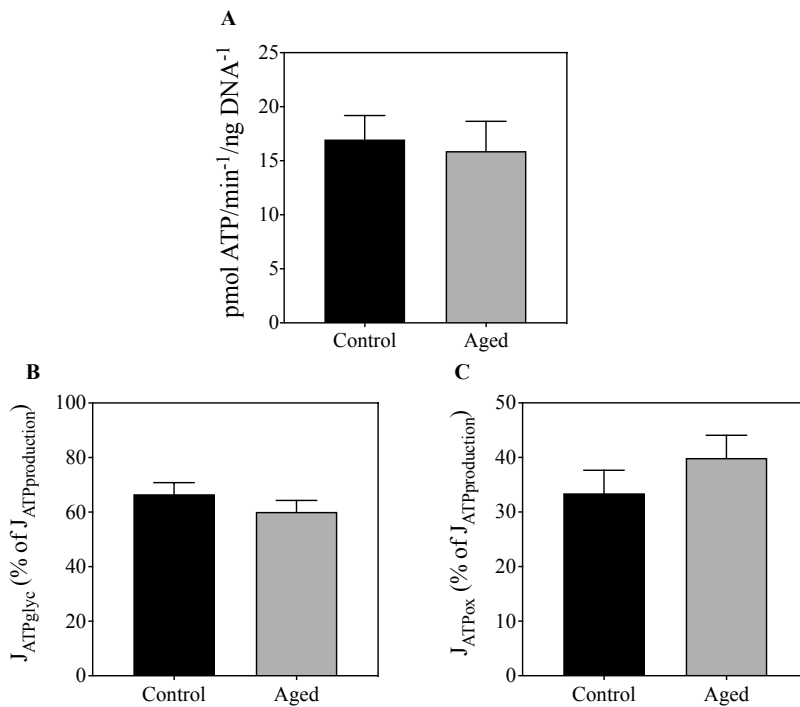


Figure 5. 4 ATP production rates of control and aged C₂C₁₂ myoblasts A) Absolute J_{ATPproduction}. B) Relative contribution of J_{ATPglyc} to J_{ATPproduction} and C) Relative contribution of J_{ATPox} to J_{ATPproduction}. Data from 3 independent experiments are presented as mean±SEM and normalised to DNA content. Differences between groups establish by independent t-test.

After reporting that replicative ageing did not cause alterations to mitochondrial function or rates of ATP production in myoblasts, the rate of proton production in control and aged myoblasts was determined (see Figure 5.5). There were no differences in the proton production rate between control and aged myoblasts (Control: 11.92±2.14 vs. Aged: 10.28±2.45 pmol H⁺/min⁻¹/ng DNA⁻¹, *P*=0.640).

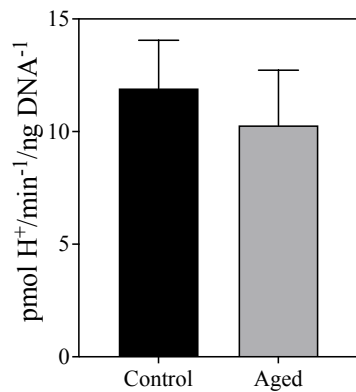


Figure 5. 5 Proton production rates in control and aged C₂C₁₂ myoblasts. Data from 3 independent experiments are presented as mean±SEM and normalised to DNA content. Differences between groups determined by independent t-test.

5.4.3 Mitochondrial bioenergetics of control and aged C₂C₁₂ skeletal myoblasts: Effects of dietary flavonoids

Having established that mitochondrial bioenergetics are similar between control and aged myoblasts the next step was to examine whether physiological flavonoid concentrations would impact indices of mitochondrial function. Flavonoids may confer beneficial effects upon mitochondria, but little is known regarding their mode of action in skeletal muscle cells. Firstly, it was important to determine potential toxic effects of flavonoids in skeletal muscle cells. After 24 h dietary flavonoid treatments (0-20 μM dose responses), there were no differences in cell number/viability (%) determined using the CyQUANT™ Cell Proliferation Assay between Q, EGCG or EPI treated cells vs. untreated control (see Figure 5.6). As a result, and for subsequent experiments, doses of 1, 5 and 10 μM were employed.

Commented [SD337]: Adjust figure numbers downwards in this chapter

Commented [CS338]: The sections go back and forth from blasts to tubes. I wonder if you would be better presenting all of the blast data and then the tube data? Not sure how difficult it would be to rearrange, but it may make the huge amount of data you have generated more easy to retain.

Commented [SD339R338]: Agree, will try this approach

Commented [SD340]: Is there a need to expand upon reasons for using flavonoids here as intervention? Would something like this would be better suited to the introduction?

Commented [CS341R340]: Good here. It is a short one liner and directs the reader.

Commented [SD342R340]: Have entered this in

Commented [SD343]: Moved viability data to here. It is not MTT, but rather the CyQuant Proliferation assay

Commented [CS344R343]: good

Commented [CS345]: Measured how e.g. ...cell viability, determined using xxx, between Q...

Commented [CS346]: Will these be spelled out in the methods?

Commented [CS347]: good

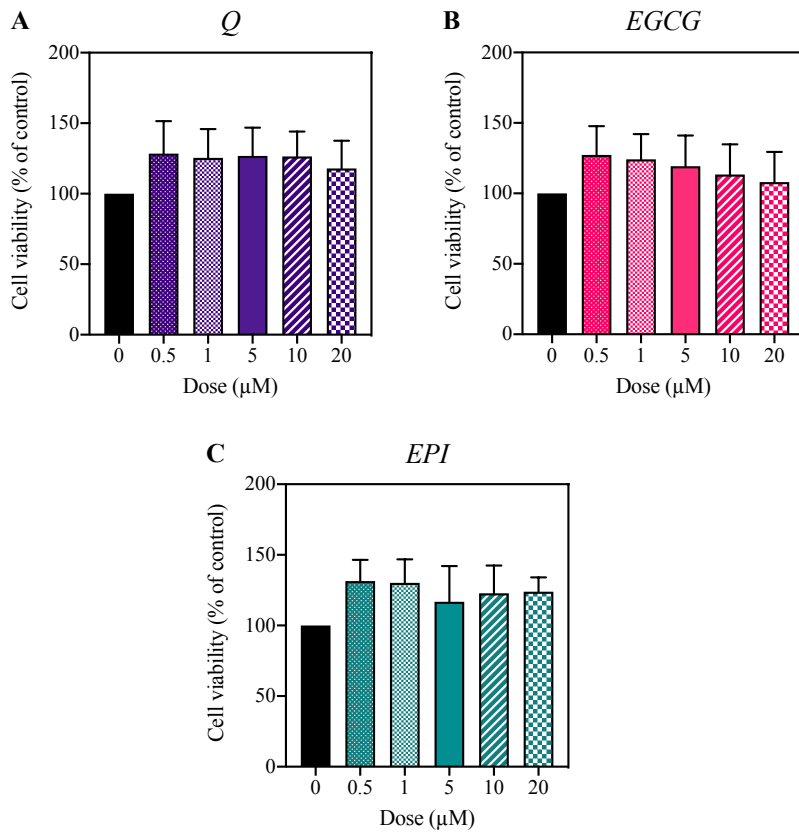


Figure 5. 6 Cell viability following 24 h differentiation +/- flavonoid treatment with A) Quercetin, B) EGCG and C) EPI. Data are means±SEM, representative of 3 independent repeats performed using 5 replicates of each condition.

There was no main effect of age or dose on basal respiration in Q (1-10 μM) or EGCG (1-10 μM) treated skeletal myoblasts (see Figure 5.7A). However, there was a significant main effect of dose on basal respiration in EPI (1-10 μM) treated myoblasts ($P=0.0284$). Multiple comparisons unveiled that basal respiration was significantly lower in aged myoblasts cultured

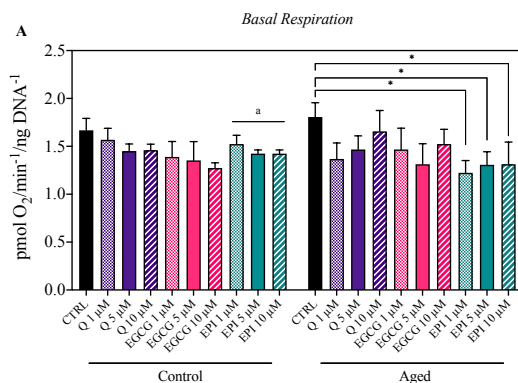
with 1, 5 and 10 μM EPI compared with CTRL (Aged CTRL: 1.81 ± 0.15 ; 1 μM EPI: 1.22 ± 0.13 ; 5 μM EPI: 1.31 ± 0.14 ; 10 μM EPI: 1.31 ± 0.23 $\text{pmol O}_2/\text{min}^{-1}/\text{ng DNA}^{-1}$; $P=0.017$, $P=0.041$ and $P=0.044$, respectively). There was a significant impact of age on proton leak in EPI treated myoblasts ($P=0.0395$) (see Figure 5.7B). However, no significant differences in proton leak were identified between conditions, regardless of the flavonoid type or dose studied. There was a significant main effect of dose on ATP production in EPI treated cells ($P=0.0492$). Multiple comparisons demonstrated a trend towards reduced oxygen consumption linked to ATP production in response to 1, 5 and 10 μM EPI in aged myoblasts ($P=0.056$, $P=0.051$, and $P=0.051$, respectively). Whereas levels of ATP-linked respiration were similar between conditions in control myoblasts. A significant main effect of age was found on coupling efficiency in myoblasts treated with Q, EGCG and EPI ($P<0.0001$). Coupling efficiency was typically greater in aged myoblasts when compared to control (see Figure 5.7D). Together, these findings demonstrate that Q and EGCG do not impact indices of mitochondrial of function. However, EPI may inhibit mitochondrial respiration in skeletal myoblasts.

Commented [CS348]: I wonder if it would make for easier reading if the triggers were all reported together. EG all of the Q data, then EGCG and finish on EPI? This may make things easier for your reader to retain.

Commented [SD349R348]: Can group flavonoids into separate smaller sections for each assay/experiment

Commented [CS350]: Unexpected? If so, put whereas, surprisingly, EPI may....

Commented [DR351R350]: 'Surprisingly' is a word for the discussion section. Results section should be factual



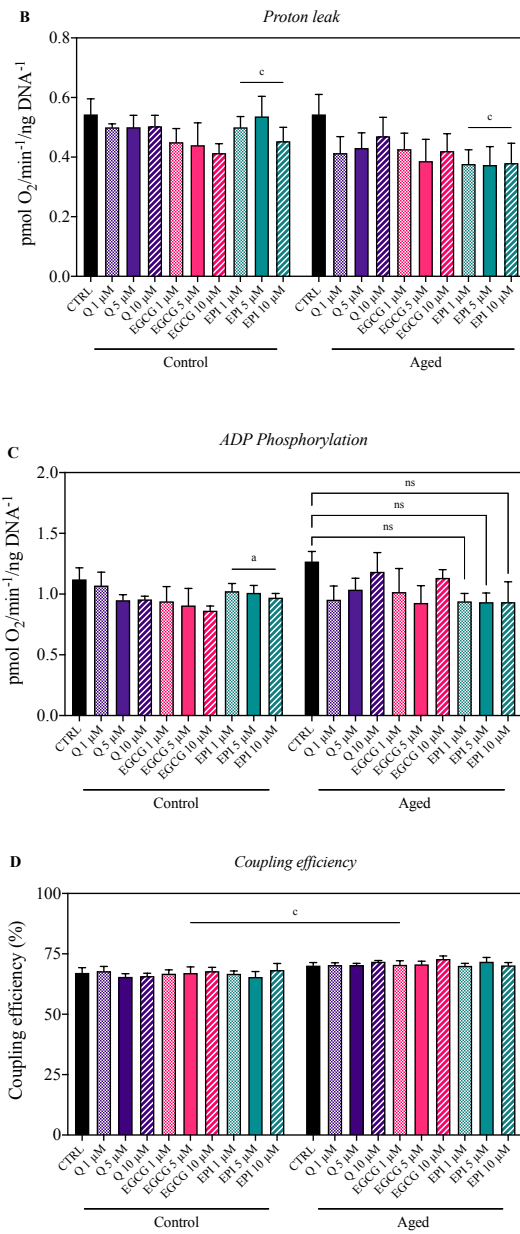


Figure 5. 7 Mitochondrial bioenergetics of control and aged skeletal muscle cells in the absence and presence of dietary flavonoids. A) Basal respiration, B) Proton leak, C) ADP

phosphorylation, D) Coupling efficiency (%). Data representative of 3 independent experiments (presented as mean±SEM) and normalised to DNA content. * $P<0.05$, significant vs. CTRL. ^a significant effect of dose. ^c significant main effect of age ($P<0.05$).

5.4.4 Rates of ATP and proton production in skeletal myoblasts

There was no significant impact of age or dose of flavonoids on absolute $J_{ATP_{glyc}}$. Similarly, there was no significant effect of age on absolute $J_{ATP_{ox}}$ production in myoblasts (see Figure 5.8). However, there was a significant main effect of dose on $J_{ATP_{ox}}$ production in EPI treated myoblasts ($P=0.036$). Both 1 and 10 μM EPI significantly lowered absolute $J_{ATP_{ox}}$ production versus CTRL in aged myoblasts (Aged CTRL: 6.1 ± 0.4 vs. 1 μM EPI: 4.3 ± 0.3 and 10 μM EPI: 4.4 ± 0.9 pmol ATP/min⁻¹/ng DNA⁻¹; $P=0.032$ and $P=0.043$, respectively). There was no main effect of dose or age found on proton production rates in control and aged myoblasts, regardless of the flavonoid investigated (data not shown).

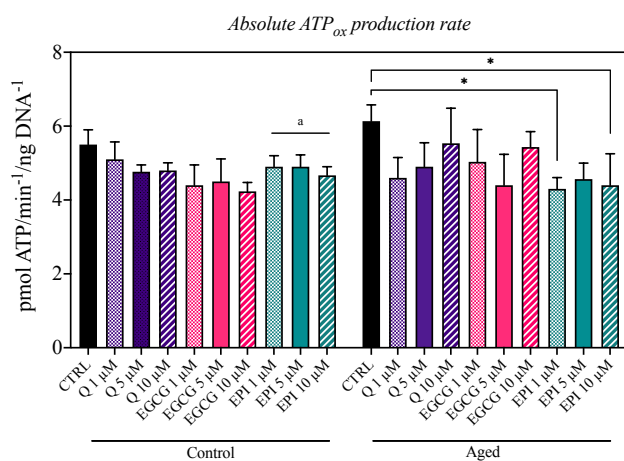


Figure 5. 8 ATP production rates of control and aged myoblasts following acute dietary flavonoid treatment. Data from 3 independent experiments are presented as mean±SEM and normalised to DNA content. * $P<0.05$, significant vs. CTRL. ^a significant main effect of dose.

The prior findings demonstrate that flavonoids have a limited direct impact on indices of mitochondrial function. Although, EPI may acutely inhibit mitochondrial bioenergetics and rates of oxidative ATP synthesis in skeletal myoblasts.

Commented [CS352]: Remember this for the discussion – need to address what the implications may be e.g. a good thing or a bad thing...

5.4.5 The impact of flavonoids on myoblast mitochondrial bioenergetics may relate to modulation of complex I activity

Initial data established that EPI may inhibit mitochondrial respiration in control and aged skeletal myoblasts (section 5.4.3). To ascertain whether flavonoid-induced inhibition of mitochondrial bioenergetics was related to effects upon the electron transfer system, the activity of complex I was studied in the absence and presence of dietary flavonoids. There was a 1.3-fold increase in complex I activity, under basal untreated (CTRL) conditions in aged cells when compared to control (Aged: 49.4 ± 3.9 vs. Control: 37.0 ± 2.9 nmol/min⁻¹/mg⁻¹ protein), though this increase was not statistically significant ($P=0.063$). In Q and EGCG treated cells, there were no main effects of age or dose on complex I activity. However, there was a significant main effect of age on complex I activity in EPI treated cells ($P=0.044$). Multiple comparisons demonstrated no significant difference between conditions, irrespective of the flavonoid studied (see Figure 5.9). Although, there was a non-significant decrease in complex I activity with 5 μ M EPI compared to CTRL conditions in aged muscle cells ($P=0.079$).

Commented [CS353]: Why not covered under control conditions above e.g. before flavonoid data? Higher complex I activity in aged vs control – how does this fit with the altered metabolic profiles basally? I would move the control data up and then repeat it here with the flavonoids.

Commented [SD354R353]: Can do this but we don't have myotube data, does it make sense to do this?

Commented [CS355R353]: Lets see what Richard thinks.

Commented [DR356R353]: The difference in complex I activity was not significant, so basically no effect of age. Will not change anything on the message regarding basal conditions. It is logic to introduce complex I activity only here because you build on previous findings

Commented [CS357]: Data?

Commented [SD358R357]: Reporting main effect of age, pairwise comparisons come later

Commented [CS359]: might this cause confusion with control used for unpassaged cells. I have added a small definition in the text above – I think this should be enough. What do you think?

Commented [SD360R359]: Thank you, having the word condition after CTRL also makes it more clear

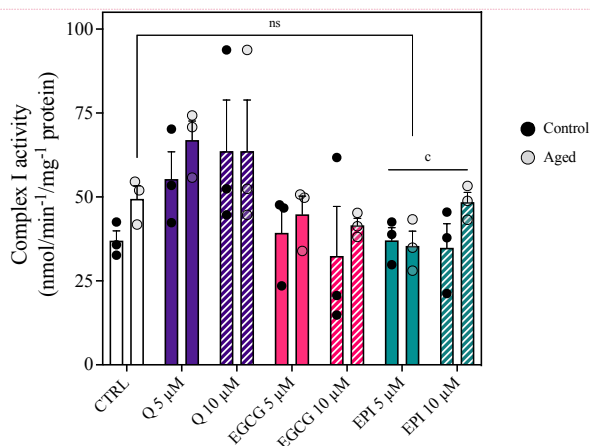


Figure 5.9 Limited impact of flavonoid treatment on complex I activity in control and aged skeletal muscle cells. Control and aged skeletal muscle cells were cultured in the absence and presence of Q, EPI or EGCG for 24 h, at 0, 5 and 10 μM . After 24 h, cells were harvested and assayed for complex I activity by spectrophotometry. Immediately following analysis, the protein content of cell lysates was determined so that complex I activity could be normalised to cell lysate protein content. Data are means \pm SEM from 3 independent experiments. A two-way ANOVA was performed with dose and age as factors to test for statistical significance between conditions, using Dunnett's test for multiple comparisons. ° significant main effect of age. Black and transparent grey solid circles represent control and aged myoblasts, respectively.

5.4.6 Intracellular nitric oxide levels are not impacted by flavonoid treatment in control and aged skeletal muscle cells

After determining the effects of flavonoids on mitochondrial respiration and complex I activity, the potential of flavonoids to contribute to NO production in control and aged muscle cells was investigated. First, NO production (measured by DAF-FM fluorescence) was compared between control and aged muscle cells under CTRL conditions. Replicative ageing reduced NO levels by 50% compared to control ($P=0.024$). The impact of flavonoids on NO levels in

Commented [CS361]: Something does not match with the legend and the bar filling for control vs aged – needs to be amended. Ignore, I have just realised, it is the dots you refer to.

Commented [DR362R361]: It indeed takes a bit of time to understand this indeed. A way out is to present an a and b figure for control and aged cells respectively. Why are the young cells not called 'young'. Using the word control (ctrl) is confusing as it could also refer to the control (non-flavonoid) conditions in aged cells?

Commented [CS363R361]: I agree with this, I think if you have a get out of jail explanation that for ease of understanding you will call the non-passaged cells young, to alleviate the issue of control unpassaged vs control untreated, then I think you would get away with it. Have that explanation in the main methods as well as in the methods of each relevant chapter and then in the first set of results where you mention them e.g. control, non-passaged cells, referred to as young for the remainder of the chapter.

Commented [DR364]: I don't think you ever explained why you want to look at NO production....

Commented [CS365R364]: See papers added above that may be useful

control and aged muscle cells was then investigated. A significant main effect of age on DAF-FM fluorescence intensity was observed in cells treated with Q, EGCG and EPI ($P<0.0005$). Multiple comparisons revealed that NO levels were similar between experimental conditions, irrespective of age (see Figure 5.10).

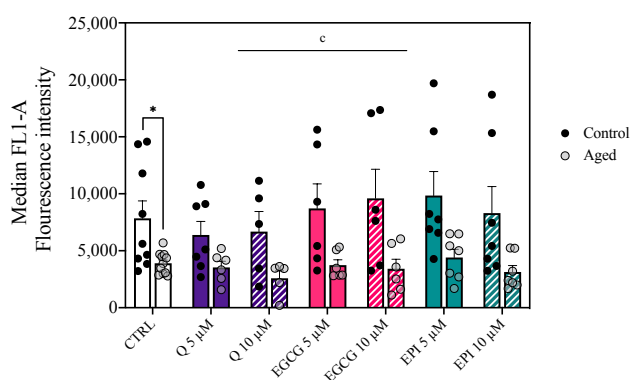


Figure 5. 10 Flavonoid supplementation does not impact intracellular nitric oxide in control and aged skeletal muscle cells. DAF-FM oxidation was determined in control and replicatively aged skeletal muscle cells in the absence and presence of Q, EPI and EGCG. Cells were treated with 0, 5 and 10 μM of flavonoids for 24 h. After 24 h, cells were trypsinised and resuspended in PBS. Median fluorescence intensity was determined with background signal (cell-free signal) subtracted. Data are presented as means \pm SEM of three independent repeats with two-three replicates per experimental condition. Black and transparent grey solid circles represent control and aged myoblasts, respectively. Statistical significance was tested for by two-way ANOVA and multiple comparisons by Tukey's test. * significant main effect of age ($P<0.05$).

5.4.7 Gene expression of control and aged skeletal myoblasts under CTRL conditions

Having described how replicative ageing and flavonoids impact mitochondrial bioenergetics and intracellular NO levels, the effects of ageing and flavonoids on skeletal myoblast gene expression were subsequently investigated. Genes associated with mitochondrial remodelling

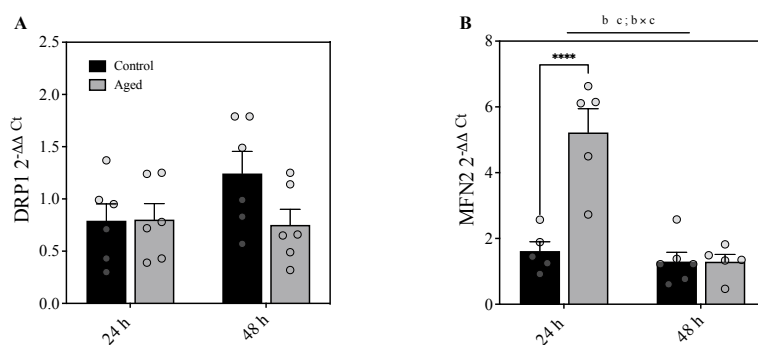
Commented [DR366]: Again, what is meant with CTRL: not treated cells, young cells? CTRL conditions suggests that you refer to untreated conditions

Commented [SD367R366]: Yes CTRL is no flavonoid, whereas control is 'young'. I can change this if it is not clear

Commented [CS368]: I still think you need an introduction to the genes studied either in this chapter or the main intro (if not already done) and then referenced in this chapter.

(TFAM, DRP1, SIRT1, MFN2 PGC-1 α and PARKIN) and the antioxidant response (NRF2, CAT, SOD2, NOX4 and eNOS) were examined.

To establish whether replicative ageing changes the expression of genes associated with mitochondrial function, comparisons were made between control and aged myoblasts under CTRL conditions. There was no significant main effect of age or time on DRP1, SIRT1 or TFAM expression (see Figure 5.11). A significant main effect of age ($P=0.0005$) and time ($P<0.0001$) was found on MFN2 expression in myoblasts, and a significant age \times time interaction ($P=0.0005$; see Figure 5.11A). Multiple comparisons revealed MFN2 expression was 3.2-fold higher in aged myoblasts over 24 h ($P<0.0001$). A main effect of age ($P=0.006$) and time ($P=0.021$) was observed on PARKIN expression in myoblasts, and a significant age \times time interaction ($P=0.0003$; see Figure 5.11C). Multiple comparisons revealed PARKIN expression was 3.9-fold higher in control compared to aged myoblasts ($P<0.0001$). A significant main effect of time ($P=0.010$) was found on PGC-1 α expression, but no differences in PGC-1 α expression were evident between control and aged myoblasts (see Figure 5.12D).



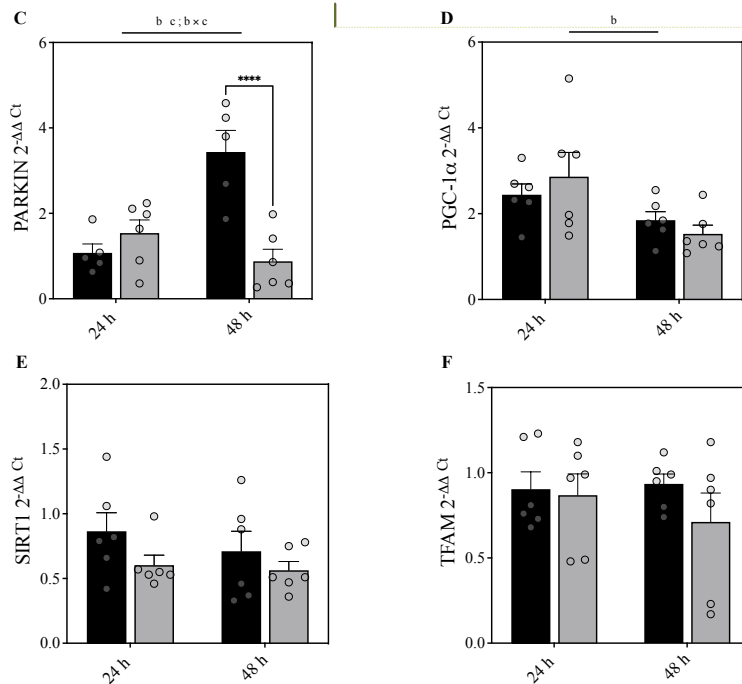
Commented [DR369]: Please avoid to use too much the same sentence in the text...was found...

Commented [SD370R369]: Fair point, will address this

Commented [SD371]: Report results section under CTRL conditions

Commented [CS372R371]: good

Commented [DR373]:



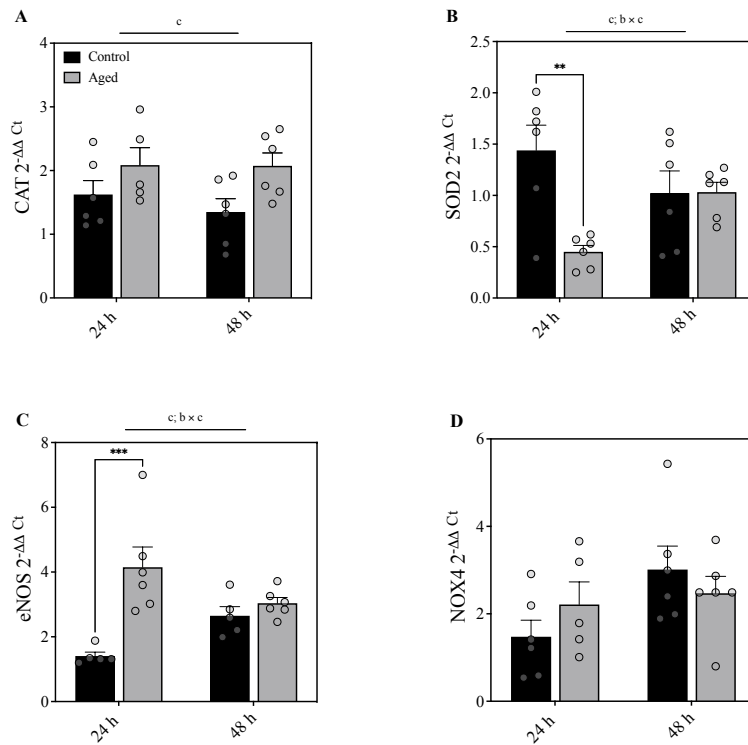
Commented [SD374]: Considering combining all graphs these into a single figure to make for easier viewing, just not 100% sure e.g. like this

Commented [DR375R374]: I would keep it like this. Combining all will in fact make viewing less easy. What I do not understand is why you measure after 24 and 48 hours. What kind of different information did you expect to find and why are they so different?

Figure 5.11 Expression of genes associated with mitochondrial remodelling in control and aged skeletal myoblasts under CTRL conditions. C₂C₁₂ myoblasts were lysed over 0-48 h of differentiation for analysis of gene expression. A) DRP1, B) MFN2, C) PARKIN, D) PGC-1 α , E) SIRT1 and F) TFAM. Data are means \pm SEM from 3 independent experiments run in duplicate. Statistical significance was determined by a two-way ANOVA, with age and time as factors. Multiple comparisons performed by Sidak's test to determine differences in gene expression between ages within each time point. ^b main effect of time; ^c main effect of age. **** P <0.0001. Control and aged myoblasts are denoted by solid black and grey bars, respectively.

Next, control and aged myoblast gene expression profiles related to the antioxidant response were compared under CTRL conditions (see Figure 5.12). There was a significant main effect of age ($P=0.016$) on CAT expression in myoblasts, but multiple comparisons revealed no differences in CAT expression between ages or across time points (see Figure 5.12A). A main

effect of age ($P=0.011$) was found on SOD2 expression in myoblasts, and a significant age \times time interaction ($P=0.009$). Over 24 h, SOD2 expression was 3.2-fold higher in control versus aged myoblasts ($P=0.001$; see Figure 5.12B). There was a significant main effect of age ($P=0.0007$) on eNOS expression, and an age \times time interaction ($P=0.007$). eNOS expression was 2.9-fold higher over 24 h in aged myoblasts compared to control ($P=0.0002$). There was no main effect of age or time on NOX4 or NRF2 expression in control and aged myoblasts (see Figure 5.12).



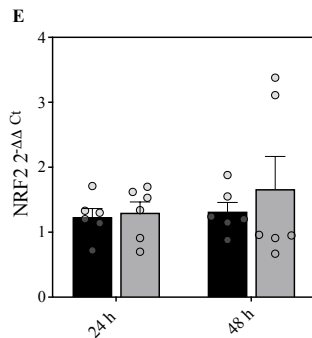


Figure 5. 12 Expression of genes associated with the antioxidant response in control and aged skeletal myoblasts under CTRL conditions. C₂C₁₂ myoblasts were lysed over 0-48 h of differentiation for analysis of gene expression. A) CAT, B) SOD2, C) eNOS, D) NOX4 and E) NRF2. Data are means±SEM from 3 independent experiments run in duplicate. Statistical significance was determined by a two-way ANOVA, with age and time as factors. Multiple comparisons performed by Sidak's test to determine differences in gene expression between ages within each time point. ^b main effect of time; ^c main effect of age. ***P*<0.01 and ****P*<0.001. Control and aged myoblasts are denoted by solid black and grey bars, respectively.

Commented [DR376]: A noticeable difference between 24 and 48 hours. I hope you will discuss this later on. This is also why it would be preferred to have a dedicated chapter on young vs aged, so you will have room in your discussion section to focus on detailed differences (without distracting the flavonoid story)

5.4.8 Summary of the effects of replicative ageing on gene expression in myoblasts

Overall, aged myoblasts presented higher and lower levels of MFN2 and PARKIN over 24 and 48 h, respectively, when compared with control. Possibly, aged myoblasts have altered mitochondrial remodelling compared to control, through reduced mitophagy and a preference toward fusion. Furthermore, aged myoblasts have lower SOD2 and higher eNOS expression over 24 h compared with control, but these effects are not apparent over 48 h.

Commented [DR377]: Why? I miss here a thorough section describing the differences (or why they do not exist) and what kind of explanation can be brought forward.

Commented [SD378R377]: I do agree this would need discussing but should it be here or the discussion?

5.4.9 Flavonoids modulate gene expression of control and aged skeletal myoblasts

5.4.9.1 Expression of mitochondrial genes following Quercetin treatment in skeletal myoblasts

Having described how replicative ageing impacts the transcriptional responses of TFAM, DRP1, SIRT1, MFN2 PGC-1 α , PARKIN, NRF2, CAT, SOD2, NOX4 and eNOS in myoblasts under CTRL conditions, the expression of these genes were quantified in the presence of Q, EGCG and EPI (see Figure 5.15 for heatmap representation). These genes were investigated to help amalgamate the mitochondrial bioenergetic data. There was a significant main effect of dose, time and age on DRP1 expression in Q treated myoblasts ($P < 0.0001$). Post-hoc comparisons revealed DRP1 expression was similar between conditions in control and aged cells (see Figure 5.13A). There was a significant main effect of dose ($P = 0.0212$) and time ($P = 0.0014$) on MFN2 expression in Q treated myoblasts. Multiple comparisons revealed no significant effect of flavonoid treatment on MFN2 in control myoblasts (see Figure 5.13B). Though, in aged myoblasts, 5 and 10 μM Q lowered MFN2 expression compared to CTRL over 24 h (3-fold, $P = 0.0148$; 4-fold, $P = 0.0051$, respectively). There was no significant main effect of dose, time or age on PARKIN expression in Q treated myoblasts. Multiple comparisons revealed no impact of Q on PARKIN expression in control and aged myoblasts. There was no main effect of dose, time or age on PGC-1 α expression in Q treated myoblasts. Post-hoc tests unveiled that PGC-1 α expression was similar between conditions in control and aged myoblasts, regardless of dose (see Figure 5.13D). Although, there was a trend toward increased PGC-1 α expression with 5 μM Q after 48 h when compared to CTRL (2-fold increase, $P = 0.058$). Regarding SIRT1 expression, there was a significant main effect of dose in Q treated cells ($P = 0.0077$), but no main effect of time or age. Multiple comparisons revealed that SIRT1 expression was similar between conditions in control myoblasts (see Figure 5.13E). In aged myoblasts, however, SIRT1 expression was significantly increased by 5 μM Q treatment over 48 h when compared to CTRL (1.5-fold, $P = 0.0221$). There was no main effect of dose, time or age on TFAM expression in Q treated myoblasts. Collectively, Q may augment

Commented [SD379]: Again, before this, add the raw CT data for con and aged cells and discuss how they differ basally, then add the delt delta for con and aged for these genes and hopefully the trends remain unchanged, then go into the impact of flavonoids on the findings and what you may expect to see, based on the earlier data.

Commented [CS380R379]: Do you refer to the heat map figure? Until you have your numbers in, it is hard to tell.

genes associated with mitochondrial biogenesis in skeletal myoblasts, although this did not culminate in altered mitochondrial respiration.

Commented [SD381]: Added line

5.4.9.2 Expression of mitochondrial genes following EGCG treatment in skeletal myoblasts

There was a significant main effect of dose, time and age on DRP1 expression in EGCG treated myoblasts ($P < 0.0001$). Post-hoc comparisons revealed DRP1 expression was similar between conditions in control and aged cells, regardless of dose (see Figure 5.13A). In EGCG treated cells, there was a significant dose \times time interaction ($P = 0.0004$). Multiple comparisons revealed no significant effect of flavonoid treatment on MFN2 in control myoblasts (see Figure 5.13B). Similarly, at 24 h, 10 μ M EGCG lowered MFN2 expression 5.9-fold versus control ($P = 0.0013$). In EGCG treated cells, a significant main effect of dose ($P = 0.0002$), time ($P = 0.0008$) and age ($P < 0.0001$) on PARKIN was found, in addition to a significant dose \times time \times age interaction ($P = 0.0086$). In control myoblasts, PARKIN expression was decreased over 48 h by 5 and 10 μ M EGCG treatment (2.2-fold, $P = 0.0213$ and 2.3-fold, $P = 0.0059$, respectively). Compared to CTRL conditions in aged cells, PARKIN expression was decreased 4.5-fold ($P = 0.001$) and 3.4-fold ($P = 0.021$) by 5 and 10 μ M EGCG over 24 h, respectively. In EGCG treated cells, a significant main effect of time ($P = 0.016$) was found, and a significant dose \times time interaction ($P = 0.032$). Post-hoc tests unveiled that PGC-1 α expression was similar between conditions in control and aged myoblasts, regardless of dose (see Figure 5.13D). There was no main effect of time or age on SIRT1 expression in EGCG treated cells. Multiple comparisons revealed that SIRT1 expression was similar between conditions in control myoblasts (see Figure 5.13E). There was no main effect of dose, time or age on TFAM expression in EGCG treated myoblasts. However, there was a significant dose \times time \times age interaction in EGCG treated cells ($P < 0.05$). Compared to CTRL, TFAM expression was 1.8-

fold lower over 48 h in control myoblasts with 10 μ M EGCG ($P=0.0046$). In aged myoblasts, TFAM expression was decreased 2-fold at 24 h by 10 μ M EGCG compared to CTRL ($P=0.0486$). Overall, EGCG attenuated the expression of genes associated with mitochondrial remodelling in skeletal myoblasts, although this did not coincide with changes in mitochondrial function.

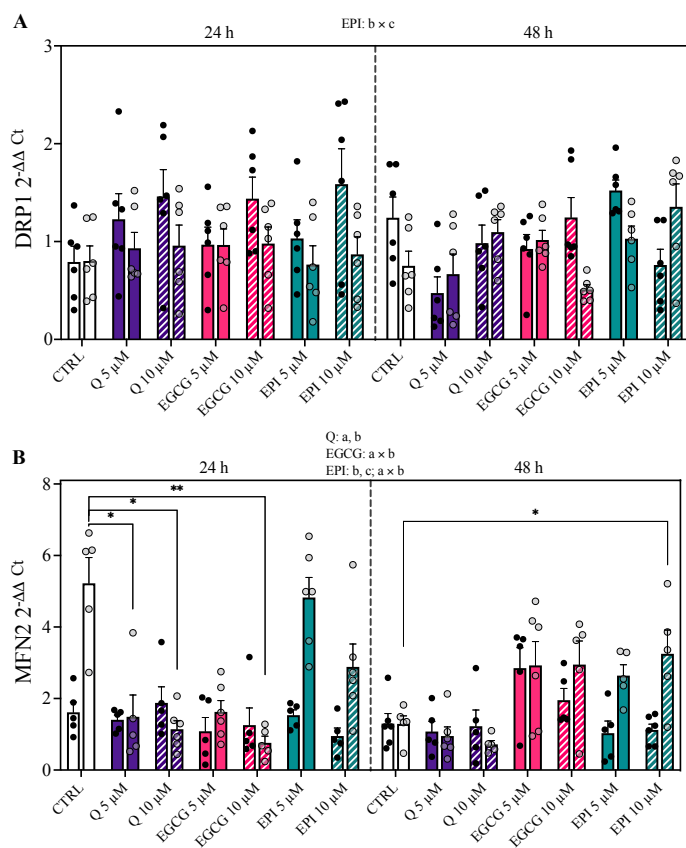
Commented [CS382]: Comment as above

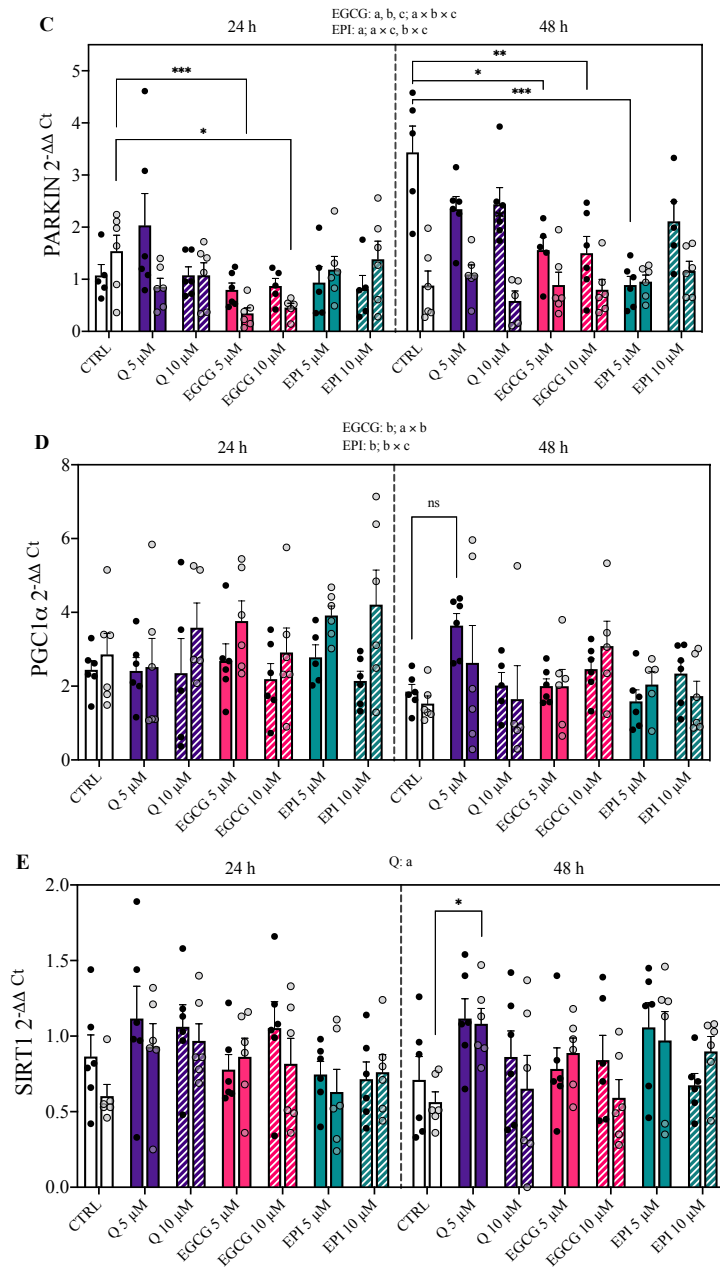
5.4.9.3 Expression of mitochondrial genes following EPI treatment in skeletal myoblasts

There was a significant main effect of dose, time and age on DRP1 expression in EPI treated myoblasts ($P<0.0001$). There was, however, a significant time \times age interaction ($P=0.019$) in EPI treated myoblasts. Post-hoc comparisons revealed DRP1 expression was similar between conditions in control and aged cells, regardless of EPI dose (see Figure 5.13A). There was a main effect of time ($P=0.0083$) and age ($P<0.0001$) on MFN2 expression in EPI treated cells, as well as a dose \times time interaction ($P=0.021$). Multiple comparisons revealed no significant effect of flavonoid treatment on MFN2 in control myoblasts (see Figure 5.13B). However, MFN2 levels were 2.5-fold higher in aged myoblasts at 48 h with 10 μ M EPI compared to CTRL ($P=0.032$). There was a main effect of dose ($P=0.034$) on PARKIN expression in EPI treated cells, and a dose \times age ($P=0.014$), and time \times age ($P=0.0009$) interaction. PARKIN expression at 48 h in control cells was decreased 3.9-fold with 5 μ M EPI versus CTRL ($P=0.0005$). There was also a main effect of time ($P=0.0001$) on PGC-1 α expression in EPI treated cells, and a significant time \times age interaction ($P=0.025$). Post-hoc tests unveiled that PGC-1 α expression was similar between conditions in control and aged myoblasts, regardless of the flavonoid dose (see Figure 5.13D). There was no main effect of time or age on SIRT1 expression in EPI treated cells. Multiple comparisons revealed that SIRT1 expression was similar between conditions in control myoblasts (see Figure 5.13E). There was no main effect of dose, time or age on TFAM expression in EPI treated myoblasts. However, there was a

significant dose \times time \times age interaction in EPI treated cells ($P < 0.05$). TFAM expression was decreased 1.8-fold with 5 μ M EPI versus CTRL conditions after 48 h ($P = 0.006$). Overall, EPI attenuated the expression of genes associated with mitochondrial remodelling over 48 h in control skeletal myoblasts, which may not be associated with mitochondrial respiration.

Commented [CS383]: As above





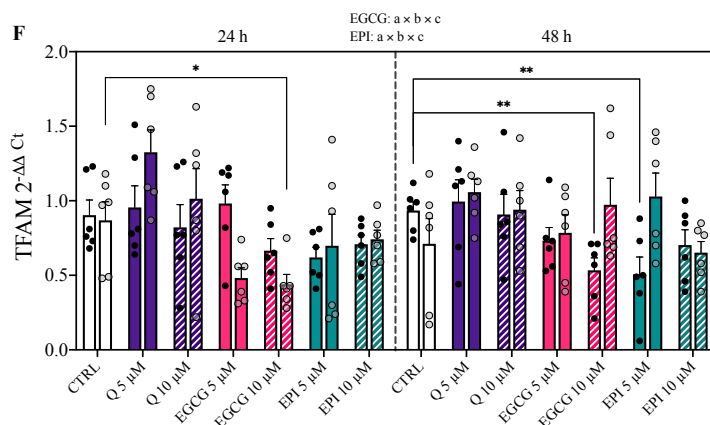


Figure 5. 13 Expression of genes associated with mitochondrial function in control and aged skeletal myoblasts following acute dietary flavonoid treatment. Myoblasts were treated with 0, 5 and 10 μ M of Q, EPI or EGCG over 48 h and lysed for analysis of gene expression. A) DRP1, B) MFN2, C) PARKIN, D) PGC1a, E) SIRT1 and F) TFAM. Data are means \pm SEM from 3 independent experiments run in duplicate. Statistical significance was determined by a three-way ANOVA, with dose, time and age as factors. Multiple comparisons performed by Dunnett's test, to determine within-age differences in gene expression between experimental conditions. ^a main effect of dose; ^b main effect of time; ^c main effect of age. * P <0.05, ** P <0.01, *** P <0.001, **** P <0.0001. Control and aged myoblasts are denoted by solid black and transparent circles, respectively.

Commented [DR384]: In the text you describe the effects per flavonoid. Why don't you use the same order here? So the bar for 24h ctrl young, attached to bar Q5, bar Q10. Then next group: 24h ctrl aged, attached to bar Q5, bar Q10. Next group: bar 48h ctrl aged, bar Q5, bar Q10. This is again you major problem: you want to show the effect of young vs aged, different flavonoid concentrations, different flavonoids and different timings. Too much messages...

Commented [SD385R384]: I know its been hard to decide best way of presenting the data, but here, at least the effects of age can be seen at each time point, along with the doses/compounds. I could present as you suggest, only consideration is the lack of direct comparison of control and aged

5.4.9.4 Expression of antioxidant related genes following Quercetin treatment in skeletal myoblasts

After reporting how flavonoids impact myoblast mRNA responses related to mitochondrial remodelling, gene transcripts associated with the antioxidant response were also examined in the presence of flavonoids. There was a significant main effect of age on catalase expression in Q treated myoblasts ($P=0.0344$), and a significant time \times age interaction ($P=0.0177$; Figure 5.14A). Over 48 h in control myoblasts, 10 μ M Q increased catalase expression \sim 1.6-fold compared to CTRL ($P=0.0468$). In aged myoblasts, 5 μ M Q increased catalase expression 2.1-

fold compared to CTRL at 48 h ($P=0.001$). For SOD2 expression, there was a significant main effect of age, and time \times age interaction in Q treated myoblasts ($P<0.05$). Levels of SOD2 were not impacted by flavonoid treatment in control myoblasts (see Figure 5.14B). Conversely, SOD2 expression was decreased 1.8-fold at 48 h following 10 μ M Q compared to CTRL ($P=0.034$) in aged cells. There was a significant main effect of dose ($P=0.0008$), time ($P=0.004$) and age ($P=0.0277$) on eNOS expression in Q treated myoblasts, and a significant dose \times age interaction ($P=0.0386$). At 48 h, eNOS expression in control myoblasts was 1.9-fold lower with 5 μ M Q versus CTRL ($P=0.035$). In aged myoblasts, 5 μ M Q decreased eNOS expression 2-fold ($P=0.0122$) and 2.3-fold ($P=0.0014$) over 24 h and 48 h, respectively. Regarding NOX4 expression, there was no significant main effect of dose, time or age in Q treated cells (Figure 5.14D). There was a significant main effect of time ($P=0.0032$) and age ($P=0.0008$) on NRF2 expression in Q treated myoblasts, and a significant dose \times time ($P=0.0144$) and time \times age interaction ($P=0.0237$). In control myoblasts, 5 μ M Q decreased NRF2 expression 2-fold versus CTRL ($P=0.005$). Overall, Q caused changes in the transcriptional activity of aged cells that imply increased cytosolic and lowered mitochondrial ROS, which, in the absence of changes in mitochondria function, warrants further investigation.

5.4.9.5 Expression of antioxidant related genes following EGCG treatment in skeletal myoblasts

There was a main effect of age ($P<0.0001$), and a dose \times age interaction ($P=0.0173$) on catalase in EGCG treated cells. Multiple comparisons revealed no impact of EGCG treatment on catalase expression. For SOD2 expression, there was a significant main effect of age, and time \times age interaction in EGCG treated myoblasts ($P<0.05$). Levels of SOD2 were increased 1.9-fold ($P=0.027$) and decreased 2-fold ($P=0.011$) by 24 h and 48 h treatment with 5 μ M EGCG,

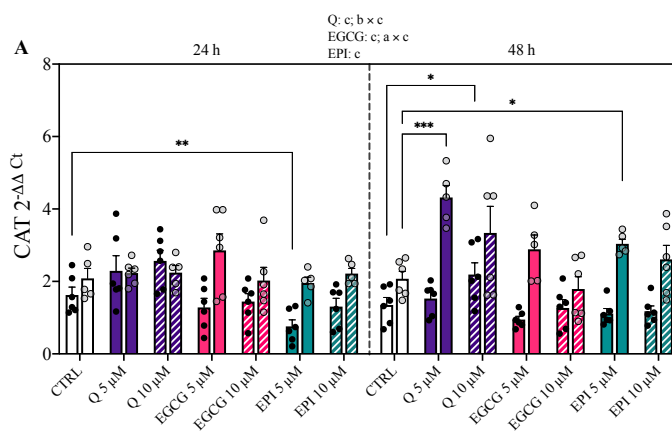
respectively (Figure 5.14B). In EGCG treated cells, a main effect of dose ($P=0.0002$) and time ($P<0.0001$), and a significant dose \times time \times age interaction ($P=0.0071$) was found for eNOS expression. Over 24 h, eNOS expression was significantly lower in aged myoblasts after 5 and 10 μM EGCG (2.9-fold, $P=0.0027$; 3.7-fold, $P=0.0027$). No differences in eNOS expression were observed in control cells after EGCG treatment (see Figure 5.14C). In EGCG treated cells, there was no main effect of dose, time or age on NOX4 expression but a significant time \times age interaction was found ($P=0.0003$). In control cells, 5 μM EGCG increased NOX4 levels over 24 h and 48 h (1.8-fold, $P=0.003$; 1.6-fold, $P=0.045$, respectively). In EGCG treated cells, there was a main effect of dose ($P=0.0037$) and time ($P=0.0162$). Both 5 μM and 10 μM EGCG augmented control NRF2 levels 1.6-fold ($P=0.028$) and 1.5-fold ($P=0.047$) over 24 h and 48 h, respectively (see Figure 5.14E). In aged myoblasts, 48 h EGCG (5 μM) increased NRF2 levels 2.6-fold compared with CTRL ($P=0.0157$). Overall, EGCG upregulated the transcription of genes associated with the antioxidant response in myoblasts, suggesting pro-oxidant effects of EGCG in myoblasts, independent of changes in mitochondrial respiration.

Commented [CS386]: Link back to prior data? ?

5.4.9.6 Expression of antioxidant related genes following EPI treatment in skeletal myoblasts

There was a main effect of age on catalase expression in EPI treated cells ($P<0.0001$). Treating control myoblasts with 5 μM EPI decreased catalase expression over 24 h versus CTRL (2.1-fold; $P=0.0027$). Conversely, over 48 h catalase expression was augmented 1.5-fold versus CTRL with 5 μM EPI ($P=0.025$) in aged cells (Figure 5.14A). On SOD2 expression, there was a significant main effect of age, and time \times age interaction in EPI treated myoblasts ($P<0.05$). Multiple comparisons revealed no impact of EPI on SOD2 expression in control and aged myoblasts. There was a significant effect of dose ($P=0.0033$) and age ($P<0.0001$) on eNOS expression in response to EPI ($P<0.0001$), and a time \times age interaction ($P=0.0180$). Over 48 h

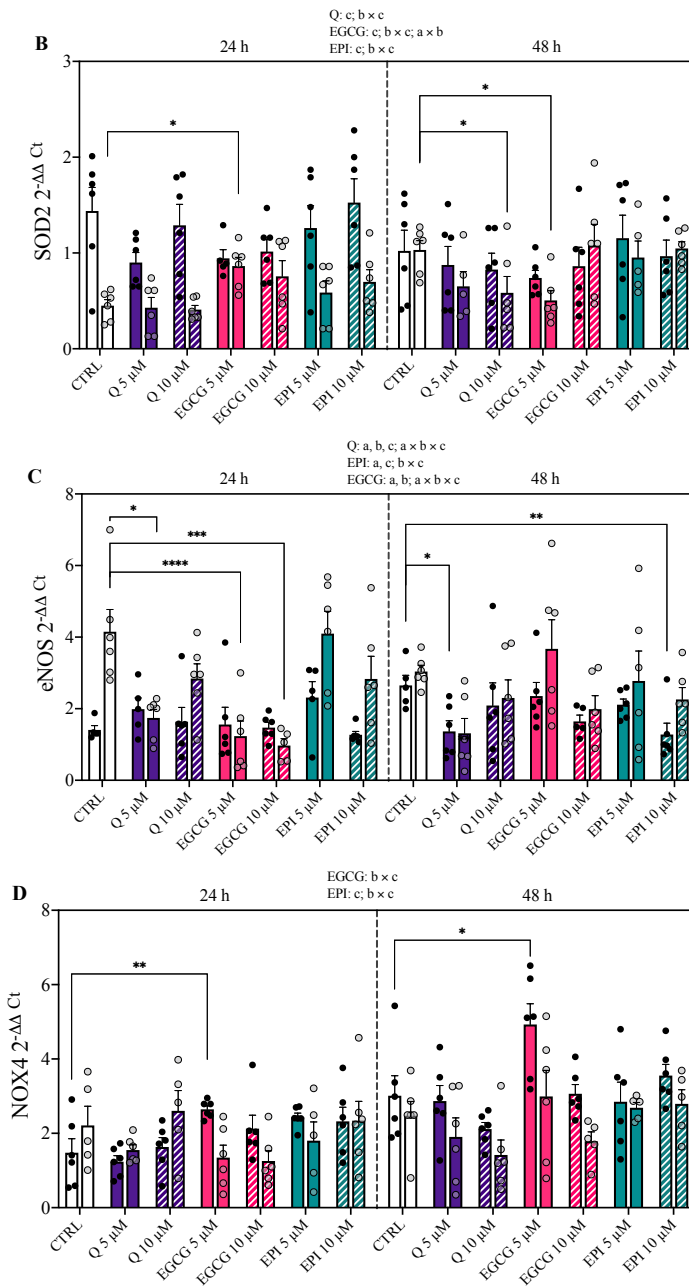
in control myoblasts, EPI treatment (10 μ M) lowered eNOS expression 2.1-fold compared to CTRL conditions ($P=0.0017$). In EPI treated myoblasts, there was a significant main effect of age ($P=0.0201$), and a time \times age interaction ($P=0.0014$) on NOX4 expression. At 24 h, NOX4 expression was 1.6-fold higher with 5 μ M EPI compared to CTRL in control cells ($P=0.020$). NOX4 expression was similar between conditions in aged myoblasts (see Figure 5.14D). There was a significant effect of dose on NRF2 expression in EPI treated myoblasts ($P=0.0035$). At 24 h, NRF2 expression was 1.6-fold higher in control myoblasts after 5 μ M EPI treatment compared to untreated CTRL ($P=0.045$; see Figure 5.14E). Whereas after 48 h 5 μ M EPI treatment of aged cells, NRF2 levels were 1.6-fold higher versus CTRL ($P=0.032$). In summary, acute EPI treatment increased antioxidant and stress responsive genes in aged myoblasts, that could relate to inhibition of mitochondrial bioenergetics.



Commented [CS387]: Would it be worth adding a summary table or figure? Showing the treatments across the rows and genes in columns and adding + / or - for increased, unchanged or decreased as a result of treatment? This may be easier to retain.

Commented [CS388]: If the presentation were separated into the treatment groups, you could have a 1 liner summary after each, re the activation or not of gene pathways.

Commented [CS389]: good



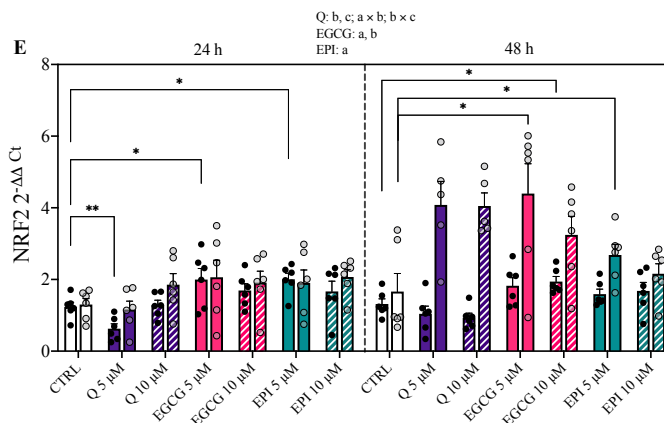


Figure 5. 14 Expression of genes associated with the antioxidant response in control and aged skeletal muscle myoblasts following acute dietary flavonoid treatment. C₂C₁₂ myoblasts were treated with 0, 5 and 10 μM of Q, EPI or EGCG over 48 h and lysed for analysis of gene expression. A) CAT, B) SOD2, C) eNOS, D) NOX4 and E) NRF2. Data are means±SEM from 3 independent experiments run in duplicate. Statistical significance was determined by a three-way ANOVA, with dose, time and age as factors. Multiple comparisons performed by Dunnett's test, to determine within-age differences in gene expression between experimental conditions. ^a main effect of dose; ^b main effect of time; ^c main effect of age. ***P*<0.05, ****P*<0.01, *****P*<0.001, ******P*<0.0001. Control and aged myoblasts are denoted by solid black and transparent circles, respectively.

5.4.10 Summary of the impact of dietary flavonoids upon control and aged skeletal myoblasts

In summary, dietary flavonoids had a limited impact on indices of mitochondrial function in skeletal myoblasts, yet EPI may evoke inhibitory effects upon mitochondrial respiration. These inhibitory effects on mitochondrial respiration in aged myoblasts could relate to a reduction in complex I activity, as opposed to a NO mediated inhibition. Interestingly, Q's effect upon

Commented [DR390]:

mRNA responses may suggest pro-oxidant effects and stimulation of mitochondrial biogenesis. In the presence of EGCG, gene expression data indicate an augmented antioxidant response and reduced mitochondrial remodelling. Lastly, EPI treatment attenuated mitochondrial remodelling in control myoblasts, but initiated an increased antioxidant response in aged myoblasts.

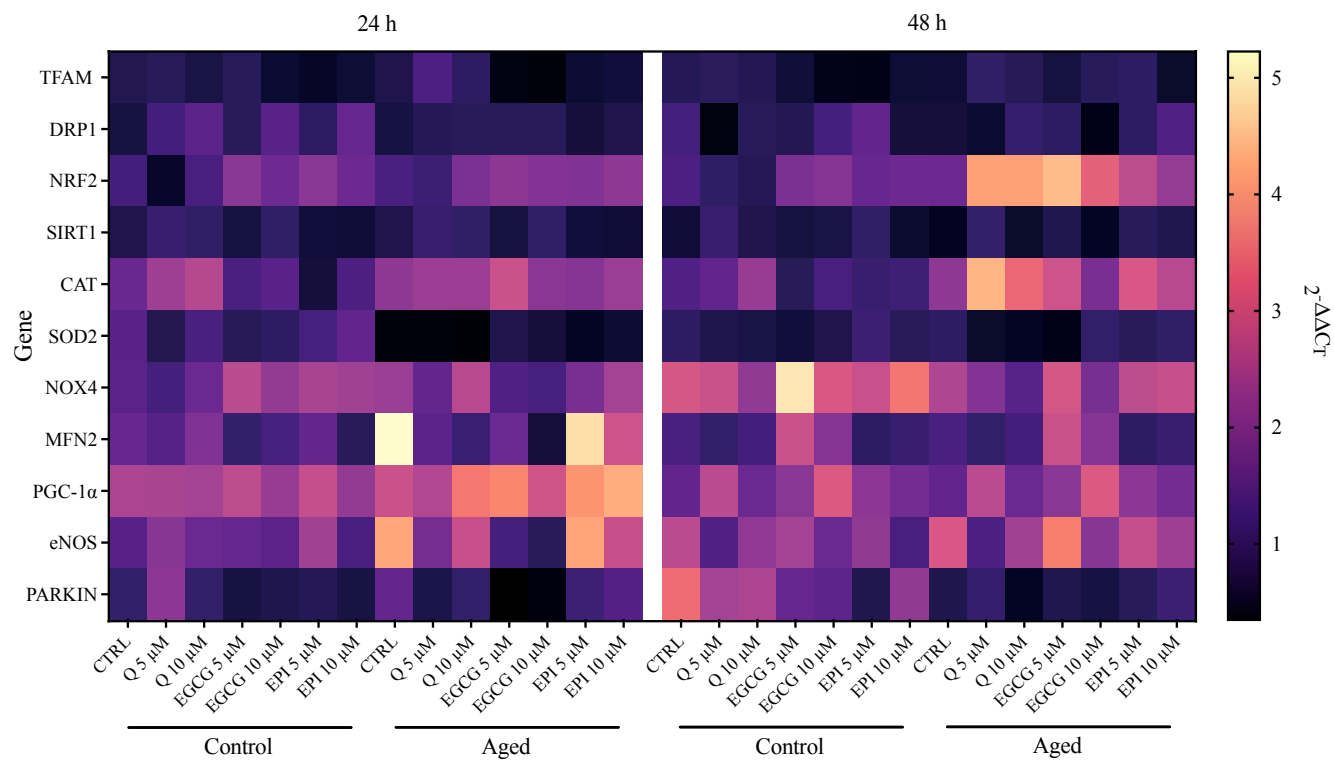


Figure 5. 15 Heatmap representation of myoblast mRNA responses in the absence of presence of flavonoids. Fold changes ($2^{-\Delta\Delta CT}$) in gene expression over 48 h presented as heat map.

5.5 Discussion

In this chapter, experiments were performed to determine whether mitochondrial function, NO bioavailability and gene expression are affected by replicative ageing, and secondly, whether these measures are impacted by dietary flavonoids. The aim of these experiments was to determine the basal phenotype of control and aged myoblasts and to subsequently determine the impact on mitochondrial function, NO bioavailability and gene expression with flavonoid treatment in the myoblast model. It was hypothesised that replicative ageing would cause mitochondrial dysfunction, lower NO bioavailability and blunt gene expression, and that these effects would be mitigated by dietary flavonoid supplementation. Overall, this chapter demonstrates that replicative ageing does not impair mitochondrial function but lowers NO bioavailability and attenuates gene expression (PARKIN and SOD2) in myoblasts (Figure 5.16). Interestingly, flavonoids evoked distinct effects on mitochondrial bioenergetics and transcription. EPI treatment increased NRF2 mRNA expression in control and aged myoblasts, but only inhibited respiration in aged myoblasts (see Figure 5.17). Therefore, EPI may act in a hormetic manner to promote beneficial adaptations via transcription. The data presented advance current knowledge of the mechanisms associated with flavonoids and their purported health benefits in skeletal muscle.

Commented [CS391]: In the interests of trying to get this back to you quickly, I have not reread the discussion.

Commented [CS392]: Just finish this by saying what it did or did not do in young

Commented [CS393]: So what would your recommendations be? Take EPI if older or not? What about any of the other flavonoids. Your get out of jail is that these are the myoblasts, so recommendations may change in tubes.

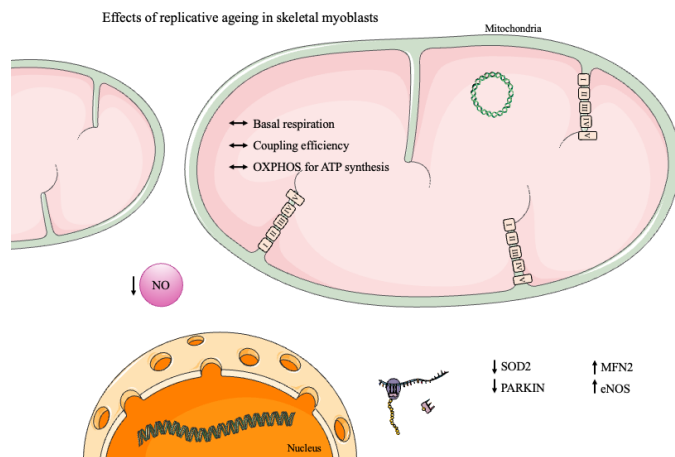


Figure 5. 16 Impact of replicative ageing upon skeletal myoblasts in this chapter. Replicative ageing does not impair indices of mitochondrial function but lowers NO bioavailability and alters gene expression (SOD2 and PARKIN lower and MFN2 and eNOS higher in aged vs. control myoblasts).

5.5.1 Replicative ageing does not compromise mitochondrial function in myoblasts

The main outcome from the current chapter was that replicative ageing does not impair mitochondrial function in cultured myoblasts, and flavonoids play a limited role in modulating mitochondrial respiration. Although advancing age has been linked with skeletal muscle mitochondrial dysfunction in rodents and humans (Gospillou et al., 2014c; Porter et al., 2015; Tonkonogi et al., 2003a), a number of studies have documented comparable mitochondrial functionality between young and aged skeletal muscle (Gospillou et al., 2014b; Hütter et al., 2007; Picard et al., 2010a). This is especially the case when mitochondrial function is interrogated when controlling for levels of physical activity (Distefano et al., 2018; Gram et al., 2015). Using an *in vitro* model of replicative ageing, the findings presented demonstrate that cellular replicative ageing is not associated with mitochondrial dysfunction, at least in myoblasts.

Commented [CS394]: This is nice 0 succinct, yet powerful observation

Commented [SD395]: check refs

5.5.2 Flavonoids do not cause alterations in myoblast mitochondrial respiration

Here, parameters of mitochondrial function were not impacted by Q or EGCG. These findings agree with oxygen consumption data from rat brain and heart mitochondria in the presence of Q (Lagoa et al., 2011), but disagree with studies demonstrating blunted state-3 supported respiration in mitochondria dosed with Q (Dorta et al., 2005; Trumbeckaite et al., 2006). The lack of change in mitochondrial respiration in cells cultured with EGCG supports previous work showing no change in parameters of mitochondrial function in isolated hepatocytes treated with analogous concentrations (10 μ M) of EGCG (Kucera et al., 2015). Although, other studies have reported EGCG administration augments state 3 respiration in human primary neurons (Castellano-González et al., 2016) and rat cardiomyocytes (Vilella et al., 2020b). Taken together, it seems that the effects of Q and EGCG on mitochondrial bioenergetics are highly cell specific. One possible explanation for differences in cell respiratory responses to Q and EGCG could relate to their potential accumulation within the mitochondrial fractions of cells. Both Q and EGCG accumulate within the organelles of T lymphocyte and neuronal cells (Fiorani et al., 2010b; Schroeder et al., 2009). However, to our knowledge, no studies have described whether Q and EGCG accrue within skeletal muscle mitochondria, and further research is required to help establish if this occurs both *in vitro* and *in vivo*. In contrast to Q and EGCG, EPI inhibited indices of mitochondrial function and oxidative ATP production in aged, but not control skeletal myoblasts. Consistent with the results in control myoblasts, one previous study reported that concentrations of EPI equivalent to those used here produced negligible effects upon C₂C₁₂ mitochondrial bioenergetics assessed during a mitochondrial stress test (Bitner et al., 2018). Furthermore, a study of isolated rat heart mitochondria in the presence of EPI unveiled 15% lower or similar state 3 respiration rates versus control when pyruvate/malate or succinate/amytal were used as substrates, respectively (Kopustinskiene et

al., 2015b). A handful of studies, however, have reported increased mitochondrial respiratory function with EPI treatment, albeit in rat beta-cells (Kener et al., 2018a; Rowley et al., 2017a). The underlying mechanism responsible for EPI-mediated respiratory inhibition in aged myoblasts is not entirely clear. However, in this study, a downward trend in complex I activity with EPI was observed in aged cells, which is consistent with data showing that complex I is a molecular target of EPI (Lagoa et al., 2011). Furthermore, EPI did not modulate NO levels in skeletal myoblasts, lending support to the idea that EPI-mediated inhibitions to mitochondrial respiration may be perpetuated by reductions in complex I activity and not increased NO. The physiological significance of acute respiratory inhibition with EPI is hard to reconcile, as it is not currently known what amounts (if any) of EPI reach mitochondria *in vivo*. Whilst chronic inhibitions to mitochondrial bioenergetics would likely be detrimental to cell function, acute respiratory inhibition could serve to stimulate a beneficiary cellular adaptive response through activation of stress signalling kinases (Garcia & Shaw, 2017; Mick et al., 2020), for example. In this manner, polyphenols (e.g. resveratrol and sulforaphane) have been proposed to act by the principle of hormesis, where these compounds stimulate stress response pathways and ultimately promote favourable adaptations (Calabrese & Baldwin, 2002; Calabrese et al., 2012; Martel et al., 2019), like that found in endothelial, neuronal and mesenchymal stem cells (J et al., 2006; Jang & Surh, 2003; Zanichelli et al., 2012).

5.5.3 Flavonoids do not rescue impairments to NO bioavailability in replicatively aged myoblasts

A second key finding of this chapter was that replicative ageing diminishes NO bioavailability, which is not rescued by flavonoid treatment. With older age, skeletal muscle NO levels reportedly decline due to reduced eNOS phosphorylation at Ser1177 (Donato et al., 2009a; Nyberg et al., 2012) and lowered nNOS expression at the mRNA and protein level (Samengo

Commented [CS396]: Good statement

et al., 2012). Similarly, the present study demonstrated that cellular ageing compromised NO bioavailability, which could be a consequence of increased ROS production (Bailey et al., 2010; Stefano et al., 2001). The observed age-related decline in NO bioavailability persisted in spite of increased eNOS mRNA in aged myoblasts, which may have served as a compensatory mechanism (Donato et al., 2009b; Thijssen et al., 2016). Such detrimental effects of ageing on NO bioavailability can have major ramifications, not only for the matching of O₂ delivery to O₂ demand within contracting muscle, but also for molecular events reliant on NO such as mitochondrial biogenesis (Lira et al., 2010; Tengan et al., 2007). In this study, flavonoids did not augment NO bioavailability in control or aged skeletal myoblasts. At the mRNA level, flavonoids tended to attenuate eNOS expression of control and aged myoblasts, yet NO levels were maintained between treatment conditions. Together, these observations emphasise the complexity involved in the regulation of eNOS activity and highlight mRNA responses may not directly translate to enzyme activity. Of the flavonoids tested, EPI has repeatedly been shown to potently stimulate NO production in endothelial cells and adult mouse tissue, and across healthy and unhealthy human populations (type 2 diabetic and heart failure patients) (Nogueira et al., 2011; Ramirez-Sanchez et al., 2010; Ramirez-Sánchez et al., 2016a; Schroeter et al., 2006; Taub et al., 2012). However, the lack of EPI-mediated change in NO levels observed here might be explained by the time course of treatment, given that peak EPI-induced NO production occurs within 10 minutes, at least in vascular endothelial cells (Ramirez-Sanchez et al., 2010). Taken together, the negligible impact of physiological concentrations of flavonoids on myoblast NO bioavailability suggests flavonoids may not afford adaptations that contribute to NO production or redox regulation in skeletal muscle myoblasts over the time-course studied.

Commented [CS397]: Nice section

Commented [CS398]: This also relates to the order of data presentation... It may be easier to explain from outside in or from inside out as suggested above.

Commented [SD399]: How can this be tied in with the PCR data and NRF2 data? Does this mean that time course was too early?

5.5.4 Replicative ageing attenuates myoblast PARKIN and SOD2 mRNA expression

Another important finding of the present study was that replicative ageing culminated in changes to the expression of genes associated with energy metabolism. Accordingly, aged myoblasts exhibited lower expression of PARKIN, suggesting reduced capacity for organelle degradation that could result in reduced competence of the mitochondrial network (Gouspillou, et al., 2014a). These data, however, contrast findings in rodent models of ageing that report increased basal mitophagy in older animals (Carter et al., 2018; Yeo et al., 2019). Besides, the abundance of MFN2 was acutely upregulated in aged myoblasts, which lends support to studies demonstrating an increased ratio of fusion:fission related proteins in ageing skeletal muscle (et al., 2013b; Leduc-Gaudet et al., 2015; Mercken et al., 2017). On the contrary, a number of studies have reported that ageing skeletal muscle mitochondria preferentially undergo fission (Iqbal et al., 2013; Joseph et al., 2012). The potential for hyper-fusion in aged myoblasts reported here would likely contribute to abnormal morphology of the mitochondrial network (Terman et al., 2009). Aged myoblasts also presented lower SOD2 expression, which supports work demonstrating that SOD2 protein content is significantly reduced in active and inactive older adults when compared to younger counterparts (Safdar et al., 2010). A reduced capacity to deal with mitochondrial superoxide by SOD2 would likely contribute to increased oxidative stress and subsequent damage to DNA and/or proteins (Dirks et al., 2006).

5.5.5 Flavonoids modulate the expression of genes associated with mitochondrial remodelling and the antioxidant response

To test whether flavonoids regulate transcription activities in control and aged myoblasts, the expression of genes associated with energy metabolism were assessed in their absence and presence. Of the genes studied associated with the antioxidant response, CAT demonstrated differential regulation by flavonoid treatment. In the presence of Q, control and aged myoblasts upregulated CAT mRNA expression, suggesting Q may act in a prooxidant manner in skeletal

myoblasts. Whereas CAT mRNA was respectively decreased and increased in control and aged cells cultured with 5 μ M EPI. Therefore, EPI's induction of CAT may depend on cellular ROS (H_2O_2) levels, although this study did not establish whether ROS are elevated in aged myoblasts. Mitochondrial SOD mRNA expression was significantly lowered by 5 μ M EGCG over 48 h in myoblasts. Given that SOD2 serves to dispense of mitochondrial superoxide, EGCG may act as an antioxidant at the level of mitochondria (Pan et al., 2015); but whether these (potential) antioxidant effects are perpetuated via an enzymatic or non-enzymatic mechanism remains to be established. These data conflict with findings showing increased SOD2 mRNA expression and protein content following EGCG administration in L6 myocytes and embryonic fibroblasts, respectively (Casanova et al., 2014; Zhang et al., 2019), although supraphysiological concentrations (25 μ M) of flavonoids were employed. In contrast to SOD2, NOX4 mRNA was increased in the presence of EGCG. NOX4 plays a key role in generating cytosolic ROS (Sakellariou et al., 2013; Serrander et al., 2007), and therefore, it is possible that the effects of EGCG on intracellular ROS are dependent on the sub cellular compartment. Together, these findings suggest that flavonoids may distinctly contribute to control of the myoblast redox state through the induction of enzymatic antioxidant systems.

The transcriptional co-activator, PGC-1 α , seems to play an important role in mediating mitochondrial adaptations to external stimuli like exercise and nutritional intervention (Lagouge et al., 2006; Lin et al., 2002; Wright et al., 2007). Together with PGC-1 α , SIRT1 functions to stimulate mitochondrial biogenesis via its deacetylase activity (Dumke et al., 2009). The increased expression of PGC-1 α and SIRT1 in myoblasts following 5 μ M Q supports previous work showing increased mitochondrial biogenesis following Q supplementation in humans and rodents (Davis et al., 2009b; Henagan et al., 2015; Nieman et al., 2010; Sharma et al., 2015b). Whilst Q appears capable of stimulating mitochondrial

biogenesis, micromolar doses of EGCG and EPI did not alter PGC-1 α mRNA levels in myoblasts. These data conflict with previous findings demonstrating blunted mitochondrial adaptations in human skeletal muscle and murine skeletal muscle cells following EPI and EGCG supplementation, respectively (Schwarz et al., 2018; Wang et al., 2016). Additionally, the lack of change in PGC-1 α with EGCG and EPI disagrees with studies documenting augmented markers of mitochondrial biogenesis with EPI and EGCG (Hüttemann et al., 2013; Lee et al., 2017; Moreno-Ulloa, Nogueira, et al., 2015; Taub et al., 2016). Although EGCG did not impact PGC-1 α mRNA expression, myoblasts cultured in the presence of EGCG exhibited lower TFAM mRNA, suggesting reduced potential for transcription of mitochondrial encoded proteins. Considering EGCG's apparent antioxidant action at the level of transcription in the mitochondria, it is plausible that the blunted TFAM expression with EGCG occurred due to lowered ROS and blunted activation of transcription factors, such as NRF2. Maintenance of mitochondrial health also involves targeted mitochondrial degradation (mitophagy), as well as fusion/fission activities that govern organelles dynamics. Evidence for reduced mitophagy in EGCG treated myoblasts was provided by decreased PARKIN expression, which may result in a more fragmented network (Bernard et al., 2007). Interestingly, aged myoblast mitochondrial fusion was differentially regulated by flavonoids. Whilst Q and EGCG attenuated MFN2 mRNA expression, EPI enhanced MFN2 mRNA in aged myoblasts. Therefore, EPI supplementation may facilitate coordinated mitochondrial membrane remodelling activities in muscle cells, with potential implications for mitochondrial function (Eisner et al., 2014; Glancy et al., 2015).

As a redox-sensitive transcription factor, NRF2 governs the transcription of multiple proteins including antioxidant enzymes and subunits of the ETS through its binding to antioxidant response elements (Gao et al., 2020; Yamamoto et al., 2018). Surprisingly, EGCG and EPI

Commented [SD400]: first time spell out?

robustly enhanced NRF2 transcription across control and aged myoblasts. Induction of NRF2 expression and activity by flavonoids is a well-documented phenomena (Huang et al., 2019; Kim et al., 2015; Li et al., 2016; Moreno-Ulloa, Nogueira, et al., 2015; Rowley et al., 2017a; Wu et al., 2006; Yang et al., 2015; Zheng et al., 2012), and together these findings raise questions about the process of flavonoid-induced NRF2 mRNA upregulation in skeletal muscle cells. Theoretically, flavonoids could promote NRF2 activation either directly, or by the formation of RONS (McMahon et al., 2010; Zhang & Hannink, 2003), via dissociation of NRF2 from its repressor Kelch-like ECH-associated protein 1 (Keap1), or even by a Keap1 independent mechanism (Gao et al., 2020). Considering that flavonoids did not impact NO production in the present study, it is plausible that a Keap1-independent mechanism was responsible for the upregulation of NRF2 mRNA, such as that afforded by signalling kinases such as AMPK (Joo et al., 2016), but this requires further investigation.

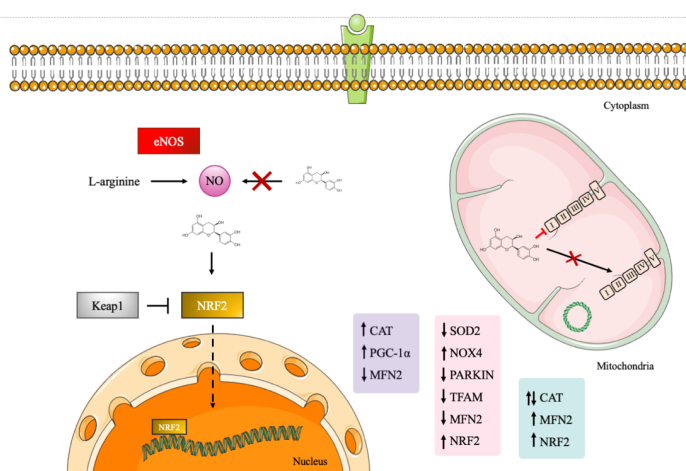


Figure 5. 17 Schematic of the potential mechanisms by which flavonoids exert their biological effects in skeletal myoblasts. Genes differentially expressed by Q, EGCG and EPI treatment are highlighted in purple, red and green, respectively.

Commented [CS401]: I think that the huge amount of data you have generated would really benefit from an infographic style figure explaining the key findings and the links in the different models, treatments and output measures. It could even be part of your abstract for this chapter, to help your readers. It could be in 4 panels for con aged, blasts and tubes. That may also then help you define the order in which you ultimately present the data.

Commented [CS402]: This is lovely. It would be good to have a similar figure earlier on how the aged and control cells differ from a metabolic perspective (mito and gene expression, but that may be too big of an ask?

Commented [SD403R402]: Will try and do this

Commented [CS404]: Very nice

5.6 Limitations

A murine skeletal muscle cell line (C₂C₁₂) was used in this study to examine the effects of (replicative) ageing and flavonoids on aspects of energy metabolism in myoblasts. The findings generated using the C₂C₁₂ myoblast model should be translated with caution given their failure to fully mimic human skeletal muscle cells with respect to metabolism (Abdelmoez et al., 2019). A second limitation of this study was the use of the fluorescent DAF-FM probe to assess NO bioavailability in muscle cells. Indeed, DAF-FM oxidation may not solely reflect NO levels but could also reflect the presence of other one electron species (Namin et al., 2013). Other key limitations were the lack of measures of protein content and localisation and/or enzyme activity, and reliance on mRNA levels to infer cellular and molecular adaptations. Like Chapter 4, this study utilised parent flavonoid compounds rather than their related *in vivo* metabolites, which may limit the translatability of the findings. Another limitation of this study was the failure to obtain information on the maximal respiratory capacities of control and aged myoblasts when using the Seahorse Analyzer to investigate mitochondrial function. Further insights into the maximal and spare respiratory capacities of myoblasts may have shed light on dysfunction that was not apparent with the measures used between control and aged cells. The respiratory data in this chapter were normalised to cell DNA content, rather than mitochondrial mass, and therefore should be interpreted with caution.

5.7 Conclusion

The novel findings in this chapter demonstrate that replicative ageing does not cause mitochondrial dysfunction but attenuates NO bioavailability and alters the expression of genes associated with energy metabolism in skeletal myoblasts. Further, this study provides evidence that the flavonoids tested did not directly impact mitochondrial function, with the exception that EPI may inhibit respiration in aged myoblasts. In addition, flavonoids did not rescue age-

related impairments to NO bioavailability, but they may indirectly regulate mitochondrial function via increased transcriptional activity in a compound- and dose-dependent manner. Of the flavonoids tested, EPI robustly induced NRF2 mRNA expression, that could relate to the inhibition of mitochondrial respiration. The reported effects of flavonoids on myoblast transcriptional responses occurred in the physiological range, suggesting that these compounds may confer favourable mitochondrial adaptations, on myoblasts, when ingested *in vivo*. Taken together, flavonoid (EGCG and EPI) supplementation may help defend against the perils of sedentary ageing by acting through the mechanism of hormesis to enhance mitochondrial health. Experimental evidence of NRF2 (in)activation and its associated signalling events is required in the presence of relevant kinase inhibitors to validate flavonoids proposed mechanism of action in skeletal myoblasts.

Commented [SD405]: Strong statement? We didn't use AMPK inhibitors to confirm AMPK is required for EPIs effects downstream... Also, EPI only inhibited O2 consumption in aged cells, where AMPK wasn't significantly increased – thus the induction of NRF2 might not be related to inhibited O2 consumption but some other mechanism

Commented [CS406R405]: I meant more to do with being bold with the language used e.g. you write: suggesting that these compounds may promote favourable adaptations – suggest and may are underwhelming and favourable doesn't really tell you how. This is your conclusion, you can be bold – but perhaps link it into an hypothesis going into the next chapter....

Commented [SD407R405]: Have tried to adjust conclusion

Commented [CS408]: This is the sort of thing you want – strong statements, but with caveats e.g. to test this you would need to do a b and c.....

Chapter 6: The effects of replicative ageing and dietary flavonoids on mitochondrial function, reactive oxygen species production and cell signalling in C₂C₁₂ skeletal myotubes

6.1 Abstract

Introduction: Sedentary ageing is associated with impaired pulmonary oxygen uptake ($\dot{V}O_2$) kinetics and exercise tolerance, that may be attributable to mitochondrial dysfunction and increased ROS production. Flavonoids are acknowledged as health promoting compounds that may impact mitochondrial function and modulate ROS production, but their effects on ageing skeletal muscle mitochondria are yet to be described.

Objective(s): 1) To determine the effect of replicative ageing on mitochondrial function, ROS production and cell signalling of C₂C₁₂ myotubes. 2) Investigate the impact of flavonoid (quercetin [Q], epigallocatechin-gallate [EGCG] or (-)-epicatechin [EPI]) supplementation on indices of mitochondrial function, ROS production and cell signalling of control and aged myotubes. It was hypothesised that replicative ageing would cause mitochondrial dysfunction, augment ROS production and blunt cell signalling, and that these effects would be mitigated by dietary flavonoid supplementation.

Methods: Control and aged C₂C₁₂ myotubes were treated with low micromolar concentrations of Q, EGCG or EPI for up to 48 h. Mitochondrial bioenergetics were investigated by respirometry after 24 h. Mitochondrial and non-mitochondrial specific ROS were measured in the absence and presence of antimycin A (AA; positive control). Genes related to mitochondrial remodelling and the antioxidant response were quantified by RT-qPCR over 48 h. Cell signalling responses were examined over 24 h +/- EPI by western blotting.

Results: Mitochondrial coupling efficiency (Control: 79.5 vs. Aged: 70.3%, $P=0.006$) and relative oxidative ATP synthesis (Control: 48.6 vs. Aged: 31.7%, $P=0.022$) were higher in control vs. in aged myotubes, but mitochondrial ROS production was lower (Control: $2.4 \times 10^{-5} \pm 0.4 \times 10^{-5}$ vs. Aged: $9.7 \times 10^{-5} \pm 1.6 \times 10^{-5}$ RFU/sec⁻¹/cell⁻¹; $P=0.035$). Age-related mitochondrial dysfunction and ROS production were not rescued by flavonoid treatment. However, flavonoid treatment augmented the expression of genes associated with mitochondrial remodelling, in a dose- and compound dependent manner. NRF2 expression was upregulated by flavonoid treatment in control myotubes (~1.8-fold increase over 24 h after 5 μ M and 10 μ M EPI vs. CTRL; $P=0.022$ and $P=0.029$, respectively) and aged myotubes (1.7-fold increase with 5 μ M EPI over 48 h vs. CTRL, $P=0.012$). In the presence of EPI, NRF2 induction appears downstream of AMPK signalling (1.9- and 2.1-fold increase with EPI over 1 h and 24 h vs. 0 h CTRL; $P=0.039$ and $P=0.012$, respectively).

Conclusion(s): Replicative ageing inhibits indices of mitochondrial function and increases mitochondrial ROS production in myotubes. Flavonoids do not rescue age-related impairments

Commented [CS409]: Very nice scene setting

Commented [CS410]: What about objectives 3/4 to determine the impact on signalling and gene expression?

Commented [SD411R410]: Shall I add these in as additional objectives and hypotheses?

Commented [DR412R410]: I would say yes, it explains why you extended your research the signalling pathways

Commented [DR413]: Explain why

to ROS production and mitochondrial function. However, flavonoids may instigate cell adaptations at the transcriptional level, partly via NRF2, that could be related to AMPK activation in the presence of EPI.

Commented [CS414]: Very nice abstract. All should take on this sort of format.

6.2 Introduction

In Chapter 5 of this thesis, replicative ageing did not compromise mitochondrial function in C₂C₁₂ skeletal myoblasts. However, it is not known whether replicative ageing captures ageing sedentary human muscle behaviour in skeletal myotubes, which is relevant because differentiated myotubes may better reflect human skeletal muscle *in vivo*. Sedentary ageing is associated with reductions in mitochondrial respiratory function (Tonkonogi et al., 2003a; Lyons et al., 2006), increased ROS production (Holloway et al., 2018) and lower mitochondrial contents (Rooyackers et al., 1996; Short et al., 2005; Zahn et al., 2006). One explanation for the observed reductions in mitochondrial content with sedentary ageing is blunted cell signalling and transcriptional responses to relevant stimuli. For example, activation of the energy sensitive AMP-activated protein kinase (AMPK) is lower after endurance exercise in aged compared to young rat muscle (Hardman et al., 2014; Reznick et al., 2007b). Further, the expression of peroxisome proliferator-activated receptor gamma coactivator 1-alpha (PGC-1 α), an important regulator of mitochondrial adaptations, is reportedly lower following exercise in older compared to younger adults (Ljubcic & Hood, 2009; Reznick et al., 2007b). Overall, targeting mitochondria and their associated metabolic pathways may help alleviate age- and (in)activity related declines in O₂ utilisation, and ultimately improve exercise tolerance.

Flavonoids are acknowledged for their potential to interact with mitochondria. Indeed, flavonoids accumulate within the mitochondrial compartments of different cell types (Fiorani et al., 2010a; Mukai et al., 2016; Schroeder et al., 2009), hinting that these compounds may afford beneficial effects at the level of organelles. Some flavonoids have been reported to modulate mitochondrial respiration (Bitner et al., 2018; Dorta et al., 2005; Rowley et al., 2017b; Vilella et al., 2020a), although findings from Chapter 5 suggest a limited role for flavonoids in directly modulating respiration in C₂C₁₂ myoblasts. Additionally, flavonoids

Commented [DR415]: This section doesn't make clear why you specifically mention AMPK and PGC-1alpha: what is so special about these enzymes in the context of mitochondrial dysfunction and ROS....

Commented [SD416R415]: Have made small adjustments

Commented [SD417]: What about NRF2

Commented [CS418]: Are any of these in skeletal muscle?

stimulate pathways responsible for mitochondrial turnover in skeletal muscle (Davis et al., 2009b; Hüttemann et al., 2013; Moreno-Ulloa et al., 2018; Murase et al., 2009). Another reported role for flavonoids relates to the modulation of cellular ROS production. Previous studies employing high micromolar doses of flavonoids have repeatedly shown antioxidant effects in skeletal muscle, brain and liver tissue (Bouitbir et al., 2012; Dorta et al., 2008; Meng et al., 2008; Rowley et al., 2017a; Shaki et al., 2017; L. Wang et al., 2016), although these doses are likely supraphysiological *in vivo* (Manach et al., 2005a). Evidently, it remains to be determined whether flavonoids modulate skeletal muscle cell mitochondria and ROS production.

Consequently, the main aims of the present study were to determine the basal phenotype of control and aged myotubes and to use dietary flavonoids to manipulate mitochondrial function, ROS production and cell signalling of aged myotubes. The study objectives were two-fold: 1) Determine the effect of replicative ageing on mitochondrial function, ROS production and cell signalling of C₂C₁₂ myotubes. 2) Investigate the impact of flavonoid (quercetin [Q], epigallocatechin-gallate [EGCG] or (-)-epicatechin [EPI]) supplementation on indices of mitochondrial function, ROS production and cell signalling of control and aged myotubes. It was hypothesised that replicative ageing would cause mitochondrial dysfunction, augment ROS production and blunt cell signalling, and that these effects would be mitigated by dietary flavonoid supplementation.

6.3 Methodology

6.3.1 Cell culture and treatment

Commercially available C₂C₁₂ murine skeletal myoblasts at passages 8-12 (referred to as 'control') and passages 47-50 (replicative aged and referred to as 'aged', having undergone

Commented [SD419]: Check allrefs are skeletal muscle based

Commented [CS420]: All rodent experiments? Please state eg in rodents

Commented [CS421]: No oversight of any of the genes you want to study nor of the signalling pathways to be investigated. If this has been done in the main intro (sorry, I cant remember), then refer the reader to the relevant sections. If not, please add a couple of paragraphs to this intro to let your reader know these parameters will be investigated and why they are relevant.

Commented [CS422]: I have taken the three words out form the aims, because until you do the experiments, you do not know if there will be any differences between the cells and therefore whether flavonoids are needed to enhance responses. Your hypothesis then puts in the specifics.

Commented [CS423]: What about objectives ¾ to determine the impact on signalling and gene expression?

Commented [SD424R423]: Shall I add these in as additional objectives and hypotheses?

Commented [DR425R423]: I would say yes, it explains why you extended your research the signalling pathways

Commented [CS426]: Good, exactly as suggested in the new comment above

Commented [CS427]: I have not looked at the methods again

130-140 population doublings) were used in this study. For standardised cell culture procedures, see section 2.3 (Chapter 2). Following the plating of cells onto appropriate well-plates in growth medium (GM), confluent C₂C₁₂ myoblasts were washed twice with phosphate-buffered saline (PBS) and switched to pre-warmed (37°C) differentiation medium (DM). After switching myoblasts to DM, they were allowed to differentiate for 72-96 h, before dosing over 24 and 48 h with Q, EGCG and EPI (0-20 µM).

Commented [CS428]: Worth putting in () after each timepoint what was measured? Eg 24 (a,b, and c were assessed) and 48 h (x and y were assessed)

6.3.2 Mitochondrial ROS production

Mitochondria derived superoxide was detected in C₂C₁₂ myotubes using the targeted MitoSOX probe. C₂C₁₂ cells were seeded at 3 × 10⁴ cells/mL into 12-well microplates, and at ~80% confluence, switch to DM. After 72 h differentiation, myotubes were dosed with 0, 5 and 10 µM Q, EGCG or EPI, for 24 h in DM. Next, myotubes were washed 2 × in PBS, and switched into pre-warmed KRH, with or without 15 µM antimycin A, an inhibitor of the mitochondrial electron transport chain (AA; serving as positive control), and incubated at 37°C for 30 minutes. Next, AA-containing KRH was removed, and MitoSOX was loaded into cells in fresh pre-warmed KRH to a final concentration of 2.5 µM. Plates were immediately transferred to a CLARIOStar plate reader (BMG Labtech, Bucks, Great Britain), and fluorescence was monitored continuously at 30-sec intervals over 30 min. Fluorescent MitoSOX oxidation products were excited at 510 nm and light emission was detected at 580 nm. The plate reader's focal height was set at 3.3 mm and gain was fixed between different experiments. Upon completion of the 30-min reading, plates were immediately fixed for the determination of protein content (see section 2.14).

Commented [CS429]: It has just struck me, perhaps a bit late, that you do not refer to treatments in any of these sections – is it worth adding a get out of jail section that states all experiments were performed with Q, EGCG etc at the doses used? If these varied, then add to each subsection.

Commented [CS430]: In what buffer? Krebs or something else?

Commented [CS431]: Details of company – I wont write this again, but please update methods accordingly

6.3.3 Cellular ROS

Cellular reactive oxygen species (ROS) were detected using the CellROX[®] Deep Red reagent by spectrophotometry. Briefly, C₂C₁₂ myoblasts were seeded at 3×10^4 cells/mL into 12-well microplates, and at ~80% confluence, switch to DM. After 72 h differentiation, myotubes were dosed with 0, 5 and 10 μ M Q, EGCG or EPI, for 24 h in DM. Next, myotubes were washed 2x in PBS, and switched into pre-warmed KRH, with or without 15 μ M antimycin A (AA), and incubated at 37°C for 30 minutes. Next, KRH was removed, and CellROX was loaded into myotubes in fresh, pre-warmed KRH buffer, to a final concentration of 2.5 μ M. Following 30 minutes incubation with the reagent, cells were washed 2 \times with PBS and immediately transferred to a plate reader (BMG Labtech, Bucks, Great Britain), where fluorescent CellROX oxidation products were excited at 640 nm and light emission detected at 665 nm. The plate reader's focal height was set at 3.3 mm and gain was optimised and fixed between experiments. Upon completion of the reading, plates were immediately fixed for the determination of cell density by the SRB assay (see section 2.14, Chapter 2), which was used to normalise obtained fluorescence values.

Commented [CS432]: In what buffer? Krebs or something else?

6.3.4 Mitochondrial Bioenergetics

Mitochondrial respiration was measured in adherent C₂C₁₂ myotubes using a Seahorse XFe96 Analyzer (Agilent, Santa Clara, CA, USA). Control (passages 9-11) and replicatively aged (passages 47-50) C₂C₁₂ myoblasts and myotubes were seeded in XFe96 well plates (Agilent, Santa Clara, CA, USA) at 10,000 cells per well in 100 μ L of GM for 24 h to allow cell attachment. After 24 h, C₂C₁₂ myoblasts were washed twice with PBS and transferred to DM. Myotubes were allowed to form over 96 h in DM, with fresh media replacement at 48 h. At 96 h, when myotube formation was evident, myotubes were dosed with Q, EGCG and EPI (0, 1, 5 and 10 μ M) in DM for a further 24 hours.

Sensor cartridges for the XFe96 Analyzer were hydrated with deionised water at 37°C in a non-CO₂ incubator in the 24 h preceding the assay. On the day of the assay, C₂C₁₂ myoblasts and myotubes were washed into 200 µL pre-warmed modified Krebs Ringer buffer (KRH) at pH 7.4. See table 2.1 (Chapter 2) for KRH composition. The cells were incubated in this buffer for 45 minutes at 37°C in a non-CO₂ incubator and then transferred to a Seahorse XFe96 extracellular flux analyser (maintained at 37°C). Following 10-minute calibration, oxygen consumption rates (OCR) were measured by a 3-4 loop cycle consisting of a 1-min mix, 2-min incubate and 3-min measure to record cellular basal respiration (see Figure 2.6, Chapter 2). After measuring basal respiration, 2 µM oligomycin was added to selectively inhibit the mitochondrial ATP synthase. Subsequently, 2 µM carbonyl cyanide-4-phenylhydrazone (FCCP) followed by a mixture of 2 µM rotenone and 2 µM antimycin A were added sequentially to, 1. uncouple oxygen consumption rates to ATP synthesis rates to determine maximal respiration or 2. inhibit complex I and III of the electron transport chain to determine non-mitochondrial respiration. Rates of oxygen consumption and extracellular acidification (ECAR) were expressed relative to the DNA content of the appropriate well (see section 6.3.6). Three independent experiments were performed to assess mitochondrial respiration, each containing four technical replicates. The Wave software native to the XF Analyzer was used to extract OCR's and ECAR.

6.3.5 ATP Production Rates

A full description of the method used for calculation of total cellular ATP production rates from ECAR and OCR is in section 2.11 (Chapter 2). Briefly, to calculate $J_{ATP_{glyc}}$, the ECAR was first converted to total proton production rate (PPR). The contribution of respiratory CO₂ to total PPR was subtracted to yield glycolytic rate of glucose catabolism terminating in lactate. This rate was multiplied by the ratio of ATP produced in glycolysis terminating in lactate per

Commented [CS433]: Remember to add the full name before the (FCCP)

Commented [CS434]: What is the F an abbreviation of?

extracellular H^+ (the P/H^+ ratio). Additional glycolytic flux generating the pyruvate that is later fully oxidised in the mitochondria generates additional ATP and is represented in the mitochondrial respiration rate (see below). Mitochondrial respiration rate was multiplied by the ratio of ATP produced in glycolysis terminating in pyruvate per O_2 consumed for each substrate (P/O_{glyc}). Glycolytic ATP production ($J_{ATP_{glyc}}$) was calculated as the sum of these two rates. To calculate $J_{ATP_{ox}}$, mitochondrial respiration rate was isolated by subtracting from the total OCR any additional oxygen consumption in the presence of rotenone and antimycin A ($OCR_{R/AA}$). Mitochondrial respiration rate was further divided into ATP-coupled and uncoupled respiration rates using the mitochondrial ATP synthase inhibitor oligomycin. The ATP-coupled respiration rate was multiplied by the portion of the P/O ratio attributable to the mitochondrial ATP synthase (P/O_{OXPHOS}). To account for oxidative substrate-level phosphorylation in the TCA cycle, the mitochondrial respiration rate was multiplied by the P/O ratio attributable to succinyl CoA synthetase (P/O_{TCA}). Oxidative ATP production ($J_{ATP_{ox}}$) was calculated as the sum of these two rates. Finally, $J_{ATP_{glyc}}$ and $J_{ATP_{ox}}$ were summed to yield the total cellular ATP production rate, $J_{ATP_{production}}$.

6.3.6 Mitochondrial bioenergetics normalisation procedures

6.3.6.1 dsDNA PicoGreen

QuantiT™ PicoGreen® dsDNA reagent (ThermoFisher, Waltham, MA, USA) was used as a fluorescent nucleic acid stain for quantifying dsDNA in solution. Upon completion of mitochondrial stress tests, C_2C_{12} myotubes were immediately removed from the Seahorse Analyzer and existing assay media (KRH buffer) carefully removed, ensuring that ~25 μL remained to avoid cell contact. Subsequently, 200 μL RIPA buffer was added to each well of the 96-well plate and plates were shaken vigorously on an orbital shaker for 10 minutes. Plates

Commented [CS435]: Same comment above re precision of remaining volume

were immediately frozen at -80°C until further processing. On the day of the assay, 96-well plates were allowed to thaw at room temperature. Meanwhile, a 1x Tris-EDTA (TE) buffer (10 mM Tris-HCl (pH 7.5), 1 mM EDTA) was prepared in DNase free H_2O and left to reach room temperature. A working concentration of QuantiT™ PicoGreen® dsDNA reagent was prepared by making a 200-fold dilution of the concentrated stock solution using TE buffer. To avoid the reagent absorbing to glass surfaces or being susceptible to photo degradation it was prepared in a plastic container and stored away from direct light. A 5-point high-range DNA standard curve was created using a 100 $\mu\text{g}/\text{mL}$ Lambda DNA stock solution diluted in 1x TE buffer supplemented with 50 RIPA buffer (see Figure 6.1). 50 μL of each DNA standard (0, 2, 20, 200, 2000 ng/mL) was added to wells of a black solid-bottom 96-well microplate (Greiner Bio-One, Kremsmünster, Austria) in duplicate. Next, 50 μL of each sample was added to appropriate wells, followed by 50 μL 1x TE buffer. Finally, 100 μL PicoGreen reagent was added to each well. Following a 5-minute incubation at room temperature in the dark, endpoint fluorescence was measured by exciting fluorescent products at 485 nm and recording emitted light at 520 nm using a multi-plate reader (OMEGA FluoSTAR, BMG Labtech). To ensure all sample readings remained in the detection range of the fluorometer, the gain was set to that of the sample containing the highest DNA concentration (i.e., the 2 $\mu\text{g}/\text{mL}$ Lambda DNA stock). DNA content in each sample was quantified by interpolating unknown X values by comparing RFU values with those on a standard curve of known dsDNA concentrations.

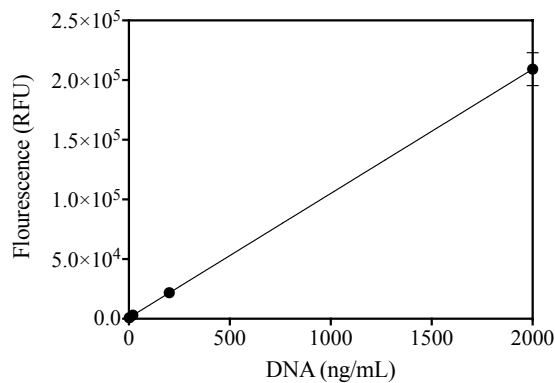


Figure 6. 1 Standard curve of Lambda dsDNA detected with QuantiT™ PicoGreen® dsDNA reagent. Cell Proliferation Assay. Lambda DNA was diluted to create standards of known concentrations (0-2000 ng/mL) and were quantified. Samples were excited at 480 nm and fluorescence emission intensity measured at 520 nm. Relative fluorescent units were plotted as a function of dsDNA and fitted with linear regression.

6.3.7 RT-qPCR – Gene expression Quantification

C₂C₁₂ myotubes were lysed in 250 uL TRIzol and total RNA was extracted using the phenol-chloroform method (see section 2.12.1, Chapter 2). RNA concentration of control and aged myotubes (n=3, in duplicate per condition; Control myotubes: 1045.1 ± 186.2; Aged myotubes: 941.2 ± 248.2 ng/uL) and purity (All samples 2.0 ± 0.0 A₂₆₀/A₂₈₀, respectively) was determined by spectrophotometry (NanoDrop™ 2000, Thermo Fisher Scientific, Waltham, USA). Samples were diluted and prepared for PCR as described in section 5.3.8. Critical threshold (C_T) values were derived from setting a threshold of 0.08 for all genes, that are outlined in Table 6.1. The amplification efficiencies were analysed for all reactions (Control myotubes: 92.6 ± 5.5; Aged myotubes: 92.1 ± 5.7 %) and values between 80-100% were accepted as efficient. To quantify gene expression, C_T values were used to quantify relative gene expression

using the comparative Delta Delta C_T ($2^{-\Delta\Delta C_T}$) equation (Livak & Schmittgen, 2001), whereby the expression of the gene of interest was determined relative to the internal reference gene (RP2 β) in the treated sample, compared with the untreated zero-hour control. RP2 β was selected as an internal reference gene because its expression was stable across experimental conditions (19.77 ± 0.60).

Table 6. 1 Primer sequences for *Mus musculus* with product length. All primers were used under the same cycling conditions.

Gene	Accession	Sequence		Product length (bp)
		Forward/Reverse or Anchor nucleotide		
Polr2b (RP2 β)	NM_153798.2	F: GGTCAGAAGGGAACCTGTGGTAT	R: GCATCATTAATGGAGTAGCGTC	197
CAT	NM_009804	AN: 324		96
SOD2	NM_013671	AN: 1769		103
Dnm1 (DRP1)	NM_152816	AN: 1337		104
MFN2	NM_113201	AN: 1709		93
Ppargc1a (PGC-1 α)	NM_008904	AN: 4601		122
Sirt1	NM_001159589.2	F: ACAATTCCTCCACCTGAG	R: GTAACCTCACAGCATCTTCAA	124
Tfam	NM_009360.4	F: TCTTGGGAAGAGCAGATGGC	R: GTCTCCGGATCGTTTCACACT	72
eNOS	NM_008713.4	F: GGTGCAAGGCTGCCAATTT	R: TAACTACCACAGCCGGAGGA	106
Nox2	NM_007807.5	F: CAGAACCAACACTTAACCTT	R: CAACCACACCAGAATGAC	84
Nox4	NM_015760.5	F: TCCCTCCTATGGGCAATGTG	R: TGCACATCAAGCCTGGACAA	177

Prkn (PARKIN)	NM_001317726.1	AN: 724	92
NRF2	NM_010902.4	F: GGACATGGAGCAAGTTTGGC R: CCAGCGAGGAGATCGATGAG	164

6.3.8 SDS-PAGE and immunoblotting – Cell signalling

Total protein and phosphoproteins levels were detected in control and aged C₂C₁₂ myotubes by Western blot (see section 2.13 (Chapter 2) for full details). Following treatment (vehicle control [CTRL] or 5 μM EPI), C₂C₁₂ myotubes were lysed and scraped in ice-cold 1x radioimmunoprecipitation assay (RIPA) buffer containing: 25 mM Tris-HCl pH 7.6, 150 mM NaCl, 1% NP-40, 1% sodium deoxycholate and 0.1% SDS, supplemented with 1x Protease Inhibitor Cocktail Set V (Merck Life Science, UK). Cell lysates were centrifuged for 15 minutes at 18,000 × g (4°C) and the supernatant was stored at -80°C before analysis for total protein. Protein concentrations of samples were determined by the Pierce™ BCA assay (section 2.15, Chapter 2), and samples were subsequently resuspended in 4x Laemmli buffer (Bio-Rad laboratories, Hertfordshire, UK) containing reducing agent (1x working concentration: 31.5 mM Tris-HCl [pH 6.8], 10% glycerol, 1% SDS, 0.005% Bromophenol Blue and 355 mM 2-mercaptoethanol). Samples were loaded (25 μg) and electrophoresed on 10% SDS-stain-free polyacrylamide gels. Semi-dry transfer of proteins to a nitrocellulose membrane was performed using the Trans-Blot® Turbo™ Transfer System. Following blocking for 1-hour in Tris-buffered saline Tween-20 (TBS-T) containing 5% non-fat dried milk (NFDM), membranes were incubated overnight with rabbit anti-phosphorylated or total antibodies: CaMKII, pThr286-CaMKII, AMPKα, pThr172-AMPK, p44/42 MAPK, pThr202/Tyr204-p44/42 MAPK, eNOS and pSer1177-eNOS, at a dilution of 1:500-1:4000 (see Table 6.2; all antibodies were tested at different dilutions for optimisation purposes before the experimental gels were run) in 5% bovine serum albumin (BSA) made up in TBS-T (Cell

Commented [DR436]: Title should indicate what you are measuring not how

Signaling Technology, London, UK). After overnight incubation, the membrane was washed 3 times in TBS-T for 5 minutes and incubated for 1 hour in HRP-conjugated anti-rabbit antibodies (Cell Signaling Technology, London, UK) at dilution of 1:5000-1:10,000, following appropriate optimisation (see Chapter 9, section 9.8-9.11). Proteins were visualised by enhanced chemiluminescence (Thermo Fisher Scientific inc, Waltham, USA) and quantified by densitometry (ChemiDoc™ MP imaging system, Bio-Rad Laboratories, Inc. CA, USA).

Commented [SD437]: Reference optimisation blots here?

Commented [CS438R437]: I think so – either have them in an appendix that you reference, or have them as the first set of blotting results in this chapter – the appendix may be better.

Table 6. 2 List of antibodies and dilutions used

Antibody	Primary Ab Dilution	Secondary Ab Dilution	Company
CaMKII	1:1000	1:5000	Cell Signaling Technology
pThr286-CaMKII	1:500	1:5000	Cell Signaling Technology
AMPK α	1:1000	1:5000	Cell Signaling Technology
pThr172-AMPK	1:1000	1:10,000	Cell Signaling Technology
p44/42 MAPK	1:2000	1:10,000	Cell Signaling Technology
pThr202/Tyr204-p44/42 MAPK	1:4000	1:5,000	Cell Signaling Technology
pSer1177-eNOS	1:500	1:5000	Cell Signaling Technology
eNOS	1:1000	1:5000	Cell Signaling Technology

6.3.9 Statistical analysis

To compare differences in outcome measures between control and aged cells only, independent t-tests were used. For the comparison of replicative ageing and flavonoid dose upon outcome measures, a two-way ANOVA was employed. A three-way ANOVA was used for comparisons of ageing, flavonoid dose and other factors such as time or antimycin A. When main effects and interactions were present, multiple comparisons were performed using Dunnett's or

Sidak's test where appropriate. For within age comparisons, a one-way ANOVA was used.

Data are presented as means \pm SEM, and significance was accepted when $P < 0.05$.

6.4 Results

6.4.1 Mitochondrial bioenergetics of control and aged skeletal muscle myotubes

Having determined the absence of an impact of serial passaging on myoblast mitochondrial bioenergetics (Chapter 5, section 5.4.1) in the absence of exogenous stressors, rates of non-mitochondrial O₂ consumption (Control: 0.15 ± 0.02 vs. Aged: 0.14 ± 0.05 , $P = 0.840$), basal respiration (Control: 0.37 ± 0.03 vs. Aged: 0.33 ± 0.05 pmol/min⁻¹/ng DNA⁻¹, $P = 0.543$), proton leak (Control: 0.07 ± 0.01 vs. Aged: 0.10 ± 0.02 pmol/min⁻¹/ng DNA⁻¹, $P = 0.304$), and ADP phosphorylation (Control: 0.29 ± 0.02 vs. Aged: 0.23 ± 0.03 pmol/min⁻¹/ng DNA⁻¹, $P = 0.183$) were examined and determined to be comparable between control and aged myotubes (see Figure 6.2). By contrast, maximal respiration (Control: 0.93 ± 0.07 vs. Aged: 0.35 ± 0.05 pmol/min⁻¹/ng DNA⁻¹, $P = 0.002$), spare respiratory capacity (Control: 0.56 ± 0.06 vs. Aged: 0.04 ± 0.02 pmol/min⁻¹/ng DNA⁻¹, $P = 0.001$) and coupling efficiency (Control: $79.5 \pm 1.0\%$ vs. Aged: $70.3 \pm 1.4\%$, $P = 0.006$) were all higher in control vs. aged myotubes, suggesting that maximal respiration, spare respiratory capacity and coupling control decline in aged vs control myotubes, but not myoblasts. Together, the data suggest that in aged myotubes, altered metabolic pathways may be required for the provision of energy as a consequence of mitochondrial dysfunction.

Commented [CS439]: No comparisons provided for young blasts vs young tubes and old blasts vs old tubes – have you done any of these analyses? Would it be worth adding e.g. these are the differences in blasts con vs aged) the fusion process causes changes in the parameters examined (or not) within con and aged. As a result of or despite no differences, con vs aged tubes then show x.

Essentially, what is the impact of fusion within the control cells and within the aged cells (blasts vs tubes) and finally are there diffs between con vs aged tubes.

Blasts vs blasts; blasts vs tubes; tubes vs tubes

If this is a huge amount of work, forget I suggested it, but I think it is an important consideration e.g. if the aged blasts are not too different from the control, but the aged tubes are, are they also different to the blasts from which they started....

Commented [SD440R439]: I would like to but this comparison isn't possible due to different normalisation strategies used for blasts and tubes in seahorse. Although I've used DNA content as normaliser, the blasts were initially relative to cell density. When this was converted to DNA content through interpolation of fluorescence from cell density to DNA from a similar assay we had in our lab (in attempt to make comparison blast vs tube), the respiration data was hugely different between blasts and tubes, and I don't trust it (at all) for a comparison between blasts and tubes

Commented [CS441R439]: Thank you.

Commented [DR442]: The lack of finding any difference: could that not be due simply because you have not looked under conditions that you stress the system, like you can ask elderly people to walk and you won't see a difference with youngsters, but don't ask them to run...

Commented [CS443]: This addresses Richard's comment, quite easily, links to the fact you have addressed it in the limitations section already and does not detract the reader from the story. However, r remove, if you are not happy with it here.

Commented [CS444]: So this is where you could first present con blasts vs tubes for these parameters. Then aged blasts vs tubes then the comparison.

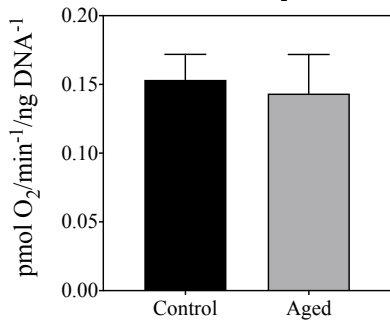
Having determined the absence of an impact of serial passaging on myoblast mitochondrial energetics, the influence of fusion on these processes were examined....

You would need to add the relevant data to each section to pre-empt tube vs tube comparisons – it would just be the text though, as you have the data in graphs already. See what you think.

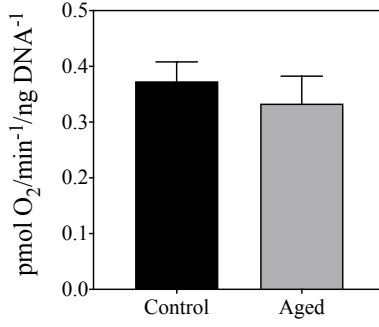
Commented [DR445]: Supports my previous assumption... a system under max stress reveals its real capacity

Commented [CS446]: This may not be the wording you would use, please change as relevant

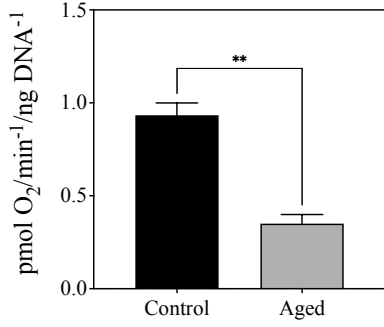
A *Non-mitochondrial O₂ consumption*



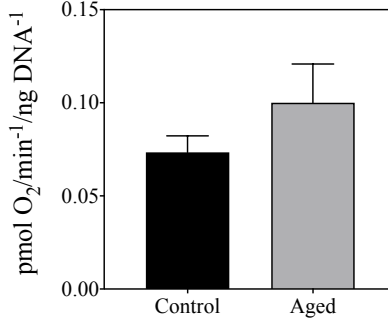
B *Basal Respiration*



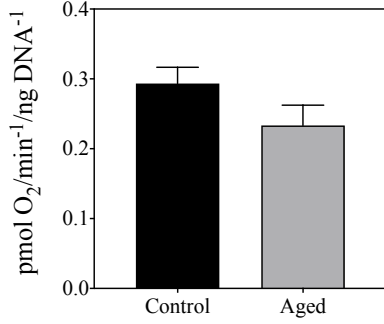
C *Maximal Respiration*



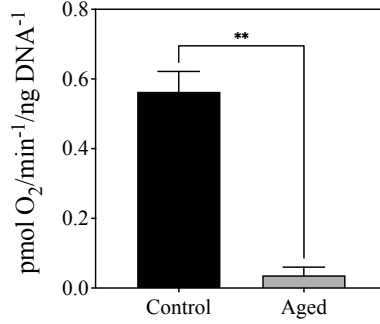
D *Proton leak*



E *ADP Phosphorylation*



F *Spare Respiratory Capacity*



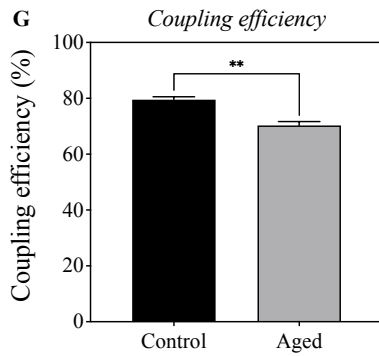


Figure 6. 2 Mitochondrial bioenergetics of control and aged C₂C₁₂ myotubes. A) Non-mitochondrial respiration, B) Basal respiration, C) Maximal respiration, D) Proton leak, E) ADP phosphorylation, F) Spare respiratory capacity G) Coupling efficiency (%). Data are mean±SEM, representative of 3 independent experiments and normalised to DNA content. ***P*<0.01, significance between groups by independent t-test.

6.4.2 Rates of ATP production: Control vs. aged myotubes

After describing differences in mitochondrial function between control and aged myotubes, rates of ATP production in myotubes were subsequently assessed. In contrast to myoblasts (Chapter 5, section 5.4.2), the relative contribution of $J_{ATP_{glyc}}$ (Control: 51.4±3.2 vs. Aged: 68.3±3.4 %) and $J_{ATP_{ox}}$ (Control: 48.6±3.2 vs. Aged: 31.7±3.4 %) to $J_{ATP_{production}}$ were now significantly higher and lower (*P*=0.022), in aged vs. control myotubes, respectively (see Figure 6.3). Overall, aged myotubes had impaired maximal respiratory capacity and reduced coupling efficiency compared to control, in parallel with a greater reliance on glycolysis for the synthesis of ATP.

Commented [CS447]: As comment earlier, add blasts vs. tubes first, then between comparisons.

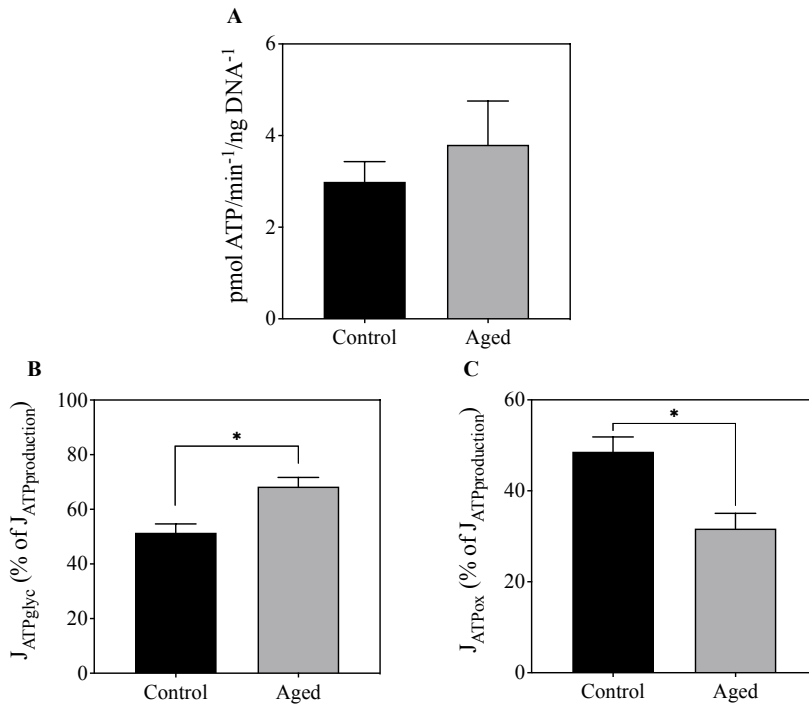


Figure 6.3 ATP production rates of control and aged C₂C₁₂ myotubes. A) Absolute J_{ATPproduction}. B) Relative contribution of J_{ATPglyc} to J_{ATPproduction} and C) Relative contribution of J_{ATPox} to J_{ATPproduction}. Data from 3 independent experiments are presented as mean±SEM and normalised to DNA content. **P*<0.05, significant between groups by independent t-test.

6.4.3 Proton production rates: Control vs. aged myotubes

Following the observation that replicative ageing caused alterations to indices of mitochondrial function, and a shift towards glycolytic ATP production in myotubes, the rate of proton production in control and aged myotubes was determined (see Figure 6.4). Although not statistically significant, rates of proton production were ~64% higher in aged vs. control myotubes (Control: 1.67±0.59 vs. Aged: 2.75±1.43 pmol H⁺/min⁻¹/ng DNA⁻¹, *P*=0.292).

Commented [CS448]: I really like panels B and C, interesting, but nicely complementary finding!

Commented [CS449]: As comment earlier, add blasts vs. tubes first, then between comparisons.

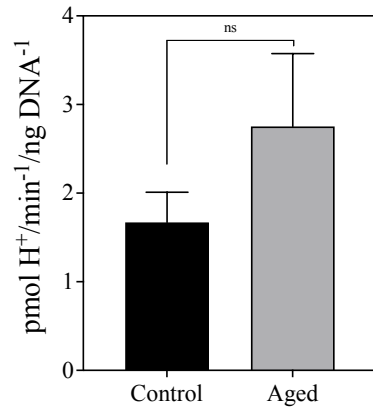


Figure 6. 4 Proton production rates in control and aged C₂C₁₂ myoblasts and myotubes. Data from 3 independent experiments are presented as mean±SEM and normalised to DNA content. Differences between groups determined by independent t-test.

Overall, the mitochondrial respiration data indicate that aged myotubes display hallmarks of mitochondrial dysfunction when compared to control. These age-related impairments to mitochondria are associated with a shift in preference away from oxidative, and towards glycolytic processes for ATP synthesis.

Commented [CS450]: This paper may be useful in the discussion, if not already used:
<https://pubmed.ncbi.nlm.nih.gov/26037248/>

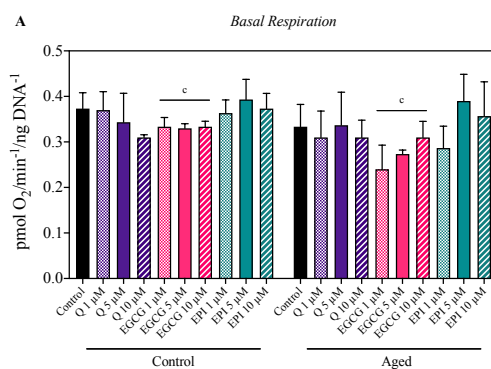
6.4.4 Mitochondrial bioenergetics of control and aged skeletal myotubes: Impact of dietary flavonoids

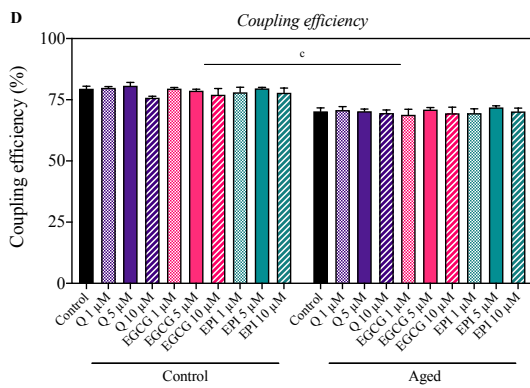
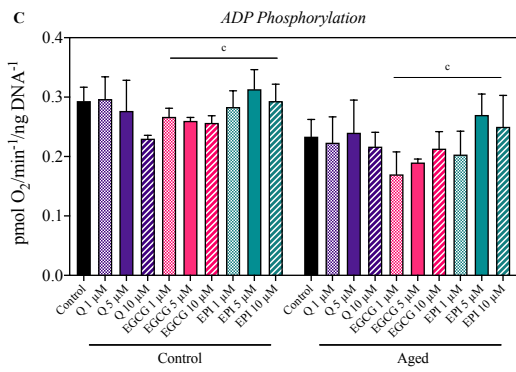
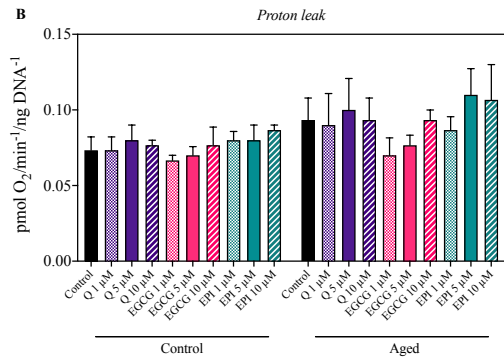
Following the data obtained in myoblasts (Chapter 5), the potential of flavonoids to mitigate age-related impairments to mitochondrial bioenergetics in myotubes was investigated. No main effect of age or dose was determined for non-mitochondrial O₂ consumption in control and aged myotubes (figure not shown). There was no main effect of age or dose on basal respiration in Q and EPI treated myotubes (see Figure 6.5A). Although, a significant main effect of age on

basal respiration in EGCG treated myotubes ($P=0.0352$) was observed. Multiple comparisons revealed that basal respiration was similar between conditions, regardless of the flavonoid studied. There were no main effects of dose or age on proton leak in Q, EGCG or EPI treated myotubes. In Q treated myotubes, there were no main effects of age or dose on ADP phosphorylation. However, there was a significant main effect of age in EGCG and EPI treated myotubes ($P=0.0009$ and $P=0.0463$, respectively). Rates of O_2 consumption linked with ADP phosphorylation were typically lower in aged myotubes compared with control (see Figure 6.5C). There was a significant main effect of age on coupling efficiency in Q, EGCG and EPI treated cells ($P<0.0001$). Multiple comparisons revealed that coupling efficiency was similar between conditions, irrespective of the flavonoid studied. Overall, flavonoids had no detectable impact on mitochondrial bioenergetics in control and aged skeletal myotubes.

Commented [CS451]: Unexpectedly?

Commented [CS452]: So where differences existed unde untreated conditions, these were not changed with flavonoids?





Commented [CS453]: Is it worth adding a few summary lines here re key findings and whether the treatments have added to knowledge vs the basal data initially presented.

Figure 6. 5 Mitochondrial bioenergetics of control and aged skeletal myotubes following 96 h differentiation and 24 h dietary flavonoid treatment. A) Basal respiration, B) Proton leak, C) ADP phosphorylation, D) Coupling efficiency (%). Data representative of 3 independent experiments and are normalised to DNA content and presented as mean±SEM. ° significant main effect of age ($P<0.05$).

6.4.5 Rates of ATP and proton production in skeletal myotubes with flavonoid treatment

After reporting that replicative ageing impaired indices of mitochondrial function that were not rescued by flavonoid treatment, calculations were made to corroborate these data with rates of ATP and proton production, with and without flavonoids. There was a significant effect of age on absolute $J_{ATP_{glyc}}$ production in Q and EGCG treated myotubes ($P=0.022$ and $P=0.015$, respectively), but no main effect of dose was observed for all compounds tested. There was a significant effect of age on absolute rates of $J_{ATP_{ox}}$ production in EGCG myotubes ($P=0.0018$). In relative terms, rates of $J_{ATP_{glyc}}$ production to total ATP were therefore significantly higher overall in aged vs. control myotubes ($P<0.001$). No significant impact of flavonoid treatment was observed on absolute and relative rates of $J_{ATP_{glyc}}$ and $J_{ATP_{ox}}$ production in control and aged myotubes (data not shown). There was a significant main effect of age on rates of proton production ($P<0.05$), though no main effect of dose was found in control and aged myotubes, regardless of the flavonoid investigated (data not shown). Similar to the negligible impact of flavonoids on mitochondrial respiration, flavonoids had no effect upon rates of ATP production or proton production in myotubes.

6.4.6 Replicative ageing augments the production of mitochondrial reactive oxygen species

Commented [CS454]: Add the actual data also, not just the P values? This may be too complex with multiple doses?

Commented [CS455]: It would be good to have another summary paragraph of key findings before moving to this section, in order to show the links in your findings and the logic in next steps.

Commented [CS456]: Should these outputs come before the gene expression data? It is more biochemical in nature? Not essential, but the links between sections are needed.

Previous findings emphasised flavonoids failed to rescue age-related impairments of mitochondrial respiration in myotubes. To further investigate the potential of flavonoids mode of action, rates of mitochondrial ROS production were examined in the presence and absence of flavonoids. Firstly, rates of mitochondrial ROS production were determined in control and aged myotubes under CTRL conditions (see Figure 6.6). A significant main effect of antimycin A ($P<0.0001$) and age ($P<0.0001$) was found on rates of MitoSOX oxidation, and a significant antimycin A \times age interaction ($P=0.0308$). In the absence of antimycin A, MitoSOX oxidation rates were higher in aged myotubes compared to control (Control: $2.4 \times 10^{-5} \pm 0.4 \times 10^{-5}$ vs. Aged: $9.7 \times 10^{-5} \pm 1.6 \times 10^{-5}$ RFU/sec⁻¹/cell⁻¹; $P=0.035$). Likewise, aged myotubes demonstrated greater rates of MitoSOX oxidation compared to control when cultured in the presence of antimycin A (Control +AA: $15.7 \times 10^{-5} \pm 4.1 \times 10^{-5}$ vs. Aged +AA: $31.0 \times 10^{-5} \pm 2.9 \times 10^{-5}$ RFU/sec⁻¹/cell⁻¹; $P<0.0001$).

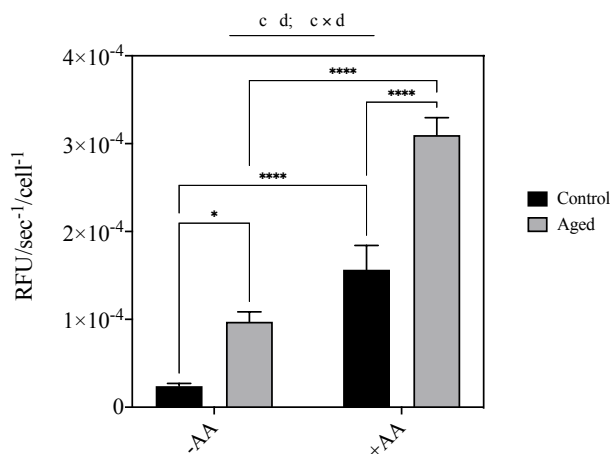


Figure 6. 6 Replicative ageing increases the rate of mitochondrial ROS production in skeletal muscle cells. MitoSOX oxidation rates were determined in control and replicatively aged skeletal myotubes in the absence or presence of antimycin A. Cells were incubated with or without antimycin A for 30 minutes, prior to the immediate loading of MitoSOX (2.5 μ M final concentration). Rates of MitoSOX oxidation were immediately measured in 30 second

Commented [CS457]: Ok, so no flavonoid data in this section. Maybe simply change the intro to this section to not focus on flavonoids and then the title can remain unchanged

intervals over 30 minutes. Data are means \pm SEM of three independent repeats with twelve replicates per condition. Statistical significance of mean differences was tested for by two-way ANOVA and adjusted for multiple comparisons: ^c main effect of age ($P < 0.05$); ^d main effect of Antimycin A ($P < 0.05$); * $P < 0.05$, ** $P < 0.01$, *** $P < 0.001$ and **** $P < 0.0001$.

6.4.7 Quercetin does not attenuate antimycin A-induced mitochondrial ROS in control and aged myotubes

Having reported that ageing increases the rate of mitochondrial ROS production in myotubes, the impact of acute flavonoid treatment on mitochondrial ROS production was determined. Firstly, Q's effect upon MitoSOX oxidation was investigated. There was a significant main effect of antimycin A on rates of MitoSOX oxidation ($P < 0.0001$), and a significant dose \times age \times antimycin A interaction ($P = 0.014$). Post-hoc tests revealed that Q treatment did not impact MitoSOX oxidation in myotubes cultured in the absence of antimycin A (see Figure 6.7). Although, rates of MitoSOX oxidation were significantly higher in control myotubes cultured in the presence of antimycin A and 10 μ M Q compared to antimycin A alone (CTRL: $15.7 \times 10^{-5} \pm 4.1 \times 10^{-5}$ vs. 10 μ M Q: $46.1 \times 10^{-5} \pm 11.7 \times 10^{-5}$ RFU/sec⁻¹/cell⁻¹; $P = 0.0363$). Therefore, Q may act in a pro-oxidant manner in control myotubes.

Commented [CS458]: Why do you detail the impacts of the flavonoids independently here, but grouped together in the previous sections?

Commented [CS459]: And so? 1 liner to conclude and lead to next flavonoid

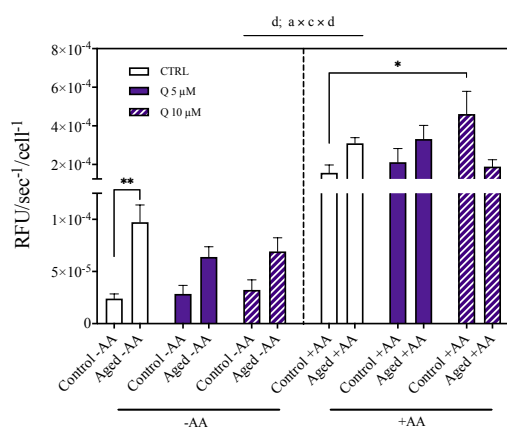


Figure 6. 7 Quercetin supplementation increases the rate of mitochondrial ROS production in control skeletal muscle cells. MitoSOX oxidation rates were determined in control and replicatively aged skeletal myotubes in the absence of presence of dietary flavonoids. Cells were treated with 0, 5 and 10 μM Q for 24 h. After 24 h, antimycin A was added to cells for 30 minutes, before 2.5 μM MitoSOX was loaded into cells in KRB. Rates of MitoSOX oxidation were measured in 30 second intervals over 30 minutes. Data are means \pm SEM of three independent repeats with two replicates per treatment. Statistical significance of mean differences was tested for by two-way ANOVA: ^a Significant main effect of dose; ^c Significant main effect of age; ^d Significant main effect of AA.

6.4.8 EGCG does not impact mitochondrial ROS production in control or aged myotubes

In EGCG treated myotubes, there was a significant main effect of age ($P < 0.0001$) and antimycin A ($P < 0.0001$) on rates of MitoSOX oxidation. Post-hoc tests revealed that MitoSOX oxidation rates were similar between conditions in control and aged myotubes (see Figure 6.8), suggesting no role for EGCG in modulating mitochondrial ROS emission.

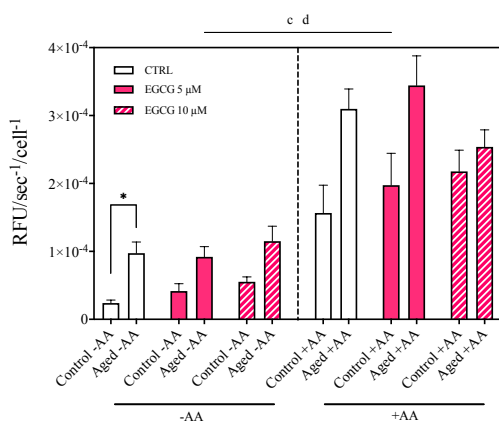


Figure 6. 8 EGCG supplementation does not impact the rate of mitochondrial ROS production in control or aged skeletal muscle cells. MitoSOX oxidation rates were determined in control and replicatively aged skeletal myotubes in the absence of presence of dietary flavonoids. Cells were treated with 0, 5 and 10 μM EGCG for 24 h. After 24 h, antimycin A was added to cells for 30 minutes, before 2.5 μM MitoSOX was loaded into cells in KRB. Rates of MitoSOX oxidation were measured in 30 second intervals over 30 minutes. Data are means \pm SEM of three independent repeats with two replicates per treatment. Statistical significance of mean differences was tested for by two-way ANOVA: ^c Significant main effect of age; ^d Significant main effect of AA.

6.4.9 EPI does not attenuate age-related increases in mitochondrial ROS production

There was a significant main effect of dose ($P=0.041$), age ($P<0.0001$) and antimycin A ($P<0.0001$) on rates of MitoSOX oxidation in EPI treated cells, and a significant dose \times age \times antimycin A interaction ($P=0.042$). Post-hoc tests revealed that 10 μM EPI treatment increased the rate of MitoSOX oxidation compared to CTRL in control myotubes cultured with antimycin A (CTRL: $15.7 \times 10^{-5} \pm 4.1 \times 10^{-5}$ vs. 10 μM EPI: $32.3 \times 10^{-5} \pm 6.0 \times 10^{-5}$ RFU/sec⁻¹/cell⁻¹; $P=0.043$). However, rates of MitoSOX oxidation were similar between treatment conditions in aged myotubes (see Figure 6.9) At 10 μM , EPI may act in a pro-oxidant manner in control myotubes.

Commented [CS460]: See comment above

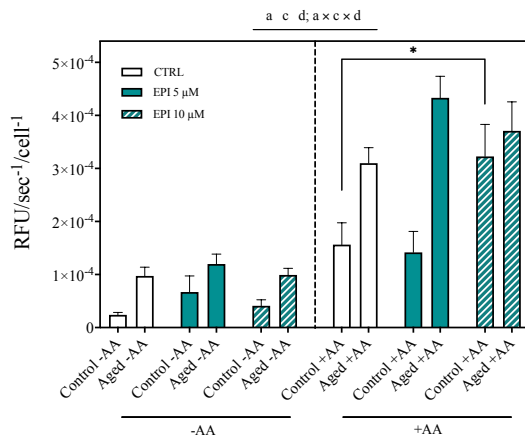


Figure 6. 9 EPI supplementation does not impact the rate of mitochondrial ROS production in control or aged skeletal muscle cells. MitoSOX oxidation rates were determined in control and replicatively aged skeletal myotubes in the absence of presence of dietary flavonoids. Cells were treated with 0, 5 and 10 μM EPI for 24 h. After 24 h, antimycin A was added to cells for 30 minutes, before 2.5 μM MitoSOX was loaded into cells in KRB. Rates of MitoSOX oxidation were measured in 30 second intervals over 30 minutes. Data are means \pm SEM of three independent repeats with two replicates per treatment. Statistical significance of mean differences was tested for by two-way ANOVA: ^a Significant main effect of dose; ^c Significant main effect of age; ^d Significant main effect of AA.

6.4.10 No role for dietary flavonoids in mitigating age-related increases in cellular ROS

Having ascertained a non-apparent role for flavonoids in regulating mitochondrial-specific ROS production, the effects of ageing and flavonoid treatment on general cellular ROS production (not specific to mitochondria) was studied. Under CTRL conditions, there was a significant main effect of age ($P=0.003$), but not antimycin A ($P=0.752$). Replicative ageing significantly increased CellROX oxidation when compared to control (Control: 7.8 ± 0.8 vs. Aged: 12.1 ± 1.5 RFU/cell⁻¹; $P=0.0226$). The presence of antimycin A did not significantly increase CellROX oxidation in control or aged skeletal muscle cells (see Figure 6.10),

Commented [SD461]: Do I add these control comparisons to the start of the chapter along with Seahorse data? Not sure because ROS work was only done in myotubes, not myoblasts

Commented [CS462R461]: It would have been good to have earlier, but as you do not have these data for blasts, I would leave it here.

providing evidence that CellROX oxidation primarily represents cytosolic, as opposed to mitochondrial derived ROS.

Commented [CS463]: nice

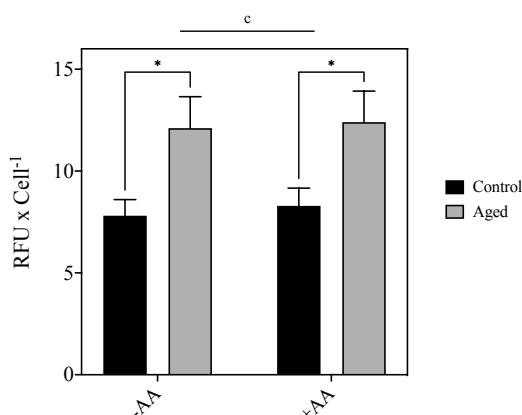


Figure 6. 10 Replicative ageing increases ROS production in skeletal muscle cells. CellROX oxidation was measured in control and replicatively aged skeletal myotubes in the absence of presence of antimycin A. Cells were incubated with or without antimycin A for 30 minutes, prior to the loading of CellROX (2.5 μ M final concentration) for 30 minutes. Rates of CellROX oxidation were subsequently measured at 640/665 nm (Ex/Em) in a plate reader. The gain was kept constant between independent experiments. Data are means \pm SEM of three independent repeats with two replicates per condition. Statistical significance was determined by a two-way ANOVA with age and antimycin A as factors. Multiple comparisons were corrected for using Sidak's test. ^c main effect of age ($P < 0.05$). * $P < 0.05$.

Next, the effects of acute flavonoid treatment on CellROX oxidation (with and without antimycin A) were determined. A significant main effect of age was observed on CellROX oxidation in the presence of Q, EGCG and EPI ($P < 0.0001$). Multiple comparisons revealed no impact of Q, EGCG or EPI treatment on CellROX oxidation in both control and aged skeletal muscle cells (see Figure 6.11). Collectively, replicative ageing augments the production of cellular and mitochondrial-specific ROS emission, which is not rescued by flavonoid treatment.

Commented [CS464]: Nice.

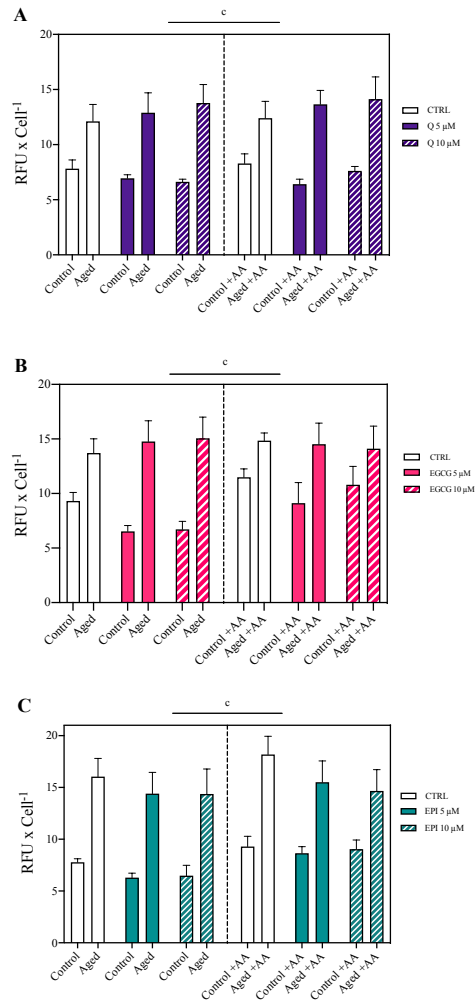


Figure 6. 11 Dietary flavonoids do not regulate ROS production in control and aged skeletal muscle cells. CellROX oxidation was determined in control and replicatively aged skeletal myotubes in the absence of presence of Q, EPI or EGCG. Cells were treated over 24 h with 0, 5 and 10 μM Q, EPI or EGC. After 24 h, cells were incubated with or without antimycin A for 30 minutes, before CellROX was loaded into cells (2.5 μM final concentration). CellROX oxidation was measured at 640/665 nm (Ex/Em) in a plate reader and normalised to cell density. A) Q treated; B) EPI treated and C) EGCG treated. Data are means \pm SEM of three

independent repeats with two replicates per treatment. Statistical significance was tested for by a three-way ANOVA, with dose, age and antimycin A as factors: ° main effect of age ($P<0.05$).

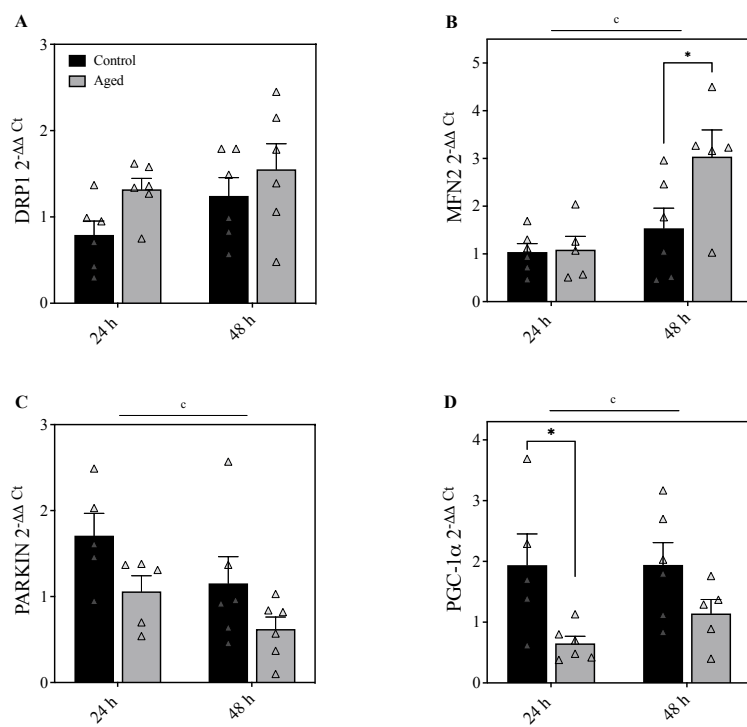
6.4.11 Flavonoids differentially modulate gene expression of control and aged skeletal myotubes

Having ascertained that replicative ageing comprises mitochondrial function and increases ROS production in myotubes, further experiments were performed. To gain more knowledge of the molecular regulation of mitochondrial function and ROS production in control and aged myotubes (in the absence and presence of flavonoids), the expression of relevant genes was determined (see Table 9.1 Chapter 9 for description of genes studied and their known function and section 1.27, Chapter 1).

To establish whether replicative ageing changes the expression of genes associated with mitochondrial remodelling, comparisons were made between control and aged myotubes under CTRL conditions. There was no significant main effect of age or time on DRP1 expression in myotubes (see Figure 6.12). A significant main effect of time ($P=0.005$) was found on MFN2 expression in myotubes. Multiple comparisons revealed MFN2 expression was 2-fold higher in aged myotubes over 48 h versus control ($P=0.024$). Although there was a main effect of age ($P=0.045$) found on PARKIN expression in myotubes, multiple comparisons revealed that no significant differences in PARKIN expression were found between control and aged myotubes, regardless of the timepoint. A significant main effect of age ($P=0.015$) was found on PGC-1 α expression in myotubes, and PGC-1 α expression was 3-fold higher in control myotubes over 24 h ($P=0.027$). There was a significant main effect of age on SIRT1 expression in myotubes ($P=0.006$). Over 48 h, SIRT1 expression was 2.1-fold higher in aged myotubes versus control

Commented [CS465]: Does this contradict itself?

($P=0.003$). A main effect of age was found on TFAM expression in myotubes ($P=0.012$). TFAM expression was 2.1-fold higher in aged myotubes compared with control ($P=0.013$). Under basal CTRL conditions, aged myotubes may have reduced capacity for mitochondrial biogenesis.



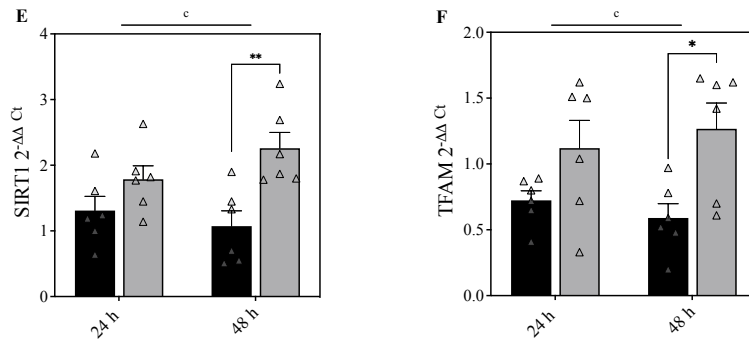
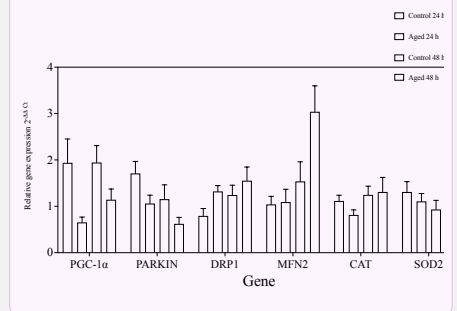


Figure 6. 12 Expression of genes associated with mitochondrial remodelling in control and aged skeletal muscle myotubes under CTRL conditions. C₂C₁₂ myotubes were lysed over 72-120 h for analysis of gene expression. A) DRP1, B) MFN2, C) PARKIN, D) PGC-1 α , E) SIRT1 and F) TFAM. Data are means \pm SEM from 3 independent experiments run in duplicate. Statistical significance was determined by a two-way ANOVA, with age and time as factors. Multiple comparisons performed by Sidak's test to determine differences in gene expression between ages within each time point. ^c main effect of age. * P <0.05 and ** P <0.01. Control and aged myotubes are denoted by solid black and grey bars, respectively.

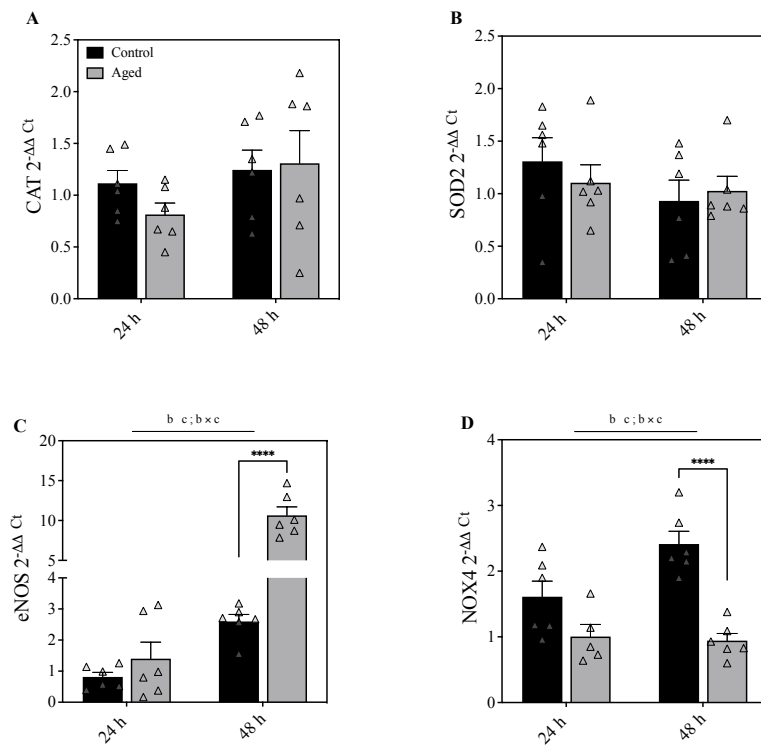
Commented [SD466]: Considering combining all grpahs these into a single figure to make for easier viewing, just not 100% sure e.g. like this



After determining the expression of genes associated with mitochondrial remodelling between control and aged myotubes under CTRL conditions, genes associated with the antioxidant response were compared. There was no significant main effect of age or time on CAT and SOD2 expression in myotubes (see Figure 6.13A/B). A significant main effect of age ($P=0.0001$) and time ($P<0.0001$) was found on eNOS expression in myotubes, and an age \times time interaction ($P<0.0001$). Multiple comparisons revealed eNOS expression was 4.1-fold higher in aged myotubes over 48 h versus control ($P<0.0001$). There was a main effect of age ($P=0.0006$) and time ($P=0.047$) for NOX4 expression in myotubes, and an age \times time interaction ($P=0.025$). NOX4 expression increased 2.6-fold over 48 h in control myotubes versus aged ($P<0.0001$). A main effect of age ($P=0.049$) and time ($P=0.048$) was found on

NRF2 expression in myotubes see (Figure 6.13E), as well as an age \times time interaction ($P=0.0006$). NRF2 expression was increased 2.8-fold in control versus aged myotubes over 48 h ($P=0.0006$). Under basal CTRL conditions, aged myotube mRNA responses are indicative of reduced NO bioavailability and lowered induction of ROS sensitive transcripts.

Commented [CS467]: Again and so? What are the potential implications of these findings from a cellular perspective. Add a line or two to summarise.



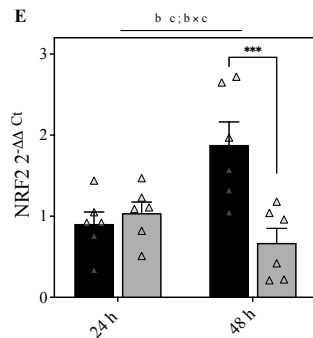


Figure 6. 13 Expression of genes associated with the antioxidant response in control and aged skeletal muscle myotubes under CTRL conditions. C₂C₁₂ myotubes were lysed over 72-120 h for analysis of gene expression. A) CAT, B) SOD2, C) eNOS, D) NOX4 and E) NRF2. Data are means±SEM from 3 independent experiments run in duplicate. Statistical significance was determined by a two-way ANOVA, with age and time as factors. Multiple comparisons performed by Sidak's test to determine differences in gene expression between ages within each time point. ^b main effect of time; ^c main effect of age. ****P*<0.001 and *****P*<0.0001. Control and aged myotubes are denoted by solid black and grey bars, respectively.

6.4.12 Summary of replicative ageing's impact upon gene expression in control and aged myotubes

Overall, aged myotubes presented higher fold changes of MFN2, SIRT1 and TFAM mRNA over 48 h when compared with control. However, aged myotubes also had reduced PGC-1α expression versus control, although basal PGC-1α expression was higher in aged vs. control myotubes. In addition, aged myotubes presented lower levels of NOX4 and NRF2 over 48 h, suggesting reduced stress compared with control. Aged myotubes may fail to instigate mitochondrial biogenesis due to lowered PGC-1α and NRF2 expression.

Commented [CS468]: TFAM lower CAT, SOD, MFN2 and PGC-1α higher in aged vs control - based on the table of data you referencing the graphical data. I think this expression is not really high for this study, although interesting.

Commented [CS469]: good

6.4.13 Mitochondrial-related gene expression following Quercetin treatment in skeletal myotubes

Once the effects of replicative ageing upon myotube gene expression were defined, the expression of genes associated with mitochondrial function and remodelling were quantified with and without dietary flavonoids. These genes were investigated to help consolidate the mitochondrial bioenergetic data. There was a significant main effect of age on DRP1 expression in Q treated cells ($P=0.0002$). Post-hoc comparisons revealed DRP1 expression was 2.6-fold lower at 48 h following 5 μM Q in control myotubes ($P=0.0054$). There was a significant main effect of dose ($P=0.0358$) on MFN2 expression, and a dose \times time interaction ($P=0.0391$) in Q treated myotubes. Multiple comparisons revealed no significant effect of Q treatment on MFN2 in control myotubes (see Figure 6.14B). Yet, in aged myotubes, 5 and 10 μM Q lowered MFN2 expression at 48 h compared to CTRL (4.3-fold, $P=0.0021$; 3.8-fold, $P=0.0027$, respectively). There was a significant main effect of age ($P<0.0001$) on PARKIN expression in Q treated myotubes, and a significant dose \times time interaction ($P=0.0085$). Multiple comparisons revealed no impact of Q on PARKIN expression in control and aged myotubes. There was a significant main effect of age ($P<0.0001$) on PGC-1 α expression in Q treated myotubes. However, multiple comparisons revealed that PGC-1 α expression was similar between conditions in control and aged myotubes (see Figure 6.14D). Regarding SIRT1 expression, there was a significant main effect of age in Q treated cells ($P<0.001$). Multiple comparisons revealed that SIRT1 expression was similar between conditions in control myotubes (see Figure 6.14E). There was a significant main effect of age on TFAM expression in Q treated myotubes ($P<0.0001$). Compared to CTRL, TFAM expression was 1.7-fold lower over 24 h in control myotubes with 10 μM Q ($P=0.0177$). However, TFAM expression was similar between conditions in aged myotubes. Overall, Q attenuated the expression of genes associated with mitochondrial remodelling, including MFN2, DRP1 and TFAM.

Commented [CS470]: nice

6.4.14 Mitochondrial-related gene expression following EGCG treatment in skeletal myotubes

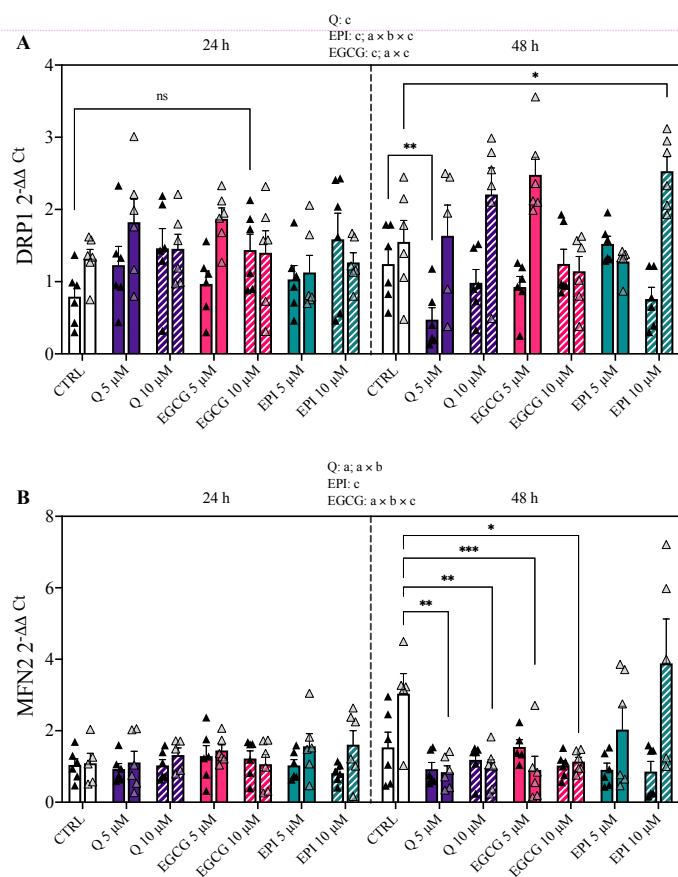
In EGCG treated cells there was a significant main effect of age on DRP1 expression ($P=0.001$), and a dose \times age interaction ($P=0.002$). Over 24 h of 10 μM EGCG treatment, there was a trend towards increased DRP1 expression in control myotubes (1.8-fold, $P=0.0575$), although this did not reach statistical significance. In EGCG treated cells, there was a significant dose \times time \times age interaction ($P=0.033$) for MFN2 expression. Multiple comparisons revealed no significant effect of EGCG treatment on MFN2 in control myotubes (see Figure 6.14B). Over 48 h, 5 and 10 μM EGCG lowered MFN2 expression 4-fold and 3.2-fold versus CTRL conditions in aged myotubes ($P=0.0006$ and $P=0.032$, respectively). In EGCG treated cells, a significant main effect of age ($P=0.0006$) on PARKIN was found, in addition to a significant dose \times time ($P=0.004$), and time \times age interaction ($P=0.046$). In control myotubes, PARKIN expression was decreased 2.4-fold over 24 h by 10 μM EGCG treatment ($P=0.021$; see Figure 6.14C). No differences in PARKIN expression were found between conditions in aged myotubes. In EGCG treated cells, a significant main effect of age ($P=0.0010$) was found on PGC-1 α , as well as a significant dose \times time ($P=0.0109$) and time \times age interaction ($P=0.025$). Post-hoc tests unveiled that PGC-1 α expression was 2.6-fold lower at 48 h in control myotubes after 10 μM EGCG compared to CTRL ($P=0.002$). Regarding SIRT1 expression, there was a significant main effect of age in EGCG treated cells ($P<0.001$). Further, there was a significant dose \times age interaction in EGCG treated cells ($P=0.012$). Multiple comparisons revealed that SIRT1 expression was similar between conditions in control myotubes (see Figure 6.14E). In aged myotubes, however, SIRT1 expression was significantly increased by 10 μM EGCG treatment over 48 h when compared to CTRL (1.7-fold, $P=0.026$). There was a significant main effect of age on TFAM expression in EGCG

treated myotubes ($P < 0.0001$). However, TFAM expression was similar between conditions in control and aged myotubes (see Figure 6.14D). Together, ECGG tended to attenuate the expression of genes associated with mitochondrial biogenesis (PGC-1 α) and degradation (PARKIN) in myotubes.

6.4.15 Mitochondrial-related gene expression following EPI treatment in skeletal myotubes

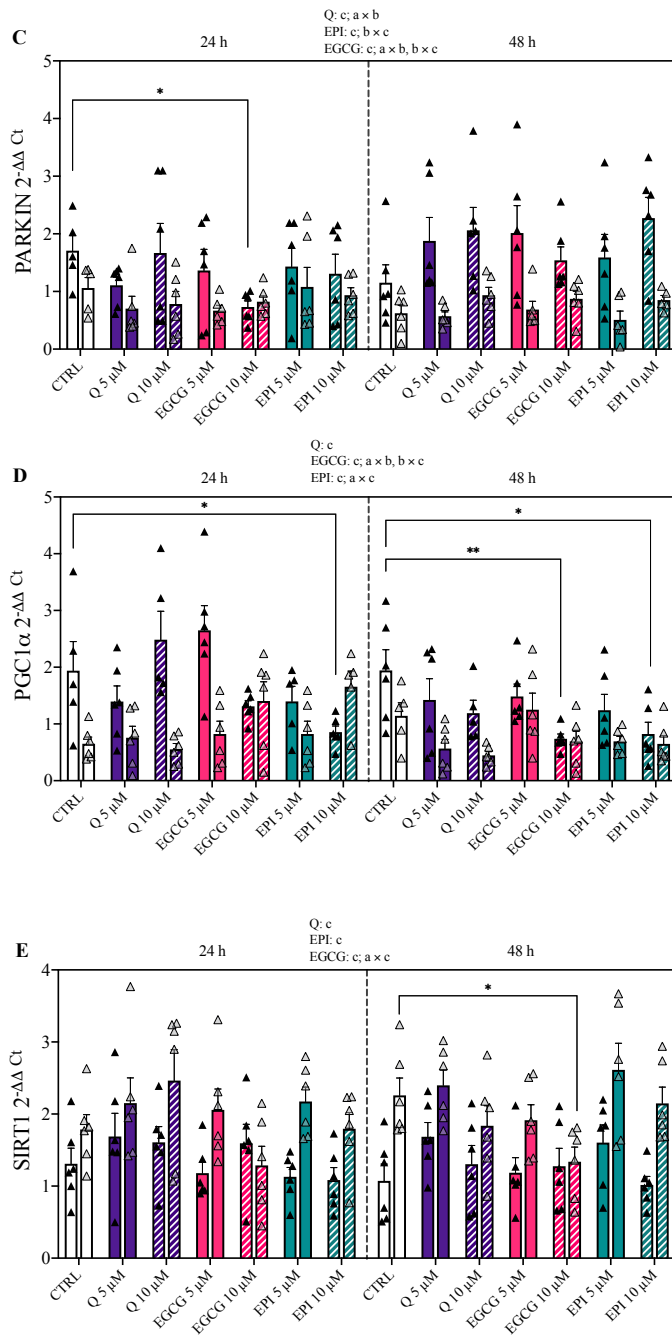
There was a significant effect of age ($P = 0.0037$), and a dose \times time \times age interaction in EPI treated myotubes ($P = 0.0015$). In aged myotubes, 10 μ M EPI increased DRP1 expression 1.6-fold over CTRL at 48 h ($P = 0.0147$), with no effect found in control myotubes (see Figure 6.14A). There was a main effect of age on MFN2 expression in EPI treated cells ($P = 0.0020$). Multiple comparisons revealed no significant effect of EPI treatment on MFN2 in control and aged myotubes (see Figure 6.14B). There was a main effect of age ($P = 0.0005$) on PARKIN expression in EPI treated cells, and a time \times age interaction ($P = 0.0370$). PARKIN expression was similar between conditions in control and aged myotubes dosed with EPI (see Figure 6.14C). There was a main effect of age ($P = 0.0013$) on PGC-1 α expression in EPI treated cells, and a significant dose \times age interaction ($P = 0.0298$). In control myotubes, PGC-1 α expression was 2.3-fold and 2.4-fold lower at 24 and 48 h following 10 μ M EPI versus CTRL ($P = 0.0265$ and $P = 0.0128$, respectively). PGC-1 α expression was 1.3-fold higher in aged myotubes after 24 h with 5 μ M EPI compared to CTRL ($P = 0.0203$). Likewise, at 48 h PGC-1 α mRNA was 1.6-fold and 1.8-fold lower versus CTRL with 5 and 10 μ M EPI ($P = 0.0352$ and $P = 0.0161$, respectively; see Figure 6.14D). Regarding SIRT1 expression, there was a significant main effect of age in EPI treated cells ($P < 0.001$). Multiple comparisons revealed that SIRT1 expression was similar between conditions in control myotubes (see Figure 6.14E). There was a significant main effect of age on TFAM expression in EPI treated myotubes ($P < 0.0001$). A

significant time \times age interaction ($P=0.009$) was also found in EPI treated myotubes. However, TFAM expression was similar between conditions in control and aged myotubes (see Figure 6.14F). Overall, EPI lowered PGC-1 α expression in aged myotubes only.



Commented [CS471]: You may want to increase the size of these and other similar graphs, which have so much data on them e.g. give them 1/2 a page each.

Commented [SD472R471]: Have increased the size



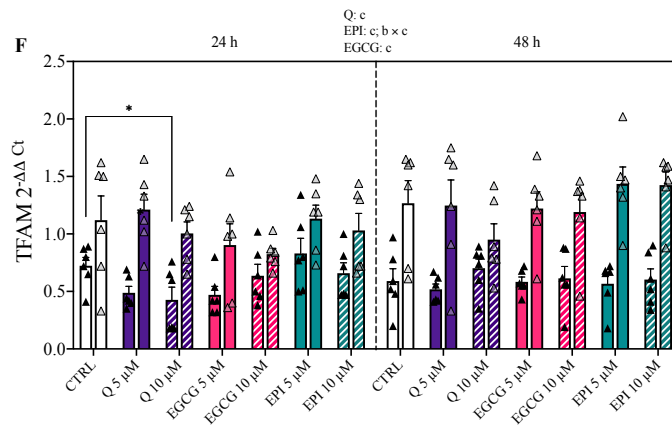


Figure 6. 14 Expression of genes associated with mitochondrial function in control and aged skeletal muscle myotubes following acute dietary flavonoid treatment. Myotubes were treated with 0, 5 and 10 μM Q, EPI or EGCG over 48 h and lysed for analysis of gene expression. A) DRP1, B) MFN2, C) PARKIN, D) PGC-1 α , E) SIRT1 and F) TFAM. Data are means \pm SEM from 3 independent experiments run in duplicate. Statistical significance was determined by a three-way ANOVA, with dose, time and age as factors. Multiple comparisons performed by Dunnett's test, to determine within-age differences in gene expression between experimental conditions. ^a main effect of dose; ^b main effect of time; ^c main effect of age. * P <0.05, ** P <0.01, *** P <0.001, **** P <0.0001. Control and aged myotubes are denoted by solid black and transparent triangles, respectively.

6.4.16 Antioxidant-related transcriptional responses following Quercetin treatment in skeletal myotubes

After describing how flavonoids impact genes linked with mitochondrial remodelling, genes associated with the antioxidant response were examined in the absence and presence of flavonoids. These were investigated to help consolidate ROS production data (see section 6.4.6-6.4.10). There was a significant main effect of dose ($P=0.030$) and age ($P<0.0001$) on catalase expression in Q treated myotubes (see Figure 6.15A). In control myotubes, catalase expression was increased 1.9-fold ($P=0.016$) and 2.1-fold ($P=0.002$) with 5 and 10 μM Q over

Commented [CS473]: Again, add the CT data for the control and aged tubes – as suggested above and then go on to delta delta for untreated, so we know what differences exist in the untreated state and then go onto the impact of flavonoids. Please amend the tube sections for genes as requested above for the blast sections

In an ideal world, you would also compare blasts to tubes in the untreated state, before going to tubes vs tubes but that may be too much to ask?

Commented [CS474]: (Section and subsection)

24 h, respectively. At 48 h, catalase expression increased 1.6-fold versus CTRL in control cells with 10 μ M Q ($P=0.046$). Levels of catalase mRNA in aged myotubes were similar between conditions, irrespective of the flavonoid tested. For SOD2 expression, there was no main effect of dose, time or age in Q treated cells (see Figure 6.15B). Although, SOD2 mRNA levels were similar between treatment groups in control myotubes. There was a significant main effect of dose ($P<0.0001$) and time ($P=0.002$) on eNOS expression in Q treated myotubes, and a significant dose \times age, and time \times age interaction ($P=0.0283$ and $P=0.031$, respectively). At 48 h, eNOS expression in control and aged myotubes was lower with 5 (Control: 3.3-fold; Aged: 19-fold, $P<0.0001$) and 10 μ M Q (Control: 6.2-fold; Aged: 19-fold; $P<0.0001$) versus CTRL (see Figure 6.15C). Regards NOX4 expression, there was a significant main effect of dose ($P=0.025$), time ($P=0.029$) and age ($P<0.0001$) in Q treated cells. Multiple comparisons revealed no difference in NOX4 expression between conditions in control myotubes (see Figure 6.15D). Yet, in aged myotubes, 24 h of 5 μ M Q treatment increased NOX4 expression 1.8-fold versus CTRL ($P=0.041$). In the presence of Q, there was a significant main effect of dose ($P=0.046$) on NRF2 expression (see Figure 6.15E), and a significant dose \times time interaction ($P<0.0001$). In control myotubes, 10 μ M Q increased NRF2 expression 2.1-fold, and decreased NRF2 1.3-fold in aged myotubes, over 24 h and 48 h versus CTRL, respectively ($P=0.002$ and $P=0.044$, respectively). Overall, Q upregulated genes (CAT, NOX4 and NRF2) associated with the antioxidant response in skeletal myotubes.

6.4.17 Antioxidant-related transcriptional responses following ECGG treatment in skeletal myotubes

In ECGG treated cells, there was a main effect of age ($P=0.023$) on catalase expression, though post-hoc tests revealed that catalase expression was similar between conditions in control and aged myotubes (see Figure 6.15A). There was a significant main effect of dose ($P=0.020$) and

time ($P=0.005$) on SOD2 expression in EGCG treated myotubes. Although, SOD2 mRNA levels were similar between treatment groups in control myotubes (see Figure 6.15B). In aged myotubes, SOD2 expression 1.2-fold lower at 48 h with 10 μM EGCG when compared to CTRL ($P=0.002$). In EGCG treated cells, a significant main effect of dose, time and age was found ($P<0.0001$), as well as a significant dose \times time \times age interaction ($P=0.003$). Over 48 h, eNOS expression was significantly lower in control myotubes after 5 and 10 μM EGCG (2.1-fold, $P=0.009$; 3.9-fold, $P<0.0001$). Similarly, eNOS expression was decreased 4.8-fold ($P<0.0001$) and 15-fold ($P<0.0001$) at 48 h in aged myotubes after 5 and 10 μM EGCG treatment, respectively (see Figure 6.15C). There was a main effect of time ($P=0.002$) and age ($P<0.0001$) on NOX4 expression in EGCG treated cells. Multiple comparisons revealed no difference in NOX4 expression between conditions in control and aged myotubes (see Figure 6.15D). In EGCG treated cells, there was a main effect of dose ($P=0.048$) and time ($P<0.0001$) on NRF2 expression. NRF2 mRNA levels were not impacted by ECGG treatment in control myotubes (see Figure 6.15E). In aged myotubes, 48 h EGCG (5 μM) treatment increased NRF2 levels 2-fold compared with CTRL ($P=0.008$). Collectively, EGCG attenuated SOD2 and eNOS expression, whilst increasing NRF2 in aged skeletal myotubes.

Commented [CS475]: And so? Potential cellular impact?

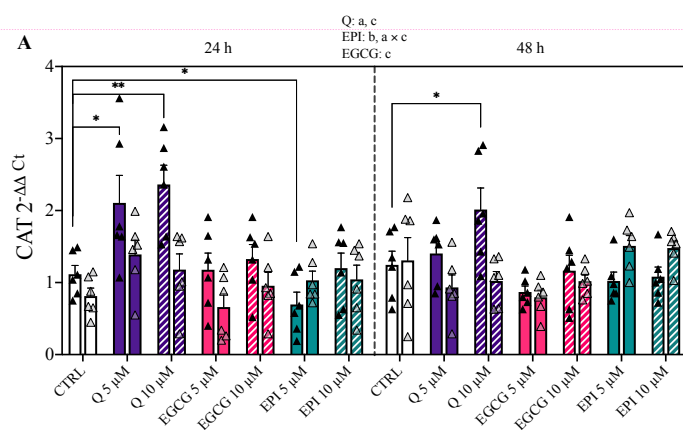
6.4.18 Antioxidant-related transcriptional responses following EPI treatment in skeletal myotubes

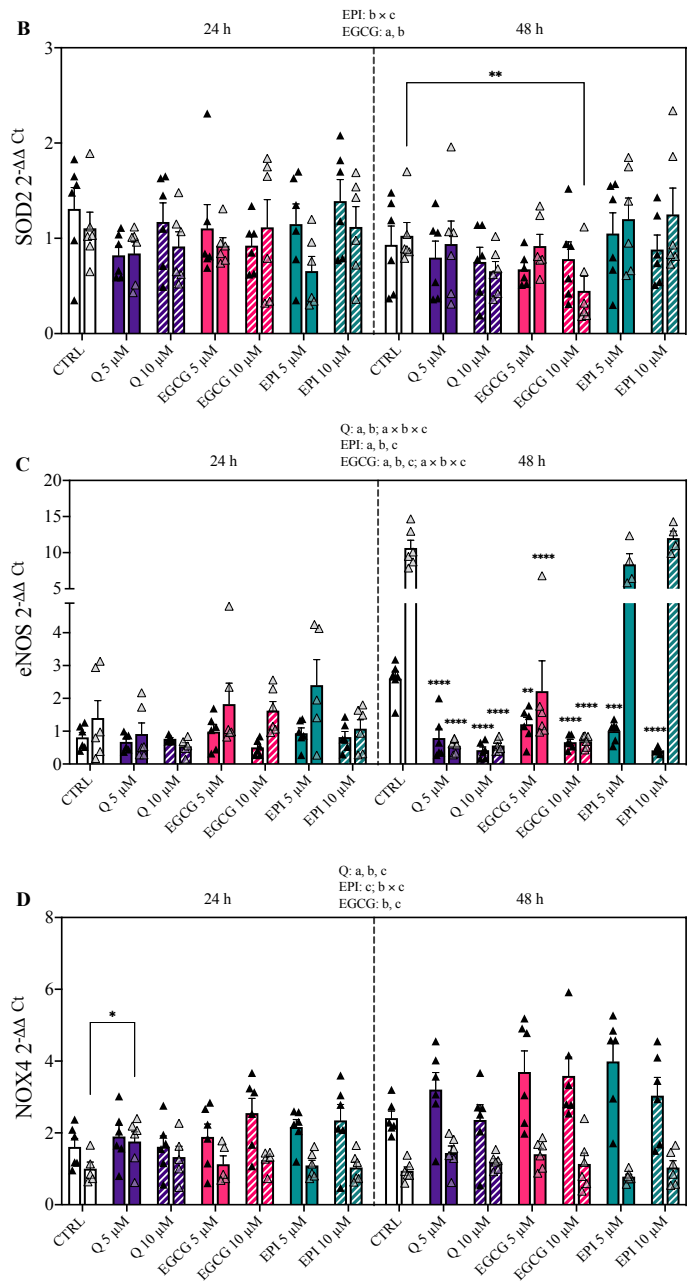
There was a main effect of time ($P=0.0098$) on catalase expression, and a dose \times age interaction ($P=0.039$) in EPI treated cells. Treating control myotubes with 5 μM EPI decreased catalase expression over 24 h versus CTRL (1.6-fold; $P=0.038$). In EPI treated myotubes, there was a significant time \times age interaction ($P=0.030$) on SOD2. Although, SOD2 mRNA levels were similar between treatment groups in control myotubes (see Figure 6.15B). There was a significant effect of dose ($P=0.032$), time ($P<0.0001$) and age ($P<0.0001$) on myotube eNOS

expression in response to EPI. At 48 h in control myotubes, 5 and 10 μ M EPI treatment lowered eNOS expression 2.6-fold ($P=0.001$) and 6.2-fold ($P<0.0001$) compared to untreated CTRL. Whereas eNOS mRNA levels were similar between conditions in aged myotubes (see Figure 6.15C). In EPI treated cells, there was a significant main effect of age ($P<0.001$), and a time \times age interaction ($P=0.015$). Multiple comparisons revealed no difference in NOX4 expression between conditions in control and aged myotubes (see Figure 6.15D). There was a significant effect of dose ($P=0.007$) and time ($P=0.0005$) on NRF2 expression (see Figure 6.15E), and a significant dose \times time interaction in EPI treated myotubes ($P=0.008$). At 24 h, NRF2 expression was \sim 1.8-fold higher in control myotubes after 5 μ M and 10 μ M EPI compared to CTRL ($P=0.022$ and $P=0.029$, respectively). In aged myotubes, 5 μ M EPI treatment over 48 h increased NRF2 levels 1.7-fold versus CTRL ($P=0.012$). Overall, EPI lowered the expression of genes associated with antioxidant activity, whilst concurrently increasing levels of NRF2 mRNA.

Commented [CS476]: And so?

Commented [CS477]: As per previous, increase space assigned to these graphs – e.g. ½ page per graph





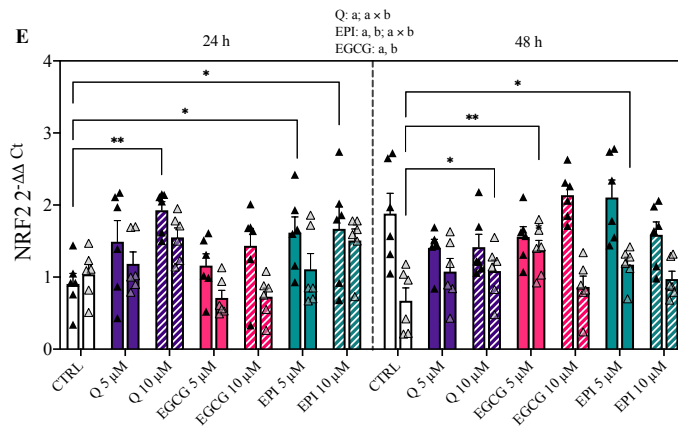


Figure 6. 15 Expression of genes associated with the antioxidant response in control and aged skeletal myotubes following acute dietary flavonoid treatment. Myotubes were treated with 0, 5 and 10 μM Q, EPI or EGCG over 48 h and lysed for analysis of gene expression. A) CAT, B) SOD2, C) eNOS, D) NOX4 and E) NRF2. Data are means \pm SEM from 3 independent experiments run in duplicate. Statistical significance was determined by a three-way ANOVA, with dose, time and age as factors. Multiple comparisons performed by Dunnett's test, to determine within-age differences in gene expression between experimental conditions. ^a main effect of dose; ^b main effect of time; ^c main effect of age. * P <0.05, ** P <0.01, *** P <0.001, **** P <0.0001. Control and aged myotubes are denoted by solid black and transparent triangles, respectively.

6.4.19 Summary of flavonoid effects upon the transcriptional responses of skeletal myotubes

Together, skeletal myotubes cultured in the presence of dietary flavonoids exhibit altered transcriptional profiles that are indicative of mitochondrial remodelling and changes in antioxidant capacity (see Figure 6.16). After Q treatment, genes associated with antioxidant stress were increased, including CAT, NOX4 and NRF2. EGCG attenuated genes associated with mitochondrial biogenesis (PGC-1 α and SIRT1), whilst blunting eNOS expression. Finally, EPI lowered PGC-1 α expression in control myotubes, and simultaneously increased

Commented [DR478]: The fact that you find quite some effects of flavonoids on transcriptional profiles related to mitochondrial remodelling offers you the possibility to present the data in three 'logic' chapters: 1. mitochondrial function in young and aged cells/myotubes; 2. A screening exercise on the transcription profiles: effects of flavonoids; 3. As we have seen effects as described in chapter 2, we decide to measure the effects of flavonoids on mitochondrial function (unfortunately transcription results do not one on one translate in functionality; which is often seen by the way)

NRF2 expression. These findings provide fundamental insight into the potential differential effects of flavonoids on cellular behaviour, basally and under ageing conditions.

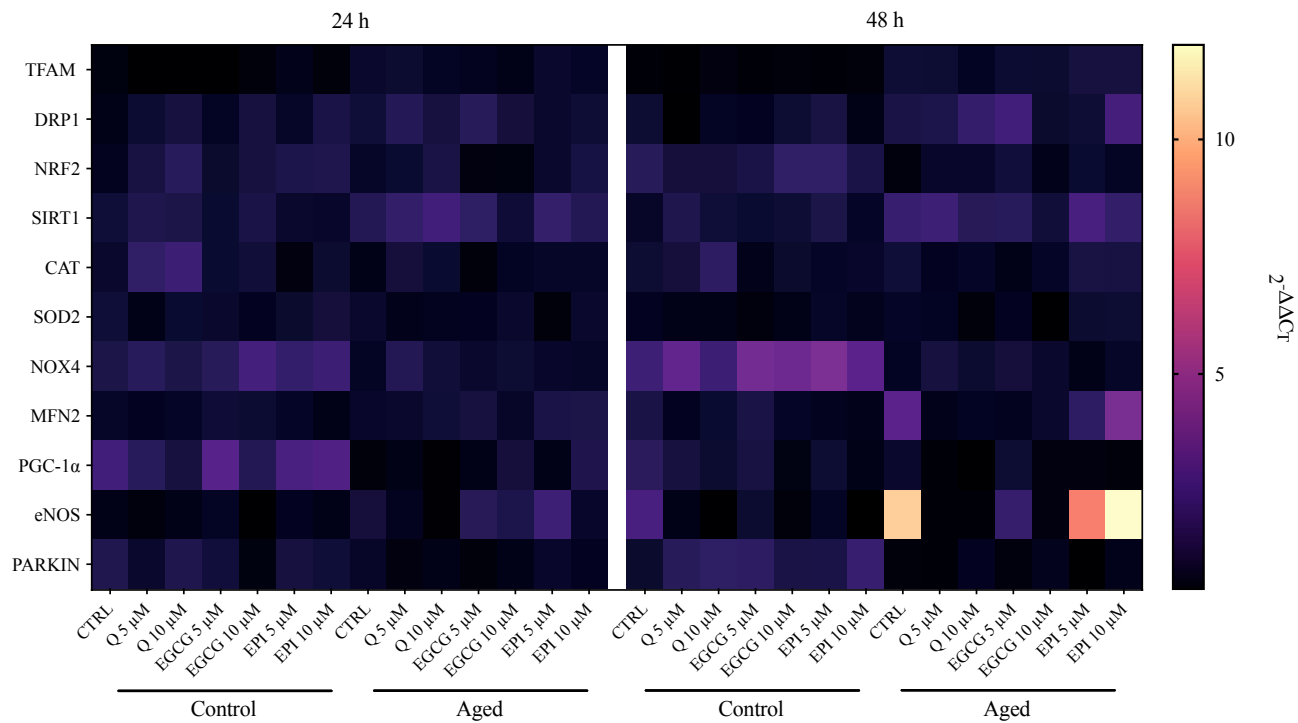


Figure 6. 16 Heatmap representation of myotube mRNA responses in the absence of presence of flavonoids. Fold changes ($2^{-\Delta\Delta CT}$) in gene expression over 48 h presented as heat map.

Commented [CS479]: Again, is this referenced in the text? Were you going to do a second set with eNOS removed to illustrate the other changes more clearly? I think we talked about this but can't remember the conclusion.

Commented [SD480R479]: Have made reference to this in the appendix

6.4.20 The effects of EPI on CaMKII protein content in control and aged myotubes

Having ascertained that EPI may inhibit indices of mitochondrial respiration (in myoblasts) and can augment the expression of NRF2 at the transcriptional level (independent of changes in ROS [emission] in myotubes), further study of EPI's impact on skeletal myotubes was conducted by assessing the canonical AMPK signalling axis. This pathway plays a central role in regulating energy metabolism. First, the potential of EPI to regulate CaMKII activity, a known upstream regulator of AMPK, was investigated. The phosphorylation of CaMKII at Thr286 was not detectable in control and aged muscle cells. There was a significant main effect of age on total CaMKII in skeletal muscle cells ($P < 0.0001$). Multiple comparisons revealed that total CaMKII was similar across time points and between conditions in control and aged cells (see Figure 6.17).

Commented [CS481]: Also in blasts, or in tubes? Please specify

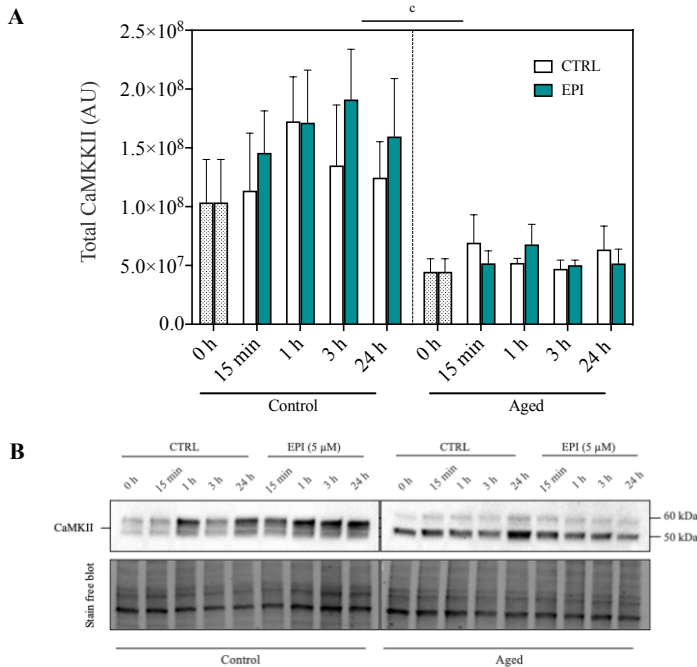


Figure 6. 17 EPI treatment does not impact CaMKII levels in control and aged muscle cells. A) Total CaMKII in control and aged myotubes in the absence (-; clear bars) or presence (+; green bars) of EPI. B) Representative images of n=3 independent experiments and associated stain free blot image. Cell lysates were analysed by SDS-PAGE and western blotting with indicated antibodies. Data are expressed as means \pm SEM; ^c significant main effect of age.

6.4.21 Acute EPI treatment augments AMPK phosphorylation in control and aged myotubes

In control and aged cells treated with EPI, there was a significant main effect of treatment ($P=0.0015$), time ($P=0.0316$) and age ($P<0.0001$), as well as a significant time \times treatment interaction ($P=0.0082$). Multiple comparisons revealed a significant increase in phosphorylation of AMPK at Thr172 at 1 h (1 h: 1.03 ± 0.17 vs. 0 h: 0.54 ± 0.09 AU; $P=0.039$) and 24 h (24 h: 1.11 ± 0.06 vs. 0 h: 0.54 ± 0.09 AU; $P=0.012$), versus 0 h CTRL with EPI in control cells. At 24 h, there was an upward trend in AMPK phosphorylation between CTRL and EPI conditions (CTRL: 0.66 ± 0.15 vs. EPI: 1.11 ± 0.07 AU; $P=0.0524$). In aged cells, post-hoc tests revealed no significant difference in AMPK phosphorylation across time amongst conditions (see Figure 6.18). However, the fold change in AMPK phosphorylation was greater in aged myotubes versus control in the presence of EPI (see Figure 6.18C).

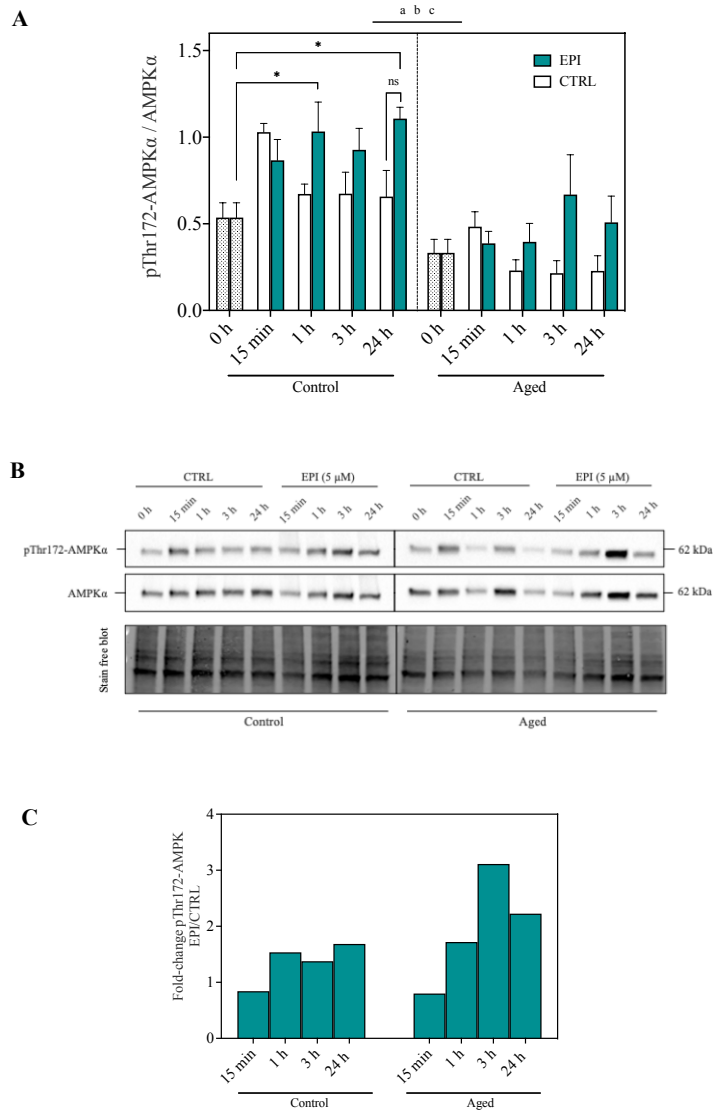


Figure 6. 18 AMPK phosphorylation at Thr172 in control and aged skeletal muscle cells. A) AMPK phosphorylation at Thr172 in control and aged myotubes in the absence (-; clear bars) or presence (+; green bars) of EPI. B) Representative images of n=3 independent experiments

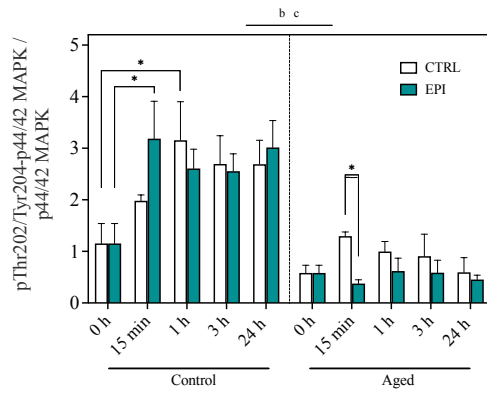
and associated stain free blot image. C) Fold change in AMPK phosphorylation with EPI vs. CTRL condition over 24 h. Cell lysates were analysed by SDS-PAGE and western blotting with indicated antibodies. Data are expressed as means \pm SEM; * P <0.05 compared to 0 h CTRL. ^a significant main effect of treatment; ^b significant main effect of time; ^c significant main effect of age.

6.4.22 EPI does not impact p44/42 MAPK (Erk1/2) phosphorylation in skeletal myotubes

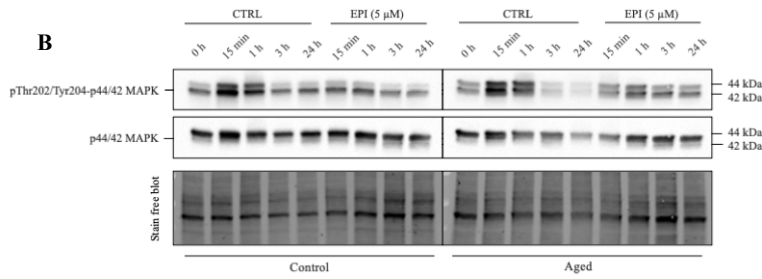
Having described how EPI impacts AMPK activation, the effects of EPI on Erk1/2 phosphorylation were investigated (see Figure 6.19). There was a significant main effect of time ($P=0.0062$), and age ($P<0.0001$) on Erk1/2 phosphorylation, and a time \times age interaction ($P=0.0244$). Post-hoc comparisons revealed Erk1/2 phosphorylation in control cells was significantly increased at 1 hour (0 h: 1.15 ± 0.39 vs. 1 h: 1.98 ± 0.11 AU; $P=0.0375$) and 15 min (0 h: 1.15 ± 0.39 vs. 15 min: 3.12 ± 0.73 AU; $P=0.0341$) versus 0 h under CTRL and EPI conditions, respectively. However, there was no difference in Erk1/2 phosphorylation between CTRL and EPI conditions both at 15 min (CTRL: 1.98 ± 0.11 vs. EPI: 3.19 ± 0.73 AU; $P=0.409$) or 1 h (CTRL: 3.12 ± 0.75 vs. EPI: 2.61 ± 0.38 AU; $P=0.946$). In aged cells, multiple comparisons revealed a significant difference between CTRL and EPI conditions at 15 min (CTRL: 1.30 ± 0.08 vs. EPI: 0.37 ± 0.07 AU; $P=0.020$).

Commented [CS482]: Interesting that all signalling molecules thus far are suppressed basally in ageing – linked to altered metabolism of old vs young shown earlier? Worth mentioning?

A



B



C

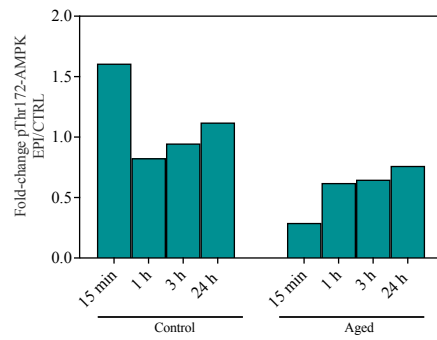


Figure 6. 19 Erk1/2 phosphorylation is not enhanced by EPI in control cells and aged muscle cells. A) ERK1/2 phosphorylation at Thr202/Tyr204 in control and aged myotubes in the absence (-; clear bars) or presence (+; green bars) of EPI. B) Representative images of n=3 independent experiments and associated stain free blot image. C) Fold change in ERK1/2

phosphorylation with EPI vs. CTRL condition over 24 h. Cell lysates were analysed by SDS-PAGE and western blotting with indicated antibodies. Data are expressed as means \pm SEM; * P <0.05 compared to 0 h CTRL. ^b significant main effect of time; ^c significant main effect of age.

6.4.23 EPI treatment does not augment eNOS phosphorylation in control and aged skeletal myotubes

Total eNOS was not detectable under experimental conditions in myotubes (see Chapter 9, Figure 9.4) and therefore pSer1177 eNOS was relativised to total lane protein. There was a significant main effect of age on phosphorylation of eNOS at Ser1177 ($P=0.0002$). Overall, eNOS phosphorylation was increased in aged versus control myotubes (see Figure 6.20). In control muscle cells, eNOS phosphorylation was non-significantly increased at 1 hour (CTRL: $1.96 \times 10^7 \pm 2.68 \times 10^6$ vs. EPI: $1.27 \times 10^7 \pm 1.21 \times 10^6$ AU; $P=0.05$) under CTRL conditions. Multiple comparisons revealed no significant impact of EPI supplementation on eNOS phosphorylation in control or aged muscle cells (Figure 6.20). Increased eNOS phosphorylation at Ser1177 may serve to compensate for reductions in NO bioavailability.

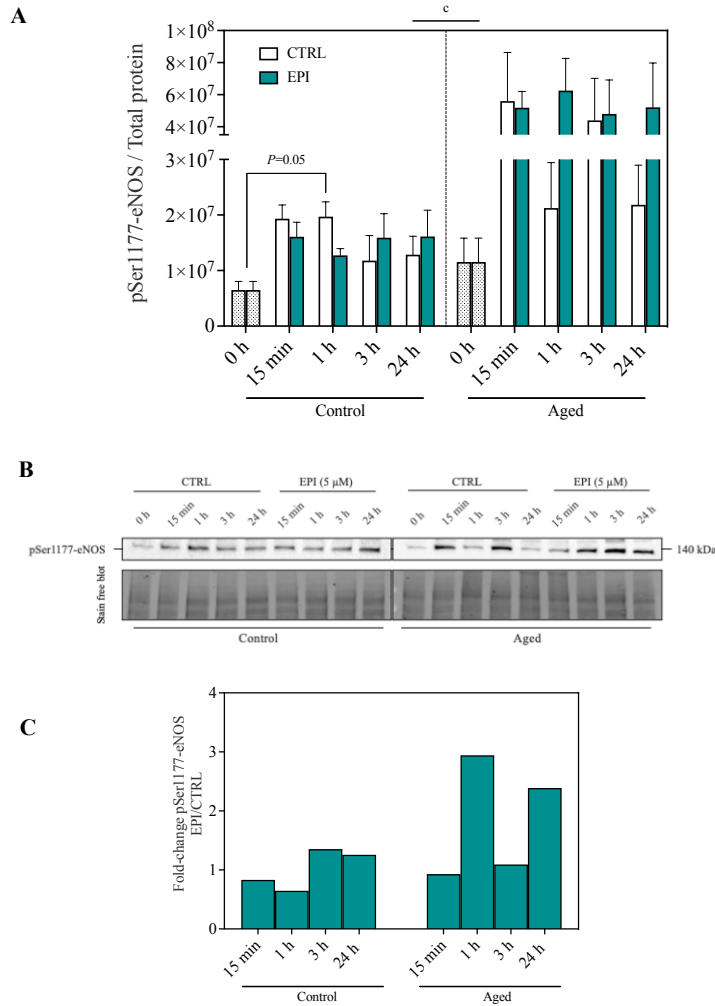


Figure 6. 20 eNOS phosphorylation is not impacted by EPI treatment. A) eNOS phosphorylation at Ser1177 in control and aged myotubes in the absence (-; clear bars) or presence (+; green bars) of EPI. B) Representative images of n=3 independent experiments and associated stain free blot image. C) Fold change in eNOS phosphorylation with EPI vs. CTRL condition over 24 h. Cell lysates were analysed by SDS-PAGE and western blotting with indicated antibodies. Data are expressed as means \pm SEM. ^c significant main effect of age.

Commented [CS483]: Again, this is such a huge section, it is worth having a summary paragraph or picture of the key signalling findings. Do you also need to consider the order of the data? Should the ROS and NO data come first, then the signalling, then the mito and then the genes? Or the f=signalling, then the mito and then the genes? Or the f=signalling, then mito, then genes then ROS and NO or something similar? Eg going from outside to in from biochem to genes or rom inside to out from signalling to changes in mito and genes to cellular responses with NO and ROS.

6.4.24 Summary of the impact of dietary flavonoids upon control and aged skeletal myotubes

In summary, dietary flavonoids have no direct impact on indices of mitochondrial function and ROS emission in control and aged skeletal myotubes. However, flavonoid treatment promotes changes in the transcriptional activity of myotubes that may reflect initiation of mitochondrial remodelling and changes in the cellular redox state. Of note, EPI augments the phosphorylation of AMPK, independent of CaMKII, in skeletal myotubes.

6.5 Discussion

In this chapter, experiments were performed to determine if indices of mitochondrial function, ROS production and cell signalling are affected by replicative ageing, and, whether these measures are impacted by dietary flavonoids. The aim of these experiments was to determine the basal phenotype of control and aged myotubes and to subsequently enhance mitochondrial function, lower ROS production and enhance cell signalling with flavonoid treatment in the myotube model. It was hypothesised that replicative ageing would cause mitochondrial dysfunction, increase ROS production and lower cell signalling, and flavonoid treatment would mitigate these effects. Overall, this chapter demonstrates that replicative ageing impairs indices of mitochondrial function and increases mitochondrial ROS production in myotubes, that are not rescued by flavonoids. Nevertheless, flavonoids evoke distinct effects on transcription, and EPI may afford beneficial adaptations through the induction of NRF2 and AMPK signalling in control and aged myotubes. The data presented advance current knowledge of the mechanisms associated with flavonoids and their purported health benefits in skeletal muscle.

6.5.1 Flavonoids do not rescue age-related impairments to mitochondrial function

Commented [CS484]: In the interests of trying to get this back to you quickly, I have not reread the discussion.

Commented [CS485]: Only skim read the discussion. It is really good, I think.

Commented [CS486]: What about the basal differences you present in con and aged and ED and LD. These data should have aims and hypotheses also.

Remember to also include the aims/objectives and hypotheses at the end of the intro and before methods.

You can accept and or reject them in the discussion.

The main outcome from the current chapter was that replicative ageing elicits impairments to mitochondrial function in cultured myotubes, that are not rescued by dietary flavonoids.

Commented [CS487]: This is nice 0 succinct, yet powerful observation

Advancing age has repeatedly been linked with skeletal muscle mitochondrial dysfunction in rodents and humans (Gospillou et al., 2014c; Porter et al., 2015; Tonkonogi et al., 2003a), although it is thought that reductions in physical activity with older age, and mitochondrial isolation procedures are major confounding factors on measures of mitochondrial function (Conley et al., 2013; Distefano et al., 2018; Gram et al., 2015; Picard et al., 2010a). Using an *in vitro* model of replicative ageing, the findings presented demonstrate that ageing is associated with mitochondrial dysfunction in myotubes, as evidenced by reductions in coupling efficiency and changes in pathways responsible for ATP synthesis (see Figure 6.21). Thus, replicatively aged skeletal myotubes appear to recapitulate features of human skeletal muscle ageing beyond muscle regeneration (Bigot et al., 2008; Sharples et al., 2011b), extending to mitochondrial dysfunction (Marcinek et al., 2005; Porter et al., 2015; Tonkonogi et al., 2003b). One important caveat on the use of replicatively aged cells to mimic metabolic features of human skeletal muscle is the lack of fusion under basal conditions (Sharples et al., 2011b). Therefore, the observed mitochondrial deficits in aged myotubes may reflect a lack of myotube formation, rather than mitochondrial dysfunction *per se*.

Commented [CS488]: Do the blast and tube data within aged differ? If not, then this holds true – if so, then you can counter this argument.

Commented [SD489R488]: Cant directly compare Seahorse data from blasts and tubes due to normalisation differences... could check non-normalised raw values and examine. Needed for defence

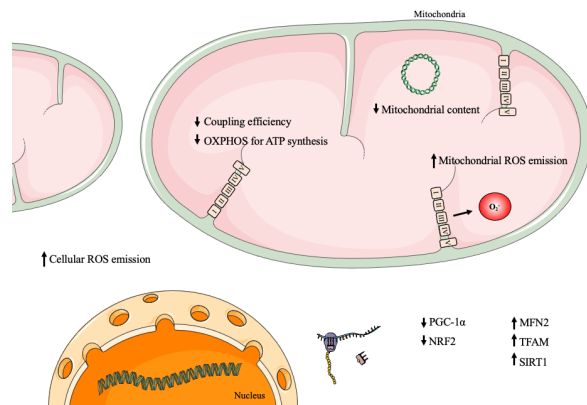


Figure 6. 21 Impact of replicative ageing upon mitochondrial form and function of skeletal myotubes.

Commented [CS490]: So this is essentially old vs control?

In the present study, micromolar concentrations of Q, EGCG and EPI did not impact indices of mitochondrial function. These findings agree with oxygen consumption data from rat brain and heart mitochondria in the presence of Q (Lagoa et al., 2011), but disagree with studies demonstrating blunted state-3 supported respiration in mitochondria dosed with Q (Dorta et al., 2005; Trumbeckaite et al., 2006). Similar to the findings with EGCG, previous studies have reported no change in parameters of mitochondrial function in isolated hepatocytes treated with similar concentrations (10 μ M) of EGCG (Kucera et al., 2015). However, evidence that EGCG increases state 3 respiration in human primary neurons (Castellano-González et al., 2016) and rat cardiomyocytes (Vilella et al., 2020b) has been documented. In line with the negligible effects of EPI on myotube mitochondrial respiration reported here, one study demonstrated analogous concentrations of EPI had no impact upon C₂C₁₂ mitochondrial bioenergetics (Bitner et al., 2018). Moreover, isolated rat heart mitochondria exhibit similar state 3 respiration rates in the presence of EPI when succinate/amytal were used as substrates (Kopustinskiene et al., 2015b). On the other hand, some studies have documented improved mitochondrial respiratory

function with EPI treatment, albeit in rat beta-cells (Kener et al., 2018a; Rowley et al., 2017a). Taken together, it seems that the effects of flavonoids on mitochondrial bioenergetics are highly cell specific. One possible explanation for differences in cell respiratory responses to flavonoids could relate to their potential accumulation within the mitochondrial compartment. Whilst Q and EGCG accumulate within the organelles of T lymphocyte and neuronal cells (Fiorani et al., 2010b; Schroeder et al., 2009) no studies have described whether flavonoids accrue within skeletal muscle mitochondria. Overall, it seems that flavonoids do not alter mitochondrial respiration over the time-course studied.

6.5.2 Flavonoids do not mitigate age-related increases in ROS production

A second key finding of this chapter was that replicative ageing increased ROS production, which was not mitigated by flavonoid treatment. Ageing has been associated with increased H₂O₂ production (Chabi et al., 2008b; Vasilaki et al., 2006) in isolated rodent skeletal muscle mitochondria, and is also linked with elevated ROS emission in human skeletal muscle when physiological concentrations of ADP are employed (Holloway et al., 2018). The present findings support the idea that (cellular) ageing is associated with increased ROS production in skeletal muscle cells. Notably, the data imply that age-related increases in ROS are both mitochondrial and cytosolic in origin. Evidence for this premise comes from studies demonstrating ageing augments the production of ROS from mitochondria (Brand et al., 2013) and from extramitochondrial enzymes such as the NADPH oxidases (Pearson et al., 2014; Sullivan-Gunn & Lewandowski, 2013). Together, these findings provide considerable evidence that replicative ageing augments ROS production in skeletal myotubes.

The antioxidant properties of dietary flavonoids have long been acknowledged, and are owed to hydroxyl substitutions in their molecular structure (Bors et al., 1990; Hodnick et al., 1988;

Silva et al., 2002). Yet, the data presented here suggest that flavonoids do not contribute to the regulation of ROS production in skeletal muscle cells. Previous research has shown that flavonoids including Q, EGCG and EPI exert potent antioxidant effects in multiple tissues, including skeletal muscle, liver and the brain (Bouitbir et al., 2012; Dorta et al., 2008; Meng et al., 2008; Rowley et al., 2017a; Shaki et al., 2017; L. Wang et al., 2016). The inconsistencies between these findings and those presented might be explained by differences in the dose of flavonoids administered, or the time course of treatments. Indeed, many of the studies that have reported antioxidant effects of polyphenols *in vitro* have employed doses that fall within the 10-100 μM range (Sandoval-Acuña et al., 2014), which may not be realistically attained *in vivo*. In addition, the direct scavenging action of flavonoids on ROS is likely to be rapid (Nijveldt et al., 2001), and therefore, measuring ROS production 24 h after flavonoid treatment may have missed any potential acute changes in the emission of ROS in muscle cells. The negligible impact of physiological flavonoid concentrations on myotube ROS production suggests flavonoid treatment may not afford adaptations that contribute to redox regulation in skeletal muscle cells over the time-course studied.

6.6 Flavonoids distinctly alter the expression of genes associated with energy metabolism

Another important finding of the present study was that replicative ageing culminated in changes to the expression of genes associated with energy metabolism. The abundance of MFN2 was acutely upregulated in aged myotubes, which lends support to studies demonstrating an increased ratio of fusion:fission related proteins in ageing skeletal muscle (Joseph et al., 2013b; Leduc-Gaudet et al., 2015; Mercken et al., 2017). Similarly, aged myotubes presented increased abundance of TFAM, which serves to increase the synthesis of OXPHOS subunits. Some (Lezza et al., 2001), but not all (Welle et al., 2003) studies have also

Commented [CS491]: This also relates to the order of data presentation.... It may be easier to explain from outside in or from inside out as suggested above.

Commented [SD492]: How can this be tied in with the PCR data and NRF2 data? Does this mean that time course was too early?

reported increased expression of TFAM in older skeletal muscle tissue. Elevations in TFAM expression in aged myotubes might function to increase the transcription of OXPHOS subunits and compensate for impairments in mitochondrial function. In spite of increased TFAM expression, aged myotubes had less abundance of PGC-1 α and NRF2 mRNA, which implies reduced capacity for mitochondrial biogenesis with replicative ageing. Similar results have been documented at the transcriptional level in ageing skeletal muscle *in vivo* (Ghosh et al., 2011; Shavlakadze et al., 2019; Su et al., 2015), suggesting aged myotubes may present lower mitochondrial content.

To test whether flavonoids regulate transcriptional responses in control and aged myotubes, the expression of genes associated with energy metabolism were assessed in their absence and presence. Of those genes studied associated with the antioxidant response, CAT demonstrated differential regulation by flavonoid treatment. In the presence of Q, control myotubes upregulated CAT expression, suggesting Q may act in a prooxidant manner through actions on H₂O₂ in myotubes. Although, rates of ROS emission were not augmented in the presence of Q. Mitochondrial SOD expression was significantly lowered by 10 μ M EGCG over 48 h in myotubes, in a similar manner to that in myoblasts (see Chapter 5). SOD2 plays an important role in quenching mitochondrial superoxide, and therefore, EGCG may attenuate mitochondrial superoxide (Pan et al., 2015). Of note, these data conflict with findings showing increased SOD2 mRNA expression and protein content following EGCG administration in L6 myocytes and embryonic fibroblasts, respectively (Casanova et al., 2014; Zhang et al., 2019), although supraphysiological concentrations (25 μ M) of flavonoids were employed. Together, these findings suggest that flavonoids may distinctly contribute to control of the cell redox state through the induction of enzymatic antioxidant systems.

Previous reports suggest Q augments mitochondrial biogenesis via activation of PGC-1 α in humans and rodents (Davis et al., 2009b; Henagan et al., 2015; Nieman et al., 2010; Sharma et al., 2015b). Yet, Q did not alter PGC-1 α or SIRT1 expression in myotubes, which could reflect differences in the dose of Q administered or failure of the myotube model to capture *in vivo* muscle tissue. Micromolar doses of EGCG and EPI actually decreased PGC-1 α mRNA levels in control myotubes. These data support previous findings demonstrating blunted mitochondrial adaptations in human skeletal muscle and murine skeletal muscle cells following EPI and EGCG supplementation, respectively (Schwarz et al., 2018; Wang et al., 2016). However, other studies have documented augmented markers of mitochondrial biogenesis with EPI and EGCG (Hüttemann et al., 2013; Lee et al., 2017; Moreno-Ulloa, et al., 2015; Taub et al., 2016). Considering the antioxidant potential of these flavonoids (Ze Xu et al., 2004a), it is possible that impaired PGC-1 α transcription in control myotubes was due to attenuated signalling through redox sensitive pathways (Gomez-Cabrera et al., 2008; Ristow et al., 2009). Maintenance of mitochondrial health also involves fusion/fission activities that govern organelles dynamics. Evidence for reduced fusion in Q and EGCG treated aged myotubes was provided by decreased MFN2 expression, which may exacerbate the age-related mitochondrial dysfunction (Sebastián et al., 2016). In the presence of EPI, aged cells demonstrated increased potential for fission by increased DRP1, with potential implications for respiratory function (Eisner et al., 2014; Glancy et al., 2015). Therefore, flavonoids may regulate organelles dynamics at the transcriptional level. However, given the negligible impact of flavonoids on respiratory function reported, it is not exactly clear how altered dynamics may impact mitochondrial health.

The transcription factor NRF2 governs the replication of antioxidant enzymes and subunits of the electron transport chain, through its binding to antioxidant response elements (Gao et al.,

2020; Yamamoto et al., 2018). Interestingly, all flavonoids tested enhanced NRF2 transcription across control and aged myotubes, which supports previous findings from Chapter 5 and others showing flavonoids are potent activators of NRF2 (Huang et al., 2019; Kim et al., 2015; Li et al., 2016; Moreno-Ulloa et al., 2015; Rowley et al., 2017a; Wu et al., 2006; G. Z. Yang et al., 2015). On the mechanism, induction of NRF2 could be attributed to the formation of ROS (McMahon et al., 2010; Zhang & Hannink, 2003), by dissociation of NRF2 from its repressor Kelch-like ECH-associated protein 1 (Keap1). Alternatively, upregulation of NRF2 may occur by an Keap1 independent mechanism (Gao et al., 2020). Here, flavonoids did not contribute to the regulation of ROS production, and therefore it is possible that a Keap1-independent mechanism was primarily responsible for the induction NRF2. One signal that may control NRF2 (independent of Keap1) in response to flavonoids is AMPK activity (Joo et al., 2016).

6.6.1 EPI augments AMPK activity in skeletal muscle cells, independent of Erk1/2

To help consolidate the findings that NRF2 expression is enhanced in parallel with dose-dependent effects on ROS emission in the presence of EPI, cell signalling responses were interrogated to help identify potential regulatory pathways. In disagreement with the hypothesis, replicatively aged myotubes displayed similar AMPK signalling responses compared to control under basal conditions. Similarly, AMPK α phosphorylation is unaffected by age at rest in rat gastrocnemius and tibialis anterior tissue (Hardman et al., 2014). Aside from AMPK, eNOS phosphorylation at Ser1177 was similar between control and aged myotubes under basal conditions, which fits with previous work demonstrating comparable eNOS phosphorylation in skeletal muscle between young and older sedentary adults (Nyberg et al., 2012). Therefore, under basal conditions, AMPK signalling may not be impaired with older age. Yet, it's possible that the activation of AMPK in response to external stimuli like nutrition may be compromised with ageing.

Commented [CS493]: I think that the huge amount of data you have generated would really benefit from an infographic style figure explaining the key findings and the links in the different models, treatments and output measures. It could even be part of your abstract for this chapter, to help your readers. It could be in 4 panels for con aged, blasts and tubes. That may also then help you define the order in which you ultimately present the data.

Commented [SD494]: Might need changing with reordering of the data

Here, EPI treatment induced AMPK activity in control myotubes, indicating that the action of EPI on NRF2 is potentially reliant upon AMPK and independent of Keap1 (Joo et al., 2016). Although AMPK signalling was enhanced with EPI in control myotubes, this effect was blunted in aged myotubes. This observation supports the premise that ageing diminishes the plasticity of skeletal muscle mitochondria due to blunted signalling responses to a given stimulus (Ljubcic et al., 2009). Activation of AMPK with EPI aligns with studies demonstrating increased AMPK activity with EPI supplementation using cultured cells, 6-week old male mice or sedentary middle-aged adults as models (Murase et al., 2009; Si et al., 2011; Taub et al., 2016). AMPK is a known metabolic governor of NRF2 activity, through its phosphorylation at Ser50 (Joo et al., 2016), and its activation is controlled by numerous factors, including the ADP/ATP ratio, Ca²⁺ levels and RONS (Auciello et al., 2014; Gowans & Hardie, 2014; Jensen et al., 2007). Although NO is known to stimulate AMPK activity (Nisoli et al., 2003; Wadley & McConell, 2007), this study found no role for EPI in regulating eNOS phosphorylation, pointing to an alternate mechanism of AMPK activation. Two regulatory kinases upstream of AMPK include CaMKII and LKB1, and evidence suggests EPI can alter the activity of both of these proteins (Moreno-Ulloa, Mendez-Luna, et al., 2015b; Murase et al., 2009). However, no impact of EPI supplementation was found on CaMKII activity, at least measured by phosphorylation at Thr286. Furthermore, the effect of EPI on NRF2 induction appears to be independent of Erk1/2 activity. Taken together, EPI-induced AMPK signalling may trigger NRF2 induction, and these effects are likely not mediated upstream by CaMKII, but rather LKB1 (see Figure 6.22). The exact pathways leading to activation of AMPK and NRF2 require further investigation.

Commented [SD495]: Toying with the idea of putting in a sentence or two about age effects on signalling under CTRL conditions before flavonoid discussion, just don't know whether its necessary, appreciate any advice. I know discussion is fairly long

Commented [CS496R495]: Paragraph before is well written, tells the story and is concise.

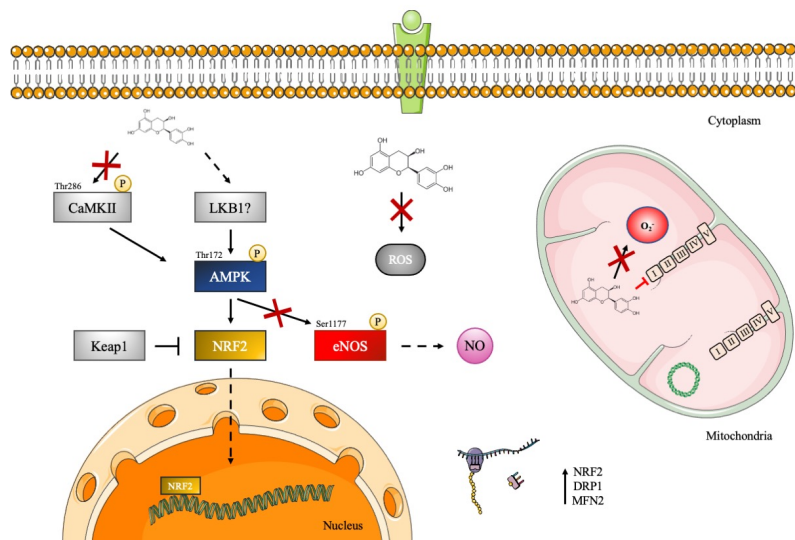


Figure 6. 22 Schematic of the potential mechanisms by which EPI exerts its biological effects in skeletal myotubes.

Commented [CS497]: This is lovely. It would be good to have a similar figure earlier on how the aged and control cells differ from a metabolic perspective (mito and gene expression, but that may be too big of an ask?)

Commented [SD498R497]: Will try and do this

6.7 Limitations

Like Chapter 5, this study used a murine skeletal muscle cell line (C₂C₁₂) to examine the effects of (replicative) ageing and flavonoids on aspects of energy metabolism. Although widely used to study mechanisms of muscle adaptation, and despite being highly practical versus primary muscle cell culture, C₂C₁₂ cells are both transcriptionally and metabolically dissimilar to primary skeletal muscle cells (Abdelmoez et al. 2019). Moreover, cultured myotubes lack the intra- and extracellular environment that is present *in vivo* (Aas et al. 2013). In this way, findings generated using the C₂C₁₂ model should be interpreted with caution. To study the effects of skeletal muscle ageing in this study, a replicative ageing model was employed. Whilst replicative ageing may indeed capture some features of ageing human skeletal muscle (Bigot

Commented [CS499]: I have not read this again.

et al. 2008; Sharples et al. 2011), this model will not capture all aspects of human skeletal muscle tissue. Furthermore, replicatively aged myoblasts do not appropriately exit the cell cycle to differentiate like control myoblasts (Sharples et al. 2011). Thus, effects of replicative ageing in myotubes could reflect a lack of myotube formation as opposed to detrimental effects of ageing *per se*. Similar to Chapters 4 and 5, this study used parent flavonoid compounds rather than their related *in vivo* metabolites. Thus, care should be taken translating the data obtained with these compounds *in vitro*. Another limitation of this study was the failure to obtain information on the maximal respiratory capacities (and consequently spare respiratory capacities) of control and aged myotubes in the presence of flavonoids when using the Seahorse Analyzer to investigate mitochondrial function. This additional data would have provided greater resolution on how ageing and flavonoids impact indices of mitochondrial function. Finally, the use of semi-quantitative western blotting techniques to confer protein activity is a limitation.

6.8 Conclusion

The novel findings in this chapter demonstrate that replicative ageing causes mitochondrial dysfunction and increases mitochondrial ROS production in myotubes. Similar to older human skeletal muscle, replicative ageing reduced mitochondrial coupling efficiency, impaired mitochondrial biogenesis and lowered reliance on OXPHOS for ATP synthesis. Notably, the data suggest flavonoids do not rescue age-related impairments to mitochondrial bioenergetics and ROS production in replicatively aged C₂C₁₂ myotubes, but flavonoids may activate AMPK signalling and transcriptional events (in a compound-dependent manner) that converge on mitochondria in C₂C₁₂ myotubes. Of the flavonoids tested, Q evoked an antioxidant response at the mRNA level, whereas EPI robustly induced NRF2 expression downstream of increased AMPK signalling. Importantly, the observed impact of flavonoids on cell adaptations occurred

Commented [CS500]: I would move the conclusion to be before the limitations, I think. But go with your preference.

Remember you also need linkers between chapters. These can be a stand alone page between each chapter (does not need to be a page of text, just we found x, therefore undertook y as the next set of studies. You have sort of done it within this chapter already e.g. first in blasts now in tubes, just remember to make it obvious between all chapter.

Commented [SD501R500]:

Commented [CS502]: Worth also stating that the impact of each is different from each other with different pathways being influenced by each, so a one size fits all approach for muscle at least is not justified from these studies.

I think you also need to start your conclusion talking about the differences in behaviour of the control vs aged cells – the findings in the aged tubes, match the paper I suggested, which were undertaken in human biopsies – so justify your basal data and thereby potentially strengthen the flavonoid data. Then go onto the comment I have made above re differences, then onto the more specific info you have already written.

in the physiological range, suggesting that these compounds may confer favourable mitochondrial adaptations when ingested *in vivo*. Therefore, EPI supplementation may help defend against the perils of sedentary ageing by acting through the mechanism of hormesis to indirectly enhance mitochondrial health. Further study of NRF2 activity in the presence of relevant inhibitors is necessary to fully describe EPI's mechanism of action in skeletal muscle cells.

Commented [CS503]: This is the sort of thing you want – strong statements, but with caveats e.g. to test this you would need to do a b and c.....

Commented [CS504]: What would your recommendations be, having undertaken this study, re young vs older people ingesting flavonoids for muscle health?

Chapter 7: The effects of replicative ageing
and dietary flavonoids on the metabolome of
skeletal myoblasts and myotubes

7.1 Introduction

Originally proposed by Oliver and colleagues in 1998, metabolomics is a powerful investigational tool that can be used to determine the phenotype of a biological sample through analysis of its present metabolites (Oliver et al., 1998). As small molecules (<1500 Daltons), metabolites are substrates or end products of enzyme-mediated reactions (Dunn et al., 2011). For fundamental reasons, the collection of metabolites within a biological sample (i.e. the metabolome) is expected (Kell, 2004), and is indeed found (Raamsdonk et al., 2001), to amplify changes observed in the transcriptome and proteome. Therefore, studying the metabolome can provide crucial insights into the molecular phenotype of a biological system in response to specific stimuli. Another asset of metabolomic investigations is that metabolites are highly conserved across mammalian species. In this way, metabolite-level information obtained from non-human species may well have relevance and translatability to human populations.

Metabolite profiling is typically performed using ^1H nuclear magnetic resonance (NMR) or liquid-chromatography mass spectrometry (LC/MS). Given that most biomolecules contain hydrogens, and the proton (^1H) has nearly 100% natural abundance and high sensitivity, ^1H -NMR is well suited for fast non-discriminative quantitative profiling based on a single internal quantification reference compound (Weljie et al., 2006; Xu et al., 2006). Briefly, ^1H -NMR is based on the interaction of nuclei of ^1H atoms with an external magnetic field. Following the application of a pulse of electromagnetic radiation at a specific “resonance” frequency, nuclei undergo ‘excitation’ and ‘relaxation’ when the radiation pulse stops. During relaxation, nuclei emit the radiofrequency waves absorbed during the excitation phase, thus generating radiofrequency peaks in a frequency spectrum (also called NMR spectrum) after Fourier’s transformation.

Commented [SD505]: Claire has not reviewed the introduction yet

Commented [MMP506R505]: Looks good – not sure how much space you have to add detail (as thesis styles differ) but one thing you may wish to expand is any evidence that you refer to in your discussion:

Such as:
Metabolites associated with changes in mitochondrial function and RONS emission

A handful of studies have investigated the impact of ageing on the plasma/serum and muscle metabolome in rodents and humans (Fazelzadeh et al., 2016; Garvey et al., 2014; Johnson et al., 2018; Uchitomi et al., 2019; Wilkinson et al., 2020). These studies have provided crucial insights into the metabolic pathways impacted by chronological ageing and highlighted potential targets for therapeutic intervention. Yet, the metabolic signature of cellular (replicative) ageing has seldom been investigated in skeletal muscle cells. Such information may help explain similarities and differences in indices of mitochondrial function between control and aged myoblasts (Chapter 5) and myotubes (Chapter 6), respectively. Developing knowledge of the metabolic pathways linked with cellular ageing will not only help establish whether *in vitro* models are useful for capturing features of skeletal muscle ageing *in vivo*, but will also enable the study of whether interventions, such as dietary agents, regulate cell function at the level of metabolites.

Flavonoid intake has long been associated with cardiometabolic health benefits (Buijsse et al., 2006; Desideri et al., 2012; Hertog et al., 1993a). Over half a century since flavonoid mechanistic research began, it is now accepted that flavonoids interact with processes associated with energy metabolism, but many questions remain unanswered. One way in which flavonoids modulate energy metabolism is through actions on mitochondrial respiration and signalling pathways typically associated with endurance exercise (Davis et al., 2009a; Dorta et al., 2005; Hüttemann et al., 2013; Lagoa et al., 2011; Lee et al., 2015). Similarly, Chapters 5 and 6 of this thesis demonstrated flavonoids may modulate the transcription of mitochondrial and antioxidant associated genes in C₂C₁₂ myoblasts and myotubes, which was potentially downstream of increased AMPK signalling. In recent years, metabolomics has been employed to further understand the molecular metabolic processes by which flavonoids perpetuate their

positive health effects. From these limited studies, evidence is emerging that flavonoid supplementation regimes contribute to changes in the cell metabolome (Chitturi et al., 2019; Chu et al., 2018; Mendes et al., 2019; Si et al., 2019a). For instance, quercetin altered the abundance of metabolites involved in the TCA cycle, antioxidant processes and membrane remodelling in human macrophages. To date, little information is available on whether dietary flavonoids impact skeletal muscle cells at the metabolite level. Considering the current gaps in knowledge regarding cellular ageing and flavonoids in skeletal muscle cells, the objective of this study was two-fold: 1) Explore how replicative ageing impacts the metabolome of skeletal muscle myoblasts and myotubes; 2) Determine whether dietary flavonoids impact the metabolic signatures of control and replicatively aged myoblasts and myotubes. This study was explorative by nature and therefore would potentially generate hypotheses to test in future research.

7.2 Materials and methods

7.2.1 Cell culture

C₂C₁₂ mouse skeletal muscle cells (ATCC, Rockville, MD, USA) at passages 9-11 (referred to as 'control') and passages 47-50 (replicative aged and herein referred to as 'aged'; [130-140 population doublings]) were used in this study. C₂C₁₂ myoblasts were resuscitated from liquid nitrogen (LN₂) in 2 mL cryovials at a cell density of 1×10^6 . Cryovials were rapidly warmed and once thawed were plated onto T75 flasks that were pre-gelatinised with 5 mL, 0.2 % gelatin. The gelatin was incubated on the flasks at room temperature (RT) for 20 minutes, before excess gelatin was aspirated. Growth medium (GM) was added (15 mL) to the pre-gelatinised T75s, prior to addition of 1×10^6 resuscitated cells. The flasks were agitated front-back and side-side to spread the cells evenly over the plate. To facilitate cell growth flasks were incubated in a humidified 5% CO₂ atmosphere at 37°C for up to 72 h.

Once the cells were 80 % confluent, they were washed twice with PBS to remove any excess serum, which is an inhibitor of trypsin. Once washed, 1 mL trypsin/T75 was added and incubated for 5 minutes at 37°C to enable cell dissociation. Following confirmation of dissociation, by microscopy, trypsin was neutralised by adding 4 mL GM (5 mL total) to the dish. To prevent cell clumping, the cells were homogenised, by slowly drawing the cell solution up and down using a syringe and 21-gauge needle. The cell suspension was prepared for cell counting in a 1:1 dilution in 0.4 % trypan blue stain (Bio Whittaker, Wokingham, UK). The cell suspension/trypan blue mix was dispensed onto a Neubauer haemocytometer (Assistent, Sondheim, Germany). Once cells were counted, they were seeded onto pre-gelatinised 6-well plates (Nunc, Roskilde, Denmark) at 40,000 cells/mL.

7.2.2 Flavonoid treatments and controls

Cell culture experiments were started (timepoint 0 h) by transitioning cells from proliferation to differentiation, by changing GM to low serum (2%) DM. In order to investigate metabolite changes in early and late differentiation, two separate dosing protocols were employed: 1) Cells were washed twice with PBS prior to switching to DM in the presence of Quercetin, EGCG or EPI at 0, 5 and 10 μ M for 24 h. 2) Cells were washed twice with PBS prior to switching to DM for 72 h. After 72 h differentiation, cells were again washed twice with PBS prior to dosing with DM in the presence of Quercetin, EGCG or EPI at 0, 5 and 10 μ M for 24 h. After 24 h treatment of myoblasts and myotubes, cells were washed three times with PBS. Following thorough aspiration of wells, plates were immediately transferred to -80°C for storage. The culture media and supplement batch were kept constant for the entire experiment. Each experimental condition was performed three times in duplicate. To control for any molecular signature arising from the pre-gelatinised 6-well plates, extra wells within the experiment were

cultured without cells. To control for the intraplate variance care was taken to design the experiment so that multiple plates contained the same conditions (see Figure 7.1).

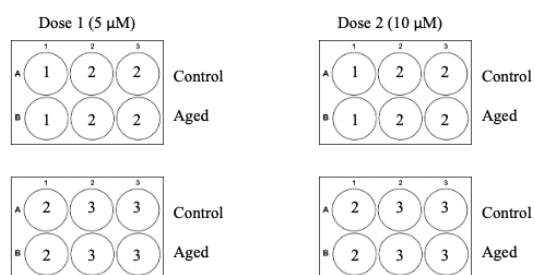


Figure 7. 1 Two plates were prepared per condition per dose (see figure) for both myoblast and myotube cultures for seven groups: 1) – DM only, 2) – Quercetin 5 μ M, 3) – EGCG 5 μ M, 4) – Epicatechin 5 μ M, 5) – Quercetin 10 μ M, 6) – EGCG 10 μ M, 7) – Epicatechin 10 μ M, and one plate for the cell free control group 8 – No cells, matrix only. Each plate contained 3x wells of “control” and 3x wells of “aged” cells = 6 samples in total for each condition. Two control plates (24 h and 96 h, for myoblast and myotube timeframes, respectively) contained replicates of cell-free media with and without 0.1% DMSO.

7.2.3 Sample preparation for ^1H NMR acquisition

Plates were thawed from -80°C and immediately placed on ice before 500 μL ice-cold acetonitrile: H_2O (50:50 v/v) solvent was pipetted into each well (see Figure 7.2). Wells were immediately scraped with a pipette tip and the cell slurry was pipetted into Eppendorf tubes. Samples were then immediately subjected to sonication at 50 KHz, 20% amplitude for 3×30 s bursts on ice. Sonicated samples were then vortexed for 20 s and centrifuged at $21,500 \times g$ for 5 minutes @ 4°C . The supernatants were then aliquoted into fresh Eppendorf tubes before being snap frozen in LN_2 . Samples were subsequently lyophilised overnight before being sealed

and stored at -80°C until further processing (2 weeks maximum). Plates were extracted in batches of 24 samples and randomised to enable appraisal of any batch effects. Immediately prior to NMR acquisition, $200\ \mu\text{L}$ of sodium phosphate buffer was added to each lyophilised sample, before centrifugation ($12,000\ \text{g}$ for 2 minutes). The sodium phosphate buffer contained $100\ \mu\text{M}$ Trimethylsilyl propionate (TSP) (d_6 deuterated, Sigma), $99.9\ \%$ $^2\text{H}_2\text{O}$ (Sigma), and $100\ \text{mM}$ $\text{Na}_2\text{HPO}_4:\text{NaH}_2\text{PO}_4$ pH 7.4 (Thermo-Fisher). Finally, $190\ \mu\text{L}$ of sample was pipetted into $3\ \text{mm}$ (outer diameter) glass SampleJet NMR tubes (Bruker).

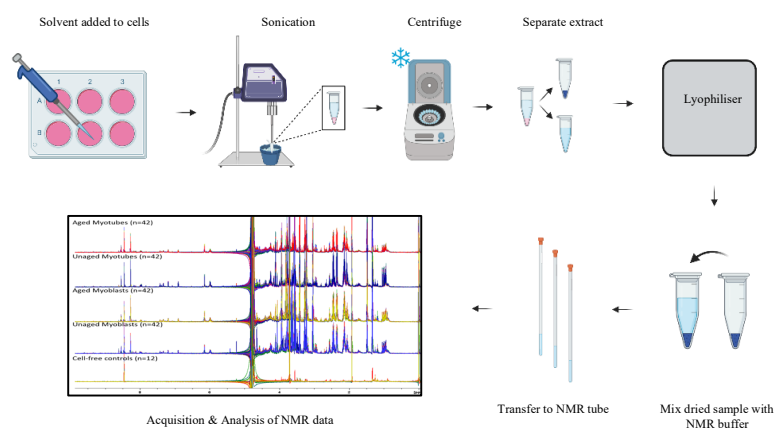


Figure 7. 2 Method of extraction from stored samples. The extraction required addition of solvent, followed by an incubation over ice to ensure solvent penetration through the sample. Homogenisation was critical for the separation of protein and small molecules. Homogenised samples were centrifuged to separate the debris and precipitants (this allowed the solution of metabolites to be extracted). The supernatant was lyophilized and metabolites were either immediately stored or prepared for analysis. Dry pellets were mixed with the appropriate buffer (see section 7.2.3) prior to acquisition.

7.2.4 ¹H NMR acquisition and sample processing

High resolution 1D ¹H NMR was acquired using 3mm outer diameter tubes in 700MHz Avance IIIHD Bruker spectrometer equipped with a TCI cryoprobe and chilled autosampler (SampleJet). A one-dimensional ¹H Carr-Purcell-Meiboom-Gill (CPMG) experiment (vendor supplied `cpmgrp1d`) was used for all spectra acquisition was used to attenuate peaks from large molecules such as proteins along with standard 1D ¹H NOESY presat (vendor supplied `noesypr1d`) to check sample quality. Spectra were evaluated for quality control (QC) by ensuring consistent water suppression, baseline correction, and peak line width of reference TSP signal according to best practice set out by the Metabolomics Standards Initiative (MSI) (Considine & Salek, 2019; Sumner et al., 2007). Initially, out of 180 samples, 168 passed QC criteria. The failed samples were re-run and all, but one subsequently passed QC criteria. Afterwards, the spectra were divided into ‘buckets’ or ‘bins’ using TameNMR software (github: <https://github.com/PGB-LIV/tameNMR>) and a ‘pattern’ file was created associating metabolites with spectral peaks. Both identified and unknown metabolites were part of the pattern file. Later, ‘binning’ of metabolites was reviewed using TameNMR software (accessed via galaxy.liv.ac.uk within University of Liverpool VPN). Peaks were binned using TameNMR through integration of each spectral region defined in the pattern file to yield a table of peak integrals that corresponded to each metabolite abundance.

7.2.5 Metabolite annotation and identification

Metabolite annotation and identification is necessary for the conversion of raw NMR spectra peaks into a biological frame of reference (e.g., relative metabolite abundances). Therefore, NMR spectra were subjected to metabolite annotation using Chenomx NMR suite 8.2 (Chenomx, CA). The software enabled the matching of 1D-¹H NMR spectra of metabolite

standards to an experimental spectrum using various matching algorithms. Where appropriate identities were confirmed using an in-house library of standards.

7.2.6 Spectral Normalisation

Initially two different methods were compared to determine optimal normalisation of the dataset. First, metabolites/bins were removed from the TameNMR generated spreadsheet and used in RStudio for one of two normalisation methods: 1) Total area (TotArea) and 2) Probabilistic quotient normalisation (PQN). After normalisation, both TotArea and PQN methods (Figure 7.3B and 7.3C, respectively) produced similar results. However, PQN was selected to be the most robust method and therefore was used in all subsequent statistical analysis (Dieterle et al., 2006). PQN is a widely used method in the NMR field that normalises each spectrum by a reference spectrum, which in this case, was the median spectrum.

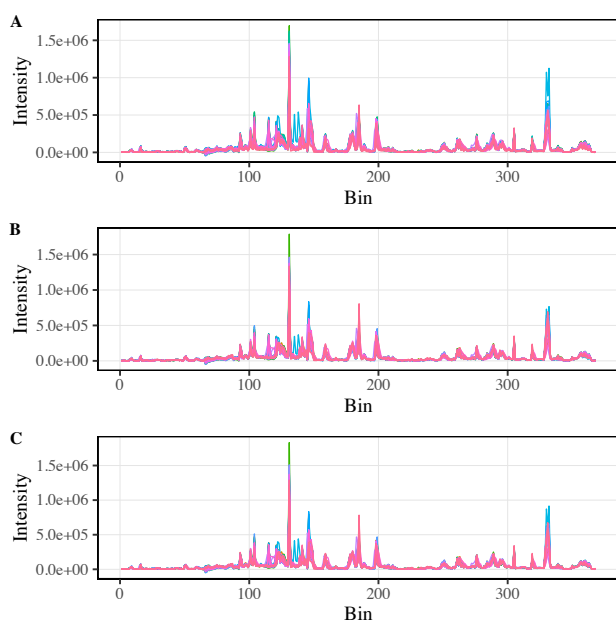


Figure 7.3 Raw and normalised data using TotArea and PQN methods. Representative of 168 NMR spectra. A) Raw data – no normalisation. B) TotArea normalisation. C) PQN. Visual inspection of the NMR spectra revealed a tighter clustering of all samples after both normalisation procedures compared to no normalisation.

7.2.7 Data scaling and centring

Scaling was performed on each variable (e.g. metabolite) across the entire dataset to enable metabolite comparisons and to minimise biological variation confounding the results (Craig et al., 2006). Two scaling methods were performed on normalised data: 1) Auto - mean centring and scaling by the standard deviation of the bin 2) 'Pareto' - mean centring and scaling by the square root of the standard deviation of the bin (Eriksson et al., 1999). The chosen method was pareto scaling. Pareto scaling was found to be the most robust method for subsequent statistical analysis as it did not appreciably increase the amount of noise in the spectra to the same degree as with auto scaling (see Figure 7.4).

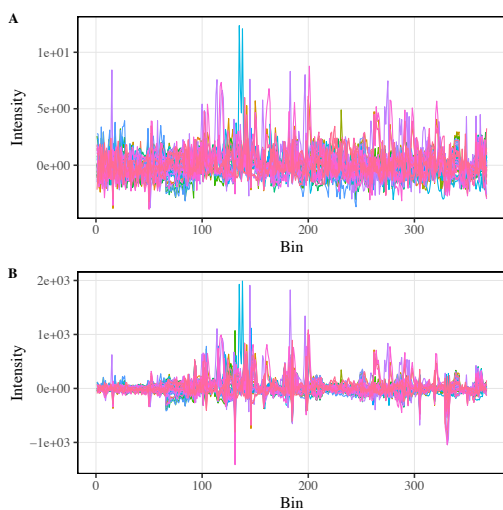


Figure 7. 4 Comparison of scaling methods. A) Normalisation by TotArea and Auto-scaling. B) Normalisation by TotArea and Pareto scaling.

7.2.8 Statistical Analysis

A flowchart of the statistical analysis performed in this study is shown in Figure 7.5. Following the aforementioned QC procedures, spectra were collated into a dataset for analysis. All further analytical steps were undertaken using a combination of published and custom-made scripts in R Studio (R Team, 2019), in addition to MetaboAnalyst (<https://www.metaboanalyst.ca>). The scaled dataset was subjected to multivariate analysis using a combination of principal component analysis (PCA) and partial least square – discriminant analysis (PLS-DA) (see section 7.2.9 and 7.2.10, respectively). Variable importance of the projection (VIP) was used to select important features from the PLS-DA models. Representative bins for the selected features were identified *via* correlation reliability score, (CRS, see further description in section 7.2.12). Differences in select metabolites between groups were determined by univariate tests (t-test/ANOVA-Tukey’s HSD depending on number of groups to contrast). Two-way ANOVA

was performed to determine differences between control and aged groups in the presence of 0, 5 and 10 μM of each flavonoid (i.e., age and dose and main factors). Finally, pathway analysis was performed via metabolite set enrichment analysis (MSEA; see section 7.2.14).

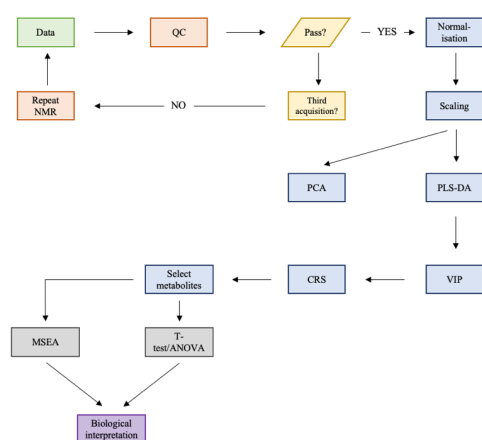


Figure 7. 5 Overview of quality control and statistical analysis workflow employed.

7.2.9 Principal component analysis

PCA is an orthogonal data transformation that returns unobserved (latent) variables named principal components (PC). Each PC is the linear combination of the original variables in such a way that the first PC explains the most variance in the data. The second component explains the most variance unexplained by the first PC and is orthogonal and uncorrelated to the first. Subsequent PCs follow the same procedure. This transformation results in a dataset where the original variables are replaced by uncorrelated PCs. In this new dataset of PCs only the first few (typically) PCs are required to explain the majority of the variance in the dataset, thus reducing the high number of starting variables with minimal information loss. In this study,

PCA was preferred as a data exploration tool to reveal and observed the hidden structures in the data. On a PCA scores plot, each point represents a sample and can gives information about the (dis)similarities between samples. This is elucidated from the distances between points on the scores plot. Furthermore, the observed structures in the PCs can be linked to the original variables (metabolites) by observing the associated loadings plot, although, selecting metabolites of interest in such datasets is often more nuanced.

7.2.10 Partial least square discriminant analysis (PLS-DA)

Partial least square - discriminant analysis (PLS-DA) is a variation of partial least square (PLS) regression. PLS is a supervised statistical model applied to multivariate datasets in order to make predictive models between two matrices (Barker & Rayens, 2003). A PLS model requires a matrix of input data (predictors) and a secondary matrix (response) where the output of the model is recorded. PLS projects both of these matrices (predictors and response) into two new matrices where the covariance between the two are minimised. PLS and PCA are somewhat similar because both create latent (unobserved) variables by using projections into new spaces. However, while PCA is an unsupervised method that projects maximum variance in latent variables called PCs, PLS is supervised (information on sample groupings retained) and projects predicted and observable variables using a linear regression model in latent variables called variables or components. PLS-DA variation uses a nominal vector as the response which allows the building of models for classification problems. PLS models are particularly suitable for data with multicollinearity in predictors such as NMR data, where a single metabolite can be represented by multiple peaks depending on its molecular structure. In this study, PLS-DA was used to build predictive models between experimental groups. PLS-DA model performance was assessed by using a 5-fold cross-validation over 50 repetitions. Classification errors were used to determine the optimal model complexity parameter (number of

Commented [MMP507]: Components?

components). From the refined model, representative metabolites could be selected to reveal those driving the differences between experimental groups.

7.2.11 Variable importance of the projection (VIP)

Bin (variable) selection from a statistical model is a crucial step for most metabolomics studies in order to extract biologically relevant information. PLS-DA and its derivative methods are designed to transform the data and make predictions. However, variable (bin) selection is not integrated into the model building process. Variable importance of the projection (VIP) scores is a method that is often preferred with datasets with multicollinearity. VIP scores in essence are weighted sum of squares of PLS weights (calculated during PLS-DA model building) which also take explained variance in PLS variates. This method is designed to be used for multivariate datasets where there is correlation between variables as well as a higher number of variables than samples. Once VIP scores are calculated, a cut-off threshold needs to be defined in order to include or exclude variables. VIP scores are calculated as such that average of all VIP scores squared is 1 (Akarachantachote et al., 2014). Hence, a cut-off of 1 was used to select variables with above average influence in the PLS-DA model. Due to the nature of NMR-derived data, metabolites with multiple signals will present multiple entries in VIP scores. Therefore, additional steps were undertaken to select the most representative bin per metabolite to take forward on the analysis pipeline (see section 7.2.12).

7.2.12 Correlation reliability score

Depending upon their molecular structure, some metabolites may have multiple NMR signals. To address the problem of selecting an appropriate representative bin for a specific metabolite, a correlation reliability score (CRS) method was employed. Multiple signals arising from a single metabolite should theoretically yield a high correlation score. However, some areas of

the NMR spectra are populated by peaks belonging to multiple metabolites. Therefore, some bins may be more representative markers for a metabolite than others. Given this challenge, bins of the same metabolite were correlated and scored to determine their reliability to report on the assigned metabolite. The CRS score is determined using the following algorithm:

1. Calculate Pearson correlation matrix for all the identified bins per metabolite.
2. For each unique metabolite extract individual bin correlation values.
3. Calculate the mean for each individual bin of the unique metabolite.
4. Multiply each score by 100 to present the percentage.

To separate candidate representative bins from non-candidate bins, previously calculated CRS scores were used to generate a passing score in the following manner:

1. Exclude all bins with a 100% CRS (single peak metabolites)
2. Calculate median and standard deviation with the remaining scores.
3. $CRS_{pass} = \text{median} - \text{standard deviation}$
4. A CRS above the threshold represents a high correlation of the bin to the rest of the signals of the same metabolite.

Finally, highest CRS scores of non-overlapping bins (where applicable) were selected so that representative metabolites were used for univariate and pathway analyses.

7.2.13 Univariate analysis

Univariate analyses were performed using Welch's t-test or two-way analysis of variance (ANOVA) where appropriate in order to compare the means of selected metabolites. To

account for type-I errors arisen from multiple hypothesis testing, *P*-values were corrected via Benjamini & Hochberg (BH) (Benjamini & Hochberg, 1995) method unless otherwise stated. Post hoc analysis was performed using two-way ANOVA adjusted for multiple tests to establish the group(s) responsible for any differences identified by the ANOVA. To visualise the significant changes in metabolites between experimental groups, boxplots were plotted.

7.2.14 Metabolite set enrichment analysis (MSEA) and interpretation

Upon the selection of metabolites through PLS-DA modelling, a qualitative metabolic set enrichment analysis (MSEA) was used based on a Fisher's exact test (Xia & Wishart, 2010). MSEA provides a probability measure for a set of metabolites likelihood of representing a pathway in a system. Given both the qualitative nature of this analysis and metabolomics showing a 'metabolic snapshot', it is not possible to annotate a pathway as being increased/decreased or up- regulated/down-regulated. MSEA's sole purpose is to provide possible leads on pathways which are to be explored and discussed further in light of complimentary data and/or further research. In this study pathway analysis was performed using metabolite sets from the KEGG database. Identified metabolite names were used to calculate the probability of individual pathways via a one-sided Fisher's exact test. Resulting *P*-values were adjusted for Type I errors with BH adjustment, and pathways with *P*-values less than 0.05 were presented as significant and discussed further.

7.3 Results

7.3.1 Age-specific differences in skeletal myoblasts

To establish potential effects of ageing in skeletal myoblasts, control and replicatively aged myoblasts were compared. **PCA** was performed to observe the major variances between all

Commented [CS508]: Are these abbreviations spelled out elsewhere in this chapter e.g. in methods or intro? If not, they will need to be spelled out here and below.

I also wonder if it is worth having a subsection somewhere in this chapter to explain the differences between the analyses used and why multiple analyses are performed and the pros/cons of each/how they support or challenge each other. This could be a flow chart, perhaps e.g. step by step protocol of what is done, what it reveals and why it is done.

Commented [SD509R508]: I will expand in greater detail in the methods section on why these analyses were used etc..

samples (Figure 7.6A). PCA scores plot of PC1 (48.36%) against PC2 (16.57%) revealed strong clustering of age in terms of separation. PC1 and PC2 explain a cumulative variance of 64.93%. Meanwhile a total of 6 components were required to explain 95% of variance in the data. When the overall metabolic profile of myoblasts is considered, control myoblasts are clustered more tightly compared to aged myoblasts on PC1. This indicates that control myoblasts have less variation compared to aged myoblasts.

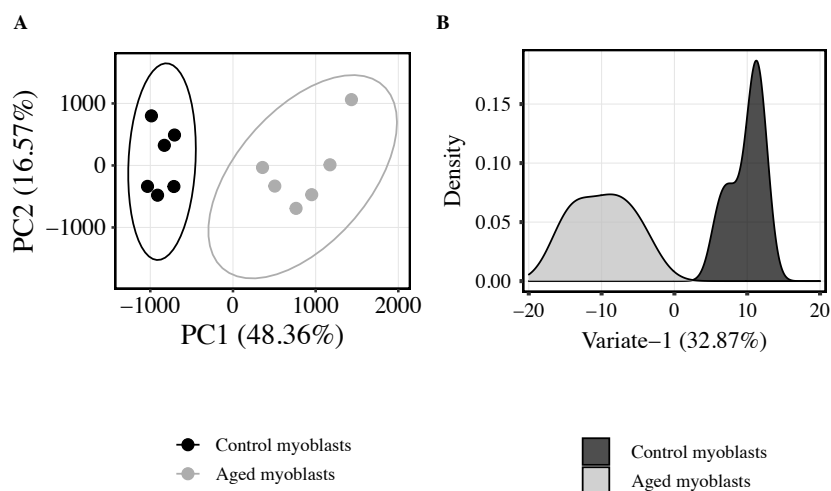


Figure 7. 6 Multivariate analyses of control and aged skeletal myoblasts. Panel A) PCA scores of control vs. aged myoblasts, coloured by age (control cells in ED black circles, $n=6$; aged cells in ED grey circles, $n=6$). Brackets report the percentage variance explained by the PC. Six PCs were required to achieve 95% explained variance. Only PC1 and PC2 are shown for simplicity/clarity. Ellipses represent 95% confidence region. Panel B) PLS-DA density plot to verify metabolite selection in myoblasts discriminated by age (control = 6 and aged = 6). Model complexity of one variate (32.87% explained variance) was determined to be optimal.

To further identify differences in the metabolic profiles of control and aged skeletal myoblasts, the differences between age were enhanced using a cross-validated PLS-DA model (Figure 7.6B). Optimal model complexity was found to be a single-variate model. Similar to the PCA plot (Figure 7.6A), a tight clustering of groups can be observed. Using VIP scoring as a criterion, metabolites influential in such discrimination were extracted.

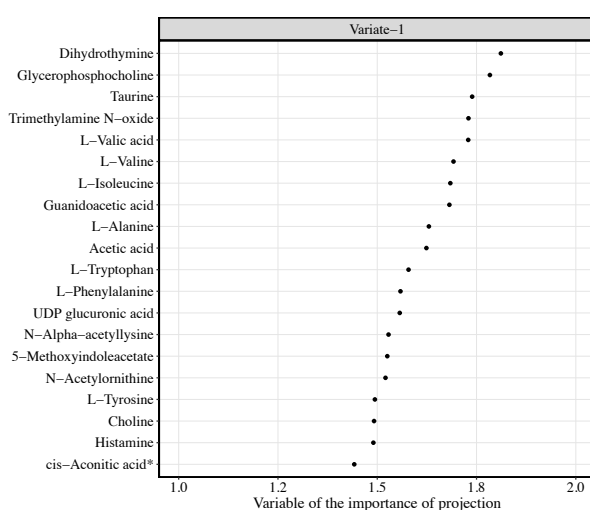


Figure 7.7 VIP scores of PLS-DA model (ROC = 1) built on age-dependent differences in skeletal myoblasts. A lower threshold of 1 was used on latent variable one to select metabolites from the model. The top 20 representative metabolites/bins are presented for clarity.

Upon observation of the VIP scores (see Figure 7.7), metabolites most influential in explaining age-specific differences in myoblasts were selected for further analyses (see Table 9.2, Chapter 9). Metabolite levels were compared via BH adjusted t-test to gain metabolite level information on age-specific differences (see Figure 7.8). The metabolite level comparison of control and aged myoblasts revealed Guanidoacetic acid, cis-Aconitic acid/L-Acetylcarnitine, Choline, Acetone, Acetic acid, Trimethylamine N-oxide, Isopropyl alcohol, L-Tyrosine, Phosphorylcholine, L-Alanine, Taurine and L-Aspartic acid were lower in aged versus control

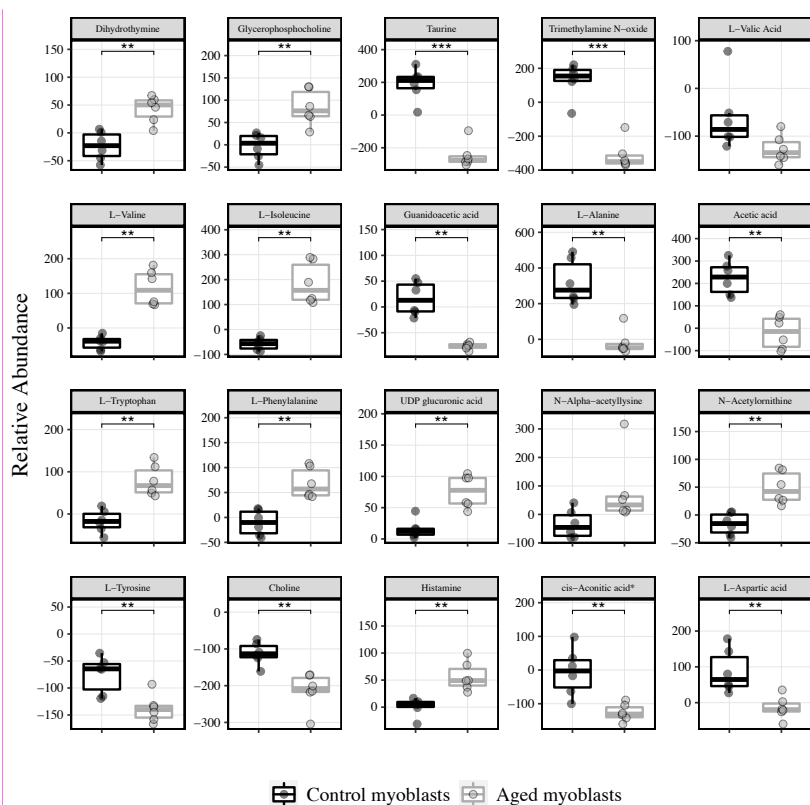
Commented [CS510]: Does this tell us anything about how the factors discriminate e.g. are they all increased in one group vs another, for example, or are they simply different and we do not get from this whether they are up or down in aged vs con?

Commented [SD511R510]: VIP scores represent the contribution a variable [metabolite] makes in the PLS DA model, provides no info on direction of change. 'VIP is calculated as a weighted sum of the squared correlations between the PLS-DA components and the original variable. The weights correspond to the percentage variation explained by the PLS-DA component in the model'

Commented [MMP512]: Report the PLS-DA model quality here (via ROC score or similar). Replace the word 'variate' with the term 'latent variable' or 'component'

Commented [CS513]: Spell out

myoblasts. The presence of isopropyl alcohol may be an artefact of cell extraction procedures. In Chapter 5 of this thesis, replicative ageing did not compromise mitochondrial function in C₂C₁₂ skeletal myoblasts. However, it is not known whether replicative ageing captures ageing human muscle behaviour as it relates to energy metabolism in the myotube model. Conversely, Carnosine, 5-Methoxyindoleacetate, Acetylcholine, Dihydrothymine, 3-Methylhistidine, Glycerophosphocholine, Uridine diphosphate glucuronic acid, L-Threonine, N-Acetylmithine, Pantothenic acid, L-Tryptophan, Histamine, L-Phenylalanine, Malic acid, L-Valine, Glycylproline, L-Isoleucine, L-Leucine and L-Glutamine were significantly higher in aged over control myoblasts.



Commented [CS514]: This is hard to retain as a list. Maybe generate the info into a figure? How do these data differ from the VIP score? Some seem to be shared between the list and the figure, but others not...

Commented [SD515R514]: Agree, these will be in appendix as whole table. Though some seem to contribute to the model, they aren't necessarily significant different versus control

Commented [CS516]: Is L valic acid not significant, or is the * simply missing? If the former, should it be removed?

Relative abundance is relative to what?

Commented [SD517R516]: Kept this metabolite because it had VIP score >1. Relative quant is standard practice for the determination of differences between treatment groups, rather than obtaining absolute quantification of single metabolites that provide useful information in this study

Figure 7. 8 Selected metabolite boxplots of control (black fill, n=6) and aged (grey fill, n=6) skeletal myoblasts. ** and *** represent *P*-value less than 0.01 and 0.001 respectively. * in the boxplot title represent denotes overlapping bin.

Selected metabolites for control and aged skeletal myoblasts were subjected to metabolite set enrichment analysis (MSEA) to extract further metabolic pathway level information. Table 9.2 (Chapter 9) summarises all metabolites selected for both control and aged cells. MSEA was performed on selected metabolites using a database curated from the KEGG pathways (Mus musculus (mouse) [KEGG organism code: mmu]), using Fisher's exact test with EASE correction and BH *P*-value adjustment for multiple testing. Ten significantly over-represented pathways were identified for control and aged skeletal myoblasts (see Table 7.1). Out of the ten pathways, metabolites present in three particular pathways including aminoacyl-tRNA biosynthesis, valine, leucine and isoleucine biosynthesis, phenylalanine, and arginine metabolism were predominately higher in aged versus control skeletal myoblasts. Overall, the metabolic signature of skeletal myoblasts is distinct between control and replicatively aged cells.

Commented [CS518]: I don't understand this – also do not see any * in the box plot titles.

Commented [SD519R518]: See bottom row, cis-aconitic acid. This means a metabolite was identified in the same bin. Thus, we cannot be 100% sure whether this is cis-aconitic acid or acetylcarnitine

Commented [CS520]: And so – Add 1 sentence to suggest the relevance of this finding – is it expected or surprising, how may it be relevant. Not a full blown discussion, but just a comment on how the progressive steps lead to this finding and its relevance.

Table 7. 1 Pathway analysis results for control and aged skeletal myoblasts. Reporting raw & BH adjusted *P* values, number of hits, pathway impact and matches.

Pathway	Raw <i>P</i> -value	BH <i>P</i> -value	Hits	Impact	Matches
Aminoacyl-tRNA biosynthesis	<0.0001	<0.0001	12	0.17	L-Phenylalanine; L-Tryptophan; L-Aspartic acid; L-Serine, L-Valine; L-Alanine, L-Leucine; L-Threonine, L-Tyrosine; L-Glutamate; L-Glutamine; L-Isoleucine
Valine, leucine and isoleucine biosynthesis	<0.0001	0.0009	4	0.00	L-Threonine; L-Leucine; L-Isoleucine; L-Valine
Alanine, aspartate and glutamate metabolism	<0.0001	0.0012	6	0.62	N-Acetyl-L-aspartate; L-Aspartic acid; L-Alanine; L-Glutamate; Pyruvate
Glyoxylate and dicarboxylate metabolism	0.0001	0.0020	6	0.07	cis-Aconitate; L-Serine; L-Glutamate; Acetate; Pyruvate; L-Glutamine
Glycine, serine and threonine metabolism	0.0001	0.0023	6	0.30	L-Serine; Choline; Betaine; Guanidinoacetate; L-Threonine; Pyruvate
Arginine biosynthesis	0.0003	0.0040	4	0.12	L-Glutamate; N-Acetylornithine; L-Aspartic acid; L-Glutamine
Histidine metabolism	0.0005	0.0061	4	0.28	L-Glutamate; Carnosine; Histamine; L-Aspartic acid
Ascorbate and aldarate metabolism	0.0016	0.0165	3	0.25	myo-Inositol; UDP-glucose; D-Glucuronolactone; UDP-glucuronate
Phenylalanine metabolism	0.0028	0.0260	3	0.36	L-Phenylalanine; Phenylacetic acid; L-Tyrosine
Phenylalanine, tyrosine and tryptophan biosynthesis	0.0036	0.0303	2	1.00	L-Phenylalanine; L-Tyrosine

Metabolites in green and red are higher and lower versus control cells, respectively. Metabolites in black are not significantly different between control and aged cells.

Commented [CS521]: What is the relevance of the font colours – I know because you have told me, but your examiners will not. Please add detail.

Commented [CS522]: It may help if you added cross lines to the table, or introduced spaces between the pathway rows, it may help the reader

7.3.2 Age-specific differences in skeletal myotubes

After describing how replicative ageing impacts the metabolic signature of skeletal myoblasts, the effects of ageing on the metabolome of myotubes were investigated. To establish potential effects of ageing in myotubes, control and replicatively aged myotubes were compared. PCA was performed to observe the major variances in the data. PCA scores plot of PC1 (48.27%) against PC2 (28.82%) showed moderate clustering of age in terms of separation (Figure 7.9A). PC1 and PC2 explains a cumulative variance of 77.09%. Meanwhile a total of 6 components were required to explain 95% of variance in the data. When the overall metabolic profile of aged cells is considered, clustering suggests control and aged myotubes display similar variance albeit with one clearly distinct sample in the aged group.

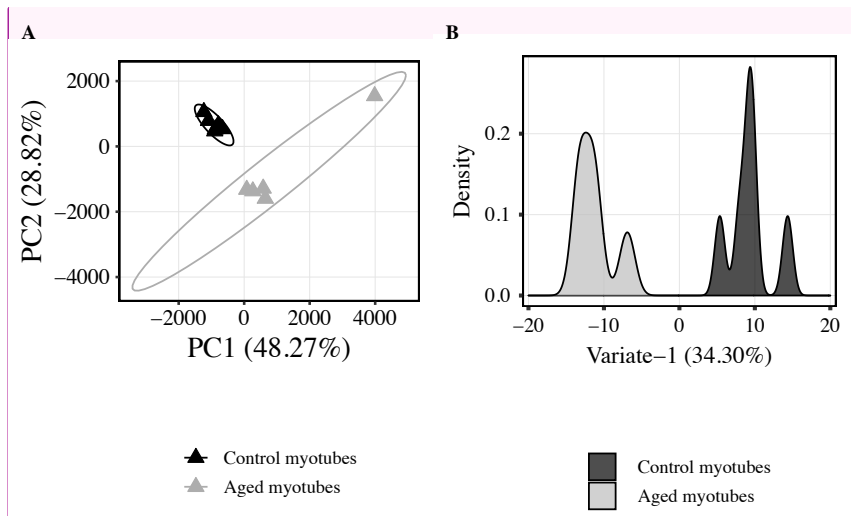


Figure 7. 9 Multivariate analyses of control and aged myotubes. Panel A) PCA scores of control vs. aged myotubes, coloured by age (control cells, black triangles in LD n=6 and aged cells, grey triangles in LD n=5). Brackets report the variance explained by the PC. Six PCs were required to achieve 95% explained variance. Only PC1 and PC2 are show in the Figure

Commented [CS523]: Have a linker e.g. summarise the key findings, as suggested above and then link those to the next steps in LD. Why are you doing the next steps?

Commented [CS524]: To me the clustering here looks better than in ED, but you have 1 outlier in the aged group. Is it therefore fair to say moderate? The young are really tightly clustered.

Commented [CS525]: Why is the profile of B in the tubes so very different from the profile of blasts e.g. what is the relevance of multiple sub-peaks?

Commented [SD526R525]: **Good question**

for simplicity/clarity. Ellipses represent 95% confidence region. Panel B) PLS-DA density plot to verify metabolite selection in myotubes discriminated by age (control, n=6 and aged, n=5). Model complexity of one variate (34.30% explained variance) was determined to be optimal.

To further identify differences in the metabolic profiles of control and aged skeletal myotubes, the differences between age were enhanced using a cross-validated PLS-DA model (Figure 7.9B). Optimal model complexity was found to be a single-variate model. Similar to the PCA plot, a tight clustering of groups can be observed. Using VIP scoring as a criterion, metabolites influential in such discrimination were extracted (see Figure 7.10).

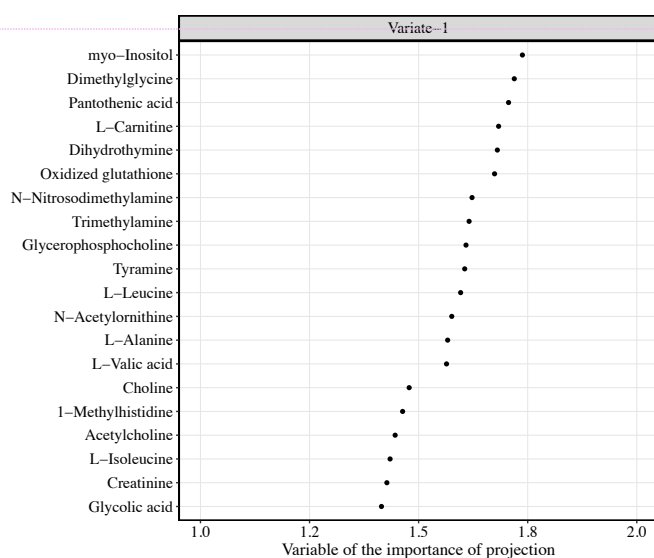


Figure 7. 10 VIP scores of PLS-DA model (ROC = 1) built on age-dependent differences in skeletal myotubes. A lower threshold of 1 was used on latent variable one to select metabolites from the model. The top 20 representative metabolites/bins are presented for clarity.

Commented [CS527]: I wonder, is it worth having a table or maybe a Venn diagram with shared metabolites from the blasts and tubes identified via VIP score – this would be interesting in terms of shared and distinct metabolites

Commented [SD528R527]: Can consider venn diagram, the appendices will contain information on vip>1 and significance etc..

Commented [MMP529]: Report the PLS-DA model quality here (via ROC score or similar). Replace the word 'variate' with the term 'latent variable' or 'component'

Upon observation of the VIP scores (Figure 7.10), metabolites most influential in explaining age-specific differences in myotubes were selected for further analyses. Metabolite levels were compared via BH adjusted t-test to gain metabolite level information on age-specific differences (see Figure 7.11). The metabolite level comparison of control and aged myotubes revealed that, Pantothenic acid, L-Carnitine, Glycerophosphocholine, L-Leucine, N-Acetylmethionine, L-Alanine, 1-Methylhistidine, L-Isoleucine, Taurine, L-Tryptophan, cis-Aconitic acid/L-Acetylcarnitine and N,N-Dimethylformamide were significantly lower in aged versus control skeletal myotubes. On the other hand, myo-Inositol, Dimethylglycine, Oxidized glutathione, Trimethylamine, Tyramine, Choline, Glycolic acid, L-Valine, L-Tyrosine, N-Alpha-acetyllysine and Pyruvic acid were significantly higher in aged versus control skeletal myotubes.

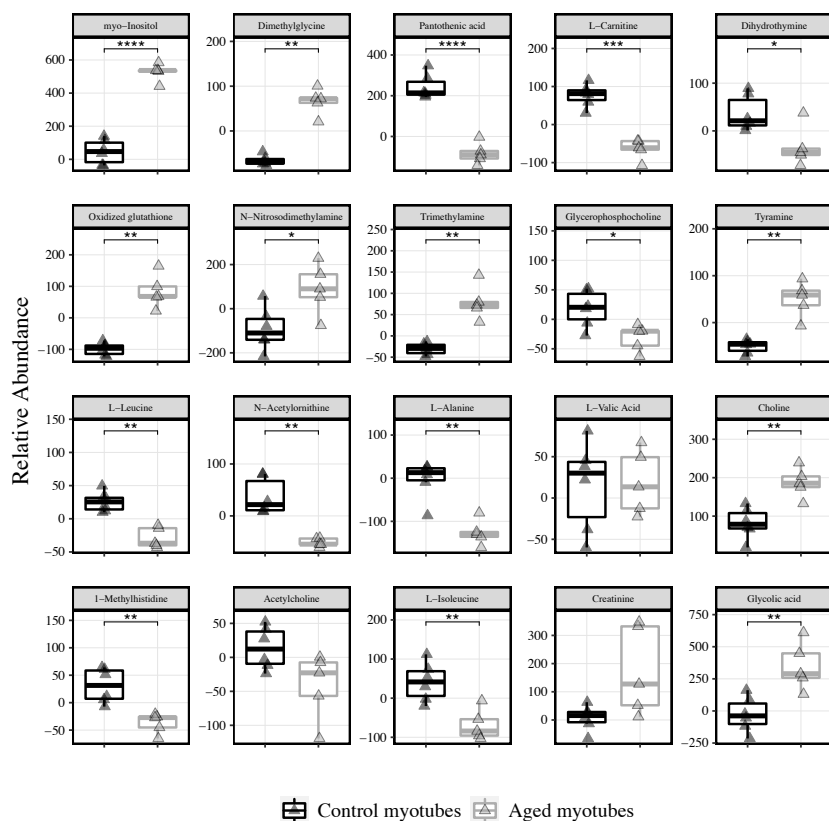


Figure 7.11 Selected metabolite boxplots of control (black outline, n=6) and aged (grey outline, n=5) skeletal myotubes. *, **, *** and **** represent *P*-value less than 0.05, 0.01, 0.001 and 0.0001, respectively. * in the boxplot title represent denotes overlapping bin.

Selected metabolites for control and aged skeletal myotubes were subjected to metabolite set enrichment analysis (MSEA) to extract further metabolic pathway level information. Table 9.3 (Chapter 9) summarises all metabolites selected for MSEA. MSEA was performed on metabolites using a database curated from the KEGG pathways (*Mus musculus* (mouse) [KEGG organism code: mmu]), using Fisher's exact test with EASE correction and BH *P*-

value adjustment for multiple testing. Three significantly over-represented pathways were identified for control and aged skeletal myotubes (see Table 7.2). Out of the three pathways, metabolites present in two pathways including aminoacyl-tRNA biosynthesis and valine, leucine and isoleucine biosynthesis were predominately lower in aged versus control skeletal myotubes.

Commented [CS530]: And so? Again, just add a brief summary line and perhaps link back to the blasts eg shared and divergent paths

Sorry, I see you have this below. Maybe reference this subsection as you generate the data above.

Table 7. 2 Pathway analysis results for control and aged skeletal myotubes. Reporting raw & BH adjusted *P* values, number of hits, pathway impact and matches.

Pathway	Raw <i>P</i> -value	BH <i>P</i> -value	Hits	Impact	Matches
Aminoacyl-tRNA biosynthesis	<0.0001	0.0006	8	0	L-Phenylalanine; L-Glutamine; L-Valine; L-Alanine; L-Leucine; L-Isoleucine; L-Tryptophan; L-Tyrosine;
Valine, leucine and isoleucine biosynthesis	0.0006	0.0250	3	0	L-Valine; L-Leucine; L-Isoleucine
Phenylalanine, tyrosine and tryptophan biosynthesis	0.0031	0.0856	2	1	L-Phenylalanine; L-Tyrosine

Metabolites in red are lower in aged versus control, whereas those in black are similar between control and aged myotubes.

7.3.3 Control vs. aged myoblasts and myotubes section summary

Following the analysis of age-specific metabolic signatures of skeletal muscle myoblasts and myotubes, it is clear that control and aged myoblasts/myotubes diverge at the metabolite level. Moreover, the age-specific differences in metabolites vary with the stage of differentiation. In skeletal myoblasts, 31 metabolites were significantly different between control and aged groups, whereas in skeletal myotubes, 26 metabolites were significantly different between control and aged groups (see Appendix Table 9.2 and 9.3, respectively). Twenty-one

metabolites were common between myoblasts and myotubes in control and aged comparisons (see Figure 7.12). Notably, the aminoacyl-tRNA biosynthesis, valine, leucine and isoleucine biosynthesis and phenylalanine, tyrosine and tryptophan biosynthesis pathways were significantly over-represented in both skeletal myoblasts and myotubes. Therefore, these pathways may capture important metabolic features of cellular ageing.

Commented [CS531]: And so? Again add a one liner relating to relevance here.
I think a venn diagram would be useful here too.

Commented [SD532R531]: Added a line of relevance

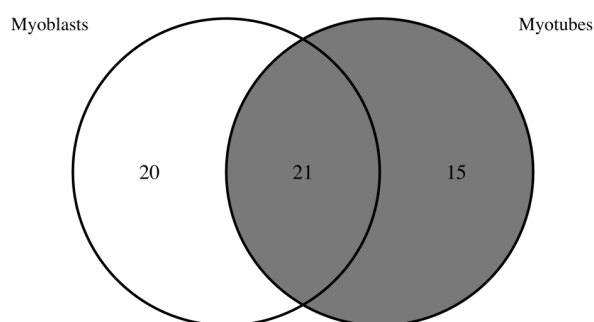


Figure 7.12 Venn diagram reporting metabolites with VIP scores >1 between control and aged myoblasts and myotubes comparisons.

7.3.4 Quercetin effects in control and aged skeletal myoblasts

Replicative ageing evoked profound changes in the metabolome of skeletal muscle myoblasts and myotubes. Considering the potential of flavonoids to modulate cellular energy metabolism, the effects of flavonoids on the metabolic signature of myoblasts and myotubes were investigated. Control and replicatively aged myoblasts were compared following 0, 5 and 10

μM Q treatment. PCA was performed to observe the major variances between all samples (Figure 7.13A). PCA scores plot of PC1 (36.09%) against PC2 (17.77%) revealed strong clustering of dose in terms of separation. PC1 and PC2 explains a cumulative variance of 53.86%. Meanwhile a total of 10 components were required to explain 95% of variance in the data. When the overall metabolic profile of myoblasts is considered, 10 μM Q treated cells are clustered more tightly compared to 5 μM Q on PC1 and PC2. This suggests cells treated with 5 μM Q have larger variation compared to those treated with 10 μM . Employing a supervised PLS-DA method, metabolites responsible for the metabolic profile differences can be extracted.

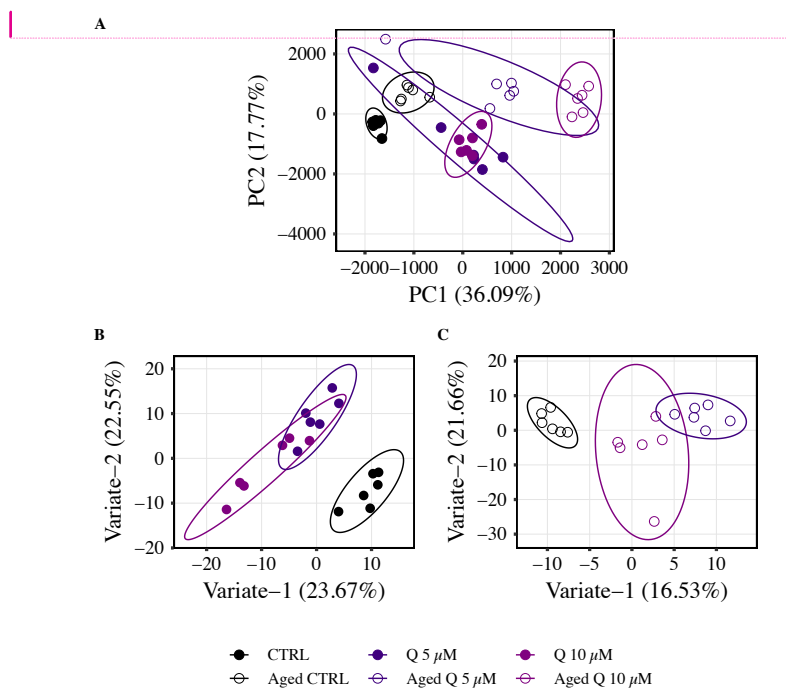


Figure 7. 13 Multivariate analysis of control and aged myoblasts +/- Q treatment. A) PCA scores of control and aged myoblasts coloured by dose. A total of ten principal components were required to achieve 95% explained variance. Brackets report the variance explained by

Commented [CS533]: Is this important? Does it suggest that there are multiple components each with little influence on variance, or could it be that a third component has a big impact also and the remainder have little influence – how can this be detailed and does it matter or am I reading too much into things?

Commented [SD534R533]: Good question. Third component could also have meaningful contribution but this will be less than PC1 and PC2

Commented [CS535]: Is there any relevance to the controls being to the left or right of the treatment groups?

Commented [CS536]: Is it ok to have PC1 and PC2 ~38%? What else is explaining the majority of the variance?

Commented [CS537]: It is good that the Qs overlap with each other and interesting that they differ from the cons for both aged and con. Also interesting that the aged con overlaps with the control Q. Is this telling us anything??

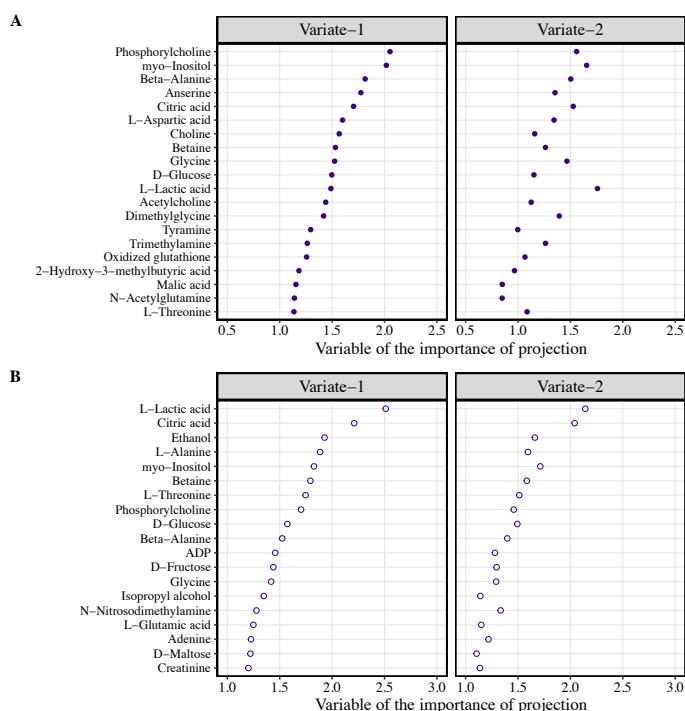
Commented [CS538]: It is hard to see the differences in the colours, particularly for the aged – could you use different symbol shapes or more distinct colours?

the PC. Only PC1 and PC2 are shown in the Figure for simplicity/clarity. Ellipses represent 95% confidence region. B) PLS-DA scores of control- and C) aged-myoblasts coloured by dose. A model complexity of two variates was employed for control and aged myoblasts. Closed and open circles represent control and aged cells, respectively.

In order to identify distinctions in the metabolic profiles, the differences between treatments were enhanced in control and aged cells using a cross-validated PLS-DA model. Optimal model complexity was found to be a two-variate model for control and aged myoblasts. Figure 7.13B and 7.13C shows the scores of these models with variate-1 plotted against variate-2 for simplicity. Similar to the PCA plot (Figure 7.13A), a tight clustering of groups can be observed. The PLS-DA model achieved a better separation between 5 μ M Q and CTRL groups in aged cells. To examine the metabolite level information, VIP scores of the PLS-DA model were calculated (see Figure 7.14).

Commented [CS539]: Is this the same as bivariate?
How is this decided?

Commented [SD540R539]: Decided based on model validation – decreasing the overall error rate of the model without trying to overfit the data. 'k-fold': 5-fold cross-validation repeated x times



Commented [CS541]: What do the different patterns for variate 1 vs 2 mean?

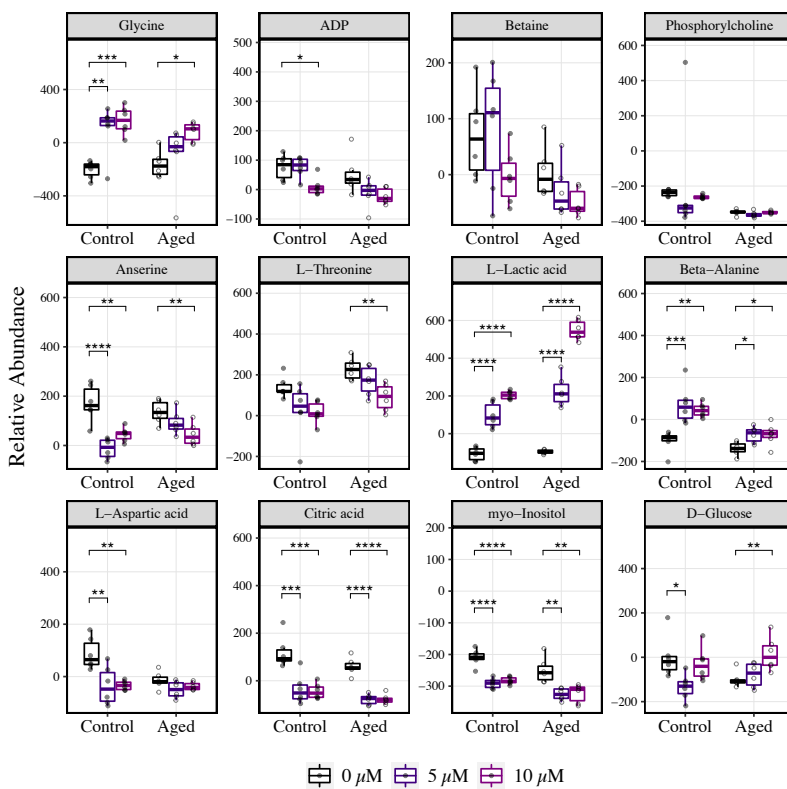
Again, is it worth doing a Venn diagram for shared and separate metabolites in con vs aged?

Figure 7.14 VIP scores of PLS-DA model built on Q treatment-dependent differences in A) control- and B) aged- skeletal myoblasts. AUC scores for control myoblasts were 0.986, 0.972 and 0.486, and 1.0, 0.5 and 1.0 for aged myoblasts for 0 μM vs. others, 5 μM vs. others and 10 μM vs. others, respectively. A lower threshold of 1 was used on latent variable one and two to select metabolites from the model. The top 20 metabolites/bins are presented for clarity.

Upon metabolite selection of treatment-specific differences, metabolite levels of control and aged myoblasts in response to 0, 5 and 10 μM Q were compared via two-way ANOVA, followed by a Tukey's HSD pairwise test and shown via boxplots (Figure 7.15). Statistical analyses of the metabolite-level comparisons can be found in Table 9.16 (Chapter 9). From the metabolite-level comparison in control cells, Glycine, Dimethylglycine, Trimethylamine, L-Lactic acid and Beta-Alanine were significantly higher following 5 and 10 μM Q treatment

versus CTRL conditions. Whereas L-Aspartic acid, Citric acid and myo-Inositol were significantly lower following 5 and 10 μM Q treatment versus CTRL. In aged cells, L-Lactic acid and Beta-Alanine were significantly higher after 5 and 10 μM Q compared with CTRL. On the other hand, Ethanol, Citric acid and myo-Inositol were significantly lower after 5 and 10 μM Q versus CTRL conditions.

Commented [CS542]: Same comment as in blasts re lists. Do you actually need this, if the data are in the box plots?



Commented [CS543]: It is interesting to note, that despite the fold changes for each metabolite, the patterns of change within a metabolite are similar between con and aged e.g. if q reduces in con it reduces in aged and vice versa. So the type of response is the same, even if the magnitude differs. Also interesting to note that there is a nice dose response in some, but not in others.

Commented [CS544]: If you change the colours in the graphs above, please also change in all graphs for consistency

Figure 7.15 Selected metabolite boxplots of control and aged skeletal myoblasts following 0, 5 and 10 μM Quercetin treatment. *, **, *** and **** represent P -value less than 0.05, 0.01, 0.001 and 0.0001, respectively. * in the boxplot title represent denotes overlapping bin.

Selected metabolites for Q-treated control and aged skeletal myoblasts were subjected to MSEA to extract further metabolic pathway level information. Tables 7.3-7.4 summarises the metabolites selected for Q-treated control and aged myoblasts, respectively. MSEA was performed on selected metabolites using a database curated from the KEGG pathways (Mus musculus (mouse) [KEGG organism code: mmu]). MSEA was performed using Fisher's exact test with EASE correction and BH *P*-value adjustment for multiple testing. Two and four significantly over-represented pathways were identified for control and aged skeletal myoblasts, respectively (Table 7.3 and 7.4, respectively). Out of the significant pathways, glycine, serine and threonine metabolism and glyoxylate and dicarboxylate metabolism were common amongst control and aged myoblasts.

Table 7. 3 Pathway analysis results for control skeletal muscle myoblasts treated with Q. Reporting raw & BH adjusted P values, number of hits, pathway impact and matches.

Pathway	Raw <i>P</i> -value	BH <i>P</i> -value	Hits	Impact	Matches
Glycine, serine and threonine metabolism	<0.0001	0.0007	6	0.62	L-Serine; Choline; Betaine; N,N-Dimethylglycine; Glycine; L-Threonine
Glyoxylate and dicarboxylate metabolism	0.0013	0.0557	4	0.20	cis-Aconitate; Citrate; L-Serine; Glycine

Metabolites in green and red are higher and lower (with both 5 and 10 μ M Q) versus CTRL conditions, respectively. Metabolites in black are not significantly different between conditions (consistently with 5 and 10 μ M Q vs. CTRL).

Table 7. 4 Pathway analysis results for aged skeletal muscle myoblasts treated with Q. Reporting raw & BH adjusted *P* values, number of hits, pathway impact and matches.

Pathway	Raw <i>P</i> -value	BH <i>P</i> -value	Hits	Impact	Matches
Aminoacyl-tRNA biosynthesis	<0.0001	0.0032	6	0.00	Glycine; L-Valine; L-Alanine; L-Leucine; L-Threonine; L-Glutamate
Valine, leucine and isoleucine biosynthesis	0.0001	0.0061	3	0.00	L-Threonine; L-Leucine; L-Valine
Alanine, aspartate and glutamate metabolism	0.0006	0.0156	4	0.20	L-Alanine; L-Glutamate; Citrate; Pyruvate
Glyoxylate and dicarboxylate metabolism	0.0009	0.0197	4	0.14	Glycine; Citrate; L-Glutamate; Pyruvate;
Glycine, serine and threonine metabolism	0.0012	0.0200	4	0.34	Glycine; Betaine; L-Threonine; Pyruvate

Metabolites in red are lower (with both 5 and 10 μ M Q) versus CTRL conditions, respectively. Metabolites in black are not significantly different between conditions (consistently with 5 and 10 μ M Q vs. CTRL).

7.3.5 Quercetin effects in control and aged skeletal myotubes

To establish potential effects of quercetin treatment in myotubes, control and replicatively aged myotubes were compared. PCA was performed to observe the major variances between all samples (Figure 7.16A). PCA scores plot of PC1 (37.04%) against PC2 (14.75%) revealed strong clustering of dose in terms of separation. PC1 and PC2 explains a cumulative variance of 51.79%. Meanwhile a total of 12 components were required to explain 95% of variance in the data. When the overall metabolic profile of myotubes is considered, 5 μ M Q treatment

Commented [CS545]: Is there an absence of colour for a reason?

Commented [SD546R545]: Yes, I thought that now there multiple conditions, colour coding will not be suitable, because I would need different shades for whether 5 or 10 μ M are increased or decreased vs. CTRL condition. Hopefully the boxplots will suffice to provide reader the direction of changes, as well as appendices showing direction of change if significant

Commented [MMP547R545]: Perhaps show colours where 5 and 10uM are showing the same direction of change with respect to control (I think only citrate is more complicated)

Commented [CS548]: What explains the remaining 50%?

Commented [SD549R548]: The remaining principle components

Commented [CS550]: So 50% of the variability is derived from another 10 components is that good/bad/indifferent? How do these things normally look?

resulted in tighter clustering compared to CTRL on PC1 and PC2. This suggests untreated CTRL myotubes have greater variation compared to the 5 μM Q condition. Employing a supervised PLS-DA method, metabolites responsible for the metabolic profile differences can be extracted.

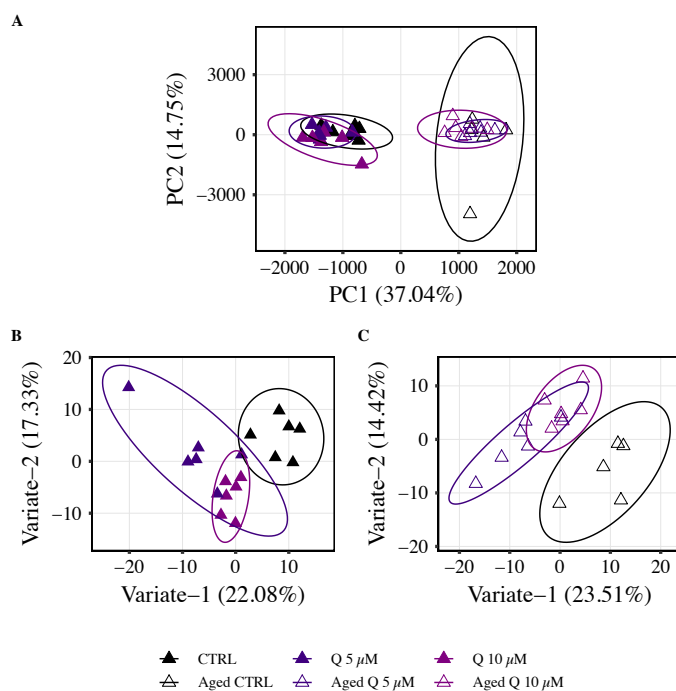


Figure 7. 16 Multivariate analysis of control and aged cells myotubes +/- Quercetin treatment. A) PCA scores of control and aged myotubes coloured by dose. A total of twelve principal components were required to achieve 95% explained variance. Brackets report the variance explained by the PC. Only PC1 and PC2 are shown in the Figure for simplicity/clarity. Ellipses represent 95% confidence region. B) PLS-DA scores of control- and C) aged-myotubes coloured by dose. A model complexity of two variates was employed for control and aged myotubes. Closed and open triangles represent control and aged cells, respectively.

In order to identify differences in the metabolic profiles, the differences between treatments in control and aged cells were enhanced using a cross-validated PLS-DA model. Optimal model complexity was found to have two- and four-components for control and aged myotubes, respectively. Figure 7.16B and 7.16C shows the scores of this model with component-1 plotted against component-2 for simplicity. Compared to the PCA plot (Figure 7.16A), a tighter clustering of groups can be observed. A clearer separation of Q treatment from CTRL can be seen along a diagonal of component-1 and component-2. Therefore, the supervised PLS-DA model was able to discriminate between treatments in control and aged myotubes, but this was not comparable to PCA. Using VIP scoring as a criterion, metabolites influential in such discrimination were extracted (see Figure 7.17).

Commented [MMP551]: As PLS-DA uses group information to produce the model this is expected (PCA just shows largest separation between samples – irrespective of groups). Therefore it would be better to rephrase this as PCA and PLSDA aren't directly comparable

Commented [CS552]: If 4 variates needed for aged, why are data from only 2 presented?

Same as before re Venn diagram

Commented [SD553R552]: For clarity of presentation, 2 variates are presented.

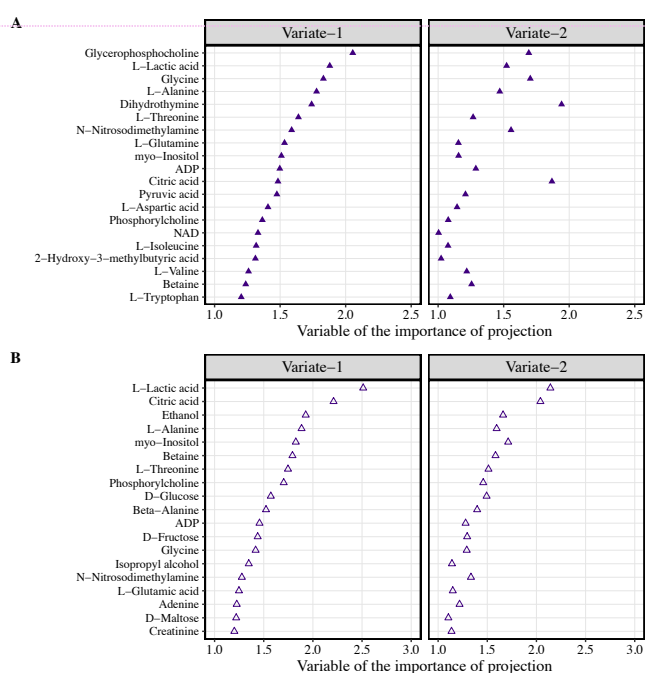


Figure 7.17 VIP scores of PLS-DA model built on Q treatment-dependent differences in A) control- and B) aged- skeletal myotubes. AUC scores for control myotubes were 1.0, 0.583 and

Commented [MMP554]: Report validation quality score (ROC?) here. Replace the word 'variate' with the term 'latent variable' or 'component'

0.912, and 0.917, 0.576 and 0.955 for aged myotubes for 0 μM vs. others, 5 μM vs. others and 10 μM vs. others, respectively. A lower threshold of 1 was used on latent variable one and two to select metabolites from the model. The top 20 metabolites/bins are presented for clarity.

Upon metabolite selection of treatment-specific differences, metabolite levels of control and aged myotubes in response to 0, 5 and 10 μM Q were compared via two-way ANOVA, followed by a Tukey's HSD pairwise test and shown via boxplots (Figure 7.18). Statistical analyses of the metabolite-level comparisons can be found in Table 9.17 (Chapter 9). From the metabolite-level comparison in control myotubes, Glycine, Isopropyl alcohol and L-Tyrosine were significantly higher following 5 and 10 μM Q compared to untreated CTRL. Whereas Phosphorylcholine was significantly lower following 5 and 10 μM Q versus CTRL. In CTRL aged myotubes, L-Tyrosine was significantly higher, whilst Phosphorylcholine and myo-Inositol were significantly lower after 5 and 10 μM Q treatment.

Commented [CS555]: As before

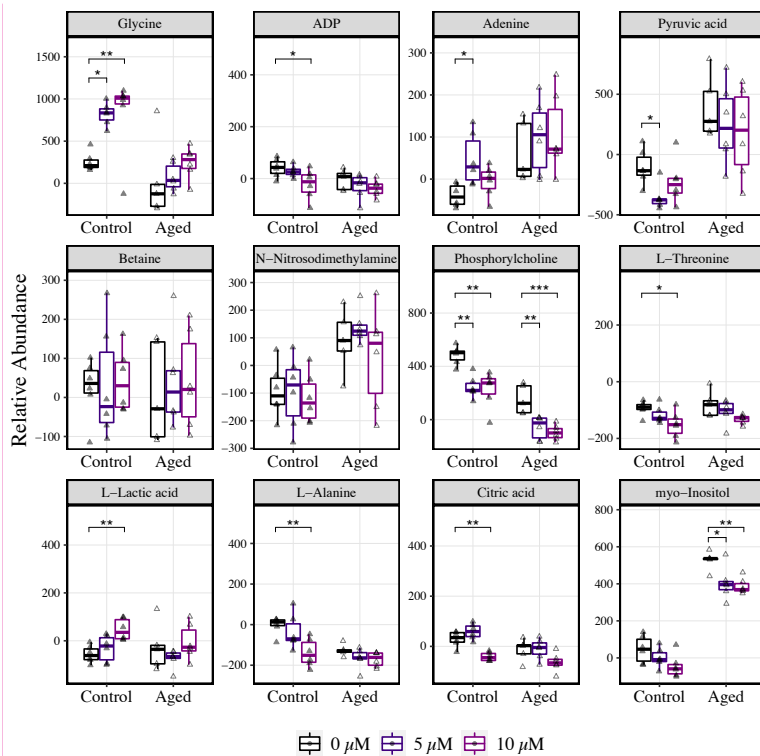


Figure 7.18 Selected metabolite boxplots of control and aged myotubes following 0, 5 and 10 μM Quercetin treatment. *, ** and *** represent P -value less than 0.05, 0.01 and 0.001, respectively. * in the boxplot title represent denotes overlapping bin.

Selected metabolites for Q-treated control and aged skeletal myotubes were subjected to MSEA to extract further metabolic pathway level information. Tables 7.5-7.6 summarise the metabolites selected for Q-treated cells in late differentiation. MSEA was performed on selected metabolites using a database curated from the KEGG pathways (Mus musculus (mouse) [KEGG organism code: mmu]). MSEA was performed using Fisher's exact test with EASE correction and BH P -value adjustment for multiple testing. Seven significantly over-represented pathways were identified for control and aged skeletal myotubes (Table 7.5 and

Commented [CS556]: Again similar profiles, generally.

Worth comparing the Q data from the box plots of blasts vs tubes – just for the metabolites impacted?

7.6, respectively). Out of the significant pathways, alanine, aspartate and glutamate metabolism, aminoacyl-tRNA biosynthesis, glyoxylate and dicarboxylate metabolism and glycine, serine and threonine metabolism were common amongst control and aged myotubes after Q treatment.

Commented [CS557]: Could this be shown better by a Venn diagram? No one will remember the text of a list of substances, but may remember a picture and certainly will be able to better compare pictures.

Table 7. 5 Pathway analysis results for control skeletal muscle myotubes treated with Q. Reporting raw & BH adjusted *P* values, number of hits, pathway impact and matches.

Pathway	Raw <i>P</i> -value	BH <i>P</i> -value	Hits	Impact	Matches
Aminoacyl-tRNA biosynthesis	<0.0001	<0.0001	10	0.00	L-Glutamine; Glycine; L-Aspartate; L-Valine; L-Alanine; L-Isoleucine; L-Leucine; L-Threonine; L-Tryptophan; L-Tyrosine
Valine, leucine and isoleucine biosynthesis	<0.0001	0.0001	4	0.00	L-Threonine; L-Leucine; L-Isoleucine; L-Valine
Alanine, aspartate and glutamate metabolism	0.0001	0.0063	5	0.34	L-Aspartate; L-Alanine; L-L-Glutamine; Citrate; Pyruvate
Glyoxylate and dicarboxylate metabolism	0.0002	0.0122	5	0.16	cis-Aconitate; Citrate; Glycine; Pyruvate; L-Glutamine
Arginine biosynthesis	0.0015	0.1174	3	0.00	N-Acetylmethionine; L-Aspartate; L-Glutamine
Glycine, serine and threonine metabolism	0.0023	0.1801	4	0.34	Betaine; Glycine; L-Threonine; Pyruvate
Citrate cycle (TCA cycle)	0.0043	0.3346	3	0.19	cis-Aconitate; Citrate; Pyruvate

Commented [CS558]: Same comment as for table above – if colour should be added, please do so for all tables. I will not ask again.

Metabolites in green are higher (with both 5 and 10 μM Q) versus CTRL conditions. Metabolites in black are not significantly different between conditions (consistently with 5 and 10 μM Q vs. CTRL).

Table 7. 6 Pathway analysis results for aged skeletal muscle myotubes treated with Q. Reporting raw & BH adjusted *P* values, number of hits, pathway impact and matches.

Pathway	Raw <i>P</i> -value	BH <i>P</i> -value	Hits	Impact	Matches
Alanine, aspartate and glutamate metabolism	<0.0001	0.0027	5	0.40	N-Acetyl-L-aspartate; L-Alanine; L-Glutamate; L-Glutamine; Citrate
Aminoacyl-tRNA biosynthesis	0.0005	0.0196	5	0.17	L-Glutamine; L-Serine; L-Alanine; L-Threonine; L-Glutamate
Glyoxylate and dicarboxylate metabolism	0.0009	0.0249	4	0.07	Citrate; L-Serine; L-Glutamate; L-Glutamine
Glycine, serine and threonine metabolism	0.0012	0.0249	4	0.23	L-Serine; Choline; L-Threonine; Creatine
Glycerophospholipid metabolism	0.0015	0.0249	4	0.08	Choline phosphate; Choline; Acetylcholine; sn-Glycero-3-phosphocholine
Nitrogen metabolism	0.0030	0.0354	2	0.00	L-Glutamate; L-Glutamine
D-Glutamine and D-glutamate metabolism	0.0030	0.0354	2	0.50	L-Glutamate; L-Glutamine

Metabolites in black are not significantly different between conditions (consistently with 5 and 10 μ M Q vs. CTRL).

7.3.6 Summary of Q effects upon the metabolome of control and aged myoblasts and myotubes

Acute Q treatment evoked shared and distinct changes in the metabolome of control and aged myoblasts. Pathways commonly impacted by Q between control and aged myoblasts included glycine, serine and threonine metabolism and glyoxylate and dicarboxylate metabolism. In

control and aged myotubes, pathways commonly impacted by Q treatment included alanine, aspartate and glutamate metabolism, aminoacyl-tRNA biosynthesis, glyoxylate and dicarboxylate metabolism and glycine, serine and threonine metabolism. Four metabolites commonly represented in control and aged myoblast and myotubes in the presence of Q were Citric acid, L-Threonine, myo-Inositol and Phosphorylcholine (see Figure 7.19).

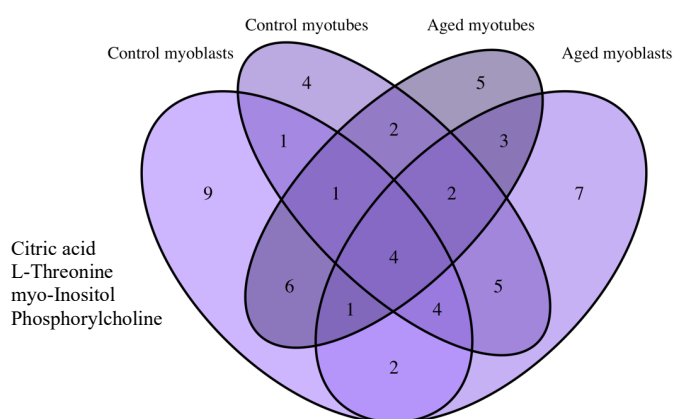


Figure 7. 19 Venn diagram reporting metabolites with VIP scores >1 between control and aged myoblasts and myotubes following Q treatment. Four metabolites were commonly represented between ages and differentiation stage (myoblast vs. myotube).

7.3.7 EGCG effects in control and aged skeletal myoblasts

[To] establish potential effects of EGCG treatment in myoblasts, control and replicatively aged cells were compared. PCA (Figure 7.20A) was performed to observe the major variances between all samples. PCA scores plot of PC1 (40.94%) against PC2 (16.04%) revealed moderate clustering of dose in terms of separation. PC1 and PC2 explains a cumulative

Commented [CS559]: As before, add a sentence for justification of the next flavonoid.

variance of 56.98%. Meanwhile a total of 12 components were required to explain 95% of variance in the data. When the overall metabolic profile of EGCG treated myoblasts is considered, 10 μ M EGCG-treated control cells were clustered tighter on PC1, but less on PC2, compared to CTRL and 5 μ M conditions. This suggests dose-dependent effects of EGCG on metabolic profiles of control myoblasts. Employing a supervised PLS-DA method, metabolites responsible for the metabolic profile differences can be extracted.

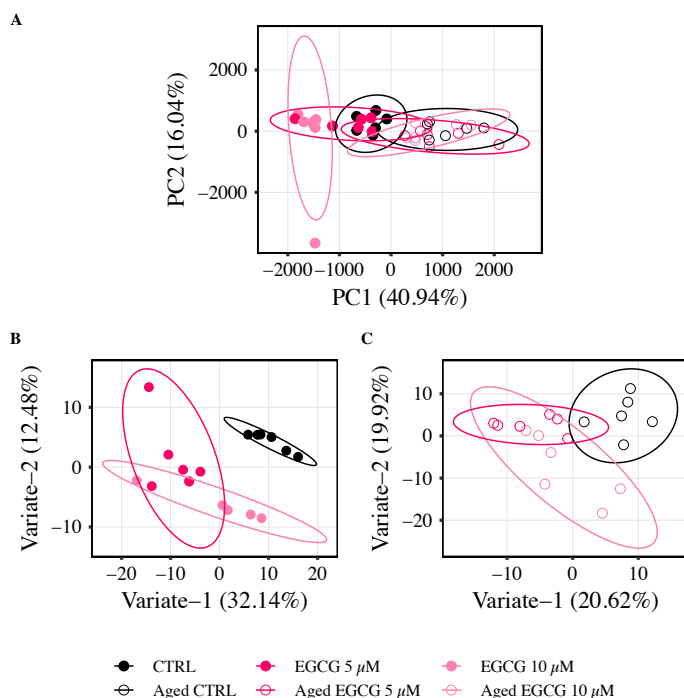


Figure 7.20 Multivariate analysis of control and aged myoblasts +/- EGCG treatment. A) PCA scores of control and aged myoblasts coloured by dose. A total of twelve principal components were required to achieve 95% explained variance. Brackets report the variance explained by the PC. Only PC1 and PC2 are shown in the Figure for simplicity/clarity. Ellipses represent 95% confidence region. B) PLS-DA scores of control- and, C) aged-myoblasts, coloured by dose. A model complexity of three- and two-components was employed for of control and aged myoblasts, respectively. Closed and open circles represent control and aged cells, respectively.

In order to identify differences in the metabolic profiles, the differences between conditions were enhanced using a cross-validated PLS-DA model. Optimal model complexity was found to be three and two-variates for control and aged myoblasts, respectively. Figure 7.20B and 7.20C shows the scores of this model with component-1 plotted against component-2 for simplicity. As expected, the supervised model exhibits a tighter clustering of groups compared to the PCA plot (Figure 7.20A). The PLS-DA model achieved a better separation between CTRL and EGCG treatment groups in control and aged myoblasts, but this was not comparable to PCA. Using VIP scoring as a criterion, metabolites influential in such discrimination were extracted (see Figure 7.21).

Commented [CS560]: Again, is this ok, if you have more than 2 variates? How do you decide which to plot?

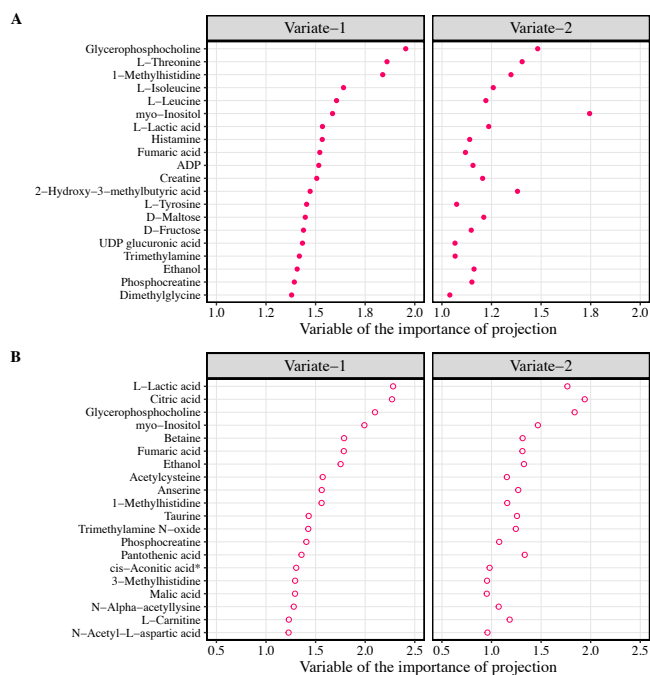


Figure 7. 21 VIP scores of PLS-DA model built on EGCG treatment-dependent differences in A) control- and B) aged- skeletal myoblasts. AUC scores for control myoblasts were 0.944, 0.889 and 0.556, and 0.972, 0.625 and 0.847 for aged myoblasts for 0 μ M vs. others, 5 μ M vs. others and 10 μ M vs. others, respectively. A lower threshold of 1 was used on latent variable one and two to select metabolites from the model. The top 20 representative metabolites/bins are presented for clarity.

Upon metabolite selection of treatment-specific differences, metabolite levels of control and aged myoblasts in response to 0, 5 and 10 μ M EGCG were compared via two-way ANOVA, followed by a Tukey's HSD pairwise test and shown via boxplots (Figure 7.22). Statistical analyses of the metabolite-level comparisons can be found in Table 9.17 (Chapter 9). From the metabolite-level comparison in control myoblasts, Phosphorylcholine, L-Lactic acid, D-Maltose and myo-Inositol were significantly higher with 5 and 10 μ M EGCG treatment compared with CTRL. Whereas 1-Methylhistidine and L-Threonine abundance were significantly lower with 5 and 10 μ M EGCG compared to untreated CTRL. When comparing metabolite levels in aged myoblasts, L-Lactic acid and Citric acid were significantly higher and lower compared to CTRL with 5 and 10 μ M EGCG, respectively.

Commented [MMP561]: Report validation quality score (ROC?) here. Replace the word 'variate' with the term 'latent variable' or 'component'

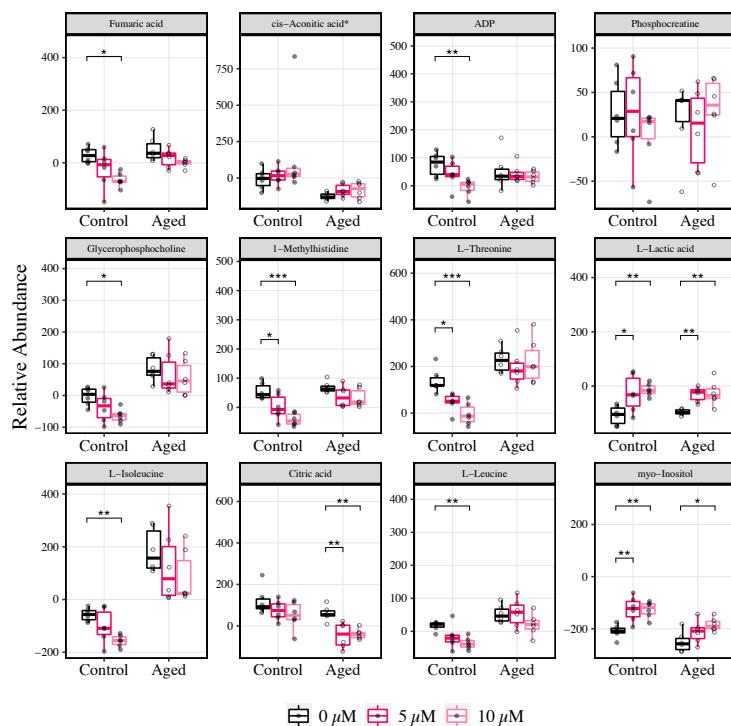


Figure 7.22 Selected metabolite boxplots of control and aged skeletal myoblasts following 0, 5 and 10 μM EGCG treatment. *, ** and *** represent P -values less than 0.05, 0.01 and 0.001, respectively. * in the boxplot title represent denotes overlapping bin. Closed and open circles represent control and aged cells, respectively.

Selected metabolites for EGCG-treated control and aged skeletal myoblasts were subjected to MSEA to extract further metabolic pathway level information. Table 7.7-7.8 summarises the metabolites selected for EGCG-treated cells in early differentiation. MSEA was performed on selected metabolites using a database curated from the KEGG pathways (Mus musculus (mouse) [KEGG organism code: mmu]). MSEA was performed using Fisher's exact test with EASE correction and BH P -value adjustment for multiple testing. Three and one significantly over-represented pathway(s) were identified for control and aged skeletal myoblasts,

respectively (Table 7.7 and 7.8). Out of the pathways, none were commonly represented amongst EGCG treated control and aged myoblasts.

Commented [CS562]: Again, at the end, it will be interesting to see what is and what is not shared with the different treatments, ages and phenotypes.

Table 7.7 Pathway analysis results for control skeletal myoblasts treated with EGCG. Reporting raw & BH adjusted *P* values, number of hits, pathway impact and matches.

Pathway	Raw <i>P</i> -value	BH <i>P</i> -value	Hits	Impact	Matches
Aminoacyl-tRNA biosynthesis	<0.0001	0.0008	8	0.17	L-Phenylalanine; L-Serine; L-Valine; L-Isoleucine; L-Leucine; L-Threonine; L-Tryptophan; L-Tyrosine
Valine, leucine and isoleucine biosynthesis	<0.0001	0.0008	4	0.00	L-Threonine; L-Leucine; L-Isoleucine; L-Valine
Glycine, serine and threonine metabolism	0.0011	0.0315	5	0.34	L-Serine; Betaine; N,N-Dimethylglycine; L-Threonine; Creatine
Phenylalanine metabolism	0.0026	0.0542	3	0.36	L-Phenylalanine; Phenylacetic acid; L-Tyrosine
Phenylalanine, tyrosine and tryptophan biosynthesis	0.0034	0.0574	2	1.00	L-Phenylalanine; L-Tyrosine

Commented [MMP563]: Again you could add colours for those treatments that show the same trend with respect to control

Metabolites in black are not significantly different between conditions (consistently with 5 and 10 μ M EGCG vs. CTRL).

Table 7.8 Pathway analysis results for aged skeletal myoblasts treated with EGCG. Reporting raw & BH adjusted *P* values, number of hits, pathway impact and matches.

Pathway	Raw <i>P</i> -value	BH <i>P</i> -value	Hits	Impact	Matches
Alanine, aspartate and glutamate metabolism	0.0003	0.0213	5	0.29	N-Acetyl-L-aspartate; L-Alanine; L-Glutamate; Citrate; Fumarate

Metabolites in red are lower (with both 5 and 10 μM EGCG) versus CTRL conditions. Metabolites in black are not significantly different between conditions (consistently with 5 and 10 μM EGCG vs. CTRL).

7.3.8 EGCG effects in control and aged skeletal myotubes

To establish potential effects of EGCG treatment myotubes, control and replicatively aged myotubes were compared. PCA (Figure 7.23A) was performed to observe the major variances between all samples. PCA scores plot of PC1 (27.19%) against PC2 (19.04%) revealed moderate clustering of dose in terms of separation. PC1 and PC2 explains a cumulative variance of 46.23%. Meanwhile a total of 11 components were required to explain 95% of variance in the data. When the overall metabolic profile of myotubes treated with EGCG is considered, 5 μM EGCG treatment resulted in tighter clustering on PC2 compared to 10 μM . This suggests 5 μM EGCG resulted in less variation compared to 10 μM EGCG in myotubes. Employing a supervised PLS-DA method, metabolites responsible for the metabolic profile differences can be extracted.

Commented [CS564]: Why?

Commented [CS565]: Why is that there generally seems to be more overlap of con with treatment in tubes vs blasts, regardless of treatment?

Commented [SD566R565]:

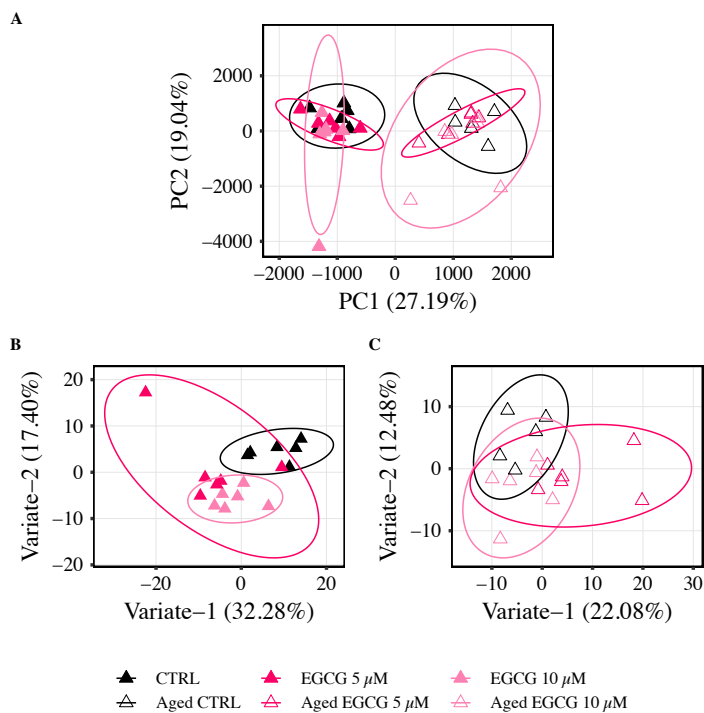


Figure 7.23 Multivariate analysis of control and aged myotubes +/- EGCG treatment. A) PCA scores of control and aged myotubes coloured by dose. A total of eleven principal components were required to achieve 95% explained variance. Brackets report the variance explained by the PC. Only PC1 and PC2 are shown in the Figure for simplicity/clarity. Ellipses represent 95% confidence region. B) PLS-DA scores of control myotubes and C) aged myotubes, coloured by dose. A model complexity of three variates was employed. Closed and open triangles represent control and aged cells, respectively.

In order to identify differences in the metabolic profiles, the differences between conditions were enhanced using a cross-validated PLS-DA model. Optimal model complexity was found to be three-variates for control and aged myotubes. Figure 7.23B and 7.23C shows the scores of this model with variate-1 plotted against variate-2 for simplicity. Compared to the PCA plot

(Figure 7.23A), a tighter clustering of groups can be observed. The PLS-DA model achieved a better separation between CTRL and EGCG treatment, especially in control myotubes, but this was not comparable to PCA. Notably, EGCG treatment was not fully decoupled from untreated CTRL in aged cells, indicating the higher degree of similarity between these conditions. Using VIP scoring as a criterion, metabolites influential in discrimination between groups were extracted (see Figure 7.24).

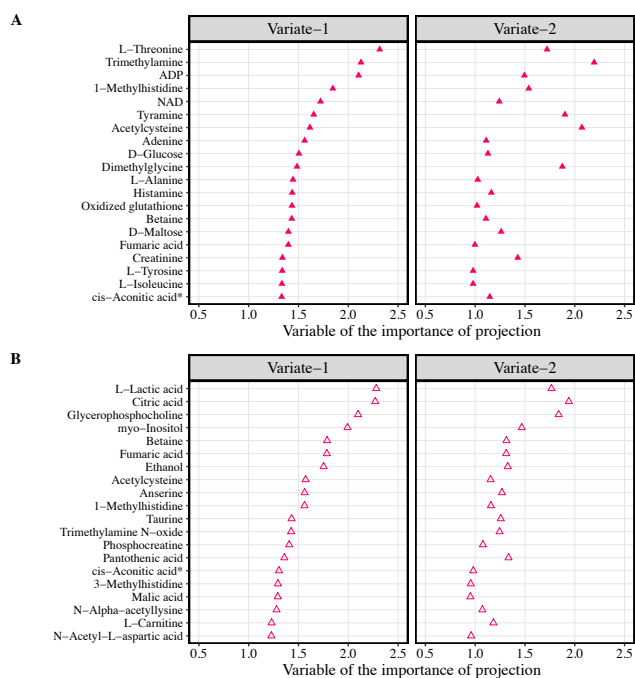
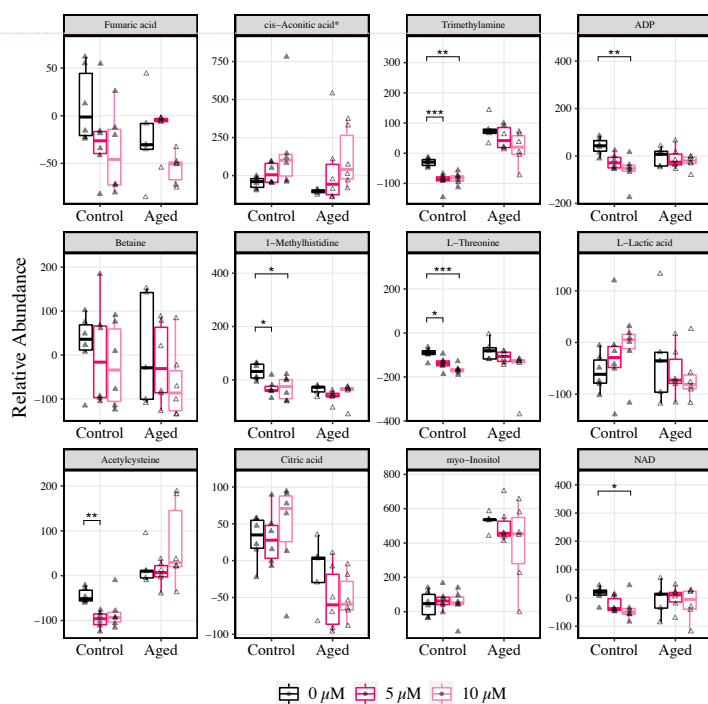


Figure 7.24 VIP scores of PLS-DA model built on EGCG treatment-dependent differences in A) control- and B) aged- skeletal myotubes. AUC scores for control myotubes were 0.931, 0.583 and 0.843, and 0.750, 0.727 and 0.955 for aged myotubes for 0 μ M vs. others, 5 μ M vs. others and 10 μ M vs. others, respectively. A lower threshold of 1 was used on latent variable one and to select metabolites from the model. The top representative 20 metabolites/bins are presented for clarity.

Commented [MMP567]: Report validation quality score (ROC?) here. Replace the word 'variate' with the term 'latent variable' or 'component'

Upon metabolite selection of treatment-specific differences, metabolite levels of control and aged myotubes in response to 0, 5 and 10 μM EGCG were compared via two-way ANOVA, followed by a Tukey's HSD pairwise test and shown via boxplots (Figure 7.25). Statistical analyses of the metabolite-level comparisons can be found in Table 9.19 (Chapter 9). From the metabolite-level comparison in control myotubes, Trimethylamine, 1-Methylhistidine, L-Threonine and Tyramine were significantly lower following 5 and 10 μM EGCG when compared with CTRL. In aged myotubes, Isopropyl alcohol abundance was significantly lowered with 10 μM EGCG versus CTRL.



Commented [CS568]: Do you determine the y axis scale?

Commented [SD569R568]: Used a 'free yscale' so that individual metabolites can be better represented in bar charts

Figure 7.25 Selected metabolite boxplots of control and aged skeletal myotubes following 0, 5 and 10 μM EGCG treatment. *, ** and *** represent P -values less than 0.05, 0.01 and 0.001, respectively. * in the boxplot title represent denotes overlapping bin. Closed and open triangles represent control and aged cells, respectively.

Selected metabolites for EGCG-treated control and aged skeletal myotubes were subjected to MSEA to extract further metabolic pathway level information. Table 7.9-7.10 summarises the metabolites selected for EGCG-treated cells in late differentiation. MSEA was performed on selected metabolites using a database curated from the KEGG pathways (Mus musculus (mouse) [KEGG organism code: mmu]). MSEA was performed using Fisher's exact test with EASE correction and BH *P*-value adjustment for multiple testing. Four and one significantly over-represented pathway(s) were identified for control and aged skeletal myotubes, respectively (Table 7.9 and 7.10). Out of the significant pathways, aminoacyl-tRNA biosynthesis was commonly represented between EGCG treated control and aged myotubes.

Table 7. 9 Pathway analysis results for control skeletal myotubes treated with EGCG. Reporting raw & BH adjusted *P* values, number of hits, pathway impact and matches.

Pathway	Raw <i>P</i> -value	BH <i>P</i> -value	Hits	Impact	Matches
Aminoacyl-tRNA biosynthesis	0.0001	0.0061	7	0.00	L-Phenylalanine; L-Valine; L-Isoleucine; L-Leucine; L-Threonine ; L-Tryptophan; L-Tyrosine
Valine, leucine and isoleucine biosynthesis	0.0006	0.0242	3	0.00	L-Threonine ; L-Leucine; L-Isoleucine
Glycine, serine and threonine metabolism	0.0009	0.0242	5	0.16	Betaine; Guanidinoacetate; N,N-Dimethylglycine; L-Threonine ; Creatine
Phenylalanine metabolism	0.0022	0.0461	3	0.36	L-Phenylalanine; Phenylacetic acid; L-Tyrosine
Phenylalanine, tyrosine and tryptophan biosynthesis	0.0031	0.0514	2	1.00	L-Phenylalanine; L-Tyrosine

Metabolites in **red** are lower (with both 5 and 10 μ M EGCG) versus CTRL conditions. Metabolites in black are not significantly different between conditions (consistently with 5 and 10 μ M EGCG vs. CTRL).

Table 7. 10 Pathway analysis results for aged skeletal myotubes treated with EGCG. Reporting raw & BH adjusted *P* values, number of hits, pathway impact and matches.

Pathway	Raw <i>P</i> -value	BH <i>P</i> -value	Hits	Impact	Matches
Aminoacyl-tRNA biosynthesis	<0.0001	0.0009	8	0.00	L-Phenylalanine; L-Glutamine; Glycine; L-Alanine; L-Isoleucine; L-Threonine; L-Tryptophan; L-Tyrosine

Metabolites in black are not significantly different between conditions (consistently with 5 and 10 μM EGCG vs. CTRL).

Commented [CS570]: Except for threonine, none of these are in the box plots – why the difference?

Commented [SD571R570]: Those metabolites with VIP scores > 1 are entered into the pathway representation analysis

7.3.9 Summary of EGCG effects upon the metabolome of control and aged myoblasts and myotubes

Acute EGCG treatment evoked changes in the metabolite signatures of control and aged myoblasts and myotubes. No pathways were overrepresented with EGCG treatment in control and aged myoblasts. However, metabolites involved in energy metabolism were significantly changed with EGCG treatment in control and aged myoblasts. In control and aged myotubes, one pathway commonly represented after EGCG treatment was aminoacyl-tRNA biosynthesis. Three metabolites commonly represented in control and aged myoblast and myotubes in the presence of EGCG were Fumaric acid, L-Isoleucine and 5-Methoxyindoleacetate (see Figure 7.26).

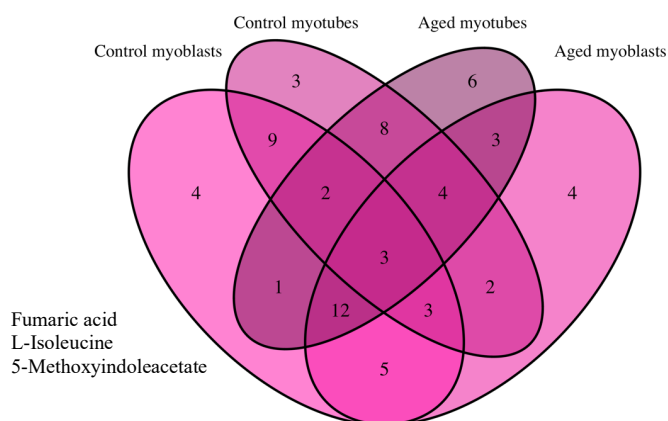


Figure 7.26 Venn diagram reporting metabolites with VIP scores >1 between control and aged myoblast and myotubes following EGCG treatment. Three metabolites were commonly represented between ages and differentiation stage (myoblast vs. myotube).

7.3.10 Epicatechin effects in control and aged skeletal myoblasts

[To] establish potential effects of EPI treatment in myoblasts, control and replicatively aged myoblasts were compared. PCA (Figure 7.27A) was performed to observe the major variances between all samples. PCA scores plot of PC1 (34.52%) against PC2 (17.67%) revealed moderate clustering of dose in terms of separation. PC1 and PC2 explains a cumulative variance of 52.19%. Meanwhile a total of 13 components were required to explain 95% of variance in the data. When the overall metabolic profile of myoblasts is considered, cells treated with 5 and 10 μ M EPI are clustered more widely on PC1 compared to respective CTRL conditions. This suggests EPI treated myoblasts have greater variation compared to CTRL.

Commented [CS572]: Should you add an intro sentence as to why you tested this flavonoid...

Commented [SD573R572]: Is this best saved for intro? Please tell me if wrong and best to give more info in this section

Employing a supervised PLS-DA method, metabolites responsible for the metabolic profile differences can be extracted.

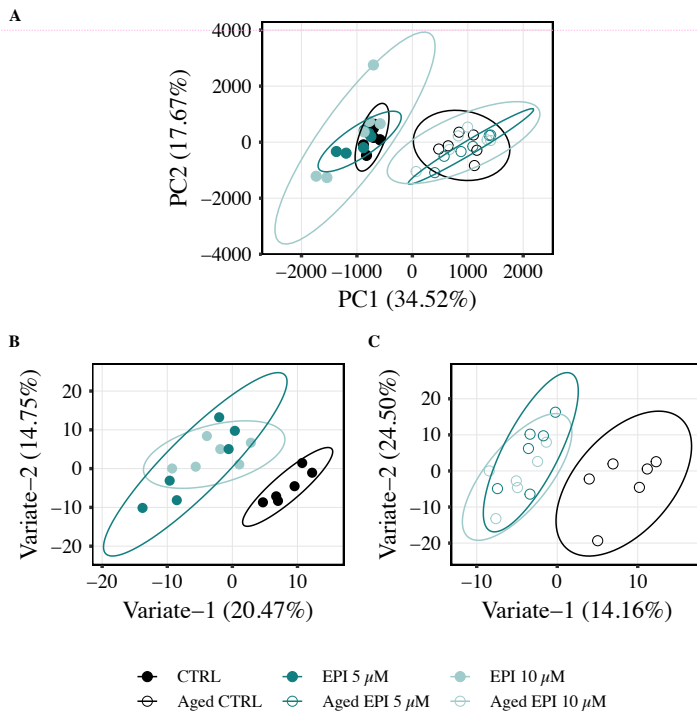


Figure 7. 27 Multivariate analysis of control and aged myoblasts +/- EPI treatment. A) PCA scores of control and aged myoblasts coloured by dose. A total of thirteen principal components were required to achieve 95% explained variance. Brackets report the variance explained by the PC. Only PC1 and PC2 are shown in the Figure for simplicity/clarity. Ellipses represent 95% confidence region. B) PLS-DA scores of control- and C) aged-myoblasts coloured by dose. A model complexity of two-variates was employed for control and aged myoblasts. Closed and open triangles represent control and aged cells, respectively.

In order to identify distinctions in the metabolic profiles, the differences between treatments were enhanced in control and aged myoblasts using a cross-validated PLS-DA model. Optimal model complexity was found to be a two-variate model for control and aged myoblasts. Figure

Commented [CS574]: Much more overlap for EPI vs con in panel A compared to Con. vs Q previously.
 Once again though, nice to see separation from Con but overlap of treatments..

Commented [MMP575]: Report validation quality score (ROC?) here. Replace the word 'variate' with the term 'latent variable' or 'component'

Commented [CS576]: The general comments raised above for Q will hold true for EPI, I will not mention them again, but if you modify anything above, based on the comments, please modify from here on also.

7.27B/C shows the scores of these models. Unlike the PCA plot (Figure 7.27A), a tight clustering of groups can be observed. The PLS-DA model achieved a better separation between 5/10 μM EPI and CTRL groups in both control and aged cells, but this was not comparable to PCA. To examine the metabolite level information, VIP scores of the PLS-DA model were calculated (see Figure 7.28).

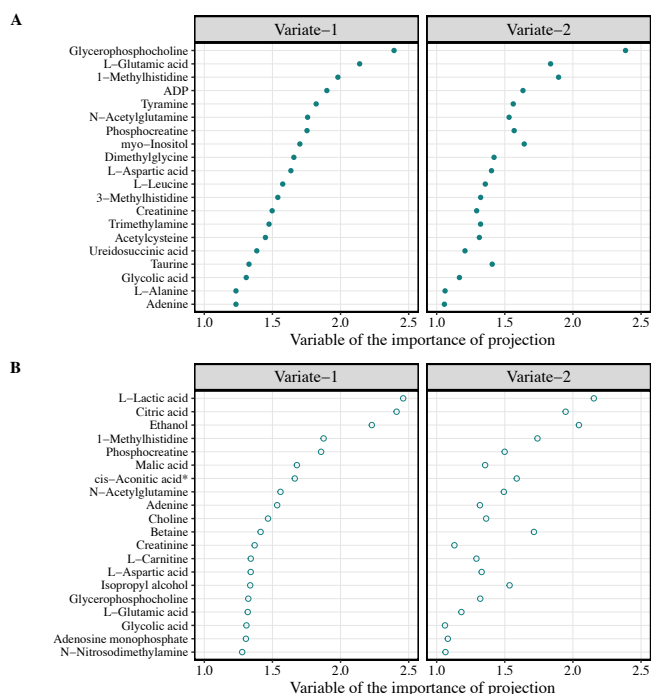
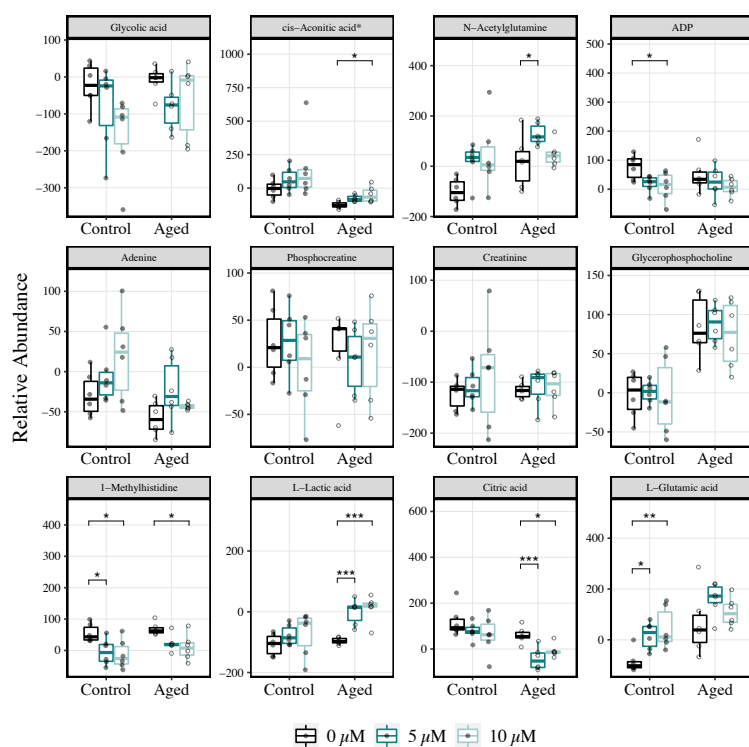


Figure 7.28 VIP scores of PLS-DA model built on EPI treatment-dependent differences in A) control- and B) aged- skeletal myoblasts. AUC scores for control myoblasts were 1.0, 0.653 and 0.847, and 0.986, 0.903 and 0.583 for aged myoblasts for 0 μM vs. others, 5 μM vs. others and 10 μM vs. others, respectively. A lower threshold of 1 was used on latent variable one and two to select metabolites from the model. The top 20 representative metabolites/bins are presented for clarity.

Commented [MMP577]: Report validation quality score (ROC?) here. Replace the word 'variate' with the term 'latent variable' or 'component'

Upon metabolite selection of treatment-specific differences, metabolite levels of control and aged myoblasts in response to 0, 5 and 10 μM EPI were compared via two-way ANOVA, followed by a Tukey's HSD pairwise test and shown via boxplots (Figure 7.29). Statistical analyses of the metabolite-level comparisons can be found in Table 9.20 (Chapter 9). From the metabolite level comparison in control myoblasts, Phosphorylcholine and L-Glutamic acid were higher after 5 and 10 μM EPI compared to CTRL. Whereas 1-Methylhistidine abundance was significantly lower after 5 and 10 μM EPI compared to CTRL. In aged myoblasts, L-Lactic acid was lower after 5 and 10 μM EPI compared to CTRL. Conversely, Ethanol and Citric acid were significantly lower with 5 and 10 μM EPI compared to CTRL.



Commented [CS578]: Far fewer sig changes with Epi compared to sig changes that were seen with Q.

Sorry to go on and on re Venn diagrams, but in the end, is it worth having one for all flavonoids (for significant metabolites) that overlap or not – be interesting to see the overall pictures in blasts and tubes for all treatments.

Commented [SD579R578]: Cant do one for all compounds combined, as it would be too many variables. However, ive put a table in the appendices that captures this information

Figure 7. 29 Selected metabolite boxplots of control and aged skeletal myoblasts following 0, 5 and 10 μM EPI treatment. *, ** and *** represent *P*-values less than 0.05, 0.01 and 0.001, respectively. * in the boxplot title represent denotes overlapping bin. Closed and open circles represent control and aged cells, respectively.

Selected metabolites for EPI-treated control and aged skeletal myoblasts were subjected to MSEA to extract further metabolic pathway level information. Table 7.11 summarises the metabolites selected for EPI-treated control myoblasts. MSEA was performed on selected metabolites using a database curated from the KEGG pathways (*Mus musculus* (mouse) [KEGG organism code: mmu]). MSEA was performed using Fisher’s exact test with EASE correction and BH *P*-value adjustment for multiple testing. Two significantly over-represented pathways were identified for control skeletal myoblasts only (Table 7.11). No significant over-represented pathways were observed for aged skeletal myoblasts. Pathways represented in control myoblasts included alanine, aspartate and glutamate metabolism and glyoxylate and dicarboxylate metabolism.

Commented [CS580]: Interesting – so generally a lower response of the cells to Epi vs Q in terms of metabolite analyses? Why?

Table 7. 11 Pathway analysis results for control skeletal myoblasts treated with EPI. Reporting raw & BH adjusted *P* values, number of hits, pathway impact and matches.

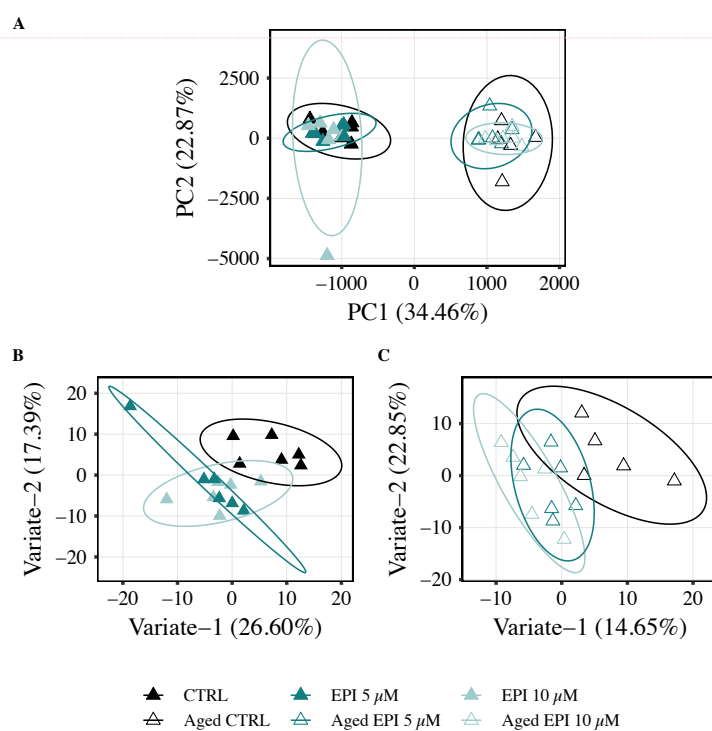
Pathway	Raw <i>P</i> -value	BH <i>P</i> -value	Hits	Impact	Matches
Alanine, aspartate and glutamate metabolism	0.0005	0.0205	5	0.16	L-Aspartate; L-Alanine; L-Glutamate; Citrate; N-Carbamoyl-L-aspartate
Glyoxylate and dicarboxylate metabolism	0.0003	0.0205	5	0.42	cis-Aconitate; Citrate; Glycine; L-Glutamate; Formate

Commented [MMP581]: Again you could add colours for those treatments that show the same trend with respect to control

Metabolites in green higher (with both 5 and 10 μM EPI) versus CTRL conditions, respectively. Metabolites in black are not significantly different between conditions (consistently with 5 and 10 μM EPI vs. CTRL).

7.3.11 Epicatechin effects in control and aged skeletal myotubes

To establish potential effects of EPI treatment in myotubes, control and replicatively aged myotubes were compared. PCA (Figure 7.30A) was performed to observe the major variances between all samples. PCA scores plot of PC1 (34.46%) against PC2 (22.87%) revealed moderate clustering of dose in terms of separation. PC1 and PC2 explains a cumulative variance of 57.33%. Meanwhile a total of 10 components were required to explain 95% of variance in the data. When the overall metabolic profile of EPI treated myotubes is considered, control myotubes are clustered tighter compared to aged myotubes on PC1. This suggests control myotubes have less variation compared to aged myotubes. Employing a supervised PLS-DA method, metabolites responsible for the metabolic profile differences can be extracted.



Commented [CS582]: As for blasts a lot less separation in the presence of EPI compared to the data derived with Q. Particularly marked in aged.

Again, maybe rethink colour or symbol choice.- especially for aged.

Figure 7. 30 Multivariate analysis of control and aged myotubes +/- EPI treatment. A) PCA scores of control and aged myotubes coloured by dose. A total of ten principal components were required to achieve 95% explained variance. Brackets report the variance explained by the PC. Only PC1 and PC2 are shown in the Figure for simplicity/clarity. Ellipses represent 95% confidence region. B) PLS-DA scores of control myotubes and C) aged myotubes coloured by dose. A model complexity of two- variates was employed for control and aged myotubes. Closed and open triangles represent control and aged cells, respectively.

In order to identify distinctions in the metabolic profiles, the differences between conditions were enhanced using a cross-validated PLS-DA model. Optimal model complexity was found to be two-variates for control and aged myotubes. Figure 7.30B/C shows the scores of this model with variate-1 plotted against variate-2 for simplicity. Compared to the PCA plot (Figure 7.30A), a tighter clustering of groups can be observed. The PLS-DA model achieved a better separation between CTRL and 10 μ M EPI groups in control and aged myotubes, but this was not comparable to PCA. However, 5 μ M EPI was not fully decoupled from CTRL, indicating the higher degree of similarity between these conditions. To examine the metabolite level information, VIP scores of the PLS-DA model were calculated (see Figure 7.31).

Commented [MMP583]: Report validation quality score (ROC?) here. Replace the word 'variate' with the term 'latent variable' or 'component'

Commented [MMP584]: As PLS-DA uses group information to produce the model this is expected (PCA just shows largest separation between samples – irrespective of groups). Therefore it would be better to rephrase this as PCA and PLS-DA aren't directly comparable (see page 36)

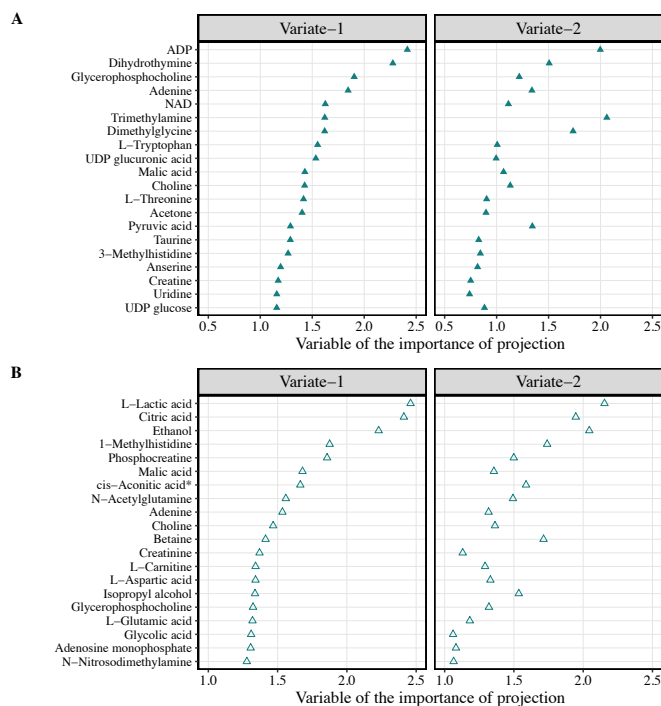


Figure 7.31 VIP scores of PLS-DA model built on EPI treatment-dependent differences in A) control- and B) aged- skeletal myotubes. AUC scores for control myoblasts were 0.847, 0.583 and 0.931, and 0.850, 1.0 and 0.682 for aged myoblasts for 0 μM vs. others, 5 μM vs. others and 10 μM vs. others, respectively. A lower threshold of 1 was used on latent variable one and two to select metabolites from the model. The top 20 metabolites/bins are presented for clarity.

Upon metabolite selection of treatment-specific differences, metabolite levels of control and aged myotubes in response to 0, 5 and 10 μM EPI were compared via two-way ANOVA, followed by a Tukey's HSD pairwise test and shown via boxplots (Figure 7.32). Statistical analyses of the metabolite-level comparisons can be found in Table 9.21 (Chapter 9). From the metabolite-level comparison in control myotubes, levels of Dimethylglycine, Trimethylamine, ADP and 1-Methylhistidine were significantly lower after 5 and 10 μM EPI compared to

CTRL. In aged myotubes, cis-Aconitic acid/L-Acetylcarnitine and L-Carnitine were significantly higher, whilst 1-Methylhistidine and myo-Inositol were significantly lower following 5 μ M EPI compared to CTRL.

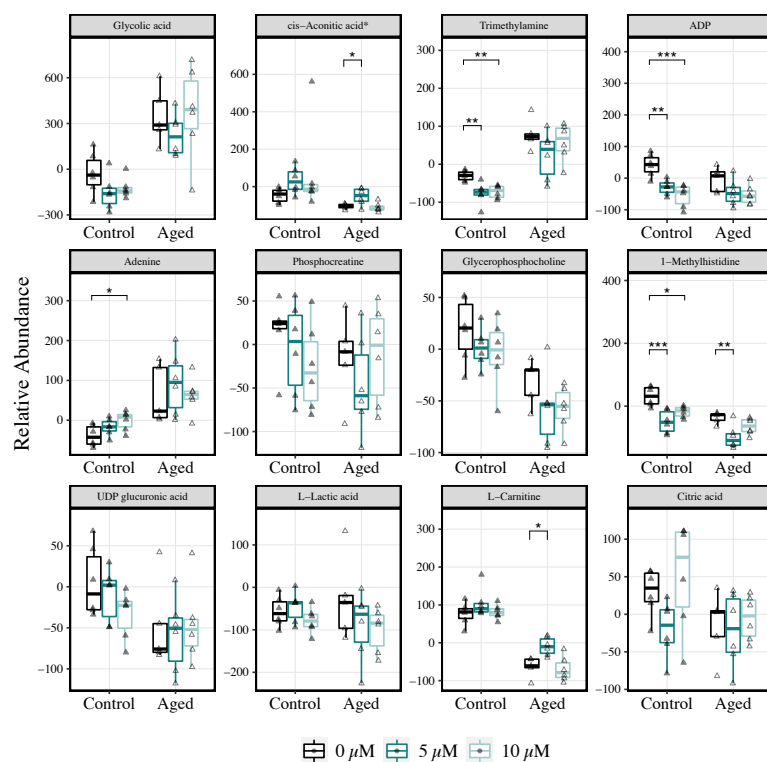


Figure 7.32 Selected metabolite boxplots of control and aged skeletal myotubes following 0, 5 and 10 μ M EPI treatment. *, ** and *** represent *P*-values less than 0.05, 0.01 and 0.001, respectively. * in the boxplot title represent denotes overlapping bin. Closed and open triangles represent control and aged cells, respectively.

Selected metabolites for EPI-treated control and aged skeletal myotubes were subjected to MSEA to extract further metabolic pathway level information. Table 7.12-7.13 summarises the

metabolites selected for EPI-treated cells in late differentiation. MSEA was performed on selected metabolites using a database curated from the KEGG pathways (Mus musculus (mouse) [KEGG organism code: mmu]). MSEA was performed using Fisher's exact test with EASE correction and BH *P*-value adjustment for multiple testing. Three and five significantly over-represented pathways were identified for control and aged skeletal myotubes, respectively (Tables 7.12-7.13). Out of the significant pathways, aminoacyl-tRNA biosynthesis and valine, leucine and isoleucine biosynthesis were common amongst EPI treated control and aged myotubes.

Table 7. 12 Pathway analysis results for control skeletal myotubes treated with EPI. Reporting raw & BH adjusted *P* values, number of hits, pathway impact and matches.

Pathway	Raw <i>P</i> -value	BH <i>P</i> -value	Hits	Impact	Matches
Aminoacyl-tRNA biosynthesis	0.0001	0.0114	6	0	L-Valine; L-Alanine; L-Isoleucine; L-Threonine; L-Tryptophan; L-Tyrosine
Valine, leucine and isoleucine biosynthesis	0.0003	0.0114	3	0	L-Threonine; L-Valine; L-Isoleucine
Ascorbate and aldarate metabolism	0.0006	0.0159	3	0.25	myo-Inositol; UDP-glucose; UDP-glucuronate

Metabolites in black are not significantly different between conditions (consistently with 5 and 10 μ M EPI vs. CTRL).

Table 7. 13 Pathway analysis results for aged skeletal myotubes treated with EPI. Reporting raw & BH adjusted *P* values, number of hits, pathway impact and matches.

Pathway	Raw <i>P</i> -value	BH <i>P</i> -value	Hits	Impact	Matches
---------	---------------------	--------------------	------	--------	---------

Aminoacyl-tRNA biosynthesis	<0.0001	<0.0001	10	0.00	L-Phenylalanine; Glycine; L-Aspartate; L-Valine; L-Alanine; L-Isoleucine; L-Leucine; L-Threonine; L-Tryptophan; L-Tyrosine
Valine, leucine and isoleucine biosynthesis	<0.0001	0.0002	4	0.00	L-Threonine; L-Leucine; L-Isoleucine; L-Valine
Glycine, serine and threonine metabolism	0.0003	0.0082	5	0.36	Choline; N,N-Dimethylglycine; Glycine; L-Threonine; Creatine
Phenylalanine metabolism	0.0011	0.0238	3	0.36	L-Phenylalanine; Phenylacetic acid; L-Tyrosine
Phenylalanine, tyrosine and tryptophan biosynthesis	0.0020	0.0329	2	1.00	L-Phenylalanine; L-Tyrosine

Metabolites in black are not significantly different between conditions (consistently with 5 and 10 μ M EPI vs. CTRL).

Commented [CS585]: Again, worth adding a summary paragraph of key findings before moving on and contrasting the data with Q? Not a discussion, just key info./take home messages

7.3.12 Summary of EPI effects upon the metabolome of control and aged myoblasts and myotubes

Acute EPI treatment evoked changes in the metabolite signatures of control and aged myoblasts and myotubes. Pathways overrepresented with EPI treatment in control myoblasts included alanine, aspartate and glutamate metabolism and glyoxylate and dicarboxylate metabolism, whereas none were overrepresented in aged myoblasts. Nevertheless, metabolites involved in energy metabolism were significantly changed with EPI treatment. In control and aged myotubes, pathways commonly impacted by EPI treatment include aminoacyl-tRNA biosynthesis and valine, leucine and isoleucine biosynthesis. Five metabolites commonly represented in control and aged myoblast and myotubes in the presence of EPI were 1-

Methylhistidine, ADP, cis-Aconitic acid, L-Acetylcarnitine and myo-Inositol (see Figure 7.33).

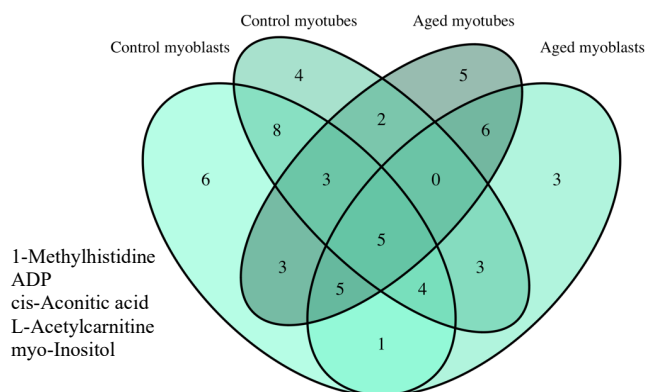


Figure 7.33 Venn diagram reporting metabolites with VIP scores >1 between control and aged myoblasts and myotubes following EPI treatment. Five metabolites were commonly represented between ages and differentiation stage (myoblast vs. myotube).

7.4 Discussion

The purpose of this study was to explore how (replicative) ageing and dietary flavonoids impact the metabolome of murine skeletal muscle myoblasts and myotubes. Using an untargeted NMR metabolomics approach, the primary outcomes were 1) replicative ageing distinctly alters the metabolome of skeletal muscle myoblasts and myotubes, that somewhat reflects ageing human muscle; 2) flavonoids elicit compound and dose-dependent effects at the metabolite level in myoblasts and myotubes and 3) flavonoid treatment partly mitigates some, but not all age-related perturbations to the metabolome in muscle cells.

Commented [CS586]: Do they? Have you definitely shown this?

Commented [SD587R586]: Adjusted this statement to better represent the findings

7.4.1 Control vs. aged myoblast comparisons (untreated CTRL conditions)

In skeletal muscle myoblasts (early differentiation), there were several major differences in metabolic signatures between control and replicatively aged cells (see Figure 7.34). The increase in aminoacyl-tRNA biosynthesis-related and BCAA metabolites in aged myoblasts suggests enhanced capacity for translation and protein synthesis. Although somewhat counterintuitive, these data support *in vivo* research demonstrating chronically activated mammalian target of rapamycin complex 1 (mTORC1) signalling, increased ribosomal protein S6 kinase beta-1 phosphorylation and elevated muscle protein synthesis in aged versus young skeletal muscle tissue (Fredriksson et al., 2008; Joseph et al., 2019; Kimball et al., 2004). Alternatively, aged myoblasts may possess greater rates of protein breakdown as seen in older adults (Trappe et al., 2004), which would help explain the elevated levels of BCAAs in aged cells. During net protein breakdown, amino acids are metabolised to precursors of the tricarboxylic acid (TCA) cycle intermediates, including glutamate that can be converted to glutamine (Wagenmakers, 1998). Compared to control myoblasts, glutamine levels were elevated in aged myoblasts, adding further evidence that protein breakdown and anaplerosis were increased compared to control. In the present study, the abundance of TCA cycle intermediates cis-Aconitate and Malic acid were lower and higher in aged versus control myoblasts, respectively. Thus, it is not clear to what extent replicative ageing impacts flux through the TCA cycle in skeletal myoblasts. When considered alongside the lack of observed mitochondrial dysfunction in aged myoblasts in Chapter 5, it is possible ageing does not impair aerobic energy metabolism in the C₂C₁₂ myoblast model.

One distinguishing feature between control and aged myoblasts was the levels of Dihydrothymine, a possible marker of DNA damage (Dawidzik et al., 2004), which were markedly increased with ageing. Interestingly, this finding is consistent with a recent metabolomics study of human skeletal muscle ageing (Wilkinson et al., 2020), adding support

to the idea that Dihydrothymine may represent a novel marker of cellular ageing. Another metabolite that increased with replicative ageing was Tryptophan. Levels of tryptophan were also reportedly increased in the gastrocnemius and soleus of aged Fischer 344 x Brown Norway male rats when compared to young. However, it is not currently clear what role tryptophan plays in the context of cellular ageing. The abundance of histamine was increased in aged myoblasts, which agrees with recent observations in aged human skeletal muscle (Wilkinson et al., 2020). A related metabolite in histidine metabolism, carnosine, was also elevated in aged myoblasts. In recent years, carnosine has been demonstrated to be a potent scavenger of free radicals such as methylglyoxal (Aldini et al., 2002; Hipkiss & Chana, 1998), thus providing a potential reason for its elevation in aged cells.

Phospholipids play an important role in regulating cell function and energy metabolism (van der Veen et al., 2017), and phosphatidylcholine accounts for ~50% of the total phospholipid pool (Takagi, 1971). Glycerophosphocholine is formed in the breakdown of phosphatidylcholine, whereas choline is essential for phosphatidylcholine synthesis by the Kennedy pathway (Kennedy & Weiss, 1956; Moessinger et al., 2014). Here, levels of acetylcholine and glycerophosphocholine were higher in aged myoblasts compared to control, whereas choline and phosphorylcholine were lower. Taken together these findings suggest increased degradation and reduced synthesis of phospholipids in aged myoblasts, which could lead to membrane fragility and cell apoptosis (Da Costa et al., 2004).

Commented [CS588]: Implications? Could this be why fusion is reduced? How could this be reversed...could then assess the impact on fusion...

Commented [SD589R588]:

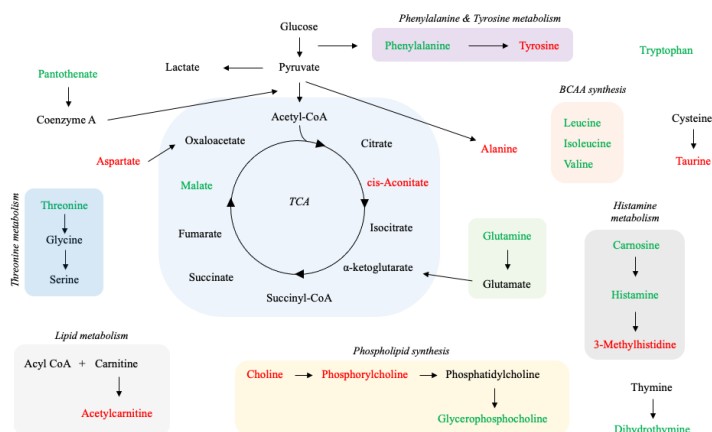


Figure 7. 34 Schematic representation of metabolic signatures of control and aged myoblasts. Metabolites in green and red are higher and lower in aged versus control, respectively. Metabolites in black are similar between control and aged.

7.4.2 Control vs. aged myotube comparisons (untreated CTRL conditions)

Similar to the effects of ageing observed in myoblasts, the metabolic signatures of control and aged myotubes (late differentiation) were profoundly different. Unlike myoblasts, the abundance of aminoacyl-tRNA and BCAA biosynthesis-related metabolites in aged myotubes was lower compared with control. These data imply a lowered potential for translation and protein synthesis in aged myotubes that may contribute to their reduced fusion capacity. Although, an important consideration when interpreting these data is that metabolite abundances were not relativised to total cellular protein. Given the fusion potential of aged myoblasts is diminished compared to control cells, we cannot exclude the possibility that metabolite abundances are conflated in control myotubes due to differences in protein content. With that said, recent dynamic proteomic profiling of control and replicatively aged myotubes

Commented [CS590]: What were the average protein concentrations like for aged and con tubes that you got for blotting? I know it is not the same experiment, but they would have been cultured similarly.....

Commented [SD591R590]: No significant differences between control and aged protein yield at each timepoint

revealed that the fractional synthetic rate of mixed proteins was 82% lower in aged versus control myotubes (unpublished Brown *et al.*, 2021), supporting the metabolite-level data presented here.

One major hallmark of cellular ageing is mitochondrial dysfunction (López-Otín *et al.*, 2013), but the effects of (replicative) ageing *in vitro* on mitochondria are not well described. Congruent with the idea that cellular ageing causes disruptions to mitochondria, levels of cis-Aconitate and L-Carnitine were lower in aged versus control myotubes (see Figure 7.35). These data suggest lowered metabolic flux through the TCA cycle and a reduced capacity for fatty acid oxidation, respectively. These findings lend support to the notion that replicative ageing impairs mitochondrial function in cultured myotubes, as found in Chapter 6. Along similar lines, pantothenic acid levels were lower in aged myotubes when compared to control. Given the importance of this metabolite in coenzyme A (CoA) synthesis, the age-related reduction in pantothenic acid supports the notion that cellular ageing disrupts pathways associated with mitochondrial energy metabolism.

As theorised in early work (Mitchell, 1966), the gradual accumulation of oxidative cellular damage is thought to play an important, but limited role in age-related tissue dysfunction (López-Otín *et al.*, 2013). Glutathione is a potent cellular antioxidant, with decreases in the ratio of reduced to oxidised glutathione being indicative of increased oxidative stress. The reported increase in abundance of oxidised glutathione in aged myotubes supports previous studies showing elevated oxidative stress in aged skeletal muscle cells (Beccafico *et al.*, 2007; Drew *et al.*, 2003b; Fulle *et al.*, 2005; Marrone *et al.*, 2018b; Mecocci *et al.*, 1999; Vasilaki *et al.*, 2006), which may be due to reduced activity of glutathione-dependent enzymes and the accumulation of hydrogen peroxide (Fulle *et al.*, 2005).

Phospholipids play an important role in regulating cell function and energy metabolism (van der Veen et al., 2017), and phosphatidylcholine accounts for ~50% of the total phospholipid pool (Takagi, 1971). Glycerophosphocholine is formed in the breakdown of phosphatidylcholine, whereas choline is essential for phosphatidylcholine synthesis by the Kennedy pathway (Kennedy & Weiss, 1956; Moessinger et al., 2014). Though speculative, our findings in myotubes could reflect lowered phosphatidylcholine turnover with cellular ageing, that may be related to lowered remodelling of the mitochondrial network (Vance, 2015). Another metabolite involved in phospholipid metabolism is myo-inositol (Holub, 1986), which has also recently been implicated in skeletal muscle ageing. Indeed, myo-inositol was reported to promote anti-ageing effects through its stimulatory effects on phosphatase and tensin homolog (PTEN)-dependent mitophagy in worm and mouse skeletal muscle (Shi et al., 2020). Therefore, it is possible that increased myo-inositol levels in aged myotubes is indicative of a compensatory mechanism to maintain mitochondrial health, although this purely speculative.

Similar to myoblasts, aged myotubes presented decreased levels of taurine in comparison to control. In skeletal muscle, taurine is involved in the control of ion channel function, membrane stability and calcium homeostasis (Camerino et al., 2004). During ageing, levels of taurine gradually decline (Pierno et al., 1998), which among many potential implications, may cause inadequate β -oxidation due to decreased pH buffering capacity (Hansen et al., 2015). Having described how replicative ageing impacts the metabolome of skeletal muscle myoblasts and myotubes, we next sought to determine how flavonoid treatment would affect the metabolic profiles of control and aged cells.

Commented [CS592]: Make an infographic with cartoon images of myoblasts and tubes and the altered metabolites and the impact they may have.

Commented [SD593R592]: Want to do this but seems very difficult given the different metabolic pathways impacted, not sure how this could be represented well in an infographic

Commented [SD594R592]: Have done it

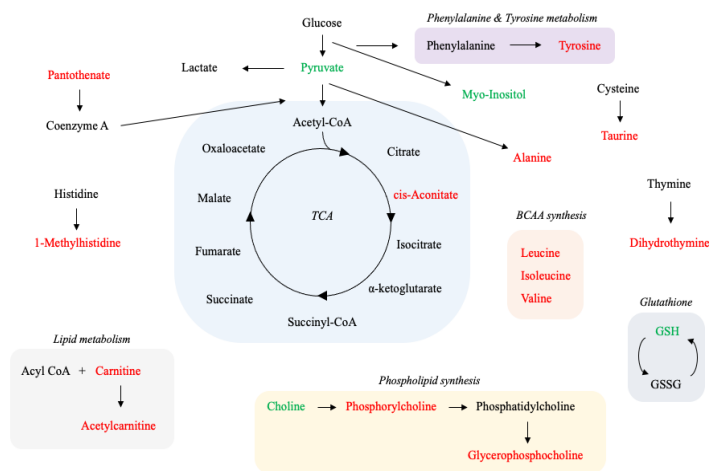


Figure 7. 35 Schematic representation of metabolic signatures of control and aged myotubes. Metabolites in green and red are higher and lower in aged versus control, respectively. Metabolites in black are similar between control and aged.

7.4.3 Quercetin effects on the metabolome of skeletal myoblasts

Following acute Q treatment, levels of citrate were lowered in both control and aged myoblasts. This observation hints that Q may lower the potential for generation of reducing equivalents through the TCA cycle. Along these lines, L-Lactic acid levels were significantly increased in response to Q treatment, suggesting elevated glycolysis as a compensatory effect for reduced energy production via OXPHOS. Yet, levels of the end product of glycolysis, pyruvate, were lower in response to Q treatment in control cells. Together these data suggest Q shifts metabolism heavily in favour of glycolysis, possibly due to impairments in pathways that converge upon the mitochondria. In this regard, previous work has demonstrated that Q accumulates within the mitochondria of Jurkat cells (Fiorani et al., 2010a) and inhibits ATP synthase in rat, bovine and porcine tissue (Di Pietro et al., 1975; Lang & Racker, 1974b; Zheng

Commented [CS595]: What tissue?

Commented [SD596R595]: Pig heart, brain, liver

& Ramirez, 2000b). However, negligible effects of Q on mitochondrial respiration were found on myoblast and myotubes in Chapters 5 and 6, respectively. The potential impediment to the phosphorylation of ADP to ATP by this compound may help explain a preference towards glycolysis to meet cellular energy demands. However, we observed a lowering of ADP levels in control myoblasts cultured with 10 μ M Q treatment, which is difficult to reconcile given the possible concurrent inhibition of OXPHOS. Further research is necessary to establish whether Q inhibits mitochondrial bioenergetics in murine skeletal muscle cells, as this will help explain the underlying processes of its therapeutic effects.

The glycine, serine and threonine metabolism pathway was overrepresented in control and aged myoblasts cultured in the presence of Q (see Figure 7.36A/B). Glycine is a non-essential amino acid that regulates homeostasis, partly via its intracellular metabolism (Koopman et al., 2017). Many macromolecules depend upon glycine availability for their synthesis, including the antioxidant glutathione (Wang et al., 2013). Indeed, glycine is required for glutathione synthesis to help maintain physiological levels of ROS (L'Honoré et al., 2018). In older humans, levels of intracellular glycine are known to be diminished, especially in frail individuals (Fazelzadeh et al., 2016). Data showing increased cellular glycine with 10 μ M Q may be a compensatory effect to cope with elevated oxidative stress, though further experimentation is required to establish whether this is the case.

Beta-alanine is formed by the degradation of l-carnosine and anserine in skeletal muscle and may also be synthesised from aspartic acid. As a non-essential amino acid, beta-alanine is an indispensable component for CoA and plays a role in intramyocellular buffering (Derave et al., 2010). Exogenous supplementation of beta-alanine has improved the physical capacity of older adults (Furst et al., 2018). Given the reported decline in levels of anserine and aspartic acid

Commented [CS597]: This was increased in aged blasts

with parallel increases in beta-alanine, it is possible Q treatment increases the requirement for beta-alanine in skeletal muscle cells. More research is needed to elucidate why Q treatment increases beta-alanine abundance in skeletal muscle cells.

Commented [CS598]: What is the overall impact, therefore, in your view of Q in blasts?

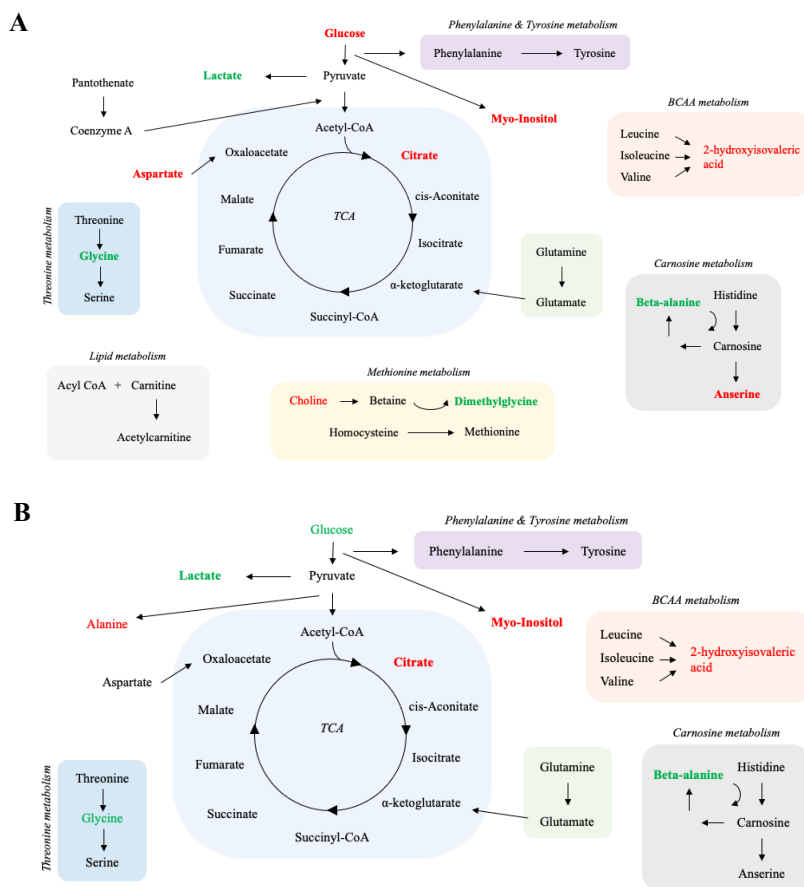


Figure 7. 36 Schematic representation of metabolic signatures in A) control and B) aged myoblasts, in the presence of 0, 5 and 10 μM Q. Metabolites in green and red are higher and lower with Q treatment vs. untreated CTRL. Metabolites in bold are significantly different vs.

CTRL with 5 and 10 μ M Q, whereas metabolites in regular font are only different vs. CTRL at one Q dose. Metabolites in black are similar between treatment conditions.

7.4.4 Quercetin effects on the metabolome of skeletal myotubes

Treatment of myotubes with Q culminated in measurable differences in metabolic signatures when compared to control conditions. Similar to the effects observed in myoblasts, Q treatment appeared to shift energy metabolism towards glycolysis and away from OXPHOS. This apparent change in fuel preference was evidenced by increased L-Lactic acid and reduced citric acid levels, at least in control myotubes. Notably, this effect was only observed with the higher dose of Q (10 μ M), implying that the effects of Q on metabolites involved in energy metabolism are largely dose dependent. Consistent with a shift in metabolic preference, prior research has demonstrated quercetin treatment reduces O₂ consumption and cellular ATP concentrations in both rat liver mitochondria and HEK293 cells (Dorta et al., 2005; Hawley et al., 2010b), although such an effect was not found in myoblasts and myotubes (Chapters 5 and 6, respectively) in this thesis. The ability of Q to interact with mitochondrial respiration may be related to its chemical structure (Dorta et al., 2005), which favours molecular interactions with components of the ETC, including ATP synthase (Di Pietro et al., 1975; Lang & Racker, 1974a; Zheng & Ramirez, 2000b). Together, these data imply that Q's impact on the metabolome is dose dependent, and may be related to its capacity to inhibit OXPHOS, with implications for downstream energy-sensitive signalling pathways (Hardie et al., 2011).

When looking at the effects of Q on phosphorylcholine, a dose dependent reduction in phosphorylcholine content was observed in both control and aged myotubes (see Figure 7.37A/B). Considering the importance of phosphorylcholine in the synthesis

Commented [SD599]: Can we refer back to seahorse data from different chapter to support this proposition

Commented [CS600R599]: This is exactly what my comments above relate to

phosphatidylcholine, our data suggest myotube phospholipid synthesis could be impeded in the presence of Q, regardless of age. This idea is supported by reduced levels of choline after Q treatment, at least in control myotubes. Phospholipids make up essential components of cell membranes, including the energy producing organelle that is the mitochondrion. The findings are in line with studies showing interactions between Q and cell membranes, and support those reporting blunted phospholipid synthesis in Q-treated hepatocytes (Gnoni et al., 2009; Saija et al., 1995).

Interestingly, quercetin treatment lowered the age-associated increase in myo-inositol abundance in myotubes, although not to levels comparable to control. Whilst the precise role of myo-inositol in cellular ageing is not well understood, it may contribute to the PTEN-dependent upregulation of mitophagy in the context of ageing (Shi et al., 2020). Therefore, quercetin may provide nutritional means to modulate myo-inositol levels in the context of cellular ageing. From what is currently known about myo-inositol, it is possible that quercetin may impact membrane phospholipid formation and signal transduction (Holub, 1986), or potentially attenuate mitophagy (Shi et al., 2020), although this requires further study.

Micromolar concentrations of Q reduced levels of control myotube metabolites involved in glycine, serine and threonine metabolism, including threonine and pyruvate. On the other hand, control myotube glycine levels were increased in the presence of Q, whilst serine remained similar between conditions. Previously it was shown that compromised mitochondrial function increases the production of glycine and augments pathways associated with glutathione synthesis (Ost et al., 2015). Collectively, these findings suggest that Q might augment control myotube glycine production in response to impediments to mitochondrial respiration and increased ROS production, but this requires further investigation.

Commented [CS601]: In both con and aged? Specify

Commented [SD602R601]: Threonine pyruvate reduced in control tubes; threonine reduced aged blasts

Commented [CS603]: In both aged and con? Tis does not make sense, why would both be compromised? Intro your Seahorse data into this argument also.

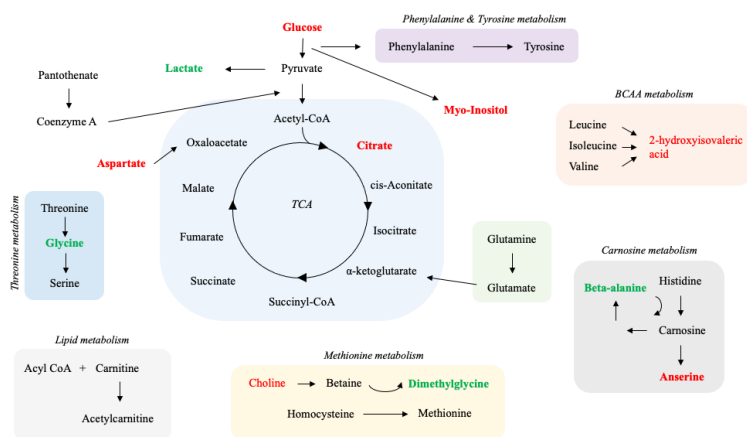
Tyrosine abundance was significantly increased in response to 5 and 10 μM Q, in both control and aged myotubes. Interestingly, levels of tyrosine were lower in aged compared to control myotubes, which supports a previous metabolomics study of human plasma across the lifespan (Darst et al., 2019). Therefore, Q may be efficacious in raising tyrosine levels in the context of cellular ageing, although it is not currently known how elevated tyrosine could mitigate the deleterious effects of ageing.

Commented [SD604]: Best here or for control/aged discussion section

Commented [CS605]: Using the image you generated in the last section of con and aged blasts and tubes, now add the Q data tot hat image e.g. use a different text colour if that helps.

What would your recommendations be for Q use and muscle adaptation with age, based on these data?

A



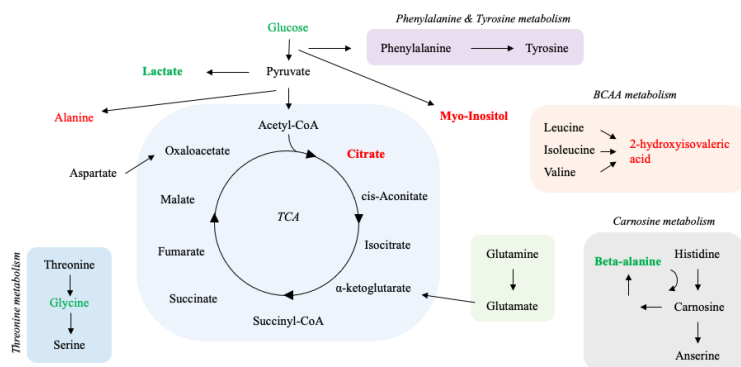
B

Figure 7. 37 Schematic representation of metabolic signatures in A) control and B) aged myotubes, in the presence of 0, 5 and 10 μ M Q. Metabolites in green and red are higher and lower with Q treatment vs. untreated CTRL. Metabolites in bold are significantly different vs. CTRL with 5 and 10 μ M Q, whereas metabolites in regular font are only different vs. CTRL at one Q dose. Metabolites in black are similar between treatment conditions.

7.4.5 EGCG effects in control and aged myoblasts

The predominant catechin derivative found in tea, EGCG, is known to have potent antioxidant effects and impact processes related to energy metabolism (Casanova et al., 2014; Most et al., 2015b; Wang et al., 2016; Ze Xu et al., 2004b). Here, control and aged myoblasts cultured in the presence of EGCG had significantly higher levels of L-Lactic acid, pointing to an increased reliance on glycolysis rather than OXPHOS for ATP synthesis. In support of this idea, EGCG treatment significantly reduced levels of citric acid and fumaric acid in control and aged myoblasts, respectively, suggesting reduced flux through the TCA cycle. The apparent inhibitory effects of EGCG on oxidative metabolism can be reconciled by previous work demonstrating reduced OXPHOS and decreased ATP levels in cancer cells cultured in the

Commented [CS606]: This seems to be a repeating theme

presence of EGCG (Valenti et al., 2013). However, not all studies have reported inhibitory effects of EGCG on mitochondrial respiration *in vitro* (Mezera et al., 2016; Pal et al., 2020a; Pournourmohammadi et al., 2017; Santamarina et al., 2015; Weng et al., 2014; Xiong et al., 2018), including the data from this thesis (Chapters 5 and 6). The discrepancies between findings are possibly explained by the cell types studied or the differences in dose administered.

Two major pathways essential for protein synthesis, aminoacyl-tRNA biosynthesis and BCAA biosynthesis, were both implicated in the effects of EGCG on the metabolome. Accordingly, levels of L-Leucine, L-Isoleucine and L-Threonine were reduced in control myoblasts cultured with physiological EGCG concentrations. These data lend support to the idea that EGCG reduced protein synthesis in skeletal myoblasts, which may be associated with increased energetic stress. Why EGCG had no impact on metabolites related to protein synthesis in aged cells remains to be determined, though it could relate to greater basal rates of protein degradation or other factors intrinsic to the aged myoblast.

One notable change found in control and aged myoblasts following EGCG treatment was increased levels of phosphorylcholine (see Figure 7.38A/B). Given the key role of phosphorylcholine in the synthesis of phosphatidylcholine, it is possible that EGCG interacts with the synthesis of phospholipids, which is facilitated by its inherent molecular structure (Sirk et al., 2009; Tamba et al., 2007). Further evidence for this idea is afforded by the observed increase in myo-inositol abundance in control and aged myoblasts. One previous study examined the effects of EGCG supplementation on the metabolome of vascular endothelial cells, and in line with the present findings, showed increased levels of metabolites associated with the synthesis of membrane lipids (Chu et al., 2018). Together, these findings highlight

that the interaction of EGCG with phospholipid metabolism may underly its associated health benefits.

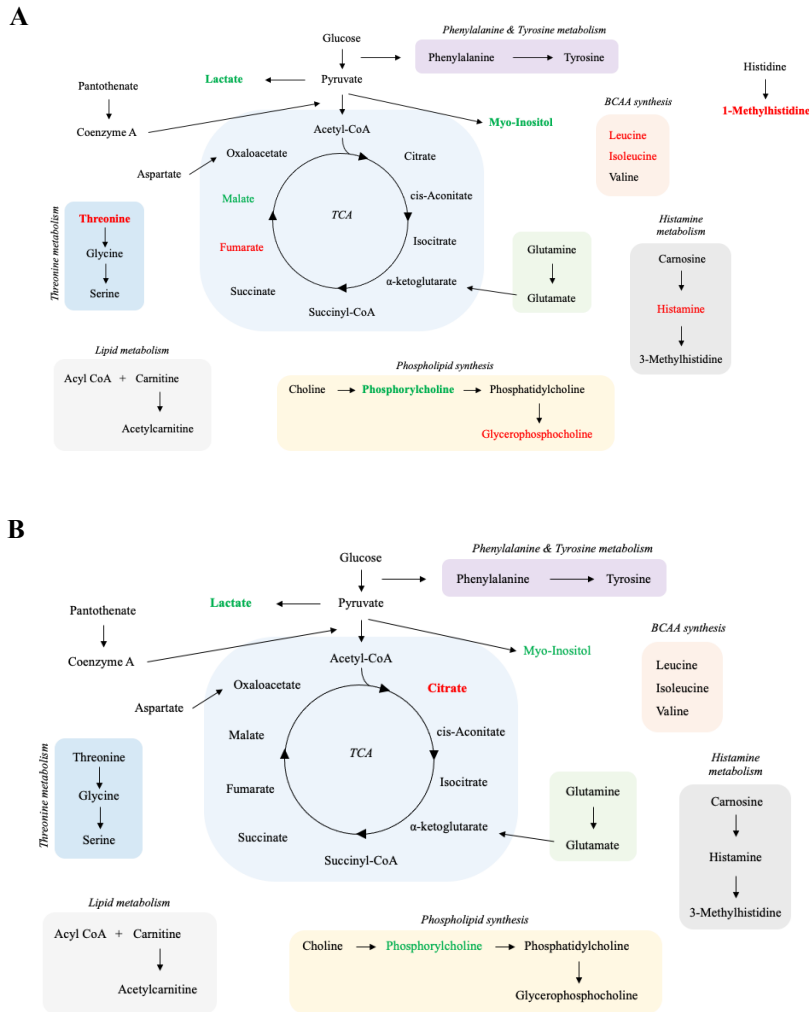


Figure 7.38 Schematic representation of metabolic signatures in A) control and B) aged myoblasts in the presence of 0, 5 and 10 μ M EGCG. Metabolites in green and red are higher and lower with EGCG treatment vs. untreated CTRL. Metabolites in bold are significantly different vs. CTRL with 5 and 10 μ M EGCG, whereas metabolites in regular font are only

different vs. CTRL at one EGCG dose. Metabolites in black are similar between treatment conditions.

7.4.6 EGCG effects in control and aged myotubes

In cultured myotubes, the impact of EGCG on metabolic signatures was somewhat limited (see Figure 7.39A/B). One pathway over-represented amongst control and aged myotubes was aminoacyl-tRNA biosynthesis. In this pathway, L-Threonine was significantly lower in response to EGCG, although only in control cells. Threonine plays an important role in protein synthesis and can also be enzymatically catabolised to produce key intermediates of energy metabolism, such as acetyl-CoA. Therefore, a decrease in Threonine abundance with EGCG may reflect suppressed protein synthesis and/or increased catabolism to support the generation of acetyl-CoA for energy production.

NAD is an essential co-factor that participates in several metabolic pathways, including beta-oxidation, glycolysis, and the TCA cycle. With advancing age, NAD levels are known to decline, highlighting this a potential therapeutic target to ameliorate age-related metabolic impairments (Gomes et al., 2013). Here, we report that 10 μ M EGCG attenuates NAD levels in control skeletal myotubes, with concurrent reductions in levels of ADP. Taken together, these data suggest that micromolar concentrations of EGCG may evoke unfavourable adaptations at the cellular level, at least in control myotubes. The effects of EGCG, and flavonoids more generally, are known to be highly dose dependent (Mattson & Cheng, 2006). Nano-micromolar concentrations of EGCG have been shown to stimulate mitochondrial respiration in rat cardiomyocytes and human foetal osteoblasts (Pal et al., 2020b; Vilella et al., 2020b), whereas **supraphysiological** doses ($>10 \mu$ M) of EGCG impair indices of mitochondrial function and increase mitochondrial ROS (James et al., 2018; Kucera et al., 2015; Li et al.,

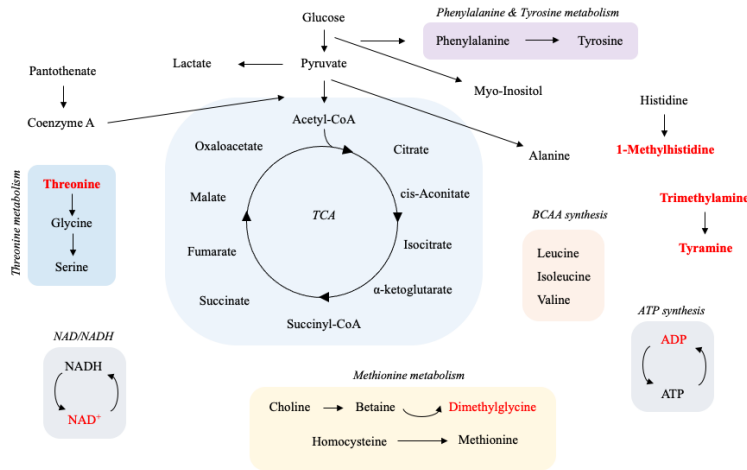
Commented [CS607]: What is considered supraphys? Add the doses

2010). This apparent biphasic response of beneficial stimulation at low doses, but toxic or null activity promoted at higher concentrations, termed hormesis, may be critical in explaining the effects of dietary flavonoids on cellular metabolites and function (Calabrese, 2008).

Other metabolites lowered by EGCG treatment in control myotubes were tyramine and 1-methylhistidine. Tyramine is a derivative of the metabolite tyrosine and is catabolised by a family of enzymes known as the monoamine-oxidases, which subsequently increases H₂O₂ generation and DNA damage (Hauptmann et al., 1996). Only a handful of studies have investigated how flavonoids impact monoamine-oxidase activity, with some reporting inhibitory effects of flavonoids (Bandaruk et al., 2012; Lin et al., 2010). Therefore, it is not entirely clear why EGCG decreased tyramine abundance in the present study and further research is necessary to explore this further. One-methylhistidine is formed from the splitting of anserine by carnosinase, and increased levels of this metabolite in skeletal muscle are indicative of drug-induced cytotoxicity (Aranibar et al., 2011a). On the other hand, in a rodent model of hypothyroidism, 1-methylhistidine levels were reduced in male and female rats versus control groups (Gołyński et al., 2016). With this said, reduced levels of methylhistidine with EGCG may be due to improved muscle cell viability, but this remains to be elucidated.

Commented [CS608]: Final update fo the figure for the key data from this section

A



B

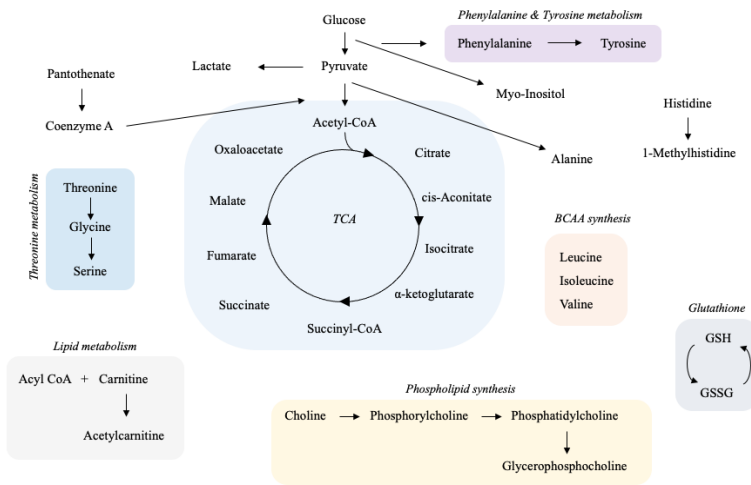


Figure 7. 39 Schematic representation of metabolic signatures in A) control and B) aged myotubes in the presence of 0, 5 and 10 μM EGCG. Metabolites in green and red are higher and lower with EGCG treatment vs. untreated CTRL. Metabolites in bold are significantly different vs. CTRL with 5 and 10 μM EGCG, whereas metabolites in regular font are only different vs. CTRL at one EGCG dose. Metabolites in black are similar between treatment conditions.

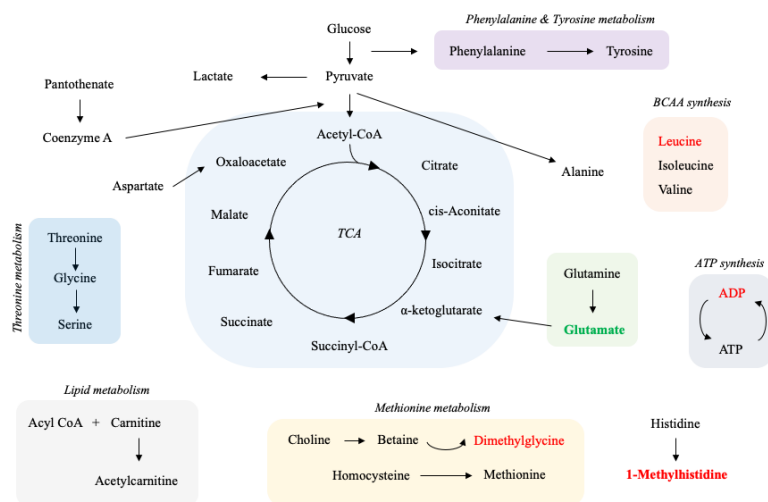
7.4.7 EPI effects in control and aged myoblasts

In the present study, physiological concentrations of EPI simultaneously increased levels of cis-Aconitic acid and decreased levels of citric acid in aged myoblasts. Thus, it may be that EPI facilitated the conversion of citric acid to cis-Aconitic acid in aged cells, although this is purely hypothetical. Alternatively, reduced citrate levels could reflect increased export of citrate from the mitochondria to the cytosol by the mitochondrial citrate transporter protein, where it has numerous metabolic fates, including supporting fatty acid and cholesterol biosynthesis (Gnoni, Priore, et al., 2009). In fact, a recent study provided evidence that EPI supplementation increased the expression of the mitochondrial citrate transporter protein in aged mice to levels observed in young animals (Si et al., 2019b). Besides changes in the abundance of TCA cycle intermediates, EPI treatment increased lactic acid production in aged myoblasts. Given the concurrent reduction in citric acid with EPI treatment, it is possible that EPI acutely inhibited mitochondrial respiration in aged myoblasts, resulting in augmented glycolysis. Accordingly, EPI inhibited mitochondrial respiration in aged myoblasts in Chapter 5.

One-methylhistidine abundance was lowered in control and aged cells by EPI treatment when compared to untreated conditions (see Figure 7.40A/B). At the present moment, there is no consensus on whether 1-methylhistidine plays a regulatory role in cellular ageing, though it has been reported as a urinary biomarker of drug-induced muscle toxicity (Aranibar et al., 2011b). The formation of 1-methylhistidine is achieved from the splitting of anserine by carnosinase. In spite of decreased levels of 1-methylhistidine in the presence of EPI, levels of anserine and beta-alanine remained unchanged. Therefore, the reasons for the observed reductions in 1-methylhistidine after EPI treatment are not clear and require further study.

Glutamic acid levels were increased in control myoblasts cultured in the presence of EPI. Two of the many important roles played by glutamic acid is the synthesis of glutathione (GSH) (Tapiero et al., 2002) and α -ketoglutarate to support the replenishment of TCA cycle intermediates by anaplerosis (Mourtzakis et al., 2008). Therefore, the reported changes in glutamic acid may reflect a response to an altered redox state and/or increased requirement for replenishment of TCA cycle intermediates. More research is required to delineate the potential antioxidant and metabolic role of EPI in skeletal muscle cells.

A



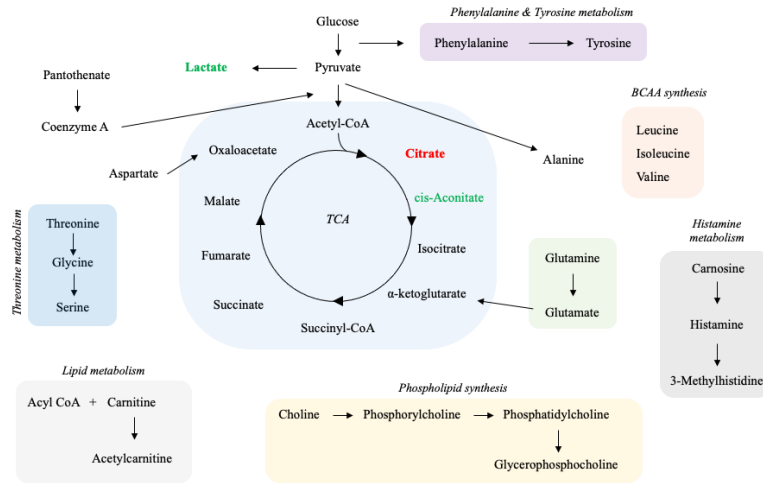
B

Figure 7. 40 Schematic representation of metabolic signatures in A) control and B) aged myoblasts in the presence of 0, 5 and 10 μM EPI. Metabolites in green and red are higher and lower with EPI treatment vs. untreated CTRL. Metabolites in bold are significantly different vs. CTRL with 5 and 10 μM EPI, whereas metabolites in regular font are only different vs. CTRL at one EPI dose. Metabolites in black are similar between treatment conditions.

7.4.8 EPI effects in control and aged myotubes

The generation of cellular ATP is achieved by OXPHOS, a conserved mechanism that is dependent upon reducing equivalents generated by the TCA cycle and β -oxidation. Levels of cis-Aconitic acid were increased in aged myotubes cultured in the presence of EPI, suggesting increased oxidative metabolism. This finding in the data is in line with some (Kener et al., 2018b; Panneerselvam et al., 2013; Rowley et al., 2017b), but not all (Bitner et al., 2018; Keller et al., 2020; Kopustinskiene et al., 2015b) studies showing enhanced state 3 supported

mitochondrial respiration following EPI supplementation in cell and rodent models. One key rate-limiting metabolite in fatty acid oxidation, carnitine, facilitates the import of long-chain fatty acids (LCFA) across the inner mitochondrial membrane (Fritz & Yue, 1963). In aged myotubes, we demonstrated increased L-Carnitine levels in the presence of EPI. Similar results have been reported previously, where adult male mice receiving a flavanol supplement (containing predominately EPI) over 14 days elevated the capacity for LCFA transport in the gastrocnemius and soleus muscles (Watanabe et al., 2014). Collectively, the reported changes in metabolites associated with oxidative metabolism suggests EPI may evoke favourable adaptations at the level of mitochondria in aged skeletal myotubes (see Figure 7.41A/B).

The ratio of ADP/ATP reflects the cellular energetic state, with increased ADP/ATP being indicative of metabolic stress, and more severely, cell death. Levels of ADP were lowered in response to EPI treatment in control, but not aged myotubes. Thus, considering the similarity in levels of ATP between experimental conditions, it is possible that EPI brought about a reduced ADP/ATP ratio, and subsequently, a more favourable metabolic milieu. Further work is required to help explain the observed changes in ADP in response to EPI, and what the potential implications of a lowered ADP/ATP ratio may be for cellular adaptation.

Other metabolites impacted by EPI, not directly related to energy metabolism were myo-inositol and methylhistidine. In response to EPI, levels of myo-inositol, which were elevated in aged myotubes, decreased towards values observed in control myotubes. Although more research is necessary to determine the role of myo-inositol in cellular ageing, this metabolite appears to be involved in phospholipid synthesis and act as a secondary messenger in signal transduction (Berridge, 2009; Chakraborty et al., 2010). Thus, our findings hint that one mechanism by which EPI may elicit health benefits is via modulation of phospholipid synthesis

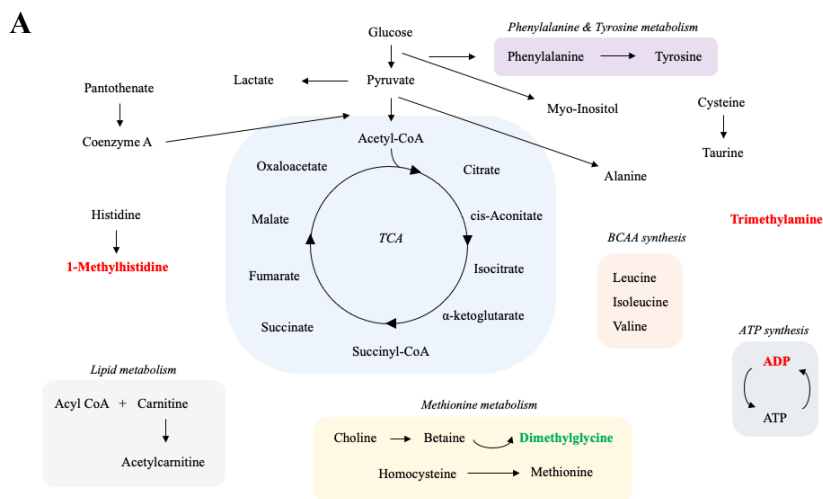
Commented [CS609]: What precisely do you mean by this?

Commented [CS610]: In what pathway? Important for PIP2/Pip3 and Akt signalling? Might be upregulated as a protective mechanism against deleterious impact of ageing.....is it then beneficial to bring levels down?

and/or Ca^{2+} or Akt **cell signalling** in skeletal muscle cells. Concerning 1-methylhistidine, reduced levels of this metabolite were found in control and aged myotubes cultured in the presence of EPI. From the current literature, it is not clear what the cellular implications of reduced 1-methylhistidine levels are, though they may relate to improved cell viability (Aranibar et al., 2011a). An alternative derivative of histidine, 3-methylhistidine, was significantly lowered in aged myotubes cultured with 10 μ M EPI. Unlike its related metabolite, 3-methylhistidine is a robust indicator of increased actin and myosin degradation (Thompson et al., 1996; Vesali et al., 2004). Thus, our data suggest that micromolar concentrations of EPI may reduce muscle protein degradation in aged cells. Evidence for such an effect comes from a recent study, where muscle atrophy 30 days after spinal cord injury was reduced from ~50% to 25% with daily EPI supplementation in female rats (Gonzalez-Ruiz et al., 2020). Clearly, further research is required to delineate the mechanisms by which EPI may regulate muscle protein **degradation**.

Commented [CS611]: Via what pathway? Add some detail for specificity here

Commented [CS612]: Again, bring the picture on of blars and tubes, young and old and add the key EPI data to it.



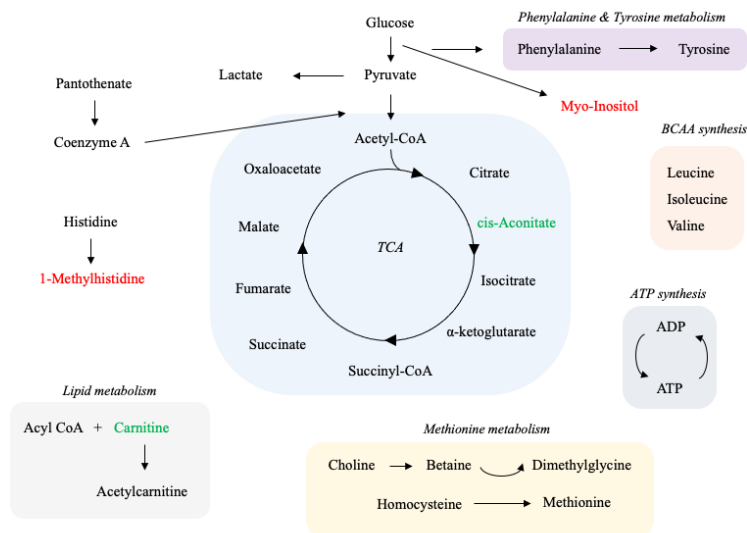
B

Figure 7. 41 Schematic representation of metabolic signatures in A) control and B) aged myotubes in the presence of 0, 5 and 10 μM EPI. Metabolites in green and red are higher and lower with EPI treatment vs. untreated CTRL. Metabolites in bold are significantly different vs. CTRL with 5 and 10 μM EPI, whereas metabolites in regular font are only different vs. CTRL at 5 μM EPI dose. Metabolites in black are similar between treatment conditions.

7.5 Limitations

A number of limitations are present in this study that limit its translatability. Firstly, despite the low micromolar doses of flavonoids used in this *in vitro* study, they may still be above the concentrations realistically attained in skeletal muscle tissue after ingestion of flavonoids *in vivo* (Manach et al., 2005b). However, the plasma concentrations of compounds used in this study have been shown to reach up to 10 μM after oral ingestion *in vivo* (Williamson & Manach, 2005). Secondly, flavonoids undergo extensive metabolism in the gastrointestinal tract and liver after ingestion *in vivo* which produces secondary metabolites that may elicit

distinct biological effects to those of the parent compound. Currently, flavonoid metabolites are not widely commercially available, and therefore the feasible approach was to use parent flavonoid compounds. Future work should try and establish whether flavonoid metabolites promote similar adaptations to those found with the parent compounds in the present study. The use of a non-targeted metabolomics approach here resulted in identification of multiple unknown metabolites, which highlights one major problem in the field of metabolomics, where (limited) metabolite annotation and accuracy is an issue for biological contextualisation (Nagana Gowda & Raftery, 2015). Finally, we used a murine skeletal muscle cell line (C₂C₁₂) to study the effects of flavonoids on the cell metabolome. This cell-based approach will not recapitulate all features of human skeletal muscle tissue and its possible regulation by dietary compounds. However, the apparent metabolite-level differences between cells cultured in the absence and presence of flavonoids illuminates key changes that may be common to murine and human skeletal muscle cells.

7.6 Conclusion

Altogether, the findings presented in this chapter reveal novel effects of replicative ageing and dietary flavonoids on murine skeletal muscle cells at the metabolite level. In myoblasts and myotubes, replicative ageing caused profound changes in the cell metabolome, highlighting novel mechanisms of (replicative) ageing *in vitro*. Flavonoids are widely known for their potential to elicit health benefits, but the prospect that these dietary compounds may impact metabolic signatures has often been overlooked. Here, we demonstrate compound- and dose-dependent effects of flavonoids on the cellular metabolome, thus advancing our understanding of their known mechanisms of action. The fact that flavonoids evoked dose-dependent changes in metabolites in control and aged muscle cells emphasises that flavonoids may be valuable in promoting health benefits in older skeletal muscle. Further research is warranted to shed light

Commented [CS613]: This is an important aspect of this chapter, but you skim over it here very quickly. It probably deserves a sentence or two in its own right.

Commented [CS614]: With both beneficial and detrimental impact.....

Commented [CS615]: See above

on the cellular adaptations brought about by flavonoids that are reflected at the level of metabolites.

Chapter 8: Thesis synthesis

8.1 Realisation of Aims

The major aims of this thesis were two-fold: 1) speed pulmonary $\dot{V}O_2$ kinetics and enhance exercise tolerance in physically inactive middle-aged adults by cocoa-flavanol supplementation (Chapter 3). 2) simultaneously enhance mitochondrial function, cell signalling and attenuate ROS production in (replicatively) aged skeletal muscle and human vascular endothelial cells using dietary flavonoids, *in vitro* (Chapter 4, 5 and 6).

Commented [CS616]: No mention of ageing in the aims – undersells your motivation a little.

See comment 4 below linked to the hypothesis. I would reformat your aim, add your hypotheses and then your underpinning objectives.

Commented [HJ617]: Link back so wording the same as abstract/intro to lit review as well as aims and hypothesis

To realise these aims, the studies in this thesis addressed the following objectives:

1. Investigate the impact of acute cocoa-flavanol supplementation on pulmonary $\dot{V}O_2$ kinetics and exercise tolerance in physically inactive middle-aged adults.
2. Examine whether flavonoids modulate ROS production, mitochondrial function and cell signalling using human vascular endothelial cells as a model system.
3. Determine whether replicative ageing and dietary flavonoids impact NO bioavailability, mitochondrial function and gene expression using C₂C₁₂ myoblasts as a model system.
4. Investigate the effects of replicative ageing and flavonoids on mitochondrial function, ROS production and cell signalling using C₂C₁₂ myotubes as a model system.
5. Explore how replicative ageing and dietary flavonoids impact the metabolome of murine skeletal muscle myoblasts and myotubes.

Objective 1: Investigate the impact of cocoa-flavanol supplementation on pulmonary $\dot{V}O_2$ kinetics and exercise tolerance in physically inactive middle-aged adults.

Objective one was addressed in Chapter 3. The hypothesis that cocoa-flavanols would speed pulmonary $\dot{V}O_2$ kinetics and enhance exercise tolerance in physically inactive middle-aged adults was only partially accepted. Acute cocoa-flavanol supplementation sped phase II $\dot{V}O_2$ kinetics by ~6 seconds compared to placebo during exercise in the moderate intensity domain. However, cocoa-flavanol supplementation did not alter the phase II $\dot{V}O_2$ kinetics during severe-intensity exercise and did not enhance exercise tolerance as assessed by time-to-exhaustion.

Objective 2: Examine whether flavonoids modulate ROS production, mitochondrial function and cell signalling using human vascular endothelial cells as a model system.

This objective was addressed in Chapter 4. The hypothesis that flavonoids would attenuate ROS production and enhance indices of mitochondrial function and cell signalling in human vascular endothelial cells was partially accepted/rejected. Although specific flavonoids attenuated ROS production in the absence and presence of antimycin A, these effects were largely dependent on the compound and dose administered. Therefore, flavonoids may act in a pro-oxidant manner at some doses, but in an antioxidant manner at others in vascular endothelial cells. In this study, flavonoids did not measurably impact indices of mitochondrial functionality. However, flavonoids did regulate the transcription of genes associated with mitochondrial remodelling and the antioxidant response. Moreover, EPI transiently activated ERK1/2 signalling and increased NO bioavailability, which occurred in parallel with induction of NRF2.

Commented [CS618]: If the human study does come last and not first, is this hypothesis a logical one following from the cell data – would it be what would be proposed as a result of the data collected? If not, then it needs to be reformatted or the order of the thesis needs to be changed.

Objective 3: Determine whether replicative ageing and dietary flavonoids impact NO bioavailability, mitochondrial function and gene expression using C₂C₁₂ myoblasts as a model system.

In chapter 5, objective three was tackled. It was hypothesised that replicative ageing would cause mitochondrial dysfunction, attenuate NO production and blunt gene expression in myoblasts, and these effects would be alleviated by flavonoid treatment. The hypothesis was partially accepted and rejected, in that control and aged myoblasts presented comparable indices of mitochondrial function. However, replicative aging diminished NO bioavailability and lowered the expression of genes like PARKIN and SOD2. In disagreement with the hypothesis, flavonoids did not modulate mitochondrial respiration, but EPI blunted respiration in aged myoblasts. Further, flavonoids did not rescue the age-related decline in NO, but did augment the expression of genes associated with mitochondrial remodelling and the antioxidant response, including NRF2.

Objective 4: Investigate the effects of replicative ageing and flavonoids on mitochondrial function, ROS production and cell signalling using C₂C₁₂ myotubes as a model system.

In Chapter 6 it was hypothesised that replicative ageing would impair mitochondrial function, increase ROS production and blunt cell signalling in myotubes. Secondly, it was hypothesised that flavonoids would mitigate mitochondrial dysfunction, lower ROS production and enhance cell signalling in replicatively aged myotubes. Hypothesis one was partially accepted and rejected. Replicative ageing impaired coupling efficiency and oxidative phosphorylation and increased the production of ROS. However, cell signalling was not significantly altered by ageing. In contrast to the second hypothesis, flavonoids did not mitigate the age-related decline in mitochondrial function or increase in ROS emission. Nevertheless, flavonoids did confer

Commented [CS619]: This contradicts your hypothesis written above

Commented [SD620R619]: Does 'partially accepted' address this or not appropriate?

beneficial cell adaptations at the level of transcription and AMPK signalling (see general findings section 8.2).

Objective 5: Explore how replicative ageing and dietary flavonoids impact the metabolome of murine skeletal muscle myoblasts and myotubes.

This objective was addressed in Chapter 7. Using an untargeted NMR metabolomics approach, metabolic signatures of control and aged skeletal myoblasts and myotubes were determined, in the absence and presence of dietary flavonoids. The metabolome of replicatively aged skeletal myoblasts revealed elevated BCAA metabolism compared to control. However, BCAA metabolism was downregulated with ageing in myotubes. Metabolites involved in oxidative metabolism like L-carnitine and cis-Aconitic acid were also attenuated in aged myotubes compared to control. Besides, novel metabolites (dihydrothymine and myo-inositol) demonstrated a potential important role in cellular ageing. Moreover, and in partial agreement with hypothesis two, flavonoids partially alleviated some age-related perturbations to metabolite signatures in myoblast and myotubes. EPI increased L-carnitine levels in aged myotubes, but not to levels reported in control. In addition, flavonoid treatment typically increased lactate abundance, suggesting inhibitions to oxidative metabolism with specific flavonoids and doses.

8.2 General findings

In Chapter 3, the effects of an acute cocoa-flavanol supplementation regime upon $\dot{V}O_2$ kinetics and exercise tolerance were investigated. This study demonstrated that cocoa-flavanols speed phase II $\dot{V}O_2$ kinetics in the moderate intensity exercise domain but did not enhance exercise

Commented [CS621]: See comment above

Commented [CS622]: How does this link to your aims above?

Commented [CS623]: Which was? If these are listed it makes life easier for your examiner. You could generate work packages or chapters with the hypotheses and objectives and how they were addressed (as you have done) and whether the hypotheses are accepted or not) as you have done.

Commented [CS624]: Vague – of the key pathways mentioned (see comment above), which were alleviated and was this beneficial.

Commented [HJ625]: My usual preference is to have this a bullet points for each study. What was the aim and then what was the main finding. I feel the rest is just repetition of what you have already said in the discussion chapters.

tolerance. Although this study could not directly explain what mechanisms were responsible for the faster phase II $\dot{V}O_2$ kinetics after CF supplementation, the potential cellular and molecular actions of flavonoids were investigated in subsequent chapters (4, 5, 6 and 7). Given the sensitivity of phase II $\dot{V}O_2$ kinetics to changes in O_2 delivery (blood flow and distribution) and utilisation (O_2 consumption within mitochondria), the following chapters investigated whether flavonoids affect vascular endothelial and skeletal muscle function *in vitro*.

The therapeutic potential of flavonoids was investigated *in vitro*, in the vascular endothelial cell. The vascular endothelial cell was used as a model cell type because of its importance in regulating blood flow and distribution during exercise, thus enabling a precise coupling of O_2 delivery to metabolic demand. The findings in this chapter demonstrated flavonoids do not play a significant role in modulating mitochondrial respiration. However, flavonoids dose-dependently regulated the production of mitochondrial derived ROS in vascular endothelial cells. In addition, EPI increased NO bioavailability and upregulated NRF2 expression. Interestingly, EPI also transiently augmented ERK1/2 signalling, independent of AMPK. Taken together, EPI induced NRF2 expression, increased NO bioavailability and dose-dependently regulated mitochondrial ROS production, in what seems an ERK1/2 dependent manner. Therefore, EPI may act through the mechanism of hormesis to promote beneficial adaptations in vascular endothelial cells.

Commented [CS626]: Nice.

Having ascertained how flavonoids modulate mitochondrial function, ROS production and signalling in the vascular endothelial cell, the next step was to investigate whether (replicative) ageing and flavonoids impact skeletal muscle cell energy metabolism. Therefore, Chapter 5

and 6 examined the impact of replicative ageing upon mitochondrial function, ROS production and cell signalling in C₂C₁₂ myoblasts and myotubes. The data in these chapters demonstrated that ageing inhibits indices of mitochondrial function (coupling efficiency and OXPHOS), augments the production of mitochondrial ROS, and blunts cell signalling in myotubes.

Commented [CS627]: Such as?

With the understanding that ageing compromises myotube mitochondrial integrity and ROS emission, Chapter 6 further elucidated whether flavonoids could mitigate age-related impairments to mitochondrial function, ROS production and cell signalling. The data in this chapter demonstrated that flavonoids do not rescue age-related impairments to mitochondrial respiration. Further, EPI may inhibit indices of mitochondrial respiration (basal respiration and OXPHOS) in aged myoblasts. It was also determined that flavonoids do not play a significant role in regulating mitochondrial ROS emission, although, they do modulate the transcriptional responses of muscle cells. One transcript commonly upregulated by flavonoid treatment, in both muscle cell models, was NRF2, a transcription factor responsible for the regulation of multiple antioxidant and mitochondrial related genes. Study of EPI's potential upstream signalling effects revealed augmented AMPK signalling, independent of NO bioavailability, which may contribute to induction of NRF2 in the presence of EPI. Notably, EPI evoked distinct signalling responses to those found in Chapter 4, implying cell-type specific effects of flavonoids. This observation implies that skeletal muscle and vascular endothelial cell models may possess different transporters or enzymes capable of facilitating flavonoid metabolism or transport into the cell. Alternatively, these cell types may or may not possess specific cell membrane receptors that perpetuate the downstream signalling effects of EPI *in vitro*. Either way, the findings in this chapter suggest that flavonoids, and EPI especially, may act through the mechanism of hormesis to promote favourable cell adaptations.

Commented [CS628]: vague

Metabolites represent the most basic level of biological regulation. To gain further knowledge of whether ageing and flavonoids are capable of modulating features of metabolism *in vitro*, Chapter 7 profiled metabolites of control and aged skeletal muscle cells in the absence and presence of flavonoids. The primary outcomes of this study highlighted that (replicative) ageing significantly alters the metabolome of control and aged skeletal myoblasts and myotubes. Metabolites involved in BCAA synthesis were increased in myoblasts by replicative ageing, whereas they were lowered in aged myotubes. Other metabolites involved in oxidative metabolism such as cis-Aconitate and L-carnitine were lower in aged vs. control myotubes, providing support to the idea that replicatively aged myotubes exhibit mitochondrial dysfunction. Interestingly, novel metabolites including dihydrothymine and myo-inositol demonstrated age-dependent regulation. Flavonoids were only partially capable of alleviating some of the age-related perturbations to the metabolome. For example, 5 μ M EPI augmented L-carnitine abundance and attenuated myo-inositol levels in aged myotubes, but not to levels comparable to control. In spite of this, flavonoids evoked distinct, compound- and dose-dependent effects on the muscle cell metabolome. Thus, even from a metabolite level perspective, cellular ageing and dietary flavonoids are capable of regulating energy metabolism.

Commented [CS629]: Such as? Add a mention of pathways facilitated or hindered to provide the reader with specificity

Commented [CS630]: Worth putting in a figure of a cell with relevant pathways altered? This would be a great summary of complex findings -if not, this is a bit vague

Commented [SD631R630]: Have got figures in metabolomic chapter, shall I put here too?

8.3 Future Directions

8.3.1 Chapter 3:

A number of avenues for future research are present following the findings in this study. Given the speeding of phase II $\dot{V}O_2$ kinetics with CF supplementation, future studies should investigate whether CFs modulate blood flow and muscle oxygenation in a similar

demographic. Additional studies investigating CFs impact upon $\dot{V}O_2$ kinetics should include acute, invasive measures of blood and/or muscle biomarkers after CF ingestion to help determine the mechanisms contributing to changes in $\dot{V}O_2$ kinetics. Considering that the ergogenic effect of CFs was exercise-intensity domain dependent, research is necessary to determine a potential fibre-type dependency mode of action of CFs on physiological responses to exercise. One noteworthy observation of this study was that $\dot{V}O_2$ kinetics were markedly faster during severe-intensity than moderate-intensity exercise. This observation contrasts expected responses to exercise in the moderate and severe-intensity domains and suggests that prior moderate-intensity exercise could prime phase II $\dot{V}O_2$ kinetics of severe-intensity exercise in physically inactive middle-aged adults. Evidently, this hypothesis should be tested in subsequent research efforts by assessing phase II $\dot{V}O_2$ kinetics during severe-intensity exercise following a priming bout of moderate-intensity exercise on separate occasions (to enhance the signal-to-noise ratio and avoid the confounding effects of prior severe-intensity exercise on phase II $\dot{V}O_2$ kinetics).

Commented [CS632]: What would such a study look like?

Commented [SD633R632]: Ive added little extra, is this for me to think about rather than action on?

Commented [CS634]: Why?

Commented [SD635R634]: Relates to type I/II fibre distinguishability, need to check up on this and provide rationale

Commented [CS636]: How?

8.3.2 Chapter 4:

In light of the data obtained in this study, future studies could strive to replicate the findings in human arterial and/or microvascular endothelial cells, especially from sedentary older individuals. This would help establish whether flavonoids can induce similar endothelial adaptations in a more relevant cell type. One next research objective could be to determine whether flavonoids regulate the production of mitochondrial ROS, using more direct, sophisticated techniques. For instance, electron magnetic resonance spectroscopy (EPR) could be valuable in confirming whether flavonoids exert antioxidant effects in vascular endothelial cells. This technique enables precise and specific superoxide measurements to delineate

superoxide concentrations of mitochondrial origin (Sergey et al., 2007). In addition, further research efforts could consider whether flavonoids regulate the activity of antioxidant enzymes in vascular endothelial cells, which would help explain changes in ROS emission. Research could also investigate how flavonoids are transported in and out of the vascular endothelial cell, as very little information is available on their transportation. Moreover, research is necessary to investigate how EPI regulates ERK1/2 activity in vascular endothelial cells, and what potential downstream proteins are involved. Finally, further research is required to establish the mechanism by which EPI induces NRF2 expression, and whether the reported change in NRF2 gene expression is also associated with increased NRF2 activity. These studies would significantly advance knowledge of EPI's mode of action and shed light on its potential therapeutic value in the context of health and disease.

Commented [CS637]: All good suggestions, but what would the impact of such findings be – why would you do these studies, what would the underlying hypotheses be?

Commented [SD638R637]: Have added some more here

8.3.3 Chapter 5:

One future step following the findings in this chapter could be to try and replicate the reported findings in cells that better reflect *in vivo* muscle tissue, such as primary human skeletal muscle cells. Another potential direction for future research is the use of transcriptomics to determine differences between control and replicatively aged myoblasts and myotubes at the transcriptional level. This would afford in depth, genome-wide insights into the molecular regulatory processes associated with cellular ageing, which were limited to a handful of genes in this thesis. One consideration for successive research is the use of more sophisticated techniques, such as EPR, to study the production of mitochondrial ROS in replicatively aged cells at greater resolution. This will add further credence to the findings reported here using a fluorescent probe. Finally, the objective of this study was to determine the effects of replicative ageing in two models, the myoblast and myotube. Future endeavours could compare

mitochondrial function and ROS production between these two models, which could highlight important considerations for subsequent research intending on using the C₂C₁₂ myoblast model.

8.3.4 Chapter 6:

Several steps could be taken following the findings obtained in this study. One first step could be to try and replicate the reported findings in cells that better reflect *in vivo* muscle tissue, such as primary human skeletal muscle cells, or cell co-culture systems (such as endothelial, adipose and skeletal muscle cells). Future studies could consider using flavonoid metabolites, rather than their parent compounds, to investigate flavonoid metabolite-dependent regulation of mitochondrial bioenergetics. Aside from using flavonoid metabolites, further research could also investigate whether nanomolar flavonoid concentrations impact muscle mitochondrial function as these concentrations may more likely be attained after consumption of flavonoid-containing foods and beverages. This is supported by the dose-dependent effects of flavonoids reported here and in the published literature. Additional research could decipher whether skeletal muscle cells metabolise flavonoids *in vitro* and *in vivo*, and also, investigate how flavonoids are transported in and out of the muscle cell. Furthermore, it is also not currently known to what extent flavonoids reach skeletal muscle tissue after ingestion *in vivo*. Subsequent research using NMR or LC/MS metabolomics may reveal whether flavonoid metabolites accumulate in muscle tissue and at what concentrations, which would help guide further efforts at describing the efficacy of flavonoids in contributing to the maintenance of skeletal muscle health. One final possible avenue for subsequent research is the use of flavonoid cocktails, where multiple compounds are administered to cells in one bolus. This cocktail of flavonoids may better represent the pool of potential compounds reaching target tissues *in vivo* after the ingestion of flavonoid containing foods or beverages.

Commented [CS639]: Of which cells?

Commented [CS640]: Are they commercially available?

Commented [CS641]: What would the benefit of this be, above and beyond your findings?

Commented [CS642]: So what would you do to find out and what would the relevance be?

8.3.5 Chapter 7:

This study was primarily exploratory in nature. Given the hypothesis-generating potential of the untargeted metabolomics pipeline, multiple avenues for future research have emerged. Firstly, it would be interesting to investigate whether the metabolome of young and aged primary human skeletal muscle cells diverges in a similar manner to that observed in control and replicatively aged murine skeletal muscle cells. Secondly, a handful of metabolites, including myo-inositol and dihydrothymine, demonstrated age-dependent effects in myoblast and myotube models. Given the scarcity of data available on these metabolites in the context of ageing skeletal muscle, further research will help describe the potential role for these metabolites in contributing to the ageing phenotype in skeletal muscle. Following the observed changes in metabolite profiles with flavonoid treatment, further research is necessary to describe the potential regulation of specific metabolic pathways by flavonoids in skeletal muscle cells. For example, flavonoids tended to augment lactate abundance, which may be indicative of increased glycolysis and reduced reliance on OXPHOS. Further, some metabolites that showed age-dependent regulation were also modulated by flavonoid treatment. For example, Q and EPI attenuated the age-related increase in myo-inositol. Whereas only EPI partially alleviated the decline in L-carnitine observed in aged myotubes. Future research should resolve how flavonoid treatment changes the levels of the aforementioned metabolites, as this knowledge will help clarify the therapeutic value of flavonoids in alleviating age-related perturbations to energy metabolism. Besides these experimental leads, further research employing a similar study design using *in vivo* flavonoid metabolites would help decipher whether the flavonoid metabolites in circulation equally impact the metabolome of muscle tissue/cells. Moreover, future studies should determine whether nanomolar flavonoid

Commented [CS643]: this is the sort of detail that should be added in line with my comments above for chapter 3

Commented [CS644]: reducing?

Commented [CS645]: Wasn't this what happened in the ageing cells basally, or am I remembering incorrectly – if so, then it is worth commenting

Commented [CS646]: Which and how. Add specific detail to maintain your reader

concentrations impact the metabolic signatures of skeletal muscle cells. Additionally, metabolite profiling of primary skeletal muscle cells in the absence and presence of flavonoids will help enhance the translatability of this research. An important consideration for future endeavours is the use of complementary analyses like metabolic flux analysis. Such an approach combines stable isotope tracing of metabolites with MS or NMR spectroscopy to help depict metabolic reaction capacities. This affords greater mechanistic insight into the dynamics of molecular metabolic reactions that may help explain differences in metabolite profiles found between experimental groups (Xu et al., 2020). Finally, it would be interesting to study whether changes in the metabolome in response to ageing or dietary flavonoids are coupled with higher levels of biological regulation, including the transcriptome and proteome. These insights would provide information on what might occur within a biological system in response to flavonoids, beyond a snapshot of what is currently happening or has happened at the metabolite level.

Commented [CS647]: Why? What would the benefit of such knowledge be and how would it be applied?

8.4 Thesis Implications and conclusion

Physical inactivity and advancing age are two major causes of poor health outcomes and non-communicable diseases (Lim et al., 2012; Peterson et al., 2009). Strategies combatting the deleterious effects of inactivity and advancing age are vital for preserving functional capacity and independence into later life. One such strategy has been the use of bioactive nutritional compounds to enhance indices of cardiometabolic health. Dietary flavonoids are considered essential for maintaining health across the life course, yet knowledge of their health effects is incomplete. This thesis has contributed original knowledge to the known health effects and modes of action associated with flavonoid supplementation. flavonoids demonstrably enhanced skeletal muscle and vascular endothelial cell function, at the level of metabolites, protein phosphorylation and mRNA expression. Given the potential for activation of cellular

Commented [CS648]: Changes were evident in both young and old cells, so is the data really only pertinent to sedentary ageing? What about potential for preventative effects or delaying the impact of ageing.....

signalling pathways and transcriptional activities in the presence of these naturally occurring compounds, flavonoids may hold therapeutic value in the context of sedentary ageing. Beyond ageing, flavonoids may also promote beneficial health benefits in younger individuals, as there were clear benefits reported in non-aged cells. These findings have raised exciting possibilities about flavonoids as signalling molecules at the cellular level, which requires further study. Furthermore, the data presented emphasise cell-dependent modes of action of flavonoids *in vitro*, which could reflect important differences in the potential efficacy of these compounds in different tissues *in vivo*. Aside from exciting mechanistic advancement, this thesis has demonstrated the potential power of flavonoid supplementation (cocoa-flavanols) in speeding phase II $\dot{V}O_2$ kinetics during moderate-intensity activity in physically inactive middle-aged adults. Therefore, flavonoid supplementation may help enhance the tolerance of daily life activities with sedentary ageing and ultimately improve quality of life. The challenge remains to fully describe flavonoid mechanisms of action, and their potential to alleviate the burden of physical inactivity and older age.

Commented [CS649]: See coment above

Commented [CS650]: Very nice

Chapter 9: Appendices

Table 9. 1 Genes of interest investigated and their known function.

Gene	Function
CAT	Protect cells from the toxic effects of hydrogen peroxide
DRP1	Mediates mitochondrial membrane fission
eNOS	Produces NO
MFN2	Mediates mitochondrial clustering and fusion
NOX4	Generates superoxide intracellularly upon formation of a complex with CYBA/p22phox
NRF2	Transcription factor that plays a key role in the response to oxidative stress
PGC-1 α	Transcriptional coactivator that regulates genes involved in energy metabolism
PRKN	Component of a multiprotein E3 ubiquitin ligase complex that mediates the targeting of substrate proteins for proteasomal degradation
RPL13a	Associated with ribosomes but is not required for canonical ribosome function (housekeeping gene)
RP2 β	Encodes the second largest subunit of RNA polymerase II (housekeeping gene)
SIRT1	NAD-dependent deacetylase that links transcriptional regulation to intracellular energetics
SOD2	Destroys mitochondrial superoxide anion radicals
TFAM	Binds to the mitochondrial light strand promoter and functions in mitochondrial transcription regulation

Commented [CS651]: Something odd has happened with your formatting here.

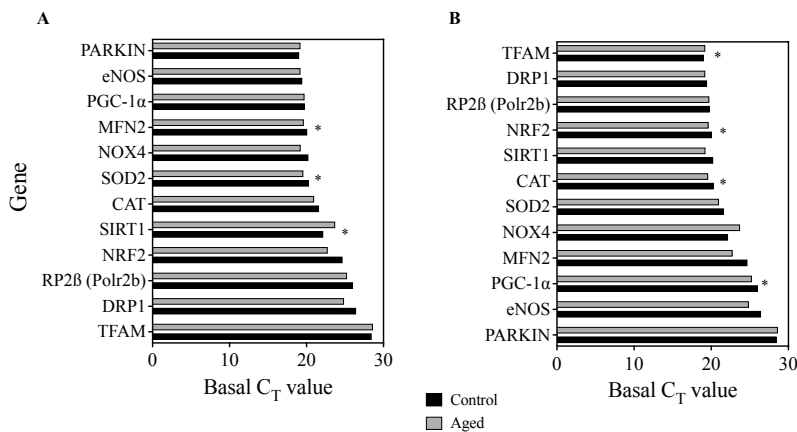


Figure 9. 1 Baseline C_T values of genes of interest in control and aged muscle A) myoblasts and B) myotubes. Control and aged myoblast/myotube are denoted by solid black and grey bars, respectively. **P*<0.05.

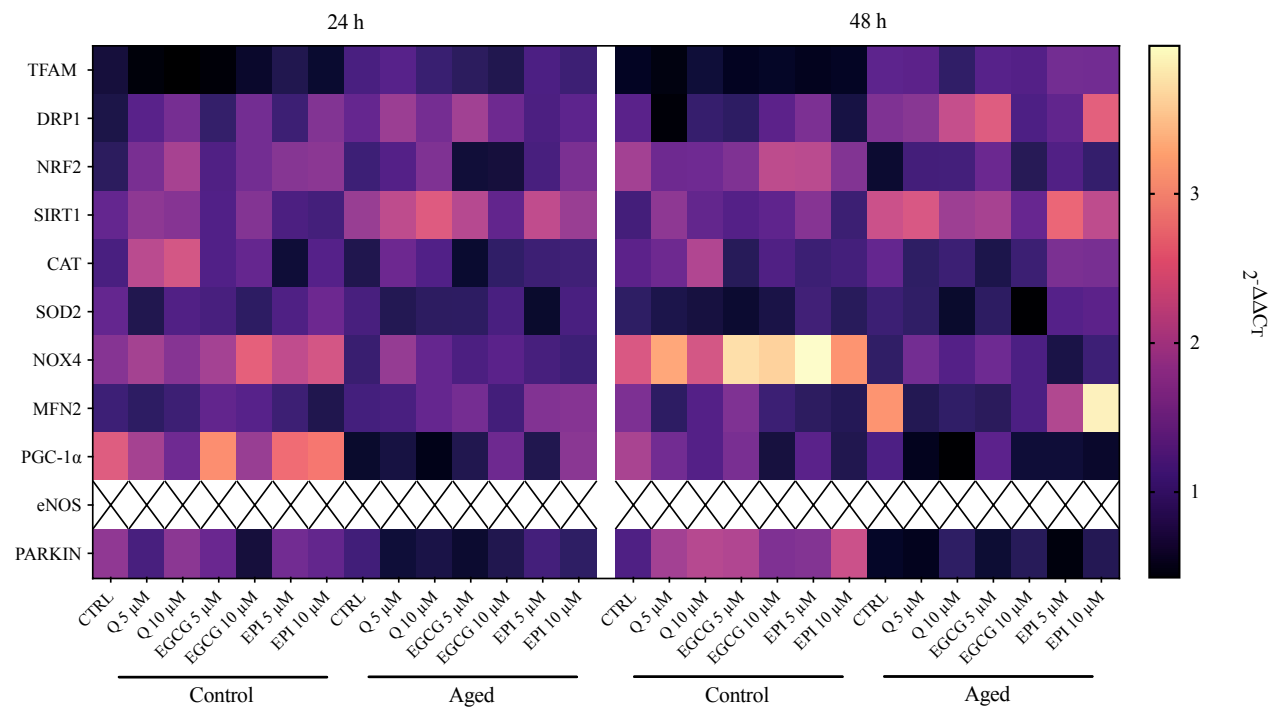


Figure 9. 2 Heatmap representation of myotube mRNA responses (without eNOS) in the absence of presence of flavonoids. Fold changes ($2^{-\Delta\Delta CT}$) in gene expression over 48 h presented as heat map.

Commented [CS652]: Again, is this referenced in the text? Were you going to do a second set with eNOS removed to illustrate the other changes more clearly? I think we talked about this but can't remember the conclusion.

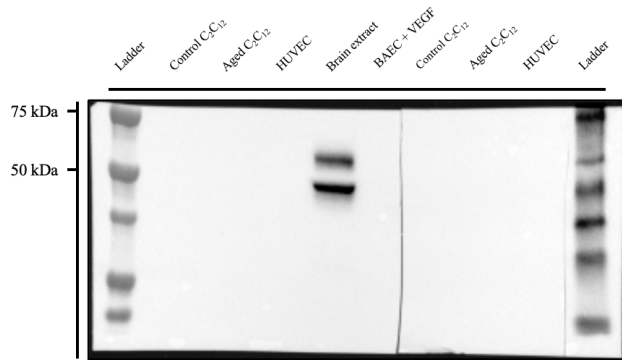


Figure 9. 3 Phosphorylation of CaMKII at Thr286 is not detectable under control conditions in C₂C₁₂ myotubes and HUVECs. Representative images of pThr286-CaMKII (60, 50 kDa) in control and aged C₂C₁₂ myotubes and HUVECs under control conditions, alongside positive control (mouse brain extract prepared from whole brain tissue of adult mice intended for use as a positive control and supplied by Cell Signaling Technology).

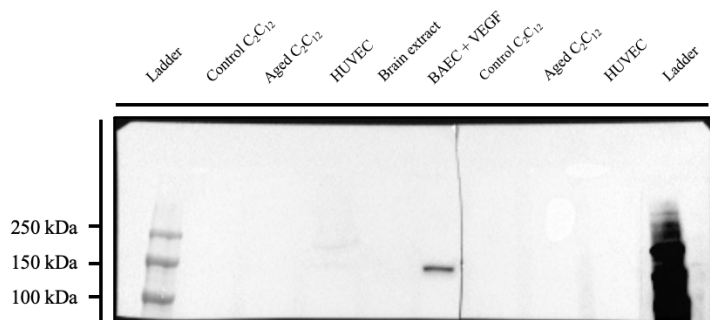


Figure 9. 4 Total eNOS is not detectable under control conditions in C₂C₁₂ myotubes. Representative images of eNOS (140 kDa) in control and aged C₂C₁₂ myotubes and HUVECs under control conditions, alongside positive control (Bovine arterial endothelial cells + vascular endothelial growth factor).

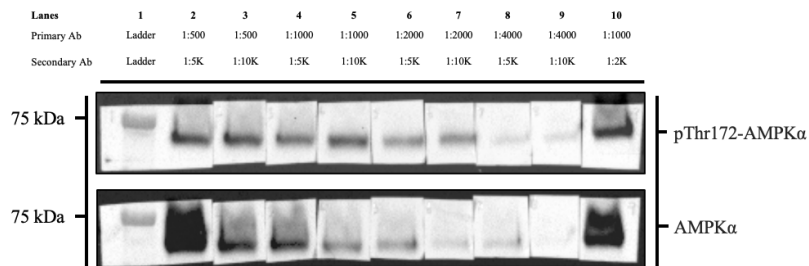


Figure 9. 5 pThr172-AMPK α and AMPK α primary and secondary antibody optimisation under control conditions in HUVECs. Representative image of pThr172-AMPK α and AMPK α (62 kDa) with primary dilution 1:500 to 1:4,000 and secondary dilution 1:2,000 to 1:10,000.

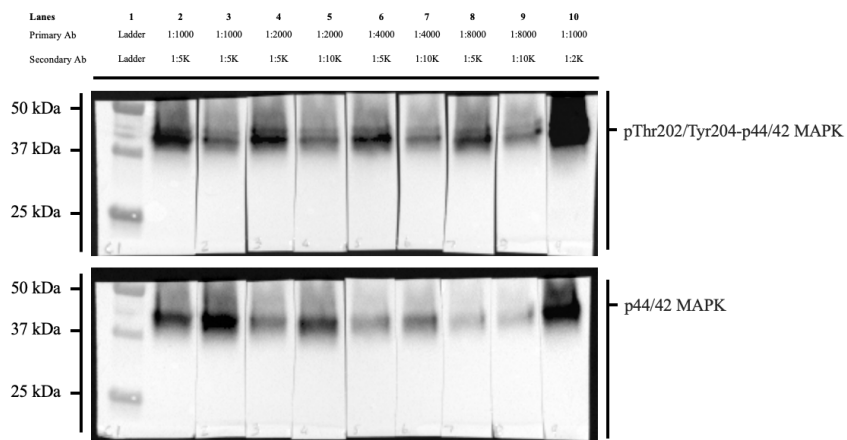


Figure 9. 6 pThr202/Tyr204-p44/42 MAPK and p44/42 MAPK primary and secondary antibody optimisation under control conditions in HUVECs. Representative image of pThr202/Tyr204-p44/42 MAPK and p44/42 MAPK (44/42 kDa) with primary dilution 1:1000 to 1:8,000 and secondary dilution 1:2,000 to 1:10,000.

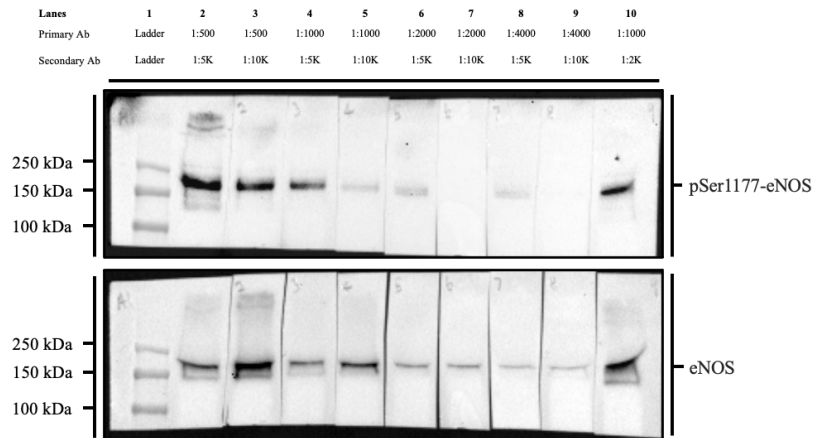


Figure 9. 7 pSer1177-eNOS and eNOS primary and secondary antibody optimisation under control conditions in HUVECs. Representative image of pSer1177-eNOS and eNOS (140 kDa) with primary dilution 1:500 to 1:4,000 and secondary dilution 1:2,000 to 1:10,000.

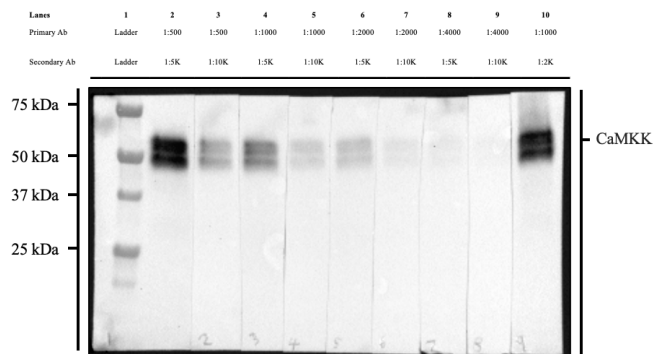


Figure 9. 8 CaMKII primary and secondary antibody optimisation under control conditions in C₂C₁₂ myotubes. Representative image of CaMKII (60, 50 kDa) with primary dilution 1:500 to 1:4,000 and secondary dilution 1:2,000 to 1:10,000.

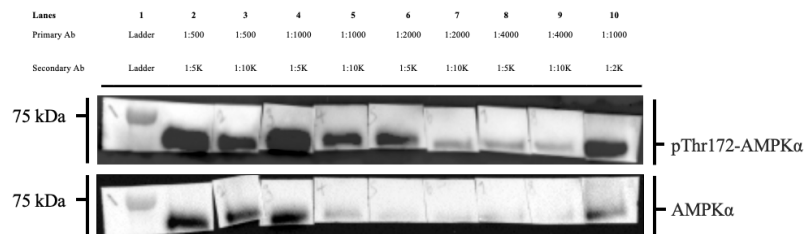


Figure 9. 9 pThr172-AMPK α and AMPK α primary and secondary antibody optimisation under control conditions in C₂C₁₂ myotubes. Representative image of pThr172-AMPK α and AMPK α (62 kDa) with primary dilution 1:500 to 1:4,000 and secondary dilution 1:2,000 to 1:10,000.

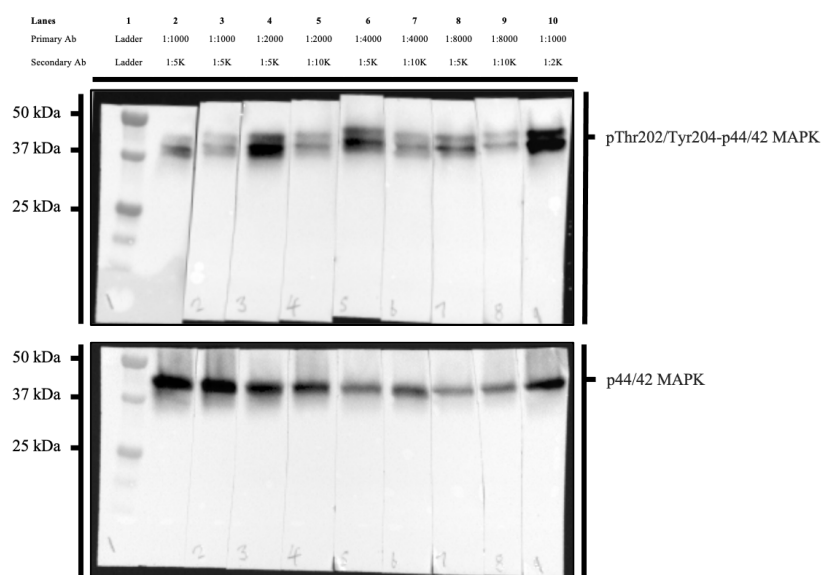


Figure 9. 10 pThr202/Tyr204-p44/42 MAPK and p44/42 MAPK primary and secondary antibody optimisation under control conditions in C₂C₁₂ myotubes. Representative image of pThr202/Tyr204-p44/42 MAPK and p44/42 MAPK (44/42 kDa) with primary dilution 1:1000 to 1:8,000 and secondary dilution 1:2,000 to 1:10,000.

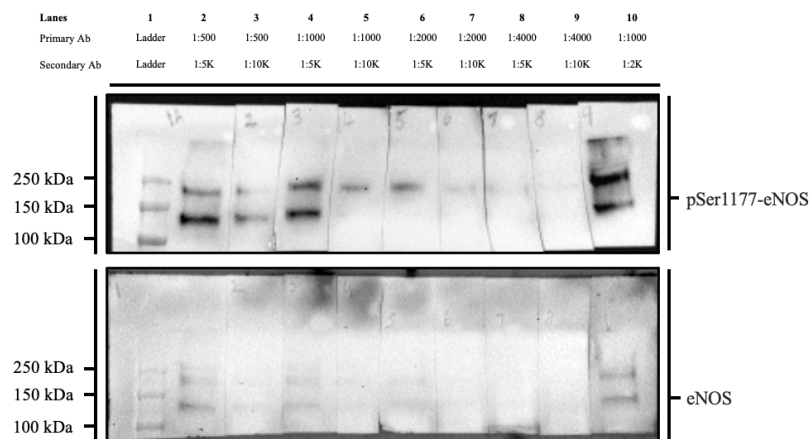


Figure 9. 11 pSer1177-eNOS and eNOS primary and secondary antibody optimisation under control conditions in C₂C₁₂ myotubes. Representative image of pSer1177-eNOS and eNOS (140 kDa) with primary dilution 1:500 to 1:4,000 and secondary dilution 1:2,000 to 1:10,000.

Table 9. 2 Metabolites with VIP scores >1 and entered for pathway analysis for comparison of control and aged skeletal myoblasts under CTRL conditions.

HMDB	Metabolite	Bin [*Overlap]	Direction of change vs. control
HMDB0000407	2-Hydroxy-3-methylbutyric acid	355/356	-
HMDB0004096	5-Methoxyindoleacetate	40	↑
HMDB0000042	Acetic acid	305	↓
HMDB0001659	Acetone	281	↓
HMDB0000034	Adenine	18/20	-
HMDB0000043	Betaine	180	-
HMDB0000033	Carnosine	46	↑
HMDB0000097	Choline	186	↓
HMDB0000072	cis-Aconitic acid	182	↓
HMDB0000122	D-Glucose	108	-
HMDB0000079	Dihydrothymine	336*	↑
HMDB0000086	Glycerophosphocholine	184	↑
HMDB0000721	Glycylproline	303	↑
HMDB0000128	Guanidoacetic acid	120	↓
HMDB0000870	Histamine	33	↑
HMDB0000161	L-Alanine	319	↓
HMDB0000191	L-Aspartic acid	222	↓
HMDB0000148	L-Glutamic acid	296	-
HMDB0000641	L-Glutamine	258	↑
HMDB0000172	L-Isoleucine	359	↑
HMDB0000687	L-Leucine	308	↑
HMDB0000159	L-Phenylalanine	36	↑
HMDB0000187	L-Serine	98	-
HMDB0000167	L-Threonine	144	↑
HMDB0000929	L-Tryptophan	44	↑
HMDB0000158	L-Tyrosine	45	-
HMDB0000883	L-Valine	354	↑
HMDB0000744	Malic acid	274	↑
HMDB0000211	myo-Inositol	141	-
HMDB0000812	N-Acetyl-L-aspartic acid	301	-
HMDB0006029	N-Acetylglutamine	297	-
HMDB0003357	N-Acetylmethionine	312	↑
HMDB0000446	N-Alpha-acetyllsine	313/314	-

HMDB0031419	N-Nitrosodimethylamine	120/190	-
HMDB0000210	Pantothenic acid	360	↑
HMDB0000209	Phenylacetic acid	42	-
HMDB0000243	Pyruvic acid	273	-
HMDB0000251	Taurine	159	↓
HMDB0000925	Trimethylamine N-oxide	180	↓
HMDB0000286	Uridine diphosphate glucose	60	-
HMDB0000935	Uridine diphosphate glucuronic acid	31	↑

↑ significantly higher and ↓ significantly lower in aged vs. control cells ($P < 0.05$). – similar between control and aged.

Table 9.3 Metabolites with VIP scores >1 and entered for pathway analysis for comparison of control and aged skeletal myotubes under CTRL conditions.

HMDB	Metabolite	Bin [*Overlap]	Direction of change vs. control
HMDB0000001	1-Methylhistidine	29	↓
HMDB0000407	2-Hydroxy-3-methylbutyric acid	355/356	-
HMDB00004096	5-Methoxyindoleacetate	40	-
HMDB0000895	Acetylcholine	285/286	-
HMDB0001890	Acetylcysteine	210	-
HMDB0000034	Adenine	18/20	-
HMDB0000097	Choline	186	↑
HMDB0000072	cis-Aconitic acid	182	↓
HMDB0000064	Creatine	103	-
HMDB0000562	Creatinine	198	-
HMDB0000079	Dihydrothymine	336/337	-
HMDB0000092	Dimethylglycine	212	↑
HMDB0000086	Glycerophosphocholine	184	↓
HMDB0000115	Glycolic acid	101	↑
HMDB0001273	Guanosine triphosphate	62/69	-
HMDB0000201	L-Acetylcarnitine	182	-
HMDB0000161	L-Alanine	319	↓
HMDB0000062	L-Carnitine	266	↓

HMDB0000641	L-Glutamine	258	-
HMDB0000172	L-Isoleucine	359	↓
HMDB0000687	L-Leucine	308	↓
HMDB0000159	L-Phenylalanine	36	-
HMDB0000929	L-Tryptophan	44	↓
HMDB0000158	L-Tyrosine	45	↑
HMDB0000883	L-Valine	354	↑
HMDB0000211	myo-Inositol	141	↑
HMDB0003357	N-Acetylmethionine	312	↓
HMDB0000446	N-Alpha-acetyllysine	313/314	↑
HMDB0031419	N-Nitrosodimethylamine	120/190	-
HMDB0001888	N,N-Dimethylformamide	200	↓
HMDB0003337	Oxidized glutathione	282	↑
HMDB0000210	Pantothenic acid	360	↓
HMDB0000243	Pyruvic acid	273	↑
HMDB0000251	Taurine	159	↓
HMDB0000906	Trimethylamine	213	↑
HMDB0000306	Tyramine	209	↑

↑ significantly higher and ↓ significantly lower in aged vs. control cells ($P < 0.05$). – similar between control and aged.

Table 9. 4 Metabolites with VIP scores >1 and entered for pathway analysis for comparison of Q treated control skeletal myoblasts.

HMDB	Metabolite	Bin [*Overlap]	Direction of change: 5 μ M vs. CTRL	Direction of change: 10 μ M vs. CTRL
HMDB0000407	2-Hydroxy-3-methylbutyric acid	355/356	↓	-
HMDB0001659	Acetone	281	-	-
HMDB0000895	Acetylcholine	285/286	-	-
HMDB0001890	Acetylcysteine	210	-	-
HMDB0000532	Acetylglycine	129*	↓	-
HMDB0000194	Anserine	129*	↓	↓
HMDB0000056	Beta-Alanine	250	↑	↑
HMDB0000043	Betaine	105/180	-	-
HMDB0000097	Choline	186	↓	-

HMDB0000072	cis-Aconitic acid	182	-	-
HMDB0000094	Citric acid	223	↓	↓
HMDB0000122	D-Glucose	108	↓	-
HMDB0000092	Dimethylglycine	212	↑	↑
HMDB0000123	Glycine	146	↑	↑
HMDB0000115	Glycolic acid	101	-	-
HMDB0000721	Glycylproline	303	-	-
HMDB0000191	L-Aspartic acid	222	↓	↓
HMDB0000190	L-Lactic acid	91	↑	↑
HMDB0000187	L-Serine	98	-	-
HMDB0000167	L-Threonine	144	-	-
HMDB0000744	Malic acid	274	-	-
HMDB0000211	myo-Inositol	141	↓	↓
HMDB0006029	N-Acetylglutamine	297	-	-
HMDB0001888	N,N-Dimethylformamide	200	↓	-
HMDB0003337	Oxidized glutathione	282	-	-
HMDB0001565	Phosphorylcholine	87	-	-
HMDB0000906	Trimethylamine	213	↑	↑
HMDB0000306	Tyramine	209	-	-

↑ significantly higher and ↓ significantly lower vs. untreated CTRL ($P < 0.05$). – similar between conditions.

Table 9. 5 Metabolites with VIP scores >1 and entered for pathway analysis for comparison of Q treated aged skeletal myoblasts.

HMDB	Metabolite	Bin [*Overlap]	Direction of change: 5 μ M vs. CTRL	Direction of change: 10 μ M vs. CTRL
HMDB0000407	2-Hydroxy-3-methylbutyric acid	355/356	-	↑
HMDB0000034	Adenine	18/20	-	-
HMDB0001341	ADP	8	-	-
HMDB0000056	Beta-Alanine	250	↑	↑
HMDB0000043	Betaine	105/180	-	-
HMDB0000094	Citric acid	223	↓	↓

HMDB0000562	Creatinine	198	-	-
HMDB0000660	D-Fructose	92	-	-
HMDB0000122	D-Glucose	108	-	↑
HMDB0000163	D-Maltose	110	-	-
HMDB0000108	Ethanol	338	↓	↓
HMDB0000123	Glycine	146	-	↑
HMDB0000863	Isopropyl alcohol	340/342	-	-
HMDB0000161	L-Alanine	319	-	↓
HMDB0000148	L-Glutamic acid	296	-	-
HMDB0000190	L-Lactic acid	91	↑	↑
HMDB0000687	L-Leucine	308	-	-
HMDB0000167	L-Threonine	144	-	-
HMDB0000883	L-Valine	354	-	-
HMDB0000211	myo-Inositol	141	↓	↓
HMDB0031419	N-Nitrosodimethylamine	120/190	-	-
HMDB0001565	Phosphorylcholine	87	-	-
HMDB0000243	Pyruvic acid	273	-	-

↑ significantly higher and ↓ significantly lower vs. untreated CTRL ($P < 0.05$). – similar between conditions.

Table 9. 6 Metabolites with VIP scores >1 and entered for pathway analysis for comparison of Q treated control skeletal myotubes.

HMDB	Metabolite	Bin [*Overlap]	Direction of change: 5 μ M vs. CTRL	Direction of change: 10 μ M vs. CTRL
HMDB0000407	2-Hydroxy-3-methylbutyric acid	355/356	-	-
HMDB0000538	Adenosine triphosphate	53	-	-
HMDB0001341	ADP	8	-	↓
HMDB0000043	Betaine	105/180	-	-
HMDB0000072	cis-Aconitic acid	182*	-	-
HMDB0000094	Citric acid	223	-	↓
HMDB0000660	D-Fructose	92	-	-
HMDB0000079	Dihydrothymine	336/337	-	-
HMDB0000086	Glycerophosphocholine	184	-	-

HMDB0000123	Glycine	146	↑	↑
HMDB0000201	L-Acetylcarnitine	182	-	-
HMDB0000161	L-Alanine	319	-	↓
HMDB0000191	L-Aspartic acid	222	-	-
HMDB0000641	L-Glutamine	258	-	-
HMDB0000172	L-Isoleucine	359	-	-
HMDB0000190	L-Lactic acid	91	-	↑
HMDB0000687	L-Leucine	308	-	-
HMDB0000167	L-Threonine	144	-	↓
HMDB0000929	L-Tryptophan	44	-	-
HMDB0000158	L-Tyrosine	45	↑	↑
HMDB0000883	L-Valine	354	-	-
HMDB0000211	myo-Inositol	141	-	-
HMDB0006029	N-Acetylglutamine	297	-	-
HMDB0003357	N-Acetylmethionine	312	-	-
HMDB0031419	N-Nitrosodimethylamine	120/190	-	-
HMDB0000902	NAD	3	-	-
HMDB0001565	Phosphorylcholine	87	↓	↓
HMDB0000243	Pyruvic acid	273	↓	-

↑ significantly higher and ↓ significantly lower vs. untreated CTRL ($P < 0.05$). – similar between conditions.

Table 9. 7 Metabolites with VIP scores >1 and entered for pathway analysis for comparison of Q treated aged skeletal myotubes.

HMDB	Metabolite	Bin [*Overlap]	Direction of change: 5 μ M vs. CTRL	Direction of change: 10 μ M vs. CTRL
HMDB0000895	Acetylcholine	285/286	-	-
HMDB0000538	Adenosine triphosphate	53	-	-
HMDB0000056	Beta-Alanine	250	-	↑
HMDB0000097	Choline	186	-	↓
HMDB0000094	Citric acid	223	-	-
HMDB0000064	Creatine	103	-	-
HMDB0000163	D-Maltose	110	-	↓

HMDB0000086	Glycerophosphocholine	184	-	-
HMDB0000721	Glycylproline	303	-	-
HMDB0000161	L-Alanine	319	-	-
HMDB0000148	L-Glutamic acid	296	-	-
HMDB0000641	L-Glutamine	258	-	↓
HMDB0000187	L-Serine	98	-	-
HMDB0000167	L-Threonine	144	-	-
HMDB0000744	Malic acid	274	-	-
HMDB0000211	myo-Inositol	141	↓	↓
HMDB0000812	N-Acetyl-L-aspartic acid	301	-	↑
HMDB0006029	N-Acetylglutamine	297	-	↑
HMDB0000446	N-Alpha-acetyllysine	313/314	-	-
HMDB0031419	N-Nitrosodimethylamine	120/190	-	-
HMDB0001888	N,N-Dimethylformamide	200	-	-
HMDB0001565	Phosphorylcholine	87	↓	↓
HMDB0000296	Uridine	88	-	-
HMDB0000286	Uridine diphosphate glucose	60	-	-

↑ significantly higher and ↓ significantly lower vs. untreated CTRL ($P < 0.05$). – similar between conditions.

Table 9. 8 Metabolites with VIP scores >1 and entered for pathway analysis for comparison of EGCG treated control skeletal myoblasts.

HMDB	Metabolite	Bin [*Overlap]	Direction of change: 5 μ M vs. CTRL	Direction of change: 10 μ M vs. CTRL
HMDB0000001	1-Methylhistidine	29	↓	↓
HMDB0000407	2-Hydroxy-3-methylbutyric acid	355/356	-	-
HMDB0004096	5-Methoxyindoleacetate	40	-	-
HMDB0000532	Acetylglycine	129	-	↑
HMDB0001341	ADP	8	-	↓
HMDB0000043	Betaine	105/180	-	-
HMDB0000033	Carnosine	46	-	-
HMDB0000094	Citric acid	223	-	-
HMDB0000064	Creatine	103	-	↑

HMDB0000660	D-Fructose	92	-	↑
HMDB0000163	D-Maltose	110	↑	↑
HMDB0000092	Dimethylglycine	212	-	↓
HMDB0000108	Ethanol	338	-	↓
HMDB0000134	Fumaric acid	48	-	↓
HMDB0000086	Glycerophosphocholine	101	-	↓
HMDB0000870	Histamine	184	-	↓
HMDB0000863	Isopropyl alcohol	340/342	-	-
HMDB0000172	L-Isoleucine	359	-	↓
HMDB0000190	L-Lactic acid	91	↑	↑
HMDB0000687	L-Leucine	308	-	↓
HMDB0000159	L-Phenylalanine	36	-	-
HMDB0000187	L-Serine	98	-	-
HMDB0000167	L-Threonine	144	↓	↓
HMDB0000929	L-Tryptophan	44	-	-
HMDB0000158	L-Tyrosine	45	-	-
HMDB0000883	L-Valine	354	-	-
HMDB0000744	Malic acid	274	↑	-
HMDB0000211	myo-Inositol	141	↑	↑
HMDB0000217	NADP	76	-	-
HMDB0003337	Oxidized glutathione	282	-	-
HMDB0000209	Phenylacetic acid	42	-	-
HMDB0001511	Phosphocreatine	199	-	-
HMDB0001565	Phosphorylcholine	87	↑	↑
HMDB0000251	Taurine	159	-	-
HMDB0000906	Trimethylamine	213	-	↓
HMDB0000925	Trimethylamine N-oxide	180	-	↑
HMDB0000306	Tyramine	209	-	↓
HMDB0000296	Uridine	88	-	-
HMDB0000935	Uridine diphosphate glucuronic acid	31	-	↓

↑ significantly higher and ↓ significantly lower vs. untreated CTRL ($P < 0.05$). – similar between conditions.

Table 9. 9 Metabolites with VIP scores >1 and entered for pathway analysis for comparison of EGCG treated aged skeletal myoblasts.

HMDB	Metabolite	Bin [*Overlap]	Direction of change: 5 μ M vs. CTRL	Direction of change: 10 μ M vs. CTRL
HMDB0000001	1-Methylhistidine	29	-	-
HMDB0000479	3-Methylhistidine	196/197	-	-
HMDB00004096	5-Methoxyindoleacetate	40	-	-
HMDB0001890	Acetylcysteine	210	-	-
HMDB0000194	Anserine	129	-	-
HMDB0000043	Betaine	105/180	-	-
HMDB0000072	cis-Aconitic acid	182	-	-
HMDB0000094	Citric acid	223	↓	↓
HMDB0000122	D-Glucose	108	-	-
HMDB0000079	Dihydrothymine	337/337	-	-
HMDB0000108	Ethanol	338	-	↓
HMDB0000134	Fumaric acid	48	-	-
HMDB0000086	Glycerophosphocholine	184	-	-
HMDB0000128	Guanidoacetic acid	120	-	-
HMDB0000863	Isopropyl alcohol	340/342	-	-
HMDB0000201	L-Acetylcarnitine	182	-	-
HMDB0000161	L-Alanine	319	-	-
HMDB0000062	L-Carnitine	266	-	-
HMDB0000148	L-Glutamic acid	296	-	-
HMDB0000172	L-Isoleucine	359	-	-
HMDB0000190	L-Lactic acid	91	↑	↑
HMDB0000687	L-Leucine	308	-	-
HMDB0000744	Malic acid	274	-	-
HMDB0000211	myo-Inositol	141	-	↑
HMDB0000812	N-Acetyl-L-aspartic acid	301	-	-
HMDB0003357	N-Acetylmethionine	312	-	-
HMDB0000446	N-Alpha-acetyllysine	313/314	-	-
HMDB0031419	N-Nitrosodimethylamine	120/190	-	-
HMDB0001888	N,N-Dimethylformamide	200	↑	-
HMDB0000210	Pantothenic acid	360	-	-
HMDB0001511	Phosphocreatine	199	-	-
HMDB0001565	Phosphorylcholine	87	-	↑

HMDB0000251	Taurine	159	-	-
HMDB0000925	Trimethylamine N-oxide	180	-	-

↑ significantly higher and ↓ significantly lower vs. untreated CTRL ($P < 0.05$). – similar between conditions.

Table 9. 10 Metabolites with VIP scores >1 and entered for pathway analysis for comparison of EGCG treated control myotubes.

HMDB	Metabolite	Bin [*Overlap]	Direction of change: 5 μ M vs. CTRL	Direction of change: 10 μ M vs. CTRL
HMDB0000001	1-Methylhistidine	29	↓	↓
HMDB0000407	2-Hydroxy-3-methylbutyric acid	355/356	-	-
HMDB00004096	5-Methoxyindoleacetate	40	-	-
HMDB0000895	Acetylcholine	285/286	-	-
HMDB0001890	Acetylcysteine	210	↓	-
HMDB0000034	Adenine	18/20	-	-
HMDB0000045	Adenosine monophosphate	16	-	-
HMDB0001341	ADP	8	-	↓
HMDB0000056	Beta-Alanine	250	-	-
HMDB0000043	Betaine	105/180	-	-
HMDB0000033	Carnosine	46	-	-
HMDB0000072	cis-Aconitic acid	182	-	-
HMDB0000064	Creatine	103	-	-
HMDB0000562	Creatinine	198	-	-
HMDB0000660	D-Fructose	92	-	-
HMDB0000122	D-Glucose	108	-	-
HMDB0000163	D-Maltose	110	-	-
HMDB0000092	Dimethylglycine	212	↓	-
HMDB0000134	Fumaric acid	48	-	-
HMDB0000115	Glycolic acid	101	-	-
HMDB0000128	Guanidoacetic acid	120	-	-
HMDB0000870	Histamine	33	-	-
HMDB0000201	L-Acetylcarnitine	182	-	-
HMDB0000161	L-Alanine	319	-	-

HMDB0000172	L-Isoleucine	359	-	-
HMDB0000687	L-Leucine	308	-	-
HMDB0000159	L-Phenylalanine	36	-	-
HMDB0000167	L-Threonine	144	↓	↓
HMDB0000929	L-Tryptophan	44	-	-
HMDB0000158	L-Tyrosine	45	-	-
HMDB0000902	NAD	3	-	↓
HMDB0003337	Oxidized glutathione	282	-	-
HMDB0000209	Phenylacetic acid	42	-	-
HMDB0000906	Trimethylamine	213	↓	↓
HMDB0000306	Tyramine	209	↓	↓
HMDB0000935	Uridine diphosphate glucuronic acid	31	-	-

↑ significantly higher and ↓ significantly lower vs. untreated CTRL ($P < 0.05$). – similar between conditions.

Table 9. 11 Metabolites with VIP scores >1 and entered for pathway analysis for comparison of EGCG treated aged skeletal myotubes.

HMDB	Metabolite	Bin [*Overlap]	Direction of change: 5 μ M vs. CTRL	Direction of change: 10 μ M vs. CTRL
HMDB0000407	2-Hydroxy-3-methylbutyric acid	355/356	-	-
HMDB0000479	3-Methylhistidine	196/197	-	-
HMDB0004096	5-Methoxyindoleacetate	40	-	-
HMDB0001890	Acetylcysteine	210	-	-
HMDB0000034	Adenine	18/20	-	-
HMDB0000045	Adenosine monophosphate	16	-	-
HMDB0000056	Beta-Alanine	250	-	-
HMDB0000033	Carnosine	46	-	-
HMDB0000097	Choline	186	-	-
HMDB0000072	cis-Aconitic acid	182	-	-
HMDB0000064	Creatine	103	-	-
HMDB0000660	D-Fructose	92	-	-
HMDB0000163	D-Maltose	110	-	-
HMDB0000079	Dihydrothymine	336/337	-	-

HMDB0000142	Formic acid	9	-	-
HMDB0000134	Fumaric acid	48	-	-
HMDB0000123	Glycine	146	-	-
HMDB0000721	Glycylproline	303	-	-
HMDB0000870	Histamine	33	-	-
HMDB0000201	L-Acetylcarnitine	182	-	-
HMDB0000161	L-Alanine	319	-	-
HMDB0000062	L-Carnitine	266	-	-
HMDB0000641	L-Glutamine	258	-	-
HMDB0000172	L-Isoleucine	359	-	-
HMDB0000159	L-Phenylalanine	36	-	-
HMDB0000167	L-Threonine	144	-	-
HMDB0000929	L-Tryptophan	44	-	-
HMDB0000158	L-Tyrosine	45	-	-
HMDB0000744	Malic acid	274	-	-
HMDB0000211	myo-Inositol	141	-	-
HMDB0003357	N-Acetylornithine	312	-	-
HMDB0000446	N-Alpha-acetyllysine	313/314	-	-
HMDB0031419	N-Nitrosodimethylamine	120/190	-	-
HMDB0001888	N,N-Dimethylformamide	200	-	-
HMDB0000217	NADP	76	-	-
HMDB0000210	Pantothenic acid	360	-	-
HMDB0000906	Trimethylamine	213	-	-
HMDB0000306	Tyramine	209	-	-
HMDB0000828	Ureidosuccinic acid	85	-	-

↑ significantly higher and ↓ significantly lower vs. untreated CTRL ($P < 0.05$). – similar between conditions.

Table 9. 12 Metabolites with VIP scores >1 and entered for pathway analysis for comparison of EPI treated control skeletal myoblasts.

HMDB	Metabolite	Bin [*Overlap]	Direction of change: 5 μ M vs. CTRL	Direction of change: 10 μ M vs. CTRL
HMDB0000001	1-Methylhistidine	29	↓	↓
HMDB0000479	3-Methylhistidine	196/197	-	-
HMDB0001890	Acetylcysteine	210	-	↓

HMDB0000034	Adenine	18/20	-	-
HMDB0000538	Adenosine triphosphate	53	-	-
HMDB0001341	ADP	8	-	↓
HMDB0000056	Beta-Alanine	250	-	-
HMDB0000043	Betaine	105/180	-	-
HMDB0000097	Choline	186	-	-
HMDB0000072	cis-Aconitic acid	182	-	-
HMDB0000094	Citric acid	223	-	-
HMDB0000562	Creatinine	198	-	-
HMDB0000079	Dihydrothymine	336/337	-	-
HMDB0000092	Dimethylglycine	212	-	↓
HMDB0000108	Ethanol	338	-	-
HMDB0000142	Formic acid	9	-	-
HMDB0000086	Glycerophosphocholine	184	-	-
HMDB0000123	Glycine	146	-	-
HMDB0000115	Glycolic acid	101	-	-
HMDB0001273	Guanosine triphosphate	62/69	-	-
HMDB0000201	L-Acetylcarnitine	182	-	-
HMDB0000161	L-Alanine	319	-	-
HMDB0000191	L-Aspartic acid	222	-	-
HMDB0000148	L-Glutamic acid	296	↑	↑
HMDB0000687	L-Leucine	308	-	↓
HMDB0000744	Malic acid	274	-	-
HMDB0000211	myo-Inositol	141	-	-
HMDB0006029	N-Acetylglutamine	297	-	-
HMDB0031419	N-Nitrosodimethylamine	120/190	-	-
HMDB0003337	Oxidized glutathione	282	-	-
HMDB0001511	Phosphocreatine	199	-	-
HMDB0000251	Taurine	159	-	-
HMDB0000906	Trimethylamine	213	-	↓
HMDB0000306	Tyramine	209	-	↓
HMDB0000828	Ureidosuccinic acid	85	-	-

↑ significantly higher and ↓ significantly lower vs. untreated CTRL ($P < 0.05$). – similar between conditions.

Table 9. 13 Metabolites with VIP scores >1 and entered for pathway analysis for comparison of EPI treated aged myoblasts.

HMDB	Metabolite	Bin [*Overlap]	Direction of change: 5 μ M vs. CTRL	Direction of change: 10 μ M vs. CTRL
HMDB0000001	1-Methylhistidine	29	-	↓
HMDB0001659	Acetone	281	-	-
HMDB0000034	Adenine	18/20	-	-
HMDB0000045	Adenosine monophosphate	16	-	-
HMDB0001341	ADP	8	-	-
HMDB0000043	Betaine	105/180	-	↓
HMDB0000097	Choline	186	-	-
HMDB0000072	cis-Aconitic acid	182	-	↑
HMDB0000094	Citric acid	223	↓	↓
HMDB0000562	Creatinine	198	-	-
HMDB0000122	D-Glucose	108	-	-
HMDB0000108	Ethanol	338	↓	↓
HMDB0000086	Glycerophosphocholine	184	-	-
HMDB0000115	Glycolic acid	101	-	-
HMDB0000863	Isopropyl alcohol	340/342	-	-
HMDB0000201	L-Acetylcarnitine	182	-	-
HMDB0000191	L-Aspartic acid	222	-	-
HMDB0000062	L-Carnitine	266	-	-
HMDB0000148	L-Glutamic acid	296	-	-
HMDB0000190	L-Lactic acid	91	↑	↑
HMDB0000744	Malic acid	274	-	-
HMDB0000211	myo-Inositol	141	-	-
HMDB0000812	N-Acetyl-L-aspartic acid	301	-	-
HMDB0006029	N-Acetylglutamine	297	↑	-
HMDB0031419	N-Nitrosodimethylamine	120/190	-	-
HMDB0001888	N,N-Dimethylformamide	200	-	-
HMDB0001511	Phosphocreatine	199	-	-
HMDB0000251	Taurine	159	-	-
HMDB0000935	Uridine diphosphate glucuronic acid	31	-	-

↑ significantly higher and ↓ significantly lower vs. untreated CTRL ($P < 0.05$). – similar between conditions.

Table 9. 14 Metabolites with VIP scores >1 and entered for pathway analysis for comparison of EPI treated control myotubes.

HMDB	Metabolite	Bin [*Overlap]	Direction of change: 5 μ M vs. CTRL	Direction of change: 10 μ M vs. CTRL
HMDB0000001	1-Methylhistidine	29	↓	↓
HMDB0004096	5-Methoxyindoleacetate	40	-	-
HMDB0001659	Acetone	281	-	-
HMDB0000034	Adenine	18/20	-	↑
HMDB0001341	ADP	8	↓	↓
HMDB0000056	Beta-Alanine	250	-	-
HMDB0000072	cis-Aconitic acid	182	-	-
HMDB0000079	Dihydrothymine	336/337	-	-
HMDB0000092	Dimethylglycine	212	↓	↓
HMDB0000108	Ethanol	338	-	-
HMDB0000134	Fumaric acid	48	-	-
HMDB0000086	Glycerophosphocholine	184	-	-
HMDB0000115	Glycolic acid	101	-	-
HMDB0000863	Isopropyl alcohol	340/342	-	↑
HMDB0000201	L-Acetylcarnitine	182	-	-
HMDB0000161	L-Alanine	319	-	-
HMDB0000172	L-Isoleucine	359	-	-
HMDB0000167	L-Threonine	144	-	-
HMDB0000929	L-Tryptophan	44	-	-
HMDB0000158	L-Tyrosine	45	-	-
HMDB0000883	L-Valine	354	-	-
HMDB0000211	myo-Inositol	141	-	-
HMDB0000902	NAD	3	-	-
HMDB0000906	Trimethylamine	213	↓	↓
HMDB0000306	Tyramine	209	-	-
HMDB0000286	Uridine diphosphate glucose	60	-	-
HMDB0000935	Uridine diphosphate glucuronic acid	31	-	-

↑ significantly higher and ↓ significantly lower vs. untreated CTRL ($P < 0.05$). – similar between conditions.

Table 9. 15 Metabolites with VIP scores >1 and entered for pathway analysis for comparison of EPI treated aged skeletal myotubes.

HMDB	Metabolite	Bin [*Overlap]	Direction of change: 5 μ M vs. CTRL	Direction of change: 10 μ M vs. CTRL
HMDB0000001	1-Methylhistidine	29	↓	-
HMDB0000407	2-Hydroxy-3-methylbutyric acid	355/356	-	-
HMDB0004096	5-Methoxyindoleacetate	40	-	-
HMDB0001341	ADP	8	-	-
HMDB0000056	Beta-Alanine	250	-	-
HMDB0000097	Choline	186	-	-
HMDB0000072	cis-Aconitic acid	182	↑	-
HMDB0000064	Creatine	103	-	-
HMDB0000163	D-Maltose	110	-	-
HMDB0000079	Dihydrothymine	336/337	-	-
HMDB0000092	Dimethylglycine	212	-	-
HMDB0000123	Glycine	146	-	-
HMDB0000201	L-Acetylcarnitine	182	-	-
HMDB0000161	L-Alanine	319	-	-
HMDB0000191	L-Aspartic acid	222	-	-
HMDB0000062	L-Carnitine	266	↑	-
HMDB0000172	L-Isoleucine	359	-	-
HMDB0000190	L-Lactic acid	91	-	-
HMDB0000687	L-Leucine	308	-	-
HMDB0000159	L-Phenylalanine	36	-	-
HMDB0000167	L-Threonine	144	-	-
HMDB0000929	L-Tryptophan	44	-	-
HMDB0000158	L-Tyrosine	45	-	-
HMDB0000883	L-Valine	354	-	-
HMDB0000211	myo-Inositol	141	↓	-
HMDB0031419	N-Nitrosodimethylamine	120/190	-	-
HMDB0003337	Oxidized glutathione	282	-	-
HMDB0000209	Phenylacetic acid	42	-	-
HMDB0000906	Trimethylamine	213	-	-

↑ significantly higher and ↓ significantly lower vs. untreated CTRL ($P < 0.05$). – similar between conditions.

Table 9. 16 Statistical analyses of control and aged myoblast metabolites following Q treatment.

Metabolite	Effect	<i>P</i>	<i>P</i> <0.05	<i>P</i> .significance
Formic acid	Dose	0.672		ns
Formic acid	Age	0.000473	*	***
Formic acid	Dose×Age	0.325		ns
Carnosine	Dose	0.525		ns
Carnosine	Age	0.000177	*	***
Carnosine	Dose×Age	0.074		ns
Fumaric acid	Dose	0.177		ns
Fumaric acid	Age	0.723		ns
Fumaric acid	Dose×Age	0.244		ns
D-Fructose	Dose	0.003	*	**
D-Fructose	Age	0.02	*	*
D-Fructose	Dose×Age	0.074		ns
Glycolic acid	Dose	0.036	*	*
Glycolic acid	Age	0.585		ns
Glycolic acid	Dose×Age	0.988		ns
Guanidoacetic acid	Dose	0.927		ns
Guanidoacetic acid	Age	0.008	*	**
Guanidoacetic acid	Dose×Age	0.701		ns
Glycine	Dose	4.99E-05	*	****
Glycine	Age	0.103		ns
Glycine	Dose×Age	0.142		ns
cis-Aconitic acid/L-Acetylcarnitine	Dose	0.812		ns
cis-Aconitic acid/L-Acetylcarnitine	Age	0.156		ns
cis-Aconitic acid/L-Acetylcarnitine	Dose×Age	0.138		ns
Choline	Dose	0.909		ns
Choline	Age	0.855		ns
Choline	Dose×Age	0.24		ns
Acetone	Dose	0.096		ns
Acetone	Age	0.002	*	**
Acetone	Dose×Age	0.661		ns
Acetic acid	Dose	0.421		ns
Acetic acid	Age	6.51E-05	*	****
Acetic acid	Dose×Age	0.736		ns
Dimethylglycine	Dose	0.108		ns
Dimethylglycine	Age	0.511		ns
Dimethylglycine	Dose×Age	0.338		ns
Acetylglycine	Dose	0.806		ns

Acetylglucine	Age	0.203		ns
Acetylglucine	Dose×Age	0.047	*	*
N-Acetyl-L-aspartic acid	Dose	0.492		ns
N-Acetyl-L-aspartic acid	Age	0.076		ns
N-Acetyl-L-aspartic acid	Dose×Age	0.659		ns
Trimethylamine	Dose	0.131		ns
Trimethylamine	Age	0.795		ns
Trimethylamine	Dose×Age	0.311		ns
Trimethylamine N-oxide	Dose	0.178		ns
Trimethylamine N-oxide	Age	4.62E-16	*	****
Trimethylamine N-oxide	Dose×Age	0.877		ns
NN-Dimethylformamide	Dose	0.377		ns
NN-Dimethylformamide	Age	0.245		ns
NN-Dimethylformamide	Dose×Age	0.362		ns
5-Methoxyindoleacetate	Dose	0.477		ns
5-Methoxyindoleacetate	Age	1.73E-06	*	****
5-Methoxyindoleacetate	Dose×Age	0.303		ns
N-Acetylglutamine	Dose	0.057		ns
N-Acetylglutamine	Age	0.003	*	**
N-Acetylglutamine	Dose×Age	0.817		ns
ADP	Dose	0.002	*	**
ADP	Age	0.002	*	**
ADP	Dose×Age	0.171		ns
Adenine	Dose	0.571		ns
Adenine	Age	0.00013	*	***
Adenine	Dose×Age	0.852		ns
Phosphocreatine	Dose	0.693		ns
Phosphocreatine	Age	0.318		ns
Phosphocreatine	Dose×Age	0.145		ns
Creatine	Dose	0.286		ns
Creatine	Age	0.003	*	**
Creatine	Dose×Age	0.688		ns
Creatinine	Dose	0.537		ns
Creatinine	Age	0.257		ns

Creatinine	Dose×Age	0.174		ns
Pyruvic acid	Dose	0.008	*	**
Pyruvic acid	Age	0.194		ns
Pyruvic acid	Dose×Age	0.644		ns
Acetylcholine	Dose	0.337		ns
Acetylcholine	Age	0.363		ns
Acetylcholine	Dose×Age	0.327		ns
N-Alpha-acetyllysine	Dose	0.072		ns
N-Alpha-acetyllysine	Age	0.093		ns
N-Alpha-acetyllysine	Dose×Age	0.671		ns
Dihydrothymine	Dose	0.026	*	*
Dihydrothymine	Age	3.15E-07	*	****
Dihydrothymine	Dose×Age	0.786		ns
Isopropyl alcohol	Dose	0.005	*	**
Isopropyl alcohol	Age	9.44E-14	*	****
Isopropyl alcohol	Dose×Age	0.034	*	*
Betaine	Dose	0.048	*	*
Betaine	Age	0.002	*	**
Betaine	Dose×Age	0.464		ns
2-Hydroxy-3-methylbutyric acid	Dose	0.001	*	***
2-Hydroxy-3-methylbutyric acid	Age	0.257		ns
2-Hydroxy-3-methylbutyric acid	Dose×Age	0.004	*	**
3-Methylhistidine	Dose	0.204		ns
3-Methylhistidine	Age	2.30E-10	*	****
3-Methylhistidine	Dose×Age	0.125		ns
Guanosine triphosphate	Dose	0.255		ns
Guanosine triphosphate	Age	0.065		ns
Guanosine triphosphate	Dose×Age	0.958		ns
N-Nitrosodimethylamine	Dose	0.085		ns
N-Nitrosodimethylamine	Age	0.814		ns
N-Nitrosodimethylamine	Dose×Age	0.187		ns
L-Tyrosine	Dose	0.045	*	*
L-Tyrosine	Age	1.44E-06	*	****
L-Tyrosine	Dose×Age	0.894		ns
Glycerophosphocholine	Dose	0.371		ns
Glycerophosphocholine	Age	2.24E-06	*	****

Glycerophosphocholine	Dose×Age	0.362		ns
Phosphorylcholine	Dose	0.905		ns
Phosphorylcholine	Age	0.015	*	*
Phosphorylcholine	Dose×Age	0.8		ns
Anserine	Dose	2.02E-06	*	****
Anserine	Age	0.178		ns
Anserine	Dose×Age	0.004	*	**
1-Methylhistidine	Dose	0.256		ns
1-Methylhistidine	Age	0.174		ns
1-Methylhistidine	Dose×Age	0.364		ns
Uridine diphosphate glucuronic acid	Dose	0.901		ns
Uridine diphosphate glucuronic acid	Age	5.89E-06	*	****
Uridine diphosphate glucuronic acid	Dose×Age	0.526		ns
L-Threonine	Dose	0.001	*	***
L-Threonine	Age	0.000423	*	***
L-Threonine	Dose×Age	0.521		ns
L-Lactic acid	Dose	8.59E-20	*	****
L-Lactic acid	Age	1.60E-10	*	****
L-Lactic acid	Dose×Age	2.80E-08	*	****
L-Alanine	Dose	3.99E-05	*	****
L-Alanine	Age	4.70E-14	*	****
L-Alanine	Dose×Age	0.069		ns
L-Carnitine	Dose	0.315		ns
L-Carnitine	Age	0.138		ns
L-Carnitine	Dose×Age	0.458		ns
Acetylcysteine	Dose	0.204		ns
Acetylcysteine	Age	0.246		ns
Acetylcysteine	Dose×Age	0.44		ns
N-Acetylorithine	Dose	0.024	*	*
N-Acetylorithine	Age	1.06E-09	*	****
N-Acetylorithine	Dose×Age	0.078		ns
Ethanol	Dose	0.005	*	**
Ethanol	Age	0.003	*	**
Ethanol	Dose×Age	0.328		ns
Pantothenic acid	Dose	0.004	*	**
Pantothenic acid	Age	0.000173	*	***
Pantothenic acid	Dose×Age	0.857		ns
Adenosine triphosphate	Dose	0.045	*	*
Adenosine triphosphate	Age	0.897		ns
Adenosine triphosphate	Dose×Age	0.958		ns

Taurine	Dose	0.208		ns
Taurine	Age	9.07E-15	*	****
Taurine	Dose×Age	0.763		ns
Tyramine	Dose	0.121		ns
Tyramine	Age	0.392		ns
Tyramine	Dose×Age	0.433		ns
L-Tryptophan	Dose	0.437		ns
L-Tryptophan	Age	8.94E-07	*	****
L-Tryptophan	Dose×Age	0.641		ns
Histamine	Dose	0.469		ns
Histamine	Age	8.37E-05	*	****
Histamine	Dose×Age	0.214		ns
L-Phenylalanine	Dose	0.478		ns
L-Phenylalanine	Age	2.38E-07	*	****
L-Phenylalanine	Dose×Age	0.21		ns
L-Serine	Dose	0.029	*	*
L-Serine	Age	0.002	*	**
L-Serine	Dose×Age	0.025	*	*
Beta-Alanine	Dose	6.58E-06	*	****
Beta-Alanine	Age	5.35E-06	*	****
Beta-Alanine	Dose×Age	0.052		ns
Malic acid	Dose	0.074		ns
Malic acid	Age	0.43		ns
Malic acid	Dose×Age	0.303		ns
L-Valine	Dose	0.128		ns
L-Valine	Age	2.79E-12	*	****
L-Valine	Dose×Age	0.169		ns
Uridine diphosphate glucose	Dose	0.054		ns
Uridine diphosphate glucose	Age	0.015	*	*
Uridine diphosphate glucose	Dose×Age	0.852		ns
Uridine	Dose	0.637		ns
Uridine	Age	0.943		ns
Uridine	Dose×Age	0.802		ns
L-Aspartic acid	Dose	0.000156	*	***
L-Aspartic acid	Age	0.011	*	*
L-Aspartic acid	Dose×Age	0.019	*	*
NADP	Dose	0.581		ns
NADP	Age	0.953		ns
NADP	Dose×Age	0.14		ns
Glycylproline	Dose	0.076		ns
Glycylproline	Age	0.000214	*	***

Glycylproline	Dose×Age	0.917		ns
Adenosine monophosphate	Dose	0.978		ns
Adenosine monophosphate	Age	0.799		ns
Adenosine monophosphate	Dose×Age	0.48		ns
Phenylacetic acid	Dose	0.367		ns
Phenylacetic acid	Age	0.000175	*	***
Phenylacetic acid	Dose×Age	0.85		ns
D-Maltose	Dose	0.009	*	**
D-Maltose	Age	0.418		ns
D-Maltose	Dose×Age	0.203		ns
L-Isoleucine	Dose	0.636		ns
L-Isoleucine	Age	1.05E-09	*	****
L-Isoleucine	Dose×Age	0.347		ns
Citric acid	Dose	7.31E-10	*	****
Citric acid	Age	0.004	*	**
Citric acid	Dose×Age	0.769		ns
L-Leucine	Dose	0.015	*	*
L-Leucine	Age	0.000142	*	***
L-Leucine	Dose×Age	0.705		ns
Ureidosuccinic acid	Dose	0.709		ns
Ureidosuccinic acid	Age	0.696		ns
Ureidosuccinic acid	Dose×Age	0.669		ns
myo-Inositol	Dose	1.06E-08	*	****
myo-Inositol	Age	8.25E-05	*	****
myo-Inositol	Dose×Age	0.952		ns
NAD	Dose	0.629		ns
NAD	Age	0.371		ns
NAD	Dose×Age	0.293		ns
D-Glucose	Dose	0.005	*	**
D-Glucose	Age	0.993		ns
D-Glucose	Dose×Age	0.015	*	*
L-Glutamine	Dose	0.442		ns
L-Glutamine	Age	1.45E-05	*	****
L-Glutamine	Dose×Age	0.713		ns
L-Glutamic acid	Dose	0.007	*	**
L-Glutamic acid	Age	0.000666	*	***
L-Glutamic acid	Dose×Age	0.378		ns
Oxidized glutathione	Dose	0.094		ns
Oxidized glutathione	Age	0.204		ns
Oxidized glutathione	Dose×Age	0.133		ns

* $P < 0.05$, ** $P < 0.01$, *** $P < 0.001$, **** $P < 0.0001$.

Table 9. 17 Statistical analyses of control and aged myotube metabolites following Q treatment.

Metabolite	Effect	<i>P</i>	<i>P</i> < 0.05	<i>P</i> .significance
Formic acid	Dose	0.905		ns
Formic acid	Age	0.835		ns
Formic acid	Dose×Age	0.069		ns
Carnosine	Dose	0.576		ns
Carnosine	Age	0.927		ns
Carnosine	Dose×Age	0.489		ns
Fumaric acid	Dose	0.883		ns
Fumaric acid	Age	0.035	*	*
Fumaric acid	Dose×Age	0.319		ns
D-Fructose	Dose	0.528		ns
D-Fructose	Age	0.026	*	*
D-Fructose	Dose×Age	0.211		ns
Glycolic acid	Dose	0.145		ns
Glycolic acid	Age	1.37E-05	*	****
Glycolic acid	Dose×Age	0.623		ns
Guanidoacetic acid	Dose	0.608		ns
Guanidoacetic acid	Age	0.000271	*	***
Guanidoacetic acid	Dose×Age	0.053		ns
Glycine	Dose	0.006	*	**
Glycine	Age	1.07E-05	*	****
Glycine	Dose×Age	0.112		ns
cis-Aconitic acid/L-Acetylcarnitine	Dose	0.109		ns
cis-Aconitic acid/L-Acetylcarnitine	Age	0.028	*	*
cis-Aconitic acid/L-Acetylcarnitine	Dose×Age	0.266		ns
Choline	Dose	0.108		ns
Choline	Age	0.608		ns
Choline	Dose×Age	0.261		ns
Acetone	Dose	0.458		ns
Acetone	Age	0.749		ns
Acetone	Dose×Age	0.315		ns
Acetic acid	Dose	0.227		ns
Acetic acid	Age	0.293		ns

Acetic acid	Dose×Age	0.46		ns
Dimethylglycine	Dose	0.234		ns
Dimethylglycine	Age	1.44E-10	*	****
Dimethylglycine	Dose×Age	0.51		ns
Acetylglycine	Dose	0.642		ns
Acetylglycine	Age	0.039	*	*
Acetylglycine	Dose×Age	0.061		ns
N-Acetyl-L-aspartic acid	Dose	0.045	*	*
N-Acetyl-L-aspartic acid	Age	0.031	*	*
N-Acetyl-L-aspartic acid	Dose×Age	0.053		ns
Trimethylamine	Dose	0.218		ns
Trimethylamine	Age	2.29E-09	*	****
Trimethylamine	Dose×Age	0.453		ns
Trimethylamine N-oxide	Dose	0.521		ns
Trimethylamine N-oxide	Age	0.047	*	*
Trimethylamine N-oxide	Dose×Age	0.937		ns
NN-Dimethylformamide	Dose	0.343		ns
NN-Dimethylformamide	Age	0.152		ns
NN-Dimethylformamide	Dose×Age	0.771		ns
5-Methoxyindoleacetate	Dose	0.316		ns
5-Methoxyindoleacetate	Age	0.018	*	*
5-Methoxyindoleacetate	Dose×Age	0.366		ns
N-Acetylglutamine	Dose	0.018	*	*
N-Acetylglutamine	Age	0.48		ns
N-Acetylglutamine	Dose×Age	0.282		ns
ADP	Dose	0.026	*	*
ADP	Age	0.008	*	**
ADP	Dose×Age	0.462		ns
Adenine	Dose	0.107		ns
Adenine	Age	0.000543	*	***
Adenine	Dose×Age	0.531		ns
Phosphocreatine	Dose	0.503		ns
Phosphocreatine	Age	0.599		ns
Phosphocreatine	Dose×Age	0.674		ns
Creatine	Dose	0.325		ns
Creatine	Age	0.856		ns
Creatine	Dose×Age	0.353		ns
Creatinine	Dose	0.512		ns
Creatinine	Age	0.016	*	*
Creatinine	Dose×Age	0.078		ns
Pyruvic acid	Dose	0.156		ns
Pyruvic acid	Age	2.12E-06	*	****
Pyruvic acid	Dose×Age	0.62		ns

Acetylcholine	Dose	0.443		ns
Acetylcholine	Age	0.711		ns
Acetylcholine	Dose×Age	0.083		ns
N-Alpha-acetyllysine	Dose	0.185		ns
N-Alpha-acetyllysine	Age	2.43E-12	*	****
N-Alpha-acetyllysine	Dose×Age	0.275		ns
Dihydrothymine	Dose	0.062		ns
Dihydrothymine	Age	1.73E-05	*	****
Dihydrothymine	Dose×Age	0.231		ns
Isopropyl alcohol	Dose	0.001	*	***
Isopropyl alcohol	Age	7.05E-13	*	****
Isopropyl alcohol	Dose×Age	0.166		ns
Betaine	Dose	0.865		ns
Betaine	Age	0.971		ns
Betaine	Dose×Age	0.979		ns
2-Hydroxy-3-methylbutyric acid	Dose	0.162		ns
2-Hydroxy-3-methylbutyric acid	Age	0.122		ns
2-Hydroxy-3-methylbutyric acid	Dose×Age	0.03	*	*
3-Methylhistidine	Dose	0.01	*	**
3-Methylhistidine	Age	0.000898	*	***
3-Methylhistidine	Dose×Age	0.311		ns
Guanosine triphosphate	Dose	0.337		ns
Guanosine triphosphate	Age	0.746		ns
Guanosine triphosphate	Dose×Age	0.777		ns
N-Nitrosodimethylamine	Dose	0.389		ns
N-Nitrosodimethylamine	Age	5.68E-05	*	****
N-Nitrosodimethylamine	Dose×Age	0.675		ns
L-Tyrosine	Dose	4.65E-06	*	****
L-Tyrosine	Age	4.95E-07	*	****
L-Tyrosine	Dose×Age	0.057		ns
Glycerophosphocholine	Dose	0.083		ns
Glycerophosphocholine	Age	0.000317	*	***
Glycerophosphocholine	Dose×Age	0.652		ns
Phosphorylcholine	Dose	5.12E-07	*	****
Phosphorylcholine	Age	5.53E-11	*	****
Phosphorylcholine	Dose×Age	0.916		ns
Anserine	Dose	0.007	*	**
Anserine	Age	0.066		ns
Anserine	Dose×Age	0.561		ns
1-Methylhistidine	Dose	0.397		ns
1-Methylhistidine	Age	0.000146	*	***

1-Methylhistidine	Dose×Age	0.403		ns
Uridine diphosphate glucuronic acid	Dose	0.885		ns
Uridine diphosphate glucuronic acid	Age	0.042	*	*
Uridine diphosphate glucuronic acid	Dose×Age	0.751		ns
L-Threonine	Dose	0.003	*	**
L-Threonine	Age	0.213		ns
L-Threonine	Dose×Age	0.958		ns
L-Lactic acid	Dose	0.011	*	*
L-Lactic acid	Age	0.262		ns
L-Lactic acid	Dose×Age	0.235		ns
L-Alanine	Dose	0.002	*	**
L-Alanine	Age	2.75E-05	*	****
L-Alanine	Dose×Age	0.075		ns
L-Carnitine	Dose	0.374		ns
L-Carnitine	Age	6.41E-10	*	****
L-Carnitine	Dose×Age	0.326		ns
Acetylcysteine	Dose	0.178		ns
Acetylcysteine	Age	1.01E-09	*	****
Acetylcysteine	Dose×Age	0.041	*	*
N-Acetylmethionine	Dose	0.12		ns
N-Acetylmethionine	Age	3.75E-08	*	****
N-Acetylmethionine	Dose×Age	0.133		ns
Ethanol	Dose	0.865		ns
Ethanol	Age	0.863		ns
Ethanol	Dose×Age	0.985		ns
Pantothenic acid	Dose	0.561		ns
Pantothenic acid	Age	4.55E-18	*	****
Pantothenic acid	Dose×Age	0.478		ns
Adenosine triphosphate	Dose	0.12		ns
Adenosine triphosphate	Age	0.466		ns
Adenosine triphosphate	Dose×Age	0.844		ns
Taurine	Dose	0.874		ns
Taurine	Age	2.91E-06	*	****
Taurine	Dose×Age	0.891		ns
Tyramine	Dose	0.896		ns
Tyramine	Age	1.63E-09	*	****
Tyramine	Dose×Age	0.414		ns
L-Tryptophan	Dose	0.015	*	*
L-Tryptophan	Age	5.22E-05	*	****
L-Tryptophan	Dose×Age	0.211		ns
Histamine	Dose	0.496		ns

Histamine	Age	0.748	ns
Histamine	Dose×Age	0.517	ns
L-Phenylalanine	Dose	0.093	ns
L-Phenylalanine	Age	0.014 *	*
L-Phenylalanine	Dose×Age	0.57	ns
L-Serine	Dose	0.128	ns
L-Serine	Age	0.136	ns
L-Serine	Dose×Age	0.549	ns
Beta-Alanine	Dose	0.012 *	*
Beta-Alanine	Age	0.061	ns
Beta-Alanine	Dose×Age	0.332	ns
Malic acid	Dose	0.439	ns
Malic acid	Age	0.829	ns
Malic acid	Dose×Age	0.125	ns
L-Valine	Dose	0.067	ns
L-Valine	Age	0.002 *	**
L-Valine	Dose×Age	0.647	ns
Uridine diphosphate glucose	Dose	0.092	ns
Uridine diphosphate glucose	Age	0.044 *	*
Uridine diphosphate glucose	Dose×Age	0.494	ns
Uridine	Dose	0.584	ns
Uridine	Age	0.784	ns
Uridine	Dose×Age	0.357	ns
L-Aspartic acid	Dose	0.033 *	*
L-Aspartic acid	Age	0.838	ns
L-Aspartic acid	Dose×Age	0.063	ns
NADP	Dose	0.775	ns
NADP	Age	0.077	ns
NADP	Dose×Age	0.676	ns
Glycylproline	Dose	0.092	ns
Glycylproline	Age	0.215	ns
Glycylproline	Dose×Age	0.694	ns
Adenosine monophosphate	Dose	0.792	ns
Adenosine monophosphate	Age	0.142	ns
Adenosine monophosphate	Dose×Age	0.806	ns
Phenylacetic acid	Dose	0.066	ns
Phenylacetic acid	Age	0.107	ns
Phenylacetic acid	Dose×Age	0.262	ns
D-Maltose	Dose	0.351	ns
D-Maltose	Age	0.555	ns
D-Maltose	Dose×Age	0.033 *	*
L-Isoleucine	Dose	0.02 *	*
L-Isoleucine	Age	1.86E-06 *	****

L-Isoleucine	Dose×Age	0.114		ns
Citric acid	Dose	1.37E-05	*	****
Citric acid	Age	0.000483	*	***
Citric acid	Dose×Age	0.266		ns
L-Leucine	Dose	0.071		ns
L-Leucine	Age	3.75E-08	*	****
L-Leucine	Dose×Age	0.192		ns
Ureidosuccinic acid	Dose	0.738		ns
Ureidosuccinic acid	Age	0.162		ns
Ureidosuccinic acid	Dose×Age	0.648		ns
myo-Inositol	Dose	0.000675	*	***
myo-Inositol	Age	1.36E-18	*	****
myo-Inositol	Dose×Age	0.358		ns
NAD	Dose	0.243		ns
NAD	Age	0.647		ns
NAD	Dose×Age	0.656		ns
D-Glucose	Dose	0.654		ns
D-Glucose	Age	0.937		ns
D-Glucose	Dose×Age	0.078		ns
L-Glutamine	Dose	0.003	*	**
L-Glutamine	Age	8.00E-04	*	***
L-Glutamine	Dose×Age	0.947		ns
L-Glutamic acid	Dose	0.558		ns
L-Glutamic acid	Age	0.148		ns
L-Glutamic acid	Dose×Age	0.147		ns
Oxidized glutathione	Dose	0.179		ns
Oxidized glutathione	Age	5.15E-12	*	****
Oxidized glutathione	Dose×Age	0.882		ns

* $P < 0.05$, ** $P < 0.01$, *** $P < 0.001$, **** $P < 0.0001$.

Table 9. 18 Statistical analyses of control and aged myoblast metabolites following EGCG treatment.

Metabolite	Effect	<i>P</i>	<i>P</i> < .05	<i>P</i> .signif
Formic acid	Dose	0.161		ns
Formic acid	Age	0.077		ns
Formic acid	Dose×Age	0.239		ns
Carnosine	Dose	0.288		ns
Carnosine	Age	1.67E-05	*	****
Carnosine	Dose×Age	0.603		ns

Fumaric acid	Dose	0.000784	*	***
Fumaric acid	Age	0.004	*	**
Fumaric acid	Dose×Age	0.476		ns
D-Fructose	Dose	0.008	*	**
D-Fructose	Age	0.05	*	*
D-Fructose	Dose×Age	0.171		ns
Glycolic acid	Dose	0.71		ns
Glycolic acid	Age	0.339		ns
Glycolic acid	Dose×Age	0.167		ns
Guanidoacetic acid	Dose	0.095		ns
Guanidoacetic acid	Age	5.26E-07	*	****
Guanidoacetic acid	Dose×Age	0.339		ns
Glycine	Dose	0.864		ns
Glycine	Age	0.071		ns
Glycine	Dose×Age	0.049	*	*
cis-Aconitic acid*	Dose	0.226		ns
cis-Aconitic acid*	Age	0.003	*	**
cis-Aconitic acid*	Dose×Age	0.447		ns
Choline	Dose	0.464		ns
Choline	Age	0.015	*	*
Choline	Dose×Age	0.335		ns
Acetone	Dose	0.505		ns
Acetone	Age	2.31E-06	*	****
Acetone	Dose×Age	0.579		ns
Acetic acid	Dose	0.205		ns
Acetic acid	Age	0.000403	*	***
Acetic acid	Dose×Age	0.872		ns
Dimethylglycine	Dose	0.041	*	*
Dimethylglycine	Age	0.003	*	**
Dimethylglycine	Dose×Age	0.554		ns
Acetylglucine	Dose	0.000758	*	***
Acetylglucine	Age	0.011	*	*
Acetylglucine	Dose×Age	0.24		ns
N-Acetyl-L-aspartic acid	Dose	0.136		ns
N-Acetyl-L-aspartic acid	Age	0.471		ns
N-Acetyl-L-aspartic acid	Dose×Age	0.802		ns
Trimethylamine	Dose	0.038	*	*
Trimethylamine	Age	0.000638	*	***
Trimethylamine	Dose×Age	0.462		ns
Trimethylamine N-oxide	Dose	0.007	*	**
Trimethylamine N-oxide	Age	9.55E-17	*	****
Trimethylamine N-oxide	Dose×Age	0.554		ns
NN-Dimethylformamide	Dose	0.287		ns

NN-Dimethylformamide	Age	0.632		ns
NN-Dimethylformamide	Dose×Age	0.267		ns
5-Methoxyindoleacetate	Dose	0.031	*	*
5-Methoxyindoleacetate	Age	1.35E-07	*	****
5-Methoxyindoleacetate	Dose×Age	0.863		ns
N-Acetylglutamine	Dose	0.236		ns
N-Acetylglutamine	Age	0.005	*	**
N-Acetylglutamine	Dose×Age	0.763		ns
ADP	Dose	0.022	*	*
ADP	Age	0.76		ns
ADP	Dose×Age	0.21		ns
Adenine	Dose	0.97		ns
Adenine	Age	0.015	*	*
Adenine	Dose×Age	0.947		ns
Phosphocreatine	Dose	0.87		ns
Phosphocreatine	Age	0.889		ns
Phosphocreatine	Dose×Age	0.415		ns
Creatine	Dose	0.006	*	**
Creatine	Age	0.115		ns
Creatine	Dose×Age	0.84		ns
Creatinine	Dose	0.003	*	**
Creatinine	Age	0.009	*	**
Creatinine	Dose×Age	0.026	*	*
Pyruvic acid	Dose	0.58		ns
Pyruvic acid	Age	0.004	*	**
Pyruvic acid	Dose×Age	0.107		ns
Acetylcholine	Dose	0.168		ns
Acetylcholine	Age	0.095		ns
Acetylcholine	Dose×Age	0.081		ns
N-Alpha-acetyllysine	Dose	0.623		ns
N-Alpha-acetyllysine	Age	0.000527	*	***
N-Alpha-acetyllysine	Dose×Age	0.353		ns
Dihydrothymine	Dose	0.096		ns
Dihydrothymine	Age	0.000269	*	***
Dihydrothymine	Dose×Age	0.506		ns
Isopropyl alcohol	Dose	0.026	*	*
Isopropyl alcohol	Age	1.18E-17	*	****
Isopropyl alcohol	Dose×Age	0.967		ns
Betaine	Dose	0.041	*	*
Betaine	Age	0.058		ns
Betaine	Dose×Age	0.845		ns
2-Hydroxy-3-methylbutyric acid	Dose	0.007	*	**
2-Hydroxy-3-methylbutyric acid	Age	8.56E-06	*	****

2-Hydroxy-3-methylbutyric acid	Dose×Age	0.752		ns
3-Methylhistidine	Dose	0.051		ns
3-Methylhistidine	Age	1.21E-10	*	****
3-Methylhistidine	Dose×Age	0.487		ns
Guanosine triphosphate	Dose	0.157		ns
Guanosine triphosphate	Age	0.001	*	***
Guanosine triphosphate	Dose×Age	0.976		ns
N-Nitrosodimethylamine	Dose	0.715		ns
N-Nitrosodimethylamine	Age	0.383		ns
N-Nitrosodimethylamine	Dose×Age	0.555		ns
L-Tyrosine	Dose	0.387		ns
L-Tyrosine	Age	3.00E-07	*	****
L-Tyrosine	Dose×Age	0.887		ns
Glycerophosphocholine	Dose	0.073		ns
Glycerophosphocholine	Age	1.65E-07	*	****
Glycerophosphocholine	Dose×Age	0.682		ns
Phosphorylcholine	Dose	1.99E-07	*	****
Phosphorylcholine	Age	7.47E-15	*	****
Phosphorylcholine	Dose×Age	0.000373	*	***
Anserine	Dose	0.011	*	*
Anserine	Age	0.888		ns
Anserine	Dose×Age	0.458		ns
1-Methylhistidine	Dose	6.10E-05	*	****
1-Methylhistidine	Age	0.00051	*	***
1-Methylhistidine	Dose×Age	0.076		ns
UDP glucuronic acid	Dose	0.026	*	*
UDP glucuronic acid	Age	2.12E-08	*	****
UDP glucuronic acid	Dose×Age	0.139		ns
L-Threonine	Dose	0.023	*	*
L-Threonine	Age	8.20E-08	*	****
L-Threonine	Dose×Age	0.056		ns
L-Lactic acid	Dose	2.49E-05	*	****
L-Lactic acid	Age	0.926		ns
L-Lactic acid	Dose×Age	0.76		ns
L-Alanine	Dose	0.225		ns
L-Alanine	Age	1.82E-08	*	****
L-Alanine	Dose×Age	0.102		ns
L-Carnitine	Dose	0.201		ns
L-Carnitine	Age	0.477		ns
L-Carnitine	Dose×Age	0.239		ns
Acetylcysteine	Dose	0.047	*	*
Acetylcysteine	Age	0.215		ns
Acetylcysteine	Dose×Age	0.798		ns

N-Acetylmethionine	Dose	0.152		ns
N-Acetylmethionine	Age	0.000137	*	***
N-Acetylmethionine	Dose×Age	0.858		ns
Ethanol	Dose	0.002	*	**
Ethanol	Age	0.393		ns
Ethanol	Dose×Age	0.623		ns
Pantothenic acid	Dose	0.164		ns
Pantothenic acid	Age	0.000809	*	***
Pantothenic acid	Dose×Age	0.185		ns
Adenosine triphosphate	Dose	0.653		ns
Adenosine triphosphate	Age	0.064		ns
Adenosine triphosphate	Dose×Age	0.187		ns
Taurine	Dose	0.018	*	*
Taurine	Age	1.51E-17	*	****
Taurine	Dose×Age	0.61		ns
Tyramine	Dose	0.22		ns
Tyramine	Age	0.000443	*	***
Tyramine	Dose×Age	0.096		ns
L-Tryptophan	Dose	0.125		ns
L-Tryptophan	Age	5.76E-08	*	****
L-Tryptophan	Dose×Age	0.854		ns
Histamine	Dose	0.03	*	*
Histamine	Age	7.14E-08	*	****
Histamine	Dose×Age	0.301		ns
L-Phenylalanine	Dose	0.153		ns
L-Phenylalanine	Age	4.62E-08	*	****
L-Phenylalanine	Dose×Age	0.858		ns
L-Serine	Dose	0.154		ns
L-Serine	Age	1.29E-06	*	****
L-Serine	Dose×Age	0.265		ns
Beta-Alanine	Dose	0.935		ns
Beta-Alanine	Age	0.004	*	**
Beta-Alanine	Dose×Age	0.187		ns
Malic acid	Dose	0.005	*	**
Malic acid	Age	0.012	*	*
Malic acid	Dose×Age	0.196		ns
L-Valine	Dose	0.433		ns
L-Valine	Age	4.86E-10	*	****
L-Valine	Dose×Age	0.996		ns
Uridine diphosphate glucose	Dose	0.553		ns
Uridine diphosphate glucose	Age	4.90E-06	*	****
Uridine diphosphate glucose	Dose×Age	0.175		ns
Uridine	Dose	0.038	*	*

Uridine	Age	0.006	*	**
Uridine	Dose×Age	0.238		ns
L-Aspartic acid	Dose	0.02	*	*
L-Aspartic acid	Age	5.93E-05	*	****
L-Aspartic acid	Dose×Age	0.369		ns
NADP	Dose	0.149		ns
NADP	Age	0.014	*	*
NADP	Dose×Age	0.273		ns
Glycylproline	Dose	0.477		ns
Glycylproline	Age	0.000451	*	***
Glycylproline	Dose×Age	0.71		ns
Adenosine monophosphate	Dose	0.584		ns
Adenosine monophosphate	Age	0.116		ns
Adenosine monophosphate	Dose×Age	0.064		ns
Phenylacetic acid	Dose	0.109		ns
Phenylacetic acid	Age	4.94E-05	*	****
Phenylacetic acid	Dose×Age	0.502		ns
D-Maltose	Dose	0.01	*	**
D-Maltose	Age	0.000158	*	***
D-Maltose	Dose×Age	0.054		ns
L-Isoleucine	Dose	0.024	*	*
L-Isoleucine	Age	1.97E-09	*	****
L-Isoleucine	Dose×Age	0.969		ns
Citric acid	Dose	0.000915	*	***
Citric acid	Age	1.96E-05	*	****
Citric acid	Dose×Age	0.391		ns
L-Leucine	Dose	0.006	*	**
L-Leucine	Age	6.08E-06	*	****
L-Leucine	Dose×Age	0.356		ns
Ureidosuccinic acid	Dose	0.557		ns
Ureidosuccinic acid	Age	0.034	*	*
Ureidosuccinic acid	Dose×Age	0.552		ns
myo-Inositol	Dose	4.94E-05	*	****
myo-Inositol	Age	2.14E-05	*	****
myo-Inositol	Dose×Age	0.31		ns
NAD	Dose	0.8		ns
NAD	Age	0.256		ns
NAD	Dose×Age	0.604		ns
D-Glucose	Dose	0.305		ns
D-Glucose	Age	4.59E-06	*	****
D-Glucose	Dose×Age	0.784		ns
L-Glutamine	Dose	0.506		ns
L-Glutamine	Age	0.013	*	*

L-Glutamine	Dose×Age	0.25		ns
L-Glutamic acid	Dose	0.099		ns
L-Glutamic acid	Age	0.000204	*	***
L-Glutamic acid	Dose×Age	0.827		ns
Oxidized glutathione	Dose	0.103		ns
Oxidized glutathione	Age	0.003	*	**
Oxidized glutathione	Dose×Age	0.113		ns

* $P<0.05$, ** $P<0.01$, *** $P<0.001$, **** $P<0.0001$.

Table 9. 19 Statistical analyses of control and aged myotube metabolites following EGCG treatment.

Metabolite	Effect	<i>P</i>	<i>P</i> <.05	<i>P</i> .signif
Formic acid	Dose	0.044	*	*
Formic acid	Age	0.94		ns
Formic acid	Dose×Age	0.575		ns
Carnosine	Dose	0.018	*	*
Carnosine	Age	0.704		ns
Carnosine	Dose×Age	0.958		ns
Fumaric acid	Dose	0.03	*	*
Fumaric acid	Age	0.313		ns
Fumaric acid	Dose×Age	0.351		ns
D-Fructose	Dose	0.149		ns
D-Fructose	Age	0.012	*	*
D-Fructose	Dose×Age	0.443		ns
Glycolic acid	Dose	0.341		ns
Glycolic acid	Age	1.02E-06	*	****
Glycolic acid	Dose×Age	0.859		ns
Guanidoacetic acid	Dose	0.561		ns
Guanidoacetic acid	Age	0.074		ns
Guanidoacetic acid	Dose×Age	0.571		ns
Glycine	Dose	0.054		ns
Glycine	Age	0.000212	*	***
Glycine	Dose×Age	0.557		ns
cis-Aconitic acid*	Dose	0.032	*	*
cis-Aconitic acid*	Age	0.62		ns
cis-Aconitic acid*	Dose×Age	0.809		ns

Choline	Dose	0.979		ns
Choline	Age	0.755		ns
Choline	Dose×Age	0.227		ns
Acetone	Dose	0.76		ns
Acetone	Age	0.293		ns
Acetone	Dose×Age	0.97		ns
Acetic acid	Dose	0.665		ns
Acetic acid	Age	0.234		ns
Acetic acid	Dose×Age	0.792		ns
Dimethylglycine	Dose	0.121		ns
Dimethylglycine	Age	5.41E-11	*	****
Dimethylglycine	Dose×Age	0.744		ns
Acetylglycine	Dose	0.236		ns
Acetylglycine	Age	0.066		ns
Acetylglycine	Dose×Age	0.787		ns
N-Acetyl-L-aspartic acid	Dose	0.158		ns
N-Acetyl-L-aspartic acid	Age	0.471		ns
N-Acetyl-L-aspartic acid	Dose×Age	0.748		ns
Trimethylamine	Dose	0.001	*	***
Trimethylamine	Age	6.81E-11	*	****
Trimethylamine	Dose×Age	0.288		ns
Trimethylamine N-oxide	Dose	0.738		ns
Trimethylamine N-oxide	Age	0.25		ns
Trimethylamine N-oxide	Dose×Age	0.452		ns
NN-Dimethylformamide	Dose	0.109		ns
NN-Dimethylformamide	Age	0.522		ns
NN-Dimethylformamide	Dose×Age	0.945		ns
5-Methoxyindoleacetate	Dose	0.083		ns
5-Methoxyindoleacetate	Age	0.014	*	*
5-Methoxyindoleacetate	Dose×Age	0.774		ns
N-Acetylglutamine	Dose	0.151		ns
N-Acetylglutamine	Age	0.409		ns
N-Acetylglutamine	Dose×Age	0.884		ns
ADP	Dose	0.004	*	**
ADP	Age	0.87		ns
ADP	Dose×Age	0.083		ns
Adenine	Dose	0.412		ns
Adenine	Age	0.000204	*	***
Adenine	Dose×Age	0.32		ns
Phosphocreatine	Dose	0.103		ns
Phosphocreatine	Age	0.918		ns
Phosphocreatine	Dose×Age	0.478		ns
Creatine	Dose	0.134		ns

Creatine	Age	0.103		ns
Creatine	Dose×Age	0.95		ns
Creatinine	Dose	0.176		ns
Creatinine	Age	0.033	*	*
Creatinine	Dose×Age	0.465		ns
Pyruvic acid	Dose	0.397		ns
Pyruvic acid	Age	1.64E-07	*	****
Pyruvic acid	Dose×Age	0.803		ns
Acetylcholine	Dose	0.952		ns
Acetylcholine	Age	0.444		ns
Acetylcholine	Dose×Age	0.618		ns
N-Alpha-acetyllysine	Dose	0.735		ns
N-Alpha-acetyllysine	Age	3.45E-08	*	****
N-Alpha-acetyllysine	Dose×Age	0.279		ns
Dihydrothymine	Dose	0.221		ns
Dihydrothymine	Age	0.011	*	*
Dihydrothymine	Dose×Age	0.37		ns
Isopropyl alcohol	Dose	0.344		ns
Isopropyl alcohol	Age	4.11E-11	*	****
Isopropyl alcohol	Dose×Age	0.138		ns
Betaine	Dose	0.357		ns
Betaine	Age	0.464		ns
Betaine	Dose×Age	0.942		ns
2-Hydroxy-3-methylbutyric acid	Dose	0.125		ns
2-Hydroxy-3-methylbutyric acid	Age	0.919		ns
2-Hydroxy-3-methylbutyric acid	Dose×Age	0.307		ns
3-Methylhistidine	Dose	0.167		ns
3-Methylhistidine	Age	0.009	*	**
3-Methylhistidine	Dose×Age	0.699		ns
Guanosine triphosphate	Dose	0.34		ns
Guanosine triphosphate	Age	0.485		ns
Guanosine triphosphate	Dose×Age	0.428		ns
N-Nitrosodimethylamine	Dose	0.95		ns
N-Nitrosodimethylamine	Age	0.000315	*	***
N-Nitrosodimethylamine	Dose×Age	0.667		ns
L-Tyrosine	Dose	0.296		ns
L-Tyrosine	Age	2.32E-08	*	****
L-Tyrosine	Dose×Age	0.566		ns
Glycerophosphocholine	Dose	0.018	*	*
Glycerophosphocholine	Age	0.002	*	**
Glycerophosphocholine	Dose×Age	0.538		ns
Phosphorylcholine	Dose	0.694		ns
Phosphorylcholine	Age	8.22E-09	*	****

Phosphorylcholine	Dose×Age	0.609		ns
Anserine	Dose	0.139		ns
Anserine	Age	0.088		ns
Anserine	Dose×Age	0.678		ns
1-Methylhistidine	Dose	0.005	*	**
1-Methylhistidine	Age	0.002	*	**
1-Methylhistidine	Dose×Age	0.183		ns
Uridine diphosphate glucuronic acid	Dose	0.474		ns
Uridine diphosphate glucuronic acid	Age	0.167		ns
Uridine diphosphate glucuronic acid	Dose×Age	0.415		ns
L-Threonine	Dose	0.002	*	**
L-Threonine	Age	0.404		ns
L-Threonine	Dose×Age	0.763		ns
L-Lactic acid	Dose	0.981		ns
L-Lactic acid	Age	0.319		ns
L-Lactic acid	Dose×Age	0.276		ns
L-Alanine	Dose	0.044	*	*
L-Alanine	Age	0.002	*	**
L-Alanine	Dose×Age	0.437		ns
L-Carnitine	Dose	0.086		ns
L-Carnitine	Age	0.002	*	**
L-Carnitine	Dose×Age	0.79		ns
Acetylcysteine	Dose	0.099		ns
Acetylcysteine	Age	2.21E-07	*	****
Acetylcysteine	Dose×Age	0.108		ns
N-Acetylmethionine	Dose	0.31		ns
N-Acetylmethionine	Age	3.51E-06	*	****
N-Acetylmethionine	Dose×Age	0.608		ns
Ethanol	Dose	0.329		ns
Ethanol	Age	0.261		ns
Ethanol	Dose×Age	0.896		ns
Pantothenic acid	Dose	0.835		ns
Pantothenic acid	Age	2.76E-14	*	****
Pantothenic acid	Dose×Age	0.399		ns
Adenosine triphosphate	Dose	0.745		ns
Adenosine triphosphate	Age	0.86		ns
Adenosine triphosphate	Dose×Age	0.791		ns
Taurine	Dose	0.671		ns
Taurine	Age	0.000193	*	***
Taurine	Dose×Age	0.191		ns
Tyramine	Dose	0.132		ns

Tyramine	Age	3.45E-11	*	****
Tyramine	Dose×Age	0.103		ns
L-Tryptophan	Dose	0.122		ns
L-Tryptophan	Age	0.003	*	**
L-Tryptophan	Dose×Age	0.464		ns
Histamine	Dose	0.01	*	**
Histamine	Age	0.783		ns
Histamine	Dose×Age	0.823		ns
L-Phenylalanine	Dose	0.079		ns
L-Phenylalanine	Age	0.022	*	*
L-Phenylalanine	Dose×Age	0.35		ns
L-Serine	Dose	0.312		ns
L-Serine	Age	0.148		ns
L-Serine	Dose×Age	0.539		ns
Beta-Alanine	Dose	0.073		ns
Beta-Alanine	Age	0.987		ns
Beta-Alanine	Dose×Age	0.987		ns
Malic acid	Dose	0.234		ns
Malic acid	Age	0.566		ns
Malic acid	Dose×Age	0.61		ns
L-Valine	Dose	0.819		ns
L-Valine	Age	0.006	*	**
L-Valine	Dose×Age	0.279		ns
Uridine diphosphate glucose	Dose	0.752		ns
Uridine diphosphate glucose	Age	0.1		ns
Uridine diphosphate glucose	Dose×Age	0.796		ns
Uridine	Dose	0.388		ns
Uridine	Age	0.867		ns
Uridine	Dose×Age	0.644		ns
L-Aspartic acid	Dose	0.099		ns
L-Aspartic acid	Age	0.276		ns
L-Aspartic acid	Dose×Age	0.269		ns
NADP	Dose	0.19		ns
NADP	Age	0.306		ns
NADP	Dose×Age	0.753		ns
Glycylproline	Dose	0.282		ns
Glycylproline	Age	0.891		ns
Glycylproline	Dose×Age	0.509		ns
Adenosine monophosphate	Dose	0.034	*	*
Adenosine monophosphate	Age	0.357		ns
Adenosine monophosphate	Dose×Age	0.724		ns
Phenylacetic acid	Dose	0.252		ns
Phenylacetic acid	Age	0.332		ns

Phenylacetic acid	Dose×Age	0.51		ns
D-Maltose	Dose	0.304		ns
D-Maltose	Age	0.14		ns
D-Maltose	Dose×Age	0.046	*	*
L-Isoleucine	Dose	0.09		ns
L-Isoleucine	Age	0.000262	*	***
L-Isoleucine	Dose×Age	0.431		ns
Citric acid	Dose	0.675		ns
Citric acid	Age	2.57E-05	*	****
Citric acid	Dose×Age	0.371		ns
L-Leucine	Dose	0.807		ns
L-Leucine	Age	0.000192	*	***
L-Leucine	Dose×Age	0.751		ns
Ureidosuccinic acid	Dose	0.361		ns
Ureidosuccinic acid	Age	0.176		ns
Ureidosuccinic acid	Dose×Age	0.822		ns
myo-Inositol	Dose	0.339		ns
myo-Inositol	Age	6.96E-11	*	****
myo-Inositol	Dose×Age	0.453		ns
NAD	Dose	0.173		ns
NAD	Age	0.564		ns
NAD	Dose×Age	0.456		ns
D-Glucose	Dose	0.138		ns
D-Glucose	Age	0.483		ns
D-Glucose	Dose×Age	0.408		ns
L-Glutamine	Dose	0.172		ns
L-Glutamine	Age	0.048	*	*
L-Glutamine	Dose×Age	0.912		ns
L-Glutamic acid	Dose	0.455		ns
L-Glutamic acid	Age	0.502		ns
L-Glutamic acid	Dose×Age	0.783		ns
Oxidized glutathione	Dose	0.411		ns
Oxidized glutathione	Age	3.42E-08	*	****
Oxidized glutathione	Dose×Age	0.977		ns

* $P < 0.05$, ** $P < 0.01$, *** $P < 0.001$, **** $P < 0.0001$.

Table 9. 20 Statistical analyses of control and aged myoblast metabolites following EPI treatment.

Metabolite	Effect	<i>P</i>	<i>P</i> <.05	<i>P</i> .signif
Formic acid	Dose	0.145		ns
Formic acid	Age	0.011	*	*
Formic acid	Dose×Age	0.786		ns
Carnosine	Dose	0.618		ns
Carnosine	Age	0.001	*	***
Carnosine	Dose×Age	0.969		ns
Fumaric acid	Dose	0.476		ns
Fumaric acid	Age	0.181		ns
Fumaric acid	Dose×Age	1		ns
D-Fructose	Dose	0.572		ns
D-Fructose	Age	0.543		ns
D-Fructose	Dose×Age	0.915		ns
Glycolic acid	Dose	0.043	*	*
Glycolic acid	Age	0.214		ns
Glycolic acid	Dose×Age	0.348		ns
Guanidoacetic acid	Dose	0.35		ns
Guanidoacetic acid	Age	0.006	*	**
Guanidoacetic acid	Dose×Age	0.469		ns
Glycine	Dose	0.327		ns
Glycine	Age	0.001	*	***
Glycine	Dose×Age	0.285		ns
cis-Aconitic acid*	Dose	0.068		ns
cis-Aconitic acid*	Age	0.000438	*	***
cis-Aconitic acid*	Dose×Age	0.708		ns
Choline	Dose	0.214		ns
Choline	Age	0.002	*	**
Choline	Dose×Age	0.421		ns
Acetone	Dose	0.148		ns
Acetone	Age	0.011	*	*
Acetone	Dose×Age	0.762		ns
Acetic acid	Dose	0.15		ns
Acetic acid	Age	0.000127	*	***
Acetic acid	Dose×Age	0.478		ns
Dimethylglycine	Dose	0.305		ns
Dimethylglycine	Age	0.005	*	**
Dimethylglycine	Dose×Age	0.284		ns
Acetylglycine	Dose	0.405		ns
Acetylglycine	Age	0.112		ns
Acetylglycine	Dose×Age	0.651		ns

N-Acetyl-L-aspartic acid	Dose	0.119		ns
N-Acetyl-L-aspartic acid	Age	0.267		ns
N-Acetyl-L-aspartic acid	Dose×Age	0.953		ns
Trimethylamine	Dose	0.211		ns
Trimethylamine	Age	0.003	*	**
Trimethylamine	Dose×Age	0.386		ns
Trimethylamine N-oxide	Dose	0.126		ns
Trimethylamine N-oxide	Age	2.96E-14	*	****
Trimethylamine N-oxide	Dose×Age	0.835		ns
NN-Dimethylformamide	Dose	0.32		ns
NN-Dimethylformamide	Age	0.366		ns
NN-Dimethylformamide	Dose×Age	0.376		ns
5-Methoxyindoleacetate	Dose	0.371		ns
5-Methoxyindoleacetate	Age	2.44E-08	*	****
5-Methoxyindoleacetate	Dose×Age	0.619		ns
N-Acetylglutamine	Dose	0.008	*	**
N-Acetylglutamine	Age	0.011	*	*
N-Acetylglutamine	Dose×Age	0.206		ns
ADP	Dose	0.019	*	*
ADP	Age	0.66		ns
ADP	Dose×Age	0.682		ns
Adenine	Dose	0.057		ns
Adenine	Age	0.004	*	**
Adenine	Dose×Age	0.24		ns
Phosphocreatine	Dose	0.673		ns
Phosphocreatine	Age	0.814		ns
Phosphocreatine	Dose×Age	0.587		ns
Creatine	Dose	0.000927	*	***
Creatine	Age	0.01	*	**
Creatine	Dose×Age	0.281		ns
Creatinine	Dose	0.585		ns
Creatinine	Age	0.723		ns
Creatinine	Dose×Age	0.685		ns
Pyruvic acid	Dose	0.016	*	*
Pyruvic acid	Age	0.007	*	**
Pyruvic acid	Dose×Age	0.283		ns
Acetylcholine	Dose	0.074		ns
Acetylcholine	Age	0.001	*	***
Acetylcholine	Dose×Age	0.823		ns
N-Alpha-acetyllysine	Dose	0.869		ns
N-Alpha-acetyllysine	Age	0.00028	*	***
N-Alpha-acetyllysine	Dose×Age	0.798		ns
Dihydrothymine	Dose	0.572		ns

Dihydrothymine	Age	0.000268	*	***
Dihydrothymine	Dose×Age	0.256		ns
Isopropyl alcohol	Dose	0.295		ns
Isopropyl alcohol	Age	3.40E-17	*	****
Isopropyl alcohol	Dose×Age	0.577		ns
Betaine	Dose	0.064		ns
Betaine	Age	0.001	*	***
Betaine	Dose×Age	0.849		ns
2-Hydroxy-3-methylbutyric acid	Dose	0.071		ns
2-Hydroxy-3-methylbutyric acid	Age	0.007	*	**
2-Hydroxy-3-methylbutyric acid	Dose×Age	0.554		ns
3-Methylhistidine	Dose	0.415		ns
3-Methylhistidine	Age	1.07E-12	*	****
3-Methylhistidine	Dose×Age	0.918		ns
Guanosine triphosphate	Dose	0.08		ns
Guanosine triphosphate	Age	0.001	*	***
Guanosine triphosphate	Dose×Age	0.869		ns
N-Nitrosodimethylamine	Dose	0.273		ns
N-Nitrosodimethylamine	Age	0.166		ns
N-Nitrosodimethylamine	Dose×Age	0.404		ns
L-Tyrosine	Dose	0.762		ns
L-Tyrosine	Age	1.15E-05	*	****
L-Tyrosine	Dose×Age	0.405		ns
Glycerophosphocholine	Dose	0.8		ns
Glycerophosphocholine	Age	5.20E-08	*	****
Glycerophosphocholine	Dose×Age	0.951		ns
Phosphorylcholine	Dose	3.90E-05	*	****
Phosphorylcholine	Age	4.75E-15	*	****
Phosphorylcholine	Dose×Age	0.002	*	**
Anserine	Dose	0.338		ns
Anserine	Age	0.168		ns
Anserine	Dose×Age	0.711		ns
1-Methylhistidine	Dose	0.000268	*	***
1-Methylhistidine	Age	0.083		ns
1-Methylhistidine	Dose×Age	0.877		ns
Uridine diphosphate glucuronic acid	Dose	0.156		ns
Uridine diphosphate glucuronic acid	Age	4.65E-06	*	****
Uridine diphosphate glucuronic acid	Dose×Age	0.712		ns
L-Threonine	Dose	0.422		ns
L-Threonine	Age	0.000117	*	***
L-Threonine	Dose×Age	0.854		ns

L-Lactic acid	Dose	0.000545	*	***
L-Lactic acid	Age	0.000435	*	***
L-Lactic acid	Dose×Age	0.096		ns
L-Alanine	Dose	0.382		ns
L-Alanine	Age	3.02E-10	*	****
L-Alanine	Dose×Age	0.184		ns
L-Carnitine	Dose	0.399		ns
L-Carnitine	Age	0.698		ns
L-Carnitine	Dose×Age	0.411		ns
Acetylcysteine	Dose	0.042	*	*
Acetylcysteine	Age	0.027	*	*
Acetylcysteine	Dose×Age	0.31		ns
N-Acetylmethionine	Dose	0.962		ns
N-Acetylmethionine	Age	6.12E-06	*	****
N-Acetylmethionine	Dose×Age	0.119		ns
Ethanol	Dose	0.003	*	**
Ethanol	Age	0.004	*	**
Ethanol	Dose×Age	0.723		ns
Pantothenic acid	Dose	0.753		ns
Pantothenic acid	Age	0.005	*	**
Pantothenic acid	Dose×Age	0.211		ns
Adenosine triphosphate	Dose	0.272		ns
Adenosine triphosphate	Age	0.39		ns
Adenosine triphosphate	Dose×Age	0.468		ns
Taurine	Dose	0.095		ns
Taurine	Age	6.54E-15	*	****
Taurine	Dose×Age	0.833		ns
Tyramine	Dose	0.131		ns
Tyramine	Age	0.005	*	**
Tyramine	Dose×Age	0.192		ns
L-Tryptophan	Dose	0.768		ns
L-Tryptophan	Age	3.17E-08	*	****
L-Tryptophan	Dose×Age	0.607		ns
Histamine	Dose	0.346		ns
Histamine	Age	2.74E-05	*	****
Histamine	Dose×Age	0.956		ns
L-Phenylalanine	Dose	0.837		ns
L-Phenylalanine	Age	1.03E-08	*	****
L-Phenylalanine	Dose×Age	0.735		ns
L-Serine	Dose	0.702		ns
L-Serine	Age	9.59E-06	*	****
L-Serine	Dose×Age	0.524		ns
Beta-Alanine	Dose	0.49		ns

Beta-Alanine	Age	0.797		ns
Beta-Alanine	Dose×Age	0.209		ns
Malic acid	Dose	0.02	*	*
Malic acid	Age	8.30E-06	*	****
Malic acid	Dose×Age	0.937		ns
L-Valine	Dose	0.922		ns
L-Valine	Age	6.37E-11	*	****
L-Valine	Dose×Age	0.768		ns
Uridine diphosphate glucose	Dose	0.269		ns
Uridine diphosphate glucose	Age	0.004	*	**
Uridine diphosphate glucose	Dose×Age	0.948		ns
Uridine	Dose	0.743		ns
Uridine	Age	0.81		ns
Uridine	Dose×Age	0.859		ns
L-Aspartic acid	Dose	0.026	*	*
L-Aspartic acid	Age	2.00E-04	*	***
L-Aspartic acid	Dose×Age	0.23		ns
NADP	Dose	0.757		ns
NADP	Age	0.972		ns
NADP	Dose×Age	0.868		ns
Glycylproline	Dose	0.902		ns
Glycylproline	Age	0.002	*	**
Glycylproline	Dose×Age	0.524		ns
Adenosine monophosphate	Dose	0.994		ns
Adenosine monophosphate	Age	0.049	*	*
Adenosine monophosphate	Dose×Age	0.394		ns
Phenylacetic acid	Dose	0.933		ns
Phenylacetic acid	Age	0.003	*	**
Phenylacetic acid	Dose×Age	0.271		ns
D-Maltose	Dose	0.49		ns
D-Maltose	Age	0.157		ns
D-Maltose	Dose×Age	0.432		ns
L-Isoleucine	Dose	0.404		ns
L-Isoleucine	Age	1.04E-11	*	****
L-Isoleucine	Dose×Age	0.646		ns
Citric acid	Dose	0.005	*	**
Citric acid	Age	6.53E-05	*	****
Citric acid	Dose×Age	0.335		ns
L-Leucine	Dose	0.076		ns
L-Leucine	Age	3.11E-05	*	****
L-Leucine	Dose×Age	0.845		ns
Ureidosuccinic acid	Dose	0.097		ns
Ureidosuccinic acid	Age	0.467		ns

Ureidosuccinic acid	Dose×Age	0.509		ns
myo-Inositol	Dose	0.043	*	*
myo-Inositol	Age	0.001	*	***
myo-Inositol	Dose×Age	0.813		ns
NAD	Dose	0.862		ns
NAD	Age	0.881		ns
NAD	Dose×Age	0.551		ns
D-Glucose	Dose	0.462		ns
D-Glucose	Age	0.006	*	**
D-Glucose	Dose×Age	0.464		ns
L-Glutamine	Dose	0.555		ns
L-Glutamine	Age	0.000665	*	***
L-Glutamine	Dose×Age	0.747		ns
L-Glutamic acid	Dose	0.006	*	**
L-Glutamic acid	Age	5.19E-05	*	****
L-Glutamic acid	Dose×Age	0.319		ns
Oxidized glutathione	Dose	0.197		ns
Oxidized glutathione	Age	0.002	*	**
Oxidized glutathione	Dose×Age	0.268		ns

* $P < 0.05$, ** $P < 0.01$, *** $P < 0.001$, **** $P < 0.0001$.

Table 9. 21 Statistical analyses of control and aged myotube metabolites following EPI treatment.

Metabolite	Effect	<i>P</i>	<i>P</i> < .05	<i>P</i> .signif
Formic acid	Dose	0.668		ns
Formic acid	Age	0.549		ns
Formic acid	Dose×Age	0.365		ns
Carnosine	Dose	0.651		ns
Carnosine	Age	0.321		ns
Carnosine	Dose×Age	0.828		ns
Fumaric acid	Dose	0.394		ns
Fumaric acid	Age	0.015	*	*
Fumaric acid	Dose×Age	0.833		ns
D-Fructose	Dose	0.975		ns
D-Fructose	Age	0.308		ns
D-Fructose	Dose×Age	0.879		ns
Glycolic acid	Dose	0.216		ns
Glycolic acid	Age	8.86E-08	*	****

Glycolic acid	Dose×Age	0.641		ns
Guanidoacetic acid	Dose	0.511		ns
Guanidoacetic acid	Age	0.01	*	**
Guanidoacetic acid	Dose×Age	0.215		ns
Glycine	Dose	0.198		ns
Glycine	Age	6.45E-06	*	****
Glycine	Dose×Age	0.185		ns
cis-Aconitic acid/L-Acetylcarnitine	Dose	0.278		ns
cis-Aconitic acid/L-Acetylcarnitine	Age	0.005	*	**
cis-Aconitic acid/L-Acetylcarnitine	Dose×Age	0.34		ns
Choline	Dose	0.073		ns
Choline	Age	0.003	*	**
Choline	Dose×Age	0.461		ns
Acetone	Dose	0.815		ns
Acetone	Age	0.883		ns
Acetone	Dose×Age	0.161		ns
Acetic acid	Dose	0.69		ns
Acetic acid	Age	0.582		ns
Acetic acid	Dose×Age	0.859		ns
Dimethylglycine	Dose	0.043	*	*
Dimethylglycine	Age	1.29E-10	*	****
Dimethylglycine	Dose×Age	0.508		ns
Acetylglycine	Dose	0.015	*	*
Acetylglycine	Age	0.121		ns
Acetylglycine	Dose×Age	0.891		ns
N-Acetyl-L-aspartic acid	Dose	0.391		ns
N-Acetyl-L-aspartic acid	Age	0.319		ns
N-Acetyl-L-aspartic acid	Dose×Age	0.678		ns
Trimethylamine	Dose	0.014	*	*
Trimethylamine	Age	2.05E-09	*	****
Trimethylamine	Dose×Age	0.624		ns
Trimethylamine N-oxide	Dose	0.513		ns
Trimethylamine N-oxide	Age	0.038	*	*
Trimethylamine N-oxide	Dose×Age	0.902		ns
NN-Dimethylformamide	Dose	0.044	*	*
NN-Dimethylformamide	Age	0.00057	*	***
NN-Dimethylformamide	Dose×Age	0.666		ns
5-Methoxyindoleacetate	Dose	0.239		ns
5-Methoxyindoleacetate	Age	6.08E-05	*	****
5-Methoxyindoleacetate	Dose×Age	0.785		ns
N-Acetylglutamine	Dose	0.643		ns

N-Acetylglutamine	Age	0.999		ns
N-Acetylglutamine	Dose×Age	0.751		ns
ADP	Dose	5.45E-05	*	****
ADP	Age	0.121		ns
ADP	Dose×Age	0.274		ns
Adenine	Dose	0.442		ns
Adenine	Age	6.40E-06	*	****
Adenine	Dose×Age	0.485		ns
Phosphocreatine	Dose	0.456		ns
Phosphocreatine	Age	0.296		ns
Phosphocreatine	Dose×Age	0.386		ns
Creatine	Dose	0.8		ns
Creatine	Age	0.56		ns
Creatine	Dose×Age	0.769		ns
Creatinine	Dose	0.906		ns
Creatinine	Age	0.239		ns
Creatinine	Dose×Age	0.106		ns
Pyruvic acid	Dose	0.261		ns
Pyruvic acid	Age	1.70E-07	*	****
Pyruvic acid	Dose×Age	0.834		ns
Acetylcholine	Dose	0.01	*	**
Acetylcholine	Age	0.08		ns
Acetylcholine	Dose×Age	0.764		ns
N-Alpha-acetyllysine	Dose	0.719		ns
N-Alpha-acetyllysine	Age	4.76E-10	*	****
N-Alpha-acetyllysine	Dose×Age	0.615		ns
Dihydrothymine	Dose	0.221		ns
Dihydrothymine	Age	0.000415	*	***
Dihydrothymine	Dose×Age	0.628		ns
Isopropyl alcohol	Dose	0.048	*	*
Isopropyl alcohol	Age	2.50E-13	*	****
Isopropyl alcohol	Dose×Age	0.474		ns
Betaine	Dose	0.299		ns
Betaine	Age	0.971		ns
Betaine	Dose×Age	0.902		ns
2-Hydroxy-3-methylbutyric acid	Dose	0.145		ns
2-Hydroxy-3-methylbutyric acid	Age	0.467		ns
2-Hydroxy-3-methylbutyric acid	Dose×Age	0.754		ns
3-Methylhistidine	Dose	0.099		ns
3-Methylhistidine	Age	4.73E-08	*	****
3-Methylhistidine	Dose×Age	0.432		ns
Guanosine triphosphate	Dose	0.237		ns
Guanosine triphosphate	Age	0.351		ns

Guanosine triphosphate	Dose×Age	0.491		ns
N-Nitrosodimethylamine	Dose	0.634		ns
N-Nitrosodimethylamine	Age	1.70E-05	*	****
N-Nitrosodimethylamine	Dose×Age	0.627		ns
L-Tyrosine	Dose	0.384		ns
L-Tyrosine	Age	7.41E-06	*	****
L-Tyrosine	Dose×Age	0.496		ns
Glycerophosphocholine	Dose	0.098		ns
Glycerophosphocholine	Age	3.52E-06	*	****
Glycerophosphocholine	Dose×Age	0.922		ns
Phosphorylcholine	Dose	0.579		ns
Phosphorylcholine	Age	1.41E-12	*	****
Phosphorylcholine	Dose×Age	0.122		ns
Anserine	Dose	0.729		ns
Anserine	Age	0.205		ns
Anserine	Dose×Age	0.8		ns
1-Methylhistidine	Dose	1.15E-05	*	****
1-Methylhistidine	Age	7.63E-06	*	****
1-Methylhistidine	Dose×Age	0.646		ns
UDP glucuronic acid	Dose	0.547		ns
UDP glucuronic acid	Age	0.013	*	*
UDP glucuronic acid	Dose×Age	0.433		ns
L-Threonine	Dose	0.211		ns
L-Threonine	Age	0.137		ns
L-Threonine	Dose×Age	0.328		ns
L-Lactic acid	Dose	0.211		ns
L-Lactic acid	Age	0.509		ns
L-Lactic acid	Dose×Age	0.335		ns
L-Alanine	Dose	0.064		ns
L-Alanine	Age	4.20E-06	*	****
L-Alanine	Dose×Age	0.728		ns
L-Carnitine	Dose	0.002	*	**
L-Carnitine	Age	3.39E-14	*	****
L-Carnitine	Dose×Age	0.283		ns
Acetylcysteine	Dose	0.624		ns
Acetylcysteine	Age	0.000112	*	***
Acetylcysteine	Dose×Age	0.965		ns
N-Acetylorithine	Dose	0.212		ns
N-Acetylorithine	Age	1.71E-07	*	****
N-Acetylorithine	Dose×Age	0.906		ns
Ethanol	Dose	0.262		ns
Ethanol	Age	0.742		ns
Ethanol	Dose×Age	0.971		ns

Pantothenic acid	Dose	0.968		ns
Pantothenic acid	Age	1.16E-14	*	****
Pantothenic acid	Dose×Age	0.703		ns
Adenosine triphosphate	Dose	0.446		ns
Adenosine triphosphate	Age	0.763		ns
Adenosine triphosphate	Dose×Age	0.757		ns
Taurine	Dose	0.286		ns
Taurine	Age	3.91E-06	*	****
Taurine	Dose×Age	0.653		ns
Tyramine	Dose	0.222		ns
Tyramine	Age	1.89E-08	*	****
Tyramine	Dose×Age	0.501		ns
L-Tryptophan	Dose	0.067		ns
L-Tryptophan	Age	4.97E-05	*	****
L-Tryptophan	Dose×Age	0.688		ns
Histamine	Dose	0.502		ns
Histamine	Age	0.687		ns
Histamine	Dose×Age	0.982		ns
L-Phenylalanine	Dose	0.128		ns
L-Phenylalanine	Age	1.09E-06	*	****
L-Phenylalanine	Dose×Age	0.555		ns
L-Serine	Dose	0.257		ns
L-Serine	Age	0.005	*	**
L-Serine	Dose×Age	0.806		ns
Beta-Alanine	Dose	0.009	*	**
Beta-Alanine	Age	0.454		ns
Beta-Alanine	Dose×Age	0.405		ns
Malic acid	Dose	0.05		*
Malic acid	Age	0.415		ns
Malic acid	Dose×Age	0.581		ns
L-Valine	Dose	0.063		ns
L-Valine	Age	5.13E-09	*	****
L-Valine	Dose×Age	0.301		ns
Uridine diphosphate glucose	Dose	0.518		ns
Uridine diphosphate glucose	Age	0.124		ns
Uridine diphosphate glucose	Dose×Age	0.605		ns
Uridine	Dose	0.347		ns
Uridine	Age	0.944		ns
Uridine	Dose×Age	0.833		ns
L-Aspartic acid	Dose	0.18		ns
L-Aspartic acid	Age	0.11		ns
L-Aspartic acid	Dose×Age	0.808		ns
NADP	Dose	0.604		ns

NADP	Age	0.049	*	*
NADP	Dose×Age	0.888		ns
Glycylproline	Dose	0.696		ns
Glycylproline	Age	0.073		ns
Glycylproline	Dose×Age	0.971		ns
Adenosine monophosphate	Dose	0.224		ns
Adenosine monophosphate	Age	0.379		ns
Adenosine monophosphate	Dose×Age	0.435		ns
Phenylacetic acid	Dose	0.107		ns
Phenylacetic acid	Age	0.003	*	**
Phenylacetic acid	Dose×Age	0.734		ns
D-Maltose	Dose	0.45		ns
D-Maltose	Age	0.837		ns
D-Maltose	Dose×Age	0.274		ns
L-Isoleucine	Dose	0.139		ns
L-Isoleucine	Age	3.71E-07	*	****
L-Isoleucine	Dose×Age	0.913		ns
Citric acid	Dose	0.085		ns
Citric acid	Age	0.043	*	*
Citric acid	Dose×Age	0.338		ns
L-Leucine	Dose	0.484		ns
L-Leucine	Age	8.57E-06	*	****
L-Leucine	Dose×Age	0.082		ns
Ureidosuccinic acid	Dose	0.261		ns
Ureidosuccinic acid	Age	0.094		ns
Ureidosuccinic acid	Dose×Age	0.999		ns
myo-Inositol	Dose	0.01	*	**
myo-Inositol	Age	4.21E-17	*	****
myo-Inositol	Dose×Age	0.428		ns
NAD	Dose	0.296		ns
NAD	Age	0.53		ns
NAD	Dose×Age	0.342		ns
D-Glucose	Dose	0.434		ns
D-Glucose	Age	0.986		ns
D-Glucose	Dose×Age	0.315		ns
L-Glutamine	Dose	0.995		ns
L-Glutamine	Age	0.007	*	**
L-Glutamine	Dose×Age	0.734		ns
L-Glutamic acid	Dose	0.046	*	*
L-Glutamic acid	Age	0.183		ns
L-Glutamic acid	Dose×Age	0.481		ns
Oxidized glutathione	Dose	0.046	*	*
Oxidized glutathione	Age	4.86E-10	*	****

Oxidized glutathione Dose×Age 0.468 ns

* $P < 0.05$, ** $P < 0.01$, *** $P < 0.001$, **** $P < 0.0001$.

Table 9. 22 Comparison of metabolites with VIP scores >1 between control and aged myoblasts treated with Q, EGCG and EPI and modelled via PLS-DA.

Metabolite	Control			Aged		
	Q	EGCG	EPI	Q	EGCG	EPI
1-Methylhistidine		X	X		X	X
2-Hydroxy-3-methylbutyric acid	X	X		X		
3-Methylhistidine			X		X	
5-Methoxyindoleacetate		X			X	
Acetic acid						
Acetone	X					X
Acetylcholine	X					
Acetylcysteine	X		X		X	
Acetylglycine	X	X				
Adenine			X	X		X
Adenosine monophosphate						X
Adenosine triphosphate			X			
ADP		X	X	X		X
Anserine	X				X	
Beta-Alanine	X		X	X		
Betaine	X	X	X	X	X	X
Carnosine		X				
Choline	X		X			X
cis-Aconitic acid	X		X		X	X
Citric acid	X	X	X	X	X	X
Creatine		X				

Creatinine			X	X		X
D-Fructose		X		X		
D-Glucose	X			X	X	X
D-Maltose		X		X		
Dihydrothymine			X		X	
Dimethylglycine	X	X	X			
Ethanol		X	X	X	X	X
Formic acid			X			
Fumaric acid		X			X	
Glycerophosphocholine		X	X		X	X
Glycine	X		X	X		
Glycolic acid	X		X			X
Glycylproline	X					
Guanidoacetic acid					X	
Guanosine triphosphate			X			
Histamine		X				
Isopropyl alcohol				X	X	X
L-Acetylcarnitine			X		X	X
L-Alanine			X	X	X	
L-Aspartic acid	X		X			X
L-Carnitine					X	X
L-Glutamic acid			X	X	X	X
L-Glutamine						
L-Isoleucine		X			X	
L-Lactic acid	X	X		X	X	X
L-Leucine		X	X	X	X	
L-Phenylalanine		X				
L-Serine	X	X				
L-Threonine	X	X		X		

L-Tryptophan		X				
L-Tyrosine		X				
L-Valine		X		X		
Malic acid	X	X	X		X	X
myo-Inositol	X	X	X	X	X	X
N-Acetyl-L-aspartic acid					X	X
N-Acetylglutamine	X		X			X
N-Acetylmethionine					X	
N-Alpha-acetyllysine					X	
N-Nitrosodimethylamine			X	X	X	X
NAD						
NADP		X				
NN-Dimethylformamide	X				X	X
Oxidized glutathione	X	X	X			
Pantothenic acid					X	
Phenylacetic acid		X				
Phosphocreatine		X	X		X	X
Phosphorylcholine	X	X		X	X	
Pyruvic acid				X		
Taurine		X	X		X	X
Trimethylamine	X	X	X			
Trimethylamine N-oxide		X			X	
Tyramine	X	X	X			
Ureidosuccinic acid			X			
Uridine		X				
Uridine diphosphate glucose						
Uridine diphosphate glucuronic acid		X				X

Table 9. 23 Comparison of metabolites with VIP scores >1 between control and aged myotubes treated with Q, EGCG and EPI and modelled via PLS-DA.

Metabolite	Control			Aged		
	Q	EGCG	EPI	Q	EGCG	EPI
1-Methylhistidine		X	X			X
2-Hydroxy-3-methylbutyric acid	X	X			X	X
3-Methylhistidine					X	
5-Methoxyindoleacetate		X	X		X	X
Acetic acid						
Acetone			X			
Acetylcholine		X		X		
Acetylcysteine		X			X	
Acetylglycine						
Adenine		X	X		X	
Adenosine monophosphate		X			X	
Adenosine triphosphate	X			X		
ADP	X	X	X			X
Anserine						
Beta-Alanine		X	X	X	X	X
Betaine	X	X				
Carnosine		X			X	
Choline				X	X	X
cis-Aconitic acid	X	X	X		X	X
Citric acid	X			X		
Creatine		X		X	X	X
Creatinine		X				
D-Fructose	X	X			X	
D-Glucose		X				
D-Maltose		X		X	X	X

Dihydrothymine	X		X		X	X
Dimethylglycine		X	X			X
Ethanol			X			
Formic acid					X	
Fumaric acid		X	X		X	
Glycerophosphocholine	X		X	X		
Glycine	X				X	X
Glycolic acid		X	X			
Glycylproline				X	X	
Guanidoacetic acid		X				
Guanosine triphosphate						
Histamine		X			X	
Isopropyl alcohol			X			
L-Acetylcarnitine	X	X	X		X	X
L-Alanine	X	X	X	X	X	X
L-Aspartic acid	X					X
L-Carnitine					X	X
L-Glutamic acid				X		
L-Glutamine	X			X	X	
L-Isoleucine	X	X	X		X	X
L-Lactic acid	X					X
L-Leucine	X	X				
L-Phenylalanine		X			X	X
L-Serine				X		
L-Threonine	X	X	X	X	X	X
L-Tryptophan	X	X	X		X	X
L-Tyrosine	X	X	X		X	X
L-Valine	X		X			X
Malic acid				X	X	

myo-Inositol	X		X	X	X	X
N-Acetyl-L-aspartic acid				X		
N-Acetylglutamine	X			X		
N-Acetylmethionine	X				X	
N-Alpha-acetyllysine				X	X	
N-Nitrosodimethylamine	X			X	X	X
NAD	X	X	X			
NADP						
NN-Dimethylformamide				X	X	
Oxidized glutathione		X				X
Pantothenic acid					X	
Phenylacetic acid		X				X
Phosphocreatine						
Phosphorylcholine	X			X		
Pyruvic acid	X					
Taurine						
Trimethylamine		X	X		X	X
Trimethylamine N-oxide						
Tyramine		X	X		X	
Ureidosuccinic acid					X	
Uridine				X		
Uridine diphosphate glucose			X	X		
Uridine diphosphate glucuronic acid		X	X			

Chapter 10: References

- Abdelmoez, A. M., Sardón Puig, L., Smith, J. A. B., Gabriel, B. M., Savikj, M., Dollet, L., Chibalin, A. V., Krook, A., Zierath, J. R., & Pilon, N. J. (2019). Comparative profiling of skeletal muscle models reveals heterogeneity of transcriptome and metabolism. *American Journal of Physiology-Cell Physiology*, *318*(3), C615–C626. <https://doi.org/10.1152/ajpcell.00540.2019>
- Adler, A., Messina, E., Sherman, B., Wang, Z., Huang, H., Linke, A., & Hintze, T. H. (2003a). NAD(P)H oxidase-generated superoxide anion accounts for reduced control of myocardial O₂ consumption by NO in old Fischer 344 rats. *American Journal of Physiology - Heart and Circulatory Physiology*. <https://doi.org/10.1152/ajpheart.01047.2002>
- Adler, A., Messina, E., Sherman, B., Wang, Z., Huang, H., Linke, A., & Hintze, T. H. (2003b). NAD(P)H oxidase-generated superoxide anion accounts for reduced control of myocardial O₂ consumption by NO in old Fischer 344 rats. *American Journal of Physiology - Heart and Circulatory Physiology*. <https://doi.org/10.1152/ajpheart.01047.2002>
- Ahmed, S., Ahmed, N., Rungtatscher, A., Linardi, D., Kulsoom, B., Innamorati, G., Meo, S. A., Gebrie, M. A., Mani, R., Merigo, F., Guzzo, F., & Faggian, G. (2020). Cocoa flavonoids reduce inflammation and oxidative stress in a myocardial ischemia-reperfusion experimental model. *Antioxidants*. <https://doi.org/10.3390/antiox9020167>
- Ahn, H. Y., Kim, C. H., & Ha, T. S. (2010). Epigallocatechin-3-gallate regulates NADPH oxidase expression in human umbilical vein endothelial cells. *Korean Journal of Physiology and Pharmacology*. <https://doi.org/10.4196/kjpp.2010.14.5.325>
- Akarachantachote, N., Chadcham, S., & Saithanu, K. (2014). Cutoff threshold of variable importance in projection for variable selection. *International Journal of Pure and Applied Mathematics*. <https://doi.org/10.12732/ijpam.v94i3.2>

- Aldini, G., Granata, P., & Carini, M. (2002). Detoxification of cytotoxic α , β -unsaturated aldehydes by carnosine: Characterization of conjugated adducts by electrospray ionization tandem mass spectrometry and detection by liquid chromatography/mass spectrometry in rat skeletal muscle. *Journal of Mass Spectrometry*.
<https://doi.org/10.1002/jms.381>
- Alexander, N. B., Dengel, D. R., Olson, R. J., & Krajewski, K. M. (2003a). Oxygen-Uptake (VO₂) Kinetics and Functional Mobility Performance in Impaired Older Adults. *The Journals of Gerontology Series A: Biological Sciences and Medical Sciences*.
<https://doi.org/10.1093/gerona/58.8.m734>
- Alexander, N. B., Dengel, D. R., Olson, R. J., & Krajewski, K. M. (2003b). Oxygen-Uptake (VO₂) Kinetics and Functional Mobility Performance in Impaired Older Adults. *The Journals of Gerontology Series A: Biological Sciences and Medical Sciences*.
<https://doi.org/10.1093/gerona/58.8.m734>
- Allgrove, J., Farrell, E., Gleeson, M., Williamson, G., & Cooper, K. (2011). Regular dark chocolate consumption's reduction of oxidative stress and increase of free-fatty-acid mobilization in response to prolonged cycling. *International Journal of Sport Nutrition and Exercise Metabolism*, 21(2), 113–123.
<https://doi.org/10.1123/ijnsnem.21.2.113>
- Anderson, S., Bankier, A. T., Barrell, B. G., De Bruijn, M. H. L., Coulson, A. R., Drouin, J., Eperon, I. C., Nierlich, D. P., Roe, B. A., Sanger, F., Schreier, P. H., Smith, A. J. H., Staden, R., & Young, I. G. (1981). Sequence and organization of the human mitochondrial genome. *Nature*. <https://doi.org/10.1038/290457a0>
- Appeldoorn, M. M., Venema, D. P., Peters, T. H. F., Koenen, M. E., Arts, I. C. W., Vincken, J. P., Gruppen, H., Keuer, J., & Hollman, P. C. H. (2009). Some phenolic compounds

increase the nitric oxide level in endothelial cells in vitro. *Journal of Agricultural and Food Chemistry*. <https://doi.org/10.1021/jf901381x>

Aranibar, N., Vassallo, J. D., Rathmacher, J., Stryker, S., Zhang, Y., Dai, J., Janovitz, E. B., Robertson, D., Reily, M., Lowe-Krentz, L., & Lehman-Mckeeman, L. (2011a).

Identification of 1- and 3-methylhistidine as biomarkers of skeletal muscle toxicity by nuclear magnetic resonance-based metabolic profiling. *Analytical Biochemistry*.

<https://doi.org/10.1016/j.ab.2010.11.023>

Aranibar, N., Vassallo, J. D., Rathmacher, J., Stryker, S., Zhang, Y., Dai, J., Janovitz, E. B., Robertson, D., Reily, M., Lowe-Krentz, L., & Lehman-Mckeeman, L. (2011b).

Identification of 1- and 3-methylhistidine as biomarkers of skeletal muscle toxicity by nuclear magnetic resonance-based metabolic profiling. *Analytical Biochemistry*.

<https://doi.org/10.1016/j.ab.2010.11.023>

Arts, Hollman, P. C. H., & Kromhout, D. (1999). Chocolate as a source of tea flavonoids.

Lancet. [https://doi.org/10.1016/S0140-6736\(99\)02267-9](https://doi.org/10.1016/S0140-6736(99)02267-9)

Arts, I. C. W., & Hollman, P. C. H. (2005). Polyphenols and disease risk in epidemiologic studies. In *The American journal of clinical nutrition*.

<https://doi.org/10.1093/ajcn/81.1.317s>

Arts, I. C. W., Jacobs, D. R., Harnack, L. J., Gross, M., & Folsom, A. R. (2001). Dietary catechins in relation to coronary heart disease death among postmenopausal women.

Epidemiology. <https://doi.org/10.1097/00001648-200111000-00015>

Auciello, F. R., Ross, F. A., Ikematsu, N., & Hardie, D. G. (2014). Oxidative stress activates AMPK in cultured cells primarily by increasing cellular AMP and/or ADP. *FEBS Letters*.

<https://doi.org/10.1016/j.febslet.2014.07.025>

Bailey, D. M., McEneny, J., Mathieu-Costello, O., Henry, R. R., James, P. E., McCord, J. M., Pietri, S., Young, I. S., & Richardson, R. S. (2010). Sedentary aging increases resting

- and exercise-induced intramuscular free radical formation. *Journal of Applied Physiology*, 109(2), 449–456. <https://doi.org/10.1152/jappphysiol.00354.2010>
- Bailey, S. J., Gandra, P. G., Jones, A. M., Hogan, M. C., & Nogueira, L. (2019). Incubation with sodium nitrite attenuates fatigue development in intact single mouse fibres at physiological PO₂. *Journal of Physiology*, 597(22), 5429–5443. <https://doi.org/10.1113/JP278494>
- Bailey, S. J., Varnham, R. L., DiMenna, F. J., Breese, B. C., Wylie, L. J., & Jones, A. M. (2015). Inorganic nitrate supplementation improves muscle oxygenation, O₂ uptake kinetics, and exercise tolerance at high but not low pedal rates. *Journal of Applied Physiology*, 118(11), 1396–1405. <https://doi.org/10.1152/jappphysiol.01141.2014>
- Bailey, S. J., Winyard, P., Vanhatalo, A., Blackwell, J. R., DiMenna, F. J., Wilkerson, D. P., Tarr, J., Benjamin, N., & Jones, A. M. (2009). Dietary nitrate supplementation reduces the O₂ cost of low-intensity exercise and enhances tolerance to high-intensity exercise in humans. *Journal of Applied Physiology*, 107(4), 1144–1155. <https://doi.org/10.1152/jappphysiol.00722.2009>
- Bandaruk, Y., Mukai, R., Kawamura, T., Nemoto, H., & Terao, J. (2012). Evaluation of the inhibitory effects of quercetin-related flavonoids and tea catechins on the monoamine oxidase-A reaction in mouse brain mitochondria. *Journal of Agricultural and Food Chemistry*. <https://doi.org/10.1021/jf303055b>
- Barker, M., & Rayens, W. (2003). Partial least squares for discrimination. *Journal of Chemometrics*. <https://doi.org/10.1002/cem.785>
- Barnett, N. L. (2014). Medication adherence: Where are we now? A UK perspective. *European Journal of Hospital Pharmacy: Science and Practice*, 21(3), 181 LP – 184. <https://doi.org/10.1136/ejhpharm-2013-000373>

- Barrientos, A., Casademont, J., Rötig, A., Miró, Ò., Urbano-Márquez, Á., Rustin, P., & Cardellach, F. (1996). Absence of relationship between the level of electron transport chain activities and aging in human skeletal muscle. *Biochemical and Biophysical Research Communications*. <https://doi.org/10.1006/bbrc.1996.1839>
- Barstow, T. J., Buchthal, S. D., Zanconato, S., & Cooper, D. M. (1994a). Changes in potential controllers of human skeletal muscle respiration during incremental calf exercise. *Journal of Applied Physiology*. <https://doi.org/10.1152/jap.1994.77.5.2169>
- Barstow, T. J., Buchthal, S., Zanconato, S., & Cooper, D. M. (1994b). Muscle energetics and pulmonary oxygen uptake kinetics during moderate exercise. *Journal of Applied Physiology*. <https://doi.org/10.1152/jap.1994.77.4.1742>
- Barstow, T. J., Lamarra, N., & Whipp, B. J. (1990). Modulation of muscle and pulmonary O₂ uptakes by circulatory dynamics during exercise. *Journal of Applied Physiology*.
- Barth, E., Stämmler, G., Speiser, B., & Schaper, J. (1992). Ultrastructural quantitation of mitochondria and myofilaments in cardiac muscle from 10 different animal species including man. *Journal of Molecular and Cellular Cardiology*. [https://doi.org/10.1016/0022-2828\(92\)93381-S](https://doi.org/10.1016/0022-2828(92)93381-S)
- Bass, A., Gutmann, E., & Hanzlíková, V. (1975). Biochemical and histochemical changes in energy supply-enzyme pattern of muscles of the rat during old age. *Gerontology*. <https://doi.org/10.1159/000212028>
- Beaver, W. L., Lamarra, N., & Wasserman, K. (1981). Breath-by-breath measurement of true alveolar gas exchange. *Journal of Applied Physiology Respiratory Environmental and Exercise Physiology*, *51*(6), 1662–1675. <https://doi.org/10.1152/jap.1981.51.6.1662>
- Beaver, W. L., Wasserman, K., & Whipp, B. J. (2016). A new method for detecting anaerobic threshold by gas exchange. *Journal of Applied Physiology*, *121*(6), 2020–2027.

- Beccafico, S., Puglielli, C., Pietrangelo, T., Bellomo, R., Fanò, G., & Fulle, S. (2007). Age-dependent effects on functional aspects in human satellite cells. *Annals of the New York Academy of Sciences*. <https://doi.org/10.1196/annals.1395.037>
- Beecher, G. R. (2003). Overview of Dietary Flavonoids: Nomenclature, Occurrence and Intake. *The Journal of Nutrition*. <https://doi.org/10.1093/jn/133.10.3248s>
- Behnke, B. J., & Delp, M. D. (2010a). Aging blunts the dynamics of vasodilation in isolated skeletal muscle resistance vessels. *Journal of Applied Physiology*, *108*(1), 14–20. <https://doi.org/10.1152/jappphysiol.00970.2009>
- Behnke, B. J., & Delp, M. D. (2010b). Aging blunts the dynamics of vasodilation in isolated skeletal muscle resistance vessels. *Journal of Applied Physiology*, *108*(1), 14-20-14–20. <https://doi.org/10.1152/jappphysiol.00970.2009>
- Bell, C., Paterson, D. H., Kowalchuk, J. M., & Cunningham, D. A. (1999). Oxygen uptake kinetics of older humans are slowed with age but are unaffected by hyperoxia. *Experimental Physiology*. <https://doi.org/10.1017/S0958067099018631>
- Bell, C., Paterson, D. H., Kowalchuk, J. M., Moy, A. P., Thorp, D. B., Noble, E. G., Taylor, A. W., & Cunningham, D. A. (2001). Determinants of oxygen uptake kinetics in older humans following single-limb endurance exercise training. *Experimental Physiology*. <https://doi.org/10.1113/eph8602209>
- Benjamini, Y., & Hochberg, Y. (1995). Controlling the False Discovery Rate: A Practical and Powerful Approach to Multiple Testing. *Journal of the Royal Statistical Society: Series B (Methodological)*. <https://doi.org/10.1111/j.2517-6161.1995.tb02031.x>
- Benson, A. P., Bowen, T. S., Ferguson, C., Murgatroyd, S. R., & Rossiter, H. B. (2017). Data collection, handling, and fitting strategies to optimize accuracy and precision of oxygen uptake kinetics estimation from breath-by-breath measurements. *Journal of*

Applied Physiology (Bethesda, Md. : 1985), 123(1).

<https://doi.org/10.1152/jappphysiol.00988.2016>

Bernard, G., Bellance, N., James, D., Parrone, P., Fernandez, H., Letellier, T., & Rossignol, R. (2007). Mitochondrial bioenergetics and structural network organization. *Journal of Cell Science*. <https://doi.org/10.1242/jcs.03381>

Berridge, M. J. (2009). Inositol trisphosphate and calcium signalling mechanisms. In *Biochimica et Biophysica Acta—Molecular Cell Research*.

<https://doi.org/10.1016/j.bbamcr.2008.10.005>

Berry, N. M., Davison, K., Coates, A. M., Buckley, J. D., & Howe, P. R. C. (2010). Impact of cocoa flavanol consumption on blood pressure responsiveness to exercise. *British Journal of Nutrition*, 103(10), 1480–1484.

<https://doi.org/10.1017/S0007114509993382>

BHF. (2017). Physical inactivity and sedentary behaviour report 2017. *British Heart Foundation*.

Bigot, A., Jacquemin, V., Debaq-Chainiaux, F., Butler-Browne, G. S., Toussaint, O., Furling, D., & Mouly, V. (2008). Replicative aging down-regulates the myogenic regulatory factors in human myoblasts. *Biology of the Cell*.

<https://doi.org/10.1042/bc20070085>

Bitner, B. F., Ray, J. D., Kener, K. B., Herring, J. A., Tueller, J. A., Johnson, D. K., Tellez Freitas, C. M., Fausnacht, D. W., Allen, M. E., Thomson, A. H., Weber, K. S., McMillan, R. P., Hulver, M. W., Brown, D. A., Tessem, J. S., & Neilson, A. P. (2018). Common gut microbial metabolites of dietary flavonoids exert potent protective activities in β -cells and skeletal muscle cells. *Journal of Nutritional Biochemistry*. <https://doi.org/10.1016/j.jnutbio.2018.09.004>

- Black, M. A., Cable, N. T., Thijssen, D. H. J., & Green, D. J. (2009). Impact of age, sex, and exercise on brachial artery flow-mediated dilatation. *American Journal of Physiology - Heart and Circulatory Physiology*. <https://doi.org/10.1152/ajpheart.00226.2009>
- Black, M. A., Green, D. J., & Cable, N. T. (2008a). Exercise prevents age-related decline in nitric-oxide-mediated vasodilator function in cutaneous microvessels. *Journal of Physiology*. <https://doi.org/10.1113/jphysiol.2008.153742>
- Black, M. A., Green, D. J., & Cable, N. T. (2008b). Exercise prevents age-related decline in nitric-oxide-mediated vasodilator function in cutaneous microvessels. *Journal of Physiology*. <https://doi.org/10.1113/jphysiol.2008.153742>
- Blau, H. M., Pavlath, G. K., Hardeman, E. C., Chiu, C. P., Silberstein, L., Webster, S. G., Miller, S. C., & Webster, C. (1985). Plasticity of the differentiated state. *Science*. <https://doi.org/10.1126/science.2414846>
- Bode-Böger, S. M., Muke, J., Surdacki, A., Brabant, G., Böger, R. H., & Frölich, J. C. (2003). Oral L-arginine improves endothelial function in healthy individuals older than 70 years. *Vascular Medicine*. <https://doi.org/10.1191/1358863x03vm474oa>
- Boffoli, D., Scacco, S. C., Vergari, R., Solarino, G., Santacroce, G., & Papa, S. (1994). Decline with age of the respiratory chain activity in human skeletal muscle. *BBA - Molecular Basis of Disease*. [https://doi.org/10.1016/0925-4439\(94\)90061-2](https://doi.org/10.1016/0925-4439(94)90061-2)
- Bondonno, N. P., Bondonno, C. P., Rich, L., Mas, E., Shinde, S., Ward, N. C., Hodgson, J. M., & Croft, K. D. (2016). Acute effects of quercetin-3-O-glucoside on endothelial function and blood pressure: A randomized dose-response study. *American Journal of Clinical Nutrition*. <https://doi.org/10.3945/ajcn.116.131268>
- Booth, F. W., Roberts, C. K., & Laye, M. J. (2012). Lack of exercise is a major cause of chronic diseases. *Comprehensive Physiology*. <https://doi.org/10.1002/cphy.c110025>

- Bors, W., Heller, W., Michel, C., & Saran, M. (1990). Flavonoids as antioxidants: Determination of radical-scavenging efficiencies. *Methods in Enzymology*. [https://doi.org/10.1016/0076-6879\(90\)86128-I](https://doi.org/10.1016/0076-6879(90)86128-I)
- Bouitbir, J., Charles, A. L., Echaniz-Laguna, A., Kindo, M., Daussin, F., Auwerx, J., Piquard, F., Geny, B., & Zoll, J. (2012). Opposite effects of statins on mitochondria of cardiac and skeletal muscles: A 'mitohormesis' mechanism involving reactive oxygen species and PGC-1. *European Heart Journal*. <https://doi.org/10.1093/eurheartj/ehr224>
- Brand, M. D., & Nicholls, D. G. (2011). Assessing mitochondrial dysfunction in cells. In *Biochemical Journal*. <https://doi.org/10.1042/BJ20110162>
- Brand, M. D., Orr, A. L., Perevoshchikova, I. V., & Quinlan, C. L. (2013). The role of mitochondrial function and cellular bioenergetics in ageing and disease. *British Journal of Dermatology*. <https://doi.org/10.1111/bjd.12208>
- Bravo, L. (2009). Polyphenols: Chemistry, Dietary Sources, Metabolism, and Nutritional Significance. *Nutrition Reviews*. <https://doi.org/10.1111/j.1753-4887.1998.tb01670.x>
- Brookes, P. S., Digerness, S. B., Parks, D. A., & Darley-Usmar, V. (2002). Mitochondrial function in response to cardiac ischemia-reperfusion after oral treatment with quercetin. *Free Radical Biology and Medicine*. [https://doi.org/10.1016/S0891-5849\(02\)00839-0](https://doi.org/10.1016/S0891-5849(02)00839-0)
- Brown, G. C. (2000). Nitric oxide as a competitive inhibitor of oxygen consumption in the mitochondrial respiratory chain. *Acta Physiologica Scandinavica*. <https://doi.org/10.1046/j.1365-201X.2000.00718.x>
- Buijsse, B., Feskens, E. J. M., Kok, F. J., & Kromhout, D. (2006). Cocoa intake, blood pressure, and cardiovascular mortality: The Zutphen Elderly Study. *Archives of Internal Medicine*. <https://doi.org/10.1001/411>

- Burnley, M., Jones, A. M., Carter, H., & Doust, J. H. (2000a). Effects of prior heavy exercise on phase II pulmonary oxygen uptake kinetics during heavy exercise. *Journal of Applied Physiology*. <https://doi.org/10.1152/jappl.2000.89.4.1387>
- Burnley, M., Jones, A. M., Carter, H., & Doust, J. H. (2000b). Effects of prior heavy exercise on phase II pulmonary oxygen uptake kinetics during heavy exercise. *Journal of Applied Physiology*. <https://doi.org/10.1152/jappl.2000.89.4.1387>
- Burns, E. M., Kruckeberg, T. W., Comerford, L. E., & Buschman, M. T. (1979). Thinning of capillary walls and declining numbers of endothelial mitochondria in the cerebral cortex of the aging primate, *Macaca nemestrina*. *Journals of Gerontology*. <https://doi.org/10.1093/geronj/34.5.642>
- Cabrera, C., Artacho, R., & Giménez, R. (2006). Beneficial Effects of Green Tea—A Review. *Journal of the American College of Nutrition*. <https://doi.org/10.1080/07315724.2006.10719518>
- Cai, H., & Harrison, D. G. (2000). Endothelial dysfunction in cardiovascular diseases: The role of oxidant stress. In *Circulation Research*. <https://doi.org/10.1161/01.RES.87.10.840>
- Calabrese, E. J. (2008). Converging concepts: Adaptive response, preconditioning, and the Yerkes-Dodson Law are manifestations of hormesis. In *Ageing Research Reviews*. <https://doi.org/10.1016/j.arr.2007.07.001>
- Calabrese, E. J., & Baldwin, L. A. (2002). Defining hormesis. *Human and Experimental Toxicology*. <https://doi.org/10.1191/0960327102ht217oa>
- Calabrese, V., Cornelius, C., Dinkova-Kostova, A. T., Iavicoli, I., Di Paola, R., Koverech, A., Cuzzocrea, S., Rizzarelli, E., & Calabrese, E. J. (2012). Cellular stress responses, hormetic phytochemicals and vitagenes in aging and longevity. *Biochimica et*

Biophysica Acta (BBA) - Molecular Basis of Disease, 1822(5), 753–783.

<https://doi.org/10.1016/j.bbadis.2011.11.002>

Calvo, S. E., Clauser, K. R., & Mootha, V. K. (2016). MitoCarta2.0: An updated inventory of mammalian mitochondrial proteins. *Nucleic Acids Research*.

<https://doi.org/10.1093/nar/gkv1003>

Camerino, D. C., Tricarico, D., Pierno, S., Desaphy, J. F., Liantonio, A., Pusch, M., Burdi, R., Camerino, C., Fraysse, B., & De Luca, A. (2004). Taurine and Skeletal Muscle Disorders. In *Neurochemical Research*.

<https://doi.org/10.1023/B:NERE.0000010442.89826.9c>

Carnevale, R., Loffredo, L., Nocella, C., Bartimoccia, S., Bucci, T., De Falco, E., Peruzzi, M., Chimenti, I., Biondi-Zoccai, G., Pignatelli, P., Violi, F., & Frati, G. (2014).

Epicatechin and catechin modulate endothelial activation induced by platelets of patients with peripheral artery disease. *Oxidative Medicine and Cellular Longevity*.

<https://doi.org/10.1155/2014/691015>

Carter, H. N., Kim, Y., Erlich, A. T., Zarrin-khat, D., & Hood, D. A. (2018). Autophagy and mitophagy flux in young and aged skeletal muscle following chronic contractile activity. *The Journal of Physiology*, 596(16), 3567–3584.

<https://doi.org/10.1113/JP275998>

Casanova, E., Baselga-Escudero, L., Ribas-Latre, A., Arola-Arnal, A., Bladé, C., Arola, L., & Salvadó, M. J. (2014). Epigallocatechin gallate counteracts oxidative stress in docosahexaenoic acid-treated myocytes. *Biochimica et Biophysica Acta - Bioenergetics*. <https://doi.org/10.1016/j.bbabi.2014.01.014>

<https://doi.org/10.1016/j.bbabi.2014.01.014>

Casey, D. P., Ranadive, S. M., & Joyner, M. J. (2015). Aging is associated with altered vasodilator kinetics in dynamically contracting muscle: Role of nitric oxide. *Journal of Applied Physiology*. <https://doi.org/10.1152/jappphysiol.00787.2014>

- Castellano-González, G., Pichaud, N., Ballard, J. W. O., Bessede, A., Marcal, H., & Guillemin, G. J. (2016). Epigallocatechin-3-gallate induces oxidative phosphorylation by activating cytochrome c oxidase in human cultured neurons and astrocytes. *Oncotarget*. <https://doi.org/10.18632/oncotarget.6863>
- Celermajer, D. S., Sorensen, K. E., Spiegelhalter, D. J., Georgakopoulos, D., Robinson, J., & Deanfield, J. E. (1994). Aging is associated with endothelial dysfunction in healthy men years before the age-related decline in women. *Journal of the American College of Cardiology*. [https://doi.org/10.1016/0735-1097\(94\)90305-0](https://doi.org/10.1016/0735-1097(94)90305-0)
- Ceolotto, G., Gallo, A., Papparella, I., Franco, L., Murphy, E., Iori, E., Pagnin, E., Fadini, G. P., Albiero, M., Semplicini, A., & Avogaro, A. (2007). Rosiglitazone reduces glucose-induced oxidative stress mediated by NAD(P)H oxidase via AMPK-dependent mechanism. *Arteriosclerosis, Thrombosis, and Vascular Biology*. <https://doi.org/10.1161/ATVBAHA.107.155762>
- Cernadas, M. R., De Miguel, L. S., García-Durán, M., González-Fernández, F., Millás, I., Montón, M., Rodrigo, J., Rico, L., Fernández, P., De Frutos, T., Rodríguez-Feo, J. A., Guerra, J., Caramelo, C., Casado, S., & López-Farré, A. (1998a). Expression of constitutive and inducible nitric oxide synthases in the vascular wall of young and aging rats. *Circulation Research*. <https://doi.org/10.1161/01.RES.83.3.279>
- Cernadas, M. R., De Miguel, L. S., García-Durán, M., González-Fernández, F., Millás, I., Montón, M., Rodrigo, J., Rico, L., Fernández, P., De Frutos, T., Rodríguez-Feo, J. A., Guerra, J., Caramelo, C., Casado, S., & López-Farré, A. (1998b). Expression of constitutive and inducible nitric oxide synthases in the vascular wall of young and aging rats. *Circulation Research*. <https://doi.org/10.1161/01.RES.83.3.279>

- Chabi, B., Ljubcic, V., Menzies, K. J., Huang, J. H., Saleem, A., & Hood, D. A. (2008a). Mitochondrial function and apoptotic susceptibility in aging skeletal muscle. *Aging Cell*. <https://doi.org/10.1111/j.1474-9726.2007.00347.x>
- Chabi, B., Ljubcic, V., Menzies, K. J., Huang, J. H., Saleem, A., & Hood, D. A. (2008b). Mitochondrial function and apoptotic susceptibility in aging skeletal muscle. *Aging Cell*. <https://doi.org/10.1111/j.1474-9726.2007.00347.x>
- Chakraborty, A., Koldobskiy, M. A., Bello, N. T., Maxwell, M., Potter, J. J., Juluri, K. R., Maag, D., Kim, S., Huang, A. S., Dailey, M. J., Saleh, M., Snowman, A. M., Moran, T. H., Mezey, E., & Snyder, S. H. (2010). Inositol pyrophosphates inhibit akt signaling, thereby regulating insulin sensitivity and weight gain. *Cell*. <https://doi.org/10.1016/j.cell.2010.11.032>
- Chance, B., & Williams, G. R. (1955). Respiratory enzymes in oxidative phosphorylation. I. Kinetics of oxygen utilization. *The Journal of Biological Chemistry*.
- Chang, M. W. F., Grillari, J., Mayrhofer, C., Fortschegger, K., Allmaier, G., Marzban, G., Katinger, H., & Voglauer, R. (2005). Comparison of early passage, senescent and hTERT immortalized endothelial cells. *Experimental Cell Research*. <https://doi.org/10.1016/j.yexcr.2005.05.002>
- Chao, C. L., Hou, Y. C., Lee Chao, P. D., Weng, C. S., & Ho, F. M. (2009). The antioxidant effects of quercetin metabolites on the prevention of high glucose-induced apoptosis of human umbilical vein endothelial cells. *British Journal of Nutrition*. <https://doi.org/10.1017/S0007114508073637>
- Chen, C. C. W., Erlich, A. T., Crilly, M. J., & Hood, D. A. (2018a). Parkin is required for exercise-induced mitophagy in muscle: Impact of aging. *American Journal of Physiology - Endocrinology and Metabolism*. <https://doi.org/10.1152/ajpendo.00391.2017>

- Chen, C. C. W., Erlich, A. T., Crilly, M. J., & Hood, D. A. (2018b). Parkin is required for exercise-induced mitophagy in muscle: Impact of aging. *American Journal of Physiology - Endocrinology and Metabolism*.
<https://doi.org/10.1152/ajpendo.00391.2017>
- Chen, X., Li, H., Wang, Z., Zhou, Q., Chen, S., Yang, B., Yin, D., He, H., & He, M. (2020). Quercetin protects the vascular endothelium against iron overload damages via ROS/ADMA/DDAHII/eNOS/NO pathway. *European Journal of Pharmacology*.
<https://doi.org/10.1016/j.ejphar.2019.172885>
- Chen, Z. P., Mitchelhill, K. I., Michell, B. J., Stapleton, D., Rodriguez-Crespo, I., Witters, L. A., Power, D. A., Ortiz De Montellano, P. R., & Kemp, B. E. (1999). AMP-activated protein kinase phosphorylation of endothelial NO synthase. *FEBS Letters*.
[https://doi.org/10.1016/S0014-5793\(98\)01705-0](https://doi.org/10.1016/S0014-5793(98)01705-0)
- Cheung, A. L. (2007). Isolation and Culture of Human Umbilical Vein Endothelial Cells (HUVEC). In *Current Protocols in Microbiology*.
<https://doi.org/10.1002/9780471729259.mca04bs4>
- Chilibeck, P. D., Paterson, D. H., Petrella, R. J., & Cunningham, D. A. (1996). The Influence of Age and Cardiorespiratory Fitness on Kinetics of Oxygen Uptake. *Canadian Journal of Applied Physiology*. <https://doi.org/10.1139/h96-015>
- Chitturi, J., Santhakumar, V., & Kannurpatti, S. S. (2019). Beneficial Effects of Kaempferol after Developmental Traumatic Brain Injury Is through Protection of Mitochondrial Function, Oxidative Metabolism, and Neural Viability. *Journal of Neurotrauma*.
<https://doi.org/10.1089/neu.2018.6100>
- Chodzko-Zajko, W. J., Proctor, D. N., Fiatarone Singh, M. A., Minson, C. T., Nigg, C. R., Salem, G. J., & Skinner, J. S. (2009). Exercise and physical activity for older adults.

In *Medicine and Science in Sports and Exercise*.

<https://doi.org/10.1249/MSS.0b013e3181a0c95c>

- Choi, S., Reiter, D. A., Shardell, M., Simonsick, E. M., Studenski, S., Spencer, R. G., Fishbein, K. W., & Ferrucci, L. (2016a). 31P magnetic resonance spectroscopy assessment of muscle bioenergetics as a predictor of gait speed in the Baltimore longitudinal study of aging. *Journals of Gerontology - Series A Biological Sciences and Medical Sciences*. <https://doi.org/10.1093/gerona/glw059>
- Choi, S., Reiter, D. A., Shardell, M., Simonsick, E. M., Studenski, S., Spencer, R. G., Fishbein, K. W., & Ferrucci, L. (2016b). 31P magnetic resonance spectroscopy assessment of muscle bioenergetics as a predictor of gait speed in the Baltimore longitudinal study of aging. *Journals of Gerontology - Series A Biological Sciences and Medical Sciences*. <https://doi.org/10.1093/gerona/glw059>
- Chou, T. C., Yen, M. H., Li, C. Y., & Ding, Y. A. (1998). Alterations of nitric oxide synthase expression with aging and hypertension in rats. *Hypertension*. <https://doi.org/10.1161/01.HYP.31.2.643>
- Chu, K. O., Chan, K. P., Chan, S. O., Ng, T. K., Jhanji, V., Wang, C. C., & Pang, C. P. (2018). Metabolomics of Green-Tea Catechins on Vascular-Endothelial-Growth-Factor-Stimulated Human-Endothelial-Cell Survival. *Journal of Agricultural and Food Chemistry*. <https://doi.org/10.1021/acs.jafc.8b05998>
- Cifuentes-Gomez, T., Rodriguez-Mateos, A., Gonzalez-Salvador, I., Alañon, M. E., & Spencer, J. P. E. (2015). Factors Affecting the Absorption, Metabolism, and Excretion of Cocoa Flavanols in Humans. *Journal of Agricultural and Food Chemistry*, *63*(35), 7615–7623. <https://doi.org/10.1021/acs.jafc.5b00443>
- Cobley, J. N., Noble, A., Jimenez-Fernandez, E., Valdivia Moya, M. T., Guille, M., & Husi, H. (2019). Catalyst-free Click PEGylation reveals substantial mitochondrial ATP

synthase sub-unit alpha oxidation before and after fertilisation. *Redox Biology*.

<https://doi.org/10.1016/j.redox.2019.101258>

- Coen, P. M., Jubrias, S. A., Distefano, G., Amati, F., Mackey, D. C., Glynn, N. W., Manini, T. M., Wohlgenuth, S. E., Leeuwenburgh, C., Cummings, S. R., Newman, A. B., Ferrucci, L., Toledo, F. G. S., Shankland, E., Conley, K. E., & Goodpaster, B. H. (2013). Skeletal muscle mitochondrial energetics are associated with maximal aerobic capacity and walking speed in older adults. *Journals of Gerontology - Series A Biological Sciences and Medical Sciences*. <https://doi.org/10.1093/gerona/gls196>
- Coggan, A. R., Spina, R. J., King, D. S., Rogers, M. A., Brown, M., Nemeth, P. M., & Holloszy, J. O. (1992). Skeletal muscle adaptations to endurance training in 60- to 70-year-old men and women. *Journal of Applied Physiology*. <https://doi.org/10.1152/jappl.1992.72.5.1780>
- Collins, Q. F., Liu, H. Y., Pi, J., Liu, Z., Quon, M. J., & Cao, W. (2007). Epigallocatechin-3-gallate (EGCG), a green tea polyphenol, suppresses hepatic gluconeogenesis through 5'-AMP-activated protein kinase. *Journal of Biological Chemistry*. <https://doi.org/10.1074/jbc.M702390200>
- Colombo, S. L., & Moncada, S. (2009). AMPK α 1 regulates the antioxidant status of vascular endothelial cells. *Biochemical Journal*. <https://doi.org/10.1042/BJ20090613>
- Conley, K. E., Amara, C. E., Bajpeyi, S., Costford, S. R., Murray, K., Jubrias, S. A., Arakaki, L., Marcinek, D. J., & Smith, S. R. (2013). Higher mitochondrial respiration and uncoupling with reduced electron transport chain content in vivo in muscle of sedentary versus active subjects. *Journal of Clinical Endocrinology and Metabolism*. <https://doi.org/10.1210/jc.2012-2967>

- Considine, E. C., & Salek, R. M. (2019). A tool to encourage minimum reporting guideline uptake for data analysis in metabolomics. *Metabolites*.
<https://doi.org/10.3390/metabo9030043>
- Cooper, J. M., Mann, V. M., & Schapira, A. H. V. (1992). Analyses of mitochondrial respiratory chain function and mitochondrial DNA deletion in human skeletal muscle: Effect of ageing. *Journal of the Neurological Sciences*, *113*(1), 91–98.
[https://doi.org/10.1016/0022-510X\(92\)90270-U](https://doi.org/10.1016/0022-510X(92)90270-U)
- Craig, A., Cloarec, O., Holmes, E., Nicholson, J. K., & Lindon, J. C. (2006). Scaling and normalization effects in NMR spectroscopic metabolomic data sets. *Analytical Chemistry*, *78*(7), 2262–2267. <https://doi.org/10.1021/ac0519312>
- Crossland, H., Pereira, S. L., Smith, K., Phillips, B. E., & Atherton, P. J. (2019). Gene-based analysis of angiogenesis, mitochondrial and insulin-related pathways in skeletal muscle of older individuals following nutraceutical supplementation. *Journal of Functional Foods*. <https://doi.org/10.1016/j.jff.2019.03.022>
- Csiszar, A., Gautam, T., Sosnowska, D., Tarantini, S., Banki, E., Tusek, Z., Toth, P., Losonczy, G., Koller, A., Reglodi, D., Giles, C. B., Wren, J. D., Sonntag, W. E., & Ungvari, Z. (2014). Caloric restriction confers persistent anti-oxidative, pro-angiogenic, and anti-inflammatory effects and promotes anti-aging miRNA expression profile in cerebrovascular endothelial cells of aged rats. *American Journal of Physiology - Heart and Circulatory Physiology*.
<https://doi.org/10.1152/ajpheart.00307.2014>
- Csiszar, A., Labinsky, N., Orosz, Z., Xiangmin, Z., Buffenstein, R., & Ungvari, Z. (2007). Vascular aging in the longest-living rodent, the naked mole rat. *American Journal of Physiology - Heart and Circulatory Physiology*.
<https://doi.org/10.1152/ajpheart.01287.2006>

- Csiszar, A., Ungvari, Z., Edwards, J. G., Kaminski, P., Wolin, M. S., Koller, A., & Kaley, G. (2002a). Aging-induced phenotypic changes and oxidative stress impair coronary arteriolar function. *Circulation Research*.
<https://doi.org/10.1161/01.RES.0000020401.61826.EA>
- Csiszar, A., Ungvari, Z., Edwards, J. G., Kaminski, P., Wolin, M. S., Koller, A., & Kaley, G. (2002b). Aging-induced phenotypic changes and oxidative stress impair coronary arteriolar function. *Circulation Research*.
<https://doi.org/10.1161/01.RES.0000020401.61826.EA>
- Culic, O., Gruwel, M. L. H., & Schrader, J. (1997). Energy turnover of vascular endothelial cells. *American Journal of Physiology - Cell Physiology*.
<https://doi.org/10.1152/ajpcell.1997.273.1.c205>
- Cunningham, D. A., & Paterson, D. H. (1994). Exercise on-transient gas exchange kinetics are slowed as a function of age. *Medicine and Science in Sports and Exercise*.
<https://doi.org/10.1249/00005768-199404000-00007>
- Da Costa, K. A., Badea, M., Fischer, L. M., & Zeisel, S. H. (2004). Elevated serum creatine phosphokinase in choline-deficient humans: Mechanistic studies in C2C12 mouse myoblasts. *American Journal of Clinical Nutrition*.
<https://doi.org/10.1093/ajcn/80.1.163>
- Darst, B. F., Kosciak, R. L., Hogan, K. J., Johnson, S. C., & Engelman, C. D. (2019). Longitudinal plasma metabolomics of aging and sex. *Aging*.
<https://doi.org/10.18632/aging.101837>
- Davis, J. M., Murphy, E. A., Carmichael, M. D., & Davis, B. (2009a). Quercetin increases brain and muscle mitochondrial biogenesis and exercise tolerance. *American Journal of Physiology - Regulatory Integrative and Comparative Physiology*.
<https://doi.org/10.1152/ajpregu.90925.2008>

- Davis, J. M., Murphy, E. A., Carmichael, M. D., & Davis, B. (2009b). Quercetin increases brain and muscle mitochondrial biogenesis and exercise tolerance. *American Journal of Physiology - Regulatory Integrative and Comparative Physiology*.
<https://doi.org/10.1152/ajpregu.90925.2008>
- Davison, G., Callister, R., Williamson, G., Cooper, K. A., & Gleeson, M. (2012). The effect of acute pre-exercise dark chocolate consumption on plasma antioxidant status, oxidative stress and immunoendocrine responses to prolonged exercise. *European Journal of Nutrition*, *51*(1), 69–79. <https://doi.org/10.1007/s00394-011-0193-4>
- Davison, K., Coates, A. M., Buckley, J. D., & Howe, P. R. C. (2008). Effect of cocoa flavanols and exercise on cardiometabolic risk factors in overweight and obese subjects. *International Journal of Obesity*, *32*(8), 1289–1296.
<https://doi.org/10.1038/ijo.2008.66>
- Dawidzik, J. B., Budzinski, E. E., Patrzyc, H. B., Cheng, H. C., Iijima, H., Alderfer, J. L., Tabaczynski, W. A., Wallace, J. C., & Box, H. C. (2004). Dihydrothymine lesion in X-irradiated DNA: Characterization at the molecular level and detection in cells. *International Journal of Radiation Biology*.
<https://doi.org/10.1080/09553000410001695877>
- Decroix, L., Soares, D. D., Meeusen, R., Heyman, E., & Tonoli, C. (2018a). Cocoa Flavanol Supplementation and Exercise: A Systematic Review. *Sports Medicine*, *48*, 867–892.
<https://doi.org/10.1007/s40279-017-0849-1>
- Decroix, L., Soares, D. D., Meeusen, R., Heyman, E., & Tonoli, C. (2018b). Cocoa Flavanol Supplementation and Exercise: A Systematic Review. *Sports Medicine*, *48*, 867-892-867–892. <https://doi.org/10.1007/s40279-017-0849-1>
- Decroix, L., Tonoli, C., Lespagnol, E., Balestra, C., Descat, A., Drittij-Reijnders, M. J., Blackwell, J. R., Stahl, W., Jones, A. M., Weseler, A. R., Bast, A., Meeusen, R., &

- Heyman, E. (2018). One-week cocoa flavanol intake increases prefrontal cortex oxygenation at rest and during moderate-intensity exercise in normoxia and hypoxia. *Journal of Applied Physiology*. <https://doi.org/10.1152/jappphysiol.00055.2018>
- DeLorey, D. S., Kowalchuk, J. M., & Paterson, D. H. (2004a). Effect of age on O₂ uptake kinetics and the adaptation of muscle deoxygenation at the onset of moderate-intensity cycling exercise. *Journal of Applied Physiology*, *97*(1), 165–172. <https://doi.org/10.1152/jappphysiol.01179.2003>
- DeLorey, D. S., Kowalchuk, J. M., & Paterson, D. H. (2004b). Effects of prior heavy-intensity exercise on pulmonary O₂ uptake and muscle deoxygenation kinetics in young and older adult humans. *Journal of Applied Physiology*. <https://doi.org/10.1152/jappphysiol.01280.2003>
- Department of Health and Social Care. (2011). Start active, stay active: Report on physical activity in the UK. *Department of Health*.
- Derave, W., Everaert, I., Beeckman, S., & Baguet, A. (2010). Muscle Carnosine Metabolism and β -Alanine Supplementation in Relation to Exercise and Training. In *Sports Medicine*. <https://doi.org/10.2165/11530310-000000000-00000>
- Desai, V. G., Weindruch, R., Hart, R. W., & Feuers, R. J. (1996). Influences of age and dietary restriction on gastrocnemius electron transport system activities in mice. *Archives of Biochemistry and Biophysics*. <https://doi.org/10.1006/abbi.1996.0375>
- Desideri, G., Kwik-Uribe, C., Grassi, D., Necozione, S., Ghiadoni, L., Mastroiacovo, D., Raffaele, A., Ferri, L., Bocale, R., Lechiara, M. C., Marini, C., & Ferri, C. (2012). Benefits in cognitive function, blood pressure, and insulin resistance through cocoa flavanol consumption in elderly subjects with mild cognitive impairment: The cocoa, cognition, and aging (CoCoA) study. *Hypertension*. <https://doi.org/10.1161/HYPERTENSIONAHA.112.193060>

- Di Pietro, A., Godinot, C., Bouillant, M. L., & Gautheron, D. C. (1975). Pig heart mitochondrial ATPase: Properties of purified and membrane-bound enzyme. Effects of flavonoids. *Biochimie*. [https://doi.org/10.1016/S0300-9084\(75\)80218-5](https://doi.org/10.1016/S0300-9084(75)80218-5)
- Dieffenbach, C. W., Lowe, T. M. J., & Dveksler, G. S. (1993). General concepts for PCR primer design. *Genome Research*. <https://doi.org/10.1101/gr.3.3.S30>
- Dieterle, F., Ross, A., Schlotterbeck, G., & Senn, H. (2006). Probabilistic quotient normalization as robust method to account for dilution of complex biological mixtures. Application in ¹H NMR metabonomics. *Analytical Chemistry*. <https://doi.org/10.1021/ac051632c>
- Dimauro, I., Pearson, T., Caporossi, D., & Jackson, M. J. (2012). In vitro susceptibility of thioredoxins and glutathione to redox modification and aging-related changes in skeletal muscle. *Free Radical Biology and Medicine*. <https://doi.org/10.1016/j.freeradbiomed.2012.09.031>
- Dirks, A. J., Hofer, T., Marzetti, E., Pahor, M., & Leeuwenburgh, C. (2006). Mitochondrial DNA mutations, energy metabolism and apoptosis in aging muscle. *Ageing Research Reviews*, 5(2), 179–195. <https://doi.org/10.1016/j.arr.2006.03.002>
- Distefano, G., Standley, R. A., Dubé, J. J., Carnero, E. A., Ritov, V. B., Stefanovic-Racic, M., Toledo, F. G. S., Piva, S. R., Goodpaster, B. H., & Coen, P. M. (2017). Chronological age does not influence Ex-vivo mitochondrial respiration and quality control in skeletal muscle. *Journals of Gerontology - Series A Biological Sciences and Medical Sciences*. <https://doi.org/10.1093/gerona/glw102>
- Distefano, G., Standley, R. A., Zhang, X., Carnero, E. A., Yi, F., Cornell, H. H., & Coen, P. M. (2018). Physical activity unveils the relationship between mitochondrial energetics, muscle quality, and physical function in older adults. *Journal of Cachexia, Sarcopenia and Muscle*. <https://doi.org/10.1002/jcsm.12272>

- Dogra, S., Spencer, M. D., Murias, J. M., & Paterson, D. H. (2013). Oxygen uptake kinetics in endurance-trained and untrained postmenopausal women. *Applied Physiology, Nutrition and Metabolism*. <https://doi.org/10.1139/apnm-2012-0173>
- Donato, A. J., Eskurza, I., Silver, A. E., Levy, A. S., Pierce, G. L., Gates, P. E., & Seals, D. R. (2007a). Direct evidence of endothelial oxidative stress with aging in humans: Relation to impaired endothelium-dependent dilation and upregulation of nuclear factor- κ B. *Circulation Research*.
<https://doi.org/10.1161/01.RES.0000269183.13937.e8>
- Donato, A. J., Eskurza, I., Silver, A. E., Levy, A. S., Pierce, G. L., Gates, P. E., & Seals, D. R. (2007b). Direct evidence of endothelial oxidative stress with aging in humans: Relation to impaired endothelium-dependent dilation and upregulation of nuclear factor- κ B. *Circulation Research*.
<https://doi.org/10.1161/01.RES.0000269183.13937.e8>
- Donato, A. J., Gano, L. B., Eskurza, I., Silver, A. E., Gates, P. E., Jablonski, K., & Seals, D. R. (2009a). Vascular endothelial dysfunction with aging: Endothelin-1 and endothelial nitric oxide synthase. *American Journal of Physiology - Heart and Circulatory Physiology*. <https://doi.org/10.1152/ajpheart.00689.2008>
- Donato, A. J., Gano, L. B., Eskurza, I., Silver, A. E., Gates, P. E., Jablonski, K., & Seals, D. R. (2009b). Vascular endothelial dysfunction with aging: Endothelin-1 and endothelial nitric oxide synthase. *American Journal of Physiology - Heart and Circulatory Physiology*. <https://doi.org/10.1152/ajpheart.00689.2008>
- Donato, A. J., Machin, D. R., & Lesniewski, L. A. (2018). Mechanisms of dysfunction in the aging vasculature and role in age-related disease. *Circulation Research*.
<https://doi.org/10.1161/CIRCRESAHA.118.312563>

- Dorta, D. J., Pigoso, A. A., Mingatto, F. E., Rodrigues, T., Pestana, C. R., Uyemura, S. A., Santos, A. C., & Curti, C. (2008). Antioxidant activity of flavonoids in isolated mitochondria. *Phytotherapy Research*. <https://doi.org/10.1002/ptr.2441>
- Dorta, D. J., Pigoso, A. A., Mingatto, F. E., Rodrigues, T., Prado, I. M. R., Helena, A. F. C., Uyemura, S. A., Santos, A. C., & Curti, C. (2005). The interaction of flavonoids with mitochondria: Effects on energetic processes. *Chemico-Biological Interactions*. <https://doi.org/10.1016/j.cbi.2005.02.004>
- Dower, J. I., Geleijnse, J. M., Gijsbers, L., Zock, P. L., Kromhout, D., & Hollman, P. C. H. (2015). Effects of the pure flavonoids epicatechin and quercetin on vascular function and cardiometabolic health: A randomized, double-blind, placebo-controlled, crossover trial. *American Journal of Clinical Nutrition*. <https://doi.org/10.3945/ajcn.114.098590>
- Drew, B., Dirks, P. A., Selman, C., Gredilla, R., Lezza, A., Barja, G., & Leeuwenburgh, C. (2003a). Effects of aging and caloric restriction on mitochondrial energy production in gastrocnemius muscle and heart. *American Journal of Physiology - Regulatory Integrative and Comparative Physiology*. <https://doi.org/10.1152/ajpregu.00455.2002>
- Drew, B., Dirks, P. A., Selman, C., Gredilla, R., Lezza, A., Barja, G., & Leeuwenburgh, C. (2003b). Effects of aging and caloric restriction on mitochondrial energy production in gastrocnemius muscle and heart. *American Journal of Physiology - Regulatory Integrative and Comparative Physiology*. <https://doi.org/10.1152/ajpregu.00455.2002>
- Duluc, L., Soleti, R., Clere, N., Andriantsitohaina, R., & Simard, G. (2012). Mitochondria As Potential Targets of Flavonoids: Focus on Adipocytes and Endothelial Cells. *Current Medicinal Chemistry*. <https://doi.org/10.2174/092986712803251467>
- Dumanoir, G. R., Delorey, D. S., Kowalchuk, J. M., & Paterson, D. H. (2010). Differences in exercise limb blood flow and muscle deoxygenation with age: Contributions to O₂

uptake kinetics. *European Journal of Applied Physiology*, 110(4), 739–751.

<https://doi.org/10.1007/s00421-010-1546-z>

Dumke, C. L., Davis, J. M., Murphy, E. A., Nieman, D. C., Carmichael, M. D., Quindry, J. C., Triplett, N. T., Utter, A. C., Gross Gowin, S. J., Henson, D. A., McAnulty, S. R., & McAnulty, L. S. (2009). Successive bouts of cycling stimulates genes associated with mitochondrial biogenesis. *European Journal of Applied Physiology*.

<https://doi.org/10.1007/s00421-009-1143-1>

Dunn, W. B., Broadhurst, D. I., Atherton, H. J., Goodacre, R., & Griffin, J. L. (2011).

Systems level studies of mammalian metabolomes: The roles of mass spectrometry and nuclear magnetic resonance spectroscopy. *Chemical Society Reviews*.

<https://doi.org/10.1039/b906712b>

Durrant, J. R., Seals, D. R., Connell, M. L., Russell, M. J., Lawson, B. R., Folian, B. J., Donato, A. J., & Lesniewski, L. A. (2009a). Voluntary wheel running restores endothelial function in conduit arteries of old mice: Direct evidence for reduced oxidative stress, increased superoxide dismutase activity and down-regulation of NADPH oxidase. *Journal of Physiology*.

<https://doi.org/10.1113/jphysiol.2009.169771>

Durrant, J. R., Seals, D. R., Connell, M. L., Russell, M. J., Lawson, B. R., Folian, B. J., Donato, A. J., & Lesniewski, L. A. (2009b). Voluntary wheel running restores endothelial function in conduit arteries of old mice: Direct evidence for reduced oxidative stress, increased superoxide dismutase activity and down-regulation of NADPH oxidase. *Journal of Physiology*.

<https://doi.org/10.1113/jphysiol.2009.169771>

- Eisner, V., Lenaers, G., & Hajnóczky, G. (2014). Mitochondrial fusion is frequent in skeletal muscle and supports excitation-contraction coupling. *Journal of Cell Biology*.
<https://doi.org/10.1083/jcb.201312066>
- Elbling, L., Herbacek, I., Weiss, R. M., Jantschitsch, C., Micksche, M., Gerner, C., Pangratz, H., Grusch, M., Knasmüller, S., & Berger, W. (2010). Hydrogen peroxide mediates EGCG-induced antioxidant protection in human keratinocytes. *Free Radical Biology and Medicine*. <https://doi.org/10.1016/j.freeradbiomed.2010.08.008>
- Eriksson, L., Johansson, E., Kettapeh-Wold, S., & Wold, S. (1999). *Introduction to multi- and megavariable data analysis using projection methods (PCA & PLS)*. Umetrics.
- Erlich, A. T., & Hood, D. A. (2019). Mitophagy Regulation in Skeletal Muscle: Effect of Endurance Exercise and Age. *Journal of Science in Sport and Exercise*.
<https://doi.org/10.1007/s42978-019-00041-5>
- Eskurza, I., Monahan, K. D., Robinson, J. A., & Seals, D. R. (2004). Effect of acute and chronic ascorbic acid on flow-mediated dilatation with sedentary and physically active human ageing. *Journal of Physiology*.
<https://doi.org/10.1113/jphysiol.2003.057042>
- Ezzati, M., & Riboli, E. (2013). Behavioral and Dietary Risk Factors for Noncommunicable Diseases. *New England Journal of Medicine*. <https://doi.org/10.1056/nejmra1203528>
- Fazelzadeh, P., Hangelbroek, R. W. J., Tieland, M., De Groot, L. C. P. G. M., Verdijk, L. B., Van Loon, L. J. C., Smilde, A. K., Alves, R. D. A. M., Vervoort, J., Müller, M., Van Duynhoven, J. P. M., & Boekschoten, M. V. (2016). The Muscle Metabolome Differs between Healthy and Frail Older Adults. *Journal of Proteome Research*.
<https://doi.org/10.1021/acs.jproteome.5b00840>

- Ferrick, D. A., Neilson, A., & Beeson, C. (2008). Advances in measuring cellular bioenergetics using extracellular flux. In *Drug Discovery Today*.
<https://doi.org/10.1016/j.drudis.2007.12.008>
- Ferrières, J. (2004). The French paradox: Lessons for other countries. *Heart (British Cardiac Society)*, 90(1), 107–111. <https://doi.org/10.1136/heart.90.1.107>
- Figueiredo, D., Teixeira, L., Poveda, V., Paúl, C., Santos-Silva, A., & Costa, E. (2016). Predictors of difficulty in medication intake in Europe: A cross-country analysis based on SHARE. *Aging and Disease*. <https://doi.org/10.14336/AD.2015.0925>
- Fiorani, M., Guidarelli, A., Blasa, M., Azzolini, C., Candiracci, M., Piatti, E., & Cantoni, O. (2010a). Mitochondria accumulate large amounts of quercetin: Prevention of mitochondrial damage and release upon oxidation of the extramitochondrial fraction of the flavonoid. *Journal of Nutritional Biochemistry*.
<https://doi.org/10.1016/j.jnutbio.2009.01.014>
- Fiorani, M., Guidarelli, A., Blasa, M., Azzolini, C., Candiracci, M., Piatti, E., & Cantoni, O. (2010b). Mitochondria accumulate large amounts of quercetin: Prevention of mitochondrial damage and release upon oxidation of the extramitochondrial fraction of the flavonoid. *Journal of Nutritional Biochemistry*.
<https://doi.org/10.1016/j.jnutbio.2009.01.014>
- Fitzgerald, M. D., Tanaka, H., Tran, Z. V., & Seals, D. R. (1997). Age-related declines in maximal aerobic capacity in regularly exercising vs. Sedentary women: A meta-analysis. *Journal of Applied Physiology*. <https://doi.org/10.1152/jap.1997.83.1.160>
- Fleischman, A., Makimura, H., Stanley, T. L., McCarthy, M. A., Kron, M., Sun, N., Chuzi, S., Hrovat, M. I., Systrom, D. M., & Grinspoon, S. K. (2010). Skeletal muscle phosphocreatine recovery after submaximal exercise in children and young and

middle-aged adults. *Journal of Clinical Endocrinology and Metabolism*.

<https://doi.org/10.1210/jc.2010-0527>

- Fraga, C. G., Litterio, M. C., Prince, P. D., Calabró, V., Piotrkowski, B., & Galleano, M. (2011). Cocoa flavanols: Effects on vascular nitric oxide and blood pressure. In *Journal of Clinical Biochemistry and Nutrition*. <https://doi.org/10.3164/jc.11-010FR>
- Fredriksson, K., Tjäder, I., Keller, P., Petrovic, N., Ahlman, B., Schéele, C., Wernerman, J., Timmons, J. A., & Rooyackers, O. (2008). Dysregulation of mitochondrial dynamics and the muscle transcriptome in ICU patients suffering from sepsis induced multiple organ failure. *PLoS ONE*. <https://doi.org/10.1371/journal.pone.0003686>
- Fritz, I. B., & Yue, K. T. N. (1963). Long-chain carnitine acyltransferase and the role of acylcarnitine derivatives in the catalytic increase of fatty acid oxidation induced by carnitine. *Journal of Lipid Research*. [https://doi.org/10.1016/s0022-2275\(20\)40302-5](https://doi.org/10.1016/s0022-2275(20)40302-5)
- Fulle, S., Di Donna, S., Puglielli, C., Pietrangelo, T., Beccafico, S., Bellomo, R., Protasi, F., & Fanò, G. (2005). Age-dependent imbalance of the antioxidative system in human satellite cells. *Experimental Gerontology*. <https://doi.org/10.1016/j.exger.2004.11.006>
- Furst, T., Massaro, A., Miller, C., Williams, B. T., LaMacchia, Z. M., & Horvath, P. J. (2018). β -Alanine supplementation increased physical performance and improved executive function following endurance exercise in middle aged individuals. *Journal of the International Society of Sports Nutrition*. <https://doi.org/10.1186/s12970-018-0238-7>
- Galleano, M., Bernatova, I., Puzserova, A., Balis, P., Sestakova, N., Pechanova, O., & Fraga, C. G. (2013). Epicatechin reduces blood pressure and improves vasorelaxation in spontaneously hypertensive rats by NO-mediated mechanism. *IUBMB Life*. <https://doi.org/10.1002/iub.1185>

- Gao, L., Kumar, V., Vellichirammal, N. N., Park, S. Y., Rudebush, T. L., Yu, L., Son, W. M., Pekas, E. J., Wafi, A. M., Hong, J., Xiao, P., Guda, C., Wang, H. J., Schultz, H. D., & Zucker, I. H. (2020). Functional, proteomic and bioinformatic analyses of Nrf2- and Keap1- null skeletal muscle. *Journal of Physiology*. <https://doi.org/10.1113/JP280176>
- Garcia, D., & Shaw, R. J. (2017). AMPK: Mechanisms of Cellular Energy Sensing and Restoration of Metabolic Balance. In *Molecular Cell*. <https://doi.org/10.1016/j.molcel.2017.05.032>
- Garvey, S. M., Dugle, J. E., Kennedy, A. D., McDunn, J. E., Kline, W., Guo, L., Guttridge, D. C., Pereira, S. L., & Edens, N. K. (2014). Metabolomic profiling reveals severe skeletal muscle group-specific perturbations of metabolism in aged FBN rats. *Biogerontology*. <https://doi.org/10.1007/s10522-014-9492-5>
- Geleijnse, J. M., Launer, L. J., Van Der Kuip, D. A. M., Hofman, A., & Witteman, J. C. M. (2002). Inverse association of tea and flavonoid intakes with incident myocardial infarction: The Rotterdam Study. *American Journal of Clinical Nutrition*. <https://doi.org/10.1093/ajcn/75.5.880>
- George, M. A., McLay, K. M., Doyle-Baker, P. K., Reimer, R. A., & Murias, J. M. (2018). Fitness level and not aging per se, determines the oxygen uptake kinetics response. *Frontiers in Physiology*. <https://doi.org/10.3389/fphys.2018.00277>
- Ghosh, S., Lertwattanak, R., Lefort, N., Molina-Carrion, M., Joya-Galeana, J., Bowen, B. P., Garduno-Garcia, J. D. J., Abdul-Ghani, M., Richardson, A., DeFronzo, R. A., Mandarino, L., Van Remmen, H., & Musi, N. (2011). Reduction in reactive oxygen species production by mitochondria from elderly subjects with normal and impaired glucose tolerance. *Diabetes*. <https://doi.org/10.2337/db11-0121>

- Glancy, B., Hartnell, L. M., Malide, D., Yu, Z. X., Combs, C. A., Connelly, P. S., Subramaniam, S., & Balaban, R. S. (2015). Mitochondrial reticulum for cellular energy distribution in muscle. *Nature*. <https://doi.org/10.1038/nature14614>
- Gnaiger, E. (2008). Polarographic Oxygen Sensors, the Oxygraph, and High-Resolution Respirometry to Assess Mitochondrial Function. In *Drug-Induced Mitochondrial Dysfunction*. <https://doi.org/10.1002/9780470372531.ch12>
- Gnoni, G. V., Paglialonga, G., & Siculella, L. (2009). Quercetin inhibits fatty acid and triacylglycerol synthesis in rat-liver cells. *European Journal of Clinical Investigation*. <https://doi.org/10.1111/j.1365-2362.2009.02167.x>
- Gnoni, G. V., Priore, P., Geelen, M. J. H., & Siculella, L. (2009). The mitochondrial citrate carrier: Metabolic role and regulation of its activity and expression. In *IUBMB Life*. <https://doi.org/10.1002/iub.249>
- Gołyński, M., Szpetnar, M., Tatara, M. R., Lutnicki, K., Gołyńska, M., Kurek, Ł., Szczepanik, M., & Wilkołek, P. (2016). Content of selected amino acids in the gastrocnemius muscle during experimental hypothyroidism in rats. *Journal of Veterinary Research*, 60(4), 489–493. <https://doi.org/10.1515/jvetres-2016-0072>
- Gomes, A. P., Price, N. L., Ling, A. J. Y., Moslehi, J. J., Montgomery, M. K., Rajman, L., White, J. P., Teodoro, J. S., Wrann, C. D., Hubbard, B. P., Mercken, E. M., Palmeira, C. M., De Cabo, R., Rolo, A. P., Turner, N., Bell, E. L., & Sinclair, D. A. (2013). Declining NAD⁺ induces a pseudohypoxic state disrupting nuclear-mitochondrial communication during aging. *Cell*. <https://doi.org/10.1016/j.cell.2013.11.037>
- Gomez-Cabrera, M. C., Domenech, E., Romagnoli, M., Arduini, A., Borrás, C., Pallardo, F. V., Sastre, J., & Viña, J. (2008). Oral administration of vitamin C decreases muscle mitochondrial biogenesis and hampers training-induced adaptations in endurance

performance. *American Journal of Clinical Nutrition*.

<https://doi.org/10.1093/ajcn/87.1.142>

Gómez-Guzmán, M., Jiménez, R., Sánchez, M., Romero, M., O'Valle, F., Lopez-Sepulveda, R., Quintela, A. M., Galindo, P., Zarzuelo, M. J., Bailón, E., Delpón, E., Perez-Vizcaino, F., & Duarte, J. (2011). Chronic (-)-epicatechin improves vascular oxidative and inflammatory status but not hypertension in chronic nitric oxide-deficient rats. *British Journal of Nutrition*.

<https://doi.org/10.1017/S0007114511004314>

Gómez-Guzmán, M., Jiménez, R., Sánchez, M., Zarzuelo, M. J., Galindo, P., Quintela, A. M., López-Sepúlveda, R., Romero, M., Tamargo, J., Vargas, F., Pérez-Vizcaino, F., & Duarte, J. (2012). Epicatechin lowers blood pressure, restores endothelial function, and decreases oxidative stress and endothelin-1 and NADPH oxidase activity in DOCA-salt hypertension. *Free Radical Biology and Medicine*.

<https://doi.org/10.1016/j.freeradbiomed.2011.09.015>

Gonzalez-Ruiz, C., Cordero-Anguiano, P., Morales-Guadarrama, A., Mondragón-Lozano, R., Sánchez-Torres, S., Salgado-Ceballos, H., Villarreal, F., Meaney, E., Ceballos, G., & Nájera, N. (2020). (-)-Epicatechin reduces muscle waste after complete spinal cord transection in a murine model: Role of ubiquitin–proteasome system. *Molecular Biology Reports*. <https://doi.org/10.1007/s11033-020-05954-x>

Gordon, J. W., Rungi, A. A., Inagaki, H., & Hood, D. A. (2001). Selected Contribution: Effects of contractile activity on mitochondrial transcription factor A expression in skeletal muscle. *Journal of Applied Physiology*, *90*(1), 389–396.

<https://doi.org/10.1152/jappl.2001.90.1.389>

Gouill, E. Le, Jimenez, M., Binnert, C., Jayet, P.-Y., Thalmann, S., Nicod, P., Scherrer, U., & Vollenweider, P. (2007). Endothelial Nitric Oxide Synthase (eNOS) Knockout Mice

Have Defective Mitochondrial β -Oxidation. *Diabetes*, 56(11), 2690 LP – 2696.

<https://doi.org/10.2337/db06-1228>

Goulding, R. P., Roche, D. M., & Marwood, S. (2017). Prior exercise speeds pulmonary oxygen uptake kinetics and increases critical power during supine but not upright cycling. *Experimental Physiology*, 102(9), 1158–1176.

<https://doi.org/10.1113/EP086304>

Goulding, R. P., Roche, D. M., & Marwood, S. (2018). “Work-to-Work” exercise slows pulmonary oxygen uptake kinetics, decreases critical power, and increases W' during supine cycling. *Physiological Reports*, 6(21). <https://doi.org/10.14814/phy2.13916>

Gouspillou, G., Bourdel-Marchasson, I., Rouland, R., Calmettes, G., Biran, M., Deschodt-Arsac, V., Miraux, S., Thiaudiere, E., Pasdois, P., Detaille, D., Franconi, J. M., Babot, M., Trézéguet, V., Arsac, L., & Diolez, P. (2014a). Mitochondrial energetics is impaired in vivo in aged skeletal muscle. *Aging Cell*.

<https://doi.org/10.1111/accel.12147>

Gouspillou, G., Bourdel-Marchasson, I., Rouland, R., Calmettes, G., Biran, M., Deschodt-Arsac, V., Miraux, S., Thiaudiere, E., Pasdois, P., Detaille, D., Franconi, J. M., Babot, M., Trézéguet, V., Arsac, L., & Diolez, P. (2014b). Mitochondrial energetics is impaired in vivo in aged skeletal muscle. *Aging Cell*.

<https://doi.org/10.1111/accel.12147>

Gouspillou, G., Bourdel-Marchasson, I., Rouland, R., Calmettes, G., Biran, M., Deschodt-Arsac, V., Miraux, S., Thiaudiere, E., Pasdois, P., Detaille, D., Franconi, J. M., Babot, M., Trézéguet, V., Arsac, L., & Diolez, P. (2014c). Mitochondrial energetics is impaired in vivo in aged skeletal muscle. *Aging Cell*.

<https://doi.org/10.1111/accel.12147>

- Gouspillou, G., Sgarioto, N., Kapchinsky, S., Purves-Smith, F., Norris, B., Pion, C. H., Barbat-Artigas, S., Lemieux, F., Taivassalo, T., Morais, J. A., Aubertin-Leheudre, M., & Hepple, R. T. (2014a). Increased sensitivity to mitochondrial permeability transition and myonuclear translocation of endonuclease G in atrophied muscle of physically active older humans. *FASEB Journal*. <https://doi.org/10.1096/fj.13-242750>
- Gouspillou, G., Sgarioto, N., Kapchinsky, S., Purves-Smith, F., Norris, B., Pion, C. H., Barbat-Artigas, S., Lemieux, F., Taivassalo, T., Morais, J. A., Aubertin-Leheudre, M., & Hepple, R. T. (2014b). Increased sensitivity to mitochondrial permeability transition and myonuclear translocation of endonuclease G in atrophied muscle of physically active older humans. *FASEB Journal*. <https://doi.org/10.1096/fj.13-242750>
- Gowans, G. J., & Hardie, D. G. (2014). AMPK: A cellular energy sensor primarily regulated by AMP. *Biochemical Society Transactions*. <https://doi.org/10.1042/BST20130244>
- Gram, M., Vigelsø, A., Yokota, T., Helge, J. W., Dela, F., & Hey-Mogensen, M. (2015). Skeletal muscle mitochondrial H₂O₂ emission increases with immobilization and decreases after aerobic training in young and older men. *Journal of Physiology*. <https://doi.org/10.1113/JP270211>
- Grassi, B., Poole, D. C., Richardson, R. S., Knight, D. R., Erickson, B. K., & Wagner, P. D. (1996). Muscle O₂ uptake kinetics in humans: Implications for metabolic control. *Journal of Applied Physiology*. <https://doi.org/10.1152/jap.1996.80.3.988>
- Grassi, B., Porcelli, S., Marzorati, M., Lanfranconi, F., Vago, P., Marconi, C., & Morandi, L. (2009). Metabolic myopathies: Functional evaluation by analysis of oxygen uptake kinetics. *Medicine and Science in Sports and Exercise*, *41*(12), 2120–2127. <https://doi.org/10.1249/MSS.0b013e3181aae96b>
- Grassi, B., Porcelli, S., Salvadego, D., & Zoladz, J. A. (2011). Slow $\dot{V}O_2$ kinetics during moderate-intensity exercise as markers of lower metabolic stability and lower

exercise tolerance. *European Journal of Applied Physiology*, 111(3), 345–355.

<https://doi.org/10.1007/s00421-010-1609-1>

Grassi, B., Rossiter, H. B., Hogan, M. C., Howlett, R. A., Harris, J. E., Goodwin, M. L., Dobson, J. L., & Gladden, L. B. (2011). Faster O₂ uptake kinetics in canine skeletal muscle in situ after acute creatine kinase inhibition. *Journal of Physiology*.

<https://doi.org/10.1113/jphysiol.2010.195164>

Grassi, D., Desideri, G., De Feo, M., Fellini, E., Mai, F., Dante, A., Di Agostino, S., Di Giosia, P., Patrizi, F., Martella, L., Allegaert, L., Bernaert, H., & Ferri, C. (2014). Long-term effects of cocoa flavonoids on endothelial function, arterial stiffness and blood pressure. *High Blood Pressure and Cardiovascular Prevention*.

Grassi, D., Desideri, G., Necozione, S., Ruggieri, F., Blumberg, J. B., Stornello, M., & Ferri, C. (2012). Protective effects of flavanol-rich dark chocolate on endothelial function and wave reflection during acute hyperglycemia. *Hypertension*.

<https://doi.org/10.1161/HYPERTENSIONAHA.112.193995>

Grassi, D., Draijer, R., Desideri, G., Mulder, T., & Ferri, C. (2015). Black tea lowers blood pressure and wave reflections in fasted and postprandial conditions in hypertensive patients: A randomised study. *Nutrients*. <https://doi.org/10.3390/nu7021037>

Grillari, J., Hohenwarter, O., Grabherr, R. M., & Katinger, H. (2000). Subtractive hybridization of mRNA from early passage and senescent endothelial cells.

Experimental Gerontology. [https://doi.org/10.1016/S0531-5565\(00\)00080-2](https://doi.org/10.1016/S0531-5565(00)00080-2)

Groschner, L. N., Waldeck-Weiermair, M., Malli, R., & Graier, W. F. (2012). Endothelial mitochondria-less respiration, more integration. *Pflugers Archiv European Journal of Physiology*. <https://doi.org/10.1007/s00424-012-1085-z>

Guo, X. D., Zhang, D. Y., Gao, X. J., Parry, J., Liu, K., Liu, B. L., & Wang, M. (2013).

Quercetin and quercetin-3-O-glucuronide are equally effective in ameliorating

endothelial insulin resistance through inhibition of reactive oxygen species-associated inflammation. *Molecular Nutrition and Food Research*.

<https://doi.org/10.1002/mnfr.201200569>

Gurd, B. J., Peters, S. J., Heigenhauser, G. J. F., LeBlanc, P. J., Doherty, T. J., Paterson, D. H., & Kowalchuk, J. M. (2008). O₂ uptake kinetics, pyruvate dehydrogenase activity, and muscle deoxygenation in young and older adults during the transition to moderate-intensity exercise. *American Journal of Physiology - Regulatory Integrative and Comparative Physiology*. <https://doi.org/10.1152/ajpregu.00537.2007>

Gurd, B. J., Peters, S. J., Heigenhauser, G. J. F., LeBlanc, P. J., Doherty, T. J., Paterson, D. H., & Kowalchuk, J. M. (2009). Prior heavy exercise elevates pyruvate dehydrogenase activity and muscle oxygenation and speeds O₂ uptake kinetics during moderate exercise in older adults. *American Journal of Physiology - Regulatory Integrative and Comparative Physiology*. <https://doi.org/10.1152/ajpregu.90848.2008>

Gureev, A. P., Shaforostova, E. A., & Popov, V. N. (2019). Regulation of mitochondrial biogenesis as a way for active longevity: Interaction between the Nrf2 and PGC-1 α signaling pathways. In *Frontiers in Genetics*. <https://doi.org/10.3389/fgene.2019.00435>

Hamer, M., Lavoie, K. L., & Bacon, S. L. (2014). Taking up physical activity in later life and healthy ageing: The English longitudinal study of ageing. *British Journal of Sports Medicine*. <https://doi.org/10.1136/bjsports-2013-092993>

Hamilton, C. A., Brosnan, M. J., McIntyre, M., Graham, D., & Dominiczak, A. F. (2001). Superoxide excess in hypertension and aging a common cause of endothelial dysfunction. *Hypertension*. <https://doi.org/10.1161/01.HYP.37.2.529>

- Handschin, C., & Spiegelman, B. M. (2006). Peroxisome proliferator-activated receptor γ coactivator 1 coactivators, energy homeostasis, and metabolism. *Endocrine Reviews*.
<https://doi.org/10.1210/er.2006-0037>
- Hansen, S. H., Birkedal, H., Wibrand, F., & Grunnet, N. (2015). Taurine and Regulation of Mitochondrial Metabolism. In J. Marcinkiewicz & S. W. Schaffer (Eds.), *Taurine 9* (pp. 397–405). Springer International Publishing.
- Hardie, D. G., Carling, D., & Gamblin, S. J. (2011). AMP-activated protein kinase: Also regulated by ADP? In *Trends in Biochemical Sciences*.
<https://doi.org/10.1016/j.tibs.2011.06.004>
- Hardman, S. E., Hall, D. E., Cabrera, A. J., Hancock, C. R., & Thomson, D. M. (2014). The effects of age and muscle contraction on AMPK activity and heterotrimer composition. *Experimental Gerontology*, 55, 120–128.
<https://doi.org/10.1016/j.exger.2014.04.007>
- Harper, A. J., Ferreira, L. F., Lutjemeier, B. J., Townsend, D. K., & Barstow, T. J. (2006). Human femoral artery and estimated muscle capillary blood flow kinetics following the onset of exercise. *Experimental Physiology*.
<https://doi.org/10.1113/expphysiol.2005.032904>
- Harrison, D. G. (1997). Endothelial Function and Oxidant Stress. *Clinical Cardiology*.
<https://doi.org/10.1002/j.1932-8737.1997.tb00007.x>
- Harvey, J. A., Chastin, S. F. M., & Skelton, D. A. (2015). How sedentary are older people? A systematic review of the amount of sedentary behavior. In *Journal of Aging and Physical Activity*. <https://doi.org/10.1123/japa.2014-0164>
- Hauptmann, N., Grimsby, J., Shih, J. C., & Cadenas, E. (1996). The metabolism of tyramine by monoamine oxidase A/B causes oxidative damage to mitochondrial DNA. *Archives of Biochemistry and Biophysics*. <https://doi.org/10.1006/abbi.1996.0510>

- Hawley, S. A., Pan, D. A., Mustard, K. J., Ross, L., Bain, J., Edelman, A. M., Frenguelli, B. G., & Hardie, D. G. (2005). Calmodulin-dependent protein kinase kinase- β is an alternative upstream kinase for AMP-activated protein kinase. *Cell Metabolism*. <https://doi.org/10.1016/j.cmet.2005.05.009>
- Hawley, S. A., Ross, F. A., Chevtzoff, C., Green, K. A., Evans, A., Fogarty, S., Towler, M. C., Brown, L. J., Ogunbayo, O. A., Evans, A. M., & Hardie, D. G. (2010a). Use of cells expressing γ subunit variants to identify diverse mechanisms of AMPK activation. *Cell Metabolism*. <https://doi.org/10.1016/j.cmet.2010.04.001>
- Hawley, S. A., Ross, F. A., Chevtzoff, C., Green, K. A., Evans, A., Fogarty, S., Towler, M. C., Brown, L. J., Ogunbayo, O. A., Evans, A. M., & Hardie, D. G. (2010b). Use of cells expressing γ subunit variants to identify diverse mechanisms of AMPK activation. *Cell Metabolism*. <https://doi.org/10.1016/j.cmet.2010.04.001>
- Heiss, C., Finis, D., Kleinbongard, P., Hoffmann, A., Rassaf, T., Kelm, M., & Sies, H. (2007). Sustained increase in flow-mediated dilation after daily intake of high-flavanol cocoa drink over 1 week. *Journal of Cardiovascular Pharmacology*. <https://doi.org/10.1097/FJC.0b013e31802d0001>
- Heiss, C., Kleinbongard, P., Dejam, A., Perré, S., Schroeter, H., Sies, H., & Kelm, M. (2005). Acute consumption of flavanol-rich cocoa and the reversal of endothelial dysfunction in smokers. *Journal of the American College of Cardiology*. <https://doi.org/10.1016/j.jacc.2005.06.055>
- Henagan, T. M., Cefalu, W. T., Ribnicky, D. M., Noland, R. C., Dunville, K., Campbell, W. W., Stewart, L. K., Forney, L. A., Gettys, T. W., Chang, J. S., & Morrison, C. D. (2015). In vivo effects of dietary quercetin and quercetin-rich red onion extract on skeletal muscle mitochondria, metabolism, and insulin sensitivity. *Genes and Nutrition*. <https://doi.org/10.1007/s12263-014-0451-1>

- Hermann, F., Spieker, L. E., Ruschitzka, F., Sudano, I., Hermann, M., Binggeli, C., Lüscher, T. F., Riesen, W., Noll, G., & Corti, R. (2006). Dark chocolate improves endothelial and platelet function. *Heart*. <https://doi.org/10.1136/hrt.2005.063362>
- Hertog, Feskens, E. J. M., Kromhout, D., Hertog, M. G. L., Hollman, P. C. H., Hertog, M. G. L., & Katan, M. B. (1993a). Dietary antioxidant flavonoids and risk of coronary heart disease: The Zutphen Elderly Study. *The Lancet*. [https://doi.org/10.1016/0140-6736\(93\)92876-U](https://doi.org/10.1016/0140-6736(93)92876-U)
- Hertog, M. G. L., Feskens, E. J. M., & Kromhout, D. (1997). Antioxidant flavonols and coronary heart disease risk. *Lancet*. [https://doi.org/10.1016/S0140-6736\(05\)60135-3](https://doi.org/10.1016/S0140-6736(05)60135-3)
- Hertog, M. G. L., Feskens, E. J. M., Kromhout, D., Hertog, M. G. L., Hollman, P. C. H., Hertog, M. G. L., & Katan, M. B. (1993b). Dietary antioxidant flavonoids and risk of coronary heart disease: The Zutphen Elderly Study. *The Lancet*. [https://doi.org/10.1016/0140-6736\(93\)92876-U](https://doi.org/10.1016/0140-6736(93)92876-U)
- Hipkiss, A. R., & Chana, H. (1998). Carnosine protects proteins against methylglyoxal-mediated modifications. *Biochemical and Biophysical Research Communications*. <https://doi.org/10.1006/bbrc.1998.8806>
- Hodnick, W. F., Mllosavljević, E. B., Nelson, J. H., & Pardini, R. S. (1988). Electrochemistry of flavonoids. Relationships between redox potentials, inhibition of mitochondrial respiration, and production of oxygen radicals by flavonoids. *Biochemical Pharmacology*. [https://doi.org/10.1016/0006-2952\(88\)90253-5](https://doi.org/10.1016/0006-2952(88)90253-5)
- Holloszy, J. O., Chen, M., Cartee, G. D., & Young, J. C. (1991). Skeletal muscle atrophy in old rats: Differential changes in the three fiber types. *Mechanisms of Ageing and Development*. [https://doi.org/10.1016/0047-6374\(91\)90131-I](https://doi.org/10.1016/0047-6374(91)90131-I)
- Holloway, G. P., Holwerda, A. M., Miotto, P. M., Dirks, M. L., Verdijk, L. B., & van Loon, L. J. C. (2018). Age-Associated Impairments in Mitochondrial ADP Sensitivity

Contribute to Redox Stress in Senescent Human Skeletal Muscle. *Cell Reports*.

<https://doi.org/10.1016/j.celrep.2018.02.069>

Holowatz, L. A., Thompson, C. S., & Kenney, W. L. (2006). L-Arginine supplementation or arginase inhibition augments reflex cutaneous vasodilatation in aged human skin.

Journal of Physiology. <https://doi.org/10.1113/jphysiol.2006.108993>

Holst, B., & Williamson, G. (2008). Nutrients and phytochemicals: From bioavailability to bioefficacy beyond antioxidants. In *Current Opinion in Biotechnology*.

<https://doi.org/10.1016/j.copbio.2008.03.003>

Holt, R. R., Lazarus, S. A., Cameron Sullards, M., Zhu, Q. Y., Schramm, D. D.,

Hammerstone, J. F., Fraga, C. G., Schmitz, H. H., & Keen, C. L. (2002). Procyanidin dimer B2 [epicatechin-(4 β -8)-epicatechin] in human plasma after the consumption of a flavanol-rich cocoa. *American Journal of Clinical Nutrition*.

<https://doi.org/10.1093/ajcn/76.4.798>

Holub, B. J. (1986). Metabolism and function of myo-inositol and inositol phospholipids. In

Annual review of nutrition. <https://doi.org/10.1146/annurev.nutr.6.1.563>

Hood, D. A., Memme, J. M., Oliveira, A. N., & Triolo, M. (2019). Maintenance of Skeletal Muscle Mitochondria in Health, Exercise, and Aging. *Annual Review of Physiology*.

<https://doi.org/10.1146/annurev-physiol-020518-114310>

Hooper, L., Kay, C., Abdelhamid, A., Kroon, P. A., Cohn, J. S., Rimm, E. B., & Cassidy, A.

(2012). Effects of chocolate, cocoa, and flavan-3-ols on cardiovascular health: A systematic review and meta-analysis of randomized trials. *American Journal of Clinical Nutrition*, 95(3), 740–751. <https://doi.org/10.3945/ajcn.111.023457>

Howald, H., Hoppeler, H., Claassen, H., Mathieu, O., & Straub, R. (1985). Influences of endurance training on the ultrastructural composition of the different muscle fiber

types in humans. *Pflügers Archiv*, 403(4), 369–376.

<https://doi.org/10.1007/BF00589248>

- Howitz, K. T., Bitterman, K. J., Cohen, H. Y., Lamming, D. W., Lavu, S., Wood, J. G., Zipkin, R. E., Chung, P., Kisielewski, A., Zhang, L. L., Scherer, B., & Sinclair, D. A. (2003). Small molecule activators of sirtuins extend *Saccharomyces cerevisiae* lifespan. *Nature*. <https://doi.org/10.1038/nature01960>
- Huang, Z., Jing, X., Sheng, Y., Zhang, J., Hao, Z., Wang, Z., & Ji, L. (2019). (-)-Epicatechin attenuates hepatic sinusoidal obstruction syndrome by inhibiting liver oxidative and inflammatory injury. *Redox Biology*. <https://doi.org/10.1016/j.redox.2019.101117>
- Hung, C. H., Chan, S. H., Chu, P. M., & Tsai, K. L. (2015). Quercetin is a potent anti-atherosclerotic compound by activation of SIRT1 signaling under oxLDL stimulation. *Molecular Nutrition and Food Research*. <https://doi.org/10.1002/mnfr.201500144>
- Hüttemann, M., Lee, I., Perkins, G. A., Britton, S. L., Koch, L. G., & Malek, M. H. (2013). (-)-Epicatechin is associated with increased angiogenic and mitochondrial signalling in the hindlimb of rats selectively bred for innate low running capacity. *Clinical Science*. <https://doi.org/10.1042/CS20120469>
- Hütter, E., Skovbro, M., Lener, B., Prats, C., Rabøl, R., Dela, F., & Jansen-Dürr, P. (2007). Oxidative stress and mitochondrial impairment can be separated from lipofuscin accumulation in aged human skeletal muscle. *Aging Cell*. <https://doi.org/10.1111/j.1474-9726.2007.00282.x>
- Hwang, J. T., Park, I. J., Shin, J. I., Lee, Y. K., Lee, S. K., Baik, H. W., Ha, J., & Park, O. J. (2005). Genistein, EGCG, and capsaicin inhibit adipocyte differentiation process via activating AMP-activated protein kinase. *Biochemical and Biophysical Research Communications*. <https://doi.org/10.1016/j.bbrc.2005.09.195>

- Ido, Y., Carling, D., & Ruderman, N. (2002). Hyperglycemia-induced apoptosis in human umbilical vein endothelial cells: Inhibition by the AMP-activated protein kinase activation. *Diabetes*. <https://doi.org/10.2337/diabetes.51.1.159>
- Iqbal, S., Ostojic, O., Singh, K., Joseph, A.-M., & Hood, D. A. (2013). Expression of mitochondrial fission and fusion regulatory proteins in skeletal muscle during chronic use and disuse. *Muscle & Nerve*. <https://doi.org/10.1002/mus.23838>
- J, G., CQ, W., HH, F., HY, D., XL, X., YM, X., BY, W., & DJ, H. (2006). Effects of Resveratrol on Endothelial Progenitor Cells and Their Contributions to Reendothelialization in Intima-injured Rats. *Journal of Cardiovascular Pharmacology*, 47(5).
- Jablonski, K. L., Seals, D. R., Eskurza, I., Monahan, K. D., & Donato, A. J. (2007). High-dose ascorbic acid infusion abolishes chronic vasoconstriction and restores resting leg blood flow in healthy older men. *Journal of Applied Physiology*. <https://doi.org/10.1152/jappphysiol.00533.2007>
- Jacobson, A., Yan, C., Gao, Q., Rincon-Skinner, T., Rivera, A., Edwards, J., Huang, A., Kaley, G., & Sun, D. (2007). Aging enhances pressure-induced arterial superoxide formation. *American Journal of Physiology - Heart and Circulatory Physiology*. <https://doi.org/10.1152/ajpheart.00413.2007>
- James, K. D., Kennett, M. J., & Lambert, J. D. (2018). Potential role of the mitochondria as a target for the hepatotoxic effects of (-)-epigallocatechin-3-gallate in mice. *Food and Chemical Toxicology*. <https://doi.org/10.1016/j.fct.2017.11.029>
- Jang, J.-H., & Surh, Y.-J. (2003). Protective effect of resveratrol on β -amyloid-induced oxidative PC12 cell death. *Free Radical Biology and Medicine*, 34(8), 1100–1110. [https://doi.org/10.1016/S0891-5849\(03\)00062-5](https://doi.org/10.1016/S0891-5849(03)00062-5)

- Jang, Y. C., Lustgarten, M. S., Liu, Y., Muller, F. L., Bhattacharya, A., Liang, H., Salmon, A. B., Brooks, S. V., Larkin, L., Hayworth, C. R., Richardson, A., & Van Remmen, H. (2010). Increased superoxide in vivo accelerates age-associated muscle atrophy through mitochondrial dysfunction and neuromuscular junction degeneration. *The FASEB Journal*. <https://doi.org/10.1096/fj.09-146308>
- Jang, Y. C., & Remmen, H. Van. (2009). The mitochondrial theory of aging: Insight from transgenic and knockout mouse models. In *Experimental Gerontology*. <https://doi.org/10.1016/j.exger.2008.12.006>
- Jefferis, B. J., Sartini, C., Lee, I.-M., Choi, M., Amuzu, A., Gutierrez, C., Casas, J. P., Ash, S., Lennon, L. T., Wannamethee, S. G., & Whincup, P. H. (2014). Adherence to physical activity guidelines in older adults, using objectively measured physical activity in a population-based study. *BMC Public Health*, *14*(1), 382. <https://doi.org/10.1186/1471-2458-14-382>
- Jendrach, M., Pohl, S., Vöth, M., Kowald, A., Hammerstein, P., & Bereiter-Hahn, J. (2005). Morpho-dynamic changes of mitochondria during ageing of human endothelial cells. *Mechanisms of Ageing and Development*. <https://doi.org/10.1016/j.mad.2005.03.002>
- Jensen, T. E., Rose, A. J., Jørgensen, S. B., Brandt, N., Schjerling, P., Wojtaszewski, J. F. P., & Richter, E. A. (2007). Possible CaMKK-dependent regulation of AMPK phosphorylation and glucose uptake at the onset of mild tetanic skeletal muscle contraction. *American Journal of Physiology - Endocrinology and Metabolism*. <https://doi.org/10.1152/ajpendo.00456.2006>
- Johnson, L. C., Martens, C. R., Santos-Parker, J. R., Bassett, C. J., Strahler, T. R., Cruickshank-Quinn, C., Reisdorph, N., McQueen, M. B., & Seals, D. R. (2018). Amino acid and lipid associated plasma metabolomic patterns are related to

healthspan indicators with ageing. *Clinical Science*.

<https://doi.org/10.1042/CS20180409>

- Jones, A. M., Wilkerson, D. P., Koppo, K., Wilmshurst, S., & Campbell, I. T. (2003). Inhibition of nitric oxide synthase by L-NAME speeds phase II pulmonary VO₂ kinetics in the transition to moderate-intensity exercise in man. In *Journal of Physiology*. <https://doi.org/10.1113/jphysiol.2003.045799>
- Jones, A. M., Wilkerson, D. P., Wilmshurst, S., & Campbell, I. T. (2004). Influence of L-NAME on pulmonary O₂ uptake kinetics during heavy-intensity cycle exercise. *Journal of Applied Physiology*. <https://doi.org/10.1152/jappphysiol.00381.2003>
- Jones, D. P. (2006). Redefining oxidative stress. In *Antioxidants and Redox Signaling*. <https://doi.org/10.1089/ars.2006.8.1865>
- Jones, H. S., Gordon, A., Magwenzi, S. G., Naseem, K., Atkin, S. L., & Courts, F. L. (2016). The dietary flavonol quercetin ameliorates angiotensin II-induced redox signaling imbalance in a human umbilical vein endothelial cell model of endothelial dysfunction via ablation of p47phox expression. *Molecular Nutrition and Food Research*. <https://doi.org/10.1002/mnfr.201500751>
- Jones, M., & Nies, M. A. (1996). The Relationship of Perceived Benefits of and Barriers to Reported Exercise in Older African American Women. *Public Health Nursing*. <https://doi.org/10.1111/j.1525-1446.1996.tb00233.x>
- Joo, M. S., Kim, W. D., Lee, K. Y., Kim, J. H., Koo, J. H., & Kim, S. G. (2016). AMPK Facilitates Nuclear Accumulation of Nrf2 by Phosphorylating at Serine 550. *Molecular and Cellular Biology*. <https://doi.org/10.1128/mcb.00118-16>
- Joseph, A. M., Adhietty, P. J., Buford, T. W., Wohlgemuth, S. E., Lees, H. A., Nguyen, L. M. D., Aranda, J. M., Sandesara, B. D., Pahor, M., Manini, T. M., Marzetti, E., & Leeuwenburgh, C. (2012). The impact of aging on mitochondrial function and

- biogenesis pathways in skeletal muscle of sedentary high- and low-functioning elderly individuals. *Aging Cell*. <https://doi.org/10.1111/j.1474-9726.2012.00844.x>
- Joseph, A. M., Adhietty, P. J., Wawrzyniak, N. R., Wohlgemuth, S. E., Picca, A., Kujoth, G. C., Prolla, T. A., & Leeuwenburgh, C. (2013a). Dysregulation of Mitochondrial Quality Control Processes Contribute to Sarcopenia in a Mouse Model of Premature Aging. *PLoS ONE*. <https://doi.org/10.1371/journal.pone.0069327>
- Joseph, A. M., Adhietty, P. J., Wawrzyniak, N. R., Wohlgemuth, S. E., Picca, A., Kujoth, G. C., Prolla, T. A., & Leeuwenburgh, C. (2013b). Dysregulation of Mitochondrial Quality Control Processes Contribute to Sarcopenia in a Mouse Model of Premature Aging. *PLoS ONE*. <https://doi.org/10.1371/journal.pone.0069327>
- Joseph, G. A., Wang, S. X., Jacobs, C. E., Zhou, W., Kimble, G. C., Tse, H. W., Eash, J. K., Shavlakadze, T., & Glass, D. J. (2019). Partial Inhibition of mTORC1 in Aged Rats Counteracts the Decline in Muscle Mass and Reverses Molecular Signaling Associated with Sarcopenia. *Molecular and Cellular Biology*. <https://doi.org/10.1128/mcb.00141-19>
- Karim, M., McCormick, K., & Kappagoda, C. T. (2000). Effects of Cocoa Extracts on Endothelium-Dependent Relaxation. *The Journal of Nutrition*. <https://doi.org/10.1093/jn/130.8.2105s>
- Katz, D. L., Doughty, K., & Ali, A. (2011). Cocoa and chocolate in human health and disease. In *Antioxidants and Redox Signaling*. <https://doi.org/10.1089/ars.2010.3697>
- Kell, D. B. (2004). Metabolomics and systems biology: Making sense of the soup. In *Current Opinion in Microbiology*. <https://doi.org/10.1016/j.mib.2004.04.012>
- Keller, A., Hull, S. E., Elajaili, H., Johnston, A., Knaub, L. A., Chun, J. H., Walker, L., Nozik-Grayck, E., & Reusch, J. E. B. (2020). (-)-Epicatechin Modulates Mitochondrial Redox in Vascular Cell Models of Oxidative Stress. *Oxidative*

Medicine and Cellular Longevity, 2020, 6392629.

<https://doi.org/10.1155/2020/6392629>

Kener, K. B., Munk, D. J., Hancock, C. R., & Tessem, J. S. (2018a). High-resolution respirometry to measure mitochondrial function of intact beta cells in the presence of natural compounds. *Journal of Visualized Experiments*. <https://doi.org/10.3791/57053>

Kener, K. B., Munk, D. J., Hancock, C. R., & Tessem, J. S. (2018b). High-resolution respirometry to measure mitochondrial function of intact beta cells in the presence of natural compounds. *Journal of Visualized Experiments*. <https://doi.org/10.3791/57053>

Kennedy, E. P., & Weiss, S. B. (1956). The function of cytidine coenzymes in the biosynthesis of phospholipides. *The Journal of Biological Chemistry*.

[https://doi.org/10.1016/S0021-9258\(19\)50785-2](https://doi.org/10.1016/S0021-9258(19)50785-2)

Kent-Braun, J. A., & Ng, A. V. (2000). Skeletal muscle oxidative capacity in young and older women and men. *Journal of Applied Physiology*.

<https://doi.org/10.1152/jappl.2000.89.3.1072>

Kicinska, A., & Jarmuszkiewicz, W. (2020). Flavonoids and Mitochondria: Activation of Cytoprotective Pathways? *Molecules (Basel, Switzerland)*, 25(13), 3060.

<https://doi.org/10.3390/molecules25133060>

Kim, C. S., Kwon, Y., Choe, S. Y., Hong, S. M., Yoo, H., Goto, T., Kawada, T., Choi, H. S., Joe, Y., Chung, H. T., & Yu, R. (2015). Quercetin reduces obesity-induced hepatosteatosis by enhancing mitochondrial oxidative metabolism via heme oxygenase-1. *Nutrition and Metabolism*. <https://doi.org/10.1186/s12986-015-0030-5>

Kim, H. S., Montana, V., Jang, H. J., Parpura, V., & Kim, J. A. (2013). Epigallocatechin gallate (EGCG) stimulates autophagy in vascular endothelial cells: A potential role for reducing lipid accumulation. *Journal of Biological Chemistry*.

<https://doi.org/10.1074/jbc.M113.477505>

- Kim, J. A., Formoso, G., Li, Y., Potenza, M. A., Marasciulo, F. L., Montagnani, M., & Quon, M. J. (2007). Epigallocatechin gallate, a green tea polyphenol, mediates NO-dependent vasodilation using signaling pathways in vascular endothelium requiring reactive oxygen species and fyn. *Journal of Biological Chemistry*.
<https://doi.org/10.1074/jbc.M609725200>
- Kim, Y., & Hood, D. A. (2017). Regulation of the autophagy system during chronic contractile activity-induced muscle adaptations. *Physiological Reports*.
<https://doi.org/10.14814/phy2.13307>
- Kim, Y., Triolo, M., Erlich, A. T., & Hood, D. A. (2019). Regulation of autophagic and mitophagic flux during chronic contractile activity-induced muscle adaptations. *Pflugers Archiv European Journal of Physiology*. <https://doi.org/10.1007/s00424-018-2225-x>
- Kimball, S. R., O'Malley, J. P., Anthony, J. C., Crozier, S. J., & Jefferson, L. S. (2004). Assessment of biomarkers of protein anabolism in skeletal muscle during the life span of the rat: Sarcopenia despite elevated protein synthesis. *American Journal of Physiology - Endocrinology and Metabolism*.
<https://doi.org/10.1152/ajpendo.00535.2003>
- Kirby, B. S., Voyles, W. F., Simpson, C. B., Carlson, R. E., Schrage, W. G., & Dineno, F. A. (2009). Endothelium-dependent vasodilatation and exercise hyperaemia in ageing humans: Impact of acute ascorbic acid administration. *Journal of Physiology*.
<https://doi.org/10.1113/jphysiol.2008.167320>
- Kitzman, D. W., & Groban, L. (2011). Exercise Intolerance. In *Cardiology Clinics*.
<https://doi.org/10.1016/j.ccl.2011.06.002>

- Knekt, P., Kumpulainen, J., Järvinen, R., Rissanen, H., Heliövaara, M., Reunanen, A., Hakulinen, T., & Aromaa, A. (2002). Flavonoid intake and risk of chronic diseases. *American Journal of Clinical Nutrition*. <https://doi.org/10.1093/ajcn/76.3.560>
- Konopka, A. R., Suer, M. K., Wolff, C. A., & Harber, M. P. (2014). Markers of human skeletal muscle mitochondrial biogenesis and quality control: Effects of age and aerobic exercise training. *Journals of Gerontology - Series A Biological Sciences and Medical Sciences*. <https://doi.org/10.1093/gerona/glt107>
- Koopman, R., Caldow, M. K., Ham, D. J., & Lynch, G. S. (2017). Glycine metabolism in skeletal muscle: Implications for metabolic homeostasis. In *Current Opinion in Clinical Nutrition and Metabolic Care*. <https://doi.org/10.1097/MCO.0000000000000383>
- Kopustinskiene, D. M., Savickas, A., Vetchý, D., Masteikova, R., Kasauskas, A., & Bernatoniene, J. (2015a). Direct effects of (-)-Epicatechin and procyanidin B2 on the respiration of rat heart mitochondria. *BioMed Research International*. <https://doi.org/10.1155/2015/232836>
- Kopustinskiene, D. M., Savickas, A., Vetchý, D., Masteikova, R., Kasauskas, A., & Bernatoniene, J. (2015b). Direct effects of (-)-Epicatechin and procyanidin B2 on the respiration of rat heart mitochondria. *BioMed Research International*. <https://doi.org/10.1155/2015/232836>
- Krogh, A., & Lindhard, J. (1913). The regulation of respiration and circulation during the initial stages of muscular work. *The Journal of Physiology*. <https://doi.org/10.1113/jphysiol.1913.sp001616>
- Krustrup, P., Söderlund, K., Mohr, M., & Bangsbo, J. (2004). The slow component of oxygen uptake during intense, sub-maximal exercise in man is associated with additional fibre

recruitment. *Pflugers Archiv European Journal of Physiology*.

<https://doi.org/10.1007/s00424-003-1203-z>

Krylatov, A. V., Maslov, L. N., Voronkov, N. S., Boshchenko, A. A., Popov, S. V., Gomez, L., Wang, H., Jaggi, A. S., & Downey, J. M. (2018). Reactive Oxygen Species as Intracellular Signaling Molecules in the Cardiovascular System. *Current Cardiology Reviews*, 14(4), 290–300. <https://doi.org/10.2174/1573403X14666180702152436>

Kucera, O., Mezera, V., Moravcova, A., Endlicher, R., Lotkova, H., Drahota, Z., & Cervinkova, Z. (2015). In vitro toxicity of epigallocatechin gallate in rat liver mitochondria and hepatocytes. *Oxidative Medicine and Cellular Longevity*. <https://doi.org/10.1155/2015/476180>

Kukidome, D., Nishikawa, T., Sonoda, K., Imoto, K., Fujisawa, K., Yano, M., Motoshima, H., Taguchi, T., Matsumura, T., & Araki, E. (2006). Activation of AMP-activated protein kinase reduces hyperglycemia-induced mitochondrial reactive oxygen species production and promotes mitochondrial biogenesis in human umbilical vein endothelial cells. *Diabetes*. <https://doi.org/10.2337/diabetes.55.01.06.db05-0943>

Kumaran, S., Panneerselvam, K. S., Shila, S., Sivarajan, K., & Panneerselvam, C. (2005). Age-associated deficit of mitochondrial oxidative phosphorylation in skeletal muscle: Role of carnitine and lipoic acid. *Molecular and Cellular Biochemistry*, 280(1), 83–89. <https://doi.org/10.1007/s11010-005-8234-z>

Laemmli, U. K. (1970). Cleavage of Structural Proteins during the Assembly of the Head of Bacteriophage T4. *Nature*, 227(5259), 680–685. <https://doi.org/10.1038/227680a0>

Lagoa, R., Graziani, I., Lopez-Sanchez, C., Garcia-Martinez, V., & Gutierrez-Merino, C. (2011). Complex I and cytochrome c are molecular targets of flavonoids that inhibit hydrogen peroxide production by mitochondria. *Biochimica et Biophysica Acta - Bioenergetics*. <https://doi.org/10.1016/j.bbabi.2011.09.022>

- Lagouge, M., Argmann, C., Gerhart-Hines, Z., Meziane, H., Lerin, C., Daussin, F., Messadeq, N., Milne, J., Lambert, P., Elliott, P., Geny, B., Laakso, M., Puigserver, P., & Auwerx, J. (2006). Resveratrol Improves Mitochondrial Function and Protects against Metabolic Disease by Activating SIRT1 and PGC-1 α . *Cell*.
<https://doi.org/10.1016/j.cell.2006.11.013>
- Lamarra, N., Whipp, B. J., Ward, S. A., & Wasserman, K. (1987). Effect of interbreath fluctuations on characterizing exercise gas exchange kinetics. *Journal of Applied Physiology*, 62(5), 2003–2012.
- Lang, D. R., & Racker, E. (1974a). Effects of quercetin and F1 inhibitor on mitochondrial ATPase and energy-linked reactions in submitochondrial particles. *BBA - Bioenergetics*. [https://doi.org/10.1016/0005-2728\(74\)90002-4](https://doi.org/10.1016/0005-2728(74)90002-4)
- Lang, D. R., & Racker, E. (1974b). Effects of quercetin and F1 inhibitor on mitochondrial ATPase and energy-linked reactions in submitochondrial particles. *BBA - Bioenergetics*. [https://doi.org/10.1016/0005-2728\(74\)90002-4](https://doi.org/10.1016/0005-2728(74)90002-4)
- Lansley, K. E., Winyard, P. G., Fulford, J., Vanhatalo, A., Bailey, S. J., Blackwell, J. R., DiMenna, F. J., Gilchrist, M., Benjamin, N., & Jones, A. M. (2011). Dietary nitrate supplementation reduces the O₂ cost of walking and running: A placebo-controlled study. *Journal of Applied Physiology*, 110(3), 591–600.
<https://doi.org/10.1152/jappphysiol.01070.2010>
- Lanza, I. R., Befroy, D. E., & Kent-Braun, J. A. (2005). Age-related changes in ATP-producing pathways in human skeletal muscle in vivo. *Journal of Applied Physiology*.
<https://doi.org/10.1152/jappphysiol.00566.2005>
- Larsen, F. J., Weitzberg, E., Lundberg, J. O., & Ekblom, B. (2007). Effects of dietary nitrate on oxygen cost during exercise. *Acta Physiologica*, 191(1), 59–66.
<https://doi.org/10.1111/j.1748-1716.2007.01713.x>

- Lavie, C. J., Ozemek, C., Carbone, S., Katzmarzyk, P. T., & Blair, S. N. (2019). Sedentary Behavior, Exercise, and Cardiovascular Health. In *Circulation Research*.
<https://doi.org/10.1161/CIRCRESAHA.118.312669>
- Leduc-Gaudet, J.-P., Picard, M., St-Jean Pelletier, F., Sgarioto, N., Auger, M.-J., Vallée, J., Robitaille, R., St-Pierre, D. H., & Gouspillou, G. (2015). Mitochondrial morphology is altered in atrophied skeletal muscle of aged mice. *Oncotarget*, *6*(20), 17923–17937.
<https://doi.org/10.18632/oncotarget.4235>
- Lee, I., Hüttemann, M., Kruger, A., Bollig-Fischer, A., & Malek, M. H. (2015). (-)-Epicatechin combined with 8 weeks of treadmill exercise is associated with increased angiogenic and mitochondrial signaling in mice. *Frontiers in Pharmacology*.
<https://doi.org/10.3389/fphar.2015.00043>
- Lee, M. S., Shin, Y., Jung, S., & Kim, Y. (2017). Effects of epigallocatechin-3-gallate on thermogenesis and mitochondrial biogenesis in brown adipose tissues of diet-induced obese mice. *Food and Nutrition Research*.
<https://doi.org/10.1080/16546628.2017.1325307>
- Lesniewski, L. A., Connell, M. L., Durrant, J. R., Folian, B. J., Anderson, M. C., Donato, A. J., & Seals, D. R. (2009). B6D2F1 mice are a suitable model of oxidative stress-mediated impaired endothelium-dependent dilation with aging. *Journals of Gerontology - Series A Biological Sciences and Medical Sciences*.
<https://doi.org/10.1093/gerona/gln049>
- Lesniewski, L. A., Zigler, M. C., Durrant, J. R., Donato, A. J., & Seals, D. R. (2012). Sustained activation of AMPK ameliorates age-associated vascular endothelial dysfunction via a nitric oxide-independent mechanism. *Mechanisms of Ageing and Development*. <https://doi.org/10.1016/j.mad.2012.03.011>

- Lezza, A. M. S., Boffoli, D., Scacco, S., Cantatore, P., & Gadaleta, M. N. (1994). Correlation Between Mitochondrial DNA 4977-bp Deletion and Respiratory Chain Enzyme Activities in Aging Human Skeletal Muscles. *Biochemical and Biophysical Research Communications*. <https://doi.org/10.1006/bbrc.1994.2732>
- Lezza, A. M. S., Pesce, V., Cormio, A., Fracasso, F., Vecchiet, J., Felzani, G., Cantatore, P., & Gadaleta, M. N. (2001). Increased expression of mitochondrial transcription factor A and nuclear respiratory factor-1 in skeletal muscle from aged human subjects. *FEBS Letters*, *501*(1), 74–78. [https://doi.org/10.1016/S0014-5793\(01\)02628-X](https://doi.org/10.1016/S0014-5793(01)02628-X)
- L'Honoré, A., Commère, P. H., Negroni, E., Pallafacchina, G., Friguet, B., Drouin, J., Buckingham, M., & Montarras, D. (2018). The role of Pitx2 and Pitx3 in muscle 1 stem cells gives new insights into P38 α MAP kinase and redox regulation of muscle regeneration. *ELife*. <https://doi.org/10.7554/eLife.32991>
- Li, G. X., Chen, Y. K., Hou, Z., Xiao, H., Jin, H., Lu, G., Lee, M. J., Liu, B., Guan, F., Yang, Z., Yu, A., & Yang, C. S. (2010). Pro-oxidative activities and dose-response relationship of (-)-epigallocatechin-3-gallate in the inhibition of lung cancer cell growth: A comparative study in vivo and in vitro. *Carcinogenesis*. <https://doi.org/10.1093/carcin/bgq039>
- Li, X., Wang, H., Gao, Y., Li, L., Tang, C., Wen, G., Zhou, Y., Zhou, M., Mao, L., & Fan, Y. (2016). Protective effects of quercetin on mitochondrial biogenesis in experimental traumatic brain injury via the Nrf2 signaling pathway. *PLoS ONE*. <https://doi.org/10.1371/journal.pone.0164237>
- Lim, S. S., Vos, T., Flaxman, A. D., Danaei, G., Shibuya, K., Adair-Rohani, H., Amann, M., Anderson, H. R., Andrews, K. G., Aryee, M., Atkinson, C., Bacchus, L. J., Bahalim, A. N., Balakrishnan, K., Balmes, J., Barker-Collo, S., Baxter, A., Bell, M. L., Blore, J. D., ... Ezzati, M. (2012). A comparative risk assessment of burden of disease and

- injury attributable to 67 risk factors and risk factor clusters in 21 regions, 1990-2010: A systematic analysis for the Global Burden of Disease Study 2010. *The Lancet*.
[https://doi.org/10.1016/S0140-6736\(12\)61766-8](https://doi.org/10.1016/S0140-6736(12)61766-8)
- Lin, J., Handschin, C., & Spiegelman, B. M. (2005). Metabolic control through the PGC-1 family of transcription coactivators. In *Cell Metabolism*.
<https://doi.org/10.1016/j.cmet.2005.05.004>
- Lin, J., Rexrode, K. M., Hu, F., Albert, C. M., Chae, C. U., Rimm, E. B., Stampfer, M. J., & Manson, J. E. (2007). Dietary intakes of flavonols and flavones and coronary heart disease in US women. *American Journal of Epidemiology*.
<https://doi.org/10.1093/aje/kwm016>
- Lin, J., Wu, H., Tarr, P. T., Zhang, C. Y., Wu, Z., Boss, O., Michael, L. F., Puigserver, P., Isotani, E., Olson, E. N., Lowell, B. B., Bassel-Duby, R., & Spiegelman, B. M. (2002). Transcriptional co-activator PGC-1 α drives the formation of slow-twitch muscle fibres. *Nature*. <https://doi.org/10.1038/nature00904>
- Lin, S. M., Wang, S. W., Ho, S. C., & Tang, Y. L. (2010). Protective effect of green tea (-)-epigallocatechin-3-gallate against the monoamine oxidase B enzyme activity increase in adult rat brains. *Nutrition*. <https://doi.org/10.1016/j.nut.2009.11.022>
- Lira, V. A., Brown, D. L., Lira, A. K., Kavazis, A. N., Soltow, Q. A., Zeanah, E. H., & Criswell, D. S. (2010). Nitric oxide and AMPK cooperatively regulate PGC-1 α in skeletal muscle cells. *The Journal of Physiology*, 588(18), 3551–3566.
<https://doi.org/10.1113/jphysiol.2010.194035>
- Lira, V. A., Okutsu, M., Zhang, M., Greene, N. P., Laker, R. C., Breen, D. S., Hoehn, K. L., & Yan, Z. (2013). Autophagy is required for exercise training-induced skeletal muscle adaptation and improvement of physical performance. *FASEB Journal*.
<https://doi.org/10.1096/fj.13-228486>

- Liu, P., Lin, H., Xu, Y., Zhou, F., Wang, J., Liu, J., Zhu, X., Guo, X., Tang, Y., & Yao, P. (2018). Frataxin-Mediated PINK1–Parkin-Dependent Mitophagy in Hepatic Steatosis: The Protective Effects of Quercetin. *Molecular Nutrition and Food Research*. <https://doi.org/10.1002/mnfr.201800164>
- Liu, X., Weaver, D., Shirihai, O., & Hajnóczky, G. (2009). Mitochondrial kiss-and-run: Interplay between mitochondrial motility and fusion-fission dynamics. *EMBO Journal*. <https://doi.org/10.1038/emboj.2009.255>
- Livak, K. J., & Schmittgen, T. D. (2001). Analysis of relative gene expression data using real-time quantitative PCR and the 2- $\Delta\Delta$ CT method. *Methods*. <https://doi.org/10.1006/meth.2001.1262>
- Ljubicic, V., & Hood, D. A. (2009). Diminished contraction-induced intracellular signaling towards mitochondrial biogenesis in aged skeletal muscle. *Aging Cell*. <https://doi.org/10.1111/j.1474-9726.2009.00483.x>
- Ljubicic, V., Joseph, A. M., Adihetty, P. J., Huang, J. H., Saleem, A., Uguccioni, G., & Hood, D. A. (2009). Molecular basis for an attenuated mitochondrial adaptive plasticity in aged skeletal muscle. *Aging*. <https://doi.org/10.18632/aging.100083>
- Loke, W. M., Hodgson, J. M., Proudfoot, J. M., McKinley, A. J., Puddey, I. B., & Croft, K. D. (2008a). Pure dietary flavonoids quercetin and (-)-epicatechin augment nitric oxide products and reduce endothelin-1 acutely in healthy men. *American Journal of Clinical Nutrition*. <https://doi.org/10.1093/ajcn/88.4.1018>
- Loke, W. M., Hodgson, J. M., Proudfoot, J. M., McKinley, A. J., Puddey, I. B., & Croft, K. D. (2008b). Pure dietary flavonoids quercetin and (-)-epicatechin augment nitric oxide products and reduce endothelin-1 acutely in healthy men. *American Journal of Clinical Nutrition*. <https://doi.org/10.1093/ajcn/88.4.1018>

- Long, L. H., Clement, M. V., & Halliwell, B. (2000). Artifacts in cell culture: Rapid generation of hydrogen peroxide on addition of (-)-epigallocatechin, (-)-epigallocatechin gallate, (+)-catechin, and quercetin to commonly used cell culture media. *Biochemical and Biophysical Research Communications*.
<https://doi.org/10.1006/bbrc.2000.2895>
- López-Otín, C., Blasco, M. A., Partridge, L., Serrano, M., & Kroemer, G. (2013). The hallmarks of aging. In *Cell*. <https://doi.org/10.1016/j.cell.2013.05.039>
- Lorenz, M., Klinkner, L., Baumann, G., Stangl, K., & Stangl, V. (2015). Endothelial NO Production Is Mandatory for Epigallocatechin-3-Gallate-induced Vasodilation: Results from eNOS Knockout (eNOS^{-/-}) Mice. *Journal of Cardiovascular Pharmacology*. <https://doi.org/10.1097/FJC.0000000000000232>
- Lorenz, M., Rauhut, F., Hofer, C., Gwosc, S., Müller, E., Praeger, D., Zimmermann, B. F., Wernecke, K. D., Baumann, G., Stangl, K., & Stangl, V. (2017). Tea-induced improvement of endothelial function in humans: No role for epigallocatechin gallate (EGCG). *Scientific Reports*. <https://doi.org/10.1038/s41598-017-02384-x>
- Lorenz, M., Wessler, S., Follmann, E., Michaelis, W., Düsterhöft, T., Baumann, G., Stangl, K., & Stangl, V. (2004a). A Constituent of Green Tea, Epigallocatechin-3-gallate, Activates Endothelial Nitric Oxide Synthase by a Phosphatidylinositol-3-OH-kinase-, cAMP-dependent Protein Kinase-, and Akt-dependent Pathway and Leads to Endothelial-dependent Vasorelaxation. *Journal of Biological Chemistry*.
<https://doi.org/10.1074/jbc.M309114200>
- Lorenz, M., Wessler, S., Follmann, E., Michaelis, W., Düsterhöft, T., Baumann, G., Stangl, K., & Stangl, V. (2004b). A Constituent of Green Tea, Epigallocatechin-3-gallate, Activates Endothelial Nitric Oxide Synthase by a Phosphatidylinositol-3-OH-kinase-, cAMP-dependent Protein Kinase-, and Akt-dependent Pathway and Leads to

- Endothelial-dependent Vasorelaxation. *Journal of Biological Chemistry*.
<https://doi.org/10.1074/jbc.M309114200>
- Losón, O. C., Song, Z., Chen, H., & Chan, D. C. (2013). Fis1, Mff, MiD49, and MiD51 mediate Drp1 recruitment in mitochondrial fission. *Molecular Biology of the Cell*.
<https://doi.org/10.1091/mbc.E12-10-0721>
- Lovelock, J. E., & Bishop, M. W. H. (1959). Prevention of freezing damage to living cells by dimethyl sulphoxide. *Nature*. <https://doi.org/10.1038/1831394a0>
- Luo, M., Tian, R., & Lu, N. (2020). Quercetin inhibited endothelial dysfunction and atherosclerosis in apolipoprotein E-deficient mice: Critical roles for NADPH oxidase and heme oxygenase-1. *Journal of Agricultural and Food Chemistry*.
<https://doi.org/10.1021/acs.jafc.0c03907>
- Lyons, C. N., Mathieu-Costello, O., & Moyes, C. D. (2006). Regulation of skeletal muscle mitochondrial content during aging. *Journals of Gerontology - Series A Biological Sciences and Medical Sciences*. <https://doi.org/10.1093/gerona/61.1.3>
- Mailloux, R. J., Jin, X., & Willmore, W. G. (2014). Redox regulation of mitochondrial function with emphasis on cysteine oxidation reactions. In *Redox Biology*.
<https://doi.org/10.1016/j.redox.2013.12.011>
- Malone, L. A., Barfield, J. P., & Brasher, J. D. (2012). Perceived benefits and barriers to exercise among persons with physical disabilities or chronic health conditions within action or maintenance stages of exercise. *Disability and Health Journal*.
<https://doi.org/10.1016/j.dhjo.2012.05.004>
- Manach, C., Scalbert, A., Morand, C., Rémésy, C., & Jiménez, L. (2004). Polyphenols: Food sources and bioavailability. In *American Journal of Clinical Nutrition*.
<https://doi.org/10.1093/ajcn/79.5.727>

- Manach, C., Williamson, G., Morand, C., Scalbert, A., & Rémésy, C. (2005a). Bioavailability and bioefficacy of polyphenols in humans. I. Review of 97 bioavailability studies. In *The American journal of clinical nutrition*. <https://doi.org/10.1093/ajcn/81.1.230s>
- Manach, C., Williamson, G., Morand, C., Scalbert, A., & Rémésy, C. (2005b). Bioavailability and bioefficacy of polyphenols in humans. I. Review of 97 bioavailability studies. In *The American journal of clinical nutrition*. <https://doi.org/10.1093/ajcn/81.1.230s>
- Manini, T. M., Everhart, J. E., Patel, K. V., Schoeller, D. A., Colbert, L. H., Visser, M., Tylavsky, F., Bauer, D. C., Goodpaster, B. H., & Harris, T. B. (2006). Daily activity energy expenditure and mortality among older adults. *Journal of the American Medical Association*. <https://doi.org/10.1001/jama.296.2.171>
- Mansouri, A., Muller, F. L., Liu, Y., Ng, R., Faulkner, J., Hamilton, M., Richardson, A., Huang, T. T., Epstein, C. J., & Van Remmen, H. (2006). Alterations in mitochondrial function, hydrogen peroxide release and oxidative damage in mouse hind-limb skeletal muscle during aging. *Mechanisms of Ageing and Development*. <https://doi.org/10.1016/j.mad.2005.11.004>
- Marcinek, D. J., Schenkman, K. A., Ciesielski, W. A., Lee, D., & Conley, K. E. (2005). Reduced mitochondrial coupling in vivo alters cellular energetics in aged mouse skeletal muscle. *Journal of Physiology*. <https://doi.org/10.1113/jphysiol.2005.097782>
- Marrone, M., La Rovere, R. M. L., Guarnieri, S., Di Filippo, E. S., Monaco, G., Pietrangelo, T., Bultynck, G., Fulle, S., & Mancinelli, R. (2018a). Superoxide anion production and bioenergetic profile in young and elderly human primary myoblasts. *Oxidative Medicine and Cellular Longevity*. <https://doi.org/10.1155/2018/2615372>
- Marrone, M., La Rovere, R. M. L., Guarnieri, S., Di Filippo, E. S., Monaco, G., Pietrangelo, T., Bultynck, G., Fulle, S., & Mancinelli, R. (2018b). Superoxide anion production

- and bioenergetic profile in young and elderly human primary myoblasts. *Oxidative Medicine and Cellular Longevity*. <https://doi.org/10.1155/2018/2615372>
- Martel, J., Ojcius, D. M., Ko, Y. F., Ke, P. Y., Wu, C. Y., Peng, H. H., & Young, J. D. (2019). Hormetic Effects of Phytochemicals on Health and Longevity. In *Trends in Endocrinology and Metabolism*. <https://doi.org/10.1016/j.tem.2019.04.001>
- Martinez Guimera, A., Welsh, C. M., Proctor, C. J., McArdle, A., & Shanley, D. P. (2018). 'Molecular habituation' as a potential mechanism of gradual homeostatic loss with age. *Mechanisms of Ageing and Development*. <https://doi.org/10.1016/j.mad.2017.11.010>
- Mattson, M. P., & Cheng, A. (2006). Neurohormetic phytochemicals: Low-dose toxins that induce adaptive neuronal stress responses. In *Trends in Neurosciences*. <https://doi.org/10.1016/j.tins.2006.09.001>
- McCreary, C. R., Chilibeck, P. D., Marsh, G. D., Paterson, D. H., Cunningham, D. A., & Thompson, R. T. (1996). Kinetics of pulmonary oxygen uptake and muscle phosphates during moderate-intensity calf exercise. *Journal of Applied Physiology*. <https://doi.org/10.1152/jappl.1996.81.3.1331>
- McMahon, M., Lamont, D. J., Beattie, K. A., & Hayes, J. D. (2010). Keap1 perceives stress via three sensors for the endogenous signaling molecules nitric oxide, zinc, and alkenals. *Proceedings of the National Academy of Sciences of the United States of America*. <https://doi.org/10.1073/pnas.1007387107>
- McNarry, M. A., Kingsley, M. I. C., & Lewis, M. J. (2012). Influence of exercise intensity on pulmonary oxygen uptake kinetics in young and late middle-aged adults. *American Journal of Physiology - Regulatory Integrative and Comparative Physiology*, 303(8). <https://doi.org/10.1152/ajpregu.00203.2012>

- Mecocci, P., Fanó, G., Fulle, S., MacGarvey, U., Shinobu, L., Polidori, M. C., Cherubini, A., Vecchiet, J., Senin, U., & Beal, M. F. (1999). Age-dependent increases in oxidative damage to DNA, lipids, and proteins in human skeletal muscle. *Free Radical Biology and Medicine*. [https://doi.org/10.1016/S0891-5849\(98\)00208-1](https://doi.org/10.1016/S0891-5849(98)00208-1)
- Melov, S., Ravenscroft, J., Malik, S., Gill, M. S., Walker, D. W., Clayton, P. E., Wallace, D. C., Malfroy, B., Doctrow, S. R., & Lithgow, G. J. (2000). Extension of life-span with superoxide dismutase/catalase mimetics. *Science*. <https://doi.org/10.1126/science.289.5484.1567>
- Mendes, L. F., Gaspar, V. M., Conde, T. A., Mano, J. F., & Duarte, I. F. (2019). Flavonoid-mediated immunomodulation of human macrophages involves key metabolites and metabolic pathways. *Scientific Reports*. <https://doi.org/10.1038/s41598-019-51113-z>
- Meng, Q., Velalar, C. N., & Ruan, R. (2008). Regulating the age-related oxidative damage, mitochondrial integrity, and antioxidative enzyme activity in Fischer 344 rats by supplementation of the antioxidant epigallocatechin-3-gallate. *Rejuvenation Research*. <https://doi.org/10.1089/rej.2007.0645>
- Mercken, E. M., Capri, M., Carboneau, B. A., Conte, M., Heidler, J., Santoro, A., Martin-Montalvo, A., Gonzalez-Freire, M., Khraiwesh, H., González-Reyes, J. A., Moaddel, R., Zhang, Y., Becker, K. G., Villalba, J. M., Mattison, J. A., Wittig, I., Franceschi, C., & de Cabo, R. (2017). Conserved and species-specific molecular denominators in mammalian skeletal muscle aging. *Npj Aging and Mechanisms of Disease*, 3(1), 8. <https://doi.org/10.1038/s41514-017-0009-8>
- Mezera, V., Endlicher, R., Kucera, O., Sobotka, O., Drahotka, Z., & Cervinkova, Z. (2016). Effects of Epigallocatechin Gallate on Tert-Butyl Hydroperoxide-Induced Mitochondrial Dysfunction in Rat Liver Mitochondria and Hepatocytes. *Oxidative Medicine and Cellular Longevity*. <https://doi.org/10.1155/2016/7573131>

- Mick, E., Titov, D. V., Skinner, O. S., Sharma, R., Jourdain, A. A., & Mootha, V. K. (2020). Distinct mitochondrial defects trigger the integrated stress response depending on the metabolic state of the cell. *ELife*. <https://doi.org/10.7554/eLife.49178>
- Miller, M. W., Knaub, L. A., Olivera-Fragoso, L. F., Keller, A. C., Balasubramaniam, V., Watson, P. A., & Reusch, J. E. B. (2013). Nitric oxide regulates vascular adaptive mitochondrial dynamics. *American Journal of Physiology - Heart and Circulatory Physiology*. <https://doi.org/10.1152/ajpheart.00987.2012>
- Mishra, P., & Chan, D. C. (2016). Metabolic regulation of mitochondrial dynamics. *Journal of Cell Biology*. <https://doi.org/10.1083/jcb.201511036>
- Mitchell, P. (1961). Coupling of phosphorylation to electron and hydrogen transfer by a chemi-osmotic type of mechanism. *Nature*. <https://doi.org/10.1038/191144a0>
- Mitchell, P. (1966). Chemiosmotic coupling in oxidative and photosynthetic phosphorylation. In *Biological reviews of the Cambridge Philosophical Society*. <https://doi.org/10.1111/j.1469-185X.1966.tb01501.x>
- Moessinger, C., Klizaitė, K., Steinhagen, A., Philippou-Massier, J., Shevchenko, A., Hoch, M., Ejsing, C. S., & Thiele, C. (2014). Two different pathways of phosphatidylcholine synthesis, the Kennedy Pathway and the Lands Cycle, differentially regulate cellular triacylglycerol storage. *BMC Cell Biology*. <https://doi.org/10.1186/s12860-014-0043-3>
- Moini, H., Arroyo, A., Vaya, J., & Packer, L. (1999). Bioflavonoid effects on the mitochondrial respiratory electron transport chain and cytochrome c redox state. *Redox Report*. <https://doi.org/10.1179/135100099101534729>
- Monagas, M., Khan, N., Andres-Lacueva, C., Casas, R., Urpí-Sardà, M., Llorach, R., Lamuela-Raventós, R. M., & Estruch, R. (2009). Effect of cocoa powder on the modulation of inflammatory biomarkers in patients at high risk of cardiovascular

disease. *American Journal of Clinical Nutrition*.

<https://doi.org/10.3945/ajcn.2009.27716>

Monahan, K. D., Feehan, R. P., Kunselman, A. R., Preston, A. G., Miller, D. L., & Lott, M.

E. J. (2011). Dose-dependent increases in flow-mediated dilation following acute cocoa ingestion in healthy older adults. *Journal of Applied Physiology*.

<https://doi.org/10.1152/jappphysiol.00865.2011>

Montezano, A. C., Burger, D., Ceravolo, G. S., Yusuf, H., Montero, M., & Touyz, R. M.

(2011). Novel nox homologues in the vasculature: Focusing on Nox4 and Nox5. In *Clinical Science*. <https://doi.org/10.1042/CS20100384>

Mookerjee, S. A., & Brand, M. D. (2015). Measurement and analysis of extracellular acid production to determine glycolytic rate. *Journal of Visualized Experiments*.

<https://doi.org/10.3791/53464>

Moreno-Ulloa, A., Cid, A., Rubio-Gayosso, I., Ceballos, G., Villarreal, F., & Ramirez-

Sanchez, I. (2013). Effects of (-)-epicatechin and derivatives on nitric oxide mediated induction of mitochondrial proteins. *Bioorganic and Medicinal Chemistry Letters*.

<https://doi.org/10.1016/j.bmcl.2013.05.079>

Moreno-Ulloa, A., Mendez-Luna, D., Beltran-Partida, E., Castillo, C., Guevara, G., Ramirez-

Sanchez, I., Correa-Basurto, J., Ceballos, G., & Villarreal, F. (2015a). The effects of (-)-epicatechin on endothelial cells involve the G protein-coupled estrogen receptor (GPER). *Pharmacological Research*. <https://doi.org/10.1016/j.phrs.2015.08.014>

Moreno-Ulloa, A., Mendez-Luna, D., Beltran-Partida, E., Castillo, C., Guevara, G., Ramirez-

Sanchez, I., Correa-Basurto, J., Ceballos, G., & Villarreal, F. (2015b). The effects of (-)-epicatechin on endothelial cells involve the G protein-coupled estrogen receptor (GPER). *Pharmacological Research*. <https://doi.org/10.1016/j.phrs.2015.08.014>

- Moreno-Ulloa, A., Miranda-Cervantes, A., Licea-Navarro, A., Mansour, C., Beltrán-Partida, E., Donis-Maturano, L., Delgado De la Herrán, H. C., Villarreal, F., & Álvarez-Delgado, C. (2018). (-)-Epicatechin stimulates mitochondrial biogenesis and cell growth in C2C12 myotubes via the G-protein coupled estrogen receptor. *European Journal of Pharmacology*. <https://doi.org/10.1016/j.ejphar.2018.01.014>
- Moreno-Ulloa, A., Nogueira, L., Rodriguez, A., Barboza, J., Hogan, M. C., Ceballos, G., Villarreal, F., & Ramirez-Sanchez, I. (2015). Recovery of Indicators of Mitochondrial Biogenesis, Oxidative Stress, and Aging With (-)-Epicatechin in Senile Mice. *Journals of Gerontology - Series A Biological Sciences and Medical Sciences*. <https://doi.org/10.1093/gerona/glu131>
- Moreno-Ulloa, A., Romero-Perez, D., Villarreal, F., Ceballos, G., & Ramirez-Sanchez, I. (2014). Cell membrane mediated (-)-epicatechin effects on upstream endothelial cell signaling: Evidence for a surface receptor. *Bioorganic and Medicinal Chemistry Letters*. <https://doi.org/10.1016/j.bmcl.2014.04.038>
- Moridani, M. Y., Scobie, H., Salehi, P., & O'Brien, P. J. (2001). Catechin metabolism: Glutathione conjugate formation catalyzed by tyrosinase, peroxidase, and cytochrome P450. *Chemical Research in Toxicology*. <https://doi.org/10.1021/tx000235o>
- Most, J., Van Can, J. G. P., Van Dijk, J. W., Goossens, G. H., Jocken, J., Hospers, J. J., Bendik, I., & Blaak, E. E. (2015a). A 3-day EGCG-supplementation reduces interstitial lactate concentration in skeletal muscle of overweight subjects. *Scientific Reports*. <https://doi.org/10.1038/srep17896>
- Most, J., Van Can, J. G. P., Van Dijk, J. W., Goossens, G. H., Jocken, J., Hospers, J. J., Bendik, I., & Blaak, E. E. (2015b). A 3-day EGCG-supplementation reduces interstitial lactate concentration in skeletal muscle of overweight subjects. *Scientific Reports*. <https://doi.org/10.1038/srep17896>

- Mourtzakis, M., Graham, T. E., Gonzalez-Alonso, J., & Saltin, B. (2008). Glutamate availability is important in intramuscular amino acid metabolism and TCA cycle intermediates but does not affect peak oxidative metabolism. *Journal of Applied Physiology*. <https://doi.org/10.1152/jappphysiol.90394.2008>
- Mukai, R., Matsui, N., Fujikura, Y., Matsumoto, N., Hou, D. X., Kanzaki, N., Shibata, H., Horikawa, M., Iwasa, K., Hirasaka, K., Nikawa, T., & Terao, J. (2016). Preventive effect of dietary quercetin on disuse muscle atrophy by targeting mitochondria in denervated mice. *Journal of Nutritional Biochemistry*. <https://doi.org/10.1016/j.jnutbio.2016.02.001>
- Muller-Delp, J. M., Spier, S. A., Ramsey, M. W., & Delp, M. D. (2002a). Aging impairs endothelium-dependent vasodilation in rat skeletal muscle arterioles. *American Journal of Physiology - Heart and Circulatory Physiology*, 283, (4 52-4).
- Muller-Delp, J. M., Spier, S. A., Ramsey, M. W., & Delp, M. D. (2002b). Aging impairs endothelium-dependent vasodilation in rat skeletal muscle arterioles. *American Journal of Physiology - Heart and Circulatory Physiology*, 283, (4 52-4).
- Mullis, K. B., & Faloona, F. A. (1987). Specific Synthesis of DNA in Vitro via a Polymerase-Catalyzed Chain Reaction. *Methods in Enzymology*. [https://doi.org/10.1016/0076-6879\(87\)55023-6](https://doi.org/10.1016/0076-6879(87)55023-6)
- Murase, T., Haramizu, S., Shimotoyodome, A., Tokimitsu, I., & Hase, T. (2006). Green tea extract improves running endurance in mice by stimulating lipid utilization during exercise. *American Journal of Physiology - Regulatory Integrative and Comparative Physiology*. <https://doi.org/10.1152/ajpregu.00752.2005>
- Murase, T., Misawa, K., Haramizu, S., & Hase, T. (2009). Catechin-induced activation of the LKB1/AMP-activated protein kinase pathway. *Biochemical Pharmacology*. <https://doi.org/10.1016/j.bcp.2009.03.021>

- Murias, J. M., Kowalchuk, J. M., & Paterson, D. H. (2011). Speeding of VO₂ kinetics in response to endurance-training in older and young women. *European Journal of Applied Physiology*. <https://doi.org/10.1007/s00421-010-1649-6>
- Murias, J. M., Kowalchuk, J. M., & Peterson, D. H. (2010a). Speeding of VO₂ kinetics with endurance training in old and young men is associated with improved matching of local O₂ delivery to muscle O₂ utilization. *Journal of Applied Physiology*, *108*(4), 913–922. <https://doi.org/10.1152/jappphysiol.01355.2009>
- Murias, J. M., Kowalchuk, J. M., & Peterson, D. H. (2010b). Speeding of VO₂ kinetics with endurance training in old and young men is associated with improved matching of local O₂ delivery to muscle O₂ utilization. *Journal of Applied Physiology*, *108*(4), 913–922. <https://doi.org/10.1152/jappphysiol.01355.2009>
- Murias, J. M., & Paterson, D. H. (2015a). Slower VO₂ kinetics in older individuals: Is it inevitable? *Medicine and Science in Sports and Exercise*. <https://doi.org/10.1249/MSS.0000000000000686>
- Murias, J. M., & Paterson, D. H. (2015b). Slower VO₂ kinetics in older individuals: Is it inevitable? *Medicine and Science in Sports and Exercise*. <https://doi.org/10.1249/MSS.0000000000000686>
- Musch, T. I., Eklund, K. E., Hageman, K. S., & Poole, D. C. (2004a). Altered regional blood flow responses to submaximal exercise in older rats. *Journal of Applied Physiology*, *96*(1), 81–88. <https://doi.org/10.1152/jappphysiol.00729.2003>
- Musch, T. I., Eklund, K. E., Hageman, K. S., & Poole, D. C. (2004b). Altered regional blood flow responses to submaximal exercise in older rats. *Journal of Applied Physiology*, *96*(1), 81-88-81–88. <https://doi.org/10.1152/jappphysiol.00729.2003>

- Nagana Gowda, G. A., & Raftery, D. (2015). Can NMR solve some significant challenges in metabolomics? *Journal of Magnetic Resonance (San Diego, Calif. : 1997)*, 260, 144–160. <https://doi.org/10.1016/j.jmr.2015.07.014>
- Namin, S. M., Nofallah, S., Joshi, M. S., Kavallieratos, K., & Tsoukias, N. M. (2013). Kinetic analysis of DAF-FM activation by NO: toward calibration of a NO-sensitive fluorescent dye. *Nitric Oxide : Biology and Chemistry*, 28, 39–46. <https://doi.org/10.1016/j.niox.2012.10.001>
- Ng, H. L. H., Premilovac, D., Rattigan, S., Richards, S. M., Muniyappa, R., Quon, M. J., & Keske, M. A. (2017). Acute vascular and metabolic actions of the green tea polyphenol epigallocatechin 3-gallate in rat skeletal muscle. *Journal of Nutritional Biochemistry*. <https://doi.org/10.1016/j.jnutbio.2016.10.005>
- Nieman, D. C., Williams, A. S., Shanely, R. A., Jin, F., McAnulty, S. R., Triplett, N. T., Austin, M. D., & Henson, D. A. (2010). Quercetin's influence on exercise performance and muscle mitochondrial biogenesis. *Medicine and Science in Sports and Exercise*. <https://doi.org/10.1249/MSS.0b013e3181b18fa3>
- Nijveldt, R. J., Van Nood, E., Van Hoorn, D. E. C., Boelens, P. G., Van Norren, K., & Van Leeuwen, P. A. M. (2001). Flavonoids: A review of probable mechanisms of action and potential applications. In *American Journal of Clinical Nutrition*. <https://doi.org/10.1093/ajcn/74.4.418>
- Nisoli, E., Clementi, E., Paolucci, C., Cozzi, V., Tonello, C., Sciorati, C., Bracale, R., Valerio, A., Francolini, M., Moncada, S., & Carruba, M. O. (2003). Mitochondrial biogenesis in mammals: The role of endogenous nitric oxide. *Science*. <https://doi.org/10.1126/science.1079368>
- Nogueira, L. de P., Nogueira Neto, J. F., Klein, M. R. S. T., & Sanjuliani, A. F. (2017). Short-term Effects of Green Tea on Blood Pressure, Endothelial Function, and

Metabolic Profile in Obese Prehypertensive Women: A Crossover Randomized Clinical Trial. *Journal of the American College of Nutrition*.

<https://doi.org/10.1080/07315724.2016.1194236>

Nogueira, L., Ramirez-Sanchez, I., Perkins, G. A., Murphy, A., Taub, P. R., Ceballos, G., Villarreal, F. J., Hogan, M. C., & Malek, M. H. (2011). (-)-Epicatechin enhances fatigue resistance and oxidative capacity in mouse muscle. *Journal of Physiology*.
<https://doi.org/10.1113/jphysiol.2011.209924>

Nyberg, M., Blackwell, J. R., Damsgaard, R., Jones, A. M., Hellsten, Y., & Mortensen, S. P. (2012). Lifelong physical activity prevents an age-related reduction in arterial and skeletal muscle nitric oxide bioavailability in humans. *Journal of Physiology*.
<https://doi.org/10.1113/jphysiol.2012.239053>

Oldendorf, W. H., Cornford, M. E., & Brown, W. J. (1977). The large apparent work capability of the blood-brain barrier: A study of the mitochondrial content of capillary endothelial cells in brain and other tissues of the rat. *Annals of Neurology*.
<https://doi.org/10.1002/ana.410010502>

Oliver, S. G., Winson, M. K., Kell, D. B., & Baganz, F. (1998). Systematic functional analysis of the yeast genome. *Trends in Biotechnology*.
[https://doi.org/10.1016/S0167-7799\(98\)01214-1](https://doi.org/10.1016/S0167-7799(98)01214-1)

Örlander, J., Kiessling, K. -H, Larsson, L., Karlsson, J., & Aniansson, A. (1978). Skeletal muscle metabolism and ultrastructure in relation to age in sedentary men. *Acta Physiologica Scandinavica*. <https://doi.org/10.1111/j.1748-1716.1978.tb06277.x>

Ornstein, L. (1964). DISC ELECTROPHORESIS-I BACKGROUND AND THEORY*. *Annals of the New York Academy of Sciences*, 121(2), 321–349.
<https://doi.org/10.1111/j.1749-6632.1964.tb14207.x>

- Ørtenblad, N., Nielsen, J., Boushel, R., Söderlund, K., Saltin, B., & Holmberg, H.-C. (2018). The Muscle Fiber Profiles, Mitochondrial Content, and Enzyme Activities of the Exceptionally Well-Trained Arm and Leg Muscles of Elite Cross-Country Skiers . In *Frontiers in Physiology* (Vol. 9, p. 1031).
- Ost, M., Keipert, S., Van Schothorst, E. M., Donner, V., Van Der Stelt, I., Kipp, A. P., Petzke, K. J., Jove, M., Pamplona, R., Portero-Otin, M., Keijer, J., & Klaus, S. (2015). Muscle mitohormesis promotes cellular survival via serine/glycine pathway flux. *FASEB Journal*. <https://doi.org/10.1096/fj.14-261503>
- Ottaviani, J. I., Borges, G., Momma, T. Y., Spencer, J. P. E., Keen, C. L., Crozier, A., & Schroeter, H. (2016). The metabolome of [2-(14C)(-)-epicatechin in humans: Implications for the assessment of efficacy, safety, and mechanisms of action of polyphenolic bioactives. *Scientific Reports*, 6, 29034. <https://doi.org/10.1038/srep29034>
- Ottaviani, J. I., Momma, T. Y., Heiss, C., Kwik-Urbe, C., Schroeter, H., & Keen, C. L. (2011). The stereochemical configuration of flavanols influences the level and metabolism of flavanols in humans and their biological activity in vivo. *Free Radical Biology and Medicine*. <https://doi.org/10.1016/j.freeradbiomed.2010.11.005>
- Pääsuke, R., Eimre, M., Piirsoo, A., Peet, N., Laada, L., Kadaja, L., Roosimaa, M., Pääsuke, M., Märtson, A., Seppet, E., & Paju, K. (2016). Proliferation of Human Primary Myoblasts Is Associated with Altered Energy Metabolism in Dependence on Ageing in Vivo and in Vitro. *Oxidative Medicine and Cellular Longevity*. <https://doi.org/10.1155/2016/8296150>
- Pal, S., Porwal, K., Rajak, S., Sinha, R. A., & Chattopadhyay, N. (2020a). Selective dietary polyphenols induce differentiation of human osteoblasts by adiponectin receptor 1-

- mediated reprogramming of mitochondrial energy metabolism. *Biomedicine and Pharmacotherapy*. <https://doi.org/10.1016/j.biopha.2020.110207>
- Pal, S., Porwal, K., Rajak, S., Sinha, R. A., & Chattopadhyay, N. (2020b). Selective dietary polyphenols induce differentiation of human osteoblasts by adiponectin receptor 1-mediated reprogramming of mitochondrial energy metabolism. *Biomedicine and Pharmacotherapy*. <https://doi.org/10.1016/j.biopha.2020.110207>
- Palomero, J., Vasilaki, A., Pye, D., McArdle, A., & Jackson, M. J. (2013). Aging increases the oxidation of dichlorohydrofluorescein in single isolated skeletal muscle fibers at rest, but not during contractions. *American Journal of Physiology - Regulatory Integrative and Comparative Physiology*. <https://doi.org/10.1152/ajpregu.00530.2012>
- Pan, H., Chen, J., Shen, K., Wang, X., Wang, P., Fu, G., Meng, H., Wang, Y., & Jin, B. (2015). Mitochondrial modulation by epigallocatechin 3-gallate ameliorates cisplatin induced renal injury through decreasing oxidative/nitrative stress, inflammation and NF-kB in mice. *PLoS ONE*. <https://doi.org/10.1371/journal.pone.0124775>
- Pandey, K. B., & Rizvi, S. I. (2009). Plant polyphenols as dietary antioxidants in human health and disease. *Oxidative Medicine and Cellular Longevity*, 2(5), 270–278. <https://doi.org/10.4161/oxim.2.5.9498>
- Panneerselvam, M., Ali, S. S., Finley, J. C., Kellerhals, S. E., Migita, M. Y., Head, B. P., Patel, P. M., Roth, D. M., & Patel, H. H. (2013). Epicatechin regulation of mitochondrial structure and function is opioid receptor dependent. *Molecular Nutrition and Food Research*. <https://doi.org/10.1002/mnfr.201300026>
- Papadimitriou, A., Peixoto, E. B. M. I., Silva, K. C., Lopes de Faria, J. M., & Lopes de Faria, J. B. (2014). Increase in AMPK brought about by cocoa is renoprotective in experimental diabetes mellitus by reducing NOX4/TGFβ-1 signaling. *Journal of Nutritional Biochemistry*. <https://doi.org/10.1016/j.jnutbio.2014.03.010>

- Park, C., So, H. S., Shin, C. H., Baek, S. H., Moon, B. S., Shin, S. H., Lee, H. S., Lee, D. W., & Park, R. K. (2003). Quercetin protects the hydrogen peroxide-induced apoptosis via inhibition of mitochondrial dysfunction in H9c2 cardiomyoblast cells. *Biochemical Pharmacology*. [https://doi.org/10.1016/S0006-2952\(03\)00478-7](https://doi.org/10.1016/S0006-2952(03)00478-7)
- Park, S. H., Kwon, O. S., Park, S. Y., Weavil, J. C., Andtbacka, R. H. I., Hyngstrom, J. R., Reese, V., & Richardson, R. S. (2018a). Vascular mitochondrial respiratory function: The impact of advancing age. *American Journal of Physiology - Heart and Circulatory Physiology*. <https://doi.org/10.1152/ajpheart.00324.2018>
- Park, S. H., Kwon, O. S., Park, S. Y., Weavil, J. C., Andtbacka, R. H. I., Hyngstrom, J. R., Reese, V., & Richardson, R. S. (2018b). Vascular mitochondrial respiratory function: The impact of advancing age. *American Journal of Physiology - Heart and Circulatory Physiology*. <https://doi.org/10.1152/ajpheart.00324.2018>
- Park, S. H., Kwon, O. S., Park, S. Y., Weavil, J. C., Hydren, J. R., Reese, V., Andtbacka, R. H. I., Hyngstrom, J. R., & Richardson, R. S. (2020). Vasodilatory and vascular mitochondrial respiratory function with advancing age: Evidence of a free radically mediated link in the human vasculature. *American Journal of Physiology. Regulatory, Integrative and Comparative Physiology*. <https://doi.org/10.1152/ajpregu.00268.2019>
- Park, S. Y., Kwon, O. S., Andtbacka, R. H. I., Hyngstrom, J. R., Reese, V., Murphy, M. P., & Richardson, R. S. (2018). Age-related endothelial dysfunction in human skeletal muscle feed arteries: The role of free radicals derived from mitochondria in the vasculature. *Acta Physiologica*. <https://doi.org/10.1111/apha.12893>
- Patel, R. K., Brouner, J., & Spendiff, O. (2015). Dark chocolate supplementation reduces the oxygen cost of moderate intensity cycling. *Journal of the International Society of Sports Nutrition*, *12*(1). <https://doi.org/10.1186/s12970-015-0106-7>

- Paterson, D. H., Jones, G. R., & Rice, C. L. (2007). Ageing and physical activity: Evidence to develop exercise recommendations for older adults. This article is part of a supplement entitled Advancing physical activity measurement and guidelines in Canada: A scientific review and evidence-based foundation for the future of Canadian physical activity guidelines co-published by Applied Physiology, Nutrition, and Metabolism and the Canadian Journal of Public Health. It may be cited as Appl. Physiol. Nutr. Metab. 32(Suppl. 2E) or as Can. J. Public Health 98(Suppl. 2). *Applied Physiology, Nutrition, and Metabolism*, 32(S2E), S69–S108. <https://doi.org/10.1139/H07-111>
- Pearson, T., Kabayo, T., Ng, R., Chamberlain, J., McArdle, A., & Jackson, M. J. (2014). Skeletal muscle contractions induce acute changes in cytosolic superoxide, but slower responses in mitochondrial superoxide and cellular hydrogen peroxide. *PLoS ONE*. <https://doi.org/10.1371/journal.pone.0096378>
- Peschek, K., Pritchett, R., Bergman, E., & Pritchett, K. (2013). The effects of acute post exercise consumption of two cocoa-based beverages with varying flavanol content on indices of muscle recovery following downhill treadmill running. *Nutrients*, 6(1), 50–62. <https://doi.org/10.3390/nu6010050>
- Peterson, J. J., Dwyer, J. T., Jacques, P. F., & McCullough, M. L. (2015). Improving the estimation of flavonoid intake for study of health outcomes. *Nutrition Reviews*. <https://doi.org/10.1093/nutrit/nuv008>
- Peterson, M. J., Giuliani, C., Morey, M. C., Pieper, C. F., Evenson, K. R., Mercer, V., Cohen, H. J., Visser, M., Brach, J. S., Kritchevsky, S. B., Goodpaster, B. H., Rubin, S., Satterfield, S., Newman, A. B., & Simonsick, E. M. (2009). Physical activity as a preventative factor for frailty: The health, aging, and body composition study. *Journals of Gerontology - Series A Biological Sciences and Medical Sciences*. <https://doi.org/10.1093/gerona/gln001>

- Phillips, B. E., Atherton, P. J., Varadhan, K., Limb, M. C., Williams, J. P., & Smith, K. (2016). Acute cocoa flavanol supplementation improves muscle macro- and microvascular but not anabolic responses to amino acids in older men. *Applied Physiology, Nutrition, and Metabolism = Physiologie Appliquee, Nutrition et Metabolisme*. <https://doi.org/10.1139/apnm-2015-0543>
- Picard, M., Ritchie, D., Wright, K. J., Romestaing, C., Thomas, M. M., Rowan, S. L., Taivassalo, T., & Hepple, R. T. (2010a). Mitochondrial functional impairment with aging is exaggerated in isolated mitochondria compared to permeabilized myofibers. *Aging Cell*. <https://doi.org/10.1111/j.1474-9726.2010.00628.x>
- Picard, M., Ritchie, D., Wright, K. J., Romestaing, C., Thomas, M. M., Rowan, S. L., Taivassalo, T., & Hepple, R. T. (2010b). Mitochondrial functional impairment with aging is exaggerated in isolated mitochondria compared to permeabilized myofibers. *Aging Cell*. <https://doi.org/10.1111/j.1474-9726.2010.00628.x>
- Picard, M., White, K., & Turnbull, D. M. (2013). Mitochondrial morphology, topology, and membrane interactions in skeletal muscle: A quantitative three-dimensional electron microscopy study. *Journal of Applied Physiology*. <https://doi.org/10.1152/jappphysiol.01096.2012>
- Pierno, S., De Luca, A., Camerino, C., Huxtable, R. J., & Camerino, D. C. (1998). Chronic Administration of Taurine to Aged Rats Improves the Electrical and Contractile Properties of Skeletal Muscle Fibers¹. *Journal of Pharmacology and Experimental Therapeutics*.
- Poole, D. C., Barstow, T. J., Mcdonough, P., & Jones, A. M. (2008). Control of oxygen uptake during exercise. *Medicine and Science in Sports and Exercise*, *40*, 462–474. <https://doi.org/10.1249/MSS.0b013e31815ef29b>

- Poole, D. C., & Jones, A. M. (2012). Oxygen uptake kinetics. *Comprehensive Physiology*, 2(2), 933–996. <https://doi.org/10.1002/cphy.c100072>
- Poole, D. C., & Musch, T. I. (2010). Mechanistic insights into how advanced age moves the site of $\dot{V}O_2$ kinetics limitation upstream. *Journal of Applied Physiology*, 108, 5-6. <https://doi.org/10.1152/jappphysiol.01237.2009>
- Poole, J. G., Lawrenson, L., Kim, J., Brown, C., & Richardson, R. S. (2003). Vascular and metabolic response to cycle exercise in sedentary humans: Effect of age. *American Journal of Physiology - Heart and Circulatory Physiology*. <https://doi.org/10.1152/ajpheart.00790.2002>
- Porter, C., Hurren, N. M., Cotter, M. V., Bhattarai, N., Reidy, P. T., Dillon, E. L., Durham, W. J., Tuvdendorj, D., Sheffield-Moore, M., Volpi, E., Sidossis, L. S., Rasmussen, B. B., & Børsheim, E. (2015). Mitochondrial respiratory capacity and coupling control decline with age in human skeletal muscle. *American Journal of Physiology - Endocrinology and Metabolism*. <https://doi.org/10.1152/ajpendo.00125.2015>
- Pournourmohammadi, S., Grimaldi, M., Stridh, M. H., Lavallard, V., Waagepetersen, H. S., Wollheim, C. B., & Maechler, P. (2017). Epigallocatechin-3-gallate (EGCG) activates AMPK through the inhibition of glutamate dehydrogenase in muscle and pancreatic β -cells: A potential beneficial effect in the pre-diabetic state? *International Journal of Biochemistry and Cell Biology*. <https://doi.org/10.1016/j.biocel.2017.01.012>
- Powers, S. K., Duarte, J., Kavazis, A. N., & Talbert, E. E. (2010). Reactive oxygen species are signalling molecules for skeletal muscle adaptation. In *Experimental Physiology*. <https://doi.org/10.1113/expphysiol.2009.050526>
- Puigserver, P., Adelmant, G., Wu, Z., Fan, M., Xu, J., O'Malley, B., & Spiegelman, B. M. (1999). Activation of PPAR γ coactivator-1 through transcription factor docking. *Science*. <https://doi.org/10.1126/science.286.5443.1368>

- R Team, C. (2019). R Core Team (2017). R: A language and environment for statistical computing. *R Found. Stat. Comput. Vienna, Austria*. URL [Http://Www. R-Project.Org/](http://www.R-Project.Org/), Page R Foundation for Statistical Computing.
- Raamsdonk, L. M., Teusink, B., Broadhurst, D., Zhang, N., Hayes, A., Walsh, M. C., Berden, J. A., Brindle, K. M., Kell, D. B., Rowland, J. J., Westerhoff, H. V., Van Dam, K., & Oliver, S. G. (2001). A functional genomics strategy that uses metabolome data to reveal the phenotype of silent mutations. *Nature Biotechnology*.
<https://doi.org/10.1038/83496>
- Ramirez-Sanchez, I., Aguilar, H., Ceballos, G., & Villarreal, F. (2012). (-)-Epicatechin-induced calcium independent eNOS activation: Roles of HSP90 and AKT. *Molecular and Cellular Biochemistry*. <https://doi.org/10.1007/s11010-012-1405-9>
- Ramirez-Sanchez, I., Mansour, C., Navarrete-Yañez, V., Ayala-Hernandez, M., Guevara, G., Castillo, C., Loredó, M., Bustamante, M., Ceballos, G., & Villarreal, F. J. (2018). (-)-Epicatechin induced reversal of endothelial cell aging and improved vascular function: Underlying mechanisms. *Food and Function*.
<https://doi.org/10.1039/c8fo00483h>
- Ramirez-Sanchez, I., Maya, L., Ceballos, G., & Villarreal, F. (2010). (-)-Epicatechin activation of endothelial cell endothelial nitric oxide synthase, nitric oxide, and related signaling pathways. *Hypertension*, *55*(6), 1398–1405.
<https://doi.org/10.1161/HYPERTENSIONAHA.109.147892>
- Ramirez-Sanchez, I., Maya, L., Ceballos, G., & Villarreal, F. (2011). (-)-Epicatechin induces calcium and translocation independent eNOS activation in arterial endothelial cells. *American Journal of Physiology - Cell Physiology*.
<https://doi.org/10.1152/ajpcell.00406.2010>

- Ramírez-Sánchez, I., Rodríguez, A., Moreno-Ulloa, A., Ceballos, G., & Villarreal, F. (2016a). (-)-Epicatechin-induced recovery of mitochondria from simulated diabetes: Potential role of endothelial nitric oxide synthase. *Diabetes and Vascular Disease Research*. <https://doi.org/10.1177/1479164115620982>
- Ramírez-Sánchez, I., Rodríguez, A., Moreno-Ulloa, A., Ceballos, G., & Villarreal, F. (2016b). (-)-Epicatechin-induced recovery of mitochondria from simulated diabetes: Potential role of endothelial nitric oxide synthase. *Diabetes and Vascular Disease Research*. <https://doi.org/10.1177/1479164115620982>
- Ramirez-Sanchez, I., Taub, P. R., Ciaraldi, T. P., Nogueira, L., Coe, T., Perkins, G., Hogan, M., Maisel, A. S., Henry, R. R., Ceballos, G., & Villarreal, F. (2013). (-)-Epicatechin rich cocoa mediated modulation of oxidative stress regulators in skeletal muscle of heart failure and type 2 diabetes patients. *International Journal of Cardiology*. <https://doi.org/10.1016/j.ijcard.2013.06.089>
- Ras, R. T., Zock, P. L., & Draijer, R. (2011). Tea consumption enhances endothelial-dependent vasodilation; a meta-analysis. *PLoS ONE*. <https://doi.org/10.1371/journal.pone.0016974>
- Rasmussen, U. F., Krstrup, P., Kjær, M., & Rasmussen, H. N. (2003). Experimental evidence against the mitochondrial theory of aging A study of isolated human skeletal muscle mitochondria. *Experimental Gerontology*. [https://doi.org/10.1016/S0531-5565\(03\)00092-5](https://doi.org/10.1016/S0531-5565(03)00092-5)
- Raymond, S., & Weintraub, L. (1959). Acrylamide Gel as a Supporting Medium for Zone Electrophoresis. *Science*, *130*(3377), 711 LP – 711. <https://doi.org/10.1126/science.130.3377.711>
- Reznick, R. M., Zong, H., Li, J., Morino, K., Moore, I. K., Yu, H. J., Liu, Z. X., Dong, J., Mustard, K. J., Hawley, S. A., Befroy, D., Pypaert, M., Hardie, D. G., Young, L. H.,

- & Shulman, G. I. (2007a). Aging-Associated Reductions in AMP-Activated Protein Kinase Activity and Mitochondrial Biogenesis. *Cell Metabolism*.
<https://doi.org/10.1016/j.cmet.2007.01.008>
- Reznick, R. M., Zong, H., Li, J., Morino, K., Moore, I. K., Yu, H. J., Liu, Z. X., Dong, J., Mustard, K. J., Hawley, S. A., Befroy, D., Pypaert, M., Hardie, D. G., Young, L. H., & Shulman, G. I. (2007b). Aging-Associated Reductions in AMP-Activated Protein Kinase Activity and Mitochondrial Biogenesis. *Cell Metabolism*.
<https://doi.org/10.1016/j.cmet.2007.01.008>
- Ried, K., Fakler, P., & Stocks, N. P. (2017). Effect of cocoa on blood pressure. In *Cochrane Database of Systematic Reviews*. <https://doi.org/10.1002/14651858.CD008893.pub3>
- Rimm, E. B., Katan, M. B., Ascherio, A., Stampfer, M. J., & Willett, W. C. (1996). Relation between Intake of Flavonoids and Risk for Coronary Heart Disease in Male Health Professionals. *Annals of Internal Medicine*. <https://doi.org/10.7326/0003-4819-125-5-199609010-00005>
- Ristow, M., Zarse, K., Oberbach, A., Klötting, N., Birringer, M., Kiehntopf, M., Stumvoll, M., Kahn, C. R., & Blüher, M. (2009). Antioxidants prevent health-promoting effects of physical exercise in humans. *Proceedings of the National Academy of Sciences of the United States of America*. <https://doi.org/10.1073/pnas.0903485106>
- Robinson, K. M., Janes, M. S., Pehar, M., Monette, J. S., Ross, M. F., Hagen, T. M., Murphy, M. P., & Beckman, J. S. (2006). Selective fluorescent imaging of superoxide in vivo using ethidium-based probes. *Proceedings of the National Academy of Sciences of the United States of America*. <https://doi.org/10.1073/pnas.0601945103>
- Rodriguez-Mateos, A., Toro-Funes, N., Cifuentes-Gomez, T., Cortese-Krott, M., Heiss, C., & Spencer, J. P. E. (2014). Uptake and metabolism of (-)-epicatechin in endothelial

cells. *Archives of Biochemistry and Biophysics*.

<https://doi.org/10.1016/j.abb.2014.03.014>

Rolfe, D. F. S., & Brown, G. C. (1997). Cellular energy utilization and molecular origin of standard metabolic rate in mammals. *Physiological Reviews*.

<https://doi.org/10.1152/physrev.1997.77.3.731>

Romano, M. R., & Lograno, M. D. (2009). Epigallocatechin-3-gallate relaxes the isolated bovine ophthalmic artery: Involvement of phosphoinositide 3-kinase-Akt-nitric oxide/cGMP signalling pathway. *European Journal of Pharmacology*.

<https://doi.org/10.1016/j.ejphar.2009.02.034>

Rooyackers, O. E., Adey, D. B., Ades, P. A., & Nair, K. S. (1996). Effect of age on in vivo rates of mitochondrial protein synthesis in human skeletal muscle. *Proceedings of the National Academy of Sciences of the United States of America*.

<https://doi.org/10.1073/pnas.93.26.15364>

Rossiter, H. B., Ward, S. A., Doyle, V. L., Howe, F. A., Griffiths, J. R., & Whipp, B. J.

(1999). Inferences from pulmonary O₂ uptake with respect to intramuscular [phosphocreatine] kinetics during moderate exercise in humans. *Journal of Physiology*. <https://doi.org/10.1111/j.1469-7793.1999.0921p.x>

Rossiter, H. B., Ward, S. A., Kowalchuk, J. M., Howe, F. A., Griffiths, J. R., & Whipp, B. J.

(2001). Effects of prior exercise on oxygen uptake and phosphocreatine kinetics during high-intensity knee-extension exercise in humans. *Journal of Physiology*, 537(1), 291–303. <https://doi.org/10.1111/j.1469-7793.2001.0291k.x>

Rossiter, H. B., Ward, S. A., Kowalchuk, J. M., Howe, F. A., Griffiths, J. R., & Whipp, B. J.

(2002). Dynamic asymmetry of phosphocreatine concentration and O₂ uptake between the on- and off-transients of moderate- and high-intensity exercise in humans. *Journal of Physiology*. <https://doi.org/10.1113/jphysiol.2001.012910>

- Rowley, T. J., Bitner, B. F., Ray, J. D., Lathen, D. R., Smithson, A. T., Dallon, B. W., Plowman, C. J., Bikman, B. T., Hansen, J. M., Dorenkott, M. R., Goodrich, K. M., Ye, L., O'Keefe, S. F., Neilson, A. P., & Tessem, J. S. (2017a). Monomeric cocoa catechins enhance β -cell function by increasing mitochondrial respiration. *Journal of Nutritional Biochemistry*. <https://doi.org/10.1016/j.jnutbio.2017.07.015>
- Rowley, T. J., Bitner, B. F., Ray, J. D., Lathen, D. R., Smithson, A. T., Dallon, B. W., Plowman, C. J., Bikman, B. T., Hansen, J. M., Dorenkott, M. R., Goodrich, K. M., Ye, L., O'Keefe, S. F., Neilson, A. P., & Tessem, J. S. (2017b). Monomeric cocoa catechins enhance β -cell function by increasing mitochondrial respiration. *Journal of Nutritional Biochemistry*. <https://doi.org/10.1016/j.jnutbio.2017.07.015>
- Russ, D. W., Krause, J., Wills, A., & Arreguin, R. (2012). "SR stress" in mixed hindlimb muscles of aging male rats. *Biogerontology*, *13*(5), 547–555. <https://doi.org/10.1007/s10522-012-9399-y>
- Rusznayk, S. T., & Szent-Gyorgyi, A. (1936). Vitamin P: Flavonols as Vitamins. *Nature*, *138*(3479), 27. <https://doi.org/10.1038/138027a0>
- Sabia, S., Singh-Manoux, A., Hagger-Johnson, G., Cambois, E., Brunner, E. J., & Kivimaki, M. (2012). Influence of individual and combined healthy behaviours on successful aging. *CMAJ*. <https://doi.org/10.1503/cmaj.121080>
- Safdar, A., Hamadeh, M. J., Kaczor, J. J., Raha, S., deBeer, J., & Tarnopolsky, M. A. (2010). Aberrant mitochondrial homeostasis in the skeletal muscle of sedentary older adults. *PLoS ONE*. <https://doi.org/10.1371/journal.pone.0010778>
- Saija, A., Scalese, M., Lanza, M., Marzullo, D., Bonina, F., & Castelli, F. (1995). Flavonoids as antioxidant agents: Importance of their interaction with biomembranes. *Free Radical Biology and Medicine*. [https://doi.org/10.1016/0891-5849\(94\)00240-K](https://doi.org/10.1016/0891-5849(94)00240-K)

- Sakellariou, G. K., Vasilaki, A., Palomero, J., Kayani, A., Zibrik, L., McArdle, A., & Jackson, M. J. (2013). Studies of mitochondrial and nonmitochondrial sources implicate nicotinamide adenine dinucleotide phosphate oxidase(s) in the increased skeletal muscle superoxide generation that occurs during contractile activity. *Antioxidants and Redox Signaling*. <https://doi.org/10.1089/ars.2012.4623>
- Samengo, G., Avik, A., Fedor, B., Whittaker, D., Myung, K. H., Wehling-Henricks, M., & Tidball, J. G. (2012). Age-related loss of nitric oxide synthase in skeletal muscle causes reductions in calpain S-nitrosylation that increase myofibril degradation and sarcopenia. *Aging Cell*. <https://doi.org/10.1111/accel.12003>
- Sanchez, M., Lodi, F., Vera, R., Villar, I. C., Cogolludo, A., Jimenez, R., Moreno, L., Romero, M., Tamargo, J., Perez-Vizcaino, F., & Duarte, J. (2007). Quercetin and isorhamnetin prevent endothelial dysfunction, superoxide production, and overexpression of p47phox induced by angiotensin II in rat aorta. *Journal of Nutrition*. <https://doi.org/10.1093/jn/137.4.910>
- Sandoval-Acuña, C., Ferreira, J., & Speisky, H. (2014). Polyphenols and mitochondria: An update on their increasingly emerging ROS-scavenging independent actions. In *Archives of Biochemistry and Biophysics*. <https://doi.org/10.1016/j.abb.2014.05.017>
- Sanguigni, V., Manco, M., Sorge, R., Gnessi, L., & Francomano, D. (2017). Natural antioxidant ice cream acutely reduces oxidative stress and improves vascular function and physical performance in healthy individuals. *Nutrition*. <https://doi.org/10.1016/j.nut.2016.07.008>
- Santamarina, A. B., Carvalho-Silva, M., Gomes, L. M., Okuda, M. H., Santana, A. A., Streck, E. L., Seelaender, M., Oller do Nascimento, C. M., Ribeiro, E. B., Lira, F. S., & Oyama, L. M. (2015). Decaffeinated green tea extract rich in epigallocatechin-3-gallate prevents fatty liver disease by increased activities of mitochondrial respiratory

- chain complexes in diet-induced obesity mice. *Journal of Nutritional Biochemistry*.
<https://doi.org/10.1016/j.jnutbio.2015.07.002>
- Sastre, J., Pallardó, F. V., & Viña, J. (2003). The role of mitochondrial oxidative stress in aging. *Free Radical Biology and Medicine*. [https://doi.org/10.1016/S0891-5849\(03\)00184-9](https://doi.org/10.1016/S0891-5849(03)00184-9)
- Scalbert, A., & Williamson, G. (2000). Dietary Intake and Bioavailability of Polyphenols. *The Journal of Nutrition*. <https://doi.org/10.1093/jn/130.8.2073s>
- Scarpulla, R. C. (2011a). Metabolic control of mitochondrial biogenesis through the PGC-1 family regulatory network. In *Biochimica et Biophysica Acta—Molecular Cell Research*. <https://doi.org/10.1016/j.bbamcr.2010.09.019>
- Scarpulla, R. C. (2011b). Metabolic control of mitochondrial biogenesis through the PGC-1 family regulatory network. In *Biochimica et Biophysica Acta—Molecular Cell Research*. <https://doi.org/10.1016/j.bbamcr.2010.09.019>
- Scarpulla, R. C., Vega, R. B., & Kelly, D. P. (2012). Transcriptional integration of mitochondrial biogenesis. In *Trends in Endocrinology and Metabolism*.
<https://doi.org/10.1016/j.tem.2012.06.006>
- Scheuermann, B. W., Bell, C., Paterson, D. H., Barstow, T. J., & Kowalchuk, J. M. (2002). Oxygen uptake kinetics for moderate exercise are speeded in older humans by prior heavy exercise. *Journal of Applied Physiology*.
<https://doi.org/10.1152/jappphysiol.00186.2001>
- Schewe, T., Steffen, Y., & Sies, H. (2008). How do dietary flavanols improve vascular function? A position paper. In *Archives of Biochemistry and Biophysics*.
<https://doi.org/10.1016/j.abb.2008.03.004>
- Schnorr, O., Brossette, T., Momma, T. Y., Kleinbongard, P., Keen, C. L., Schroeter, H., & Sies, H. (2008). Cocoa flavanols lower vascular arginase activity in human

- endothelial cells in vitro and in erythrocytes in vivo. *Archives of Biochemistry and Biophysics*. <https://doi.org/10.1016/j.abb.2008.02.040>
- Schreuder, T. H. A., Green, D. J., Nyakayiru, J., Hopman, M. T. E., & Thijssen, D. H. J. (2015). Time-course of vascular adaptations during 8 weeks of exercise training in subjects with type 2 diabetes and middle-aged controls. *European Journal of Applied Physiology*. <https://doi.org/10.1007/s00421-014-3006-7>
- Schriner, S. E., Linford, N. J., Martin, G. M., Treuting, P., Ogburn, C. E., Emond, M., Coskun, P. E., Ladiges, W., Wolf, N., Van Remmen, H., Wallace, D. C., & Rabinovitch, P. S. (2005). Extension of murine life span by overexpression of catalase targeted to mitochondria. *Science*. <https://doi.org/10.1126/science.1106653>
- Schroeder, E. K., Kelsey, N. A., Doyle, J., Breed, E., Bouchard, R. J., Loucks, F. A., Harbison, R. A., & Linseman, D. A. (2009). Green tea epigallocatechin 3-gallate accumulates in mitochondria and displays a selective antiapoptotic effect against inducers of mitochondrial oxidative stress in neurons. *Antioxidants and Redox Signaling*. <https://doi.org/10.1089/ars.2008.2215>
- Schroeter, H., Heiss, C., Balzer, J., Kleinbongard, P., Keen, C. L., Hollenberg, N. K., Sies, H., Kwik-Urbe, C., Schmitz, H. H., & Kelm, M. (2006). (-)-Epicatechin mediates beneficial effects of flavanol-rich cocoa on vascular function in humans. *Proceedings of the National Academy of Sciences of the United States of America*, *103*(4), 1024–1029. <https://doi.org/10.1073/pnas.0510168103>
- Schwarz, E., & Neupert, W. (1994). Mitochondrial protein import: Mechanisms, components and energetics. In *BBA - Bioenergetics*. [https://doi.org/10.1016/0005-2728\(94\)90125-2](https://doi.org/10.1016/0005-2728(94)90125-2)
- Schwarz, N. A., Blahnik, Z. J., Prahadeeswaran, S., McKinley-Barnard, S. K., Holden, S. L., & Waldhelm, A. (2018). (-)-Epicatechin Supplementation Inhibits Aerobic

Adaptations to Cycling Exercise in Humans. *Frontiers in Nutrition*.

<https://doi.org/10.3389/fnut.2018.00132>

Schweizer, M., & Richter, C. (1994). Nitric oxide potently and reversibly deenergizes

mitochondria at low oxygen tension. *Biochemical and Biophysical Research*

Communications. <https://doi.org/10.1006/bbrc.1994.2441>

Sebastián, D., Sorianello, E., Segalés, J., Irazoki, A., Ruiz-Bonilla, V., Sala, D., Planet, E.,

Berenguer-Llargo, A., Muñoz, J. P., Sánchez-Feutrie, M., Plana, N., Hernández-

Álvarez, M. I., Serrano, A. L., Palacín, M., & Zorzano, A. (2016). Mfn2 deficiency

links age-related sarcopenia and impaired autophagy to activation of an adaptive

mitophagy pathway. *The EMBO Journal*. <https://doi.org/10.15252/embj.201593084>

Sergey, D., K., G. K., & G., H. D. (2007). Measurement of Reactive Oxygen Species in

Cardiovascular Studies. *Hypertension*, *49*(4), 717–727.

<https://doi.org/10.1161/01.HYP.0000258594.87211.6b>

Serrander, L., Cartier, L., Bedard, K., Banfi, B., Lardy, B., Plastre, O., Sienkiewicz, A.,

Fórró, L., Schlegel, W., & Krause, K.-H. (2007). NOX4 activity is determined by

mRNA levels and reveals a unique pattern of ROS generation. *The Biochemical*

Journal, *406*(1), 105–114. <https://doi.org/10.1042/BJ20061903>

Sesso, H. D., Gaziano, J. M., Liu, S., & Buring, J. E. (2003). Flavonoid intake and the risk of

cardiovascular disease in women. *American Journal of Clinical Nutrition*.

<https://doi.org/10.1093/ajcn/77.6.1400>

Shaki, F., Shayeste, Y., Karami, M., Akbari, E., Rezaei, M., & Ataee, R. (2017). The effect

of epicatechin on oxidative stress and mitochondrial damage induced by

homocysteine using isolated rat hippocampus mitochondria. *Research in*

Pharmaceutical Sciences. <https://doi.org/10.4103/1735-5362.202450>

- Sharma, D. R., Sunkaria, A., Wani, W. Y., Sharma, R. K., Verma, D., Priyanka, K., Bal, A., & Gill, K. D. (2015a). Quercetin protects against aluminium induced oxidative stress and promotes mitochondrial biogenesis via activation of the PGC-1 α signaling pathway. *NeuroToxicology*. <https://doi.org/10.1016/j.neuro.2015.10.002>
- Sharma, D. R., Sunkaria, A., Wani, W. Y., Sharma, R. K., Verma, D., Priyanka, K., Bal, A., & Gill, K. D. (2015b). Quercetin protects against aluminium induced oxidative stress and promotes mitochondrial biogenesis via activation of the PGC-1 α signaling pathway. *NeuroToxicology*. <https://doi.org/10.1016/j.neuro.2015.10.002>
- Sharples, A. P., Al-Shanti, N., Lewis, M. P., & Stewart, C. E. (2011a). Reduction of myoblast differentiation following multiple population doublings in mouse C 2C 12 cells: A model to investigate ageing? *Journal of Cellular Biochemistry*. <https://doi.org/10.1002/jcb.23308>
- Sharples, A. P., Al-Shanti, N., Lewis, M. P., & Stewart, C. E. (2011b). Reduction of myoblast differentiation following multiple population doublings in mouse C2C12 cells: A model to investigate ageing? *Journal of Cellular Biochemistry*. <https://doi.org/10.1002/jcb.23308>
- Shavlakadze, T., Morris, M., Fang, J., Wang, S. X., Zhu, J., Zhou, W., Tse, H. W., Mondragon-Gonzalez, R., Roma, G., & Glass, D. J. (2019). Age-Related Gene Expression Signature in Rats Demonstrate Early, Late, and Linear Transcriptional Changes from Multiple Tissues. *Cell Reports*, 28(12), 3263-3273.e3. <https://doi.org/10.1016/j.celrep.2019.08.043>
- Shen, Y., Croft, K. D., Hodgson, J. M., Kyle, R., Lee, I. L. E., Wang, Y., Stocker, R., & Ward, N. C. (2012). Quercetin and its metabolites improve vessel function by inducing eNOS activity via phosphorylation of AMPK. *Biochemical Pharmacology*. <https://doi.org/10.1016/j.bcp.2012.07.016>

- Shi, D., Xia, X., Cui, A., Xiong, Z., Yan, Y., Luo, J., Chen, G., Zeng, Y., Cai, D., Hou, L., McDermott, J., Li, Y., Zhang, H., & Han, J. D. J. (2020). The precursor of PI(3,4,5)P3 alleviates aging by activating daf-18(Pten) and independent of daf-16. *Nature Communications*. <https://doi.org/10.1038/s41467-020-18280-4>
- Short, K. R., Bigelow, M. L., Kahl, J., Singh, R., Coenen-Schimke, J., Raghavakaimal, S., & Nair, K. S. (2005). Decline in skeletal muscle mitochondrial function with aging in humans. *Proceedings of the National Academy of Sciences of the United States of America*. <https://doi.org/10.1073/pnas.0501559102>
- Si, H., Fu, Z., Babu, P. V. A., Zhen, W., LeRoith, T., Meaney, M. P., Voelker, K. A., Jia, Z., Grange, R. W., & Liu, D. (2011). Dietary epicatechin promotes survival of obese diabetic mice and *Drosophila melanogaster*. *Journal of Nutrition*. <https://doi.org/10.3945/jn.110.134270>
- Si, H., Wang, X., Zhang, L., Parnell, L. D., Admed, B., LeRoith, T., Ansah, T. A., Zhang, L., Li, J., Ordovas, J. M., Si, H., Liu, D., & Lai, C. Q. (2019a). Dietary epicatechin improves survival and delays skeletal muscle degeneration in aged mice. *FASEB Journal*. <https://doi.org/10.1096/fj.201800554RR>
- Si, H., Wang, X., Zhang, L., Parnell, L. D., Admed, B., LeRoith, T., Ansah, T. A., Zhang, L., Li, J., Ordovas, J. M., Si, H., Liu, D., & Lai, C. Q. (2019b). Dietary epicatechin improves survival and delays skeletal muscle degeneration in aged mice. *FASEB Journal*. <https://doi.org/10.1096/fj.201800554RR>
- Silva, M. M., Santos, M. R., Caroço, G., Rocha, R., Justino, G., & Mira, L. (2002). Structure-antioxidant activity relationships of flavonoids: A re-examination. *Free Radical Research*. <https://doi.org/10.1080/198-1071576021000016472>
- Sindler, A. L., Delp, M. D., Reyes, R., Wu, G., & Muller-Delp, J. M. (2009). Effects of ageing and exercise training on eNOS uncoupling in skeletal muscle resistance

arterioles. *Journal of Physiology*, 587(15), 3885–3897.

<https://doi.org/10.1113/jphysiol.2009.172221>

- Singh, N., Prasad, S., Singer, D. R. J., & MacAllister, R. J. (2002a). Ageing is associated with impairment of nitric oxide and prostanoid dilator pathways in the human forearm. *Clinical Science*. <https://doi.org/10.1042/CS20010262>
- Singh, N., Prasad, S., Singer, D. R. J., & MacAllister, R. J. (2002b). Ageing is associated with impairment of nitric oxide and prostanoid dilator pathways in the human forearm. *Clinical Science*. <https://doi.org/10.1042/CS20010262>
- Sirk, T. W., Brown, E. F., Friedman, M., & Sum, A. K. (2009). Molecular binding of catechins to biomembranes: Relationship to biological activity. *Journal of Agricultural and Food Chemistry*. <https://doi.org/10.1021/jf900951w>
- Spencer, J. P. E. (2003). Metabolism of Tea Flavonoids in the Gastrointestinal Tract. *The Journal of Nutrition*. <https://doi.org/10.1093/jn/133.10.3255s>
- Spencer, J. P. E., Abd El Mohsen, M. M., Minihane, A. M., & Mathers, J. C. (2008). Biomarkers of the intake of dietary polyphenols: Strengths, limitations and application in nutrition research. In *British Journal of Nutrition*. <https://doi.org/10.1017/S0007114507798938>
- Spencer, J. P. E., Chowrimootoo, G., Choudhury, R., Debnam, E. S., Srail, S. K., & Rice-Evans, C. (1999). The small intestine can both absorb and glucuronidate luminal flavonoids. *FEBS Letters*. [https://doi.org/10.1016/S0014-5793\(99\)01160-6](https://doi.org/10.1016/S0014-5793(99)01160-6)
- Spencer, J. P. E., Kuhnle, G. G. C., Williams, R. J., & Rice-Evans, C. (2003). Intracellular metabolism and bioactivity of quercetin and its in vivo metabolites. *Biochemical Journal*. <https://doi.org/10.1042/BJ20021972>
- Spencer, M. D., Murias, J. M., Lamb, H. P., Kowalchuk, J. M., & Paterson, D. H. (2011a). Are the parameters of VO₂, heart rate and muscle deoxygenation kinetics affected by

- serial moderate-intensity exercise transitions in a single day? *European Journal of Applied Physiology*. <https://doi.org/10.1007/s00421-010-1653-x>
- Spencer, M. D., Murias, J. M., Lamb, H. P., Kowalchuk, J. M., & Paterson, D. H. (2011b). Are the parameters of VO₂, heart rate and muscle deoxygenation kinetics affected by serial moderate-intensity exercise transitions in a single day? *European Journal of Applied Physiology*. <https://doi.org/10.1007/s00421-010-1653-x>
- Spier, S. A., Delp, M. D., Meininger, C. J., Donato, A. J., Ramsey, M. W., & Muller-Delp, J. M. (2004). Effects of ageing and exercise training on endothelium-dependent vasodilation and structure of rat skeletal muscle arterioles. *Journal of Physiology*, *556*(3), 947–958. <https://doi.org/10.1113/jphysiol.2003.060301>
- Stahmann, N., Woods, A., Carling, D., & Heller, R. (2006). Thrombin Activates AMP-Activated Protein Kinase in Endothelial Cells via a Pathway Involving Ca²⁺/Calmodulin-Dependent Protein Kinase Kinase β . *Molecular and Cellular Biology*. <https://doi.org/10.1128/mcb.00383-06>
- Stefano, T., Agostino, V., Lorenzo, G., Guido, S., Giampaolo, B., Armando, M., & Antonio, S. (2001). Age-Related Reduction of NO Availability and Oxidative Stress in Humans. *Hypertension*, *38*(2), 274–279. <https://doi.org/10.1161/01.HYP.38.2.274>
- Stellingwerff, T., Godin, J. P., Chou, C. J., Grathwohl, D., Ross, A. B., Cooper, K. A., Williamson, G., & Actis-Goretta, L. (2014). The effect of acute dark chocolate consumption on carbohydrate metabolism and performance during rest and exercise. *Applied Physiology, Nutrition and Metabolism*, *39*(2), 173–182. <https://doi.org/10.1139/apnm-2013-0152>
- Stessman, J., Hammerman-Rozenberg, R., Cohen, A., Ein-Mor, E., & Jacobs, J. M. (2009). Physical activity, function, and longevity among the very old. *Archives of Internal Medicine*. <https://doi.org/10.1001/archinternmed.2009.248>

- St-Pierre, J., Buckingham, J. A., Roebuck, S. J., & Brand, M. D. (2002). Topology of superoxide production from different sites in the mitochondrial electron transport chain. *Journal of Biological Chemistry*. <https://doi.org/10.1074/jbc.M207217200>
- Strobel, N. A., Peake, J. M., Matsumoto, A., Marsh, S. A., Coombes, J. S., & Wadley, G. D. (2011). Antioxidant supplementation reduces skeletal muscle mitochondrial biogenesis. *Medicine and Science in Sports and Exercise*. <https://doi.org/10.1249/MSS.0b013e318203afa3>
- Su, J., Ekman, C., Oskolkov, N., Lahti, L., Ström, K., Brazma, A., Groop, L., Rung, J., & Hansson, O. (2015). A novel atlas of gene expression in human skeletal muscle reveals molecular changes associated with aging. *Skeletal Muscle*, 5(1), 35. <https://doi.org/10.1186/s13395-015-0059-1>
- Sullivan-Gunn, M. J., & Lewandowski, P. A. (2013). Elevated hydrogen peroxide and decreased catalase and glutathione peroxidase protection are associated with aging sarcopenia. *BMC Geriatrics*. <https://doi.org/10.1186/1471-2318-13-104>
- Sumner, L. W., Amberg, A., Barrett, D., Beale, M. H., Beger, R., Daykin, C. A., Fan, T. W.-M., Fiehn, O., Goodacre, R., Griffin, J. L., Hankemeier, T., Hardy, N., Harnly, J., Higashi, R., Kopka, J., Lane, A. N., Lindon, J. C., Marriott, P., Nicholls, A. W., ... Viant, M. R. (2007). Proposed minimum reporting standards for chemical analysis. *Metabolomics*. <https://doi.org/10.1007/s11306-007-0082-2>
- Sun, D., Huang, A., Yan, E. H., Wu, Z., Yan, C., Kaminski, P. M., Oury, T. D., Wolin, M. S., & Kaley, G. (2004). Reduced release of nitric oxide to shear stress in mesenteric arteries of aged rats. *American Journal of Physiology - Heart and Circulatory Physiology*. <https://doi.org/10.1152/ajpheart.00854.2003>
- Sun, Q., Townsend, M. K., Okereke, O. I., Franco, O. H., Hu, F. B., & Grodstein, F. (2010). Physical activity at midlife in relation to successful survival in women at age 70 years

or older. *Archives of Internal Medicine*.

<https://doi.org/10.1001/archinternmed.2009.503>

Sundberg, C. W., Prost, R. W., Fitts, R. H., & Hunter, S. K. (2019). Bioenergetic basis for the increased fatigability with ageing. *Journal of Physiology*.

<https://doi.org/10.1113/JP277803>

Taddei, S., Galetta, F., Viridis, A., Ghiadoni, L., Salvetti, G., Franzoni, F., Giusti, C., & Salvetti, A. (2000a). Physical activity prevents age-related impairment in nitric oxide availability in elderly athletes. *Circulation*.

<https://doi.org/10.1161/01.CIR.101.25.2896>

Taddei, S., Galetta, F., Viridis, A., Ghiadoni, L., Salvetti, G., Franzoni, F., Giusti, C., & Salvetti, A. (2000b). Physical activity prevents age-related impairment in nitric oxide availability in elderly athletes. *Circulation*.

<https://doi.org/10.1161/01.CIR.101.25.2896>

Tak, E., Kuiper, R., Chorus, A., & Hopman-Rock, M. (2013). Prevention of onset and progression of basic ADL disability by physical activity in community dwelling older adults: A meta-analysis. In *Ageing Research Reviews*.

<https://doi.org/10.1016/j.arr.2012.10.001>

Takagi, A. (1971). Lipid composition of sarcoplasmic reticulum of human skeletal muscle.

Biochimica et Biophysica Acta (BBA) - Lipids and Lipid Metabolism, 248(1), 12–20.

[https://doi.org/10.1016/0005-2760\(71\)90069-5](https://doi.org/10.1016/0005-2760(71)90069-5)

Takahashi, M., & Hood, D. A. (1996). Protein Import into Subsarcolemmal and

Intermyofibrillar Skeletal Muscle Mitochondria. *Journal of Biological Chemistry*.

<https://doi.org/10.1074/jbc.271.44.27285>

- Takehara, Y., Kanno, T., Yoshioka, T., Inoue, M., & Utsumi, K. (1995). Oxygen-dependent regulation of mitochondrial energy metabolism by nitric oxide. *Archives of Biochemistry and Biophysics*. <https://doi.org/10.1006/abbi.1995.0005>
- Tamba, Y., Ohba, S., Kubota, M., Yoshioka, H., Yoshioka, H., & Yamazaki, M. (2007). Single GUV method reveals interaction of tea catechin (2)-epigallocatechin gallate with lipid membranes. *Biophysical Journal*. <https://doi.org/10.1529/biophysj.106.097105>
- Tapiero, H., Mathé, G., Couvreur, P., & Tew, K. D. (2002). II. Glutamine and glutamate. *Biomedicine and Pharmacotherapy*. [https://doi.org/10.1016/S0753-3322\(02\)00285-8](https://doi.org/10.1016/S0753-3322(02)00285-8)
- Taub, P. R., Ramirez-Sanchez, I., Ciaraldi, T. P., Perkins, G., Murphy, A. N., Naviaux, R., Hogan, M., Maisel, A. S., Henry, R. R., Ceballos, G., & Villarreal, F. (2012). Alterations in Skeletal Muscle Indicators of Mitochondrial Structure and Biogenesis in Patients with Type 2 Diabetes and Heart Failure: Effects of Epicatechin Rich Cocoa. *Clinical and Translational Science*. <https://doi.org/10.1111/j.1752-8062.2011.00357.x>
- Taub, P. R., Ramirez-Sanchez, I., Patel, M., Higginbotham, E., Moreno-Ulloa, A., Román-Pintos, L. M., Phillips, P., Perkins, G., Ceballos, G., & Villarreal, F. (2016). Beneficial effects of dark chocolate on exercise capacity in sedentary subjects: Underlying mechanisms. A double blind, randomized, placebo controlled trial. *Food and Function*. <https://doi.org/10.1039/c6fo00611f>
- Tebay, L. E., Robertson, H., Durant, S. T., Vitale, S. R., Penning, T. M., Dinkova-Kostova, A. T., & Hayes, J. D. (2015). Mechanisms of activation of the transcription factor Nrf2 by redox stressors, nutrient cues, and energy status and the pathways through which it attenuates degenerative disease. In *Free Radical Biology and Medicine*. <https://doi.org/10.1016/j.freeradbiomed.2015.06.021>

- Tengan, C. H., Kiyomoto, B. H., Godinho, R. O., Gamba, J., Neves, A. C., Schmidt, B., Oliveira, A. S. B., & Gabbai, A. A. (2007). The role of nitric oxide in muscle fibers with oxidative phosphorylation defects. *Biochemical and Biophysical Research Communications*, 359(3), 771–777. <https://doi.org/10.1016/j.bbrc.2007.05.184>
- Terman, A., Kurz, T., Navratil, M., Arriaga, E. A., & Brunk, U. T. (2009). Mitochondrial Turnover and Aging of Long-Lived Postmitotic Cells: The Mitochondrial–Lysosomal Axis Theory of Aging. *Antioxidants & Redox Signaling*, 12(4), 503–535. <https://doi.org/10.1089/ars.2009.2598>
- Tew, G. A., Klonizakis, M., & Saxton, J. M. (2010). Effects of ageing and fitness on skin-microvessel vasodilator function in humans. *European Journal of Applied Physiology*. <https://doi.org/10.1007/s00421-009-1342-9>
- Thijssen, D. H. J., Carter, S. E., & Green, D. J. (2016). Arterial structure and function in vascular ageing: Are you as old as your arteries? In *Journal of Physiology*. <https://doi.org/10.1113/JP270597>
- Thijssen, D. H. J., De Groot, P., Kooijman, M., Smits, P., & Hopman, M. T. E. (2006). Sympathetic nervous system contributes to the age-related impairment of flow-mediated dilation of the superficial femoral artery. *American Journal of Physiology - Heart and Circulatory Physiology*. <https://doi.org/10.1152/ajpheart.00240.2006>
- Thompson, M. G., Palmer, R. M., Thom, A., Garden, K., Loble, G. E., & Calder, G. (1996). N(τ)-methylhistidine turnover in skeletal muscle cells measured by GC-MS. *American Journal of Physiology - Cell Physiology*. <https://doi.org/10.1152/ajpcell.1996.270.6.c1875>
- Thomson, R. L., Buckley, J. D., & Brinkworth, G. D. (2016). Perceived exercise barriers are reduced and benefits are improved with lifestyle modification in overweight and

- obese women with polycystic ovary syndrome: A randomised controlled trial. *BMC Women's Health*. <https://doi.org/10.1186/s12905-016-0292-8>
- Tonkonogi, M., Fernström, M., Walsh, B., Ji, L. L., Rooyackers, O., Hammarqvist, F., Wernerman, J., & Sahlin, K. (2003a). Reduced oxidative power but unchanged antioxidative capacity in skeletal muscle from aged humans. *Pflugers Archiv European Journal of Physiology*. <https://doi.org/10.1007/s00424-003-1044-9>
- Tonkonogi, M., Fernström, M., Walsh, B., Ji, L. L., Rooyackers, O., Hammarqvist, F., Wernerman, J., & Sahlin, K. (2003b). Reduced oxidative power but unchanged antioxidative capacity in skeletal muscle from aged humans. *Pflugers Archiv European Journal of Physiology*. <https://doi.org/10.1007/s00424-003-1044-9>
- Towbin, H., Staehelin, T., & Gordon, J. (1979). Electrophoretic transfer of proteins from polyacrylamide gels to nitrocellulose sheets: Procedure and some applications. *Proceedings of the National Academy of Sciences*, 76(9), 4350 LP – 4354. <https://doi.org/10.1073/pnas.76.9.4350>
- Trappe, T., Williams, R., Carrithers, J., Raue, U., Esmarck, B., Kjaer, M., & Hickner, R. (2004). Influence of age and resistance exercise on human skeletal muscle proteolysis: A microdialysis approach. *Journal of Physiology*. <https://doi.org/10.1113/jphysiol.2003.051755>
- Tribolo, S., Lodi, F., Winterbone, M. S., Saha, S., Needs, P. W., Hughes, D. A., & Kroon, P. A. (2013). Human metabolic transformation of quercetin blocks its capacity to decrease endothelial nitric oxide synthase (eNOS) expression and endothelin-1 secretion by human endothelial cells. *Journal of Agricultural and Food Chemistry*. <https://doi.org/10.1021/jf402511c>

- Trumbeckaite, S., Bernatoniene, J., Majiene, D., Jakštas, V., Savickas, A., & Toleikis, A. (2006). The effect of flavonoids on rat heart mitochondrial function. *Biomedicine and Pharmacotherapy*. <https://doi.org/10.1016/j.biopha.2006.04.003>
- Uchitomi, R., Hatazawa, Y., Senoo, N., Yoshioka, K., Fujita, M., Shimizu, T., Miura, S., Ono, Y., & Kamei, Y. (2019). Metabolomic Analysis of Skeletal Muscle in Aged Mice. *Scientific Reports*. <https://doi.org/10.1038/s41598-019-46929-8>
- Ungvari, Z., Bailey-Downs, L., Gautam, T., Sosnowska, D., Wang, M., Monticone, R. E., Telljohann, R., Pinto, J. T., De Cabo, R., Sonntag, W. E., Lakatta, E. G., & Csiszar, A. (2011). Age-associated vascular oxidative stress, Nrf2 dysfunction, and NF- κ B activation in the nonhuman primate macaca mulatta. *Journals of Gerontology - Series A Biological Sciences and Medical Sciences*. <https://doi.org/10.1093/gerona/qlr092>
- Ungvari, Z., Labinskyy, N., Gupte, S., Chander, P. N., Edwards, J. G., & Csiszar, A. (2008a). Dysregulation of mitochondrial biogenesis in vascular endothelial and smooth muscle cells of aged rats. *American Journal of Physiology - Heart and Circulatory Physiology*. <https://doi.org/10.1152/ajpheart.00012.2008>
- Ungvari, Z., Labinskyy, N., Gupte, S., Chander, P. N., Edwards, J. G., & Csiszar, A. (2008b). Dysregulation of mitochondrial biogenesis in vascular endothelial and smooth muscle cells of aged rats. *American Journal of Physiology - Heart and Circulatory Physiology*. <https://doi.org/10.1152/ajpheart.00012.2008>
- Ungvari, Z., Orosz, Z., Labinskyy, N., Rivera, A., Xiangmin, Z., Smith, K., & Csiszar, A. (2007). Increased mitochondrial H₂O₂ production promotes endothelial NF- κ B activation in aged rat arteries. *American Journal of Physiology - Heart and Circulatory Physiology*. <https://doi.org/10.1152/ajpheart.01346.2006>

- Ungvari, Z., Tarantini, S., Donato, A. J., Galvan, V., & Csiszar, A. (2018). Mechanisms of vascular aging. *Circulation Research*.
<https://doi.org/10.1161/CIRCRESAHA.118.311378>
- Valenti, D., De Bari, L., Manente, G. A., Rossi, L., Mutti, L., Moro, L., & Vacca, R. A. (2013). Negative modulation of mitochondrial oxidative phosphorylation by epigallocatechin-3 gallate leads to growth arrest and apoptosis in human malignant pleural mesothelioma cells. *Biochimica et Biophysica Acta - Molecular Basis of Disease*. <https://doi.org/10.1016/j.bbadis.2013.07.014>
- Van Der Loo, B., Labugger, R., Skepper, J. N., Bachschmid, M., Kilo, J., Powell, J. M., Palacios-Callender, M., Erusalimsky, J. D., Quaschnig, T., Malinski, T., Gygi, D., Ullrich, V., & Lüscher, T. F. (2000a). Enhanced peroxynitrite formation is associated with vascular aging. *Journal of Experimental Medicine*.
<https://doi.org/10.1084/jem.192.12.1731>
- Van Der Loo, B., Labugger, R., Skepper, J. N., Bachschmid, M., Kilo, J., Powell, J. M., Palacios-Callender, M., Erusalimsky, J. D., Quaschnig, T., Malinski, T., Gygi, D., Ullrich, V., & Lüscher, T. F. (2000b). Enhanced peroxynitrite formation is associated with vascular aging. *Journal of Experimental Medicine*.
<https://doi.org/10.1084/jem.192.12.1731>
- van der Veen, J. N., Kennelly, J. P., Wan, S., Vance, J. E., Vance, D. E., & Jacobs, R. L. (2017). The critical role of phosphatidylcholine and phosphatidylethanolamine metabolism in health and disease. In *Biochimica et Biophysica Acta—Biomembranes*.
<https://doi.org/10.1016/j.bbamem.2017.04.006>
- Vance, J. E. (2015). Phospholipid Synthesis and Transport in Mammalian Cells. In *Traffic*.
<https://doi.org/10.1111/tra.12230>

- Vanhatalo, A., Bailey, S. J., Blackwell, J. R., DiMenna, F. J., Pavey, T. G., Wilkerson, D. P., Benjamin, N., Winyard, P. G., & Jones, A. M. (2010). Acute and chronic effects of dietary nitrate supplementation on blood pressure and the physiological responses to moderate-intensity and incremental exercise. *American Journal of Physiology - Regulatory Integrative and Comparative Physiology*, 299(4).
<https://doi.org/10.1152/ajpregu.00206.2010>
- Vasilaki, A., Mansouri, A., Van Remmen, H., van der Meulen, J. H., Larkin, L., Richardson, A. G., McArdle, A., Faulkner, J. A., & Jackson, M. J. (2006). Free radical generation by skeletal muscle of adult and old mice: Effect of contractile activity. *Aging Cell*.
<https://doi.org/10.1111/j.1474-9726.2006.00198.x>
- Vasilaki, A., McArdle, F., Iwanejko, L. M., & McArdle, A. (2006). Adaptive responses of mouse skeletal muscle to contractile activity: The effect of age. *Mechanisms of Ageing and Development*. <https://doi.org/10.1016/j.mad.2006.08.004>
- Vasilaki, A., Van Der Meulen, J. H., Larkin, L., Harrison, D. C., Pearson, T., Van Remmen, H., Richardson, A., Brooks, S. V., Jackson, M. J., & McArdle, A. (2010). The age-related failure of adaptive responses to contractile activity in skeletal muscle is mimicked in young mice by deletion of Cu,Zn superoxide dismutase. *Aging Cell*.
<https://doi.org/10.1111/j.1474-9726.2010.00635.x>
- Vesali, R. F., Klaude, M., Thunblad, L., Rooyackers, O. E., & Wernerman, J. (2004). Contractile protein breakdown in human leg skeletal muscle as estimated by [2H3]-3-methylhistidine: A new method. *Metabolism: Clinical and Experimental*.
<https://doi.org/10.1016/j.metabol.2004.02.017>
- Vichai, V., & Kirtikara, K. (2006). Sulforhodamine B colorimetric assay for cytotoxicity screening. *Nature Protocols*. <https://doi.org/10.1038/nprot.2006.179>

- Vilella, R., Sgarbi, G., Naponelli, V., Savi, M., Bocchi, L., Liuzzi, F., Righetti, R., Quaini, F., Frati, C., Bettuzzi, S., Solaini, G., Stilli, D., Rizzi, F., & Baracca, A. (2020a). Effects of standardized green tea extract and its main component, EGCG, on mitochondrial function and contractile performance of healthy rat cardiomyocytes. *Nutrients*.
<https://doi.org/10.3390/nu12102949>
- Vilella, R., Sgarbi, G., Naponelli, V., Savi, M., Bocchi, L., Liuzzi, F., Righetti, R., Quaini, F., Frati, C., Bettuzzi, S., Solaini, G., Stilli, D., Rizzi, F., & Baracca, A. (2020b). Effects of standardized green tea extract and its main component, EGCG, on mitochondrial function and contractile performance of healthy rat cardiomyocytes. *Nutrients*.
<https://doi.org/10.3390/nu12102949>
- Vincent, A. E., White, K., Davey, T., Philips, J., Ogden, R. T., Lawless, C., Warren, C., Hall, M. G., Ng, Y. S., Falkous, G., Holden, T., Deehan, D., Taylor, R. W., Turnbull, D. M., & Picard, M. (2019). Quantitative 3D Mapping of the Human Skeletal Muscle Mitochondrial Network. *Cell Reports*, 26(4), 996-1009.e4.
<https://doi.org/10.1016/j.celrep.2019.01.010>
- Vita, J. A., Treasure, C. B., Nabel, E. G., McLenachan, J. M., Fish, R. D., Yeung, A. C., Vekshtein, V. I., Selwyn, A. P., & Ganz, P. (1990). Coronary vasomotor response to acetylcholine relates to risk factors for coronary artery disease. *Circulation*, 81(2), 491–497. <https://doi.org/10.1161/01.CIR.81.2.491>
- Wach, A., Pyrzyńska, K., & Biesaga, M. (2007). Quercetin content in some food and herbal samples. *Food Chemistry*. <https://doi.org/10.1016/j.foodchem.2005.10.028>
- Wadley, G. D., & McConell, G. K. (2007). Effect of nitric oxide synthase inhibition on mitochondrial biogenesis in rat skeletal muscle. *Journal of Applied Physiology*.
<https://doi.org/10.1152/jappphysiol.00549.2006>

- Wagenmakers, A. J. M. (1998). Protein and amino acid metabolism in human muscle. *Advances in Experimental Medicine and Biology*. https://doi.org/10.1007/978-1-4899-1928-1_28
- Wan, L. L., Xia, J., Ye, D., Liu, J., Chen, J., & Wang, G. (2009). Effects of quercetin on gene and protein expression of NOX and NOS after myocardial ischemia and reperfusion in rabbit. *Cardiovascular Therapeutics*. <https://doi.org/10.1111/j.1755-5922.2009.00071.x>
- Wang, L., Wang, Z., Yang, K., Shu, G., Wang, S., Gao, P., Zhu, X., Xi, Q., Zhang, Y., & Jiang, Q. (2016). Epigallocatechin Gallate Reduces Slow-Twitch Muscle Fiber Formation and Mitochondrial Biosynthesis in C2C12 Cells by Repressing AMPK Activity and PGC-1 α Expression. *Journal of Agricultural and Food Chemistry*. <https://doi.org/10.1021/acs.jafc.6b02193>
- Wang, W., Wu, Z., Dai, Z., Yang, Y., Wang, J., & Wu, G. (2013). Glycine metabolism in animals and humans: Implications for nutrition and health. *Amino Acids*. <https://doi.org/10.1007/s00726-013-1493-1>
- Ward, S. A. (2007). Muscle-energetic and cardio-pulmonary determinants of exercise tolerance in humans. *Experimental Physiology*, *92*(2), 321–322. <https://doi.org/10.1113/expphysiol.2006.034389>
- Wasilewski, R., Ubara, E. O., & Klonizakis, M. (2016). Assessing the effects of a short-term green tea intervention in skin microvascular function and oxygen tension in older and younger adults. *Microvascular Research*. <https://doi.org/10.1016/j.mvr.2016.05.001>
- Watanabe, N., Inagawa, K., Shibata, M., & Osakabe, N. (2014). Flavan-3-ol fraction from cocoa powder promotes mitochondrial biogenesis in skeletal muscle in mice. *Lipids in Health and Disease*. <https://doi.org/10.1186/1476-511X-13-64>

- Wei, H., Liu, L., & Chen, Q. (2015). Selective removal of mitochondria via mitophagy: Distinct pathways for different mitochondrial stresses. In *Biochimica et Biophysica Acta—Molecular Cell Research*. <https://doi.org/10.1016/j.bbamcr.2015.03.013>
- Weljie, A. M., Newton, J., Mercier, P., Carlson, E., & Slupsky, C. M. (2006). Targeted profiling: Quantitative analysis of ¹H NMR metabolomics data. *Analytical Chemistry*. <https://doi.org/10.1021/ac060209g>
- Welle, S., Bhatt, K., Shah, B., Needler, N., Delehanty, J. M., & Thornton, C. A. (2003). Reduced amount of mitochondrial DNA in aged human muscle. *Journal of Applied Physiology*, *94*(4), 1479–1484. <https://doi.org/10.1152/jappphysiol.01061.2002>
- Weng, Z., Zhou, P., Salminen, W. F., Yang, X., Harrill, A. H., Cao, Z., Mattes, W. B., Mendrick, D. L., & Shi, Q. (2014). Green tea epigallocatechin gallate binds to and inhibits respiratory complexes in swelling but not normal rat hepatic mitochondria. *Biochemical and Biophysical Research Communications*. <https://doi.org/10.1016/j.bbrc.2013.12.110>
- Whipp, B. J., & Rossiter, H. B. (2013). The kinetics of oxygen uptake: Physiological inferences from the parameters. In *Oxygen Uptake Kinetics in Sport, Exercise and Medicine* (pp. 1–406). <https://doi.org/10.4324/9780203613771>
- Whipp, B. J., & Ward, S. A. (1992). Pulmonary gas exchange dynamics and the tolerance to muscular exercise: Effects of fitness and training. *The Annals of Physiological Anthropology = Seiri Jinruigaku Kenkyūkai Kaishi*, *11*, 207–214. <https://doi.org/10.2114/ahs1983.11.207>
- Whipp, B. J., Ward, S. A., Lamarra, N., Davis, J. A., & Wasserman, K. (1982). Parameters of ventilatory and gas exchange dynamics during exercise. *Journal of Applied Physiology Respiratory Environmental and Exercise Physiology*. <https://doi.org/10.1152/jappl.1982.52.6.1506>

- Whipp, B. J., Ward, S. A., & Rossiter, H. B. (2005). Pulmonary O₂ uptake during exercise: Conflating muscular and cardiovascular responses. *Medicine and Science in Sports and Exercise*. <https://doi.org/10.1249/01.mss.0000177476.63356.22>
- WHO, W. H. O. (2010). Global recommendations on physical activity for health. *Geneva: World Health Organization*. <https://doi.org/10.1080/11026480410034349>
- Wilkinson, D. J., Rodriguez-Blanco, G., Dunn, W. B., Phillips, B. E., Williams, J. P., Greenhaff, P. L., Smith, K., Gallagher, I. J., & Atherton, P. J. (2020). Untargeted metabolomics for uncovering biological markers of human skeletal muscle ageing. *Aging*. <https://doi.org/10.18632/aging.103513>
- Williamson, G., Kay, C. D., & Crozier, A. (2018). The Bioavailability, Transport, and Bioactivity of Dietary Flavonoids: A Review from a Historical Perspective. In *Comprehensive Reviews in Food Science and Food Safety*. <https://doi.org/10.1111/1541-4337.12351>
- Williamson, G., & Manach, C. (2005). Bioavailability and bioefficacy of polyphenols in humans. II. Review of 93 intervention studies. In *The American journal of clinical nutrition*. <https://doi.org/10.1093/ajcn/81.1.243s>
- Wong, C. C., Botting, N. P., Orfila, C., Al-Maharik, N., & Williamson, G. (2011). Flavonoid conjugates interact with organic anion transporters (OATs) and attenuate cytotoxicity of adefovir mediated by organic anion transporter 1 (OAT1/SLC22A6). *Biochemical Pharmacology*. <https://doi.org/10.1016/j.bcp.2011.01.004>
- Woodman, C. R., Price, E. M., & Laughlin, M. H. (2002). Aging induces muscle-specific impairment of endothelium-dependent dilation in skeletal muscle feed arteries. *Journal of Applied Physiology*, *93*(5), 1685–1690. <https://doi.org/10.1152/jappphysiol.00461.2002>

- Wright, D. C., Han, D. H., Garcia-Roves, P. M., Geiger, P. C., Jones, T. E., & Holloszy, J. O. (2007). Exercise-induced mitochondrial biogenesis begins before the increase in muscle PGC-1 α expression. *Journal of Biological Chemistry*.
<https://doi.org/10.1074/jbc.M606116200>
- Wu, C. C., Hsu, M. C., Hsieh, C. W., Lin, J. B., Lai, P. H., & Wung, B. S. (2006). Upregulation of heme oxygenase-1 by Epigallocatechin-3-gallate via the phosphatidylinositol 3-kinase/Akt and ERK pathways. *Life Sciences*.
<https://doi.org/10.1016/j.lfs.2005.11.013>
- Wu, M., Neilson, A., Swift, A. L., Moran, R., Tamagnine, J., Parslow, D., Armistead, S., Lemire, K., Orrell, J., Teich, J., Chomicz, S., & Ferrick, D. A. (2007). Multiparameter metabolic analysis reveals a close link between attenuated mitochondrial bioenergetic function and enhanced glycolysis dependency in human tumor cells. *American Journal of Physiology - Cell Physiology*. <https://doi.org/10.1152/ajpcell.00247.2006>
- Xia, J., & Wishart, D. S. (2010). MSEA: a web-based tool to identify biologically meaningful patterns in quantitative metabolomic data. *Nucleic Acids Research*, 38(suppl_2), W71–W77. <https://doi.org/10.1093/nar/gkq329>
- Xiong, L. G., Chen, Y. J., Tong, J. W., Gong, Y. S., Huang, J. A., & Liu, Z. H. (2018). Epigallocatechin-3-gallate promotes healthy lifespan through mitohormesis during early-to-mid adulthood in *Caenorhabditis elegans*. *Redox Biology*.
<https://doi.org/10.1016/j.redox.2017.09.019>
- Xu, J., Martien, J., Gilbertson, C., Ma, J., Amador-Noguez, D., & Park, J. O. (2020). Metabolic flux analysis and fluxomics-driven determination of reaction free energy using multiple isotopes. *Current Opinion in Biotechnology*, 64, 151–160.
<https://doi.org/10.1016/j.copbio.2020.02.018>

- Xu, Q., Sachs, J. R., Wang, T. C., & Schaefer, W. H. (2006). Quantification and identification of components in solution mixtures from 1D proton NMR spectra using singular value decomposition. *Analytical Chemistry*.
<https://doi.org/10.1021/ac0606857>
- Yaffe, D., & Saxel, O. (1977). A Myogenic Cell Line with Altered Serum Requirements for Differentiation. *Differentiation*. <https://doi.org/10.1111/j.1432-0436.1977.tb01507.x>
- Yamamoto, M., Kensler, T. W., & Motohashi, H. (2018). The KEAP1-NRF2 system: A thiol-based sensor-effector apparatus for maintaining redox homeostasis. In *Physiological Reviews*. <https://doi.org/10.1152/physrev.00023.2017>
- Yan, J., Feng, Z., Liu, J., Shen, W., Wang, Y., Wertz, K., Weber, P., Long, J., & Liu, J. (2012). Enhanced autophagy plays a cardinal role in mitochondrial dysfunction in type 2 diabetic Goto-Kakizaki (GK) rats: Ameliorating effects of (-)-epigallocatechin-3-gallate. *Journal of Nutritional Biochemistry*.
<https://doi.org/10.1016/j.jnutbio.2011.03.014>
- Yang, D., Liu, X., Liu, M., Chi, H., Liu, J., & Han, H. (2015). Protective effects of quercetin and taraxasterol against H₂O₂-induced human umbilical vein endothelial cell injury in vitro. *Experimental and Therapeutic Medicine*.
<https://doi.org/10.3892/etm.2015.2713>
- Yang, G. Z., Wang, Z. J., Bai, F., Qin, X. J., Cao, J., Lv, J. Y., & Zhang, M. S. (2015). Epigallocatechin-3-gallate protects HUVECs from PM_{2.5}-induced oxidative stress injury by activating critical antioxidant pathways. *Molecules*.
<https://doi.org/10.3390/molecules20046626>
- Ye, Q., Ye, L., Xu, X., Huang, B., Zhang, X., Zhu, Y., & Chen, X. (2012). Epigallocatechin-3-gallate suppresses 1-methyl-4-phenyl-pyridine-induced oxidative stress in PC12

- cells via the SIRT1/PGC-1 α signaling pathway. *BMC Complementary and Alternative Medicine*. <https://doi.org/10.1186/1472-6882-12-82>
- Yeo, D., Kang, C., Gomez-Cabrera, M. C., Vina, J., & Ji, L. L. (2019). Intensified mitophagy in skeletal muscle with aging is downregulated by PGC-1 α overexpression in vivo. *Free Radical Biology and Medicine*, *130*, 361–368. <https://doi.org/10.1016/j.freeradbiomed.2018.10.456>
- Yu, X., Xu, Y., Zhang, S., Sun, J., Liu, P., Xiao, L., Tang, Y., Liu, L., & Yao, P. (2016). Quercetin attenuates chronic ethanol-induced hepatic mitochondrial damage through enhanced mitophagy. *Nutrients*. <https://doi.org/10.3390/nu8010036>
- Zahn, J. M., Sonu, R., Vogel, H., Crane, E., Mazan-Mamczarz, K., Rabkin, R., Davis, R. W., Becker, K. G., Owen, A. B., & Kim, S. K. (2006). Transcriptional profiling of aging in human muscle reveals a common aging signature. *PLoS Genetics*. <https://doi.org/10.1371/journal.pgen.0020115>
- Zane, A. C., Reiter, D. A., Shardell, M., Cameron, D., Simonsick, E. M., Fishbein, K. W., Studenski, S. A., Spencer, R. G., & Ferrucci, L. (2017). Muscle strength mediates the relationship between mitochondrial energetics and walking performance. *Aging Cell*. <https://doi.org/10.1111/accel.12568>
- Zanichelli, F., Capasso, S., Di Bernardo, G., Cipollaro, M., Pagnotta, E., Carteni, M., Casale, F., Iori, R., Giordano, A., & Galderisi, U. (2012). Low concentrations of isothiocyanates protect mesenchymal stem cells from oxidative injuries, while high concentrations exacerbate DNA damage. *Apoptosis*, *17*(9), 964–974. <https://doi.org/10.1007/s10495-012-0740-3>
- Ze Xu, J., Venus Yeung, S. Y., Chang, Q., Huang, Y., & Chen, Z.-Y. (2004a). Comparison of antioxidant activity and bioavailability of tea epicatechins with their epimers. *British Journal of Nutrition*. <https://doi.org/10.1079/bjn20041132>

- Ze Xu, J., Venus Yeung, S. Y., Chang, Q., Huang, Y., & Chen, Z.-Y. (2004b). Comparison of antioxidant activity and bioavailability of tea epicatechins with their epimers. *British Journal of Nutrition*. <https://doi.org/10.1079/bjn20041132>
- Zhang, D. D., & Hannink, M. (2003). Distinct Cysteine Residues in Keap1 Are Required for Keap1-Dependent Ubiquitination of Nrf2 and for Stabilization of Nrf2 by Chemopreventive Agents and Oxidative Stress. *Molecular and Cellular Biology*. <https://doi.org/10.1128/mcb.23.22.8137-8151.2003>
- Zhang, Q., Wu, Y., Guan, Y., Ling, F., Li, Y., & Niu, Y. (2019). Epigallocatechin gallate prevents senescence by alleviating oxidative stress and inflammation in WI-38 human embryonic fibroblasts. *RSC Advances*. <https://doi.org/10.1039/c9ra03313k>
- Zhao, J., Lendahl, U., & Nistér, M. (2013). Regulation of mitochondrial dynamics: Convergences and divergences between yeast and vertebrates. In *Cellular and Molecular Life Sciences*. <https://doi.org/10.1007/s00018-012-1066-6>
- Zheng, J., & Ramirez, V. D. (2000a). Inhibition of mitochondrial proton F₀F₁-ATPase/ATP synthase by polyphenolic phytochemicals. *British Journal of Pharmacology*. <https://doi.org/10.1038/sj.bjp.0703397>
- Zheng, J., & Ramirez, V. D. (2000b). Inhibition of mitochondrial proton F₀F₁-ATPase/ATP synthase by polyphenolic phytochemicals. *British Journal of Pharmacology*. <https://doi.org/10.1038/sj.bjp.0703397>
- Zheng, Y., Morris, A., Sunkara, M., Layne, J., Toborek, M., & Hennig, B. (2012). Epigallocatechin-gallate stimulates NF-E2-related factor and heme oxygenase-1 via caveolin-1 displacement. *The Journal of Nutritional Biochemistry*, 23(2), 163–168. <https://doi.org/10.1016/j.jnutbio.2010.12.002>
- Zhou, X., Bohlen, H. G., Unthank, J. L., & Miller, S. J. (2009). Abnormal nitric oxide production in aged rat mesenteric arteries is mediated by NAD(P)H oxidase-derived

peroxide. *American Journal of Physiology - Heart and Circulatory Physiology*.

<https://doi.org/10.1152/ajpheart.00325.2009>

Zielonka, J., & Kalyanaraman, B. (2010). Hydroethidine- and MitoSOX-derived red fluorescence is not a reliable indicator of intracellular superoxide formation: Another inconvenient truth. In *Free Radical Biology and Medicine*.

<https://doi.org/10.1016/j.freeradbiomed.2010.01.028>